WOODHEAD PUBLISHING SERIES IN ENERGY

Handbook of advanced radioactive waste conditioning technologies

Edited by Michael I. Ojovan

Belgoprocess

WP WOODHEAD PUBLISHING

Handbook of advanced radioactive waste conditioning technologies

Related titles:

Geological repository systems for safe disposal of spent nuclear fuels and radioactive waste
(ISBN 978-1-84569-542-2)
The long-term fate of spent nuclear fuel and radioactive waste materials is of critical importance to the nuclear industry. Long-term safety must be assured without active human oversight, based on the requirement that we do not pass the burden of nuclear waste onto future generations. Geological disposal systems and technology, utilising both natural geological barriers and engineered barrier systems, have therefore been developed to isolate spent nuclear fuel and radioactive materials from the human environment. This book critically reviews state-of-the-art technologies, scientific methods and engineering practices directly related to the design, operation and safety of geological repositories.

Advanced separation techniques for nuclear fuel reprocessing and radioactive waste treatment
(ISBN 978-1-84569-501-9)
Advanced separations technology is key to ensuring the environmental protection, criticality-safety and non-proliferation (security) of radioactive materials. Separation techniques are applied in reprocessing nuclear fuels for further power generation as well as in radioactive waste treatment for radiological-content reduction of materials due for storage and disposal. Initial sections review materials management issues and the characterisation and behaviour of the main radioactive materials produced by nuclear power generation. Further sections cover irradiated fuel treatment, such as the PUREX process, and radioactive waste treatment, such as supercritical fluid extraction. Final sections cover next generation processes, including partitioning and transmutation, and applications.

Understanding and mitigating ageing in nuclear power plants
(ISBN 978-1-84569-511-8)
Plant life management (PLiM) is a safety-based methodology for the management of nuclear power plants over their entire lifetime. It is used by plant operators and regulators to assess the condition of nuclear power plant, and to establish the technical and economic requirements for safe, long-term operation. This book critically reviews the fundamental ageing-degradation mechanisms that affect nuclear power plant structures, systems and components (SSC), along with relevant analysis and modelling methods and mitigation paths. Coverage of plant maintenance and replacement routes is extended through chapters on the development of advanced materials and components, as well as through reactor-type specific PLiM practices.

Details of these and other Woodhead Publishing books can be obtained by:

- visiting our web site at www.woodheadpublishing.com
- contacting Customer Services (e-mail: sales@woodheadpublishing.com; fax: +44 (0) 1223 832819; tel: +44 (0) 1223 499140 ext. 130; address: Woodhead Publishing Limited, 80 High Street, Sawston, Cambridge CB22 3HJ, UK)

If you would like to receive information on forthcoming titles, please send your address details to: Francis Dodds (address, tel. and fax as above; e-mail: francis.dodds@woodheadpublishing.com). Please confirm which subject areas you are interested in.

Woodhead Publishing Series in Energy: Number 12

Handbook of advanced radioactive waste conditioning technologies

---

Edited by
Michael I. Ojovan

Belgoprocess

WP
WOODHEAD
PUBLISHING

Oxford Cambridge Philadelphia New Delhi

Published by Woodhead Publishing Limited
80 High Street, Sawston, Cambridge CB22 3HJ, UK
www.woodheadpublishing.com

Woodhead Publishing, 1518 Walnut Street, Suite 1100, Philadelphia,
PA 19102-3406, USA

Woodhead Publishing India Private Limited, G-2, Vardaan House,
7/28 Ansari Road, Daryaganj, New Delhi – 110002, India
www.woodheadpublishingindia.com

First published 2011, Woodhead Publishing Limited
© Woodhead Publishing Limited, 2011
The authors have asserted their moral rights.

This book contains information obtained from authentic and highly regarded sources. Reprinted material is quoted with permission, and sources are indicated. Reasonable efforts have been made to publish reliable data and information, but the authors and the publisher cannot assume responsibility for the validity of all materials. Neither the authors nor the publisher, nor anyone else associated with this publication, shall be liable for any loss, damage or liability directly or indirectly caused or alleged to be caused by this book.

Neither this book nor any part may be reproduced or transmitted in any form or by any means, electronic or mechanical, including photocopying, microfilming and recording, or by any information storage or retrieval system, without permission in writing from Woodhead Publishing Limited.

The consent of Woodhead Publishing Limited does not extend to copying for general distribution, for promotion, for creating new works, or for resale. Specific permission must be obtained in writing from Woodhead Publishing Limited for such copying.

Trademark notice: Product or corporate names may be trademarks or registered trademarks, and are used only for identification and explanation, without intent to infringe.

British Library Cataloguing in Publication Data
A catalogue record for this book is available from the British Library.

ISBN 978-1-84569-626-9 (print)
ISBN 978-0-85709-095-9 (online)
ISSN 2044-9364 Woodhead Publishing Series in Energy (print)
ISSN 2044-9372 Woodhead Publishing Series in Energy (online)

The publisher's policy is to use permanent paper from mills that operate a sustainable forestry policy, and which has been manufactured from pulp which is processed using acid-free and elemental chlorine-free practices. Furthermore, the publisher ensures that the text paper and cover board used have met acceptable environmental accreditation standards.

Typeset by Toppan Best-set Premedia Limited
Printed by TJI Digital, Padstow, Cornwall UK

Contents

Contributor contact details

(* = main contact)

Editor and Chapter 1

M. I. Ojovan
Department of Materials Science and Engineering
University of Sheffield
Sir Robert Hadfield Building
Mappin Street
Sheffield S1 3JD
UK
E-mail: m.ojovan@sheffield.ac.uk

Chapter 2

M. Garamszeghy
Ontario Power Generation Inc.
700 University Ave, H17
Toronto, ON M5G 1X6
Canada
E-mail: miklos.garamszeghy@sympatico.ca

Chapter 3

J. Deckers
Belgoprocess
Gravenstraat 73
2480 Dessel
Belgium
E-mail: jan.deckers@belgoprocess.be

Chapter 4

F. Glasser
Department of Chemistry
University of Aberdeen
Meston Walk
Aberdeen AB24 3UE
UK
E-mail: f.p.glasser@abdn.ac.uk

Chapter 5

A. S. Aloy
V. G. Khlopin Radium Institute
2nd Murinskiy Prospect, b. 28
194021 St Petersburg
Russia
E-mail: aloy@khlopin.ru

Chapters 6 and 9

C. M. Jantzen
Savannah River National Laboratory
Aiken, SC 29808
USA
E-mail: carol.jantzen@srnl.doe.gov

Chapter 7

M. Laraia
International Atomic Energy Agency (IAEA)
Wagramerstrasse 5
PO Box 200
A-1400 Vienna
Austria
E-mail: M.Laraia@iaea.org

Chapter 8

E. R. Vance* and D. S. Perera
Institute of Materials Engineering
Australian Nuclear Science and Technology Organisation (ANSTO)
Menai, NSW 2234
Australia
E-mail: erv@ansto.gov.au
pereradan@gmail.com

Chapter 10

H. Kinoshita
Department of Materials Science and Engineering
The University of Sheffield
Mappin Street
Sheffield S1 3JD
UK
E-mail: H.Kinoshita@sheffield.ac.uk

Chapter 11

G. Ouzounian and R. Poisson*
Agence Nationale pour la Gestion de Déchets Radioactifs (Andra)
1–7 rue Jean Monnet
92298 Chatenay Malabry
France
E-mail: Richard.Poisson@andra.fr
Gerald.Ouzounian@andra.fr

Chapter 12

I. G. Crossland
Crossland Consulting
Nympsfield GL10 3UB
UK
E-mail: i.g.crossland@btinternet.com

Chapter 13

V. V. Rondinella
European Commission Joint Research Centre
Institute for Transuranium Elements
Postfach 2340
76125 Karlsruhe
Germany
E-mail: vincenzo.rondinella@ec.europa.eu

Chapter 14

D. Bacon* and E. Pierce
Pacific Northwest National Laboratory
PO Box 999
Richland, WA 99352
USA
E-mail: Diana.Bacon@pnl.gov

Chapter 15

P. Gowin, J. Kinker, A. Kosilov*, I. Upshall and Y. Yanev
International Atomic Energy Agency (IAEA)
Wagramerstrasse 5
P.O. Box 200
A-1400 Vienna
Austria
E-mail: A.Kossilov@iaea.org
A.Kossilov@inode.at

Woodhead Publishing Series in Energy

1 **Generating power at high efficiency: Combined cycle technology for sustainable energy production**
Eric Jeffs

2 **Advanced separation techniques for nuclear fuel reprocessing and radioactive waste treatment**
Edited by Kenneth L. Nash and Gregg J. Lumetta

3 **Bioalcohol production: Biochemical conversion of lignocellulosic biomass**
Edited by K.W. Waldron

4 **Understanding and mitigating ageing in nuclear power plants: Materials and operational aspects of plant life management (PLiM)**
Edited by Philip G. Tipping

5 **Advanced power plant materials, design and technology**
Edited by Dermot Roddy

6 **Stand-alone and hybrid wind energy systems: Technology, energy storage and applications**
Edited by J.K. Kaldellis

7 **Biodiesel science and technology: From soil to oil**
Jan C.J. Bart, Natale Palmeri and. Stefano Cavallaro

8 **Developments and innovation in carbon dioxide (CO_2) capture and storage technology Volume 1: Carbon dioxide (CO_2) capture, transport and industrial applications**
Edited by M. Mercedes Maroto-Valer

9 **Geological repository systems for safe disposal of spent nuclear fuels and radioactive waste**
Edited by Joonhong Ahn and Michael J. Apted

10 **Wind energy systems: Optimising design and construction for safe and reliable operation**
Edited by John D. Sørensen and Jens N. Sørensen

11 **Solid oxide fuel cell technology: Principles, performance and operations**
Kevin Huang and John Bannister Goodenough

12 **Handbook of advanced radioactive waste conditioning technologies**
Edited by Michael I. Ojovan

13 **Nuclear reactor safety systems**
Edited by Dan Gabriel Cacuci

14 **Materials for energy efficiency and thermal comfort in buildings**
Edited by Matthew R. Hall

15 **Handbook of biofuels production: Processes and technology**
Edited by Rafael Luque, Juan Campelo and James Clark

16 **Developments and innovation in carbon dioxide (CO_2) capture and storage technology Volume 2: Carbon dioxide (CO_2) storage and utilisation**
Edited by M. Mercedes Maroto-Valer

17 **Oxy-fuel combustion for power generation and carbon dioxide (CO_2) capture**
Edited by Ligang Zheng

18 **Small and micro combined heat and power (CHP) systems: Advanced design, performance, materials and applications**
Edited by Robert Beith

19 **Hydrocarbon fuel conversion technology: Advanced processes for clean fuel production**
Edited by M. Rashid Khan

20 **Modern gas turbine systems: High efficiency, low emission, fuel flexible power generation**
Edited by Peter Jansohn

21 **Concentrating solar power (CSP) technology: Developments and applications**
Edited by Keith Lovegrove and Wes Stein

22 **Nuclear corrosion science and engineering**
Edited by Damien Féron

23 **Power plant life management and performance improvement**
Edited by John Oakey

24 **Direct-drive wind and marine energy systems**
Edited by Markus Mueller

25 **Advanced membrane science and technology for sustainable energy and environmental applications**
Edited by Angelo Basile and Suzana Nunes

26 **Irradiation embrittlement of reactor pressure vessels (RPVs)**
Edited by Naoki Soneda

27 **High temperature superconductors (HTS) for energy applications**
Edited by Ziad Melhem

28 **Infrastructure and methodologies for the justification of nuclear power programmes**
Edited by Agustín Alonso Santos

1

Radioactive waste characterization and selection of processing technologies

M. I. OJOVAN, University of Sheffield, UK

Abstract: The generic approach of radioactive waste management is to use more reliable natural and engineered barrier systems for more hazardous waste. The guidance for treatment and conditioning of radioactive waste is based on data obtained on waste material characterization. Characterization of radioactive waste gives important waste material parameters and enables its classification according to national regulations. Although classification schemes are country dependent, there is a generic consensus that end points (e.g. storage and disposal) and conditioning methods (e.g. immobilization and packaging) depend on the level of radioactivity and radionuclide lifetime. Radioactive waste processing routes are specified herein using the new International Atomic Energy Agency (IAEA) radioactive waste classification scheme which is based on long-term safety of waste.

Key words: radioactive waste, classification, processing, treatment, immobilization, conditioning, disposal.

1.1 Introduction

Although many of the radioactive substances currently used are of artificial origin, radioactivity is a natural phenomenon with natural sources of radiation in the environment. Radiation and radioactive materials have many beneficial applications, ranging from power generation to industrial and agricultural irradiators and radiolabelled compounds in medicine and scientific research. Radioactive waste associated with those applications is generated in a wide range of concentrations of radionuclides and in a variety of physical and chemical forms. There is a variety of alternatives for processing waste or storage prior to disposal as well as several alternatives for the safe disposal of waste, ranging from near-surface to geological disposal. Wide differences in waste compositions may result in an equally wide variety of options for the management of the waste; therefore a proper scheme of waste classification is required before any waste processing.

Many schemes have been developed to classify or categorize radioactive waste according to its physical, chemical and radiological properties, most of which are of relevance to particular facilities or given circumstances in which radioactive waste is managed. Nevertheless there is a generic consensus that the end points (e.g. storage and disposal) and conditioning methods (e.g. immobilization and packaging in containers) depend on the level of radioactivity and radionuclide lifetime. This approach has found reflection in the generic classification scheme developed by the International Atomic Energy Agency (IAEA) in the General Safety Guide GSG-1 [1], which has evolved via a long process of consultations and accounted for current worldwide practice on radioactive waste management. This publication is providing consistent and reliable guidance on the classification of the whole range of radioactive waste, beginning from waste having such low levels of activity concentration that it is not required to be managed or regulated as radioactive waste, and ending with highly radioactive waste resulting from nuclear fuel reprocessing and nuclear fuel in the case when it is considered radioactive waste. The IAEA classification scheme is focused on disposal where the multi-barrier principle holds [2]. The key issue with any disposal option is safety, which is achieved mainly by concentration and containment involving the isolation of suitably conditioned radioactive waste in a disposal facility. Containment uses many barriers around the radioactive waste to restrict the release of radionuclides into the environment. Such an approach is termed the multi-barrier concept and is often called matreshka after the popular Russian doll, which inside of each larger doll has a smaller one, so that the total number of dolls is large (Fig. 1.1).

The restricting barriers can be either natural or engineered, e.g. obtained via processing. The generic approach is to use more reliable barriers for more hazardous waste, including engineered barriers which result from the radioactive waste treatment and conditioning process. The IAEA waste classification [1] can be thus used to develop generic guidance for waste processing methods. This is particularly important as many countries use IAEA standards and approaches in developing national radiation and

1.1 Russian doll 'matreshka' as a symbol of the multi-barrier concept.

nuclear safety regulations. Therefore we will first analyse the new IAEA waste classification scheme and then use it as guidance for waste treatment and conditioning.

1.2 Radioactive waste classification

Two main parameters of the IAEA classification scheme [1] are radionuclide half-life and radioactivity content. In terms of radioactive waste safety, a radionuclide with a half-life longer than that of ^{137}Cs (30.17 years) is considered to be long lived whereas those with half-life shorter than about 30 years are considered short lived. In terms of radioactive waste safety, radioactivity contents are analysed compared with exemption levels [3]. The activity content term is a generic name that covers activity concentration, specific activity and total activity and is used in classification schemes accounting for the generally heterogeneous nature of radioactive waste [1]. The activity content can range from negligible to very high, that is, a very high concentration of radionuclides or a very high specific activity. The higher the activity content, the greater the need to contain the waste and to isolate it from the biosphere, e.g. the more stringent are the requirements for safety barriers.

The IAEA classification scheme first defines exempt waste (EW). EW is that radioactive waste which contains such small concentrations of radionuclides that it does not require provisions for radiation protection, irrespective of whether the waste is disposed of in conventional landfills or recycled. The EW meets the criteria for clearance, exemption or exclusion from regulatory control for radiation protection purposes which are given in IAEA publications [3, 4]. The criteria for exemption were established by the IAEA following recommendations and principles of the International Commission on Radiological Protection (ICRP). The criteria used to derive exemption levels for radioactive materials are an expected individual effective dose not higher than 10 μSv/y and a collective effective dose not higher than 1 person Sv/y. Exemption levels were established for both concentration and total amount of radionuclides based on the individual and collective dose. These were determined for each radionuclide taking account of all possible pathways to humans including assessment of individual and collective doses. Exemption levels are published in the International Basic Safety Standards for Protection against Ionizing Radiation and for the Safety of Radiation Sources [4]. Sources of radiation are exempt from control if at a distance of 0.1 metres the dose rate is below 1 μSv/h. Clearance levels are defined by the national regulatory authorities; however, since these take into account internationally approved recommendations, quantified clearance levels (with some exceptions) are similar in all countries. EW is thus in practice considered as a non-radioactive material and waste.

The IAEA classification scheme defines five classes of radioactive waste: very short lived waste (VSLdW), very low level waste (VLLW), low level waste (LLW), intermediate level waste (ILW) and high level waste (HLW).

VSLdW is that radioactive waste which can be stored for decay over a limited period of no longer than a few years with subsequent clearance from regulatory control. Clearance procedure is done according to existing national arrangements, after which VSLdW can be disposed of, discharged or used. VSLdW includes waste containing primarily radionuclides with very short half-lives which are most often used for research and medicine.

VLLW is that radioactive waste which does not necessarily meet the criteria of EW, but which does not need a high level of containment and isolation and is therefore suitable for disposal in near-surface landfill-type facilities with limited regulatory control. Typical VLLW includes soil and rubble with low levels of activity concentration.

LLW has higher activity contents than VLLW but with limited amounts of long-lived radionuclides in it. Such waste requires robust isolation and containment for periods of up to a few hundred years and is suitable for disposal in engineered near-surface facilities. LLW covers a very broad range of waste with long-lived radionuclides only at relatively low levels of activity concentration.

ILW is that radioactive waste which, because of its radionuclides content, particularly of long-lived radionuclides, requires a greater degree of containment and isolation than that provided by near-surface disposal. However, ILW needs no provision, or only limited provision, for heat dissipation during its storage and disposal. ILW may contain long-lived radionuclides, in particular alpha-emitting radionuclides that will not decay to a level of activity concentration acceptable for near-surface disposal during the time for which institutional controls can be relied upon. Therefore ILW requires disposal at greater depths, of the order of tens of metres to a few hundred metres. A precise boundary between LLW and ILW cannot be universally provided, as limits on the acceptable level of activity concentration will differ between individual radionuclides or groups of radionuclides. Waste acceptance criteria for a particular near-surface disposal facility depend on its actual design and operation plan for the facility (e.g. engineered barriers, duration of institutional control, site-specific factors). A limit of 400 Bq/g on average (and up to 4000 Bq/g for individual packages) for long-lived alpha-emitting radionuclides has been adopted in many countries. For long-lived beta- and/or gamma- emitting radionuclides, such as ^{14}C, ^{36}Cl, ^{63}Ni, ^{93}Zr, ^{94}Nb, ^{99}Tc and ^{129}I, the allowable average activity concentrations may be considerably higher (up to tens of kBq/g) and may be specific to the site and disposal facility [1]. A contact dose rate of 2 mSv/h has been generally used to distinguish between LLW and ILW [5], though contact radiation dose rate is not used to distinguish waste classes in the current IAEA classification scheme, which is based primarily on long-term safety [1].

HLW is that radioactive waste with levels of activity concentration high enough to require shielding in handling operations and generate significant quantities of heat by the radioactive decay process. HLW can be also the waste with large amounts of long-lived radionuclides that need to be considered in the design of a disposal facility. Disposal in deep, stable geological formations usually several hundred metres or more below the surface is the generally recognized HLW disposal option.

As can be seen, the IAEA classification scheme is rather generic and has very few exact limits in defining radioactive waste classes. Existing national regulations give more exact figures. For example, the UK classification scheme [2] defines VLLW as waste which can be disposed of with ordinary refuse, each 0.1 m^3 of material containing less than 400 kBq of beta/gamma activity or single items containing less than 40 kBq. LLW is defined as waste containing radioactive materials other than those suitable for disposal with ordinary refuse, but not exceeding 4 GBq/te of alpha or 12 GBq/te of beta/gamma activity. ILW is waste with radioactivity levels exceeding the upper boundaries for LLW, but which do not need heating to be taken into account in the design of storage or disposal facilities. HLW is waste in which the temperature may rise significantly as a result of its radioactivity, so this factor has to be taken into account in designing storage or disposal facilities. Russia is at the stage of introducing a VLLW class [6]; currently its national regulations define only LLW, ILW and HLW classes. LLW is waste with specific radioactivity $<10^3$ Bq/g for beta, $<10^2$ Bq/g for alpha and <10 Bq/g for transuranic radionuclides; ILW is waste with specific radioactivity from 10^3 to 10^7 Bq/g for beta, from 10^2 to 10^6 Bq/g for alpha, and from 10 to 10^5 Bq/g for transuranic radionuclides; and HLW is waste with specific radioactivity $>10^7$ Bq/g for beta, $>10^6$ Bq/g for alpha and $>10^5$ Bq/g for transuranic radionuclides [2]. Note that there is a generic trend to use lower activity contents for longer-lived radionuclides as boundaries between LLW, ILW and HLW, e.g. alpha and transuranic elements, in the Russian classification scheme.

1.3 Radioactive waste characterization

The nature and composition of the waste must be thoroughly characterized and understood for processing, storage and disposal. Characterization of radioactive wastes is carried out to determine important waste parameters and to enable segregation of radioactive waste for exemption, reuse and choice of disposal option, e.g. near-surface or deep geological facility. A compendium of available characterization methods and techniques including relevant testing procedures (standards) is given in [7]. Based on characterization data, radioactive waste is categorized for processing [8]. Finally, characterization of radioactive waste enables its classification according to national regulations.

Characterization of radioactive waste accounts for ionizing radiation and any potential for escape and contamination of the surrounding environment. Characterization equipment usually includes sampling tools, radiological and spectrometric (spectroscopic) measuring devices, physical/chemical analysis and separation devices. Universal radiometers – dosimeters are used to characterize γ, β and α radiation fields. Detailed information on radionuclide content in radioactive waste is obtained by analysing representative samples using γ-, β- and α-spectrometers. Materials containing low concentrations of radionuclides are most difficult to analyse. High-purity germanium detectors are typically used for highly sensitive γ-spectrometry of such materials. These detect the electrical current induced by electron-hole pairs created by γ-rays in the depletion regions of reverse-biased *p–n* junctions. β- and α-spectrometers may use either the scintillation phenomenon, which converts energy lost by ionizing radiation into pulses of light in either solid or liquid materials, or electron-hole production in semiconductor devices. The most sensitive liquid scintillation analysis involves dissolving samples in solvents containing scintillating additives and analysis of light emission caused by ionizing β- or α-particles emitted by sample radionuclides. Processing of the resulting spectra enables both qualitative identification of separate radionuclides and quantitative determination of their content in the analysed materials.

1.4 Radioactive waste processing

Different types of radioactive waste follow different processing routes schematically shown in Fig. 1.2 for solid and in Fig. 1.3 for liquid radioactive wastes. After characterization, the radioactive waste is first processed, then stored and disposed of [2]. Processing of radioactive waste includes any operation that changes the characteristics of radioactive waste and includes pre-treatment, treatment and conditioning. Pre-treatment of radioactive waste is the initial step in waste management that occurs after waste generation. Treatment of radioactive waste includes all operations intended to improve safety or economy by changing the radioactive waste characteristics. The three basic treatment objectives are: (1) volume reduction, (2) radionuclide removal from waste, and (3) change of physical and chemical composition [2]. Examples of treatment processes include incineration of combustible waste, compaction of dry solid waste, evaporation, filtration or ion exchange of liquid waste streams (radionuclide removal), and neutralization, precipitation or flocculation of chemical species (change of composition). Often several of these processes are combined to provide effective

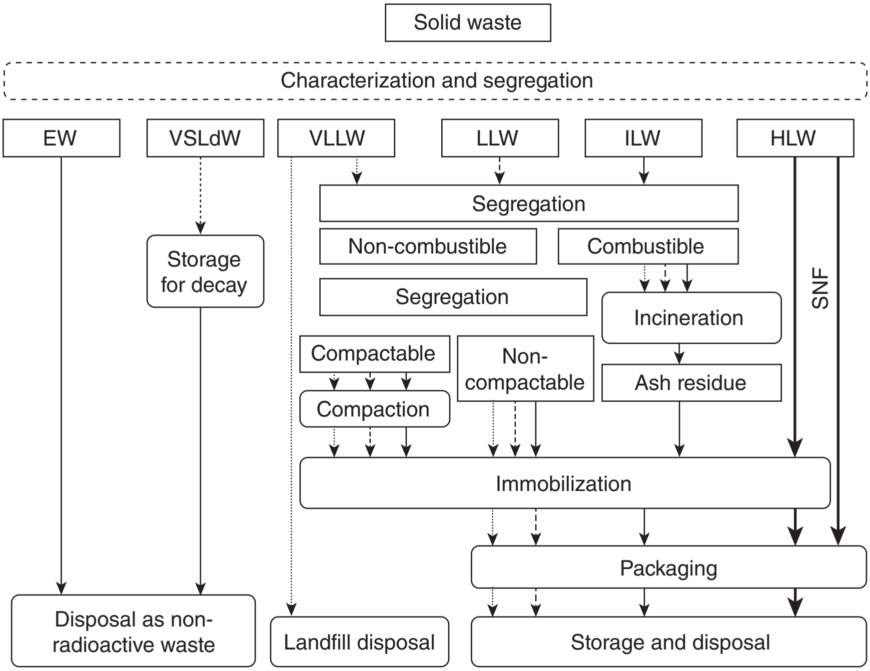

1.2 Schematic representation of solid radioactive waste management operations.

decontamination of a liquid waste stream. Treatment may result in several types of secondary radioactive waste which need to be managed, including, e.g., contaminated filters, spent ion exchangers and sludges.

Conditioning transforms the radioactive waste into a form suitable for handling, transportation, storage and disposal. Conditioning as a rule includes immobilization of radionuclides, placing the waste into containers and providing additional packaging. Immobilization in contrast to conditioning comprises the conversion of a waste into a wasteform by solidification, embedding or encapsulation. Common immobilization methods include solidification of liquid LLW and ILW, e.g. in cement, bitumen or glass, and vitrification of liquid HLW in a glass matrix or embedding of solid HLW into a metal matrix. These, in turn, may be packaged in containers ranging from common 200-litre steel drums to highly engineered thick-walled containers depending on the nature and level of radioactivity. In many instances, treatment and conditioning take place in close conjunction with one another. Packing is preparation of radioactive waste for safe handling, transportation, storage and disposal by means of enclosing it in a suitable container. An over-pack is a secondary or outer container for one or more waste packages, used for handling, transportation, storage or disposal.

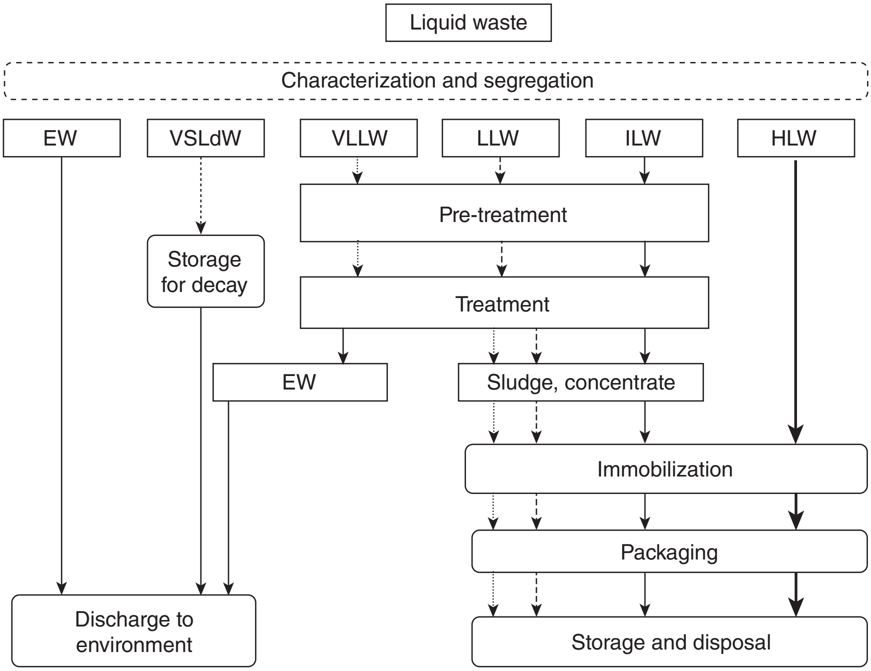

1.3 Schematic representation of liquid radioactive waste management operations.

1.5 Selection of conditioning technologies

Conditioning technologies used are different and depend on the class of waste processed, as shown schematically in Fig. 1.4. VLLW typically does not require immobilization, although some packaging could be used. LLW is typically immobilized using cements, although glasses provide better retention of contaminants, with very large volumes of LLW immobilized using vitrification in Hanford, USA [9]. ILW with a higher hazard than LLW can be immobilized using glasses, bitumen, cements and geopolymers. LLW and ILW can be packed in high-integrity metal and concrete containers. The most hazardous waste such as HLW requires the most durable and reliable wasteforms, e.g. ceramics and glasses and containers such as stainless steel canisters for vitrified HLW and copper containers for spent nuclear fuel declared as waste.

1.5.1 VSLdW

VSLdW contains only very short half-life radionuclides with half-lives typically of the order of 100 days or less. Typical VSLdW from industrial and

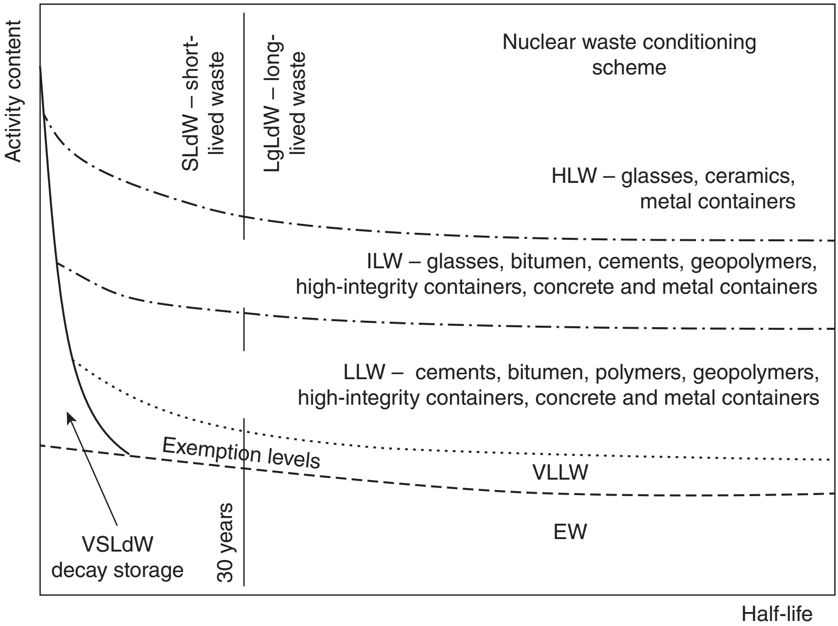

1.4 Radioactive waste conditioning as a function of radioactive waste class.

medical applications contain ^{192}Ir and ^{99m}Tc, although they could contain other radionuclides with very short half-lives. Due to natural radioactive decay VSLdW will gradually transform into EW, so VSLdW can be stored for relatively short periods of time until the activity has naturally decreased below clearance levels. After that storage period, often termed 'storage for decay' or 'delay for decay', the cleared waste can be managed as any conventional (non-radioactive) waste. Storage for decay is thus the typical method used in the management of solid, liquid and gaseous waste containing very short half-life radionuclides.

1.5.2 VLLW

VLLW is generated as a result of operation and decommissioning of nuclear facilities and also originates from the mining or processing of ores and minerals. Its activity contents are only slightly above the levels specified for the clearance of materials from regulatory control. Most typically this waste is solid. Although VLLW cannot be exempt from regulatory control, the extent of the provisions necessary to ensure its safe disposal is rather limited. VLLW disposal facilities can range from simple covers to trenches or more complex disposal systems. Landfill facilities could safely accommodate waste containing artificial radionuclides with levels of activity concentrations one or two orders of magnitude above the levels for EW, for waste containing short-lived radionuclides and with limited total activity.

1.5.3 LLW

Although LLW may contain high concentrations of short-lived radionuclides, significant radioactive decay of these will occur during the period of reliable containment and isolation provided by the site, the engineered barriers and institutional control of which is typically assumed to last for a period of up to around 300 years. LLW can contain only low concentrations of long-lived radionuclides and so it is suitable for near-surface disposal when robust containment and isolation for limited periods of time up to a few hundred years are required. Near-surface disposal facilities can be in the form of simple or complex engineered facilities, and may involve disposal at varying depths, typically from the surface down to 30 m depending on safety approaches and national practices.

The most common methods of liquid (aqueous) LLW treatment are evaporation, chemical precipitation, ion exchange and membrane methods. Evaporation of aqueous or organic solutions concentrates radionuclides and results in a very high waste volume reduction factor as well as a high decontamination factor. The resulting concentrate is then conditioned. Chemical precipitation involves the precipitation of insoluble compounds using chemicals such as barium chloride, sodium sulphate, potassium ferrocyanide, copper sulphate, etc. The resultant sludge that contains the bulk of radioactivity requires conditioning. Ion exchange uses extraction of radionuclides by selective ion exchange resins and inorganic ion exchangers. The spent ion exchangers are subsequently conditioned. Membrane methods include processes such as reverse osmosis, nano- and ultrafiltration. The used membranes and the concentrates are conditioned. In practice several methods are often used in combination, e.g. evaporation followed by ion exchange.

The most common solid LLW treatment methods are compaction/supercompaction and incineration. Compaction aims to reduce the volume and increase the stability of solid waste for transport, storage and disposal. The volume reduction achievable depends on the nature of the waste and the equipment used, with the highest reduction for high-force compactors termed supercompactors. Incineration can be applied to both solid and liquid combustible LLW. It achieves the highest volume reduction and yields a chemically stable form – ash residue, which needs further stabilization such as by supercompaction followed by cementation. Secondary wastes from incineration are conditioned before disposal. Metallic wastes can be melted, resulting in a high reduction of volume and often in purification from radioactive contaminants. Secondary wastes generated in this process, e.g. slag and spent filter materials, need conditioning.

Treated or untreated LLW is typically immobilized to produce a more stable physical and chemical wasteform. Cementation and bituminization are the most typical immobilization technologies used for liquid LLW, whereas solid LLW is typically cemented [2]. Geopolymers are also used for LLW immobilization [10]. The LLW wasteform is typically placed in concrete containers. Processed or unprocessed LLW may also be placed into high-integrity containers capable of providing containment for long periods of time. Steel, plastic (high-density polyethylene) and concrete containers have been developed for this purpose [11].

1.5.4 ILW

ILW contains long-lived radionuclides in quantities that need a greater degree of containment than LLW, e.g. it requires disposal in a facility at a depth of between a few tens and a few hundreds of metres. Disposal at such depths provides a longer period of isolation from the accessible environment if both the natural barriers and the engineered barriers of the disposal system are selected properly. In particular, there is generally no detrimental effect of erosion at such depths in the short to medium term. Another important advantage of disposal at such depths is that the likelihood of inadvertent human intrusion is greatly reduced. ILW may require shielding to provide adequate protection for workers, but needs no or only limited provision for heat dissipation during its storage and disposal. ILW typically comprises metals that have been irradiated in reactor cores, graphite waste, ion exchange resins and fuel cladding waste resulting from spent fuel reprocessing. Processing methods for ILW are similar to those for LLW. Conditioning methods could include more durable wasteforms and containers compared with those used for LLW. Additional shielding may be required to limit radiation dose rates near ILW containers.

1.5.5 HLW

HLW has substantial high activity levels and requires extensive personnel protection, shielding, remote handling and consideration of the effects of radiogenic heat generation. HLW requires deep underground disposal. Typically, this waste arises from spent nuclear fuel (SNF) reprocessing or is the spent fuel itself. It can include some highly radioactive disused sealed radioactive sources (SRS) such as those used in industrial irradiators. SNF and liquid HLW from reprocessing are highly radioactive and heat generating, and need to be cooled and shielded. Prior to processing, liquid HLW is stored in cooled high-integrity double-walled stainless steel tanks housed in special vaults. Processing of liquid HLW involves chemical treatment and evaporation followed by vitrification using borosilicate or phosphate glasses, or incorporation in ceramic compositions. The HLW solid product (wasteform) is contained in stainless steel canisters. Solid HLW in the form of SNF after removal from the reactor requires shielding and heat removal, which are provided by water in storage pools built at the reactor. After several years of cooling, SNF is transferred to a separate storage facility, either wet (pools) or dry (vaults or casks). Prior to disposal the SNF is emplaced in highly durable metallic (copper) containers. Solid HLW in the form of disused SRS is immobilized using metal matrices and encapsulation in stainless steel casings. These may further be grouted in steel drums or other suitable overpack.

A summary guidance on processing was recently given in the IAEA publication on policies and strategies for radioactive waste management [11]. Table 1.1 gives generic guidance on treatment and conditioning options for radioactive wastes with detailed information found in the chapters of this book.

It can be seen that both more reliable conditioning technologies (immobilization, packaging) and end points (disposal options) are used for each increase of waste class, e.g. level of waste hazard. This is in line with the so-called geochemical approach on nuclear waste disposal. The geochemical approach considers disposal of nuclear waste as a process with many uncertainties on the long-term (geological) scale. Moreover, it takes into account that any geological environment disturbed by a repository may support faster than usual degradation of engineering barriers. Justification of wasteforms is based not only on chemical durability and resistance to radiation damage in laboratory conditions but also on geochemical compatibility with the host rock. The use of more durable wasteforms for more hazardous waste is therefore extremely important [12].

1.6 Sources of further information and advice

The handbook chapters described below give detailed information on sources of further reading. Table 1.2 gives a chapter- by-chapter summary of treatment and conditioning options.

1.7 Acknowledgements

This book has become possible due to the enthusiasm of Woodhead Publishing Ltd and its Commissioning Editor Ian Borthwick to whom I would like to express my gratitude. Mike Garamszeghy of Ontario Power Generation, a known expert in waste processing technologies, prepared the

Table 1.1 Summary of treatment and conditioning options for radioactive wastes

Waste	Form	Treatment	Conditioning		End point
			Immobilization	Packaging	
VSLdW	Solid	Storage for decay	–	–	Disposal as non-radioactive waste
	Liquid	Storage for decay	–	–	Discharge to environment
VLLW	Solid	Storage for decay, fragmentation	–	–	Surface trench, landfill, near-surface disposal
	Liquid	Storage for decay, evaporation, membrane methods, ion exchange	Cementation	Simple packages, e.g. excepted and industrial packages	Surface trench, landfill, near-surface disposal
LLW	Solid	Compaction, supercompaction, incineration, melting, fragmentation	Grouting	Metal and concrete containers, high-integrity containers	Near-surface disposal
	Liquid	Chemical treatment, ion exchange, membrane methods, evaporation	Cementation, bituiminization, polymers and geopolymers immobilization, vitrification	Metal and concrete containers, high-integrity containers	Near-surface disposal
ILW	Solid	Compaction, supercompaction, fragmentation	Grouting	Metal and concrete containers, high-integrity containers	Intermediate depth disposal, deep geological disposal
	Liquid	Chemical treatment, ion exchange, membrane methods, evaporation	Cementation, bituiminization, polymers and geopolymers immobilization, vitrification	Metal and concrete containers, high-integrity containers	Intermediate depth disposal, deep geological disposal
HLW	Solid e.g. SRS	–	Metal matrix immobilization	Stainless steel capsules	Intermediate depth disposal, deep geological disposal
	SNF	–	–	Metallic, e.g. copper container	Deep geological disposal
	Liquid	Evaporation in conjunction with immobilization	Vitrification, ceramics immobilization	Stainless steel canisters	Deep geological disposal

Table 1.2 Application of the chapters of this book to various waste classes

Chapter		Waste classes
1	Radioactive waste characterization and selection of processing technologies (Ojovan)	All waste classes
2	Compaction processes and technology for treatment and conditioning of radioactive waste (Garamszeghy)	LLW, ILW
3	Incineration and plasma processes and technology for treatment and conditioning of radioactive waste (Deckers)	LLW, ILW
4	Application of inorganic cements to the conditioning and immobilisation of radioactive wastes (Glasser)	LLW, ILW
5	Calcination and vitrification processes for conditioning of radioactive wastes (Aloy)	ILW, HLW
6	Historical development of glass and ceramic waste forms for high level radioactive wastes (Jantzen)	HLW
7	Decommissioning of nuclear facilities and environmental remediation: generation and management of radioactive and other wastes (Laraia)	VSLdW, VLLW, LLW, ILW
8	Development of geopolymers for nuclear waste immobilisation (Vance and Perera)	LLW, ILW
9	Development of glass matrices for high level radioactive wastes (Jantzen)	ILW, HLW
10	Development of ceramic matrices for high level radioactive wastes (Kinoshita)	HLW
11	Development of waste packages for the disposal of radioactive waste: French experience (Ouzounian and Poisson)	LLW, ILW
12	Development and use of metal containers for the disposal of radioactive wastes (Crossland)	LLW, ILW, HLW
13	Failure mechanisms of high level nuclear waste forms in storage and geological disposal conditions (Rondinella)	HLW
14	Development of long-term behavior models for radioactive waste forms (Bacon and Pierce)	All waste classes
15	Knowledge management for radioactive waste management organisations (Gowin, Kinker, Kosilov, Upshall and Yanev)	All waste classes

first chapter for the Handbook, on compaction technologies (Chapter 2). Jan Deckers of Belgoprocess, who has long-term experience in thermal treatment technologies, overviewed the incineration and plasma techniques (Chapter 3). Fred Glasser of the University of Aberdeen, who is one of the founders of the scientific bases for the use of cements in nuclear waste immobilization, kindly agreed to give an overview of all types of cementitious materials (Chapter 4). Albert Aloy of KRI, the leading Russian scientist in vitrification, has shared his views on using glasses and vitrification (Chapter 5). Carol Jantzen of SRNL, former President of the American Chemical Society, in addition to her chapter on glassy wasteforms (Chapter 9) has proposed a comprehensive overview on development of vitrification technology (Chapter 6). The IAEA staff members and experts in nuclear waste management Mike Laraia (Chapter 7) and Andrey Kossilov (Chapter 15) have prepared generic overviews on decommissioning and nuclear knowledge management respectively. Eric Vance and Dan Perera of ANSTO, known for Synroc-type ceramic developments, have prepared a chapter on novel waste immobilizing materials – geopolymers (Chapter 8). Hajime Kinoshita of ISL, well known for his pioneering works on ceramics for actinides, has prepared a comprehensive overview on ceramics (Chapter 10) which could itself serve as a handbook. Gerald Ouzounian and Richard Poisson of ANDRA have given an excellent French perspective on containers for waste conditioning (Chapter 11). Ian Crossland of the UK not only has prepared a nice chapter on metallic containers (Chapter 12) but also has given much advice in finding experts ready to assist. Vincenzo Rondinella of the EC JRC Institute for Transuranium Elements has described failure mechanisms of wasteforms accounting for radiation and corrosion effects (Chapter 13). Lastly, Diana Bacon with Eric Pierce of PNNL, who have contributed to safety analysis reports of many repositories, kindly agreed to prepare a generic overview on safety analysis methodology (Chapter 14).

All the authors of this book are outstanding experts and acknowledged leaders in nuclear waste management and nuclear materials. I am expressing my deepest thanks to all of them for sharing their knowledge. I hope that the reader will find the information useful.

1.8 References

1. IAEA. Classification of radioactive waste: General Safety Guide GSG-1. IAEA, Vienna (2009).
2. M.I. Ojovan, W.E. Lee. *An Introduction to Nuclear Waste Immobilisation,* Elsevier Science Publishers, Amsterdam, 315 pp. (2005).
3. IAEA. Application of the Concepts of Exclusion, Exemption and Clearance, IAEA Safety Standards Series No. RS-G-1.7, IAEA, Vienna (2004).
4. IAEA. International Basic Safety Standards for Protection against Ionizing Radiation and for the Safety of Radiation Sources. Safety Series No. 115, IAEA, Vienna (1996).
5. IAEA. Classification of Radioactive Waste, Safety Series No. 111-G-1.1, IAEA, Vienna (1994).
6. A. Lavrinovich. Communication at IAEA Workshop RER3007/9008/01. Waste Management Operators on Treatment/Processing Problematic Waste from NPPs and Nuclear Facilities Decommissioning. Ljubljana, Slovenia, 6–9 April 2010.

7. A. Aloy, S. Amoravian, R. Burcl *et al.* Strategy and methodology for radioactive waste characterization. IAEA TECDOC-1537, IAEA, Vienna (2007).
8. J. Burclova, Z. Drace, J.L. Gonzales Gomez *et al.* Categorizing operational radioactive wastes. IAEA TECDOC-1538, IAEA, Vienna (2007).
9. M.I. Ojovan, W.E. Lee. *New Developments in Glassy Nuclear Wasteforms*, Nova Science Publishers, New York, 131 pp. (2007).
10. Z. Drace, M.I. Ojovan. The behaviours of cementitious materials in long term storage and disposal: an overview of results of the IAEA coordinated research programme. *Mater. Res. Soc. Symp. Proc.* **1193**, 663–672 (2009).
11. P. Bredell, Z. Drace, S. Hudson *et al.* Policies and strategies for radioactive waste management. IAEA Nuclear Energy Series, NW-G-1.1, STI/PUB/1396, 68 pp., IAEA, Vienna (2009).
12. B.E. Burakov, M.I. Ojovan, W.E. Lee. *Crystalline Materials for Actinide Immobilisation*, Imperial College Press, London, 198 pp. (2010).

2

Compaction processes and technology for treatment and conditioning of radioactive waste

M. GARAMSZEGHY,
Ontario Power Generation Inc., Canada

Abstract: Compaction is a versatile, commonly used, relatively low-cost method to reduce the volume of radioactive solid waste by the application of a compression force, such as a hydraulic ram. The process does not destroy organic material, convert the waste to an inorganic form or reduce the total mass. Rather, compaction works by increasing the density of the waste product.

Compacting devices that are specifically designed for radioactive waste applications are widely available. In addition, other presses and compacting devices designed for general rubbish and other materials often can be used for radioactive waste after appropriate modifications for radiation protection, such as exhaust filtering or remote operation.

Volume reduction factors in the range of 3 to 10 are typical. These depend mostly on the waste material being treated and on the pressure applied. Prior sorting and size reduction of the waste can improve the overall efficiency by removing non-compressible items.

Compaction technology has been applied to radioactive wastes for several decades, since the dawn of the nuclear age, and is still one of the most widely practiced waste treatment methods in most countries. The technology has evolved from simple, manually operated, mechanical compression devices to fully automated, high throughput, dedicated industrial-scale facilities. It can be applied on both a small scale and a large scale, depending on the requirements of the situation.

This chapter describes various compaction processes, their application, resulting waste products, advantages and limitations.

Key words: compaction, supercompaction, low-level waste, treatment and conditioning.

2.1 Applicable waste streams in compaction processes and technology

Compaction is a versatile process and can be applied to a wide variety of wastes, either as a primary treatment or for further treatment of a secondary waste. It is mostly applied to dry wastes. However, specialized versions of the process have been developed for wet wastes. Table 2.1 summarizes

Table 2.1 Application of compaction technology to various waste streams

Waste stream	Low-force	High-force	Hot pressing	Pelletization
Dry active waste (paper, plastic, etc.)	√	√		√
Metallic waste	√[1]	√[2]		
Incinerator ash		√		
Ion-exchange resins		√[3]	√	√
Wood		√		
Concrete		√		
Glass[4]	√	√		
Soil/sand		√		
Wet wastes			√	√
Air filters	√	√		
Liquid filters		√[3]		
Thermal insulation	√	√		
Intermediate-level wastes[5]		√		

[1] Light-gauge (thin) metals only, e.g. paint cans.
[2] Can be heavy-gauge metals, such as pipes and technological components.
[3] Requires drying of wastes first to reduce quantity of secondary liquid wastes.
[4] For example, light bulbs, laboratory glassware, etc.
[5] For example, fuel hulls and other technological components from spent fuel reprocessing.

the applicability of various compaction technologies to different waste streams.

2.2 Compaction processes and technology

Compaction technologies can generally be categorized by the degree of pressure applied to the wastes. Compaction performance is generally measured by the ‘volume reduction factor’, VRF, which is defined as the ratio of the volume prior to compaction compared to the volume of the waste after compaction. For example, a VRF of 4 indicates that the final waste product occupies only one-quarter of the volume that the original waste did.

Increasing the compaction pressure will generally result in a higher (better) VRF, with an upper limit being achieved when the waste has been compressed to its ultimate density (i.e. all of the void space in the waste has been compressed out). Increasing the compaction pressure beyond this point will not result in any improvement in the VRF.

The different technologies are described below.

2.2.1 Low-force compaction

Introduction

Low-force compaction is the most commonly used form of the technology. It generally involves applied compaction forces of less than about 5 MN (500 tonnes), with most applications being less than about 0.5 MN (50 tonnes) for a 200 L drum. This results in pressures of a few megapascals being exerted on the waste material. Low-force compaction is used for soft, easily compressible, low-level waste materials only.

Technology description and application

There are three main types of low-force compaction currently used around the world:

- In-drum compactors
- In-box compactors
- Balers.

The most common type is the 'in-drum compactor'. A typical example is shown in Fig. 2.1. With the in-drum compactor, waste materials are placed inside the drum (typically a standard 200 L drum), and compressed *in situ* by a mechanically or hydraulically operated piston ram that fits inside the drum. The ram is then retracted, more waste is added, and the compaction cycle repeats until no more waste can be placed in the drum. The compactor typically operates with a compaction force of up to about 0.5 MN, and has a moderate volume reduction factor of 2 to 5 for most materials. When full, the drum containing the compacted waste is then capped. The distinguishing feature of the process is that the container (drum) remains intact during the process.

In-drum compaction is often used as a pre-treatment step prior to high-force compaction in order to increase the amount of waste compacted in each high-force compaction cycle and reduce the number of sacrificial drums required by the high-force compactor.

A variation of the in-drum compactor is the 'in-box compactor'. Shown in Fig. 2.2, the in-box compactor operates with a force of 2 to 5 MN (200 to 500 tonnes). This force is spread out over the area of a 2.5 m^3 steel box rather than a 200 L drum. As such, it operates at similar pressure to the in-drum compactor and results in similar volume reduction factors. The

2.1 In-drum compactor (example courtesy of NUKEM Technologies GmbH).

primary advantage is the larger box format, which can accommodate larger items (e.g. HEPA filters, etc.) without prior size reduction. In addition, the 2.5 m^3 box provides more efficient storage than the 200 L drum.

The third type of common low-force compactor is the 'baler'. A typical example is shown in Fig. 2.3. This device compresses material into a cubic shape without the use of a steel drum or box. For contamination control purposes, it is often compressed into a plastic bag or cardboard box, which offers no additional structural support. The bale is then fastened with steel or plastic strapping to maintain its shape once the pressure has been removed. The baler generally operates at a lower compaction force (<0.2 MN) than other equipment used for radioactive wastes, and has a lower volume reduction factor.

Baling technology is commonly used in non-nuclear industries (e.g. paper recycling). It has been used in the nuclear industry, but has been

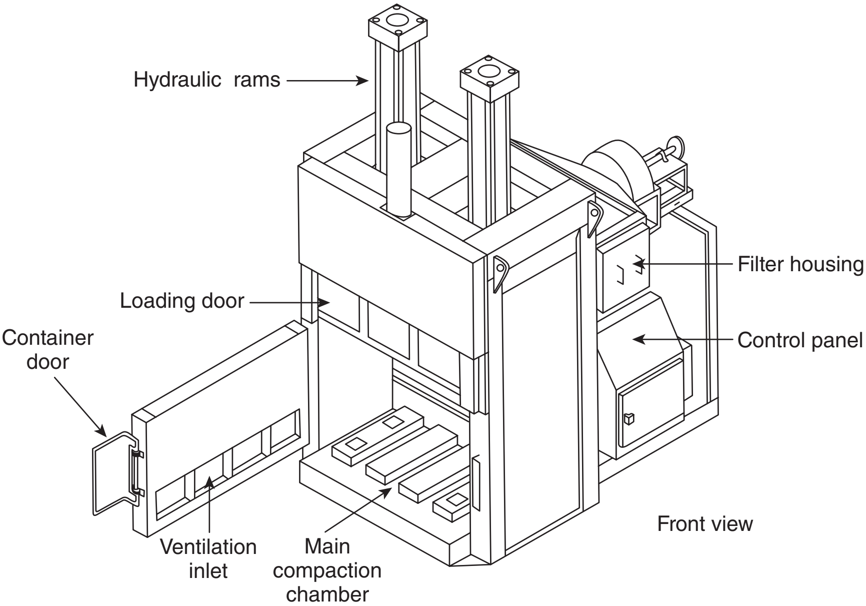

2.2 In-box compactor (example courtesy of Container Products Corporation).

largely replaced for radioactive waste treatment by other compaction technologies.

2.2.2 High-force (super) compaction

Introduction

Supercompaction is used at over 50 radioactive waste processing facilities around the world. It is a mechanical volume reduction process where waste is placed in a sacrificial metal container (drum or box) and the container is then crushed in an hydraulic press operating at 10 MN (1000 tonnes) or greater. This force is sufficient to crush the container and its contents, including heavy-gauge metal (such as pipes, valves and motors), concrete blocks and wood, as well as normally compactible materials (paper, plastic, rubber, etc.). The resulting pellet or ‘puck’ is then placed in a container or overpack for storage. Volume reduction (VR) factors of 2 to greater than 10 are typical, depending on the mix of material being processed.

Incinerator ash and spent ion exchange resins are also supercompacted in some facilities, although VR factors typically less than 2 can be expected.

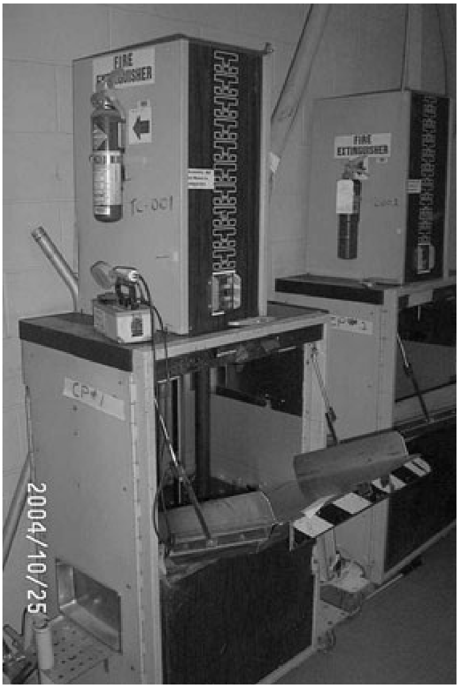

2.3 Radioactive waste baler.

Technology description and application

A supercompactor is a large hydraulic press that crushes a drum or other receptacle containing essentially all types of solid waste with a force of 10 MN to 50 MN (1000 to 5000 tons). The container is held in a mold during the compaction stroke of the supercompactor, which sizes the container's outer dimensions. The compressed drum is then stripped from the mold and the process is repeated. Two or more crushed containers (pellets or pucks) are then sealed inside an overpack container for storage and ultimate disposal.

A system may be mobile or stationary in concept, supplied as a basic system, manually controlled, with a minimum of auxiliary equipment to an elaborate computer-controlled system, which selects drums to be processed, measures weight and radiation levels, compresses the drums, places the crushed drums in overpack containers, seals the overpacks, and records the overpack content, weight and radiation level via a microprocessor-based inventory control system. In general, mobile units have a minimum of auxiliary equipment and the production rate may be less and labor and

2.4 Typical stationary, drum-type, high-force compactor system.

radiation exposure may be more than for a stationary installation per unit of throughput. A typical stationary system is shown in Fig. 2.4.

Most of the systems in operation today are designed to use 100 L to 200 L drums as the sacrificial waste container. Larger 1 m^3 box systems are also available as stationary installations at two sites (Energy Solutions, US, and Sellafield, UK).

As summarized in Table 2.2, more than 50 supercompactors have been sold worldwide by a number of suppliers. Most suppliers will build fixed base, transportable or mobile units, but a high percentage of the transportable and mobile units have never been moved. Most of the mobile units require a number of operations to be performed manually, some with mechanical assistance. In addition, environmental chambers are simplistic in mobile units, and some desirable features possible with fixed base units may not be available for mobile units.

The overall operation of a typical high-force compaction facility is shown schematically in Fig. 2.5. In order to make the facility run smoothly, there are a number of support services that need to be integrated into the facility, including handling of full and empty containers (e.g. conveyor systems), collection and treatment of secondary liquids (mostly those which have been squeezed out of the wastes), and characterization systems (e.g. radioactivity, X-ray, mass, pellet height measurement, etc.).

Most of the supercompactor installations in the world are 15 MN to 20 MN units handling beta-gamma LLW with a radiation level less than 200 mSv/h. A few have been designed to handle alpha-bearing waste and/or higher radiation level material. Two stationary units, one in England and one in the US, are 50 MN units that will handle drums and boxes up to about 1 m^3 (109 cm × 91 cm × 122 cm high).

Table 2.2 Summary of supercompaction facilities

Country	Facility	Supplier	Press force	Remarks	Number of drums processed	Year operational
Austria	Seibersdorf	GNS	20 MN		2600	1995
Belgium	Mol-CILVA	Fontijne	20 MN	Capacity 8000 drums/y	15,000	1993
China	China Inst. Atomic Energy	Nukem	20 MN			2001
	Framatome	ACB-Nantes	15 MN			1999
France	EdF Bugey	HANSA Projekt	20 MN	Mobile/used also on other locations	75,000	1990
	La Hague/Cogema	ACB-Nantes	15 MN			1986
		ACB-Nantes	25 MN	ILW		1997
		ACB-Nantes	25 MN	ILW		1997
	Soulaines	ACB-Nantes	15 MN			1991
Germany	Amersham Buchler	HANSA	20 MN			
	Brunsbüttel	HANSA Projekt	20 MN		8300	1983
	Energie Nord / Lubmin	GNS	20 MN	Fakir 7		
	GNS-Dortmund facility	GNS	20 MN			
	Gundremmingen	GNS	20 MN	Fakir 4		
	Jülich	GNS	15 MN	Fakir 6	14,000	1996
	Karlsruhe-Forschungszentrum	Fontijne	15 MN	Scrapped 2001	110,000	1984
		Fontijne	15 MN	Commissioned 2001		2001
		Fontijne	20 MN			1997
		Nukem	30 MN			1993
	KWU-Karlstein	Nukem	16 MN			1988
	Philippsburg	Fontijne	20 MN			1994
	Würgassen	Siemens	40 MN		4000	1997
Italy	ENEA Casaccia	Fontijne	20 MN			1990
		HANSA Projekt	20 MN	Mobile system	25,000	1988
Japan	Tokyo Electric Power	NGK	20 MN			

Lithuania	Ignalina NPP	Nukem	20 MN			2008
Netherlands	Covra-Vlissingen	Fontijne	15 MN		25,000	1993
Russia	Balakova	Nukem	20 MN		0	2002
	Leningrad NPP	Nukem	20 MN			2007
	RADON Moscow	Fontijne	15 MN		130,000	1980/1997
S.Korea	Korean Electric Power	HANSA Projekt	20 MN	Mobile system	21,000	1992
Slovakia	Bohunice	Nukem	20 MN			2000
Spain	El Cabril	GNS	20 MN	Fakir 3		1992
Taiwan	Taipower at Kuosheng plant	Fontijne	20 MN			1990
		HANSA /Hitachi	20 MN			
UK	Sellafield-WTC	Fontijne	20 MN			1996
		SEG	50 MN	1 m^3 box system		1995
	Sellafield-SDP	Fontijne	20 MN	ILW		2000
		Fontijne	20 MN	ILW		2001
	UK AEA	HANSA	20 MN			1986
	UK AEA Dounreay	Fontijne	20 MN	Mobile system		1990
Ukraine	Chernobyl NPP	Nukem	20 MN			2007
	Chmelnitzki	Nukem	20 MN			2001
	South Ukraine NPP	Nukem	20 MN			2001
USA	ATG Hanford	ATG design	15 MN		7000/y, 63,000 to date	1992
	BWX Technologies (B & W)	Fontijne-Stock	15 MN	Operational at Naval Fuel Plant	2000/y	1986
	DOE-Rocky Flats	HANSA /INET	20 MN	Never fully operational	900	1989
	Energy Solutions	Bliss	15 MN			1987
	Energy Solutions	SEG design	50 MN	1 m^3 box system	800,000 containers	1990
	Hanford WRAP	Williams White	20 MN		600	1996
	INEEL	Fontijne	20 MN		0	2001
	Northern States Power	HANSA /INET	20 MN	Mobile, but never moved	6000	1985
	Savanna River Site	Bliss	10 MN	Former West Valley	27,800	1986
	Studsvik, Inc.	HANSA /INET	20 MN		33,000	

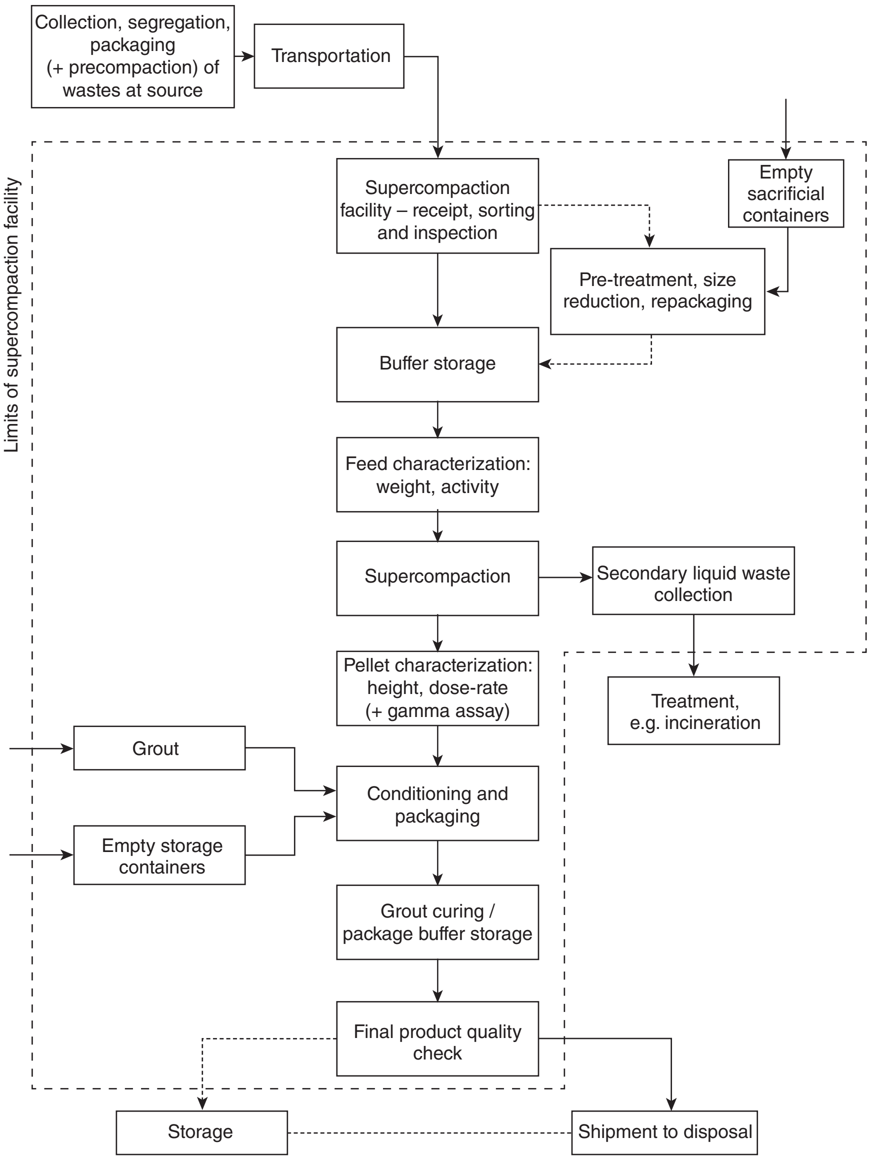

2.5 Typical reference supercompaction facility.

2.2.3 Other compaction processes

Introduction

There are several other waste treatment processes that employ compaction as part of the overall process, such as hot pressing and pelletization. These are generally limited to specific applications and are described below.

Technology description and application

Hot pressing

Hot isostatic pressing is applied to wet wastes, such as ion exchange resins. In this process, the ion exchange resins are first dewatered or dried to a residual water content (water of hydration) of less than 50% in a drying vessel. Different resin types (e.g. bead type and powdered type) can be mixed in this vessel with other wet wastes, such as sludges and evaporator bottoms with higher water content, along with various chemical additives or binder materials to produce a stable waste product. The waste is then loaded into special metal containers (cartridges) which are then capped with a lid and then immediately transferred into a high-force compactor. The resulting pellets are then measured for dose rate, height and weight, and then packed for storage and/or disposal. The resulting products must be packed into watertight containers to avoid resin swelling due to rehydration from contact with water.

Hot pressing can treat multiple waste streams and will potentially produce a solid monolithic waste form, depending on waste types. Volume reduction factors on the order of 6 typically can be achieved for ion exchange resins.

Pelletization

Pelletization technology is suitable for conversion of wet waste, such as ion exchange resins, sludge, evaporator concentrates, etc., into a dry solid waste. For this process the raw waste is dried into a powder form, extruded or compacted in a mold, and then chopped or cut into small pieces. The name pelletization is derived from the eventual form of the waste, which appears as small pellets. The treatment of ion exchange resins requires a chemical binder, whereas other waste types may not. Pelletization is primarily used at some Japanese nuclear power plants for the conditioning of ion exchange resins and evaporator concentrates.

2.3 End waste forms and quality control of compaction processes

The final product of compaction is a compressed waste in a container. High-force compacted wastes are typically placed in a secondary container

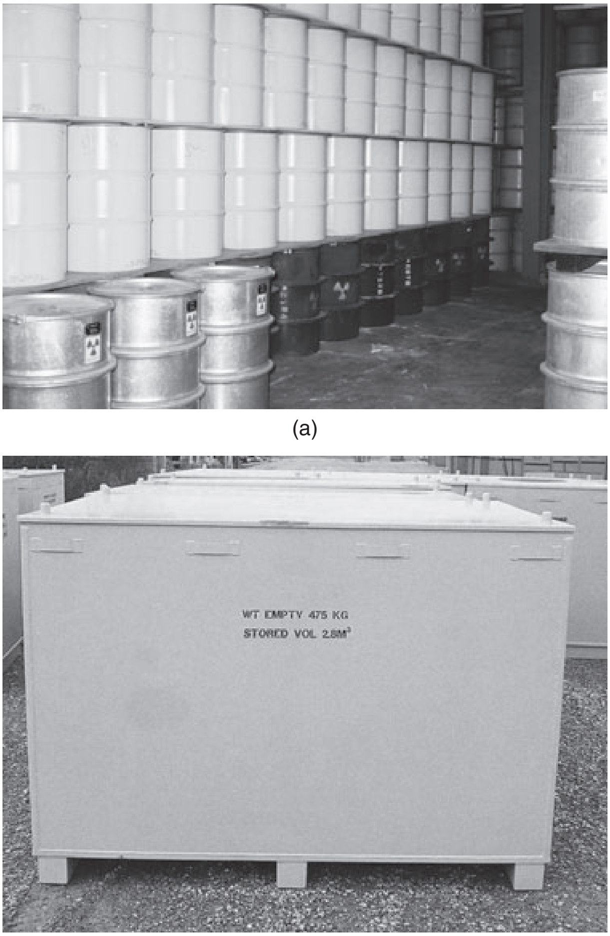

(a)

(b)

2.6 Typical containers for low-force compacted wastes: (a) drums, (b) boxes, (c)bales.

(overpack) prior to storage or disposal. Low-force compacted wastes are generally stored or disposed without further packaging.

2.3.1 Low-force compaction

The products of low-force compaction are typically 200 L steel drums, 2.5 m^3 steel boxes or bales of various shapes and sizes. The steel drums or boxes are suitable for direct storage or disposal. The bales are generally not considered suitable for long-term storage or disposal without further pack-

(c)

2.6 Continued

aging (e.g. emplacement in a secondary container), due to the low structural integrity and potential combustibility of the bale. Typical drums, boxes and bales of compacted waste are shown in Fig. 2.6.

Quality control measures for low-force compaction typically consist of inspection of the incoming waste to ensure that prohibited materials (such as liquids and heavy metallic objects) have been removed. Inspection of the product can consist of mass, radiation and contamination measurements, as well as a visual inspection of the final container. Since compaction is a mechanical process, some deformation of the container (e.g. dents) may appear. This is a normal part of the process, and as long as it does not hinder the handling of the container, it should not be a cause for rejection of the container.

2.3.2 High-force compaction

Typical volume reduction capability of supercompaction is shown in Table 2.3. In most real cases, a container of waste will have more than one waste type (e.g. x% plastic, y% paper, z% metal). The achievable final density for each container and the resulting VRF will depend on the specific mixture in the container. Example results of crushing standard 208 L drums containing electric motors and hardwood in a 15 MN machine are shown in Fig 2.7.

The individual pellets produced by high-force compaction are generally placed in a secondary container or overpack, such as a larger drum, as

Table 2.3 Typical volume reduction factors for supercompaction

Material description	Initial density (kg/m^3)	Final density (kg/m^3)	VRF
Rags, paper	261	1242	4.8
Newspaper, magazines	200	1006	5.0
Plastic sheets (wadded)	126	1200	9.5
Hardwood	376	1142	3.0
Scrap metal	781	3312	4.2
Small electric motors	968	3680	3.8
Concrete paving blocks	800	1296	1.6
Glass	378	1558	4.1

(a)

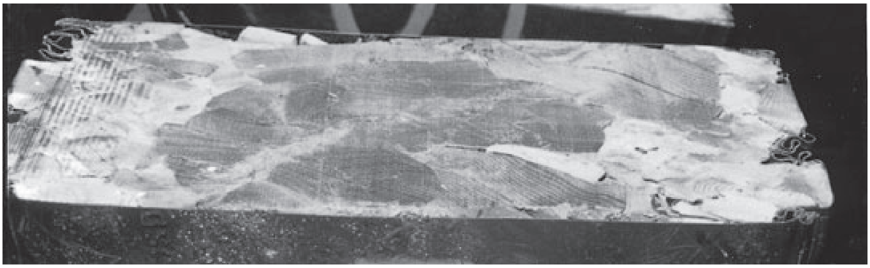

(b)

2.7 Typical compaction results: (a) electric motors after supercompaction, (b) hardwood after supercompaction (courtesy of Fontijne Holland).

shown in Fig 2.8. Other secondary containers, such as large rectangular boxes, are also used, as shown in Fig. 2.9. In many cases, the void space in the secondary container is backfilled with granular material or cement grout to improve the structural stability and to provide a waste form that is more resistant to radionuclide leaching.

2.8 Cutaway view of an overpack drum with high-force compacted pellets.

Most of the existing and planned supercompaction facilities are based on the use of 200 L (55 US gallon) drums as a sacrificial container, with a 280 L or 300 L overpack. Several European facilities use a 100 L drum as the sacrificial container, with a 200 L overpack. One facility in the US and one in the UK are designed to supercompact 1 m^3 boxes into 1.6 m^3 overpack boxes (see Table 2.2).

Conditioning is required in some countries to control the void space in the overpacks to meet waste acceptance criteria for long-term storage and/or disposal. Typically this is done using a cement grout. In some cases (such as at the COVRA facility in the Netherlands), the hardened grout acts as a cap and a separate lid is not required for the overpack. Backfilling of overpacks with contaminated dry granular material, such as charcoal, low-level ion exchange resins, grit blasting material, etc., has also been done. This has the added advantage of disposal of the granular material at no incremental cost.

2.9 High-force compacted pellets in an ISO disposal container (photo courtesy of UKAEA Dounreay).

2.3.3 Other compaction processes

Hot pressing

Hot pressing produces a pellet similar to high-force compaction, that is then enclosed in a secondary container.

Pelletization

Pelletization produces loose, dry pellets, a few centimeters in size. These can be packed loosely into a secondary container. The secondary container can then be either subject to high-force compaction for further volume reduction, or backfilled with grout to condition the waste. Note that special care must be taken with grout mixtures so as not to cause the dry pellets to rehydrate and expand.

2.4 Pre-treatment in compaction processes

Various pre-treatment steps are often employed in conjunction with compaction. These are described briefly below. In addition, low-force compaction is often applied as a pre-treatment for high-force compaction involving soft materials (paper, plastic, etc.) in order to minimize the number of sacrificial containers required.

2.4.1 Shredding

Wastes can be shredded prior to compaction. This provides two main advantages:

- Size reduction of larger items to ensure that they fit into the waste container and to remove void spaces
- Converting the waste into more uniform feedstock, allowing for more efficient packing and better automated handling.

Shredders are available for handling a wide range of materials, from soft (such as paper and plastic) to hard (such as metal components and piping). The systems can be automated to a large degree and integrated into a waste container feeding system. However, shredding by its very nature can be a very dirty operation that can lead to the production of airborne particulates and other forms of spreadable contamination. Because of this, it generally needs to be conducted in a carefully controlled environment with containment and filtered exhaust.

2.4.2 Mechanical size reduction

Mechanical size reduction must be employed when a waste item will not fit into a waste container due to its size and/or geometry. There are numerous techniques that are applied depending on the material in question, such as sawing, plasma/flame cutting, shearing, etc. These are standard techniques that can be carried out either manually or remotely as the situation requires. As with shredding, proper containment and control of contamination is required.

2.4.3 Drying

Wet wastes may require pre-drying prior to compaction in order to minimize the amount of secondary liquid produced as a result of the compaction process. For high-force compaction especially, any liquid contained in the waste will be squeezed out by the compaction. This will often include 'non-visible' moisture, such as that absorbed on rags. Compaction processes which include heating as part of the technique, such as hot pressing, will often include an integrated drying step as part of the process.

2.4.4 Containerization

High-force compaction employs the use of a sacrificial container, which is compacted along with the waste. Therefore, wastes must be packaged in suitable containers prior to compaction. 'Suitable' in this case means being of the correct size to fit the press, and being constructed of materials and in a way that allows it to be compacted effectively (e.g. heavily reinforced containers are generally not suited to being compacted, but may be required for in-container compaction).

2.5 Secondary wastes of compaction processes and technology

Compaction will squeeze out any gas or liquid contained in the wastes. As such, containment and secondary treatment systems are required as part of an integrated compaction system. In the case of high-force compaction, pre-puncturing of the sacrificial container is often used to establish a controlled 'escape path' for gases and liquids. If this is not done, an escape path may be randomly created, rupturing the container in an uncontrolled fashion. This may cause, for example, liquids to squirt out in unpredictable locations.

2.5.1 Gaseous emissions

Ventilation systems are required around most compaction installations to collect and control the gases that are squeezed out during the compaction process, as well as any particulate matter that may be generated. The ventilation and treatment system typically consists of:

- A negative pressure enclosure to prevent outleakage of potentially radioactive gas and particulate
- A HEPA filtration system on the exhaust to remove particulate
- An activated charcoal absorber bed if certain radioactive gases, such as iodines, are present
- A molecular sieve absorber if gases such as tritium are present
- A monitor system to measure the amount of radioactivity in the effluent gases.

The negative pressure containment system can range from a simple 'fume hood' to a fully airlocked chamber, depending on the needs of the installation.

2.5.2 Liquid

Liquid collection and treatment systems are required for many compaction systems, especially high-force systems, to manage liquids squeezed out of the waste by the compaction process. The liquid collection system typically consists of a pan and drain system that will collect drippings from under the waste container as it is being compacted. Depending on the waste being treated, the liquid can be a multi-phase layered aqueous/organic 'soup' that can include water, solvents, oils, paints, biological materials and other liquids that may be present either by design or inadvertently in the wastes.

Treatment methods depend on the liquid, but generally involve:

- Incineration (if available this is often the simplest because it can tolerate a wide range of mixtures)
- Phase separation, followed by treatment of each phase by an appropriate method
- Immobilization in a tolerant matrix (i.e. one that can handle a wide range of liquids).

The liquid treatment process can be quite complex, especially if there are several phase layers in the mixture.

Periodic rinsing and decontamination of the compaction area is also often required, resulting in the generation of water that must be collected and treated.

2.6 Advantages and limitations of compaction processes and technoligy

Compaction technology is widely employed in various configurations. It can be a cost-effective way to reduce volumes of radioactive and other wastes for transportation, storage and disposal. In its simplest form (low-force compaction), it is a 'reversible' process (i.e. the wastes can be un-compacted for further treatment, such as incineration).

The main limitations of the technology in general are that it does not stabilize the waste by changing its composition and it does not reduce the mass of the waste but only creates a denser waste package (i.e. same mass in a smaller volume). For example, organic materials such as paper and plastic are not converted to a more stable inorganic form and will over long time periods break down, potentially releasing gases and other decomposition products. In some repository environments, the presence of organic materials may be an issue.

Some specific aspects that must be considered in the design of a compaction facility include the following:

- Pre-sorting and segregation of wastes is often important. For example:
  - Large, non-compactible components (e.g. very thick steel pieces, solid concrete, etc.) can damage the press equipment and should be segregated from the waste stream.
  - Physical and chemical reactivity of the material being compacted may be affected. For example, pyrophoric or explosive materials may ignite. Compressed gas cylinders or pressurized aerosol cans may explosively rupture.

Such materials must be removed prior to compaction. In addition, the compaction equipment should be provided with appropriate fire suppression systems.
- Absorbed or incidentally contained liquids can be released during compaction and should be collected in an appropriate drip tray system.
- Air enclosed in the primary waste packages will be released during compaction. This can lead to airborne contamination, which requires an appropriate air filtration system.
- Special precautions need to be taken into account when compacting material showing a tendency to expand or spring back after release of the compaction pressure, including many plastics and rubber. Compaction of waste in steel containers or using 'anti-springback' constraints (e.g. straps or bands) can reduce or eliminate the springback effect.

The radiological properties of the waste, such as dose rate, are important in the design of the overall facility. Compaction can be designed for a wide range of wastes from low level to high level. However, as the radiological hazard increases, additional sophistication in the form of remote handling and shielding is required. In case of high-dose-rate wastes, the ability to perform maintenance remotely is often required (e.g. to remove a stuck waste container).

2.6.1 Low-force compaction

The principal advantages of low-force compaction are:

- The relatively low investment and operating cost, resulting in quick payback from reduced waste disposal costs
- Ease of use
- Reasonable volume reduction factors for most compressible materials
- Wide availability of equipment 'off-the-shelf' in various configurations to suit most applications.

The main disadvantages are:

- Limited to compaction of 'soft' materials (e.g. paper, plastic, thin metals, etc.)
- 'Springback' effect of some materials, such as rubber and some types of plastic.

2.6.2 High-force compaction

The advantages and disadvantages of various high-force compaction technologies are summarized in Table 2.4. In general, high-force compaction offers significant advantages over low-force compaction:

- Ability to compact a much wider range of materials than is possible using low-force compaction, including some not normally considered to be compactible, such as technological components (pumps, motors, etc.)
- Higher volume reduction factors
- More stable waste form (e.g. higher density, lower moisture content, grouted overpacks, etc.).

Table 2.4 Comparison of supercompaction options

Option	Advantages	Disadvantages
Stationary 20 MN Drum SC	• Wide variety of proven systems and vendors to choose from • Lower investment cost than 50 MN system • Fully automated systems available • Efficient processing if automated • Lower maintenance than for 50 MN system (lower forces on cylindrical mold walls than on cubical walls of 50 MN system) • Wide availability and low cost of sacrificial containers • Lower container weight for handling purposes	• Higher maintenance cost due to automation and usually additional equipment • Requires handling of five times more containers than 50 MN system • Larger objects must be cut into smaller pieces to fit drum • Storage efficiency of drum type overpacks can be low
Stationary 50 MN Box SC	• May be a fully automated process • Different types/sizes of containers may be processed • Up to 1 m^3 square containers processible (larger objects can be handled and fewer containers required than for drum systems) • Efficient processing if automated • Higher throughput than for drum systems • Usually a higher overpack filling efficiency • Cubical overpack leads to more efficient stacking in disposal/storage vault and lower emplacement volume	• High investment cost • Only one proven system/vendor • Higher maintenance cost due to automation and usually additional equipment • Larger facility and throughput than 20 MN system • Requires large waste volumes to be economically viable (capacity could be shared between several waste producers)

Table 2.4 Continued

Option	Advantages	Disadvantages
Mobile 20 MN Drum SC	• Can be moved from one location to another • No or limited capital investment for rental system • Available for rent and/or lease which may reduce costs • Low cost or no structure other than the press truck containment	• Limited auxiliary equipment • More manual handling with increased labor and higher safety risk • Protective clothing may be necessary for operators • With some units only one size of drum may be processed • Lower throughput than fixed system • Weather conditions may disrupt operations • Cold weather could require a heated enclosure • Control of contamination spread difficult and costly

However, the main drawback of high-force compaction systems is that they are much more costly and technologically more complex to operate compared to low-force compaction systems. Because of this, they are generally suited to high-throughput operations, such as a centralized waste processing facility.

2.6.3 Other compaction processes

The main advantages of hot pressing and pelletization processes are that they are specifically designed to treat wet wastes, such as ion exchange resins, sludge and evaporator concentrates. The primary disadvantage is that they can be technologically complex, and therefore expensive to procure and operate.

2.7 Future trends

Mechanical compaction technology based on hydraulic presses as applied to radioactive wastes has been available for several decades. It is a mature technology, which also has a solid non-nuclear industrial experience. Future trends in the area of radioactive waste processing by compaction mainly involve:

- Improved automation of integrated processes
- Application to a wider range of wastes (such as intermediate level wastes from spent fuel reprocessing, larger components such as decommissioning wastes, and wet wastes such as ion-exchange resins)
- Improved final waste product through:
  - use of better final conditioning techniques
  - optimized design of final containers
  - optimized packing of wastes into final containers
  - use of pre-treatment techniques such as shredding
- Specialized configurations, such as presses designed to compact piping from reactor decommissioning and other applications.

2.8 Sources of further information and advice

Further information on compaction processes can be found in the references listed below, as well as on various Internet-based resources, such as www.iaea.org, www.radwaste.org, www.rwin.org.uk and www.world-nuclear.org. Information on various equipment and applications can also be obtained from the equipment manufacturers and vendors, such as those listed in Table 2.2, including NUKEM (www.nukem.de), Hansa Projekt (www.h-p-a.de), ACB Nantes (www.acb-ps.com), GNS (www.gns.de), Fontijne (www.fontijnegrotnes.com), Siemens (www.siemens.de), Container Products Corporation (www.c-p-c.com) and many others.

2.9 Bibliography

Blinn, K. and Sander, H., 2000. Innovative super compaction system. Paper presented at WM'00 Conference, 27 February – 2 March 2000, Tucson, AZ.

Garcia, R.S., 1996. Commercially Available Low-Level Radioactive and Mixed Waste Treatment Technologies. Report DOE/LLW-240 prepared for the United States Department of Energy (USDOE), October 1996.

International Atomic Energy Agency (IAEA), 1993. Containers for Packaging of Solid Low and Intermediate Level Radioactive Wastes. IAEA Technical Reports Series No. 355, July 1993.

International Atomic Energy Agency (IAEA), 1994. Status of Technology for Volume Reduction and Treatment of Low and Intermediate Level Solid Radioactive Waste. IAEA Technical Reports Series No. 360, May 1994.

International Atomic Energy Agency (IAEA), 2001. Handling and Processing of Radioactive Waste from Nuclear Applications. IAEA Technical Reports Series No. 402, November 2001.

International Atomic Energy Agency (IAEA), 2006. Innovative Waste Treatment and Conditioning Technologies at Nuclear Power Plants. IAEA TECDOC Series No. 1504, August 2006.

International Atomic Energy Agency (IAEA), 2007. Retrieval and Conditioning of Solid Radioactive Waste from Old Facilities. IAEA Technical Reports Series No. 456, March 2007.

Nakashio, N., *et al.*, 2007. Trial operation of the advanced volume reduction facilities for LLW at JAEA. *Journal of Nuclear Science and Technology*, Vol. 44, No. 3, pp. 441–447.

Ojovan, M.I. and Lee, W.E., 2005. *An Introduction to Nuclear Waste Immobilisation*, Elsevier Science Publishers, Amsterdam, 315 pp.

Williams, P., 1992. Super-compaction of dry active waste: an overview. *Waste Management*, Vol. 2, pp. 301–312.

Williams, P., Bowles C.R., Brandt, R.T. and Fogel, D.M., 1986. Start-up and Operation of a Super-compactor at a RVRC. Stock Equipment Company, March 1986.

3

Incineration and plasma processes and technology for treatment and conditioning of radioactive waste

J. DECKERS, Belgoprocess, Belgium

Abstract: Radioactive waste can be treated by thermal treatment, resulting in a robust end waste form with a high volume reduction factor (VRF). Not only is the VRF of importance but also the growing requirements for improved quality of the final waste form. Virtually all waste streams can be treated by the described treatment technologies, resulting in a conditioned product free from organics and liquids, and meeting without doubt the acceptance criteria for safe storage and disposal. In this chapter the most commonly used thermal treatment, namely incineration, and the emerging plasma technology are handled, each illustrated with an existing industrial operation facility.

Key words: radioactive waste, incineration, plasma, ALARA principles, conditioned waste, volume reduction factor (VRF).

3.1 Introduction

Large amounts of radioactive waste, with varying characteristics, are generated from the operation and maintenance of nuclear power plants, the nuclear fuel cycle, research laboratories, pharmaceutical and medical facilities. It is in the interest of the waste producers and future generations that a high volume reduction factor (VRF) of the waste is achieved in order to minimise the volume and overall costs of storage and waste disposal. Not only is the VRF of importance but also the growing requirements for improved quality of the final waste form. Virtually all of the waste streams can be treated by a thermal treatment technology, resulting in a conditioned product free from organics, liquids and moisture, and meeting without doubt the acceptance criteria for safe storage and disposal.

In this chapter, applicable waste streams to be treated by thermal processes are described. For thermal technologies the most commonly used, namely incineration, and the emerging plasma technology are handled, each illustrated with an existing industrial operation facility. For both technologies the robust end waste forms are described as well as their advantages and limitations.

In conclusion one can say that incineration is a well-proven technology with well-performing off-gas cleaning systems which can treat a variety of waste streams. The emerging plasma technology is very suitable for treating historical waste containing mixtures of inorganic, organic, liquids, sludge, etc., with limited preparation and minimum risks of radioactive contamination.

3.2 Applicable waste streams in incineration processes and technology

The waste composition greatly affects the choice of thermal technologies, as well as the nominal capacity of the machine, the construction material, and the design of the off-gas cleaning system.

3.2.1 Solid organic radioactive waste

This low-level solid waste stream is quite often heterogeneous in nature. Depending on the sorting and segregation facilities available, either at the generation point or at the waste management facility, eliminating or controlling this heterogeneity may not be practical. As such, the heterogeneous nature of the waste stream usually translates to a high variability of heat content (from as low as 16 MJ/kg for wood to 42 MJ/kg for some plastics). This high heat content can make the control of some thermal processes difficult. Special attention should also be given to spent ion-exchange resins which contain a lot of absorbed water and make the thermal treatment process more difficult.

3.2.2 Solid inorganic radioactive waste

Solid inorganic waste can be all types of granulates such as concrete, mineral insulation material, glass and metal pieces. The higher melting points of this waste stream must be considered. Most thermal technologies cannot generate the minimum heat for melting these wastes. However, small granular inorganic pieces can be accepted, but bigger pieces will block or obstruct the mechanical systems for ash discharge in incineration systems.

3.2.3 Liquid organic and aqueous radioactive waste

As with solid organic waste, an evaluation should also be made for liquid waste (organic liquids, oil, solvents, borated aqueous waste, etc.). These liquids can contain solid particles and corrosive products. Sludge containing organic and inorganic materials should also be considered. Aqueous waste can also contain dissolved organic or complexing agents which can seriously disturb the conventional water treatment process, so it is more appropriate to 'burn' these liquids. The water is evaporated and the organics and complex agents are oxidised. Modern thermal technologies will permit organic liquids such as oils, solvents, aqueous and scintillation liquids to be treated together with the solid waste stream.

3.2.4 Specific activity of incoming waste and radiological releases

The waste to be treated has a certain specific activity for alpha, beta and gamma emitters. A maximum contact dose rate of 2 mSv/h, which can be correlated to a certain permissible radioactivity content in the waste, is often applied as an acceptance criterion for thermal treatment of low-level waste for the following reasons:

- Since thermal technology concentrates the radioactivity of the incoming waste stream, consideration must be given to special requirements for handling and disposing of the end product. If the specific activity is close to the threshold for a higher waste disposal category, then volume reduction could result in a waste form that has the higher category disposal requirements and higher costs. In this case, volume reduction may not be desirable, and consideration should be given to setting limits on the activity concentration for wastes destined for a given processing method to avoid generation of waste forms of a higher disposal category.
- If the incoming waste stream has a high specific activity, the levels of contamination of the internal parts of the thermal treatment system increase along with the dose rates and increase the protection requirements for maintenance activities.
- For licensing purposes, the specific activity of the incoming waste will need to known in order to model and calculate the maximum radiological release and the potential radiological impact on critical population group and environment. This will have an effect on the permissible activity levels of the incoming waste. However, nowadays thermal technologies and their off-gas systems are very effective at capturing the radionuclides and may result in negligible releases.

3.3 Incineration process and technology

3.3.1 Basic description

Process description

Radioactive wastes are commonly incinerated in multiple-stage systems. In the first chamber, or primary combustion chamber (PCC), the waste undergoes a combination of pyrolysis, gasification and combustion under controlled air conditions. The mixture of combustible gases, soot, CO, CO_2 and H_2O is passed to a secondary combustion chamber (SCC) where they are burned out in an oxygen-rich environment to primary components such as CO_2 and H_2O. The solid residue in the form of ash remains in the PCC and undergoes a further burn-out. Depending on the oxygen content in the PCC one can have pyrolysis, gasification and combustion. Pyrolysis is in fact a flameless process in which organic material at an elevated temperature in the absence of oxygen or air is decomposed into volatile components. The main outputs are light hydrocarbons, benzene, toluene and tars. Gasification is the decomposition of organic material at higher temperatures and in an oxygen-deficient environment and forms mainly CO and H_2 gases. In general, organics are thermally unstable and fracture at temperatures of 500–600°C.

For the design of a thermal treatment facility, which is not only limited to incinerators, one should take into account the rule of the 3T's for obtaining good combustion efficiencies:

- *Temperature*. In order to decompose and destroy completely the organic components, the temperature should be high enough. This is particularly important for the SCC: the higher the temperature the higher the reaction kinetics for achieving complete combustion.
- *Time*. The duration of combustion in the PCC and the SCC should be long enough to burn out the ash and the flue gases. For example, the EC Directive 200/76/EC requires a residence time of at least 2 seconds in the afterburner chamber.
- *Turbulence*. Particularly in the SCC, there should be good turbulence for obtaining intensive mixing between unburned gases coming from the PCC and the air added to the SCC in order to achieve complete combustion.

Main components of an incinerator system

Radioactive waste incinerators can be designed using horizontal combustion chambers, vertical (shaft) chambers, or a combination of the two. The combustion chambers have refractory-lined cylindrical steel vessels or rectangular steel structures. The refractory lining has different layers. The inner layer is a real refractory brickwork or castable, resistant to generally 1300°C or higher. The other layers are insulation refractories and the outside layer can be industrial rockwool in order to obtain low enough contact temperatures of the outer wall. Well-designed refractories have a lifetime of 10 years or more depending on mode of operation. However, small repairs within this period may need to be carried out, e.g. at the bottom of the PCC.

The combustion chamber burners may be operated with propane, natural gas or fuel oil. The function of the burner in the PCC is more for heating the system before adding waste. The burner for the SCC is also for heating and for keeping the temperature at a minimum level (850°C), so this burner can modulate between high or low fire as a function of the outlet temperature.

In a successful incinerator design, careful consideration is given to the provision of adequate access and appropriate location of air supplies; the combustion temperature is carefully controlled and the gas residence times are comparatively long.

The end product of incineration of radioactive materials is ash, the composition and characteristics of which vary with the combustion process used, as well as with the composition of the initial waste feed. In essence, the end products of incineration are the elemental oxides of the initial substance composition and the non-combustibles that were originally present in the waste feed. Ideally, ash should contain no fixed carbon, which is achievable as long as the carbon burn-out can take place in an oxygen-rich atmosphere and for a sufficiently long time.

Ash can be discharged from the primary chamber by gravity, by mechanical or hydraulic means. Regardless of the system used for ash transport and removal, consideration needs to be given to control of radiological contamination and radiation exposure to personnel.

Incinerators also produce fly-ash, which is an easily dispersible material collected from the incineration off-gas system. The fly-ash can be collected in a separate drum or together with the incinerator ash.

As in all thermal treatment processes there is an extended off-gas system. First the hot gases have to be cooled to temperatures that are compatible with the components of the off-gas treatment system. Subsequently dust, fly-ash and chemical pollutants as well as any remaining radionuclides have to be removed. Off-gas systems of incinerators or other thermal facilities for radioactive waste should have sufficient redundant equipment in order to go to safe shutdown and to prevent any spread of radioactivity. Therefore off-gas systems incur significant cost, which can reach 50% of the total investment. An example of an off-gas treatment system is described below.

Waste feed preparation

Each incinerator concept has its unique requirements for the solid waste feed form. Solid waste materials can be fed into the combustion chamber simply by gravity (vertically) or by mechanical devices (horizontally). While some systems require careful sorting of the waste feed, other systems may accept organic waste feed form almost 'as is'. Some systems require that waste be shredded; other systems require pre-packaging the waste feed in bags or cardboard boxes free from external contamination. The incinerator system should also cope with heterogeneous waste feed varying between 4 MJ /kg and 42 MJ/kg.

Pre-sorting in order to eliminate materials that would not be compatible with either the combustion system design or the off-gas treatment capabilities may be required. As an example, the following waste items or materials may need to be controlled (either eliminated, minimised or limited), depending on the incinerator type and the ash removal system limitations:

- Non-combustibles or granulates
- Metal objects
- Plastics with high halogen contents (PVC, PTFE)
- Materials with excessive heating value
- Excessive radioactivity.

A final inspection of waste prior to incineration is usually completed to ensure that the waste does not include undesirable items. Activity detectors, metal detectors and X-ray devices are routinely utilised to detect undesirable items.

Incineration can treat waste with a variety of feed characteristics. Dry solid organic wastes from power plants remain the principal feed for incinerators. Note that the rated throughput of an incinerator is normally based on this typical waste feed. However, organic and aqueous liquids can also be processed and are usually co-processed with the solid waste. In summary, the following waste streams can be generically treated by incineration, depending on the incinerator concept employed:

- Dry solid wastes
- Ion-exchange resins
- Organic liquids
- Aqueous liquids.

Special waste streams are low-activity spent ion-exchange resins and are now routinely processed by modern incinerators. Considerable operational experience has been collected. Usually, the resins would be co-processed together with dry solid wastes, and there would be a set limit for the resin types, mass and radioactivity. If incineration of resins has not been considered in the incinerator design phase, their processing may affect performance and the rated throughput of the incinerator.

Organic liquid waste can be fed into the combustion or post-combustion chamber; most incinerators are furnished with nozzles or burners for incineration of these liquids. Organic liquids may be a mixture of oils, lubricants, etc., and may contain a certain fraction of water. When incinerating these liquids sudden variations in thermal power should be taken into account.

Aqueous liquids may also be co-processed in an incinerator. It is to be recognised in the system design that aqueous liquids have effectively a negative heating value, and their feed into the incinerator must be strictly controlled.

3.3.2 Operational experience

Existing facilities

Incineration is a mature and proven technology and has demonstrated successful operation and accumulated credible operating experience. Most incinerators are controlled air multi-stage incinerators and are operating on a commercial and industrial scale. Table 3.1 gives an overview of different incinerator plant currently in operation in some countries.

Table 3.1 Incinerator facilities in operation in some courtries

Country	Facility/site	In-service date	Capacity	Notes
Austria	Seibersdorf Research Centre	1983	40 kg/h solid	
Belgium	CILVA, Belgoprocess	1995	80 kg/h solid, 50 kg/h liquid	Commercial treatment: solids, liquids and ion-exchange resins
Canada	Ontario Power Generation, Western Waste Management Facility	2002	2 t/d solid, 45 l/h liquid (licence limit)	Continuous feed, starved air system
France	Socodei Centraco	1999	2000 t/y solid, 1100 t/y liquid	Commercial LLW treatment facility
Germany	Karlsruhe	Since 1980s	40 kg/h liquid, 50 kg/h solid	Solids and liquids
Japan	PNC, Tokai-Mura	1991	50 kg/h solid	
Netherlands	COVRA, Vlissingen-Oost	1994	60 kg/h solid, 40 l/h liquid	Two incinerators, one for liquids, one for animal carcasses and other solids

Table 3.1 Continued

Country	Facility/site	In-service date	Capacity	Notes
Russia	TORCH, Sergiev Posad	1982	100 kg/h solid, 30 l/h liquid	Solids and liquids
Slovakia	Jaslovske Bohunice BSC	2001	50 kg/h solid, 10 kg/h liquid	Used in campaigns for LLW
Spain	ENRESA El Cabril	1992	50 kg/h total, solid and liquid	Located at LLW disposal facility
Sweden	Studsvijk	1977	150 kg/h total solid	
Ukraine	Zaporozhye NPP	1993	40 kg/h solid, 20 kg/h liquid	New incinerator, similar to Belgoprocess, under contruction
USA	Energy Solutions, Beer Creek, Oak Ridge	1989	2 incinerators, approx. 400 kg/h each	Commercial LLW treatment facility

Description of a specific radwaste incinerator

An example of a controlled air multi-stage incinerator is the CILVA incinerator at Belgoprocess in Belgium which started nuclear operation in 1995. Figure 3.1 shows the flow diagram of the incineration system which treats the following types of radioactive waste:

- Uncompacted and compacted solid waste such as clothing, gloves, rags, cotton, rubber and plastics (PVC quantity 3% average, caloric value of about 25 MJ/kg)
- Frozen animal carcasses
- Spent ion-exchange resins in wet or dry condition
- Organic liquid waste such as scintillation liquids and organic solvents (caloric value up to 42 MJ/kg)
- Aqueous liquid waste whether or not containing organic components and solid particles
- Spent oil (caloric value of about 42 MJ/kg).

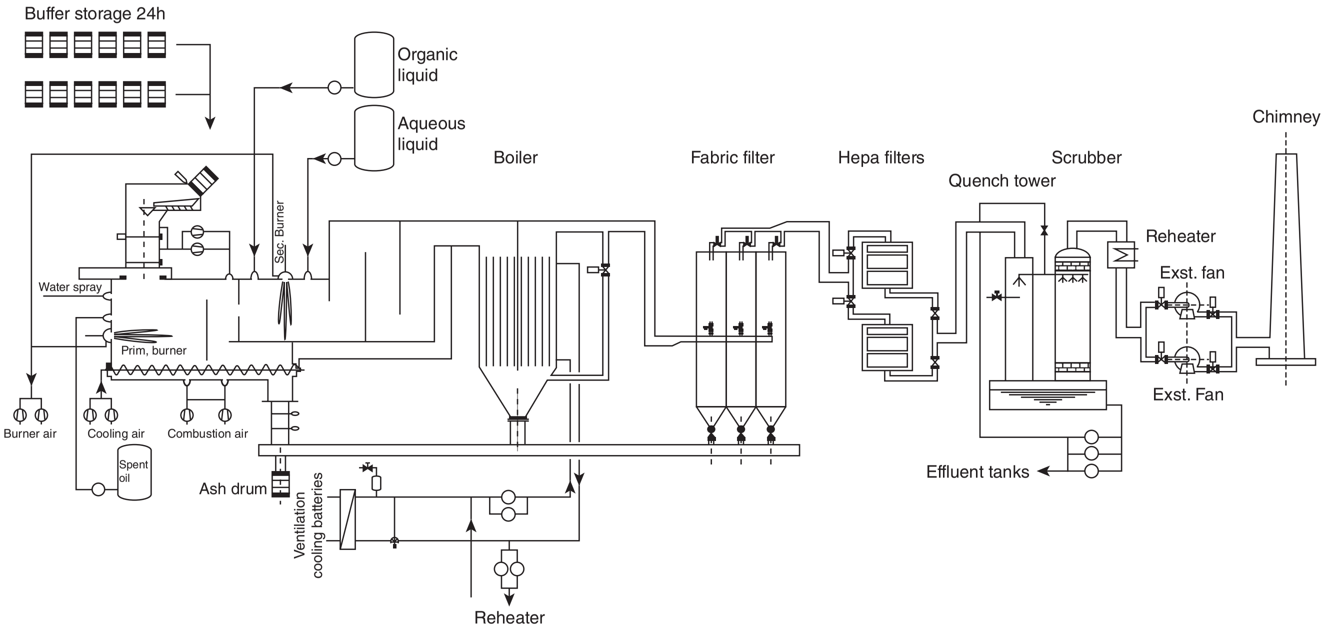

3.1 CILVA Belgoprocess low-level waste incinerator facility, Belgium.

Based on a weekly operating time of 100 h the capacity is about 8 tons/week of solid waste, besides 1 to 5 tons of liquid wastes. The radioactivity limit of the waste is 40 GBq/m^3 for beta–gamma emitters and 40 MBq/m^3 for alpha emitters, with a maximum dose rate at the surface of each package of 2 mSv/h. The collected ashes and fly-ashes, which contain the concentrated radioactivity, are supercompacted and embedded with grout.

The incineration system consists of the following main components:

- A primary combustion chamber in which the radioactive waste undergoes a combined process of combustion and pyrolysis in a temperature range of 900–950°C
- A secondary combustion chamber in which the unburned gases and soot particles are mixed with excess air to complete oxidation to primary combustion components
- A boiler to cool the off-gases
- Off-gas filtration and radiological purification, consisting of a bag-house with bag filters and high efficiency particulate air (HEPA) filters
- A wet off-gas scrubbing system, consisting of a quench tower and a counter-current scrubbing tower to remove HCl and SO_2.

The feeding of the waste, the incineration process and the off-gas treatment operate as follows.

Waste feed system

The solid and liquid waste transport packages are stored in the warehouse. At the solid waste pre-treatment line, the waste is checked for dose rate and absence of metal particles. Then the waste is loaded into incinerator feed containers which provide 24 h buffer capacity and automatic transfer to the incinerator.

The solid waste is fed into the incinerator through two locks. The first lock is the glove box from where the waste is automatically transferred via a vibrating table to the second lock, comprising two successive slide doors connected to the incinerator. These two locks create a double barrier between the ambient atmosphere and the primary combustion chamber.

The organic and aqueous liquids and the spent oil are transferred to special storage and incinerator feed tanks. From there the liquids are directly pumped into the injection lances installed in the primary and secondary combustion chambers, where they are atomised by means of compressed air.

PCC

The radioactive waste undergoes a combined process of combustion and pyrolysis. The PCC operates in a specific temperature range of 900–950°C. The primary burner operates with gas-oil and is sized to accommodate the thermal load during weekly start-up. During the combustion cycle the burner can run from low to high fire. The burner is normally shut off with the typical high energetic waste.

In the ash bed of the PCC two augers are turning backward and forward to obtain high combustion burnout residues through sufficient residence time and good contact with combustion air. At the end of the PCC, the ashes, at a temperature of about 70°C, fall into a hopper, from where they are discharged into a 200-litre drum through sliding doors.

Fly-ashes from the boiler and the bag filter are transferred by means of a vibrating tube to the same drum. From the ash drums containing the concentrated radioactivity, a sample is taken for radiological characterisation. Afterwards the fly-ashes are supercompacted and conditioned with grout in a separate part of the CILVA facility.

SCC

The unburned gases and soot particles entering the SCC are mixed with excess air to complete oxidation to primary components such as CO_2, SO_2 and HCl. The excess air supply is regulated by an oxygen analyser–controller at the outlet of the SCC. The set point is about 8% O_2. Due to the special shape of the SCC there is an intense mixing between unburned gases and excess air, creating a high turbulence. This process gives a combustion efficiency of 99.99%. The SCC is sized to provide a minimum of 2 seconds' residence time at the design waste feed rate and at a temperature of 1050°C. The secondary burner operates with gas-oil and modulates between high and low fire as a function of the outlet temperature of the SCC.

Waste heat boiler

The combustion gases leaving the SCC are cooled to 200°C in the three-pass hot water boiler. The hot water circulates in a closed circuit and the waste heat is transferred to exhausted ventilation air of the CILVA facility via cooling batteries. A system to recuperate heat of 500 KW for heating the building is also implemented.

Flue gas purification

The bag-house consists of three compartments or three times 50%. Two compartments are in service while one serves as standby. Particulate matter is captured by surface filtration of membrane filter bags, consisting of a PTFE membrane laminated to a PTFE fibreglass fabric. The bags can withstand operating temperatures of 260°C.

The filter media are cleaned online by means of pulsed jets of compressed air triggered by a differential pressure switch. The collected particles are shaken off from the surface of the bags. The hopper at the bottom of the bag-house receives the released particulate matter and emptying is accomplished through a rotary discharge valve at the vibrating tube.

Having passed the fabric filter, the gases enter the HEPA filters, consisting of two parallel compartments. One compartment serves as standby. The outlet temperature is 170°C. The wet gas scrubbing assembly consists of a quench tower to cool the gases to about 50°C, a counter-current scrubbing tower with caustic liquid for removal of HCl and SO_2, and a demister. The flue gases are heated up by 10°C in order to decrease the relative humidity and to avoid condensation. Two extraction fans in parallel ensure the evacuation of the purified flue gases into the atmosphere. One fan serves as a standby. The negative pressure in the PCC is controlled by frequency regulation by varying the motor speed of the extraction fans.

For chemical releases (see Table 3.2) the values given in EC directive 2000/76/CE are taken into account as reference limits. The particulate matter, which is the main carrier for radioactive material, must have detection limits <1 mg/Nm^3. The low content of carbon monoxide (<10 mg/Nm^3) proves the high combustion efficiency (CO_2/CO_2 + CO) of the incinerator, which is more than 99.99%.

Table 3.2 Chemical releases

Release (mg/Nm^3)[1]	EC Directive 2000/76/EC	
	Daily average values	Incinerator typical measurement campaign
Total dust	10	<1
CO	50	16
TOC	10	<2
HCl	10	1
HF	1	0.18
SO_2	50	15
NO_X	400	190
Heavy metals:		
ΣCd, Ti	0.05[2]	<0.037
Hg	0.05[2]	<0.01
ΣSb, As, Pb, Cr, Cu, Mn, Ni, V, Sn	0.5[2]	<0.028
Dioxins and furanen (ng/Nm^3)	0.1[3]	0.04

[1] Emissions are standardised at the following conditions: temperature 273 K; pressure 101.3 kPa; 11% O_2; dry gas. . . .

[2] Average values over sample period, min. 30 min, max. 8 hours.

[3] Average values over sample period, min. 6 hours, max. 8 hours.

The radioactivity of the scrubber water of a typical isotope, Co-60, is lower than the detection limit (<1 Bq/l). Even the radioactivity of a typical semi-valuable isotope, such as Cs-137, is lower than the detection limits, which proves that almost all the radioactivity is captured before the bag filters, so the radioactivity discharge in the stack is several orders of magnitude below the licensed values.

3.4 Plasma process and technology

3.4.1 Basic description

Plasma process

Plasma is considered by many to be the fourth state of matter, following the more familiar states of solid, liquid and gas. Plasma consists of a collection of free-moving electrons and ions, and energy is needed to strip electrons from atoms to make plasma. With insufficient sustaining power, plasma recombines into neutral gas. Heat energy, where added to liquid, converts the liquid into gas. The addition of heat energy to a gas converts the gas into plasma. Lightning is an example of the plasma state of matter. Lightning is not a flame; it is rather a very high temperature beam of energy.

Plasma knowledge was not exploited until the period of NASA's space programme during the 1960s. Considerable developments in plasma technology were achieved in an effort to produce an intense heat source for carrying out reliability tests on re-entry heat shields of spacecraft and missiles.

After more than four decades, plasma technology is being utilised worldwide in many industrial processes, e.g. metal cutting, metallurgical applications, vitrification of fly-ash from municipal incinerators, treatment of problematic chemical wastes, etc. Thousands of hours of successful testing on surrogate radioactive waste on different plasma systems have been carried out. The first full-scale industrial plant for treatment of low-level radioactive waste started up at the beginning of 2004.

Plasma, this unique fourth state of matter, is a highly desirable heat source for treatment of radioactive waste. Because of its high temperature (up to 10,000°C), it can treat the radioactive waste 'as is'. The inorganic materials are melted into a glassy slag containing most of the radioactive isotopes, while the organic materials are vaporised into a syngas and afterwards oxidised in an afterburner.

Plasma torches

The plasma torch is a design comprising several concentrically arranged tubes that are water cooled. The outermost tube can be cladded with refractory material to enable the burner to withstand the high temperatures within the processing chamber. Plasma torches contain the following main components:

- Torch with the electrodes
- Power supply unit
- Control and instrumentation system
- Cooling water circuits
- Process gas supply (e.g. N_2, air or O_2).

Two main torch types can be distinguished:

- Transferred torches
- Non-transferred torches.

For transferred torches, the plasma torch transfers electrical energy from the anode to the molten slag which serves as the cathode. By this principle the energy is transferred directly into the waste material to be heated more efficiently. A non-transferred torch contains two metallic tubular electrodes (upstream and downstream with respect to the plasma flow direction) separated by a gas injection chamber. An electrical arc flows between the negative and positive electrodes and therefore the gas flow injected into the chamber is ionised. The result is a high-temperature gas flow coming from the downstream electrode in a plasma jet.

Transferred torches normally induce higher temperatures to the waste material, but temperatures of non-transferred ones are still enough to treat a variety of heterogeneous waste with different melting points. Power ratings typically range from 100 kW to several megawatts. Process conditions can be varied from inert (e.g. Ar or N_2) to oxidising status (e.g. air or pure O_2) through the selection of the plasma gas.

Sensitive components on plasma torches are the electrodes. The first electrodes had lifetimes of only several hours. Nowadays electrode lifetimes vary from hundreds to several thousands of hours.

Feeding systems

The choice of feed systems has a direct effect on processing parameters. One distinguishes two main feed systems:

- Batch feed system
- Continuous feed system.

In a batch feed system the whole 200-litre drum containing the radioactive waste such as the metals, concrete debris and organic material is fed via a drum feeder into the primary chamber. In case the waste contains a lot of organic material, the off-gas system should be sized for the large instantaneous flue gas flow caused by the vaporisation of the organic material.

Metering with a shredder gives a more continuous feed and smoothes and reduces peak off-gas flow rates. Shredders allow a 200 l drum to be fed into a primary chamber that is otherwise too small to accept a whole drum.

Slag production

The waste, containing, for example, metals, concrete debris, different types of inorganic granulates and organic materials, is fed to the primary chamber containing the plasma torch. Due to the intense heat of the plasma flame the metals are melted and partially or fully oxidised. Concrete debris, sand, inorganic granulates, insulation material such as mineral rockwool and even asbestos are melted. Their crystalline structure is destroyed and they are transformed into a chemically inert and amorphous glassy slag. The liquids and organic materials in the waste are vaporised so an organic-free residue is obtained.

As in conventional radwaste incinerators, the non-volatile isotopes such as those of Co, U and Pu stay in the slag residues while part of the typical semi-volatile isotope Cs-137 transfers to the off-gas system. Experiments with non-radioactive caesium prove that Cs is a slag-seeking material and that carry-over of Cs is limited. The operational results on radioactive plasma systems confirm that there is no accumulation of Cs in the off-gas. The collected fly-ashes are sent back to the plasma furnace where most of the Cs is captured in the slag.

Thermal oxidation and off-gas treatment

As in conventional radwaste incinerators, the flue gases leaving the primary treatment chamber are passed through a secondary (thermal oxidiser) chamber followed by an appropriate off-gas treatment. In the secondary chamber the gases containing hydrocarbons, whether or not linked with sulphur or halogens, CO and H_2 are oxidised to primary components such as CO_2, H_2O, HCl and SO_2. Off-gas treatment systems for radwaste have proved their high cleaning performance, safety and reliability (see also the chapter on incineration).

Off-gas cleaning is a multi-step procedure to eliminate chemical compounds such as fly-ash, HCl and SO_2, and radioactivity, in the released off-gas to a safe level which complies with both applicable conventional and radiological regulations. Due to the high temperature of the plasma torch, more NO_x is produced which also has to be eliminated by DENOX systems depending on the release criteria. The entire system is maintained under pressure by redundant extractor fans.

3.4.2 Operational experience

The first full-scale plasma system, the ZWILAG facility in Switzerland, was taken into nuclear operation at the beginning of 2004. The maximum capacity of the facility is 200 kg/h burnable waste and 300 kg/h fusible waste. Two campaigns per year of about 10 weeks are organised to treat the stored waste. In each campaign about 500 drums will be processed. The process principles are shown in Fig. 3.2. The use of two campaigns is not due to technological restrictions but for logistical and organisational purposes.

From the horizontal drum feeder the waste falls on the molten slag. Inorganic material is melted and becomes slag. Organic material is vaporised and the incompletely burned flue gas is sent to the secondary chamber. The rotating crucible (centrifuge) in the primary processing chamber moves the molten slag. Centrifugal forces keep the slag from the pour hole during processing. Pouring is achieved by opening the closing system of the throat and slowing down the centrifuge. The slag moves towards the centre and pours through the throat into a mould. The mould is located directly below the throat in the slag collection chamber.

After complete oxidation in a secondary chamber, the flue gases emitted from the centrifuge chamber are routed to an off-gas treatment system, which can be divided into a wet physical and a wet chemical process. Inside the wet physical process, containing normally a quench, acid scrubber and wet electrostatic filter, a large portion of the gaseous and particulate materials is separated. After passing through the HEPA filter elements, the caustic scrubber absorbs the remaining portions of acids, gaseous contaminants and sulphur dioxide.

The entire gas stream is propelled through the off-gas treatment system by redundant flue gas extraction fans. They have a dual function of enabling transportation of the flue gases and ensuring that the required continuous negative pressure inside the entire system is maintained. Any nitrogen oxides still remaining in the flue gas are removed in the DENOX system through selective catalytic reduction. The clean gas attained by this purification method is continuously subjected to conventional emissions monitoring prior to being released into the environment from the building's integral flue stack.

Another plasma facility has been ordered for the Kozloduy Nuclear Power Plant site in Bulgaria. The plasma furnace is planned to have a non-transferable torch and an off-gas system based on the off-gas from the conventional radwaste incinerator at Belgoprocess. The radioactive waste, whether or not in 200-litre drums and containing organic and inorganic waste, such as steel parts, concrete debris and insulation, will first be shredded in order to obtain a more continuous waste feed. It is also foreseen to

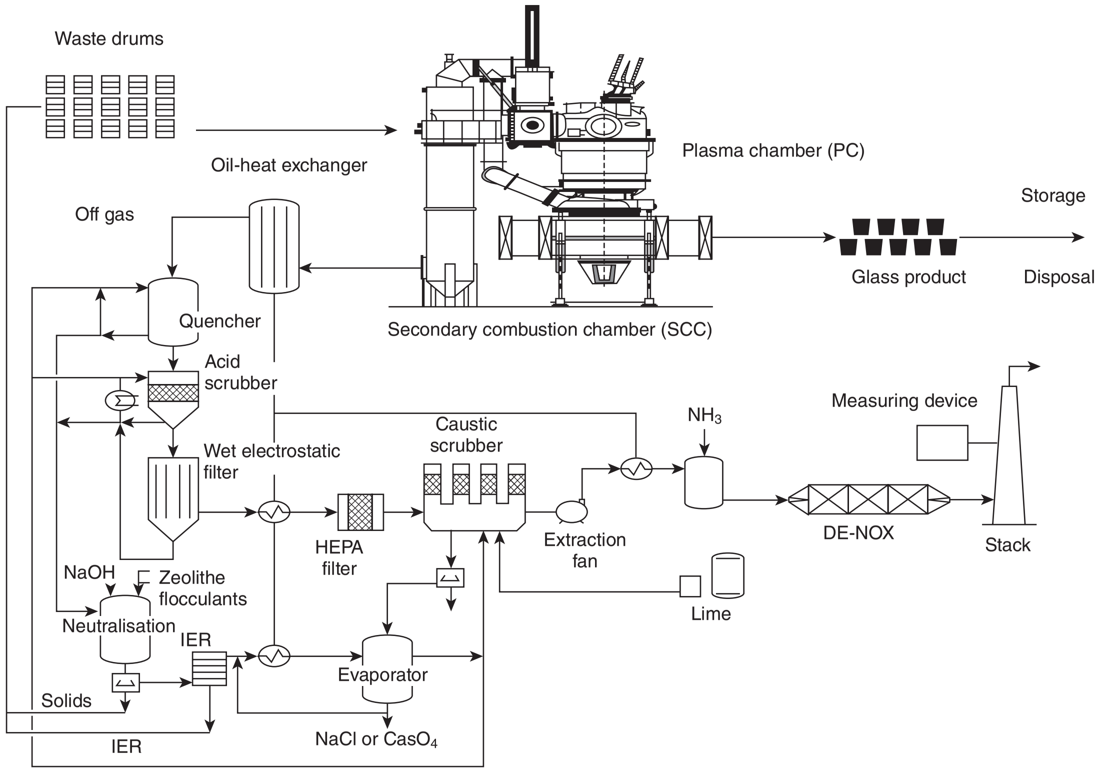

3.2 Flow diagram of ZWILAG plasma facility.

treat organic liquids and drummed spent ion-exchange resins. Start-up is planned for the beginning of 2013.

3.5 End waste form and quality control in incineration (plasma) processes

With thermal treatment processes a high VRF is obtained. But the driving force is not only a higher VRF in comparison with non-thermal waste treatment processes. The final waste packages also have to fulfil certain acceptance criteria. For example, they cannot contain any more than trace amounts of organic solid residues, sludge or moisture. Applying a thermal treatment process gives indeed a final product which is stable and free from organics and liquids and meets without doubt the acceptance criteria for long-term storage or final disposal.

Depending on the type of thermal treatment process, there are different possibilities for final waste packages. Such final packages, free from external radioactive contamination, can be stored safely and isolated from the environment in dedicated storage facilities for conditioned waste.

Due to the high volume reduction factor, which can be between 30 and 100, the ash or slag contains the concentrated radioactivity. One should take into account the fact that the ash stays in the category of low-level waste, so operational limits regarding radioactivity content for the incoming waste should be set up. Higher radioactivity content can lead to medium active waste, which needs additional precautions and incurs more expensive storage costs.

3.5.1 Waste form from incineration

Residues from an incineration process such as ashes and fly-ashes are collected in standard 200-litre drums. These drums can be supercompacted so an additional VRF is obtained and voids are eliminated. The supercompacted pucks are then loaded into a final overpack and embedded in grout or concrete as a final conditioning step. This final package, free from external radioactive contamination, can be stored safely in a dedicated storage facility.

3.5.2 Waste form from plasma treatment

Depending on the total plasma system and the final waste requirements, one can obtain heterogeneous or homogeneous final slag.

Heterogeneous slag

If the waste contains significant amounts of metals, a melt consisting of melted metals and a slag will be obtained. When pouring this melt into a mould different layers will be produced. The melted metals with higher density are found at the bottom and the less dense slag at the top of the mould. This is called a heterogeneous slag. After cooling, the mould can be put into an overpack and further eventually embedded in concrete. In most countries this type of heterogeneous slag is an accepted final product because a minimal waste volume is obtained free from any organic substances and free from moisture. This type of process is easy to operate and requires minimum mechanical components and thus less investment costs. The waste can be treated ‘as is’ with limited addition of additives.

Homogeneous slag

Similar to vitrification, a homogeneous durable glassy slag can be obtained, without the need for an additional conditioning step, which fulfils the stringent criteria for final disposal of conditioned radioactive waste. This type of process needs more additional equipment, e.g. movable torch control, a rotating crucible in the primary processing chamber, and additional equipment for oxidation/reduction control, and is more difficult to operate. Better prior knowledge of the waste to be fed and slag-forming additives such as glass may be necessary in order to obtain a homogeneous slag.

3.6 Advantages and limitations of incineration (plasma) processes

Advantages and limitations are set out below for the common technologies and in particular for the incineration and plasma technology.

3.6.1 Common advantages

- Very high volume reduction factor (VRF), up to 100, of the processed waste, especially when processing power-plant dry solid LLW. The VRF of plasma treatment is reduced when inorganic material is also treated.
- The end product is a stable and chemically inert residue that is free of organic materials and can be conditioned by various commonly used methods into a waste form suitable for long-term storage and disposal.
- Both systems can be equipped with the same type of well-proven off-gas systems.
- High throughput available process.
- Process continuity (i.e. process can operate on a continuing basis).

3.6.2 Advantages of incineration

- Incineration is a mature and well-proven technology and the most commonly used thermal treatment process for radioactive waste coming from the nuclear industry.
- It has high versatility, in that it can process a broad spectrum of dry solid organic wastes, organic liquid and aqueous wastes and to some extent also spent resins.

3.6.3 Advantages of plasma treatment

- One single process can treat the waste ‘as is’. There is no need for costly sorting infrastructure and other treatment facilities for non-burnable waste.
- The process fulfils without doubt ALARA principles. There is no need for pretreatment of the waste and entire waste drums are fed unopened, virtually eliminating direct radiation exposure and contamination risks to personnel.
- A robust waste form, similar to that from the vitrification process, can be obtained free from any organic material.
- It is an environmentally friendly process and so better accepted by the public. The heat source is a plasma instead of fuel or gas, thus there is less production of flue gases and the greenhouse gas CO_2.

3.6.4 Common limitations

- Relatively high capital cost for investment, so it appears uneconomic unless there is a sufficient minimum annual waste stream that needs to be continuously processed during the lifetime of the incineration system.
- Public acceptability of plasma and in particular incineration may be difficult in certain jurisdictions.
- Combustion process controls need to be carefully designed to compensate for the process variables (i.e. waste characteristics and heating value of a batch feed, ingress of air, etc.) to ensure safety of the combustion process.

3.6.5 Limitations of incineration

- Due to the heterogeneity of the waste stream, waste sorting, segregation, and for some systems also shredding is required. Metal objects in the waste feed, if not removed, may create mechanical operational problems.

- Well-proven combustion and de-ashing systems need to be utilised to eliminate the need for manual interventions that are associated with exposure to radioactive contamination.

3.6.6 Limitations of plasma treatment

- If a homogeneous slag, similar to that from vitrification, is desired, the process is expensive to construct and operate.
- There is limited full-scale plant experience. The first plasma unit for LLW came into commercial operation in 2004. However, other facilities are in advanced stages of start-up or under contruction.

3.7 Future ternds

3.7.1 Selection of thermal treatment technology

Table 3.3 shows a summary of the applicability of different current thermal technologies for different types of radioactive waste, solid as well as liquid. Depending on the technology, the waste has to be sorted into organic and inorganic material. Cutting and sorting of waste create potential contamination risks and are costly operations. Some technologies can accept only a limited variety of waste streams or only one kind of material. In selecting a thermal technology one should take into account the following facts:

- Can the selected technology treat different waste streams?
- What type of preparation or sorting has to be done?

Thermal treatment plants are expensive investments, so the more diverse waste streams they can treat the better the return from the investment.

Existing commercial incinerators have already proved capable of treating different waste streams at the same time:

- Organic solid waste
- Organic liquid waste such as solvents, oils and scintillation liquids
- Aqueous liquids
- Mixtures of organic and inorganic sludges
- Spent resins.

But for incinerators, inorganic material such as iron and concrete debris should be pre-sorted. In particular for historical waste, which is present in many nuclear facilities all over the world, waste treatment plants should be available to treat this waste with limited preparation efforts. Plasma technology is the upcoming technology which can treat the waste ‘as is’ with limited preparation efforts, so it fulfils ALARA principles, produces a final

Table 3.3 Thermal technologies for common waste types

Technology	Waste type						
	Organic liquids	Inorganic liquids	Organic solids	Inorganic solids	Mixed organic–inorganic solids	Mixed organic–inorganic liquids	Spent resins
Incineration	A	A	A	NA*	NA*	A	A
Melting	NA	NA	NA	A	NA	NA	NA
Plasma	A	A	A	A	A	A	A
Pyrolysis	A	NA	A**	A**	A**	A	A
Vitrification	NA	A	A**	A**	A**	NA	A

Legend:
A Technology is applicable to this waste type.
NA Technology is not applicable to this waste type.
* Small inorganic pieces are acceptable without causing damage or plugging of the system.
** Applicable only for granular or powder form of this waste type.

product with a high VRF and meets acceptance criteria for conditioned waste free from organics and liquids. The first industrial plasma facility has proved successful in operation and others are under construction.

3.7.2 Servicing for thermal treatment of radioactive waste

Many countries have a limited nuclear programme and have solid and liquid organic radioactive waste which has to be disposed of in a proper way. Due to the limited quantities produced each year, it is not always economically justified for these countries to build their own waste treatment facilities.

Small incinerators do not incur proportionally small investments. Plants with capacities ranging from 40 kg/h solid to approximately 150 kg/h will have more or less equivalent capital costs. Also, smaller capacity incinerators do not require a smaller off-gas treatment system. This is due to the fact that the high instantaneous heat release of the waste and resulting off-gas production will still dictate the size and design of the off-gas system. Therefore countries that do not have these facilities tend to negotiate with neighbouring countries that have the thermal technology or surplus in their own facility. After treatment the residues in the form of ash are sent back to the country of origin.

3.8 Sources of further information and advice

Interesting and general literature concerning the thermal treatment of radioactive waste can be found in the different Tecdocs and Technical Reports published by the International Atomic Energy Agency. The publications give the reader an overview of the technologies that exist in different countries:

International Atomic Energy Agency, Status of technology for volume reduction and treatment of low and intermediate level solid radioactive waste, TRS No. 360, Vienna (1994)

International Atomic Energy Agency, Treatment and conditioning of radioactive organic liquids, TECDOC-656, Vienna (1992)

International Atomic Energy Agency, Predisposal management of organic radioactive waste, TRS No. 427, Vienna (2004)

International Atomic Energy Agency, Application of ion exchange processes for treatment of radioactive waste and management of spent ion exchangers, TRS No. 408, Vienna (2002).

Particular and more detailed information about incineration and plasma treatment of radioactive waste can be found in the proceedings of various international conferences, e.g.:

International Conference on Incineration and Thermal Treatment Technologies IT3, University of Maryland

International Conference on Waste Management and Environment Remediation, ASME 2001, ICEM.

3.9 Bibliography

Camacho S.L. *et al.*, 'Plasma heat: worldwide developments using a demonstrated, unique heat source for waste treatment and industrial applications', *Proc. Int. Conf.*, Tucson, AZ, 2000.

Deckers J., Luycx P., 'First operation experience of the CILVA incinerator for radioactive waste treatment', *Incineration and Thermal Treatment Technologies, Proc. Int. IT3 Conf.*, San Francisco, 1997, University of Maryland, College Park, MD (1997).

Deckers J., Mols L., 'Thermal treatment of historical radioactive solid and liquid waste', *Proc. Int. Conf. Waste Management and Environment Remediation*, ASME, ICEM 2007, CD-ROM (2007).

Deckers J., Vanbrabant R., Womack R., Shuey M., 'Plasma treatment of problematic waste', *Proc. Int. Conf. Waste Management and Environment Remediation*, ASME, ICEM 2001, CD-ROM (2001).

Guihard B., 'Industrial and environmental applications of non transferred plasma', *Incineration and Thermal Treatment Technologies, Proc. Int. IT3 Conf.*, New Orleans, 2002.

Hanus G., Williams J., Zirbes M., 'Plasma gasification/vitrification', *Proc. Int. Conf. Waste Management and Environmental Remediation*, ASME, ICEM 2010, CD-ROM (2010).

Heep W., 'The ZWILAG plasma facility', *Proc. Int. Conf. KONTEC 2007*, Dresden, Germany.

International Atomic Energy Agency, Application of thermal technologies for processing of radioactive waste, TECDOC-1527, Vienna (2006).

Massit H., Atabek R., 'Plasma arc vitrification – a complementary solution for low level radioactive waste treatment and conditioning', *Proc. Int. Conf. Safewaste 2000*, Montpellier, France.

Ojovan M.I., Lee W.E., *An Introduction to Nuclear Waste Immobilisation*, Elsevier, Amsterdam, 315 pp. (2005).

Roos M. Contract for JV Iberdrola/Belgoprocess for Kozloduy Plasma Melting facility, available from http://www.world-nuclear-news.org (accessed April 2009).

Wenger J.P., Ineichen R. *et al.*, 'Startup of the ZWILAG Plasma Radwaste Treatment System', *Proc. Int. Conf. Waste Management and Environment Remediation*, ASME, ICEM 2001, CD-ROM (2001).

Womack R., 'Using the centrifugal method for the plasma-arc vitrification of waste', *JOM*, Vol. 51, No. 10, October 1999.

4

Application of inorganic cements to the conditioning and immobilisation of radioactive wastes

F. GLASSER, University of Aberdeen, UK

Abstract: Portland cement is extensively used in the construction of nuclear waste facilities and as a matrix for shielding and immobilisation of radioactive species. It affords both a physical and chemical potential for immobilisation. These potentials are quantified and related to specification, fabrication and performance. However, performance in the long term depends on the cement formulation as well as the geochemistry of the disposal environment and interactions between cement and its near field environment including inactive waste components and other containment materials. Future performance can be estimated using data from natural analogues, experience of the performance of historic structures and by modelling. Comparison of Portland cement with other non-Portland cements is also made.

Key words: Portland cement, special cements, radionuclide binding, barrier formation, pH, fly ash, slag, cement mineralogy, cement ageing, performance, durability.

4.1 Overview

This review concentrates on the application of Portland and modified Portland cements to the conditioning and immobilisation of radioactive waste. It explains briefly background data on the composition and manufacture of Portland cement as an aid to understanding the complex technology underlying its use. Brief mention is made of other matrices, including special cements, mainly by comparing them with Portland cement.

Portland cement is a manufactured product based on calcium oxide and typically containing 62–68% CaO by weight. The exact *chemical* composition of Portland cement is not directly specified, although chemical limits may be placed on the maximum permissible content of some of its constituent oxides, as determined by conventional chemical analysis. However, the representative chemistry of commercial Portland cement normally falls in a narrow range, shown in Table 4.1 in terms of oxide weight %.

The manufacturing process has as its objective transforming the appropriate chemical composition and initial mineralogy to a particular series of

Table 4.1 Typical composition of Portland cement, oxide wt%

Oxide	%	Oxide	%
CaO	63–66	MgO	0.5–3.5
SiO_2	21–24	SO_3	1–3
Al_2O_3	4–8	Others	<2[b]
Fe_2O_3	1–6[a]		

[a] Deliberately kept low, *ca.* 1% or less in white cement.
[b] Mainly TiO_2, Na_2O, K_2O and MnO. Chromium, as Cr(VI), may be restricted to ppm levels.

compounds, often termed 'minerals'.* It is these minerals, produced by thermal activation, which give rise to the characteristic properties we associate with Portland cement, namely the formation of a strongly cohesive cement, even in the presence of excess water, as well as (1) the ability to bond to a wide variety of mineral products and metals and (2) to protect metals such as iron and ferrous alloys against corrosion by virtue of the high internal pH and low permeability of the matrix.

Portland cement is made worldwide and its production exceeds 2×10^9 tonnes per year. It is thus widely available in enormous quantities. Portland cement is normally supplied to a national or regional specification, with guarantees of strength gain when mixed and hydrated under standard conditions. These guarantees do not necessarily extend to all aspects of nuclear operations, which often use exotic formulations of which manufacturers and engineers have no experience, for example, of cement mixed and hydrated with salt-rich wastes.

However, an important trend in the industry is to manufacture only a relatively few types of cement but subsequently modify these for special purposes using admixtures and supplementary cementing materials. These additions are often made at the point of use, so formulators have gained much experience which is potentially valuable to the nuclear industry.

4.2 Manufacture of Portland cement

The intention of this section is to provide a brief overview of the production process, especially as it might influence product properties relevant to nuclear applications. The term 'Portland' is historic and derives from a

---

*The International Mineralogical Association (IMA) recommends that 'mineral' should only be applied to phases formed in nature, but the broader usage of the term is well established and usefully conveys a structure without also specifying a precise chemistry, so it is used here.

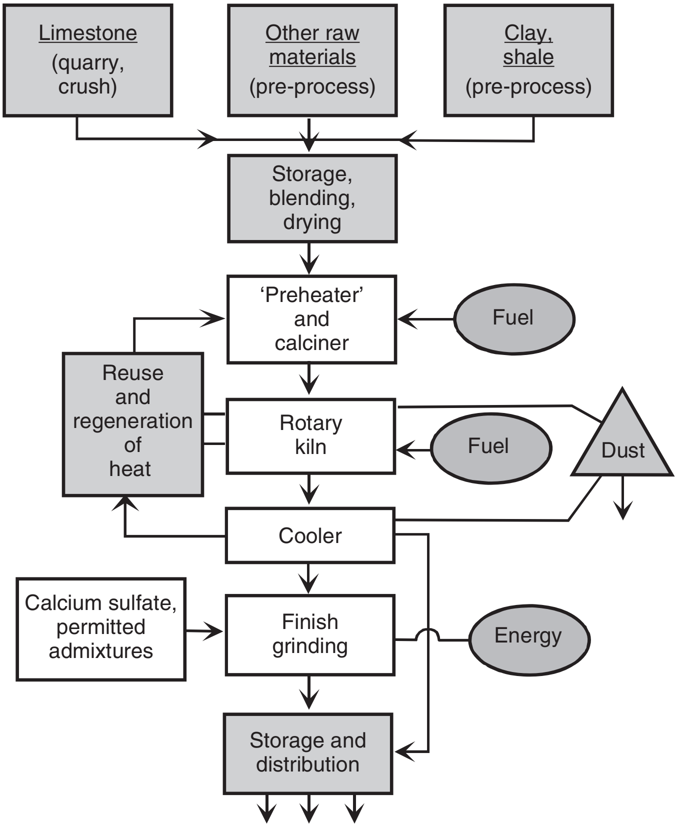

4.1 Dry process for manufacture of Portland cement: the clinkering cycle.

supposed similarity of the final product to the colour and texture of natural stone from Portland, England.

The industrial process for the manufacture of Portland cement [1] is energy intensive and is finely tuned to maximise output, ensuring a product that not only conforms to specifications but also requires minimum energy for its production. Figure 4.1 shows a schematic of the cement-making process during which raw materials are transformed into Portland cement. The high-temperature processing stages include calcination in the preheater, kiln and cooler.

Typically, but not exclusively, limestone and shale are used as the precursor raw materials. The raw materials are ground and mixed to give 'raw meal', the target composition of which is usually monitored by on-line X-ray fluorescence analysis. Thermogravimetry may be used to determine moisture contents and enable the batch composition to be recalculated to a water- and carbonate-free basis.

Knowledge of the relevant high-temperature-phase equilibria allows the relations between chemical composition and mineralogy of the final product to be calculated, and the operation of the process is regulated to attain as closely as possible a high-temperature-phase equilibrium and hence to achieve the target mineralogy. This relation utilises equations first devised by Bogue, the so-called Bogue calculation. However, a wide variety of raw materials may be used in the cement-making process: what is crucial to the product properties is the completeness of reaction and the mineralogy achieved after pyroprocessing, termed ‘burning’.

The usual fuel used in cement making is coal, although gas, petroleum coke and combustible industrial, agricultural and community wastes are all widely used to provide the necessary thermal energy. The current trend to replace fossil fuel with combustible wastes seems likely to gain in importance. These wastes are many and variable, including waste biomass, industrial oils and solvents, paper and municipal waste, etc.

The ash composition of the fuel has to be factored into the overall composition of the cement so, if waste is combusted, its trace element concentrations – except possibly of volatiles – are reflected in the clinker composition. For example, the combustion of rubber tyres in the kiln contributes to and enhances the zinc content of cements. This zinc oxide content is not, however, believed to be detrimental to the quality of the finished product. Manufacturers will avoid using wastes known to contain significant quantities of toxic, hazardous or undesirable species. For example, chromium oxide is undesirable on account of its carcinogenic properties, and municipal sewage sludge on account of its phosphorus content, which may impair subsequent hydration and strength gain of the cement. Chloride is also rigidly excluded because of its potential to corrode steel. Nevertheless, since cement is made from minerals abundant in nature, trace element concentrations of commercial cements can be expected to vary, depending on the origin and geochemistry of the raw materials. So trace element concentrations result from both the fuel and the raw materials.

Once the raw materials are crushed, milled and blended to achieve a homogeneous feed, and any oversize material returned to the mill, the dry fines are fed continuously first into a suspension preheater, followed by an inclined rotary kiln as shown schematically in Fig. 4.1. Some older kilns using semi-wet and wet feeds are still in use but are less fuel efficient than the dry process described here and are being phased out.

The intention of pyroprocessing is to minimise free lime and maximise the phases shown in Table 4.2. This is achieved by a combination of chemical and particle size control, the tumbling action of the rotary kiln, and pyroprocessing followed by blending the kiln output. Blending the kiln

Table 4.2 Mineral composition of Portland cement

Phase designation	Mineral name	Approximate formula	Amount (wt%)
Alite	Ye'elimite	Ca_3SiO_5	30–60
Belite	Larnite	Ca_2SiO_4	15–40
Ferrite	Brownmillerite	$Ca_4(Fe,Al)_2O_5$	2–8
Tricalcium aluminate	(none)	$Ca_3Al_2O_6$	3–8
Lime	Lime	CaO	0–3
Calcium sulfate	Gypsum, anhydrite	$CaSO_4$ (or its dihydrate)	1–4

output, termed 'clinker', helps cater for short-term fluctuation in the kiln output.

A major component of finished cement is tricalcium silicate, ideally Ca_3SiO_5. It is not stable at temperatures below 1250°C, hence high temperatures are required for its formation during the final stages of 'burning'. To combine the high calcium oxide content and enhance tricalcium silicate formation, peak temperatures must preferably exceed about 1330°C, so that partial fusion occurs. Thus maximum kiln temperatures are usually on the order of 1450°C. In the suspension preheater, and extending into the rising temperature part of the rotary kiln, water and carbon dioxide from calcium carbonate – the usual source of calcium oxide – are eliminated, while in the hotter zone of the rotary kiln, with the formation of melt, assimilation of unconsumed reactants occurs while di- and tricalcium silicates crystallise. As the reactants undergo partial fusion, the melt phase is important to assimilate and dissolve the remaining reactants, such as free lime and silica, the latter normally present in the reactants as quartz, with simultaneous precipitation of solids stable at high temperatures (Table 4.2).

During cooling the melt phase, typically rich in Al and Fe oxides, crystallises, giving the characteristic texture and microstructure of Portland cement, consisting of 5–30 micron size crystals of di- and tricalcium silicate embedded in a fine-grained matrix of calcium aluminate and calcium aluminoferrite phases. This sequence of phase formation also gives rise to the characteristic indurated product with its characteristic microstructure obtained after cooling, termed 'clinker'.

Despite the high chemical lime content of clinker, free lime, CaO, is usually reduced to <1–2 wt% in the course of reaction. Thus the clinker consists mainly (95%) of four solids as shown in Table 4.2: alite, belite, tricalcium aluminate and ferrite. The ferrite phase is a solid solution, $Ca_2(Fe,Al)_2O_5$. Although the clinker product is *inhomogeneous* on a micron scale, its relative homogeneity on the *macroscale* is assured by blending and fine grinding in the final finishing stage.

The combustion process contributes additional CO_2 to the kiln exit gas stream, with the result that about 0.8 tonnes of carbon dioxide are emitted per tonne of cement clinker, even in a modern fuel-efficient plant. Burning conditions are normally kept on the oxidising side of neutral, with the result that the iron oxide component of the raw materials is normally retained mainly as ferric, Fe(III), iron. Reducing conditions have sometimes been used to partially convert Fe(III) to Fe(II) and thereby lessen the pigmenting impact of ferric iron on the colour of the product, but this is not general industrial practice because reducing kiln conditions also tend to increase sulfur emissions as elemental sulfur. Sulfate sulfur in the raw materials is partially volatilised in the hot zone and alkali sulfate/carbonate solid solutions often condense onto cooling clinker.

To activate cement clinker requires fine grinding. Several wt% of calcium sulfate are usually interground with the clinker, as shown in Table 4.2. The addition may be made as gypsum, hemihydrate and/or active anhydrite, the choice depending on cost and availability. The manufacturer will generally adjust both the fineness of grinding, as determined by surface area measurement or particle size analysis, as well as the sulfate content, to give the desired setting characteristics (see below) and minimise shrinkage, with the result that the as-supplied product has a surface area in the range 2000–5000 cm^2/g, or perhaps even higher for special purposes. The fine, free-flowing powder is marketed in bulk or bags as Portland cement.

The high surface area of Portland cement, as well as the tendency of its components to react with moisture and carbon dioxide, implies that the product is perishable. If finished cement is to be stored, it has limited 'shelf life', particularly in conditions where moisture uptake can occur or, more subtly, where internal moisture transfer can occur. Significant water is stored in cement in the form of surface moisture, as hydrated calcium sulfate, etc., and it is important that this moisture is not transferred to the anhydrous silicates and aluminates in the course of transport and storage.

Prehydrated cement is not always easy to recognise but amongst its characteristics are 'caking' of the normally free-flowing product, a tendency to false set during hydration and slow strength gain, with lower than expected final strengths. Prehydration is not normally a problem in operations which use cement continuously but intermittent operation, as often occurs in the nuclear industry, can lead to problems.

A number of variants of 'Portland cement' are commercially available. These are generally achieved by: (1) changing the cement composition, while staying within the target specification, (2) changing the mean particle size and surface area in the course of grinding, and (3) adding approved reactive or inert blending materials, termed '*supplementary cementing materials*' if they react with cement or, if the additive is inert, '*fillers*'. National specifications differ in how much supplementary material requires labelling:

in Europe it is 5% maximum if the product is declared as 'Portland cement'. If this limit is exceeded, the cement must be declared and labelled under the relevant specification. Examples of permitted additives include coal-combustion fly ash, glassy iron blast furnace slag and ground limestone – (itself mainly calcium carbonate), metakaolin and natural pozzolanic materials.

The problem of cement specification is also complicated by differing requirements of different user groups. For example, the oil and gas industry has special requirements and operates under different specifications than the construction sector.

Because product specification and labelling requirements vary with application area and from country to country, the clinker compositions and fineness are also governed by many national or regional specifications. As noted, both specification and availability vary depending on national outlook and on markets, but in any event are subject to periodic review and change.

The complex and often somewhat indirect nature of prescriptive specification arises from the fact that the specification is usually defined in terms of achieving a particular rate of strength gain, using a standard formulation cured under standard conditions. This criterion may not be relevant in all nuclear applications. However, the situation is further complicated because many specifications employ a dual approach: as well as prescriptive specifications, they permit 'performance-based' formulations. That is, if the user can prove that a particular formulation is fit for purpose, it is permitted. This permissive option is of particular interest to the nuclear sector since it often uses cement in non-structural applications for which existing specifications may not be appropriate.

For example, the nuclear industry does not generally set as high a priority on rapid strength gain and high final strength as does the construction sector. But it often has other requirements for cement and concrete. As a result, it sometimes uses unconventional formulations about which relatively little is known concerning long-term performance. Before committing to unconventional formulations, the industry should consider on a case-by-case basis whether conventional formulations would be acceptable. A strong case has to be made before unconventional formulations are approved and the burden of robust proof of performance may rest on the industry.

The existing body of specifications dominates the thinking of engineers and cannot fail to be consulted by regulators, so if unconventional formulations are used, robust proof of performance should preferably be developed by following the same path as has been used for the development of existing formulations.

In this respect, the ASTM specifications are broadly representative of most national specifications; they recognise the cement types shown in Table 4.3. The European Community recognises 17 distinct classes, although

Table 4.3 ASTM classification of Portland cements

Type/designation according to C150	Special characteristics/ intended use	Type/designation according to ASTM C1157
I	Normal, general purpose	GU
IA	Normal, air-entraining	
II	Moderate sulfate resistance	MS
IIA	Moderate sulfate resistance, air-entraining	
III	High early strength	HE
IIIA	High early strength, air-entraining	
IV	Low/moderate heat of hydration	LH/MH respectively
V	High sulfate resistance	HS

(1) this classification also includes both cements and blended cements, and (2) not all 17 classes are necessarily available in all markets. In fact not all the ASTM classes are readily available, especially type IV.

The cement types shown in Table 4.3 are mainly achieved by varying the relative proportions of the four principal clinker minerals as well as by the fineness of grinding, measured by specific surface area.

European specifications broadly recognise the same generic types as the ASTM with one conspicuous exception: there is no agreement on a uniform specification for sulfate-resistant cement and the older national pre-EC specifications persist.

The important consideration for nuclear engineering is that only a few, probably not more than four or five, types of Portland cement are in commercial production. If oil well cements are taken into account the list may grow to about eight types. But good reasons have to be advanced if special cement clinkers specified to include cements intended for high-temperature, high-pressure service, as in the oil or gas industry, are to be used in more normal environments.

Instead, blending of the basic clinker types can be used to alter the properties of cementitious systems. Thus relatively few basic cement types are extensively tailored to special applications by adding supplementary cementing materials. The nuclear industry has been particularly concerned by the possibility of sulfate attack and has been a large user of so-called ‘sulfate resistant’ cement types: we return to this aspect of performance subsequently.

The nuclear industry has concentrated on two types of additive: (1) large quantities of reactive inorganic admixtures, such as fly ash, glassy iron blast furnace slag or, at lower dosages, silica fume, and/or (2) relatively small quantities of admixtures, either organic or inorganic, used to control the properties of cement while still in its fluid state. Examples of the organic admixtures include tailored molecular configurations designed to entrain air or to achieve self-compaction: these are discussed in Sections 4.6 and 4.10. Examples of inorganic admixtures include mainly corrosion inhibitors (for protection of embedded steel) such as calcium nitrite. And of course, wastes requiring to be immobilised may contain large quantities of process chemicals derived from waste streams, both organic and inorganic. For the present we restrict discussion to those additives used deliberately to influence cement matrix properties.

When admixes and supplementary materials are included in the batch close to the point of use, it is important for the customer to ensure that batching is done by competent operators and that an appropriate quality assurance plan is in place to ensure conformity with the specification. Many problems arising at operational sites and blamed on cement quality are in fact due to failure adequately to batch and mix the components of complex formulations. Inadequate emplacement procedures or some combination of sub-optimum circumstances are also common failings. Conventional civil engineering applications use 'good practice' codes and these codes ought to be more widely consulted and, where appropriate, implemented by the nuclear industry, to avoid the many pitfalls.

4.3 Application of Portland cement

In most practical applications, cements are not used 'neat' but are normally diluted with mineral aggregates. Fine, millimetre-sized, aggregates are mixed with cement and water to give a product termed '*mortar*' while mixtures of cement with both fine and coarse aggregate are termed '*concrete*'. The boundary between 'fine' and 'coarse' aggregate is not fixed but for present purposes may be taken as approximately 2 mm. Any free-flowing cement–fine particle–water mixture is termed 'grout' although to flow and penetrate well, grouts are normally made with fine millimetre- or sub-millimetre-sized aggregates. Since cement is the chemically most reactive fraction of mortars and concrete, 'cement' may therefore be the essential binder of a grout, mortar or concrete.

Mineral aggregates are used in construction because (1) they lower the cost without significantly lowering the strength of the hardened product, (2) they dilute the heat of hydration of cement which could, if not managed, lead to excessive thermal excursion, especially in large masses, and (3) they help restrain and reduce the impacts of normal physical shrinkage which occurs in the course of cement hydration.

The freshly mixed cement product, grout, mortar or concrete, usually has a period of workability lasting several hours, during which the mix remains fluid and may be emplaced by pouring or pumping without detriment to its long-term properties. Unconventional formulations sometimes exhibit *false set* in which stiffening occurs but where agitation is sufficient to break down the structures forming in the aqueous phase, thus restoring fluidity at least temporarily, or even *flash set* where set occurs prematurely and is not reversible.

In general the rheology of fresh mixes is a complex subject requiring expert input [2]. However, fresh cement mixtures are notably non-Newtonian and may exhibit thixotropic behaviour in the fluid state. For this reason, the filling of complex moulds, infiltration of drum contents, etc, require an understanding of mix rheology. The rheology can be much influenced by admixes. For example, limestone and various organic admixtures have been combined into cement batches to assist its self-compaction in the course of emplacement. In nuclear waste applications, it is usually important to eliminate voids in mass concrete and a two-way pull develops: either to use admixtures, as a way of ensuring better product homogeneity, or to avoid additives entirely owing to concern about the impact of introducing a 'cocktail' of chemicals, often of essentially unknown molecular constitution, which may act as complexants for radionuclides or break down in the cement matrix to yield potential complexants. We address this question subsequently.

The duration of the period of fluidity of fresh mixes is affected by temperature, generally decreasing with rising temperature, but the time to setting, known as the 'set time', can be regulated by means of admixtures; both accelerating and retarding admixtures are known. The widespread use of calcium sulfate as a set retarder has been noted, so cements will normally be supplied containing a set retarder, the action of which has to be overcome if it is desired to change the properties.

More than a century of experience has demonstrated that the amounts of sulfate required to ensure set control will not impair long-term strength development, but experience of other substances used to control fluid rheology and accelerate or retard subsequent set and strength gain is more limited. Experience does, however, suggest that some admixtures, particularly set retarders, may adversely affect long-term strength gain. An example in nuclear waste management is borate, which precipitates calcium and for reasons not fully understood, interferes with subsequent strength gain. Thus care is required in the selection of admixtures, particularly exotic admixtures, including in this context substances which may be present in waste, to ensure that they do not impair long-term performance. For example, citric acid has been used successfully as a retarder for Portland cement at low dose rates, and apparently does not affect ultimate strength development, but dosage is critical: excessive concentrations of citric acid will not only delay set but also inhibit long-term strength development. Set interference is not confined to soluble substances: for example, ferric floc, often used as a scavenger in the nuclear industry to sorb radionuclides, is a strong retarder for cement hydration; as it is not soluble, its interference set arises from physical, not chemical, causes.

In some cases the admixture has a beneficial effect on cement but adversely affects other components: for example, calcium chloride is a good accelerator for early strength gain and does not detract from final strengths but is nevertheless an undesirable admixture because it promotes corrosion of embedded metals, notably steel and ferrous alloys. In most cases we rely on empirical experience of the impact of waste components on set and strength gain but often lack evidence to assess their impacts in the longer term, over centuries.

Normal cements and concretes gradually stiffen with time until by 2–6 hours after mixing, they no longer flow. This point is known as 'initial set' and is somewhat more scientifically measured by using a weighted needle – the Vicat needle – to measure depth of penetration of the needle at a fixed load. The Vicat needle is used to define two times: an 'initial' and a 'final' set, the latter corresponding approximately to the onset of strength gain.

Final strengths vary with water:cement ratio, cement content and time. However, unconfined compressive strengths for commercially available ready-mix concretes are typically in the range 32.5–50 MPa, measured at 28 days. However, these mixtures may contain relatively low cement contents, perhaps ~275–325 kg/m^3. Higher specifications are readily achievable and commercially available; for example, the concrete frames of multi-storey buildings are often formulated with concretes having compressive strengths in the range 60–120 MPa. At the higher strengths, it becomes important to use rather more cement and to match the compressive strength of the aggregate to that of the matrix, so high-strength aggregates are also required.

However, compressive strength is often of secondary importance in nuclear applications; the porosity and permeability are often more important. These two factors – porosity and permeability – are not interchangeable (as is sometimes supposed). We have to consider the intrinsic properties of the matrix as well as superimposed fabrication variables. Examples will suffice. Concrete road surfaces are subject to freeze–thaw damage which is limited by providing a network of fine but well-spaced pores in which water vapour can condense and freeze without physical disruption of the matter. Such concrete can have a very low permeability despite considerable porosity. In this example the pores are created by fabrication: an air-entraining agent is added and air injected to a fresh mix giving stabilised small bubbles. An extreme example of the influence of fabrication arises in making foamed concrete by adding aluminium (metal) powder to fresh cement. Thus highly porous but impermeable blocks with bulk densities as low as ~800–1200 kg/m^3 are marketed. The porosity–permeability relationships are explored in more detail in Section 4.5.

4.4 Hydration of Portland cement

Portland cement is an example of an 'hydraulic' cement. That is, the fluid cement will continue to set and harden normally, even when emplaced underwater. This contrasts with other inorganic cements, for example gypsum-based cements, which will simply disperse in an excess of water and never achieve cohesion and strength. The strong cohesion characteristic of Portland cement hydrates is noteworthy and is relied upon in the formation of underwater constructions.

Because clinker solids are highly unstable in the presence of water, they react rapidly with much evolution of heat as shown in Fig. 4.2. The overall hydration process is complex and details are given in specialist monographs [3]. Briefly, within seconds of mixing, the mix water becomes strongly alkaline. The high content of hydroxide ions disrupt metal–oxygen bonds in anhydrous clinker minerals and in glassy supplementary materials, such as fly ash or slag, so hydration progresses by attack of water on the surfaces of grains. The evolution of the microstructure around a slag grain is shown schematically in Fig. 4.3.

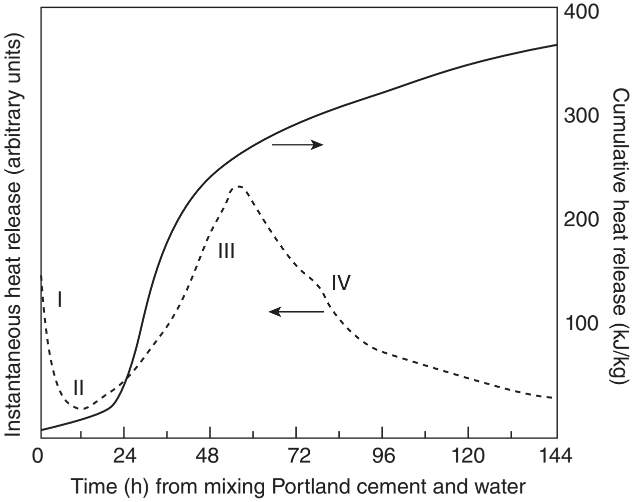

4.2 Heat evolution from Portland cement, showing both the instantaneous and cumulative heat evolution in the course of early hydration.

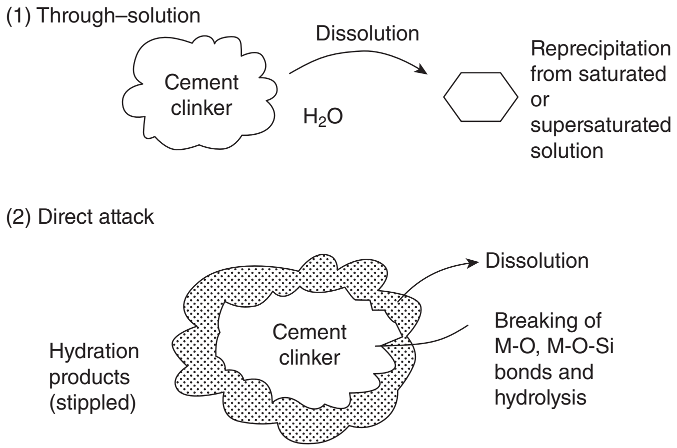

4.3 Schematic representation of the hydration mechanisms of Portland cement.

The rate at which the reaction progresses as a function of time is uneven. In general, significant attack is most rapid on cement. The initial reaction between cement and water is exothermic and is often attributed to a 'heat of wetting' of the solids, although it is probable that the initial dissolution of soluble components, with resulting increase in pH of the aqueous solution, is also an exothermic process with the result that the increased ion–dipole interactions in the aqueous phase, resulting from the rise in pH and increased ionic strength of the solution, also contribute to the initial exotherm. The most soluble components are calcium, liberated from clinker, alkali present in soluble form, and sulfate, from calcium sulfate. If calcium sulfate is initially present as anhydrite and hemihydrate, or mixtures, both rapidly convert to gypsum; the calcium sulfate rehydration reactions are also exothermic.

However, the solubilities of the main cement compounds, calcium silicates and aluminates, are incongruent: that is, the ions present in the solid do not dissolve at the same rate, as indicated by the stoichiometry of the dissolving solids. Thus the ratio of Ca/Si in solution at all stages of hydration is very much greater than the ratio in either tricalcium silicate (3.0) or dicalcium silicate (2.0). So dissolution must inevitably leave a solid silica-rich product. The residual silica-rich products of dissolution tend in part to accumulate as a coating on the surface of reactant grains, thus slowing the hydration reaction. These events are difficult to quantify because of the amorphous nature of the products and their low amounts but relate to heat output, as shown in Fig. 4.2. The initial rapid heat evolution, event I, is, as noted, the so-called heat of wetting (but in reality, more complex). This is followed by a '*dormant period*', II, often of several hours' duration, during which heat evolution is slow. Its duration is controlled by formation of surface films on clinker grains and their eventual disruption. Water diffuses through this film of hydrates and reaction continues by disruption of the protective layer and direct attack of water on mineral grains. The duration of the dormant period is normally a few hours and the mix remains fluid during this time, allowing it to be transported and emplaced. However, after a few hours – the exact time is affected by temperature as well as the nature and content of admixtures such as calcium sulfate – hydration recommences spontaneously. The heat output rises and, as the solid hydrate products accumulate and fill the spaces between the grains, the mix loses fluidity and physical set occurs. These physical phenomena correlate with events III and IV in Fig. 4.2. The reasons why hydration recommences spontaneously are not fully understood; one theory is that the initial insoluble products of dissolution form a semi-permeable envelope on cement grains, and that osmosis of liquid water through the membrane eventually leads to increased internal osmotic pressure, with disruption of the membrane and, upon exposure of fresh clinker surfaces to water, resumption of hydration.

The hydration of slag and of fly ash, although slow relative to that of cement, appears to progress at a more constant rate per unit surface area. Thus any physical benefits from adding slag and fly ash may only become apparent after several months and then only if moisture is conserved to sustain slow reaction. The heat of hydration of slag is often assumed to be less than that of cement but this is not so: the heat is simply liberated over a much longer period. Thus, comparing equivalent geometries, the actual temperature rise of slag blends is less than that of a cement-only formulation.

In summary, two main mechanisms of hydration occur: direct attack on the clinker minerals by water with formation of hydration products *in situ*, and dissolution of mineral grains, followed by precipitation of hydrated solids from saturated or supersaturated aqueous phase at some distance. In general, as hydration proceeds and liquid water diminishes and becomes discontinuous, 'through solution' mechanisms gradually become less important than direct attack.

As solid hydration products accumulate, they increasingly fill the spaces between and around grains of solid reactants. Liquid water is increasingly bound into solids while the remaining aqueous phase is increasingly subdivided by the growth of solid hydration products, both crystalline and amorphous. Eventually the remaining aqueous phase becomes trapped in isolated pores and is termed '*pore water*'. Many of the properties of cement relevant to nuclear wastes relate to this pore water. For example, it is technically incorrect (but understandable) to claim that Portland cement has a high pH: it is actually the occluded pore water in equilibrium with cement solids that has the high pH. However, the pore water is everywhere in intimate contact with cement solids which buffer and sustain the high pH, and on that account we use the term 'cement pH'. The pore water can be expressed from hardened cement by using a high-pressure press, colloquially termed a 'squeezer', equipped with a suitable collection device. Analysis of the fluid gives an insight into its chemistry and we know that it concentrates much of the Na and K present in cements. Since anions other than hydroxide, OH, are relatively insoluble in the cement environment, the (Na,K) components are effectively present as their hydroxides. Hence pH may be elevated in excess of that conditioned by the solubility of $Ca(OH)_2$, the exact pH depending on pore water volume, cement alkali content and a degree of reaction.

The hydration products of Portland cement have been much studied and they consist of relatively few solid phases. Table 4.4 lists the most important

Table 4.4 Products of hydration of Portland cement

Designation	Composition	Notes
$Ca(OH)_2$, portlandite, CH	$Ca(OH)_2$ crystalline	Found in all Portland cements but its quantity is reduced, or even eliminated, in blended cements
C-S-H calcium silicate hydrate, gel, cement gel	$C_3S_2H_8$[a]	Ca/Si ratio variable: 1.7–1.8 in Portland cement but less, ranging to as low as 1.0, in blended cements. Water content is also variable, decreasing with temperatures >40°C
Hydrogarnet	C_3AH_6	Forms solid solutions, $Ca_3Al_2(OH)_{12-4x}(SiO_4)_x$
AFm, monosulfo-aluminate	$C_4A\$H_{12}$[b]	Forms solid solutions with OH replacing SO_4 as well as ordered compounds with partial replacement of (SO_4, OH) by CO_3
AFt	$C_6A\$_3H_{30-32}$[b]	Typically an early-formed hydration product, diminishing in amount as hydration approaches completion
$CaSO_4{\cdot}nH_2O$	Gypsum ($n = 2$) Hemihydrate ($n = 0.5$) Anhydrite ($n = 0$)	Compositions are normally undersaturated with respect to calcium sulfate, which is usually consumed within the first days of hydration

[a] Approximate; the molar Ca/Si ratio in contact with $Ca(OH)_2$ is reported to be 1.6–1.9.
[b] \$ = sulfur.

of these. The principal hydrate, comprising perhaps two-thirds of the bulk of the fully hydrated paste, is an amorphous phase, a gel-like calcium silicate hydrate, whose formula is in shorthand notation C-S-H; since it ranges in Ca/Si ratio, the shorthand representation does not specify a ratio or water content. The remaining three phases are crystalline and correspond more closely to defined stoichiometry. Of these, $Ca(OH)_2$ is next in abundance, comprising perhaps 20–25% of the fully hydrated paste. The carriers of most of the alumina and sulfate, in shorthand AFm and AFt, together comprise about 5–10% of the paste.

The formation of $Ca(OH)_2$ and AFt begins very early in the course of hydration; electron micrographs disclose the characteristic needles of AFt and the plate-like morphology of $Ca(OH)_2$ develops within minutes of adding water. Development of C-S-H and AFm probably also begins early, although the bulk of the C-S-H only forms after the end of the dormant period. Because the early-formed phases can grow into water-filled space, they often have well-developed crystal morphologies. C-S-H, on the other hand, mostly develops later and reported morphological features reported for C-S-H, such as fibrillar and crumpled foils, are characteristic of poorly crystallised substances. These morphologies are in part real, but mainly result from C-S-H growing without restraint into liquid-filled pores. In well-made, low-porosity cements, C-S-H may appear to be massive and featureless in electron micrographs, and morphological features do not appear until resolution is increased to the nanometre range. At this scale, C-S-H consists of strongly adherent nanoparticles, perhaps platelet-shaped; individual platelets are about 10–20 nm in maximum dimension. Figure 4.4 shows the nanostructure inferred from atomic force microscopy. The exceedingly fine scale implies a high surface area, perhaps 50–200 m^2/g for water as the sorbate with high surface capacity for sorption and desorption of charged species.

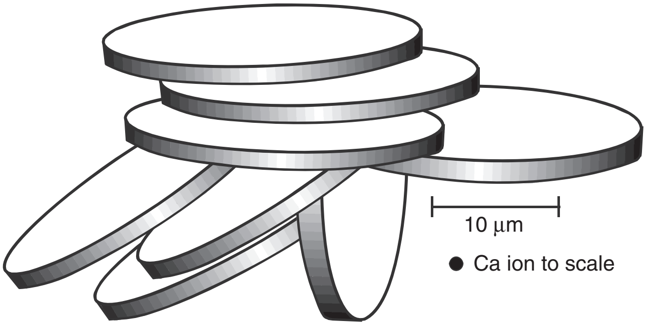

4.4 Platelet nanostructure of C-S-H.

Modern Portland cements typically reach 70–80% hydration by 28 days and >95% hydration by 1 year at 20°C. Thus, in the absence of alteration, we are reasonably confident about extrapolating the present-day properties into the future. Historic Portland cements, on the other hand, were often made with coarse clinker, at least in part, and the hydration process is seen to be continuing around coarse clinker grains even after a century or more. However C-S-H, although metastable with respect to crystalline calcium silicate phases, persists. Its persistence at 10–25°C has been observed in Roman concretes and in geological occurrences: see Section 4.11.

However, the last fraction of cement clinker to hydrate makes a disproportionate contribution to the physical properties; it may not contribute greatly to strength but does contribute to space filling and markedly reduces product permeability. Accordingly, civil engineers place much emphasis on *cure* – preservation of water within the hardening matrix until hydration reactions approach completion – to obtain the lowest possible permeability associated with the formulation. This lesson is directly transferable to the nuclear sector, where good cure is essential if low permeability is to be achieved.

The total heat of hydration of cement is substantial and may require management to avoid an excessive thermal excursion. The heat released in the course of hydration could in theory be conducted away to a suitable heat sink. But the need to cast large monoliths and thick sections, coupled with the rather poor thermal conductivity of cement and mineral aggregates, may result in achieving near-adiabatic conditions in the course of hydration. What is of concern in the course of adiabatic hydration is the associated temperature rise. As noted, the quantitative rise is dependent not only on scale but also on geometry: for example, large but thin slabs rarely experience significant thermal excursions unless they are well insulated. Small-scale laboratory simulations do not necessarily give a true picture of the thermal evolution and resulting temperature excursion at full scale.

Temperature rises in massive sections or monoliths can have serious consequences with respect to future volume instability and tendency to crack. There are two main contributions to cracking: (1) normal thermal expansion and contraction of the solid components, leading to stresses which cannot be contained, and (2) thermally-induced phase changes within the cement matrix: we discuss the potential thus created for phase changes subsequently.

The short-term heats of hydration liberated as a function of time are shown in Table 4.5. We need not concern ourselves about exact numerical values, which may vary by 5–10%, as well as with temperature and cement fineness. Except for low heat of hydration cements, Type IV, the short-term thermal outputs of commercial cements are broadly similar. There is some

Table 4.5 Approximate heat liberation from Portland cement hydrated at 20°C, determined by ASTM C186

ASTM type	Heat evolution kJ/kg at (days)	
	(7)	(28)
I	349	400
II	344	398
III	370	406
IV	233	274
V	310	–

scope, but not much, for controlling the thermal excursion in monoliths by selection of cement type. For this reason, supplementary cement materials, are commonly used to limit early-age heat release.

For a modern Portland cement, the 28-day total heat evolution tends to be about 80% or more of the total heat liberation; the remainder is released slowly over months or years. Of course the aggregate in mortars and concretes acts as a heat sink and helps control the resulting temperature excursion.

Commercial computer programs taking geometry into account are available to model the temperature excursion and assist management of heat evolution in large masses. These programs are generally reliable for commercial Portland and blended cements in which part of the cement is replaced at normal levels by supplementary cementing materials, such as fly ash and slag. But the programs suffer from database limitations at high loadings of supplementary cementing materials, as may be used in the nuclear industry.

However, these programs will not help fix the maximum acceptable temperature rise. In the precast concrete industry, where concrete is sometimes deliberately warm-cured, there is general agreement that temperatures should not be allowed to exceed 50–60°C in the course of early hydration. Note that this limit is expressed as a fixed temperature, not as a differential temperature, and theoretical justification exists for this definition. The restriction relates to Portland cement and derives mainly from empirical experience. Less experience is available concerning desirable limits for Portland cement blends containing large quantities of supplementary materials, as will be discussed subsequently.

The amount of water added to form the fresh mix is crucial to the subsequent performance of hardened cement matrices. Reasons for this are easily explained: too little water and the mix will not achieve sufficient fluidity for emplacement and compaction; also, much clinker may remain unhydrated. On the other hand, too much water, in excess of that which is required to satisfy the chemical hydration demands of the cement components, will result in a fluid mix but one which, upon hardening, will give rise to a weak and permeable product. It is uncommon to find too little water being used in cement mixes because the resulting mass remains crumbly and dry and cannot readily be emplaced and compacted. But in the absence of specification and control, it is relatively commonplace to find excessive water being used to promote initial fluidity with scant regard for the consequences. Water in excess of that required for hydration creates pores. Thus the water content, normally expressed as a weight ratio of water to cement, the w/c ratio, is a compromise between (1) obtaining satisfactory targeted values of initial properties, such as mix fluidity, permitting emplacement and compaction, (2) achieving desirable properties at intermediate stages, such as the need to avoid segregation of denser aggregate in the course of handling before hardening can occur, and (3) final or long-term properties, such as strength, permeability and resistance to penetration by aggressive agents. As a result, there is no single 'magic number' for the w/c (water/cement) ratio and its optimisation is further complicated by the presence of supplementary cementitious materials such as silica fume, slag, fly ash, etc. In general, slag and fly ash do not significantly affect the water demand; indeed, fly ash may actually reduce water demand. But higher replacement levels, particularly of silica fume, >4–6%, markedly increase water demand.

This optimum value of the w/c ratio can be benchmarked by another quantity: the amount of water required to hydrate all the cement. The numerical value of the water requirement for complete hydration depends in part on what criteria are used to distinguish between 'bound', i.e. chemically combined, water, and 'free' water, i.e. water trapped in pores within the hardened matrix. Hardened cement is intrinsically nanoporous and water in nanopores may differ in properties from bulk water, so bound water is not easy to define in terms of operational criteria. A robust procedure is to equate 'free' water with non-evaporable water: the latter is measured by the weight loss between water retained after drying over saturated calcium chloride solution at 20°C and ignition at 900°C. Measured in this way, the bound water requirement for complete hydration, in weight terms (weight of cement/weight of water), is in the range 0.32 to 0.38, depending on cement composition and hydration temperature. Differences between cements, particularly in their alumina and sulfate contents, fineness and completeness of hydration, affect the balance of hydration products and thereby give rise to variation in this ratio amongst commercial cements.

In practice, fluidity sufficient for the initial emplacement and compaction is generally achieved only at significantly higher water : cement ratios than the minimum required for hydration, as defined above. Also, aggregates (if present) may absorb some water, so that constructional concretes intended to have low permeability tend to have water : cement ratios in the range 0.40

to 0.55 (or more). But in general water in excess of that required for hydration will lead to development of porosity in the hardened product, and as porosity increases, so will permeability. Optimisation of the physical barrier functions should normally be achieved at the lowest practicable w/c ratio but, on the other hand, high permeability may be desirable, for example to permit escape of gas overpressures. But the characteristics of the solid product depend on initial formulation and this requires careful specification.

In recent decades the development and application of 'superplasticisers' (SP) – organic, water-dispersible surfactants – have enabled concretes to be formulated to low w/c ratios, yet achieve adequate fluidity for emplacement and compaction. While superplasticisers have been embraced enthusiastically by the construction industry, there has been considerable resistance to their use in the nuclear industry because of concerns that the SP, or its degradation products, will complex and solubilise radioactive species. We discuss this issue subsequently.

Once cement has hardened, it is difficult to determine accurately what water content had been used to make the fresh mix. Signs of too much water having been used include *laitance* (segregation of free water at an exposed upper surface; laitance may be either temporary or permanent); gravitational settling of denser and coarser components, such as coarse mineral aggregate; and higher than expected porosity, despite adequate cure. However, these indicators are difficult to quantify and, in general, once a concrete is deemed to be unsatisfactory, it is difficult or impossible to remediate it short of replacement. Hence the constant emphasis on the need for correct formulation and of quality controls during production to avoid having to remediate unsatisfactory cement and concrete.

At the mixing stage, and for some hours after mixing, mix fluidity is maintained. This period of fluidity is essential to permit its placement. Indeed, one of the great advantages of Portland cement is its ability to flow, so that it can, for example, completely fill drums containing metal scrap, or infiltrate complex networks of rigid reinforcement, or be formed into geometrically complex shapes. The flow of fresh concrete is markedly non-Newtonian and tamping or vibration is often required to assist its consolidation and compaction. However, vibration energy is readily dissipated in fresh concrete and it is easy to over-vibrate some regions, resulting in segregation, while others regions may, at the same time, be insufficiently vibrated and fail to be compacted. Thus it is not always appropriate to use vibration, but if vibration is used considerable operator skill is required to ensure satisfactory results.

In recent decades, much emphasis has been placed on the development of '*self-compacting*' (SC) concretes. These are usually formulated to contain finely ground limestone (itself mainly calcium carbonate) either interground with the cement or added at the mixing stage, and superplasticiser.

The term 'self-compacting' is to some extent a misnomer but SC formulations usually require much less compaction than traditional formulations. The improved surface appearance and absence of voidage in a good self-compacting concrete has revolutionised the production of well-consolidated concretes and could with benefit be considered for nuclear applications, for example the formation of impermeable barriers, despite the potentially detrimental impact arising from the presence of organic admixtures.

The hydration and hardening processes of cement are generally accompanied by physical shrinkage. The principal cause of shrinkage arises because the volume occupied by the solid hydration products and residual water is less than that of the initial volume of solids and mix water. Although many of the anhydrous crystalline phases have much higher densities than the hydrated products of reaction, liquid water is efficiently chemically combined into the hydrates and, as a result, the overall volume of solids tends to diminish in the course of hydration relative to that of the precursor anhydrous solids and water. This type of shrinkage is termed '*chemical shrinkage*'. Other types of dimensional change can occur in hardened cements, notably shrinkage in the course of alternating wet–dry cycles.

The consequences of shrinkage, especially stress accumulation and cracking, are scale-dependent. Small laboratory-sized specimens often remain relatively uncracked as a result of small linear shrinkages, but bigger masses, for example tank fillings, or massive constructions such as walls, slabs and fills, may readily exceed stress levels which can be restrained by the low tensile strength of the matrix and, as a result, they crack. This scale effect is well known from conventional civil engineering where cracking is dealt with in four ways: by (1) control of thermal excursions, (2) provision of regularly spaced expansion and contraction joints, (3) use of shrinkage-reducing admixtures, and (4) restraint arising from high tensile strength reinforcement, e.g. steel. All but one of these methods is concerned with avoidance. However, in the present context of applications to the nuclear sector, it may be undesirable to use organic shrinkage-reducing admixtures (to which the same objections attach as to the use of superplasticisers) and it may be undesirable to introduce joints in nuclear constructions intended for low permeability. So avoidance is much preferable to joints and/or subsequent repair.

Much attention has been given to controlling dimensional change in hydrating cement pastes. So-called shrinkage compensated cements have been developed: these seek to compensate for normal shrinkage by adding an expansive inorganic component, such that normal shrinkage is compensated in whole or part by an expansive component. Unfortunately, it has proven difficult to make the expansive component 'kick in' at the right point in time, with the result that a robust system, which gives consistent results across a range of hydration temperatures and w/c ratios, has not been achieved. Probably the best expectation, consistent with conservative practice, is to accept that the cement formulation will contract in the course of setting, but that the amount of shrinkage will be controlled and limited to less than 0.05% of linear dimension, thus reducing or eliminating cracking. Additional restraint may be provided by reinforcement and/or expansive admixtures. In that respect, extensive experience of the design and construction of water-retaining structures gives useful guidance to the nuclear sector [4].

4.5 Porosity and permeability

As we have shown, cements contain two types of pores: intrinsic and extrinsic. The *intrinsic* pores are associated with C-S-H gel and are mainly in the nanoscale range. On account of their very small size, nanoscale permeability presents a high frictional resistance to flow and therefore does not contribute significantly to the transport properties of the matrix. The transport properties are dominated by the *extrinsic* porosity, mainly on the micro- and macro-scale, as well as its interconnectivity. The intrinsic porosity results from a number of factors, the most important of which is the water/cement ratio and degree of maturity of the matrix. We have previously emphasised the role of the w/c ratio; once this ratio exceeds that is required to hydrate the cement, excess water remains trapped in pores. There are other sources of porosity, for example air entrainment and bubble formation, insufficient or poorly mixed cement, failure of all cement completely to fill gaps between aggregates, etc. Matrices are often microcracked and this may be treated as a special case of porosity. But in the main, porosity is a function of specification and fabrication and can thus be controlled.

In nuclear applications, permeation is a key to quantification of the barrier function. The porosity is only indirectly related to the permeability and indeed, porosity is often incorrectly used where permeability correctly describes the desired property. For example, lightweight concretes are frequently formed by generating gas in the still-plastic cement matrix; as a result, the cement may be highly porous but the pores are in the main isolated, so the product retains the low permeability characteristic of an impermeable matrix. If we ignore the added pores resulting from extrinsic factors such as air entrainment, percolation, the ability of liquid or gas readily to permeate the matrix, appears to increase rapidly above about 16 ± 2% porosity. Thus, where pores are introduced as a result of adding an excess of mix water, it is generally found that permeability increases exponentially as the porosity increases above this value. As a rule-of-thumb, for Portland cement concrete, if we take a permeability of 1.0×10^{-12} m/s as the upper acceptable limit, the water/cement ratio should not be allowed to exceed 0.60. In the w/c range 0.40–0.60, of course, adequate cure is essential so that the maximum possible quantity of water is transferred from liquid to the combined state.

4.6 Supplementary cementitious materials

Portland cement can be supplemented by other materials, which are usually treated as partial replacements for Portland cement. These materials are not cementitious, or are only weakly cementitious, in their own right but require activation by some other material. Upon activation, they participate in the cementitious reactions and become part of the cementitious matrix. Portlandite, calcium hydroxide, perhaps furnished by Portland cement, can be used as an activator for most supplementary materials. Portland cement is often preferred as the activator because, although it furnishes only ~25% portlandite, (1) it gives better early strength development, and (2) it gives C-S-H which helps fill pore space and is thus a conservative choice of binder. However, the supplementary materials, while very varied in composition and mineralogy, share several characteristics: they are cheap and widely available and they are less basic, i.e. more acidic, than Portland cement. By 'basic' is meant consisting, on average, of less electropositive oxides than cement, giving rise to a potential for reaction with hydroxide ions (OH) from a basic cement. Table 4.6 lists the source and constitution

Table 4.6 Supplementary cementing materials

Designation	Source/origin	Chemistry/mineralogy	Comments
Fly ash	Combustion of pulverised coal. Collected from exit gas stream	Lime content highly variable. Much crystalline matter, some or all of which is inert. Glass content variable	Classified according to lime content; low = class F, high = class C[a]
Slag	Iron blast furnace	Mainly glassy. Contains sulfide. Quenched and granulated prior to use	Other types of metallurgical slags are often unsuitable
Silica fume	Ferrosilicon production	Micron/submicron amorphous silica particles	Particles tend to agglomerate and are difficult to disperse
Natural 'pozzolans'	Not available everywhere	Contain either or both reactive silica and zeolites	Natural sources: abundant but inhomogeneous

[a] This classification of ash types is obsolete but continues in widespread use.

of the principle supplementary materials. Many other materials have potential pozzolanic activity and have been suggested for use but are often not widely available, or are available only in small amounts, are of inconsistent quality, or have potential for adverse reaction with cement.

Many of the materials listed in Table 4.6, e.g. silica fume, slag and fly ash, are themselves industrial by-products. Only natural pozzolanic materials (a term deriving from the Italian locality, worked since Roman times as a source of ashes which are activated by portlandite) are used in essentially unmodified form. However, all these materials, natural as well as synthetic, are highly variable in composition, mineralogy, granulometry, etc., and on that account need to be subject to quality control. Trade associations will generally ensure that waste materials such as fly ash and slag marketed for blending with cement have an appropriate granulometry, are free from deleterious impurities and are sufficiently reactive with cement to attain minimum standards of strength gain. However, fly ashes meeting these criteria embrace a wide range of compositions and crystallinity and at long ages, after reaction with cement, may confer a wide range of properties on the resulting cement matrix, especially when used at high replacement levels. Slag also varies considerably in composition depending on the geochemistry of the iron ores, as well as the extent to which ore has been pre-processed before smelting, the fuel used and the nature of the iron-making process. However, quenched slags are mineralogically relatively simpler than fly ash as they consist overwhelmingly (>90%) of one phase: glass. But none of these replacement materials should be thought of in the same class as Portland cement: they are much less homogeneous and vary in chemical composition. Because they differ significantly from Portland cement in composition and granulometry, high substitution for cement can be expected to induce a wide range of properties to the composite matrix after reaction.

One should beware of generalised statements about the impact of supplementary materials, especially when used at high replacement levels, on the porosity and permeability of the solids. A critical and often overlooked consideration is the long-term evolution of pH as many fly ashes, used at high replacement levels, appear to have sufficient capacity – not necessarily revealed in tests of a few months' or years' duration – to react with portlandite and high Ca/Si ratio C-S-H thus lowering the absolute value of pH to ~10 and reducing the pH buffering capacity per unit mass.

This is not to imply that supplementary cement materials are undesirable, only that extra care is required in selection and assessment, especially of long-term properties such as the evolution of internal pH. Scaling effects also need to be considered. For example, it is claimed that high slag blends, with 20% or more replacement of cement by slag, lessen the thermal excursion during initial set. Indeed, this has historically been one of the justifications for the use of high-slag blends in nuclear applications. While a reduction in exothermicity is observed on the laboratory scale, the heat of hydration of iron blast furnace slag is actually comparable with that of plain Portland cement. The thermal excursion attending early hydration may be reduced by the sluggish hydration kinetics of slag relative to those of cement. But the activation energy for slag hydration is relatively low, much less than for cement, so the near-adiabatic self-heating encountered in large masses (the heat being furnished initially from the cement activator) markedly accelerates slag hydration, with the result that at full scale, the net thermal excursion may not be significantly reduced by adding slag: depending on geometry, some or all of the benefit of using slag to lessen the thermal excursion may be lost. However, slag has other impacts on matrix properties, as will be discussed.

Supplementary materials may affect the internal pH and redox potential (Eh) of cements but to varying extents. Regarding pH impacts, slag is generally a net consumer of portlandite but the consumption is sensitive to slag composition, replacement level and fractional slag reactivity: at high replacement levels, only ~50% of slag may react in 20 years. Fly ashes containing significant glass content, itself an aluminosilicate composition, tend to be relatively high consumers of portlandite, with the result that free portlandite may be completely reacted and the Ca/Si ratio of C-S-H lowered even at moderate (~50%) replacement. The impact of fly ash on the continued persistence of portlandite is sensitive to replacement level and amount of glass in the fly ash, as well as by its composition and reactivity. As with slag, the full extent of pH lowering is unlikely to be achieved in short-term tests on account of slow reaction kinetics. But predictions are that the pH buffering capacity will decrease with time to pH < 11, perhaps to or below the limit for steel passivation.

Although well-characterised natural systems, the Eh function of cements is arguably less well appreciated [5]. The Eh function measures the ability of substances to participate in oxidation and reduction reactions while the poising capacity measures the capacity to participate. An example is helpful: Portland cement itself is slightly on the oxidising side of neutral, its Eh relative to the potential to discharge hydrogen from water being several hundred millivolts positive but the numerical value is poorly poised. That is, it does not contain any chemically reactive oxidising–reducing couples, with the result that its oxidation potential is readily influenced by added electroactive materials. For example, corroding steel will scavenge and consume the relatively small quantities of dissolved oxygen in cement pore fluid and thereafter, generate a reducing environment in the vicinity of embedded steel. But if the service environment is oxidising, oxygen, perhaps dissolved in percolating water, could renew the oxygen supply and create an oxidising environment. Many constructional concretes used in air but with embedded steel thus have a strong Eh gradient, oxidising at the surface exposed to air but reducing in the vicinity of embedded steel.

Fly ash contains unburnt carbon and much iron as both ferrous and ferric, so in theory fly ash should lower the redox potential and provide internal poising capacity. But both the carbon and ferrous iron minerals in fly ash are inert, with the result that fly ash does not significantly affect the internal redox state in the course of laboratory measurements typically extending at most to a few years. Slag, however, is redox-active with relatively rapid kinetics. While still in the blast furnace, slag scavenges sulfur from the metal and, as a result, iron blast furnace slag typically contains about 1% sulfide sulfur. This sulfur is mainly dissolved in the glassy slag but becomes available for subsequent reaction in the course of slag hydration. Provided sufficient sulfide is available to overcome the relatively weak poising capacity of cement, the internal redox potential of slag-rich blends will decrease, from perhaps +100 to 200 mV in cement to –200 to –300 mV (relative to a standard hydrogen electrode) in slag-rich blended cement matrices. The reactions are complex: sulfate in the cement activator appears to react with sulfide in an alkaline environment giving thiosulfate and it is likely that the observed low redox potential arises from couples involving sulfide, thiosulfate and sulfate [6]. Thus not only is the redox potential lowered in slag-rich blends but the poising capacity is also increased by sulfide in the unreacted slag. The low redox potential achieved in high-slag matrices is believed to reduce many soluble higher-valent species to lower-valent and less soluble speciations, e.g. Tc(VII) is reduced to Tc(IV). The activity of reduced S species may perhaps be sufficient to combine some radioactive species, e.g. Pb, Ni, Bi, etc., as sulfides.

4.7 Mineral aggregates

An important class of mineral additives to cement are aggregates. The quantitative importance of aggregates to the constitution of mortars and concretes can scarcely be underestimated: most constructional concretes have densities in the range 2200–2500 kg/m^3 but, of this total, cement contents are likely to be low, in the range 230–450 kg, the balance being mainly mineral aggregates and water. Since water : cement ratios are usually in the range 0.4–0.6, aggregates comprise perhaps 75–90 mass% of concrete and are thus its most abundant constituent.

Aggregates are generally products of natural origin and, except for washing, are essentially unrefined and show all the variation characteristics of naturally occurring rocks. Aggregates may be produced from unconsolidated gravel but may also be obtained by crushing rocks of igneous, metamorphic or sedimentary origin. Reclaimed crushed concrete is sometimes used, but care is required as fragments of adhering cement increase the water demand with potentially deleterious consequences for the permeability. Synthetic and semi-synthetic aggregates are known but not in common use.

Aggregates are nominally chosen to be inert towards cement but in most cases the inertness is a matter of sluggish reaction kinetics, with the result that reaction is thermodynamically favourable, although perhaps not perceptible over a few decades or even centuries at or near ambient temperatures. However, elevated temperatures accelerate reaction; the necessary thermal energy for activation in nuclear waste applications could be supplied by a geothermal gradient, from inclusion of heat-generating wastes, or as a consequence of the initial thermal excursion or some combination of processes and events.

As noted, aggregates play an important role in constructional concretes: to reduce cost and dilute the impacts of thermal excursions and shrinkage of the cement paste. These functions are relevant in nuclear applications, although dilution of cement may also have adverse consequences, such as lowering the mass of active pH buffering components per unit volume. But, given the relatively long time-scale expected in many nuclear applications, the assumption that aggregates remain inert requires critical examination.

We know from experience that some aggregates are reactive with cement on relatively short time-scales of years or decades. Table 4.7 gives guidance on potentially reactive aggregates together with a brief explanation of the origin of the reactivity [7]. The consequences of reaction are often manifested by physical expansion and cracking. For example, the reaction of siliceous aggregates with cement arises from hydrolysis of Si–O bonds with subsequent imbibition of water. This reaction is expansive and the results

Table 4.7 Aggregates known to be reactive with Portland cement

Source of reaction	Occurrence of reactive material	Process and consequences of reaction
Glassy silica, strained or crypto-crystalline quartz	Widespread in sedimentary and low-grade metamorphic rocks	Si–O–Si bonds are hydrolysed with formation of silanol (Si–OH) bonds. Product imbibes water with swelling
Tridymite, cristobalite	Igneous rocks: occasionally in sedimentary or hydrothermally altered rocks	As above. These high-temperature, low-density silica forms are susceptible to attack, resulting in physical expansion
Dolomite, $CaMg(CO_3)_2$	Dolomitic limestones and dolomite of sedimentary origin	Mg is selectively extracted at high pH forming brucite, $Mg(OH)_2$, and other Mg products. Reaction is expansive

are physical cracking and distress as monoliths expand. The resulting cracking enhances subsequent secondary attack, for example resulting from freeze–thaw, ingress of salts and oxygen from the service environment, etc., with the result that deterioration, once initiated by cement–aggregate interactions, tends to accelerate with time. Hence the problem of unsuitable aggregates is best dealt with by specification with a view to avoidance.

The generic type of reaction is termed 'alkali–aggregate reaction', or AAR. In principle all rocks containing free silica are susceptible to AAR but it has long been known that reactive silica tends to concentrate in certain rock types, e.g. in sedimentary rocks which contain opal, chert and flint. Some dolomites may also contain silica impurity in reactive form. Nevertheless, many rocks in these categories have given perfectly satisfactory service, so some better discrimination is needed to avoid reactive types. Rapid identification of susceptible aggregates has proven to be difficult. Petrographic examination in polarised light has been used to determine the occurrence of strain in silica grains and, since strain is associated with reactivity, suspect aggregates can be rejected based on optical examination using a polarising light microscope. It is sufficient to examine a relatively small random sample of grains. However, skilled petrographers are in short supply and methods requiring human skill or judgement are not now fashionable. Various rapid tests have been proposed or adopted, such as autoclaving mortar prisms and measuring the linear expansion achieved in short-term trials, but experience has shown that the test is not generally reliable.

Chemical extraction tests have been devised based on the amount of readily soluble silica in aggregates, and thus identify susceptible aggregates, but the tests appear not to show good discrimination between aggregates known from experience to be either safe or deleterious.

The AAR type of reaction between cement and siliceous aggregate arises from several sources: (1) the general instability of 'acidic' substances such as silica in the 'basic' environment of cement, and (2) the tendency of the mineral aggregate first to undergo hydrolysis, followed by imbibition of water in the cement environment. It is known qualitatively that high pH and high temperature both enhance the rate of hydrolysis of Si–O–Si bonds. These bonds occur in well-crystallised, dense silica but are kinetically resistant to hydrolysis, so these aggregates are normally acceptable. But once hydrolysis commences, the resulting product, hydrated amorphous silica, takes up additional water by imbibition, causing physical expansion. The concrete cannot contain the resulting expansive stresses even if reinforced and, as a result, the matrix expands with cracking.

The designation 'alkali–aggregate reaction' is to some extent a misnomer inasmuch as 'alkalis' – sodium and potassium – are not strictly necessary to initiate and sustain the reaction: calcium hydroxide is often sufficient.

Nevertheless, the presence of alkalis effectively *as hydroxides* elevates the internal pH of the cement matrix to above the pH threshold obtained in the presence of $Ca(OH)_2$, pH = about 12.6 at 20°C, so an effective means of mitigating reaction is to use low-alkali cements. Water is a key component for the swelling reaction and so keeping concretes dry is another option to prevent AAR: thus AAR frequently affects concretes used outdoors but only rarely does so in dry internal applications.

Still less is known about the characterisation of dolomite where the kinetics of Ca/Mg ion exchange control reaction kinetics. Reactions of the type

$$MgO\ _{\text{(from dolomite)}} + Ca(OH)_2\ _{\text{(from cement)}} = Mg(OH)_2 + 2CaCO_3$$

occur, giving rise to damaging physical expansion as they occur within an already hardened matrix.

In designing nuclear waste concretes to be used with siliceous aggregates, low-alkali cement should always be specified. But this option obviously needs to be exercised *before* construction and, in any event, will not deal with alkalis that may migrate into concrete from the service environment. Unfortunately the option of keeping concrete dry is unlikely to be available in the context of geological disposal. AAR is also enhanced by elevated temperature, so particular care is required in aggregate selection if the cement is expected to perform in warm or hot conditions. However, even cold conditions do not necessarily confer immunity to AAR; Icelandic experience affords numerous examples of AAR-damaged concrete. Other sources of silica and silicate minerals are also suspect. Geologically young granites containing tridymite and cristobalite phases of silica, instead of the more usual quartz, are also potentially reactive, as are fine-grained igneous rocks such as rhyolites. These also liberate alkali following crushing.

As noted, much less is known about factors controlling dolomite, $CaMg(CO_3)_2$, reactivity and selection. Some dolomites are known from experience to be highly reactive with cement and should be avoided. While some have suggested that the source of reaction is silica impurity within dolomite, it appears that magnesium from dolomite can also replace calcium in portlandite, etc., and that the resulting reaction to form brucite is physically expansive. However, factors controlling dolomite reactivity are not well characterised and dolomite aggregate is probably best avoided to achieve long-lived constructions.

Some rock types containing no free silica have also been the source of dimensional instability, for example altered dolerites and basalts. The alteration occurs over geological time but its significance only becomes apparent when the rock is used as aggregate for concrete. It is thought that layer-lattice minerals such as chlorite exhibit ion exchange with cement and cement pore fluid, and the exchanges initiate shrink–swell processes in the course of wet–dry cycles, as a result of which the aggregate grains debond from the cement matrix. The physical spaces thus created, as well as the cracks between the spaces, facilitate ingress of aggressive agents and enhance the susceptibility to freeze–thaw cycles.

In general, the importance of lessons learned from the AAR problem has been underestimated in respect of its impact on the design and formulation of concretes for the nuclear industry. It should be noted in this context that many concrete structures made with suspect aggregates have shown no sign of expansion for decades. But once expansion begins – and its onset may be delayed by years or decades – it is progressive, so an inevitable cycle is initiated leading to structural distress, cracking and loss of coherence and strength. Subsequent investigation into the causes of expansion reveals that reactive aggregate was used but its belated recognition does not permit remediation.

While some of the secondary mechanisms of deterioration described above, e.g. freeze–thaw, may not be high on the hazard list for nuclear structures, other hazards such as wet and warm conditions are likely to be encountered in the course of nuclear waste disposal. In view of the longevity expected from nuclear waste applications, aggregate selection should receive a higher priority than is generally accorded. The sole aggregate type which is in (or very nearly in) equilibrium with Portland cement is calcite, $CaCO_3$. Limestone, mainly $CaCO_3$, is widely distributed in nature and is available in high purity with respect to its $CaCO_3$ content. It thus represents a logical choice of aggregate for nuclear structures intended for long life. It has the added benefit of providing additional buffering against acid attack, should acid be generated in the post-closure phase.

4.8 Service environments and cement performance in its service environment

A rational approach to predicting future performance requires definition of the geochemical parameters of the near field and impact, if any, of the waste and of other barriers. An example suffices: the foregoing discussion may give the impression that cement is bound to degrade because it is prone to a very large number of degradation mechanisms. This may be so, but cement matrices are also surprisingly tolerant to many types of environmental exposure and resistant to degradation under a wide range of conditions.

In the general case, cement is a material whose internal state is quite different from that of most natural environments, so it is only to be expected that reaction will occur between cement and its service environment. And, as we have noted, attention to specification of the service environment and care in the delivery of construction will enable a wide range of problems to be avoided, or at least mitigated, leaving us to address a shortened list.

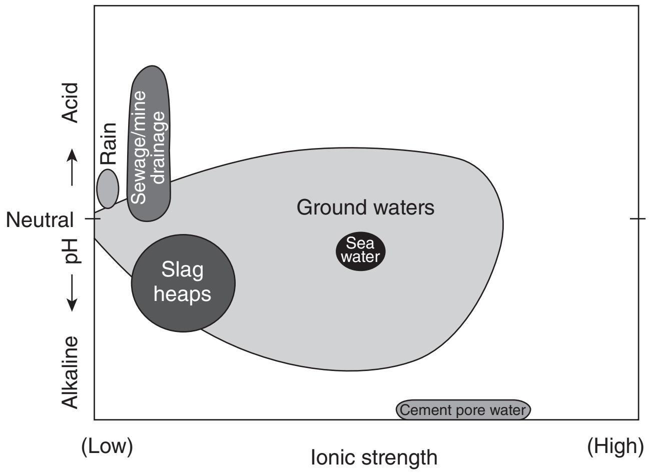

4.5 Comparison of natural environments with those in Portland cement, as functions of pH and ionic strength of permeating fluid.

The contrast between the internal environment of cements and natural environments is shown in Fig. 4.5. Cement pore water has a moderately high ionic strength and high pH, so its composition lies near the lower right corner of the figure. Natural environments are highly varied but only rarely do waters approach the high pH of Portland cement. High ionic strength waters, on the other hand, are well known; for example, sea water and formation brines may have ionic strengths approaching or even exceeding that of sea water or cement pore fluid.

Rain water has low ionic strength and is slightly acidic, on account of its content of dissolved carbon dioxide. Once rain water reaches the surface and percolates soil and rock, it tends to dissolve mineral matter and also increases its soluble organic content. Thereafter its pH–ionic strength evolution depends on local geology, vegetation, land use and climate, together with interactions between percolating water and connate water: the latter may be conditioned by ancient paleoclimates. All these features, processes and events may give rise to the large envelope labelled ‘ground water’ in Fig. 4.5. A few of many special cases are shown; for example, drainage from mining activity, where oxidation of sulfide, either still *in situ* or in spoil, can lead to formation of free sulfuric acid and very low aqueous pH. Care may be required in managing repository sites not to push the site into some special regime, often quite different from that anticipated in performance assessments based on analysis of the site in its undisturbed condition.

In this context it is useful to distinguish two classes of reaction: (1) internal, between cement and other components of the cementitious system, including waste and other added components such as aggregates, and (2) external, cement and the service environment in which it is expected to perform. The distinction is important because we have some control over the engineering formulation of the cement matrix and can choose to add certain constituents or not, as, for example, by selecting the aggregate mineralogy. Thus a range of problems regarding future performance can be anticipated and managed with mitigation, by appropriate specification and design. But we often have less (or even no) control over the service environment, especially in the longer term.

Before discussing performance, it is well to recognise that performance is an abstract concept and can only be quantified if we define its *attributes*. These attributes should be defined so that they can be quantified in terms of accessible variables. Once this has been done, performance can be assessed through the time-dependent changes to the relevant parameters. Figure 4.6 shows an example.

The selected attribute, or performance parameter, is measured or modelled as a function of time. The initial value is chosen to exceed the requirement but declines with time; when it reaches a certain conservatively chosen predetermined value, the material is said to have reached the end of its

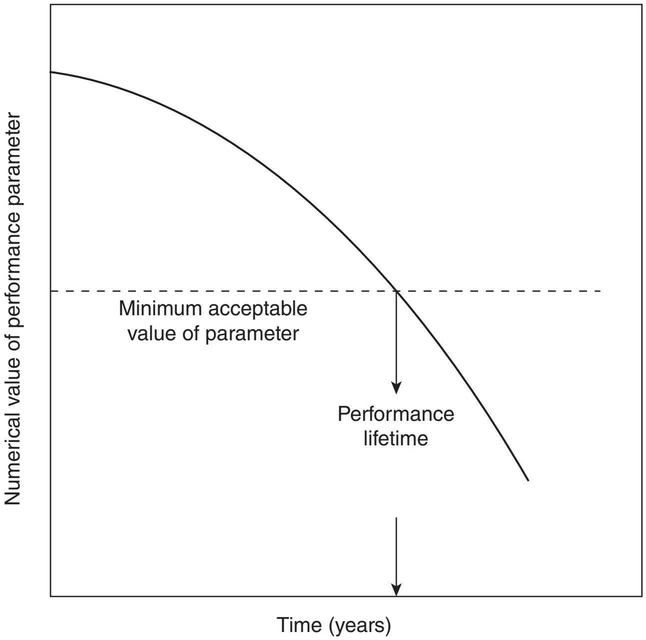

4.6 Concept and definition of performance lifetime in terms of selected attributes.

performance life. This approach forces us to think about the parameters defining performance, how they can be measured and – even more important – their future evolution, correlation into a multivariant framework and integration into the overall performance assessment model (PA).

However, we often have less than ideal control over the potential for reaction in the disposal environment in the sense that the environment is often undefined, or only partially defined, at the time when cementation is commenced. For example, waste may be cemented into monoliths which are stored pending a decision on a permanent disposal site.

The characteristics of the disposal site should be considered at as early a stage as possible, preferably as an integral part of the decision to use cementation followed by geological disposal and as part of the site selection process. Clearly, many factors enter site assessment; some are addressed in other IAEA publications, as well as in various national programmes, and cannot be considered in detail here. But the proposed environments for disposal of cement conditioned waste are known to include a wide range of geological and geochemical conditions: clay and soils at shallow depth and, in deeper sites, salt, clay, granite, volcanic tuffs in varying states of alteration, etc., as well as a wide range of groundwater geochemistry. The host geochemistry may not be in equilibrium with local rocks and the future evolution of the site can thus impact in very different ways on the PA model.

Moreover, the wastes themselves may superimpose a unique geochemical signature on the immediate disposal environment, often termed the 'near field'. For example, Portland cement, with its high pH and content of slightly soluble calcium, may superimpose its chemical signature on the host rock, including both the near and far fields. This chemical signature is one of the unique features of cement and is sometimes envisaged as giving rise to an 'alkaline plume' which migrates away from the repository in response to groundwater movement and reactions leading to its neutralisation.

These influences may affect the ability of the near field to immobilise and retard radionuclides. For shallow sites, soil often replaces rock as the host, but the principles remain the same. The compatibility relations and impacts of cement upon its near-field environment probably do not receive the priority which they deserve. Given the wide range of options for disposal and the varied environments, the approach taken here is not to describe particular environments, but instead to isolate generic factors likely to affect performance and quantify the factors and their impacts.

The above discussion is qualitative and the question often arises about how to quantify the interaction between cement and the near field. Given the complexity of the problem, the time scales involved and the general lack of detailed knowledge, it is again best to identify the cement properties associated with performance, agree parametric limits and seek (or develop) generic models and apply them in an iterative manner.

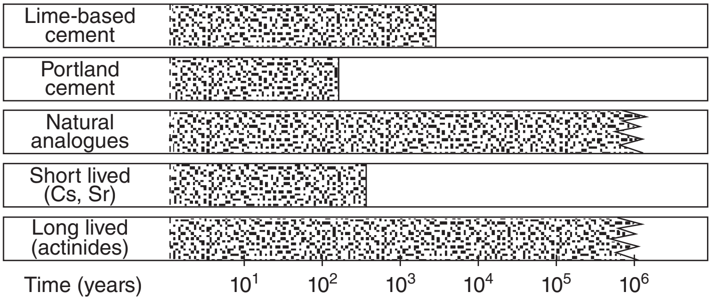

4.7 Timelines characteristic of Portland cement and comparison with radioactive decay.

In this context, the single most difficult factor to elucidate is the dependence of performance on time. Figure 4.7 compares a few relevant time benchmarks. Experience of artificial lime-based cements extends back perhaps nearly 10,000 years. Most surviving examples of ancient lime-based constructions use hydrated lime, perhaps mixed with aggregate, as a flooring plaster, often over a sub-base of lime-based rubble concrete. Contemporary examination shows these to have completely carbonated, i.e. the original high pH has been lost, and leached, i.e. they have become friable. Roman cements have often survived. They are based on reaction between hydrated lime and a pozzolanic material, either man-made or, more usually, naturally occurring, such as hydrothermally altered volcanic ash. As such they do not differ much in bulk composition from modern cements although using different raw materials and having initially different granulometry and mineralogy.

Portland cement, on the other hand, is a nineteenth-century development of which we have at most 150 years of experience, but some transfer of knowledge from lime-based structures is possible. Experience of above-grade concrete shows deep penetration of the carbonation front, perhaps 1–2 mm/y depending on rainfall, humidity and exposure. On the other hand, natural analogues of Portland cement exist, notably in Jordan. The Jordanian site has probably persisted for 10^5–10^6 years, but is still discharging springs at pH in excess of 12. It is intensely fractured and the local rainfall – at present about 500 mm/y–percolates the cement rock. The deposit is presently at about 30°C and the fractured cement rock shows considerable signs of self-healing. It is probable that the rock scavenges much of the carbon dioxide in percolating water, although on account of the huge mass of rock, springs emerging from the base of the deposit where it is intersected by a deep river valley are still at high pH, *ca.* 12.5–13. Historical and natural analogues thus suggest that model predictions, of a long dissolution lifetime for cement conditioning by effective contact between circulating water and rock, is achieved.

These examples may be compared with time-scales for immobilisation. If we take 10 half-lives as the benchmark for containment of a particular radioisotope, cement needs to perform for 300–500 years to contain short half-life isotopes such as Cs and Sr but much longer for actinides and other long-lived isotopes for which the performance lifetime should preferably extend over ~10^6 years. Depending on the weight attached to the various historical or natural analogues, it is therefore reasonable to suppose that persistence of high pH might, under favourable circumstances, extend to ~10^6 years.

4.9 Standards and testing

Concrete is frequently used in structural applications in nuclear waste repositories where it is not in direct contact with waste, for example to stabilise trench walls or, in deeper repositories, to stabilise shafts and drifts and form roadways, etc., and eventually, in final closure, to form plugs and anti-intrusion barriers. These emplacements are structural in the classic engineering sense of the term and, where structural applications are paramount, relevant national specifications and normal civil engineering codes of practice should apply as an integral part of the design and construction brief. If deviations from these codes occur, justification needs to be given. Regulatory and public confidence is improved if relevant standard tests and test methods can be applied to verify performance, together with independent verification that compliance has been achieved in the course of construction and formation, etc.

However, there are a great many uses of cement and concrete which are either non-standard or have at most a limited structural function. These may not be catered for by existing specifications and codes. For example, the barrier function of cements to contain and isolate nuclear wastes, together with verification of present and future performance, is not explicitly defined in existing civil engineering specifications: historically no justification existed that was sufficient to require a specification. Thus there is a clear gap in guidance for cement specification and use.

The nuclear industry has made a number of tentative approaches to developing its own standards, for example those of the Materials Characterization Center [8]. However, while these specifications appear to work well for ceramic and glass waste forms, they are arguably less appropriate to cements, the reasons being (1) the high chemical reactivity of cements which alters fundamentally the composition of the leachant solution, and (2) the difficulty of determining performance in the presence of specific aggressive agents. As an example of the latter, it is well known from experience that sulfate and chloride dissolved in ground water are damaging, chloride mainly because it depassivates embedded steel. The ingress of sulfate and chloride is often slow and damage may not be apparent for years. So how can attack be simulated and, at the same time, accelerated? One method – often used for sulfate attack – is to use concentrated sodium sulfate as the attacking medium. However, a threshold in attack mechanism occurs at about 1 to 2 g/l sulfate concentration: above this limit, gypsum (calcium sulfate dihydrate) appears as a product of attack while at lower sulfate concentrations the attack product is mainly ettringite, a hydrated calcium sulfoaluminate. Increasing sulfate concentration speeds attack but alters the mechanism: it is not possible realistically to extrapolate data obtained at high concentrations to lower concentrations. Damage conditions can be thought of as a series of fences dividing different mechanistic regions; all too often, the fences are invisible in the first instance.

In the case of chloride, attempts have been made to approach chloride ingress as a diffusion process with application of Fick's laws. The approach seems sound but in fact many factors, including differences in ionic potential between cement pore fluid and its service environment, drive diffusion, so what is measured is not a true diffusion constant but a conditional constant: its evolution with time is not well established.

In recent years it has also become fashionable to speed chloride diffusion using electrochemical assistance. In one form of the test, concrete is cast in the form of a cylinder with a central electrode. Using a chloride electrolyte, a DC voltage is superimposed across the cylinder such that the central electrode is anodic and the passage of current monitored. The method accelerates penetration but a number of pitfalls exist: for example, using relatively high voltages risks formation of free hydrogen and chlorine.

Therefore more work needs to be done to isolate generic features of cement performance and seek a consensus on ways to evaluate future performance, preferably with a significant degree of acceleration. To achieve regulatory approval it is important to provide appropriate models and experimental techniques appropriate to evaluate at least key performance parameters, and preferably to find ways of (1) achieving a measure of acceleration in the course of testing, (2) permit generic information to be derived, and (3) give results which can be extrapolated into the future together with fundamental justification.

We are also a long way from achieving quantification of matrix formulation. Several case studies are presented to show the present situation.

Case 1: Differences in matrix properties arising from use of supplementary materials e.g., slag

Part of the variability in cement systems arises from the use of supplementary cementing materials at high replacement levels for Portland cement. These supplementary materials, as noted, vary widely in composition, granulometry, particle morphology and performance. For the most part, they are formally wastes deriving from other processes where control of their composition is a secondary goal: priority is given to ensuring quality of the primary product, in this instance, iron. While the engineering community imposes specifications on slag used for cement, many of the properties of special interest to nuclear waste disposal are not necessarily specified. For example, iron blast furnace slag is mainly glassy but the glass contains a significant fraction of oxide ions replaced by sulfide ions. When the resulting slag reacts with cement and water, sulfide ions are released; the released sulfide reacts with sulfate, furnished by the cement, forming species such as thiosulfate. The resulting complex sulfur chemistry leads to the development of chemically reducing conditions within cement matrices [6]. However, while specifications may fix a maximum sulfur content, usually not exceeding ~1% S, they do not usually fix a minimum, so the ability of slag to condition the oxidation–reduction potential of the cement matrix may vary greatly from one slag to another. Standard methods of determining the impact of slag on redox potential and its overall poising capacity are needed.

Case 2: Variability of fly ash

Coal combustion fly ash is also a very variable by-product. The ash composition reflects the mineral content of the coal, and the content of CaO (often present as mixtures of free lime and $CaCO_3$ in high-lime ashes) is particularly variable, depending on provenance. Thus large variations in fly ash composition and mineralogy are encountered worldwide. The low-lime ashes are characteristically rich in silica, alumina and iron oxide and have a high glass content, whereas the lime-rich ashes are more crystalline, with little or no glass, and may even contain some of the same crystalline minerals found in clinkers, e.g. dicalcium silicate, calcium aluminates, free lime and ferrite. Indeed, some lime-rich ashes are weakly cementitious when mixed with water and can be used for low-strength construction.

A potential concern about the lime-poor ashes is that, by reacting with calcium hydroxide furnished by cement activator, the ash will lower the internal pH. This process is described in more detail in subsequent sections, but the conclusions for nuclear waste are that (1) supplementary cementing materials have potential advantages in cemented waste matrices, such as control over thermally-induced cracking, but (2) specifications imposed by civil engineers, based on presently available data, may not provide sufficient information to predict long-term performance. Certainly blended cements should not be specified for use on the basis of improvement in short-term properties without also considering longer-term impacts. *But an agreed procedure is needed to calculate the long-term impact of fly ash on the pH conditioning ability of cement solids.*

4.10 Organic materials added to Portland cement

Various special chemicals may be added to improve the properties of cement. Foremost amongst these are 'plasticisers'. These are high molecular weight substances, either soluble or dispersible in water, and are added to improve the flow and space-filling properties of fluid grouts and concretes, etc., without the need to increase the w/c ratio. When cement admixtures were first developed, they were based on waste materials such as sulfoligns from paper making. However, as the molecular basis of the plasticising action has become clearer, and as the industry has become convinced of their usefulness, molecules have increasingly been tailored for specific purposes. As a result, we have a wide range of organics commercially available for use as superplasticisers: a summary is presented in Table 4.8.

It should be noted that most commercial superplasticiser (SP) formulations contain a complex mixture of molecular species and molecular weights. Thus it is not usually possible to do more than specify the type of functional groups. Their plasticising action arises from the presence of a functional ionic group and it is possible that this is removed by hydrolysis, resulting in insolubilisation of the residue. The concern of the nuclear industry is that the plasticiser, or its degradation products, or both, may be soluble and act as complexants for radwaste species.

Such concerns need to be taken seriously but set into context. Firstly, while cements are regarded as 'inorganic' they are not totally free from organics. These organics derive from various sources: from organics present in natural gypsum or added to the grinding mill, as so-called 'grinding aids', for example commercial grades of triethanolamine. Fly ash used as a supplementary cementing material may contain several percent partially graphitised carbon as well as pyrolysis products deriving from the precursor coal. Cumulatively, the total organic content of commercial cements from all these sources is low but nevertheless perceptible. The potentially harmful consequences of using superplasticisers thus have to be set against an

Table 4.8 Superplasticisers used in Portland cement formulations

Functional chemical group	Comments
Lignosulfonate	'First generation', known since about 1940. By-product of paper industry
Sulfonates	Melamine or naphthalene condensates
Sulfonates	Condensates with formaldehyde
Polycarboxylates	More effective than first-generation materials
Polyacrylates	More effective than first-generation materials
Polyphosphonates	Relatively new to the market; not much data

appropriate background, of the organics already present being supplemented, so the relatively low dose rate of SPs used, typically not more than 1% by weight of cement, adds to an already complex background. But the present position seems to be that concerns about the addition of organics, while easily raised, are not easily dispelled.

Amongst other materials added to cement, steel is of special concern. Steel reinforcements are commonly used in composite construction: essentially, concrete carries the compressive load while steel copes with tensile loads. Waste containers and packages often rely on steel, e.g. with waste emplaced in steel drums. The high pH of Portland cement creates a passivating environment for mild steel and a range of ferrous alloys, so that in the absence of oxygen, corrosion rates are generally low, on the order of $0.1–1.0 \times 10^{-3}$ mm/year. Under conditions of passivation, iron and steel corrosion proceeds, albeit very slowly, with discharge of hydrogen from water as iron is oxidised [9]. Historical analogues, admittedly based on pure (wrought) iron rather than modern low-carbon mild steel, support this picture of passivation and of slow but ongoing corrosion from experience of several centuries.

However, loss of high pH brings a change in regime with the onset of more rapid corrosion: we treat this problem in more detail subsequently. The boundary between active corrosion and passivation is often fixed at about pH 11 but the transition between regimes of passivation and active corrosion is also affected by impurities, the single most important of which is chloride. Chloride raises the pH threshold necessary to achieve passivation and is thus an undesirable constituent. If the performance assessment depends significantly on steel lifetimes, the presence of chloride needs to be taken into account to develop a realistic corrosion scenario.

4.11 Service environments and lessons from historic concrete

The range of natural conditions being proposed for nuclear waste disposal is highly variable. Cements and concretes in nuclear waste applications are typically associated with underground disposal, either shallow or deep, but it should be recalled that interim storage facilities may be located in whole or in part above ground and that some plant closures may involve construction of above-ground facilities.

The couplings between waste constructions and natural environments are such that technology transfer from civil engineering is possible. In considering this transfer and its limits, it may be noted that (1) until very recently, civil engineers relied heavily on practical experience for design and formulation of durable concrete, (2) owing to changing practices, changing cement compositions, etc., ‘historic cement’ may not be the same as that currently being supplied into the market, and (3) formulations used in civil engineering are strongly influenced by initial cost, perhaps unduly so. Consequently, while we should not ignore historic constructions or empirical experience, we should take care that transfer is subject to critical assessment. For example, the Pantheon is often cited as an example proving the durability of concrete construction. Its free-standing concrete dome, spanning ~42 m, is now about 1800 years old, and is still freely accessible to visitors to Rome. Its dome is built of lime-activated pozzolanic volcanic ash concrete. The density of the concrete-making aggregate is also graded to reduce the concrete density progressively towards the top of the dome. Without detracting from the achievement of its construction and longevity, I also note that Rome has many other failed concrete structures of about the same period and we are unsure why the Pantheon almost alone survives intact. The historic relevance is also limited by the fact that the concrete is above ground, where an entirely different regime of degradation arises compared to structures below ground. Moreover, we are unlikely again to use the same concrete formulations as the Romans: contemporary records suggest that the concrete required physical support for up to 2 years, on account of its slow strength development.

Nevertheless, we have much empirical experience of concrete degradation in the below-ground environment and in wet environments. Table 4.9 lists some of the commonly encountered environments and conditions which are aggressive to concrete or adversely affect performance. Some of

Table 4.9 Cement performance in the service environment

Factor	Origin and impacts
Thermal stresses	Service temperature and thermal gradients lead to stress and diffusion. Possible freeze–thaw damage
Moisture regime	Changes in moisture regime may occur, possibly coupled to thermal regime. Drying shrinkage, partly reversible upon rewetting. In wet regimes, flow may be 'flow past' or 'flow through', or mixed. Soluble salts may migrate and concentrate in zones of evaporation
Geochemical regime	Groundwaters may contain aggressive chemicals. These may also be liberated from the inactive waste inventory
Gas evolution and radiolysis	See Table 4.10
Disturbance and intrusion	Seismic hazard. Physical toughness of cements intended as anti-intrusion barriers. Fire hazard with spalling and damage
Accident	Fires furnish a threat to underground concrete construction

these hazards are well known to engineers: an example already discussed is the relatively poor resistance of Portland cements to sulfate-containing waters. Others are relatively novel, e.g. radiolysis, and only limited technology transfer is possible.

Civil engineers have recently taken a more positive interest in quantitative modelling of concrete durability [10] and of the underlying transport properties [11]. However, an enormous leap in the quality of our knowledge base is required to develop models embracing chemistry, kinetics and mechanics. Both physical and chemical modes of deterioration have to be included, as well as equilibrium and non-equilibrium aspects. Nevertheless, and despite the relatively low investment thus far made in modelling, significant progress has been made and we return to modelling subsequently. It is important to promote such developments because only modelling allows the time factor to be compressed without unrealistically and artificially increasing the intensity of chemical, mechanical and/or thermal stresses applied – with largely unknown consequences – in the course of accelerated testing. Of course, predictions made by modelling have to be subject to a verification process, and we discuss this later.

Nevertheless, concretes in nuclear applications may also be exposed to stresses not encountered in conventional civil engineering. Table 4.10 lists some of the more exotic factors which are a challenge to the nuclear engineer. Fortunately, most exposures will be impacted by only a limited combination of these factors.

Each identified hazard requires appropriate responses. For example, temperature excursions resulting from waste packages may have to be limited

Table 4.10 Stresses on cement unique to radioactive waste immobilisation

Nature of stress	Comments
Ionising radiation	Set of fresh cement is adversely affected by high radiation fluxes. All cement, fresh or set, is subject to radiolysis of water at a rate comparable to pure water. However, the oxygen liberated may be stored in cement, probably as peroxide species and with unknown impact on internal redox potential, and hydrogen overpressure may be of concern
Heat, thermal excursions	Temporary excursion may arise from liberation of heat of hydration of cement substances. A more prolonged thermal pulse may arise from heat-generating waste or in accident scenarios, such as fires
Reactive metals	Evolution of hydrogen from electropositive metals, with potential for overpressure in sealed systems. Swelling pressure generated from solid corrosion products

by controlling the density of the distribution of heat-generating waste in the repository. Other factors, such as the potential for storage of both hydrogen and oxygen in cement substances, have not been integrated sufficiently well and integrated with the general post-closure redox potential and the corrosion scenario to permit quantitative evaluation.

Several national programmes have made the decision that, because of the difficulty of experimental verification of cement performance above 100°C, as well as the paucity of thermodynamic data and speciation at elevated temperature, repositories have to be designed so that temperatures will not exceed this limit. We deal subsequently with the impact of prolonged high temperature on cement properties. Alternatively, if high temperatures are unavoidable, cements may have to be specially designed for the particular service. Gas overpressures may require vented systems and/or 'headroom' for gas accumulation. For example, NIREX (UK) have formulated a high-porosity grout containing *ca.* 40% pores, capable of giving high pH conditioning while remaining permeable to permit gas migration and thus avoid local gas pressure build-up. A high content of $Ca(OH)_2$ ensures high porosity while at the same time giving a large reserve of reliable pH conditioning solid. A holistic approach to all the options is required, including applicability to the geochemistry of a particular site and water inventory.

4.12 Non-Portland cement

Table 4.11 lists some other types of inorganic cement, ranked according to decreasing internal pH. Not all these cements are commercially available, but they could readily be formulated from commercially available reactants.

'Geopolymer' cements have no exact definition but include a class of materials made by mixing (1) a reactive source of alumina and silica, such as fly ash or metakaolin, with (2) an activator such as a concentrated aqueous solution of sodium or potassium hydroxide and silicate. The solid matrix consists of a hydrous aluminosilicate gel which binds much of the added alkali. However if these cements are warm-cured at temperatures above 40–60°C, the gel crystallises at least in part: various zeolites and framework structures such as sodalite and zeolite P, etc., have been reported to form. Crystallisation generally leads to reduced strength. It would appear that the setting reactions are strongly exothermic. Virtually nothing is known about the long-term performance of these materials. It has been claimed that the Egyptian pyramids of antiquity are constructed of geopolymer [12]. These claims might be used to support their durability but are insufficiently validated.

The need to use caustic (Na,K)OH as an activator for geopolymers presents distinct safety issues in handling. Apparently alkali is well bound

Table 4.11 Special cements

pH function	Type	Availability	Comments
Very high, >13	‘Geopolymers’	Not commercial	Difficult to handle, caustic. Little known about long-term properties
Moderate, 11–12	High alumina (HAC or CAC); calcium sulfoaluminate	Commercial	Long history of use (CAC). Become porous if set normally but used at elevated temperature. High heat of hydration and fast strength gain
Moderate, 11–12	Fluoroaluminate, $Ca_{12}Al_{14}O_{33}F_2$	Available from specialist suppliers	Extremely rapid strength gain. Compatible with either PC or CAC cements
Slightly alkaline	MgO-based cements	Sub-commercial	Has been used as special backfill, as at Carlsbad NM, USA
Neutral to acidic types	Phosphate, oxyhalide and oxysulfates	Sub-commercial/ available in small quantities	Corrosive to steel (oxyhalides), somewhat soluble (sulfate and halide types). Phosphates expensive but have potential

in these materials, but ‘well bound’ cannot at present be quantified. Moreover, the internal environment has a very high pH, often ≥14, during the initial formation and setting. Given our relatively poor knowledge of the speciation of radwaste components, uncertainties in redox conditions and the potential for adverse impacts on other construction materials, these matrices do not seem to have sufficient potential to justify their use. Modelling species behaviour at extreme pH also introduces uncertainties owing to the difficulty of making reliable activity corrections at extremes of the pH scale.

Two types of alkaline cement, calcium aluminate (shorthand CAC, or HAC) cement and ‘sulfoaluminate’ (shorthand C$A), cement, are well known, the sulfoaluminate cement having been made commercially in China since about 1975. Both these cement types are made by pyroprocessing: calcium sulfoaluminate in a rotary kiln, like Portland cement, and CAC cement either by sintering or by fusion to a melt, followed by rapid solidification with partial crystallisation of the melt.

Commercial C$A cement sets very rapidly and requires a retarder to ensure an adequate period of workability, whereas CAC does not normally require set control admixtures. Both cement types normally shrink slightly upon hardening, but it is reported that shrinkage compensation is readily and consistently achieved with C$A cements by controlled additions of calcium sulfate, although zero dimensional change or slight but controlled expansion has not been consistently achieved. Both these cement types gain strength more rapidly than Portland cement but, conversely, they liberate their high heat of hydration in a relatively short time. Like Portland cement, both cement types are compatible with mineral aggregates and so can be used to form grout, mortar and concrete. Both are hydraulic and can be used in wet situations without impairing normal set and strength gain.

The consequences of high set temperatures to loss of strength are, however, severe in both C$A and CAC materials. Consequently, the thermal pulse during hardening needs careful management and long-term service temperatures need to be low. CAC is particularly sensitive to long-term service in warm humid environments: it undergoes a slow phase transformation, resulting in strength reduction and enhanced porosity. The critical upper limit may be as low as 8°C. CAC is, however, often used in sewer linings as it is more resistant to dilute sulfuric acid than an equivalent Portland cement. The slightly lower internal pH (about one unit) of both types of aluminate cements relative to Portland cement is still sufficiently high to give adequate corrosion protection to embedded steel yet low enough greatly to reduce problems arising from adverse reaction with mineral aggregates. Fluoro-aluminate cements, based on the crystalline phase $C_{12}A_7 \cdot CaF_2$, have been marketed as repair materials. The fluoroaluminate is supplied as a dry powder; after mixing with water, a short period of workability is obtained. Once set occurs, strength gain follows very rapidly; the process is strongly exothermic. However, and like C$A and CAC types, it bonds strongly to Portland cement.

MgO, magnesium oxide, has also been used as cement. Commercially, MgO is derived from thermal decomposition of natural magnesite, $MgCO_3$, at about 500–600°C; heating at higher temperatures lowers the subsequent reactivity of the MgO product with water. Limited experience with the semi-commercial MgO product suggests that it can be formed and handled like Portland cement. The precursor, fine-grained MgO, hydrates in water or moist air, initially with formation of brucite, $Mg(OH)_2$. Because brucite is much less soluble than $Ca(OH)_2$, its pH conditioning ability is low and limited to slightly above pH 9 at 25°C. Upon subsequent exposure to air or moist carbon dioxide, brucite will carbonate to yield a series of basic salts, e.g. magnesium hydroxycarbonates such as hydromagnesite, apparently without loss of strength and coherence. The internal pH of these cements, while on the alkaline side of neutral, is probably insufficient to protect embedded steel against corrosion. Nevertheless, if a low alkalinity cement is required, magnesium oxide is a contender. It has been used as a sacrificial backfill material in the saline repository at Carlsbad NM with the aim of elevating pH in the vicinity of the waste while at the same time having low dissolution rates, and hence long performance life in brine.

Table 4.11 also lists the composition of several 'acidic' cements based on phosphates. The acidity (or basicity) of a calcium phosphate depends on its Ca/P ratio, the end-member acidity being achieved by phosphoric acid, H_3PO_4. Reaction of phosphoric acid, or of an acid phosphate with high P/Ca ratio, with a basic substance, such as $Ca(OH)_2$ or a calcium-rich phosphate salt, initiates the cementing reaction. A large number of calcium phosphates and phosphate hydrates exist and many of their reactions are cementitious, thus permitting a choice of Ca/P ratio and reactants. The final product may be acidic, neutral or basic, depending on its Ca/P ratio and completeness of reaction, with basicity generally increasing with an increase in the Ca/P ratio. Although commercial experience of their use is limited, one interesting and potentially useful phosphate host is hydroxyapatite, $Ca_3(PO_4)_3(OH)$. In nature, the apatite structure is very durable. The structure is also very flexible with respect to substituent ions, often containing trivalent lanthanides substituted for Ca, so, by analogy, trivalent actinides are also potential substituents. Apatite comprises the mineral substance of bones and teeth and typically has low solubility combined with excellent stability in natural environments.

Oxysulfate and oxychloride cements are readily formed and have more than a century of use. For example, Sorel's cement, consisting of magnesium oxychloride hydrates, is made by mixing reactive MgO powder with a saturated solution of magnesium chloride: the fluid mass sets and hardens with formation of an interlocking matrix of magnesium hydroxyhalide hydrate crystals. The white colour and fine grain size of this cement have led to its historic use as an interior flooring plaster or replacing gypsum plaster in the casting of crisp decorative features in relief, etc. In general, the acidic cements, especially oxychloride and oxysulfate cements, are somewhat too soluble for performance in wet environments and are also corrosive to steel and, on that account, are unlikely contenders for immobilisation matrices.

4.13 Immobilisation mechanisms

Cements make both physical and chemical contributions to immobilisation. Amongst the various matrices used for radioactive wastes, the *chemical* contribution exhibited by cements is unique and we are as yet some way from having a complete quantitative understanding of the various mechanisms involved. The chemical action of cements has only been characterised in recent years but valuable data on the specific species–waste interactions have also been contributed from studies of toxic and hazardous wastes. The physical mechanisms of immobilisation include surface sorption. In particular, the binding phase of Portland cement, a calcium silicate hydrate gel-like phase, shorthand C-S-H, has a high specific surface, perhaps 50–200 m^2/g for water vapour, and a known tendency to sorb both cations and anions, e.g. Cs and sulfate.

The chemical immobilisation potential of cement for inorganic species ranges widely, from very weak to very strong. For example, cement has weak potential for monovalent cations such as Cs but rather stronger potential for multivalent cations and a very variable potential for anionic speciations. Moreover, the high pH imposed by cement on the internal environment helps control both oxidation state and speciation. Speciation has generally been less well studied in alkaline solutions than in acid solutions, one reason being the lower solubilities often encountered at high pH. Each element, and for some elements each oxidation state and speciation, may have to be studied. A review summarises the available knowledge of sorption processes, which are of special importance to immobilisation in the concentration range below the precipitation threshold [13].

Table 4.12 serves as an introduction to the nature of retention mechanisms in cement systems, with selected examples. Owing to the abundance in cement of C-S-H, with its non-crystalline and nanoporous structure, considerable, but non-specific, sorption potential exists. The effective surface area of C-S-H is difficult to determine as measurements give different

Table 4.12 Reactions between Portland cement and radwaste species

Binding mechanism	Characteristic features and comments
Sorption	Characteristically encountered at low species concentration but with low capacity. High surface area C-S-H is the main source of sorption for Cs
Structural substitution (radwaste substitution competitive for sites)	Crystalline components of cement offer potential anion and cation sites for uptake of radioactive species, e.g. Cl in AFm, Ni in hydrotalcite-like phase, etc.
Characteristic phase formation (radwaste species essential)	Ca-U-OH phase X for U and $CaSn(OH)_6$ for tin
Oxy/hydroxyl precipitates	Often metastable and short-lived, e.g. $Cr(OH)_3$. Difficult to identify on account of low crystallinity
Mixed mechanisms	Combinations of the above, often concentration-dependent

results depending on technique and, for studies made by gas sorption (the BET method), the nature of the sorbate (with or without dipole moment). For dipolar sorbates such as water vapour, C-S-H surface areas of up to 750 m^2/g have been reported.

The nanostructure of C-S-H is, as previously noted, believed to consist of small platelets of gel, perhaps 10–20 nm in maximum dimension, adhering strongly to each other. Figure 4.4 shows a schematic view. The arrangement of platelets appears to afford a variety of sites suitable for sorption of both cations and anions (and possibly neutral speciations). Under these circumstances the nature of 'surface' and its distinction from bulk becomes problematic; the uptake process is often described as 'sorption' but without the intention of being mechanism specific. However, C-S-H particles suspended in solution also have net surface change, as indicated by their zeta potential. For high Ca/Si ratios, as occur in plain cement, the zeta potential is positive, i.e., C-S-H preferentially attracts anions. However, as the Ca/Si ratio decreases, the zeta potential decreases, passing through zero and eventually becoming negative at low Ca/Si ratios <1.0. The zeta potential may well represent the 'surface' contribution of sorption but if so, bulk effects must also operate because it is established beyond doubt that C-S-H will uptake both cations and anions, the arithmetic sign of the zeta potential notwithstanding. It should also be noted that sorption of radionuclides measured on commercial cements and cement substances (and possibly on some laboratory preparations) are of necessity measured on 'dirty' systems where impurities, cationic as well as anionic, compete for available sorption sites. For example, commercial cements furnish an abundant supply of anions – hydroxide, sulfate, carbonate, aluminate and silicate – all of which can compete for anion sites.

The crystalline phases of cement exhibit a range of structures. Broadly, these are of two types: layer-lattice structures and columnar structures. Portlandite and AFm phases have a layer-lattice type of structure shown in Fig. 4.8. $Ca(OH)_2$ is the prototype; it is formed of layers of Ca ions bonded top and bottom to two sheets of hydroxyl ions. Each Ca is connected to six OH, and each OH is in turn connected to three calcium ions. As a result, individual layers have the net composition $Ca(OH)_2$ and are electrically neutral. Thus layers are held to each other by van der Waals forces. The rather short van der Waals layer spacing makes it energetically difficult to introduce substituents between layers and the residual surface forces are also weak. Consequently, portlandite does not exhibit significant sorptive power for radionuclides; its role is to buffer high pH and supply hydroxide groups necessary to promote other mechanisms of immobilisation.

AFm has a structure derivative from that of portlandite. In AFm, one in three calcium atoms are replaced by a trivalent ion, normally Al but with minor Fe(III). This substitution of a divalent by a trivalent charge

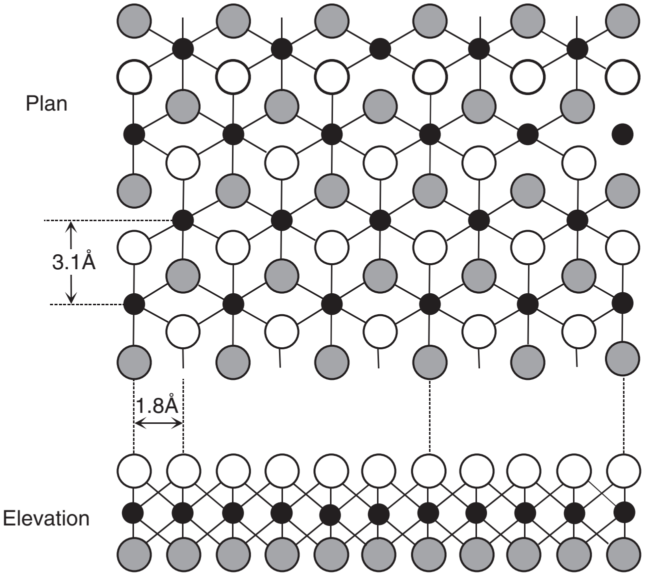

4.8 Crystal structure of $Ca(OH)_2$ in two orientations. Dark circles are Ca atoms, open and lightly shaded atoms are oxygen.

unbalances the layer charge. In theory, this unbalance could be compensated by introducing vacancies, but in practice, anions are substituted in the interlayer space which, as a consequence, expands the layer spacing relative to portlandite. To complete occupancy of the additional interlayer space thus created, water molecules are also incorporated. This structure, designated 'AFm', participates readily in ion exchanges partly on account of the enhanced layer spacing. In normal cement, the anions found in interlayer space are hydroxide, sulfate and carbonate, but in many saline environments chloride also competes for exchangeable anion sites. Additional anionic species present in the waste have to compete for these sites: some, such as MoO_4^{-2} (molybdate), are strongly incorporated. On the other hand, the di- and trivalent cations in the main layer can also be substituted, e.g. by Cr(III) for (Al,Fe). We have little quantitative data either on the partition functions for trace species in AFm or on reaction kinetics, although it is likely that interlayer sites exhibit rapid exchange while substitutions involving the main layers are kinetically slow.

The last of the main phases, AFt, or ettringite, has a structure built of columns constructed of alternating calcium and aluminium polyhedra, both in octahedral coordination to water, crosslinked by additional water and, for charge balance, sulfate ions. The sulfate ions compete with carbonate in cements, but in nature the occurrence of borate ettringite also points to possible borate substitution in intra-columnar sites. Additional possibilities arise because Al can also be substituted by silica, while at the same time additional carbonate is accommodated in channel sites, giving rise to thaumasite, a mineral essentially isostructural with ettringite but, unusually, accommodating Si in hexacoordinate (octahedral) positions.

From the range of substitutions observed in nature, as well as in commercial cements, numerous possibilities must exist for ionic substitution of radionuclides in the several mineral phases of cement. If blended cements are also included, the mineral suite is affected, giving additional possibilities of 'tailoring' cements selectively to bind specific radionuclides or groups of nuclides.

However, two additional binding mechanisms may operate, both involving precipitation of the radionuclide. Firstly, an oxide or hydroxide of the cation may precipitate. Examples include zirconium, Hf and Th, which precipitate in the alkaline cement environment as amorphous hydroxides of indefinite composition. Amorphous precipitates are probably unstable in the thermodynamic sense but if so, crystalline products have not been reported. However, precipitation may also involve reaction with one or more of the constituents of cement, and the eventual fate of the amorphous precipitates may simply be to persist until they can react further with cement phases. For example, Sn(IV), like Zr, is readily precipitated at high pH, as its hydrous oxide. But under oxidising conditions and within a few weeks or months at 25°C, the initially formed tin-containing precipitate reacts with calcium, furnished by the cement substance, forming crystalline $CaSn(OH)_6$. Cr(III) is another example: it readily precipitates in the high pH pore fluid as $Cr(OH)_3 \cdot nH_2O$. But in the longer term, it is likely that Cr(III) substitutes for Al in the AFm, and possibly in AFt, while Cr(VI) partially substitutes for sulfate in AFt. Thus initially-formed precipitates may be metastable and a complete account of the speciation may be time-dependent. Experimenters may determine that species solubility is time-dependent but it is not usually possible to infer specific mechanisms or precipitate forms from this dependence.

The precipitation of chemically complex phases, not normally found in cement, is often at variance with predictions made using meagre databases. For example, it is virtually certain that the solubility of Sn as crystalline $CaSn(OH)_6$ is less than that of the hydrous oxide by at least an order of magnitude. But data for $CaSn(OH)_6$ do not seem to have been incorporated in databases until recently, with the result that predictions of species solubility are often based on those solids for which data are available. It could be argued correctly that this approach, which tends to overestimate solubility, is conservative. Unfortunately it also obscures the true boundary between sorption, which presumably continues to operate below the solubility threshold, and precipitation, with resulting distortion of the contribution of

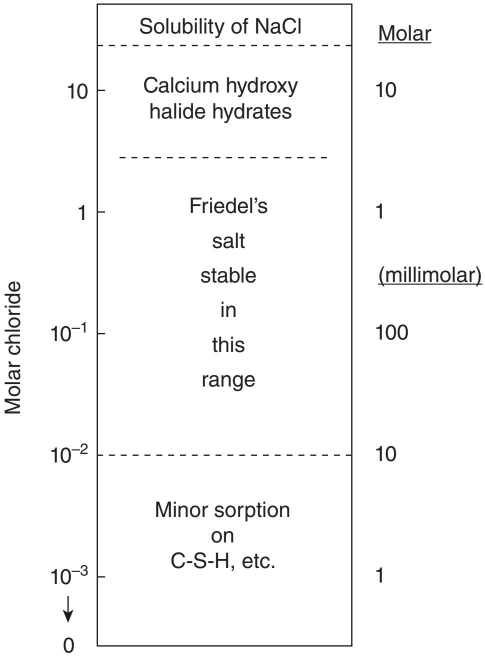

4.9 Binding mechanism for chloride in the cement environment as a function of chloride concentration.

sorption to immobilisation and incorrect application of the Kd (or Rd)* concept, which is meant to apply to sorption.

As noted, the nature of the binding mechanism is often concentration dependent. Figure 4.9 shows an example for chloride. The diagram is constructed for pH about 12.5 and for 25°C. To embrace the wide range of relevant concentrations, these are shown on a log scale. At very low concentrations, typical of fresh cement mixed with potable water, the main mechanism for removal of chloride is the weak potential of C-S-H to sorb chloride in the presence of high concentrations of competing ions, mainly OH. However, at higher loadings, above a few millimolar, chloride increasingly substitutes in the AFm phase of cements with formation of Friedel's salt, the chloride-substituted AFm [14].

Friedel's salt is stable over several orders of magnitude concentration change but eventually, above about 5 molar, it reacts with calcium salts in alkaline conditions with formation of calcium hydroxyhalides. A complete

---

*Kd and Rd refer to the distribution ratio of the concentrations achieved in solid and coexisting aqueous phases. Where data are obtained reversibly, as in a sorption/desorption cycle, the numerical ratio is Kd but where data are determined in one direction only, Rd; only the former is presumed to be an equilibrium value.

overview at low concentrations is presented in [15]. The position of boundaries in Fig. 4.9 is approximate: what is important is that (1) the binding mechanism is concentration dependent, and (2) the binding capacity is dependent on mechanism, with the sorptive contribution being typically less than contributions that involve the bulk, such as ion exchanges and phase transformation.

In an ideal world, diagrams of this type, or data sufficient for their calculation, would be available for every element/species of significance. But this is not so and, in the absence of data, many assessments of repository performance use a single distribution coefficient for each species, combined with a 'snapshot' approach to depict the impact of time. For example, a set of distribution coefficients showing the distribution of each radwaste species between solid and aqueous phases is taken at different stages of cement degradation.

4.14 Deterioration processes affecting Portland cement: processes and features

As noted, cements are almost invariably metastably in their disposal environment and will therefore react with their service environment, possibly undergoing deterioration. Many books on the subject adopt a largely empirical approach but cement science is moving towards a more quantitative approach [16].

It is convenient to mark the progress of cement deterioration by dividing the overall process into four stages, as shown in Fig. 4.10.

Commercial Portland cements contain on the order of 1.0 wt% total sodium and potassium oxides. These are relatively soluble: some binding of

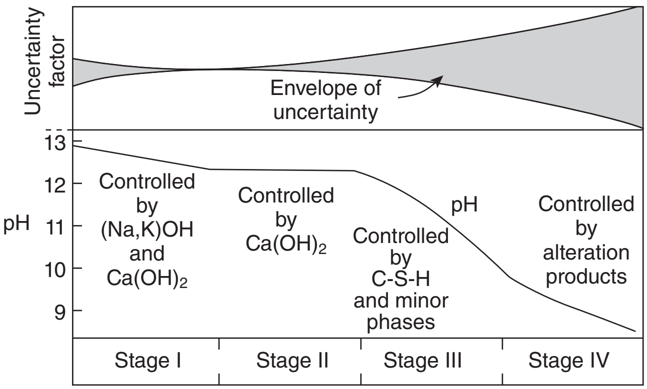

4.10 Evolution of cements in disposal environments and associated uncertainties.

alkalis occurs in the solid phases but the normal cement solids are relatively ineffective at binding alakli, with the result that sodium and potassium are prominent components of the cement pore fluid. The relative insolubility of anions other than hydroxide means that as a good approximation, sodium and potassium are present as their hydroxides. As long as their concentration in pore fluid exceeds about 0.05 M, the alkalis will condition an internal pH higher than would be expected from portlandite, $Ca(OH)_2$, alone. At 25°C, the threshold pH conditioned by portlandite is about 12.5 but the pore fluid pH of commercial Portland cements often exceeds this value. This period, during which pH is dominated by alkali hydroxides and their coexistence with portlandite, is termed stage 1. The pH in this region is variable because cements differ in alkali and water contents, so the available alkali is extracted into different masses of water, depending on formulation and the extent of hydration. Moreover, there are no solubility-limiting phases in the relevant concentration range to limit alkali dissolution, although many national specifications place an upper limit to sodium and potassium contents of clinker. But because stage I is difficult to define precisely, the uncertainty envelope (Fig. 4.10, top panel) is broadened to reflect this inherent variability.

However, alkalis are not well-bound into cement and, as a consequence, are readily lost by leaching. The progress of leaching from monoliths is normally very uneven: the outer layers may have lost all, or nearly all, their alkali while inner portions are still contributing a flux of alkalis diffusing towards surfaces undergoing leaching. Thus the initial stage of leaching tends to give rise to a Fickian concentration profile for (Na,K). Therefore the lifetime of pH conditioning by alkali for monoliths, assuming that cracking is not significant, depends largely on geometry and the physical quality of the matrix. Nevertheless, considering time-scales for immobilisation, there is general agreement that much of the leachable alkali will be lost early in the history of the cement. However, during this period, while active leaching by alkali is occurring, the solubility of portlandite is greatly suppressed. This can be explained by the impact of the common ion effect on solubility products. Portlandite dissolves with formation of calcium and hydroxide ions:

$$Ca(OH)_2 = Ca^{2+} + 2OH^-$$

The solubility can be expressed in more general terms by a solubility product constant, K_{sp}, where square brackets indicate species concentrations:

$$K_{sp} = [Ca]\ [OH]^2$$

To maintain the solubility product in the presence of alkali hydroxides, the equilibrium calcium concentration has to reduce. From the form of the equation, even low concentrations of alkali hydroxides have a very significant impact on reducing calcium solubility and hence leach rates. Thus not only is calcium largely immobilised during stage I but leaching is also much reduced relative to predictions made using an alkali-free model. But because the time dependence of the common ion (hydroxide) effect is difficult to evaluate in monoliths, considerable uncertainty is attached to the duration of this stage.

The transition between stages I and II is gradual. But stage II is chemically the most simple to evaluate and is marked by a constant solid phase assemblage consisting of portlandite, calcium-saturated C-S-H, AFm and AFt phases. As long as portlandite persists, the pH and composition of the pore fluid – the source of leachate – is constant throughout the stage and can be well quantified. This state is also quite robust. A hydrated Portland cement contains about 20–25% portlandite and thus a considerable reservoir of solid mass capable of conditioning pH is present. Note that the pH does not depend on the amount of portlandite, only on its presence. This state is well characterised by decades of study and, although many of these studies focus on non-nuclear areas, the data and conclusions are potentially transferable – for example, data on the performance of natural analogues.

As degradation proceeds with loss of portlandite, the most important phase controlling pH is C-S-H. Since C-S-H has a variable composition, its pH conditioning ability varies, from high at Ca/Si ratios ~1.5 and above, to moderate ($\mathrm{pH} = 10.5$) at Ca/Si ~1.0. Because stage III has a degree of freedom, it is not possible to give a single set of characterisation parameters. Also, in real life, mass loss is typically balanced at least in part by mass gain of species such as sulfate and carbonate and, without a detailed analysis of the ground water chemistry, it is not possible to state what, if any, phases will precipitate or the balance between precipitation and dissolution. Of course precise calculations can be made for specific compositions but in a realistic repository, where the system to be calculated has a degree of openness, uncertainties tend to accumulate as reaction progresses. Thus an increasing envelope of uncertainty attaches to the nature and amount of the remaining solids, their porosity, permeability and pH-conditioning ability. These trends continue into stage IV, which is marked by the final exhaustion of the phases originally present in cement and their partial to total replacement by alteration products. The nature and amount of alteration products is of course environment-specific and hence the envelope of uncertainty continues to expand.

Mostly, therefore, we will concentrate on stage II. Its duration coincides with the effective exhaustion of the characteristic pH-conditioning ability of cements. It is also a state which will be characteristic of all Portland cements worldwide and will not be much influenced by the presence of waste or by the conditions of the local disposal environment. Finally, the kinetics of reaction and progression through stages are not intrinsic properties of cement but depend on formulation into concrete and the properties of composites, as well as the specific conditions of exposure in the service environments. However, when the initial leachant composition approaches that of pure water, numerous leaching studies have shown that for a constant geometry, calcium leaching is proportional to the square root of time.

4.15 Deterioration processes: carbonation

4.15.1 Overview

An important set of processes relevant to deterioration of Portland cement arises in the course of its reaction with carbon dioxide. Carbon dioxide, used here in the generic sense to include dissolved species such as carbonate and bicarbonate, can react with cement in three ways depending on mode of delivery and local environment: (1) as calcium carbonate incorporated into the cement, perhaps as aggregate or fine-grained supplementary cementing material, or with waste, (2) in gaseous form, perhaps from air or from the local atmosphere, by decomposition, or (3) dissolved in ground water.

Each type of reaction requires a different approach, but a general characteristic of all three classes of reaction is that the reaction is driven by an approach to thermodynamic equilibrium. Consequently, the energetics of reaction are an important aid to analysis and prediction. The approach to equilibrium is subject to controls, often externally superimposed, and mass balance has to be preserved, locally as well as globally.

Table 4.13 sums up the principal exchanges that accompany carbonation. Both internal and externally conditioned reactions are involved. The internal reactions are perhaps the simplest to envisage. When a cement is blended with finely ground limestone, itself consisting mainly of calcium carbonate, some of the calcium carbonate dissolves and reacts with other cement substances, At the low carbonate activity conditioned by the solubility of $CaCO_3$, the reaction is driven by the greater stability of the carbonate form of AFm relative to the sulfate or (sulfate, hydroxy) AFm forms. Sulfate thus displaced from AFm by carbonate substitution goes to form more AFt (ettringite) and, to conserve mass balances, calcium hydroxide diminishes. C-S-H is, however, unaffected by the reaction which, although it involves only the minor phases present, has a beneficial effect on space filling by cement solids. The physical density of ettringite is lower than that of its precursors, so the enhanced ettringite content arising from carbonate addition, other factors being equal, tends to fill space and thereby reduce porosity. However, the maximum amount of reactive calcite is low, only a few wt%.

Table 4.13 Carbonation reactions in Portland cement

Process description	Nature of exchanges in the process	Kinetic and mass transport restrictions and requirements
Reaction with CO_2 gas	Gain of CO_2. Decomposition of cement hydrates with formation of calcium carbonate, etc.	Inward migration of carbonation 'front' with time. Loss of high pH. Possible internal migration of calcium ions towards minimum of calcium solubility
Reaction of cement solids with added calcium carbonate	Reaction of solid $CaCO_3$ with formation of calcium carboaluminate hydrates. Redistribution of sulfate	As above. Ideally all reactions occur internally
Reaction of cement substance with dissolved CO_2	At one extreme, 'aggressive' CO_2 dissolves cement substance, while at the other, calcium carbonate is precipitated without much leaching	Occurs upon contact of cement with external water. Geochemistry of the water is crucial to predictions, but, since waters generally have complex chemistry, other cations and anions may also be involved

When calcite is interground with clinker, its reaction is rapid, within 1–7 days, and goes nearly to completion before the cement gains strength, with the result that any volume changes are readily accommodated: the reaction is not macroscopically expansive. If calcite is used as a coarse aggregate, two possibilities exist: either the cement used also contained calcite as a supplementary material or it did not. If it contained supplementary calcite, its potential for reaction will already have been saturated and no potential for further reaction with $CaCO_3$ aggregate will exist. If, on the other hand, the cement did not contain added calcite, a reaction with aggregate will ensue but is typically slow on account of the relatively small contact area. Reaction is masked by formation of carboaluminates at or near the interface between cement and aggregate. This slow reaction allows time for recrystallisation and the reaction is not believed to result in macroscopic expansion.

These early carbonation reactions do not of course affect C-S-H although, as noted, changes may occur to the amount of $Ca(OH)_2$ as required to conserve mass balances. As a consequence of the formation of carboaluminates, the total buffering capacity of the cement in terms of pH control is reduced, but overall the reduction is not significant for Portland cement. However, the importance of this reaction to form carboaluminate increases as the available alumina content increases, so it may have greater impact on the pH conditioning of blended compositions containing aluminous supplementary materials, such as slag and fly ash. However, no quantitative calculations appear to have been made.

4.15.2 Reaction between cement and gaseous carbon dioxide

Arguably the simplest carbonation process in chemical terms is that involving reaction between Portland cement and gaseous carbon dioxide. Phases present in cement, such as $Ca(OH)_2$, react readily with CO_2 forming $CaCO_3$ and 'water', either liquid or vapour, depending on conditions. As we will show, the physical state of water (gas, liquid) has an important role in controlling reaction kinetics, because the diffusion of gas is much more rapid than that of dissolved CO_2, which may have to diffuse along a tortuous water-filled path to reach uncarbonated cement.

The initial attack of CO_2 occurs on portlandite but once $Ca(OH)_2$ has been carbonated, carbon dioxide activities rise and C-S-H is attacked. The pH conditioning is well maintained by calcium-rich C-S-H but as the C-S-H gel phase is attacked, its Ca/Si ratio decreases and the pH conditioning ability of the matrix undergoes a corresponding reduction. The equations for reaction with C-S-H and other calcium substances in cement are similar, although several solid products are formed from C-S-H and, as a result, it is more difficult to write balanced equations for its carbonation than for $Ca(OH)_2$. For example, the C-S-H phase initially carbonates with reduction of its Ca/Si ratio, formation of water and $CaCO_3$ but once the Ca/Si ratio of C-S-H decreases to about 0.85, hydrous silica gel also forms. We return to these complex mineralogical changes subsequently. This reaction is almost invariably driven by ingress of carbonation from an external source, so it is commonplace to find mineralogically zoned structures developing at intermediate stages of reaction. This situation is depicted in Fig. 4.11, as a snapshot in time, showing carbonation commencing at a free interface and progressing inward with time. A simplistic analysis of the reaction might tend to suggest that the inward diffusion of CO_2 could be represented by Fick's law and a single diffusion coefficient applied to calculation of the kinetics of carbonation with time. However, the resistance of cement to ingress of gas is related to its permeation which, in turn, is a function of matrix quality. Differences in matrix quality – for, quite clearly, CO_2 could be expected to diffuse more rapidly through porous matrices than dense matrices – might suggest that the diffusion coefficient would be more correctly described as an *apparent* or *conditional* diffusion constant, to reflect the important kinetic role of factors which are not generic, such as matrix porosity and permeability. In fact, observations of constructional concrete often suggest that the rate of carbonation is at least approximately

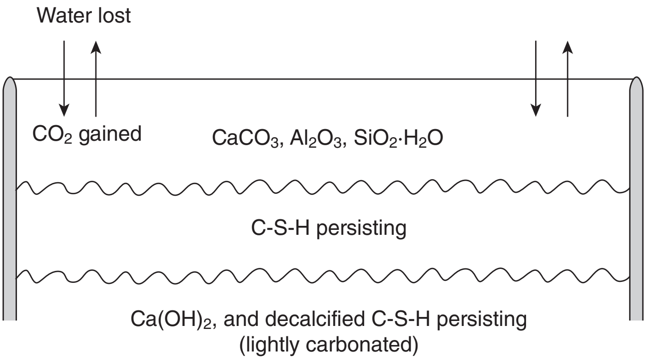

4.11 Carbonation from the vapour phase showing development of a zoned structure.

proportional to the product (α × square root of time) where α is a constant, thus supporting a Fickian interpretation. However this agreement is in part fortuitous. A condition for application of Fick's law, namely that diffusion is occurring through a homogeneous matrix, is not satisfied, as is evident, for example, from the development of mineralogical zoning shown in Fig. 4.11. The observed zoned structure arises from superimposition of the Gibbs phase rule onto a Fickian diffusion profile. At its simplest, and in order of decreasing CO_2 activity, four zones are created: (1) a near-surface zone in which all cement phases have been carbonated, composed of calcium carbonate and gel-like substances containing silica, alumina and iron oxide; (2) a zone in which portlandite is completely carbonated but in which C-S-H persists; (3) a zone in which portlandite is completely reacted and C-S-H is being decalcified, decreasing its Ca/Si ratio; and finally (not shown in Fig. 4.11) (4) a zone of unaffected cement paste.

As noted, the kinetics of carbonation are partly controlled by loss of water. Should flooding of the pore system occur in the zone where water is being actively released, reaction slows: diffusion of CO_2 through water is much slower than in the vapour phase. It is likely that flooding will only occur in well-made, low-permeability matrices, so that the rate will be controlled not only by inward diffusion of CO_2 but also by the outward diffusion of water and the water balance between liquid and vapour. Especially when considering mass transport in partially saturated concrete, it is important to remember that the water content generated locally by carbonation is dynamic. Accelerated tests are particularly susceptible to introduction of artefacts arising from water balances.

It is common to determine the depth of carbonation in cement and concrete by means of the 'phenolphthalein test'. In the test, a sample of fresh cement from a known depth, perhaps obtained by exposing fresh surface or by controlled depth drilling, is wetted with a test solution containing the

Table 4.14 Composition of cement used for carbonation calculation shown in Fig. 4.12

Oxide component	Weight %
CaO	68.5
SiO_2	22.0
Al_2O_3	4.50
$CaSO_4$[a]	5.00

[a] Equivalent to 2.9% SO_3.

indicator. The phenolphthalein changes colour at about pH 11, high pH giving an intense purple colour and low pH giving a colourless form. However, lightly carbonated cement may still contain a sufficiently high ratio of C-S-H, or traces of $Ca(OH)_2$, or of both, sufficient to form a purple colour. Thus the depth of carbonation, as revealed by the phenolphthalein test, is not quantitative for carbonation, but it does indicate the point where declining pH is no longer likely to passivate embedded steel. The test also tends to be inconclusive when applied to inhomogeneous concretes and in permeable concretes, where mineralogical and pH gradients are diffuse.

The actual progress of carbonation with preservation locally of mass balances has been modelled in detail for the cement composition given in Table 4.14. The cement was allowed completely to hydrate at w/c weight ratio = 0.5 at 25°C prior to carbonation. Although the calculation is done for a single composition, it highlights many of the generic aspects of carbonation, as can be seen from the calculation, shown in Fig. 4.12.

The calculation is done by superimposing a gradient of CO_2 across the cement, adding sufficient mass of CO_2 at each pressure to allow the reaction to proceed locally to completion. Water is automatically added or removed (mostly the latter) to maintain a balance amongst the solids. Thus the calculation simulates ingress of CO_2 such that a gradient of CO_2 partial pressures occurs. The maximum CO_2 pressure is that of the standard atmosphere, corresponding to $P_{CO_2} = 10^{-3.5}$ bar, but in fact the calculation is essentially unchanged up to at least 1 bar total CO_2 pressure. The progressive carbonation and its impact on changing phase distribution can be simulated by constructing a vertical line, initially coincident with the left-hand edge of the diagram (corresponding to zero CO_2), and sweeping the line to the right. Note that of the various solids, the first to respond to rising P_{CO_2} is the AFm phase, with progressive stabilisation of the hemi- and monocarboaluminate compositions. Indeed, many cements will contain sufficient intrinsic carbonate effectively to start at this stage. Ongoing carbonation attacks portlandite initially, followed by C-S-H and AFt. Additional scales show numerical

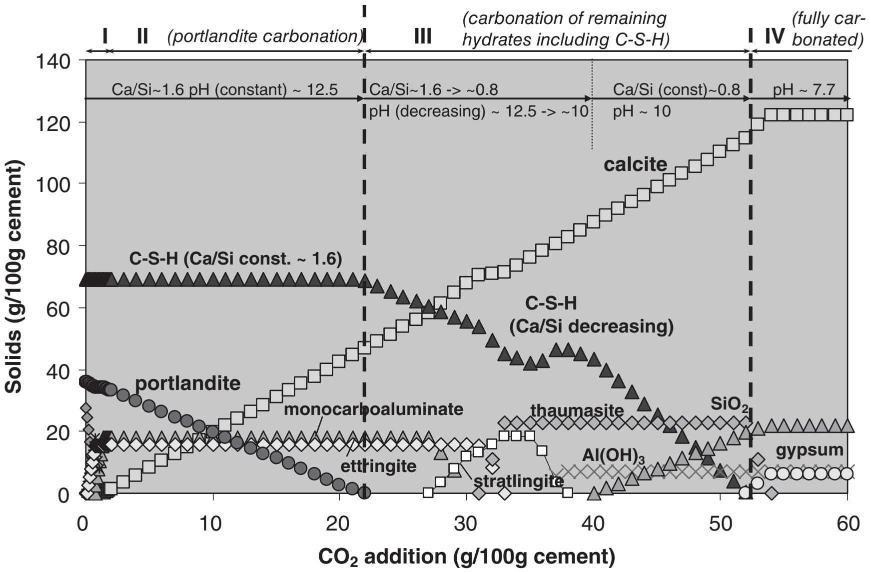

4.12 Progressive carbonation of a model cement at 25°C (after Matschei and Glasser [16]).

values of P_{CO_2} as well as the mass of CO_2 required to be added to attain specific phase transformations. Note the high buffering capacity of cements in this respect, as measured by the mass of CO_2 required to reach the end state. The predicted sequence of zoning agrees well with field observations and with laboratory studies, particularly in earlier stages of carbonation. The prediction of spontaneous thaumasite formation in later stages is only partly confirmed by field studies but, because many investigators have failed to distinguish between ettringite and thaumasite (the two phases have similar structures), some uncertainty attaches to the literature reports showing ettringite but not thaumasite or mixtures of the two AFt phases.

In the course of atmospheric carbonation, leaching does not occur. Furthermore, the external dimensions of cement masses remain essentially constant. Therefore changes in the specific volume of solids attending carbonation must affect the porosity. The specific volume of solids for the companion calculation to Fig. 4.12 showing volume changes is presented in Fig. 4.13.

The action of adding carbon dioxide can be simulated by superimposing a vertical construction line on the diagram and sweeping this line to the right, noting its intesection with the concentration scale. The intercept of the line shows what phases are formed, and the intersection length of the line segments relative to the whole show the amounts of each. The sum of

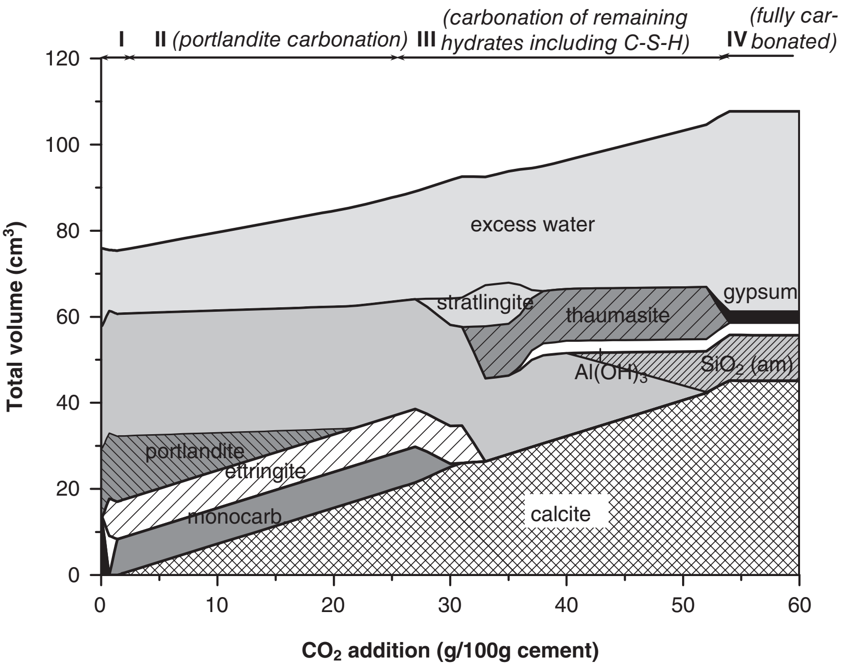

4.13 Specific volume of solids in the carbonation process.

the volumes of the solids gives the total solid volume, which increases, on average, but only slightly, throughout the carbonation process. Note that the carbonation process is attended by loss of water, which must escape to maintain reaction. The change in porosity attending carbonation is not well agreed in the literature, but calculation shows that the porosity drops as the degree of carbonation increases, albeit not on a regular trend. We do not at present know how porosity changes affect permeability but it is likely that the impact is variable, depending on retention of water and the potential for internal transport and recrystallisation of the solid products. Escape of water is often a rate-limiting step, so the kinetics of carbonation are only partly related to the porosity and permeability of the cement because, if water is retained, recrystallisaton of the matrix is facilitated. But, because flooding of the pore network reduces reaction rate, most studies have used lower humidities, <80%, to discourage flooding and facilitate reaction. Under conditions of carbonation in unsaturated regimes, recrystallisation has much less impact on the microstructural changes, although quantitative data are lacking. The above calculation has been made for only one cement composition, but it is expected from scoping studies that the features and processes described will be generic for all Portland cements.

4.15.3 Reactions of dissolved carbon dioxide with portland cement

Arguably the most complicated examples of carbonation arise from reaction of cement with natural waters. A spectrum of water compositions exists in nature: at one extreme, typically encountered in slightly alkaline waters, carbonation mainly results in transfer of CO_2 to the solid, with formation of $CaCO_3$: leaching occurs but is less than accumulation of carbonate, with the result that a thickening layer including calcium carbonate develops. The precipitated calcium carbonate acts as a semi-protective membrane, with the result that reaction slows with time. At the other extreme, so-called 'aggressive carbon dioxide' yields acidic solutions which attack and dissolve cement substance, in extreme cases without precipitation of solid $CaCO_3$. A further complication arises because the calcium carbonate product may appear as one of three polymorphs or mixtures of polymorphs: calcite, aragonite and vaterite. Of the three polymorphs, vaterite is the least dense; it is metastable and characteristic of rapid precipitation from locally supersaturated solutions. Calcite has an intermediate density while aragonite, the densest of the three and actually only stable at high pressures, is nevertheless frequently observed as a product of cement carbonation, especially in saline waters. Calcite is the most stable phase and subsequent example calculations assume it is to be the favoured phase.

Natural waters containing only dissolved CO_2, without significant content of other ions, are relatively uncommon: a host of other cations and anions normally dissolved in fresh and ground waters. These interact with carbon dioxide and cement to give rise to a wide range of products. In general these can be divided into two types of process: dissolution reactions, which remove solid matter from cement, and precipitation. To keep matters simple, calculations do not include other 'foreign' ions such as halides, sulfate, etc.

Kinetic factors may also mediate reactions and need to be taken into account. To illustrate the role of kinetics in controlling interface reactions, let us examine kinetics relevant to the situation shown in Fig. 4.14. A flat cement surface is exposed to an atmosphere which, for simplicity, is assumed to be in contact with an atmosphere of constant partial pressure of carbon dioxide at constant temperature. For reference, we may note that the carbon dioxide content of the standard atmosphere is presently about 380 ppm, equivalent to 0.28 mm Hg, but rising steadily on account of the combustion of fossil fuel. Even this low partial pressure, which we will equate with activity, is sufficient to react with all cement phases. The calcium product of carbonation is assumed to be calcite, calcium carbonate. However, reaction kinetics are strongly influenced by the partial pressure of water vapour in the atmosphere. Thus carbonation will be found to proceed most rapidly at relative humidity in the range 50–80% but to slow at either extreme end of

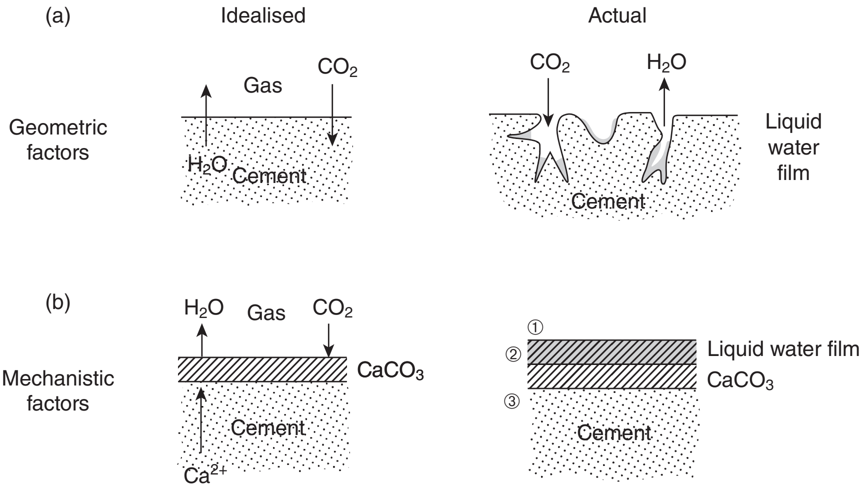

4.14 Mechanism of carbonation showing (a) how geometric roughness and capillary condensation of water affect surface available for transport and (b) (ignoring surface roughness) how transport occurs.

the humidity scale. This sensitivity to relative humidity arises because, on the one hand, gaseous CO_2 does not react with cement but must first dissolve in a film of water and, on the other, the effective surface area available for CO_2 to dissolve is reduced as pores are increasingly flooded. Thus the first step of the reaction is:

$$CO_{2(\text{gas})} + H_2O = CO_{2(\text{aqueous})}$$

The solubility of carbon dioxide in water is temperature dependent but in the standard atmosphere at 25°C, is approximately 1.5 g/l. Thus, for example, rain water is approximately saturated with respect to CO_2 at the temperature and pressure at which its droplets were formed.

The numbered processes in the lower right-hand corner of Fig. 4.14 refer to (1) dissolution of molecular CO_2 and ionisation in water to HCO_3^- and CO_3^{2-}, and (2) transport of Ca, OH, HCO_3^- and CO_3^{2-} through a thickening product layer of $CaCO_3$.

The cement surface shown in Fig. 4.14 releases soluble components to the aqueous phase: as a result, its pH increases. And since both CO_2 solubility increases with rising pH, and dissolution kinetics are accelerated by hydroxide ions, the dissolution process accelerates. As long as the cement is able to contribute soluble sodium and potassium, the pH is approximately fixed by formation of a carbonate–bicarbonate buffer system, at about pH 10–11. This corresponds to an increase of 3–4 orders of magnitude in [OH] concentration relative to rain water (the pH of which is slightly acidic, between pH 6 and 7). As noted, this increased OH concentration both enhances CO_2 solubility and catalyses the conversion of dissolved molecular CO_2 to hydrated CO_2, with its subsequent and relative rapid equilibration to bicarbonate and carbonate speciations. Precipitation of $CaCO_3$ is initiated by interaction of carbonate with $Ca(OH)_2$. Note that CO_2 is being gained at one interface, between air and liquid, while calcium can only enter the aqueous phase at a different interface, i.e., that between solid and aqueous phase. For thin water films, the time taken to transport species through the water layer is negligible. However, the physical position of the two interfaces can be physically separated and this sometimes leads to cement corrosion, although in this case without change in oxidation state.

Certain natural waters have long been known to be aggressive towards cement. These have been characterised empirically as follows. Dissolved CO_2 is known to be present in three speciations in ground water: (1) as dissolved CO_2, sometimes referred to as carbonic acid or 'free carbon dioxide'; (2) as $CaHCO_3$, calcium bicarbonate, a sparingly soluble hypothetical compound giving bicarbonate, HCO_3^{2-}, ions in aqueous solutions; and (3) as carbonate ions, CO_3^{2-}. And, as we have seen, part of the total carbon species is available to form calcium carbonate, while part, the so-called 'aggressive CO_2', is available to dissolve calcium. The aggressive content is defined as that amount of CO_2 in excess of that necessary to maintain the equilibrium:

$$CaCO_3 + H_2CO_3 = Ca(HCO_3)_{2(\text{aqueous})}$$

This aggressive content is sometimes designated H_2CO_3* and is easily estimated from a good water analysis, although such analyses often need to be done *in situ* to avoid subsequent reactions with atmospheric carbon dioxide, changes in temperature, etc. Pisters [17] developed the semi-quantitative classification shown in Table 4.15. The classification includes a range of other chemical factors, some of which will be discussed subsequently. But it represents a clear attempt to define aggressivity of CO_2 in a different way

Table 4.15 Classification of aggressivity of natural waters to Portland cement

Function	Weakly aggressive	Strongly aggressive	Very strongly aggressive
pH	5.5–6.5	4.5–5.5	<4.5
Aggressive CO_2, mg/l	15–30	30–60	>60
Ammonium, mg/l	15–30	30–60	>60
Magnesium, mg/l	100–300	300–1500	>1500
Sulfate, mg/l	200–600	600–2500	>2500

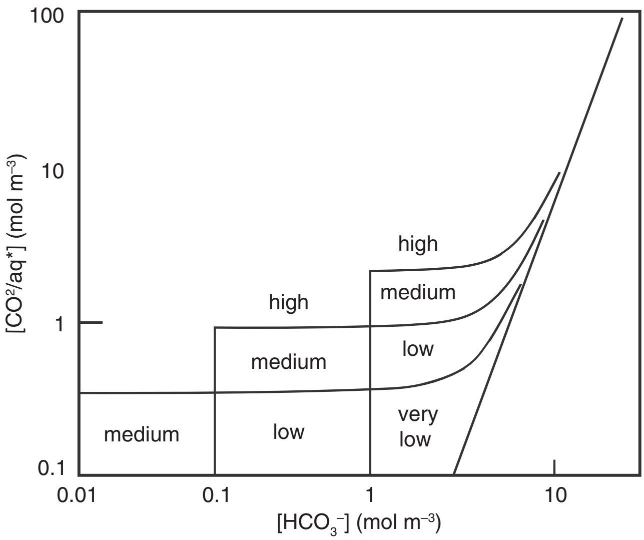

4.15 Classification of aggressivity of natural waters containing dissolved carbon dioxide (after Lea and Desch [18]).

than, for example, sulfate, where the aggressivity is defined in terms of total concentration, not of specific species.

Lea and Desch [18] approached the problem in a similar way. They plotted total bicarbonate as a function of aggressive CO_2 with the results shown in Fig .4.15. The diagram is truncated at the right-hand side by a sloping line which represents the limiting case. The division of waters is somewhat arbitrary but the general principle is sound: that H_2CO_3* unbalanced by bicarbonate is aggressive and gives rise to dissolution of calcium. The process of constructing nomographs was further refined by Roger [19] to enable more quantitative calculations.

However, the advent of modern computational methods suggests that the entire calculation could best be done on a computer: this approach was developed by Cowie and Glasser [20] using the routine MINEQL. Figure 4.16 shows the solubility of calcite as a function of log P_{CO_2}. The solid circle marks an invariant point at which $Ca(OH)_2$ and $CaCO_3$ coexist with an aqueous phase. As long as solid $Ca(OH)_2$ is present, the aqueous calcium content is fixed, at about 1.2 g/l $Ca(OH)_2$ at 25°C) and the CO_2 activity is also fixed, at about 10^{-13} bar. However, once portlandite has reacted, the condition of invariancy is removed and, assuming a supply of CO_2 at higher pressure than this value, aqueous calcium concentrations will decrease, initially in an almost linear trend with increasing P_{CO_2}. Eventually the calcite solubility passes through a minimum, at which point the pH will have decreased to about 9.9. Thus, on this limb of the calcite solubility curve,

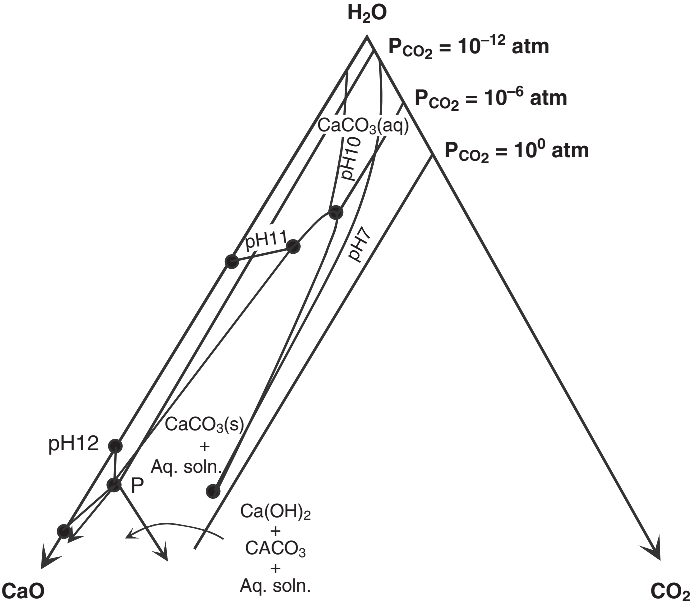

4.16 Part of the system $CaO–CO_2–H_2O$ showing solid phase solubility as a function of P_{CO_2} (three isobars are shown) at 25°C (after Cowie and Glasser [20]).

between its invariant point with calcium hydroxide and the solubility minimum, CO_2 added to the system will increase P_{CO_2}, decreasing pH but also *decreasing* the solubility of calcite. Note that we are treating P_{CO_2} as the independent variable: it is important to the analysis that independent and dependent variables are clearly identified. As it is not difficult to exceed P_{CO_2} of log 10^{-13} in natural environments, this part of the curve has great importance to the evolution of cement in the presence of carbon dioxide in ground water. We might term this portion of the curve the 'passivation limb' as it is increasingly favourable to conservation of solid mass.

However, once P_{CO_2} increases beyond 10^{-6} bar, the content of aggressive CO_2 increases, slowly at first but more rapidly thereafter. The pH continues to decrease, and the solubility of Ca to increase, as a linear function of log P_{CO_2}. As this occurs, the aqueous phase becomes increasingly aggressive: i.e., calcite solubility increases with increasing P_{CO_2}. The actual numerical values are, however, difficult to read from this type of presentation and a companion figure, Fig. 4.17, shows more clearly the species solubilities as a function of pH.

In the foregoing analysis, the system was treated as chemically simple: only P_{CO_2} was allowed to vary and only one temperature was depicted. The effect of temperature is not complicated: the positions of boundaries and

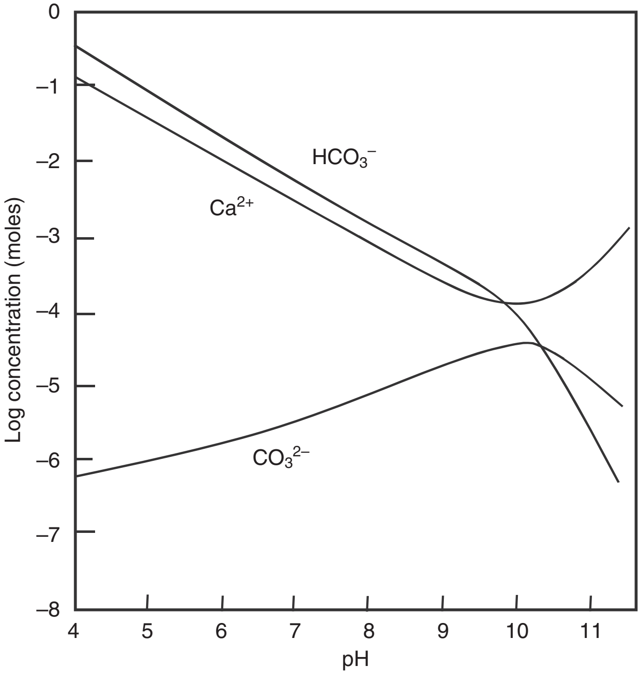

4.17 CO_2 speciation and solubility of Ca as functions of pH. The value of P_{CO_2} is variable: see Fig. 4.16.

of pH shift slightly and progressively with temperature but the basic features of Fig. 4.17 remain unchanged in the range 0–100°C. However, the introduction of other substances, notably of acids and bases, will change the relationships. Neutral salts such as sodium chloride may also impact on the solubility but, at low concentrations, tend to have limited impact. The presence of acids is particularly important: lowering pH at constant P_{CO_2} activity tends to increase significantly the severity of attack, other factors remaining constant. This exposition is generic, but most commercially available routines for the computation of chemical equilibria will be able rapidly to undertake quantitative calculations of a user-defined scenario.

A conclusion emerging from this study is that groundwater conditions where ‘aggressive CO_2’ is present are not compatible with good performance lifetimes for concrete barriers. The cement will act sacrificially to neutralise excess acidity, but as a consequence its performance lifetime will be shortened, perhaps unacceptably so. Nor is it sufficient totally to rely on site groundwater analyses to calculate the aggressivity: the impacts of disturbances in the course of construction and during the operational phase of the repository, as well as releases from wastes, may have to be assessed.

4.16 Miscellaneous interactions of cement in its service environment

A number of modes of deterioration of cement have been suggested as being important. We consider briefly two: microbiological attack and the role of complexants derived from organic wastes.

The high pH of cement inhibits the multiplication of all known microbiological species. Many species can survive but not flourish at pH ~12. This does not mean that microbiology can be neglected: particularly in warm, humid climates, attack on cement is observed. Usually the observed deterioration involves (1) a complex symbiosis, in which microflora and microfauna cooperate, (2) sunlight, as input of energy within photosynthesis is essential for growth, and (3) formation of a chemically-insulating layer, isolating the colony from the high pH of cement. For example, the colony frequently develops a mechanical anchor and chemically low permeability, based on calcium oxalate or one of its hydrates, using calcium from the cement. But the condition of energy availability, from light, is also not typical of repository conditions, although it could be a problem in long-term interim storage facilities. Problems have also arisen with respect to sulfur cycles in concrete tanks used for storage of sulfur-laden crude oils but the author is not aware of conditions in a repository which would initiate this reaction. Perhaps a more serious problem is that sulfur oxidation in the host geology, mediated by bacteria, could give rise to sulfate and sulfuric acid which then attack concrete. For repositories situated in clay and shale containing sulfide, care needs to be taken not to trap oxygen during the operational and closure phases, thus avoiding the problem.

Concerning complexants arising from waste, it is clear that chemical chelating agents such as EDTA, as used in reprocessing and decontamination, are a potential problem. EDTA is not degraded by cement and its concentration in waste streams needs to be controlled. However, a more subtle problem is that degradation of some nominally innocuous waste at high pH, e.g. paper, could generate complexants. Under oxidising conditions, cellulosics may degrade with formation of isosaccharinic acid (ISA) and related saccharides. These, in turn, complex and solubilise actinides. However, investigation shows that order-of-magnitude increases in actinide concentrations are only obtained at unrealistically high concentrations of ISA.

4.17 Summary and conclusions

When cement and concrete are mentioned in connection with radioactive waste treatment most engineers automatically think either of shielding against radiation, drum fillings and/or dense impermeable barriers limiting advection and diffusion of radioactive species. These applications represent important uses of cement. But, in addition, the properties of cement systems are very flexible, and cements also find application in such diverse functions as the formation of porous barriers designed to prevent gas overpressures and as radiation shields. In some applications, such as formation of physical barriers, they compete with other materials, e.g. bentonite clay.

Much technology transfer has been possible between civil and nuclear engineering, especially with respect to material properties, formulation, testing and performance on time-scales up to perhaps 100 years. However, predicting performance at longer time-scales has been more problematical. Nuclear science has had to develop its own approaches, although recent interest of civil engineers on performance in the time frame 100–300 years has provided interesting links.

But nuclear applications still contain unique features with respect to cement–waste species interactions: cement has a chemical potential which finds expression in diverse ways, for example by insolubilising radionuclides. This action is quite specific to the chemical nature and speciation of radionuclides and has only been quantified for a few species: the mechanistic balance between sorption, precipitation and lattice inclusion is often incompletely known. The high pH of cement also protects and preserves some metals, e.g. ferrous alloys, against corrosion.

The many complex processes affecting degradation of cement are being modelled. Many of these models are 'partial' models inasmuch as they deal only with selected aspects of performance. However, as knowledge grows and the relevant databases expand, models are becoming increasingly sophisticated and more relied upon for long-term property prediction. Natural analogues provide comfort that model predictions are broadly correct in concluding that in an appropriate geological setting, cement can maintain its integrity and give protection for long (>1000 year) time-scales.

4.18 References

1. P.C. Hewlitt (ed.), *Lea's Chemistry of Cement and Concrete*, 4th edn. Edward Arnold, London, 1998.
2. D. Beampré and S. Mindess, 'Rheology of fresh concrete: principles, measurement and application', in *Materials Science of Concrete*, Amer. Ceram. Soc., Westerville, OH, 1998.
3. H.F.W. Taylor (ed.), *Cement Chemistry*, 2nd edn. Thomas Telford, London, 1997.
4. H.W. Reinhardt (ed.), *Penetration and Permeability of Concrete*. E. and F.N. Spon, London, 1997.
5. J.L.Dreaver (ed.), *The Geochemistry of Natural Waters*, 3rd edn. Prentice-Hall, Upper Saddle River, NJ, 1997.

6. 'Chemical, mineralogical and microstructural changes occurring in hydrated slag–cement blends', in *Materials Science of Concrete III* (ed. J.S. Skalny), Amer. Ceram. Soc., Westerville, OH, 1991.
7. F.P. Glasser, '*Chemistry of the alkali–silica reaction*', in *The Alkali–Silica Reaction in Cement and Concrete* (ed. R. Swamy), Blackie, Glasgow, 1991.
8. Report DoE/TIC 11,400, Materials Characterization Center, Pacific Northwest Laboratory, Richland, WA, 1982.
9. A. Bentur, S. Diamond and N.S. Berke, *Steel Corrosion in Concrete*. E. and F.N. Spon, London, 1997.
10. F.P. Glasser, J. Marchand and E. Samson, 'Durability of concrete-degradation phenomena involving detrimental chemical reactions', in *Proc. 12th Int. Congr. on the Chemistry of Cements*, Montreal, 2007.
11. B. Mobasher and J. Skalny (eds), *Transport Properties and Concrete Properties*. Amer. Ceram. Soc., Westerville, OH, 2007.
12. J. Davidovitz and M. Morris, *The Pyramids*. Dorset Press, New York, 1988.
13. M.H. Bradbury and L.R. van Loon, 'Cementitious near-field sorption data bases for performance assessment of a L/ILW disposal facility in a palfris marl host rock'. CEM-94, Update 1, Paul Scherrer Inst., Bericht Nr. 98-01, 1998.
14. M. Balonis, B. Lothenbach, G. LeSaout and F.P. Glasser, 'Impact of chloride on the mineralogy of hydrated Portland cement systems'. *Cement and Concrete Res.*, **40**(7), 1009–1022, 2010.
15. K.L. Scrivener and J.F. Young (eds), *Mechanisms of Chemical Degradation of Cement-Based Systems*. E. and F.N. Spon, London, 1995.
16. T. Matschei and F.P. Glasser, 'Interactions between Portland cement and carbon dioxide', In *Proc. 12th Int. Congr. on the Chemistry of Cement*, Montreal, 2007.
17. H. Pisters, 'Reaction of corrosive water with cement'. *Vom Wasser* **30**, 208–221, 1963.
18. F.M. Lea and C.H. Desch, *The Chemistry of Cement and Concrete*, 2nd edn. Edward Arnold, London, 1956.
19. D.E. Roger, 'Determination of carbon dioxide and aggressive carbon dioxide in waters'. *NewZealand J. Sci.*, **16**, 875–893, 1973.
20. J. Cowie and F.P. Glasser, 'The reaction between cement and water containing dissolved carbon dioxide'. *Advances in Cement Res.*, **4**, 119–134, 1991/92.

5

Calcination and vitrification processes for conditioning of radioactive wastes

A. S. ALOY, Khlopin Radium Institute, Russia

Abstract: The object of this chapter is to provide information and references for those vitrification systems which are now at different stages of implementation. It then describes the main parameters and performance of Joule-heated ceramic melters (JHCM) used successfully around the world. The chapter reviews the basics of the potentially attractive cold-crucible induction melting (CCIM) and microwave (MW) heating as advanced technologies of the very near future. Bulk vitrification and plasma touch combined with CCIM are described as well. Advantages and limitations of each technology and existing techniques are discussed.

Key words: vitrification, calcination, melters, radioactive waste, glassy materials.

5.1 Introduction

The purpose of calcination processes, which proceed when the material is heated, is to convert waste solutions into a mixture of dry solid oxides named calcine. Calcine could be stored as an interim product or be further treated at higher temperatures to produce glass using a vitrification process.

A vitrification process can be defined as any thermal process producing a vitreous product and is internationally accepted as the technology of choice for the immobilization of radioactive wastes (RWs) of different natures and origins. In general, vitrification of wastes significantly reduces the volume of material which may have to be transported, stored and placed in final disposal.

However, vitrification of RW is not just a single technology, but rather a family of technologies. For example, Joule-heated ceramic melters (JHCM) are heated by passing a current through the pre-melted chemicals. High-frequency melters use either induction heating or microwave energy to form a melt. Plasma torch melters use torches to generate extremely high temperatures.

Each of these is compatible with some type of wastes or other materials to be vitrified. The effectiveness of each choice could be estimated taking into account the origin and activity of waste, reduction factor compared to initial volume, available equipment operated and maintained remotely, volume of secondary waste, cost of facility and cost of operation.

The main topic of this chapter is vitrification processes of liquid and solid wastes that have been implemented and are now used on an industrial scale or are very close to that. Also, it briefly describes the Idaho calcination process, the only one used in the world to convert liquid high-level waste (HLW) to an interim calcine product for long-term storage, and the French calcination process followed by vitrification in the Atelier Vitrification de Marcoule (AVM) process.

5.1.1 Applicable waste streams/waste forms

Vitrification of various, typically high-level liquid wastes generated from reprocessing of spent nuclear fuel (SNF) or accumulated and stored in special tanks in the USA and Russia has become widely accepted. HLW is the acidic aqueous waste solution from the first cycle of SNF reprocessing operations and the product of its treatment. Depending on the type of nuclear power plant (NPP), the fission product spectrum can differ significantly. Typical compositions of HLW from a light water reactor (LWR) fuel with burn up to 40 GW *d per tonne in solution concentrated to 250 l/t fuel processed are given in Table 5.1.

Table 5.1 Typical composition of HLW from LWR fuel (UK), 40 kW/kg, 40 MW *d/kg, five-year cooled, in mg/kg U in fuel

Element	mg/kg U	Element	mg/kg U
Cr	225	Rh	525
Fe	850	Pd	1,826
Ni	162	Ag	36
Ge	1.46	Cd	115
As	0.041	In	2.9
Se	66.84	Sn	105
Rb	410	Sb	25.5
Sr	963	Te	646
Y	529	Cs	2,901
Zr	4,226	Ba	2,043
Mo	4,040	REE[a]	24,163.7
Tc	1,020	U	25
Ru	2,878	TUE[b]	567
Volume approx. 0.250 l/kg uranium processed			

[a] Rare earth elements.
[b] Transuranic elements.
Source: Nuclear Energy Agency (1997).

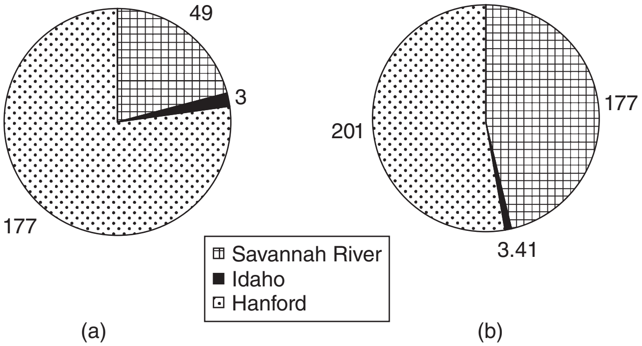

5.1 (a) Number of storage tanks and (b) total volume (million liters) of HLW at three DOE sites (Gerdes and Ross, 2009).

Other categories of HLW represent materials that have been formed as a result of nuclear defense complex activity. Instead of the pure acidic solutions after reprocessing SNF, these wastes are composed of one or more of the following components:

- Liquid in the form of alkaline supernatant
- Salt cake as a crystalline mixture of chemical salts
- Sludges or slurries which are usually heterogeneous and contain a wide variety of cations and anions.

The numbers of storage tanks and total volumes of HLW at three US Department of Energy (DOE) sites are shown in Fig. 5.1. Based on a long history of success on an industrial scale, vitrification is proposed not only for HLW but also for the very large volumes of low-level waste found throughout the US DOE defense complex. In Russia vitrification of low- and intermediate-level liquid waste (LILW) generated in routine operation of NPP has also been proposed (Sobolev *et al.*, 1996). Concerning the product, as a result of the vitrification process very durable borosilicate glass is a preferred waste form in most countries. A wide range of chemical compositions have been studied and evaluated (IAEA, TRS 257, 1985). Typical proportions of major component oxides are 35–55 wt% SiO_2, 10–20 wt% alkali metal oxides and 7–20 wt% B_2O_3 with the waste loading in the final product in the range 15–35 wt%. Borosilicate glasses are less corrosive than phosphate ones and devitrification of them occurs under higher temperatures. During the fabrication of borosilicate glasses, problems can occur because of phase separation, especially of alkali molybdate or sulfate. In Russia a sodium-alumina-phosphate glass has been implemented on an industrial scale for the vitrification process of HLW in JHCM (IAEA, TRS 339, 1992). This was mainly due to the relatively low formation temperature of this glass (~900°C), resulting in lower volatilization of Cs and Ru, and also due to its relatively high solubility for Al_2O_3.

For each application of the vitrification process, fabrication of an acceptable final waste form is extremely important. Final waste products should satisfy certain criteria: they should maintain their mechanical integrity, and have good resistance to irradiation, adequate thermal conductivity and, ideally, a low leach rate. Calcines do not fulfill all of these criteria to a sufficient degree and therefore are considered as interim products.

5.2 Calcination and vitrification processes

Calcinations of HLW consist of heating the waste in special equipment up to 500–700°C, when decomposition of nitrates takes place. As a result calcine is formed, which represents a mixture of solid oxides. Due to calcination the initial volume of HLW can be reduced by a factor of 7–10 and the resulting product can be used for long-term storage under control or converted into a more stable material, like glass, suitable for final disposal.

The calcination process proceeds with consumption of energy (endothermic reaction) and there are different ways of providing the energy required. There are apparatuses of the spray type or with a fluidized bed, in the form of a rotary horizontal tube or as a crucible, where the melting process can be performed simultaneously (the in-pot process).

A number of the processes require the feed solution to be sprayed via the nozzles into either a fluidized bed or a heated calciner column. An atomizing gas is normally used, either air or superheated steam. The design of these nozzles is critical and much development work has taken place to improve the designs for reliable operation. For example, in the spray calciner effective operation depends on good atomization to break up the feed solutions into small enough droplets to permit drying and calcination during the short residence time in the calciner column.

On an industrial scale, fabrication of calcine for interim storage has been implemented only in the Idaho National Laboratory (USA) using the fluidized bed method. The bed was maintained at 400–500°C due to in-bed combustion of kerosene. The bed height was maintained at a constant level by adjusting the rate of product withdrawal and transferring it to storage bins located within near-surface storage vaults. Each bin is 3 m in diameter and 12–18 m high. Calcine has a high thermal stability (up to 800°C) but low thermal conductivity (0.13–0.2 W/m°C) and very high leach rates. Three different compositions of calcines are shown in Table 5.2.

A specially designed calciner is used in the AVM process to preconcentrate HLW feed prior to the melter. Special airtight seals located at each end allow longitudinal expansion of the tube and ensure the tightness. The

Table 5.2 Composition of major calcine types produced at the Idaho National Laboratory, USA

Component	Alumina (wt%)	Zirconia (wt%)	Zirconia-Na (wt%)
Al_2O_3	82–95	13–17	10–16
Na_2O	1–3	–	6–8
ZrO_2	–	21–27	16–19
CaF_2	–	50–56	33–39
CaO	–	2–4	13–17
B_2O_3	0.5–2	3–4	2–3
NO_3	5–9	0.5–2	7–9.5
CdO	–	–	–
Other	0.5–1.5	0.5–1.5	0.5–1.5
Fission products	<1	<1	<1
Activity (Ci/g)	~0.02	~0.007	~0.005

Source: IAEA (1977).

tube is divided into four zones, and an electric resistance furnace heats each externally. The first two zones are devoted to evaporation and each of the last two is for calcination. The waste is fed by gravity from the metering wheel into the upper part of the calciner and the calcined product is discharged by gravity from the outlet of the calciner at its lower end directly into the melter (IAEA STR-314, 2002).

The AVM process is a continuous two-step process that has been implemented at the AVM since 1978. It involves calcining the HLW solution in a rotary calciner that feeds the calcined products to a metallic melter, while glass formers in the form of primary glass (frit) are introduced into the melter simultaneously. The HLW feeding flow rate is controlled with a rotary wheel, which is fed by means of a double-stage airlift. The melter is composed of a metallic pot heated by induction. Both the products and the glass frit react with the molten glass located in the pot. Glass pouring is performed by heating a pouring nozzle equipped with an induction heater, and stops when the decreasing glass level inside the pot reaches the upper level of the nozzle. The AVM process has been operated successfully in France for 30 years and three vitrification plants based on this process have been constructed at Marcoule and La Hague. A similar plant also been constructed at Sellafield, UK (Riley *et al.*, 2009).

5.2.1 JHCM

The present vitrification technologies of real HLW are essentially only of two types: the two-stage AVM process described above, and the single-stage

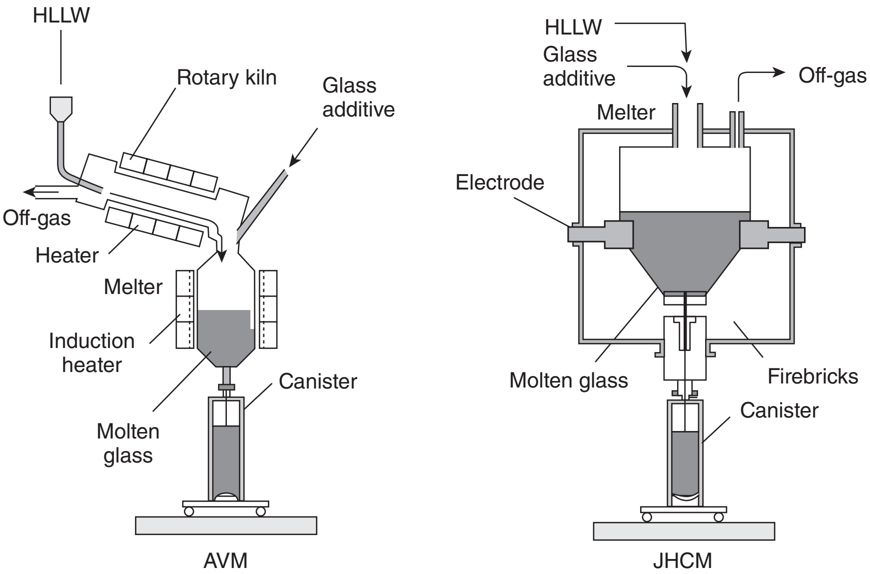

5.2 Schematic view of AVM and JHCM vitrification melters (adapted from IAEA, STR-314, 2002).

Joule-heated ceramic melter (JHCM). Their conceptual views are shown in Fig. 5.2.

Vitrification of liquid HLW in JHCM systems implies that several individual stages of the process, such as evaporation, drying, calcination, and reactions of the waste components with glass-forming additives, i.e., frits, occur in the melter simultaneously. The liquid waste and the frit are fed directly into the melter, forming a cold cap on the surface of the melt pool, lined with ceramic refractory bricks.

To start the process each melter is equipped with electric resistance heating rods, which are placed behind the refractory of the melter plenum. When these heat up and the simulated glass filled earlier in the ceramic pool becomes electrically conductive, the main electrodes are turned on.

The glass melt is heated by Joule heating, resulting from the electric current passing through the electrodes that are immersed in the melt. The energy dissipated in the melt keeps the molten glass at the high temperatures required. Inconel-690 electrodes are used for borosilicate glass production, but in the case of the more corrosive phosphate glass in Russia EP-500 melter molybdenum is adopted for the electrodes. The melter (Fig. 5.3) represents a rectangular pool with total surface area about 12 m^2 lined with refractory melted bricks. The melter is encased in a sealed stainless steel housing. The throughput of the EP-500 melter is 500 l/h of liquid HLW.

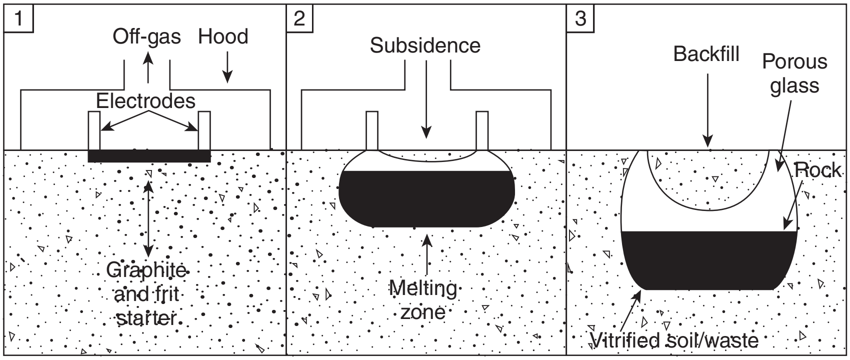

5.3 Schema of *in situ* vitrification process (from Roberts *et al.*, 1993).

Vitrification of HLW using JHCM has been an evolutionary process with quite different glass compositions. Both defense waste slurries, accumulated in special tanks, and HLW after SNF reprocessing have been used as feed to the melters.

The typical JHCM melter design has a flat bottom, but variations exist that have been designed to overcome technical challenges. Example variations in JHCM design include adding a sloped bottom and agitating the melt pool. The first problem is connected with the very low solubility of the noble metals (Rh, Pd, Ru) in the borosilicate glasses. Settling and accumulation of noble metals on the flat bottom of the JHCM can result in marked changes in electrical resistance and viscosity of melt. As a result, failure of the melter could take place either by electrical short circuit between the electrodes or by plugging of the drain device. The melter solves this problem by having a special internal configuration of the molten glass pool that pushes separated noble metal particles toward the glass pouring outlet where they concentrate and are preferably discharged during the initial phase of pouring (Grunewald *et al.*, 2000).

The second modification in the design was initiated to increase glass production. Vitrification productivity is affected by several factors, most of which involve feed composition and melt mixing. The mass fraction of salts in the feed solution affects the amount of energy that has to be used to evaporate water from the waste instead of heating the melt. Intense air bubbling of the molten glass helps to prevent sedimentation of insoluble waste components and significantly increases the production rate, mainly through heat transfer improvement (Perez *et al.*, 2005).

The PAMELA melter in Belgium has a reported production rate of 21 kg/m^2 h, and the radioactive Liquid Fed Ceramic Melter at Pacific Northwest National Laboratory has operated at production rates of 14 to 40 kg/m^2 h. The DWPF melter (2.6 m^2 melt area) has a design-basis production rate of 40 kg/m^2 h, and its typical attained production rate is 24.5 kg/m^2 h. The target production rate for the Waste Treatment Plant at Hanford was 40 kg/m^2 h in 1996, though extensive plenum heating is usually required to meet this production rate (Fox, 2007).

Volatilization of components from a JHCM could be affected by parameters such as cold cap size, plenum temperature and feed composition. In general, the volatility of various species in a JHCM is relatively low due to the cold top surface of the melt pool.

Further developments of ceramic melter technologies have been associated with improvements in their design with the primary purpose of extending the service life of the electrodes, improving safety and reliability of the glass pouring system, successful handling of poorly soluble waste components, such as noble metals and silver, and preventing plugging of the off-gas lines.

The service life of the electrodes located in the melt pool was extended by optimization of air cooling of the electrodes, making it possible to maintain the electrode surface temperature below 1000°C while the temperature in the melt was 1200°C. It was shown that, at this temperature mode, during eight years of operation, the electrodes had not been affected by any noticeable corrosion (Fleisch *et al.*, 2008). Corrosion testing showed (Smith *et al.*, 2005) that chromium-nickel alloy MA 758 is a better choice than either Inconel 690 or MA 754 for higher-temperature or high-sulfate applications.

The improved pouring system of the German Vitrification Plant includes a circular Inconel 690 insert with 12 channels to protect the pour spout from plugging with solid particles. There is a conceptual design for developing replacement electrodes to increase melter operational life up to 20 years (Japan Atomic Energy Agency, 2008).

The extensive operational experience with the JHCM vitrification technology shows that this technology is simple and reliable. It is appropriate for generating a wide range of various glasses, including borosilicate, aluminosilicate and phosphate glass. With effective convection of the molten glass pool, these glasses can incorporate significant quantities of poorly soluble materials, such as spinels and noble metals that generate suspensions in the glass.

5.2.2 Cold-crucible induction melter (CCIM)

Induction glass melting technology can be realized using two approaches: hot-crucible (described above) and cold-crucible. The principle of induction heating based on Faraday's law for the electromotive force (E) generated by an ideal solenoid having N close-packed coils, each coil generating a magnetic flux Φ, is given by:

$$E = -N\frac{\mathrm{d}\Phi}{\mathrm{d}t} \quad (5.1)$$

where t is the time. Φ is related to the current in the coil by the expression

$$\Phi = \mu I n A \quad (5.2)$$

where μ is the magnetic permeability of the material inside the solenoid, I the current in the solenoid, n the number of coils per unit length and A the area of the central coil.

Thus, E depends on the frequency of the alternating-current (AC) generator, the current in the inductor coils, the magnetic permeability of the heated material, and the dimensions of the crucible and inductor.

Eddy currents of intensity I proportional to E/R, where R is the resistance of the material in which the eddy current occurs, are induced in the materials inside the solenoid. The power dissipated within the solenoid is

$$P = E^2/R \quad (5.3)$$

This simplified expression defines the ideal case. In practice, other dissipative phenomena, such as heating of the coils because of their resistance, also occur. This makes it necessary to cool the inductor coils to prevent them from overheating (Guilbeau *et al.*, 2004).

In CCIM to melt the batch charge the crucible is formed by metal tubes with good heat conductivity (usually copper or stainless steel) placed within the inductor coils. The crucible tubes are water-cooled so that their temperature does not exceed 200°C, even during melting. A protective layer of solid glass, called ‘skull’, forms between melt and crucible. This protective layer, of the same chemistry as the melt, blocks leaking of the melted glass between the crucible tubes and protects the crucible from corrosion due to melt aggressive components. This increases crucible lifetime considerably.

CCIM technology is based on heating of conductive melt in a high-frequency electromagnetic field. Frequencies of 0.30, 0.44, 1.76 and 5.28 MHz are commonly used. The electromagnetic field penetrates through the gaps between the cold-crucible tubes and induces eddy currents. The eddy currents heat and stir the melt directly. The initial melt can be formed by inductively heating a solid conductive material, such as graphite or silicon carbide.

Development of CCIM technology for the next generation of RW melters started in Russia and France at the beginning of the 1980s. The Russian design philosophy is to emphasize smaller high-frequency (MHz) units, whereas the French approach is to use larger diameter, relatively lower-frequency (kHz) melters. To maximize the use of the inductive energy for glass melting, in Russia the feed material is paste (moist), while in France it is calcine. Another difference is a mechanical stirring of the melt (France) and only a convective stirring in the Russian design.

CCIM technology has been identified in numerous studies as a potential alternative to JHCM vitrification, but little data is available for engineering and economic evaluation. Gombert *et al.* (2002b) presented a system design and description of major components for CCIM as next-generation HLW melters. The system configuration and each of the components has distinct functions and must respond to certain design requirements to ensure overall system performance.

Approximately 86% of the energy transferred by the induction coil is deposited in the small skin-depth layer. Thus, design of an induction coil is not trivial. It should be configured (diameter, number and spacing of turns) to maximize efficiency of energy transfer from the generator to the melt. The design is constrained by the physical dimensions of the crucible, the electrically conductive properties and volume of the melt, the desired thermal profile of the melt, and the output electrical properties of the generator itself. Because of the large amount of energy conducted through the coil and the electrical resistivity of common conductive materials used to make the coil such as copper, a coil as part of a CCIM system will likely require active thermal cooling. Induction coils may also require a mechanical support structure due to both their size and weight.

The energy balance with a CCIM is sharply different from that of a JHCM. First, in a JHCM, essentially all of the applied power is dissipated directly in the glass melt. Second, in a JHCM, refractory brick and several layers of low-density silica insulating board surround the melt. The outer metal containment may be water-cooled, but the multiple insulating layers drastically reduce the total heat transfer. In the CCIM, there may be a 1000°C+ temperature gradient across a 2–5 mm layer of solidified glass 'cold-skull' between the melt and the cooled crucible. This lower energy efficiency is not necessarily a significant cost issue, but the energy balance, thermal profile, and operational energy deposition model must be understood to do detailed design. This knowledge should be a primary focus in laboratory and pilot-scale development of the CCIM technology.

Modeling of CCIM provides data needed to perform detailed engineering design of the induction generator power level and output electrical interface, the geometry and cooling requirement for induction coils of various melter configurations, the melter constraints on a slurry feed system and output pour timing and volume, and key design parameters of the feedback control system. Models also offer reference values for designing and operating a control system (Gombert *et al.*, 2002a).

An advanced new model provides the capability to calculate temperature distribution and convection cell characteristics in large high-efficiency industrial scale melters. As the melter diameter increases, the inductor current frequency must also decrease to maintain electrical efficiency. Thus, the processes and characteristics of heat transfer and melt flow change considerably, which drives the design and configuration. Application of this model to the design of large melters with different geometries and configurations would allow cost-effective and expeditious evaluation, optimization, and design selection (Roach *et al.*, 2008).

A full-scale vitrification plant using CCIM has been operational in Russia (SIA 'Radon') since 1999 for treatment of low and intermediate institutional radioactive waste. It has three high-frequency (1.76 MHz) CCIM producing borosilicate glass (Sobolev *et al.*, 2003). Application of the same plant for vitrification of NPP operational waste is also under consideration (Lifanov *et al.*, 2003).

In France CCIM technology has been developed progressively since the 1980s and is well documented in numerous publications. It opens a new perspective in terms of glasses with HLW formulation that can be produced in a CCIM (Petitjean *et al.*, 2002). A totally new range of matrices for various applications has been developed and studied. Based on all the benefits from CCIM, a new project, 'Vitrification 2010', was started in 2005 with the aim of putting into active operation a CCIM instead of an AVM hot-pot vitrification line R7 in 2010 (Chauvin *et al.*, 2009).

In India, an engineering-scale CCIM using a frequency of 200 kHz was locally developed for the inactive demonstration of the technology. The melter was operated continuously to assess its performance. Industrially adaptable melter operating procedures for start-up, melting and pouring operations were established. Glass melting capacities up to 200 kg/m^2 h were accomplished. The electrical and thermal efficiencies were found to be in the range of 70–80% and 10–20% respectively (Sugilal and Sengar, 2008).

5.2.3 Microwave (MW) vitrification

Microwave or dielectric heating is defined as heating by the energy of an electromagnetic field with ultra high frequencies. Ultra high frequencies range from 300 to 300,000 MHz and are primarily used in communications applications. Mostly 915 MHz and 2450 MHz are used for microwave heating (Ku *et al.*, 2002).

The electromagnetic field forces charged particles, e.g. dipole molecules of water, to oscillate with the frequency of the induced field. For a microwave frequency of 2450 MHz the dipoles within the material realign themselves approximately 2.5 billion times per second. Due to dielectric losses associated with the internal friction, each molecule or dipole becomes a source of heat, thereby heating the entire volume of the material. Effectiveness of conversion of microwave energy into thermal energy depends on the operational frequency of the generator, the electrical field

Table 5.3 Summary of microwave active elements of interest for glass production

Compound	*T* (°C)	Compound	*T* (°C)
Fe_3O_4	1258	NiO	1305
CuO	1012	V_2O_5	714
MnO_2	1287	WO_3	1270
Co_2O_3	1014	$NaH_2PO_4 \cdot 2H_2O$	678

Source: adapted from Stennett and Hyatt (2009).

density and the electro-physical properties of the processed material (Appleton *et al.*, 2005).

The electro-physical properties of the material dictate its capability to absorb energy. To heat the material with the energy of an electromagnetic field, at minimum, one of the components of the material has to possess a high absorbing capacity. Several MW active compounds that could provide fast heating of suitable glass are shown in Table 5.3. The temperature values indicate the maximum reported temperatures achieved by heating in a conventional MW oven. Due to the selectivity of energy absorption, the material can be heated to high temperatures in a 'cold' container.

Depths of penetration of microwave energy into various materials significantly differ. Specifically, depths of penetration into water for 915 MHz and 2450 MHz are 12 cm and 4.3 cm, respectively. Most metals have a low depth of penetration of the electromagnetic field, about a few microns, thereby limiting energy impact on metals and preventing losses of energy emission for the energy transferred in metal waveguides (Jantzen and Cadieux, 1991).

The major components of microwave heating equipment include: (1) MW generator and waveguide system, (2) a process unit with a container for the final product, and (3) an off-gas system and a system for monitoring process parameters.

Most glass-forming oxides have a low absorbing capacity for this type of heating. Some intensifying glass additives, for example ferromagnetic additives, are occasionally used to heat the feed and generate glass. However, oxide mixtures of most radioactive waste usually have a sufficient quantity of components for microwave heating of the feed to reach glass-forming temperatures. In some cases commercially available microwave ovens have been used; in others a special apparatus was designed to perform experimental work.

Almeida *et al.* (2007) prepared iron-phosphate glasses by melting mixtures of magnetite or ferrite with a phosphate precursor in a microwave oven, and some properties were compared with glasses of the same nominal composition produced in an electric furnace. Mössbauer spectroscopy, X-ray diffraction, and differential thermal analysis were used to characterize these materials.

It was shown that glasses produced in a microwave oven present $Fe^{2+}/(Fe^{3+} + Fe^{2+})$ ratios higher than those observed in glasses produced in electric furnaces. The assumption to explain the Fe^{3+} reduction was based on the different heating rates in both cases but the possible effects of microwave radiation on the 3d level of Fe was evinced also.

Vitrification of sodium-iron phosphate ($10Na_2O–30Fe_2O_3–60P_2O_5$ (mol%) composition) was performed in a microwave oven by Stennett and Hyatt (2009). These glasses for HLW immobilization were chosen because they exhibit lower melting temperatures and high solubility for transition metal oxides and some of them demonstrate equivalent or superior chemical durability to borosilicate systems (Day *et al.*, 1998).

The bench-scale MW equipment was developed to perform vitrification of simulated waste from NPP with VVER reactor in the form of sodium borophosphate glass (Komarov *et al.*, 2005). The main parameters of the equipment used are given in Table 5.4. As a result of the tests a 200-liter drum with 320 kg of the final glassy-like product was obtained. Visual examination of the whole block showed the presence of structural nonuniformity over the volume, the properties of the product changing from layer to layer.

Development and characterization of borosilicate glasses for immobilization of Pu-containing alkaline sludges using a specially designed MW device with 5 kW power was made in the frame of the Russian Pu excess disposition program (Aloy *et al.*, 2001). The main factor of the optimization process

Table 5.4 The basic characteristics of the scale-up microwave equipment

Microwave generator power (kW)	At least 50
Microwave power regulation	Smooth
Microwave power regulation range (%)	At least 10–100
Working frequency of the microwave generator (MHz)	915 ± 10
Crucible-container volume (liters)	200
Power grid:	
Voltage (V)	380
Number of phases	3
Power consumption (kVa)	No more than 75
Maximum heating temperature (°C)	1300
Temperature measurement method:	
Inside contact-free melter	IR pyrometer
Outer walls of melter	Thermocouples

Source: Komarov *et al.* (2005).

Table 5.5 Composition of glass produced in microware equipment

Oxide	Component (wt%)	Oxide	Component (wt%)
UO_2	13.34	Fe_2O_3	9.37
Na_2O	16.47	MnO_2	7.76
SiO_2	34.23	Cr_2O_3	0.58
B_2O_3	7.9	NiO	1.03
Al_2O_3	8.76		
Total			100.00

Source: Aloy *et al.* (2001).

was that the glasses must meet durability requirements while remaining remotely obtained in hot cells. As a result the glass with composition shown in Table 5.5 was selected for testing at the radiochemical plant due to its higher durability and better technological properties.

In comparison with traditional heating methods, microwave heating has the following advantages: (1) a waveguide makes it easy to apply energy to the processed material and avoid significant losses; (2) the process can be stopped and restarted at any time, without any additional technological operations, as the heating rate is very fast; (3) the heat source does not have contact with the processed material, which can often be corrosive or radioactive if radioactive waste is being processed; and (4) the main power equipment can be placed at a large distance from the process unit, which is especially important for handling radioactive materials; it simplifies operations, as well as minimizing contamination of the equipment and radiation exposure of the personnel.

5.2.4 Bulk vitrification

One of the first examples of bulk vitrification was a process called in-situ vitrification (ISV). This is a technology that treats contaminated soils *in situ* by melting the soil to form a durable glass which crystallizes when solidified. The ISV process immobilizes inorganic materials such as radionuclides and heavy metals. Vitrification eliminates the danger of damage to the surface barrier from soil settlement caused by decomposition of combustible material and settling of the compressible waste (Roberts *et al.*, 1993).

Soil melting in the ISV process is accomplished by passing electrical current through contaminated soils via electrodes disposed in the soil. Because dry soil is not very electrically conductive, a mixture of graphite and glass frit is placed between each electrode to serve as a starter path. An electrical potential is applied to the electrodes to establish an electrical current in the starter path. The flow of current heats the starter path and surrounding soil to well above the initial soil-melting temperatures of 1100–1400°C. Once the soil becomes molten, it becomes more electrically conductive, and the molten region grows outward and downward. The ISV process is demonstrated in Figure 5.3. Power is applied until the melt encompasses the contaminated region.

During the ISV process, the water present in the pores of the soil near the melt is heated to boiling, and combustibles are combusted or pyrolyzed (depending on the availability of oxygen). Both of these processes produce significant quantities of gas. If the permeability of the soil is low due to its tight structure or the presence of solid regions (e.g., metal drums, concrete walls, etc.), the gas generated can cause a significant increase in pressure below the melt. When this pressure becomes greater than the static head of the melt, there is the possibility that it can rupture the sintered soil layer surrounding the melt and send a bubble of gas into the melt. As the gas bubble rises through the melt, its volume increases due to decreasing pressure until it reaches the surface. Such behavior is dangerous to personnel and equipment and can lead to the potential for uncontrolled release of contaminants into the atmosphere as the off-gas hood is pressurized. For these reasons, it is important to avoid pressure buildups beneath the melt.

In the case of In-Container Vitrification™ (ICV™), also referred to as the 'bulk vitrification' process, the melting zone moves bottom-up. This process (Fig. 5.4) combines glass-forming additives, low active solids and chemicals which are melted using a Joule-heating method in a refractory-lined steel container (Mauss and Raymond, 2005).

Melting begins at the bottom of the container and then progresses using a feed-while-melt (FWM) process. FWM refers to the capability to continue to add waste and glass formers to the ICV™ container during the entire melting process. In this 'bottom-up' melting process, a conductive 'starter path' is arranged just above a bottom refractory liner surface, with two graphite electrodes set at opposite ends of the container, in contact with the starter path. A mixture of glass formers and waste material is spread on top of the starter path, and power is then applied to the electrodes, causing the starter path material to melt via Joule heating. This heat propagates upward and outward, eventually melting the surrounding glass former and waste mixture. Additional glass former/waste material is periodically fed onto the surface of, and incorporated into, the melt pool. FWM continues and the volume of the melt increases until the container is filled. Because it continually compensates for the volume reduction inherent in a melting process, the FWM technique maximizes waste loading by production of a full box of vitrified waste. Treatment by bulk vitrification, interim storage, transport, and final long-term disposal are achieved entirely within the same ICV™ container. A disadvantage of this technology is penetration of the low-viscosity molten ionic salt (MIS) which contains technetium into a

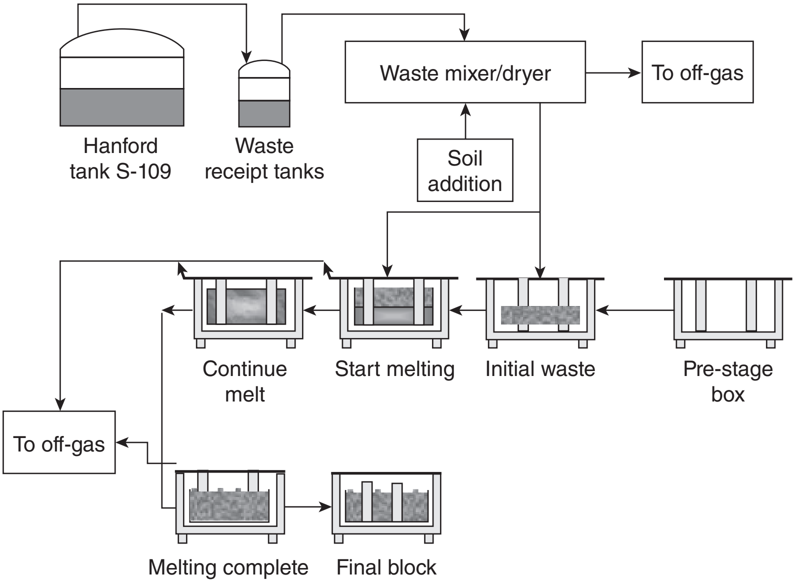

5.4 Simplified in-container vitrification flow diagram (adapted from Mauss and Raymond, 2005).

porous refractory block. Laboratory and crucible-scale tests showed that a variety of methods, individually or in combination, can decrease MIS penetration (Bagaasen *et al.*, 2008).

A viable variant of 'bulk vitrification' is based on a self-sustaining thermochemical process (Ojovan and Lee, 2003). Self-sustaining vitrification processes utilize the energy released during exothermic chemical reactions that can occur in a mixture of radioactive waste and specially designed powder metal fuel (PMF) to melt the waste and form a glass-like material without requiring an external power supply. This process is controlled by the composition of the initial mixture of waste and PMF. The composition of the PMF is crucial; it is designed to release sufficient heat to sustain waste melting and to produce a mineral or glass-like end product. Appropriate PMF composition and PMF/waste ratios have been determined through computer simulation. Both minimization of carryover of hazardous components and retention of contaminants in the final waste form have been achieved using suitable PMF compositions. Self-sustaining vitrification does not require expensive equipment and is economically justified, particularly for small volume hazardous wastes. Double-walled crucible containers made of carbon steel of 3, 5 and 10 dm^3 volumes have been used (Fig. 5.5).

Self-sustaining vitrification uses the energy released during exothermic chemical reactions similar to the well-known thermite reactions. However,

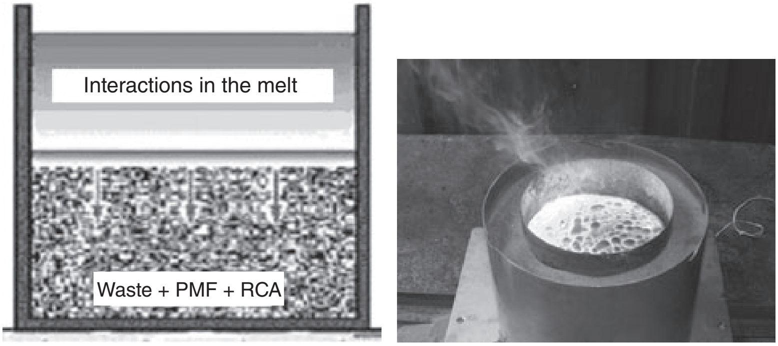

(a) (b)

5.5 Self-sustaining vitrification: (a) schematic; (b) process occurring in a double-well container crucible (adapted from Ojovan and Lee, 2003).

for self-sustaining vitrification other compositions are used, which are mixtures of wastes with a specially designed powder metal fuel (PMF). The powder metal fuel is prepared to utilize chemical reactions to: (1) melt the radioactive waste, (2) form a glass-like (glass composite) material without requiring an external power supply, and (3) bind hazardous contaminants into the final waste form. Conventionally the overall reaction of self-sustaining vitrification can be written as

$$\text{Waste} + \text{PMF} \rightarrow \text{waste form} + \text{heat} \qquad (5.4)$$

The waste is usually in the form of a mixture of metal oxides including the hazardous ones (e.g. heavy metal oxides, radionuclide compounds). PMF is a specially designed blend of heat-generating components. As for thermite reactions, self-sustaining vitrification is controlled by the parameters of the initial mixture (waste + PMF). However, unlike thermite compositions, PMF compositions must ensure efficient immobilization of hazardous components into the final waste form. In addition, during the vitrification process release of contaminants due to volatilization or through emission of contaminated aerosols must be minimized. A suitable PMF composition takes into account both the immobilizing process and material parameters.

After stirring the waste with PMF, the mixture is ignited by remote electrical igniters, causing the self-sustaining vitrification reaction. The final stage of the process is quenching and cooling. The fill material such as sand or feldspar between two drums ensures slow cooling of the vitrified product. Since the initial volume of the mixed composition after melting is reduced as a rule by a factor of 2–3, the self-sustaining vitrification can be carried out several times using the same crucible.

5.2.5 Combined plasma torch incineration and CCIM vitrification

Some 'exotic' radioactive waste, containing a large amount of chlorinated organics or a mixture of plastics with concrete and metals, can not be conditioned by existing vitrification processes. To solve this problem a single innovative process coupling a refractory-free furnace with a water-cooled jacket and an oxygen twin plasma torch has been developed (Poitou *et al.*, 2001). The goal is to achieve in the same reactor the incineration of the waste, the vitrification of the mineral fraction, and combustion of the toxic off-gases. A schematic view of an advanced hybrid system is presented in Fig. 5.6.

At the beginning of the process the crucible is filled with borosilicate glass frit. The plasma is first used to start the melting of the glass frit. Then high frequency (HF) power is turned on to melt the whole batch of the frit.

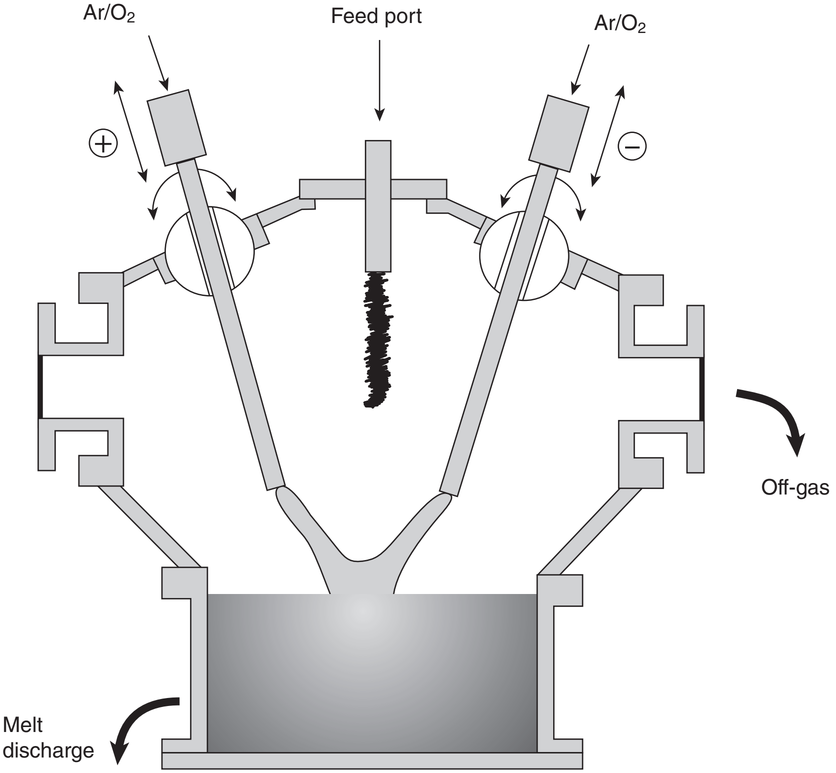

5.6 Schematic view of twin torch and refractory-free furnace (adapted from Poitou *et al.*, 2001).

After complete melting, the torches are moved back from the bath surface to avoid high levels of volatilization. HF power is then maintained at a sufficient level to heat the molten glass at around 1300°C. Glass pouring is possible after the end of the process. (Girold *et al.*, 2006).

Analysis of the material balance during tests on a semi-industrial scale shows good incorporation in glass of the mineral elements of the waste and an appropriate level of off-gas treatment.

5.3 End waste forms and quality control in calcination and vitrification processes

Much work on glass formulation and properties has been conducted worldwide to ensure that vitrified waste will not have problems with durability, phase separation, crystallinity or homogeneity (IAEA TRS 257, 1985). In the USA glass development continues as feed streams to a JHCM are varied, ensuring that the vitrified wastes are more durable than the HLW reference standard Environmental Assessment (EA) glass via application of the Product Consistency Test (ASTM, 2002).

Because analytical works with real radioactive materials are very expensive and dangerous, the main characterization procedures are performed using simulated compositions. The results are combined to produce a database for quality control requirements independent of the process parameters (Ojovan and Lee, 2007). This has an important impact on vitrification plant operation. To guarantee that end waste forms meet quality requirements, control parameters include monitoring of temperatures in the melt pool, the plenum space, discharge areas, refractories and cooling water circuits. Control of the feed rate is typically dictated by the amount of cold cap coverage. Monitoring of the cold cap coverage is difficult but possible using remote infrared cameras or millimeter-wave measuring devices. Melter plenum pressure is controlled to keep a slight vacuum on the melter in order to protect the process cells from contamination.

Improvements in some process parameters are based on step-by-step cold tests, which can be divided into two major stages. First, operational testing has to identify the performance of the process itself to produce the glass product with the claimed requirements. Second, the performance of process equipment must be confirmed for all remote operations.

5.3.1 Advantages and limitations

At the present time, vitrification on an industrial scale is being carried out using the JHCM or AVM process with 'hot' crucible for HLW and CCIM for LILW. The advantages of hot-crucible induction melting technology with respect to JHCM include decreased melt volume and residence time, ability to handle high concentrations of insoluble noble metals, decreased material compatibility issues (i.e., lack of electrodes) and improved resistance to potential electric 'shorting' failures. The primary disadvantages are the relatively short life of the melting pot and corresponding secondary waste generation, and the temperature limitation to ~1150°C, due to the properties of Inconel-690 alloy. Heat transfer to the melt from the hot crucible wall has a limiting influence on the total productivity of the process.

CCIMs have the following benefits: absence of direct contact between melter material and melt because of the formation of a solid skull that protects the crucible material from glass corrosive components; high specific capacity; small size and weight; high-temperature operation (up to 1600°C) that permits the preparation of new, more stable glasses; short occurrence time of the glass charge in the melter; possibility of remote repair and removal; and high crucible lifetime.

Due to higher temperatures, CCIMs may require a potentially more complicated and expensive off-gas system. This problem can be decreased if the solids fed into the melter form a layer on the surface of the molten glass, partly blocking the emission of the volatile components. Dry-feed requires a calciner in the feed system, which makes the operational mode more complicated. Liquid feeding is possible too, but the efficiency of process vitrification in CCIM becomes very low because of great energy loss.

Power consumption in CCIM is more than twice that of JHCM, and cooling water demand is approximately five times that of JHCM.

JHCM operation in full-scale HLW vitrification plants in a number of countries over more than 10 years has demonstrated a high level of reliability and robustness to different feed compositions and process variations. The temperature is well monitored at several points in the melter and is controlled with the electrodes and plenum heaters. Power and utility supply systems for remote operation are well established.

The limitation of JHCM is connected with the presence of corrosive species in the melt due to the performance of refractory materials and electrodes. A relatively large amount of HLW glass may remain in the melter and refractories after use, offering difficulties for size reduction of the melter to minimize secondary waste for disposal.

5.4 Future trends

Future trends, in general, have two main streams. The first is based on the necessity for the development of new, more refractory glass or glass–ceramic waste forms, taking into account the fact that a high content of specific elements (Ce, Mo, Zr, actinide) can not be vitrified essentially in standard borosilicate glass. Production of these new glass families (aluminum silicate, titanium silicate, lanthanum borosilicate, etc.) takes place at temperatures of 1200–1300°C and even higher. The second trend is linked to improvements in melter systems. There are several areas of R&D for improving JHCM technology, which include forced convection via mechanical stirring or bubbling (for improved melt rate and throughput), aggressive cooling of electrodes to allow operating temperatures up to 1350°C (which would in turn allow access to higher waste loadings and improve robustness to feed variations), redesign of bottom drains and melter bottom geometry (to improve tolerance for crystals and noble metals in the melter), and reduction in the thickness of refractories by using shell cooling and provisions for emergency draining (to reduce the disposal costs of failed melters). The potential also exists for developing replacement electrode materials that can operate in the submerged melt pool environment (Fox, 2007, p. 10).

Innovative CCIM are focused in three primary areas: (1) mathematical modeling of a two-frequency integrated inductively heated melter system for optimization of the drain design; (2) development and testing of a melter with an inductively heated bottom draining device for glass melt casting; and (3) design, development, and testing of an innovative system for casting process by pressure control (Lopukh *et al.*, 2009).

5.5 References

Almedia F.J.M., Martinelli J.R., Partiti C.S.M. (2007), 'Characterization of iron phosphate glasses prepared by microwave heating', *Journal of Non-Crystalline Solids*, vol. 353, 4783–4791.

Aloy A.S., Iskhakova O.A., Koltsova T.I., Trofimenko A.V., Jardine L.J. (2001), 'Development and characterization of borosilicate glasses for immobilization of plutonium-containing alkaline sludges', *Mater. Res. Soc. Symp. Proc.*, Vol. 663, 189–198.

Appleton T.J., Colder R.I., Kingman S.W., Lowndes I.S., Read A.G. (2005), 'Microwave technology for energy-efficient processing of waste', *Applied Energy*, Vol. 81, 85–113.

ASTM (2002), 'Standard test methods for determining chemical durability of nuclear waste glasses: the product consistency test (PCT)', ASTM C-1285.

Bagaasen L.M., Hrma P.R., Kim D.-S., Schweiger M.J., Matyas J., Rodriguez C.P., Witwer K.S. (2008), 'Method to reduce molten salt penetration into bulk vitrification refractory materials', *WM'08 Conference*, no. 8275, Phoenix, AZ (CD).

Chauvin E., Ladirat C., Quang R.Do (2009), 'French industrial vitrification plant: 30 years old and still innovating', *Mater. Res. Soc. Symp. Proc.*, Vol. 1193, 249–257.

Day D.E., Wu Z., Ray C.S., Hrma P. (1998), 'Chemically durable iron phosphate glass wasteforms', *Journal of Non-Crystalline Solids*, 241(1), 1–12.

Fleisch J., Gruenewald W., Roth G., Schwaab E., Tobie W., Weishaupt M. (2008), 'Cold test operation of the German VEK vitrification plant', *WM'08 Conference*, no. 8326, Phoenix, AZ (CD).

Fox K.M. (2007), 'Technical comparison of Joule heated ceramic melter and cold crucible induction melter technologies to vitrification of high-level nuclear wastes', SRNL-PSE-2007-00132, p. 16.

Gerdes K.D., Ross S.L. (2009), 'The United States Department of Energy's Environmental Management Program', *Mater. Res. Soc. Symp. Proc.*, Vol. 1193, 645–654.

Girold C., Lemort F., Pinet O. (2006), 'The vitrification as pathway for long life organic waste treatment', *WM'06 Conference*, Tucson, AZ (CD).

Gombert D., Hawkes G., Richardson J.G. (2002a), 'Modeling of cold crucible induction-heated melters', *SPECTRUM Conf. Proc.*, Reno, NV (CD).

Gombert D., Richardson J., Aloy A., Day D. (2002b), 'Cold-crucible design parameters for next generation HLW melters', *WM'02 Conference*, Tucson, AZ (CD).

Grunewald W., Roth G., Tobie W. (2000), 'Cold demonstration of the VEK vitrification technology in full-scale mock-up facility', *WM'00 Conference*, Tucson, AZ (CD).

Guilbeau K., Giordana A., Ramsey W.G., Aloy A., Soshnikov R.A., Shulyak N. (2004), 'Induction-melting technology', *American Ceramic Society Bulletin*, 83(7), 38–40.

International Atomic Energy Agency (1977), 'Techniques for the solidification of high-level wastes', *Technical Reports Series* no. 176, IAEA, Vienna.

International Atomic Energy Agency (1985), 'Chemical durability and related properties of solidified high-level waste forms', *Technical Reports Series* no. 257, IAEA, Vienna.

International Atomic Energy Agency (1992), 'Design and operation of high-level waste vitrification and storage facilities', *Technical Reports Series* no. 339, IAEA, Vienna.

International Atomic Energy Agency (2002), 'Radioactive waste management', STR-314, Vol. 10, IAEA, Vienna, p. 43.

Jantzen C.M., Cadieux J.R. (1991), in *Microwaves: Theory and Applications in Materials Processing*, ed. Clark D.E., Gac F.D. and Sutton W.H., American Ceramic Society, Westerville, OH, pp. 441–449.

Japan Atomic Energy Agency (2008), 'Vitrification melter improvement – Development of long-life high level radioactive liquid waste vitrification melter', http://jolisfukyu.tokai-sc.jaea.go.jp/fukyu/mirai-en/2008/8_1.html

Komarov V.I., Molokhov M.N., Sorokin A.A., Kharitonov K.A., Balashov A.V., Borisov G.B., Volchok Yu.Yu., Nazarov A.V., Khrubasik A. (2005), 'Microwave vitrification of radioactive wastes', *Atomic Energy*, 98(4), 278–283.

Ku H.S., Siores E., Taube A., Ball J.A.R. (2002), 'Productivity improvement through the use of industrial microwave technologies', *Computers and Industrial Engineering*, 42, 281–290.

Lifanov F.A., Ojovan M.I., Stefanovsky S.V., Burcl R. (2003), 'Cold crucible vitrification of NPP operational waste', *Mater. Res. Soc. Symp. Proc.*, Vol. 757.

Lopukh D.B., Roach J.A., Martynov A.P., Chepluk S.I., Vavilov A.V., Richardson J.G. (2009), 'Development of cold crucible induction melter system with an innovative electromagnetically heated bottom draining device for radioactive waste vitrification' Engineering Conferences International (ECI), Charleston, South Carolina (CD) www.engconfint.org.

Mauss B., Raymond R. (2005), 'Status and direction of the bulk vitrification program for the supplemental treatment of low activity tank waste at Hanford', *WM'05 Conference*, Tucson, AZ (CD).

Nuclear Energy Agency (1997), 'Actinide separation chemistry in nuclear waste streams and materials', NEA/NSC/DOC (97) 19.

Ojovan M.I., Lee W.E. (2003), 'Self sustaining vitrification for immobilization of radioactive and toxic waste', *Glass Technology*, 44(6), 218–224.

Ojovan M.I., Lee W.E. (2007), *New Developments in Glassy Nuclear Waste Forms*, Nova Science Publishers, New York.

Perez L.M., Chapman C.C., Mohr R.H., Matlack K.S., Pegg I.L. (2005), 'Development and demonstration of an air bubbler design to meet high-level waste melter production rate requirements of the Hanford waste treatment and immobilization plant', *ICEM'05*, no. 1260, Glasgow, Scotland (CD).

Petitjean V., Fillet C., Boen R., Veyer C., Flament T. (2002), 'Development of vitrification process and glass formulation for nuclear waste conditioning', *WM'02 Conference*, Tucson, AZ (CD).

Poitou S., Fiquet O., Bourdeloie C., Gramondi P., Rebollo F., Girold C., Charvillat J.-P., Boen R., Jouan A., Ladirat C., Nabot J.-P., Ochem D., Baronnet J.-M. (2001), 'Plasma arc and cold crucible furnace vitrification for medium level waste: a review', *Global'01*, Paris.

Riley A., Walker S., Gribble N.R. (2009), 'Composition changes and future challenges for the Sellafield waste vitrification plant', *Mater. Res. Soc. Symp. Proc.*, Vol. 1193, 267–273.

Roach J.A., Lopukh D.B., Martynov A.P., Polevodov B.S., Chepluk S.I. (2008), 'Advanced modeling of cold crucible induction melting for process control and optimization', *WM'08 Conference*, no. 8359, Phoenix, AZ (CD).

Roberts J.S., Strachan C.W., Luey J. (1993), 'Investigation potential for occurrence of molten soil displacement events during in situ vitrification of combustible wastes', *Proc. Symp. Waste Management, WM'93*, Tucson, AZ, Vol. 1, 867–871.

Smith E.C., Diener G.A., Joseph I., Bowan B.W., Pegg I.L. (2005), 'Waste vitrification melter throughput enhancement through increased operating temperature', *WM'05 Conference*, Tucson, AZ (CD).

Sobolev I.A., Dmitriev S.A., Turlak H.A. *et al.* (1996), 'SIA "Radon" experience in radioactive waste vitrification', *Enomar*, Moscow, pp. 1–35.

Sobolev I.A., Dmitriev S.A., Lifanov F.A., Kobelev A.P., Popkov V.N., Polkanov M.A., Savkin A.E., Varlakov A.P., Karlin S.V., Stefanovsky S.V., Karlina O.K., Semenov K.N. (2003), 'High temperature treatment of intermediate-level radioactive wastes – SIA radon experience', *WM'03 Conference*, Tucson, AZ (CD).

Stennett M.C., Hyatt N.C. (2009), 'Microwave processing of glasses for waste immobilization', *Mater. Res. Soc. Symp. Proc.*, Vol. 1124, 147–152.

Sugilal G., Sengar P.B.S. (2008), 'Cold crucible induction melting technology for vitrification of high level waste: development and status in India', *WM'08 Conference*, Phoenix, AZ (CD).

6

Historical development of glass and ceramic waste forms for high level radioactive wastes

C. M. JANTZEN, Savannah River National Laboratory, USA

Abstract: The initial development of borosilicate, aluminosilicate, phosphate and ceramic glass formulations for the solidification of HLW took place in the US, Canada, Europe and the USSR over the course of the 1950s and 1960s. Borosilicate glass formulations were first investigated in the US between 1956 and 1957 by Goldman and colleagues at the Massachusets Institute of Technology (MIT). However, the main bulk of research into the vitrification process was conducted in the UK and Europe in the 1960s. Between 1952 and 1962, Canadian scientists began developing aluminosilicate glass formulations at the Chalk River Nuclear Laboratories (CRNL), and in 1967, Tuthill and others launched research into phosphate waste glasses at Brookhaven National Laboratory (BNL). This chapter describes the research and development process, the advantages and disadvantages of each method, and their various applications.

Key words: borosilicate, aluminosilicate, phosphate, ceramic, glass matrices, vitrification.

6.1 Introduction

Development of glasses for the solidification of HLW began at different times in the US, Canada, Europe, and the USSR. Different glass formulations (borosilicate, aluminosilicate, and phosphate glasses) and processing strategies were developed as discussed in Chapter 9. The borosilicate glass formulations were developed in the US between 1956 and 1957. The aluminosilicate (nepheline syenite based) glass formulations were simultaneously being developed in Canada in 1957. Phosphate-based glasses were the last to be investigated for solidification of nuclear waste. At that time, a systems evaluation of phosphate glasses demonstrated that the positive aspects of processing, e.g. low melting temperatures, were outweighed by other negative processing aspects, e.g. melt corrosivity, and by poor product performance. The aluminosilicate glasses, phosphate glasses, and ceramic waste forms are still being investigated for certain types of nuclear waste because the systems evaluation for these waste forms is favorable under certain conditions. However, repeated systems evaluations of borosilicate waste glass formulations and the associated processing technology have found this family of glasses to be applicable to a wide range of waste compositions

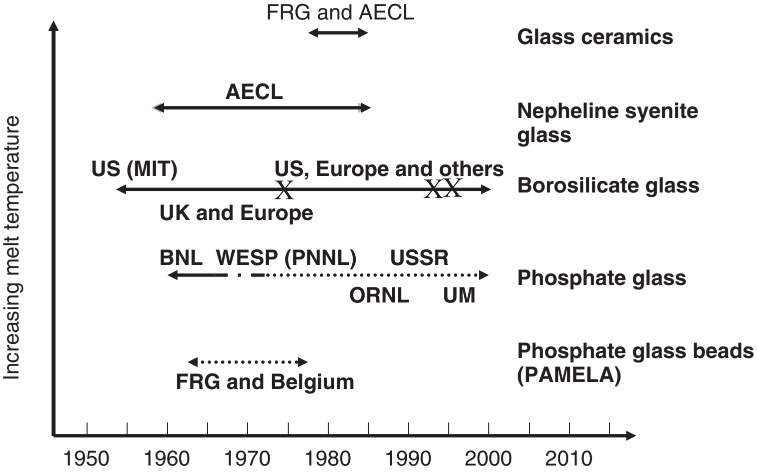

6.1 Waste glass vitrification timeline.

melted by various processing methodologies. The favorable systems evaluations of borosilicate waste glasses have led to their acceptance as the reference nuclear waste form in 10 countries including Canada [1].

Figure 6.1 is an attempt to unify the development of vitreous waste forms by year and country since the late 1950s. The historical development of the glass formulations and the importance of a whole systems evaluation (waste form performance vs. processing aspects) will be summarized below with special reference to the development in the US. Figure 6.1 shows the relative processing temperature of the various glass, glass ceramic, and ceramic waste forms and the timeline of development for each. Solid lines mean active development in the US and/or Canada while dotted lines indicate inactive development of a waste form in the US and/or Canada but active development in other countries. Significant development by certain laboratories is indicated as discussed below.

Borosilicate glasses are alkali-aluminosilicate type glasses which are fluxed with boron. The lower alumina content and the presence of boron lowers the melt viscosity and hence the processing temperature (~1150°C) relative to that of the aluminosilicate glasses. The boron increases the solubility of many waste constituents in the silica-based glass [2] while maintaining thermal and mechanical stability [3] and decreasing chemical durability only slightly [3, 4] relative to the highly durable but more difficult to produce aluminosilicate glasses.

The typical borosilicate waste glasses currently in use for solidification of nuclear waste are quite different from Pyrex or Vycor type borosilicate glasses (Fig. 6.2). Since the borosilicate waste glasses are between 18–25 wt% actinides fission products and other waste species, much of the chemistry is still dominated by the chemistry of the Na_2O–B_2O_3–SiO_2 system. The range

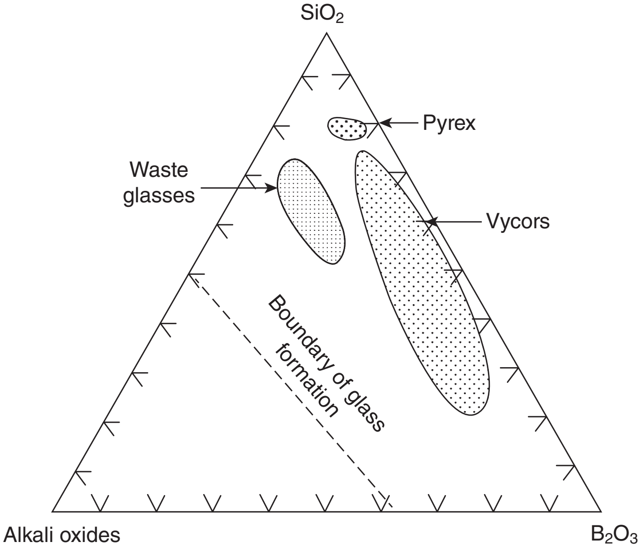

6.2 Pseudoternary phase diagram of the alkali oxide–silica–boron oxide system. Compositional ranges of borosilicate glasses including Pyrex, Vycor and borosilicate nuclear waste glasses are superimposed (after reference 20).

of compositions for commercial and defense borosilicate waste glasses expressed as a function of Na_2O–B_2O_3–SiO_2 are shown on the ternary phase diagram in Fig. 6.2. Note that Pyrex has a higher silica content than the waste glasses and, hence, melts at a higher temperature. The alkali content of the waste glasses is higher than that of Pyrex or Vycor while the boron content overlaps that of some Vycors.

A systems evaluation of the borosilicate waste glasses indicates that these glasses exhibit good chemical durability, thermal stability, mechanical stability and waste solubility while being processed at temperatures of 1150°C which limits the volatility of the radionuclides and hazardous species. The borosilicate waste melts are generally less corrosive than commercial glass melts, such as Pyrex, due to the lower temperature of fabrication. The technology used for commercial waste glass fabrication can, therefore, easily be adapted. Borosilicate glasses exhibit favorable product performance as well as ease of processability.

6.2 Borosilicate glass development in the United States

The initial borosilicate glass formulations were developed in the US between 1956 and 1957 by Goldman and others at the Massachusetts Institute of Technology (MIT) [5–7]. They examined calcium-aluminosilicate porcelain glazes to which B_2O_3 had been added to achieve a pourable glass melting at 1300°C. The quality of these glasses did not suffer from the incorporation of such substances as ZrO_2 and Fe_2O_3 which were present in the nuclear waste solutions. Eliassen and Goldman [6] felt that the most promising vitreous systems for future development were borosilicate based, e.g. $CaO–Al_2O_3–B_2O_3–SiO_2$ and $Na_2O–CaO–Al_2O_3–B_2O_3–SiO_2$.

Although the early borosilicate glass formulations were developed in the US, vitrification process development and testing during the early 1960s was carried out primarily in the UK and Europe [8–10]. In the mid-1960s the Waste Solidification Engineering Prototypes (WSEP) program demonstrated the overall ease of processability and compositional flexibility of borosilicate type glasses [11], and Pacific Northwest Laboratories (PNL) demonstrated the advantages of ceramic Joule-heated melters [8]. Other waste producers in the US such as the Savannah River Site (SRS) built upon both the European and US experience and chose borosilicate glass as the reference solid waste form as early as 1975 [12]. The SRS started up its Joule-heated melter, the Defense Waste Processing Facility (DWPF), in April 1994 and ran simulated waste and frit until radioactive operation started in March 1996. These startup dates are shown in Fig. 6.1 with an 'X' indicating the 1975 decision at SRS to pursue borosilicate glass as a waste form. The West Valley Demonstration Project (WVDP) started operating shortly after the DWPF in 1994 and finished its mission in 2002. The Hanford Vitrification Facility known as the Waste Treatment Plant (WTP) is still under construction.

6.3 Borosilicate glass development in France

Laboratory research on containment matrices for radioactive waste from nuclear energy began in France in 1957. Borosilicate glass quickly proved to be more suitable for incorporating the 40-odd elements created by uranium fission (as well as additives and corrosion products resulting from fuel reprocessing) into a homogeneous matrix.

The first industrial vitrification facility, PIVER (Pilote Verre, a batch vitrification process that did not employ a separate calcination step), began operating in 1969. Before it was shut down in 1972, PIVER produced 164 glass blocks, weighing a total of 12 tons, from 24 m^3 of concentrated fission product solutions containing 6×10^6 Ci. The facility resumed operation a few years later to vitrify HLW solutions arising from the reprocessing of fast breeder reactor fuel, producing 10 glass blocks of 90 kg each with very high specific activity. In 1989, PIVER was named a Nuclear Historic Landmark by the American Nuclear Society.

Faced with increasing demand, research was undertaken in the 1970s to develop a continuous vitrification process to obtain a final glass waste form by first evaporating and calcining the feed solution in a rotary furnace, then melting the calcine with glass frit in an induction-heated metal melter. The Marcoule Vitrification Facility (AVM or Atelier de Vitrification de Marcoule) was commissioned in 1978 to vitrify fission product solutions from the French UP1 reprocessing plant. By the end of 1995, AVM had logged nearly 64,800 hours of operation and vitrified 1920 m^3 of solution containing 401 million curies, producing 857.5 tons of glass in 2412 canisters, each containing 360 kg of glass.

The successful operating record and experience gained with AVM allowed the start-up of a commercial-scale high level waste vitrification plant in France. Two similar facilities, R7 and T7, are on line at the La Hague reprocessing plant. R7 was commissioned in 1989 and T7 in 1992. Fission-product oxides are incorporated in quantities ranging from 12% to 18% of the R7T7 glass package (this value ranges from 6% to more than 20% depending on waste composition and type of glass). In the La Hague vitrification facilities, the metal pot is heated to 1150°C using a 200-kW power generator operating at a frequency of 4 kHz. The glass inside the metal pot is melted by conduction upon contact with the metal wall. Glass can react with metals at the process temperature, with the result that melting pots corrode and must be periodically replaced. They currently have an average lifetime of 5000 hours with R7T7 glass. The melter lifetime has been extended considerably since the vitrification unit was commissioned, however, by modifying the composition of the nickel-based alloy from which the pots are made and by optimizing the management of the thermal power dissipated in the glass during the process. The unit also includes equipment for process off-gas treatment, comprising a particle separator, a condenser, and scrubbing columns.

For future use, the CEA has developed a process in which the glass is melted by induction heating inside a water-cooled crucible. The use of this cold crucible induction melter (CCIM) will allow glass or glass ceramic materials (GCMs) to be produced at higher temperatures and higher melt rates with no risk of corrosion, as the melter shell is made of the same glass and remains at a lower ‘frozen’ temperature. A nonradioactive prototype CCIM melter 55 cm in diameter and 70 cm high has been operating together with a calciner for several years at Marcoule. A unit of this type could advantageously replace the current melter in the future.

6.4 Borosilicate glass development in the United Kingdom

Borosilicate glass has been under development in the UK over the last 40 years, with initial work having been carried out at Harwell in the 1950s. Process development was temporarily halted in the 1960s due to lack of an economic incentive for treating the HLW and a high degree of confidence in the integrity of the HLW storage tanks. Work on the Harvest vitrification process was restarted in the 1970s. In 1981 it was decided to adopt the continuous French AVM melting process instead of the Harvest batch vitrification process in which calcination and vitrification took place in the same reaction vessel.

From 1983 a Full Scale Inactive Facility (FSIF) was constructed and operated by British Nuclear Fuels Ltd at Sellafield to develop the vitrification process for BNFL HLW. A parallel program developed and fine-tuned the glass composition(s) required to vitrify the waste. These programs culminated in the construction, commissioning and active operation of the Waste Vitrification Plant (WVP) at Sellafield in 1991.

The WVP plant consists of a high active (HA) liquor storage and distribution cell, two parallel vitrification lines consisting of vitrification and pouring cells, and container decontamination and monitoring/control cells, and is based on the French AVM procedure. The process incorporates a rotary calciner through which HA liquor is fed and partially denitrated. The calcine is mixed with glass frit (glass beads 1 to 2 mm in diameter) and fed into an elliptical Inconel melter that is inductively heated. In December 2005 a third vitrification line began operation in parallel with the existing two. This allows two vitrification lines to operate while the third line is under maintenance. The first two lines were retrofitted with ‘thick wall’ melters which have increased throughput.

6.5 Aluminosilicate glass development in Canada

Aluminosilicate-based glass formulations were investigated from 1955 to 1962 at the Chalk River Nuclear Laboratories (CRNL) funded by Atomic Energy of Canada Ltd (AECL) [13–15]. These glasses were fused from crushed nepheline syenite rock (abundant in Canada) and mixed with waste at temperatures above 1350°C. The waste being immobilized was a HLW UO_2 fuels recycle waste and the major radionuclides were ^{242}Pu and ^{238}U, but the activity was primarily generated by ^{137}Cs and ^{90}Sr [16–19]. Two sets of glass blocks based on ground nepheline syenite rock with 15% CaO were buried without secondary containers, one in 1959 and one in 1960. This ended the active stage of research and development on aluminosilicate glasses until the blocks were exhumed in 1978 and the chemistry and glass surfaces examined.

The aluminosilicate or nepheline syenite type glasses underwent continued development in Canada from the late 1950s into the 1980s when the exhumed blocks were characterized and studied as indicated in Fig. 6.1. The major advantage of aluminosilicate waste glasses is their excellent chemical durability, thermal stability, and mechanical stability due to the high silica and alumina content. The disadvantages were the high melt temperature of

1350°C which caused volatilization of hazardous species and limited waste loading [2]. Melt corrosivity is comparable to that of commercial Pyrex glass but greater than that of borosilicate glasses due to the higher fabrication temperature of the aluminosilicate glasses. A system evaluation of the aluminosilicate glasses, therefore, indicates that they have superior product characteristics but are difficult to process [20].

A new HLW glass program was initiated in 1976 [21] and focused on interim storage of spent fuel and its immobilization since no spent fuel reprocessing was being considered. The reference waste form examined from 1976 to 1981 was a dilute borosilicate glass with ≤3 wt% fission products to keep the heat of radioactive decay in the canister low. When a new nuclear fuel waste management program was established in 1981 the glass forming systems being investigated were $Na_2O–B_2O_3–SiO_2$ and $Na_2O–Al_2O_3–B_2O_3–SiO_2$ [14, 22, 23].

6.6 Phosphate glass development in the United States, Russia, Germany and Belgium

The major research into phosphate waste glasses in the US was started at Brookhaven National Laboratory around 1967 by Tuthill and others [24]. The delay in the development of phosphate glasses for use in waste disposal has been attributed to the lack of industrial usage of these types of glasses and hence the lack of commercial experience and technology such as exists for the various silica-based glasses [2]. The attractive low melting temperature of the phosphate glasses is offset by the corrosivity of the melt and the ease with which these glasses devitrify [2]. Phosphate glasses were also attractive because molybdenum and sulfate were more soluble than in borosilicate glass [25]. This was particularly applicable to wastes in Germany and hence the Pilot Anlage Mol zur Erzeugung Lagerfähiger Abfälle (PAMELA) process [26] was developed in the early 1960s. In this process, phosphate glass is formed as small beads which are then placed in a metal matrix in a steel canister (see Fig. 6.1). The small size of the beads, plus the high thermal conductivity provided by the metal matrix, ensure that the phosphate glass does not devitrify.

Development of the phosphate beads in Germany began in the early 1960s and subsequent solidification in a continuous metallic melter at Eurochemic in Mol, Belgium, continued until the late 1970s. About 1976 Karlsruhe and Eurochemic changed to a borosilicate waste glass produced by a Joule-heated ceramic melter, after experience in the glass industry and at PNL [8] had demonstrated that this type of melter had a higher capacity per physical size, produced a more uniform glass, and had fewer problems with volatile losses than other melting techniques. The time interval for development of phosphate beads in a metal matrix was, therefore, relatively short (Fig. 6.1).

In 1966 the WSEP program was initiated at PNL. WSEP was a pilot plan designed for a radioactive demonstration of three solidification processes, two for borosilicate glass and one for phosphate glass [11]. Eleven canisters of radioactive phosphate waste glass were solidified. The results of the WSEP program showed that phosphate glass has several shortcomings when compared with borosilicate glasses. These shortcomings included the following: (1) high ruthenium volatility during preparation (denitration) of the liquid waste slurry; (2) additions of ferric nitrate and sodium hydroxide required to adjust the melting point and melt viscosity; (3) extreme corrosivity of the phosphate melt which required the use of platinum melters; (4) extreme corrosivity of the phosphate melt which placed limitations on the temperature of the melt poured into the canisters; (5) low solubility of certain waste components including alumina, alkaline earth oxides, sulfates and fission products; (6) segregation of fission products in the glass; (7) rapid thermal devitrification at temperatures above 500°C; and (8) a factor of 1000 increase in the leach rate of the glass after devitrification.

At the conclusion of the WSEP program in 1972 phosphate glasses were abandoned for waste solidification in the US as indicated in Fig. 6.1. In 1984 lead-iron phosphate (LIP) glasses were proposed as a new, very stable and easily prepared medium for the immobilization of all types of high-level liquid waste [23, 27–30]. The developers demonstrated that the corrosion rate of the LIP waste glass was 10^2–10^3 times lower than the corrosion rate of a comparable borosilicate waste glass. In addition, they determined that: (1) melt temperatures could be as low as 800°C since the glasses had low melt viscosities in the 800–1050°C range; (2) the glasses did not devitrify up to temperatures as high as 550°C; and (3) the glasses were not adversely affected by large doses of gamma radiation in water at 135°C. The developers suggested that the improved chemical durability and thermal stability of this phosphate glass over previous WSEP formulations were due to the Fe_2O_3 content of the glass [28–30] and the structural role of iron in the glass which strengthens the cross-bonding between the polyphosphate chains [30, 31]. A highly stable waste form is realized when the iron concentration is adjusted to a content of $Fe_2O_3/(PbO{\cdot}P_2O_5) \sim 9$ wt% and the PbO content is between 45 and 66 wt%. Comparing the LIP glass formulations to WSEP phosphate glasses demonstrates that the LIP glasses have higher PbO content and a lower waste loading. The iron and phosphate levels are, however, comparable. Likewise, melt corrosivitiy [29, 30, 32, 33] and incompatibility with certain canister materials [32, 33] were observed. Low waste component solubility even at elevated temperatures (>1150°C) produced non-homogeneous glasses which gave leach rates comparable to those of borosilicate glass [32, 33]. Thermal stability was poor as evidenced by rapid thermal devitrification above 550°C [34].

Iron phosphate (Fe-P or IPG) glasses were studied from about 1995 to the present at the bench scale. Most of the research and development was championed at the University of Missouri in Rolla in the US while pilot-scale testing has been performed in Russia. Some of the characteristics of FeP glasses that are improvements over previous phosphate glass formulations are as follows:

- Excellent chemical durability [35–37]
- High solubility [37, 38] for many heavy metals (uranium, chromium, zirconium, cesium, molybdenum, etc.), noble metals, rare earths and sulfate
- Low melting temperatures (950–1100°C), rapid melting rates (a few hours), tolerance of a wide range of furnace atmospheres (oxidizing to reducing), and high melt fluidity (viscosity typically below 1 poise)
- Low corrosion of oxide refractories [39] commonly used in glass melting furnaces, such as high alumina, zircon, and mullite
- Low corrosion of Inconel alloys [40] commonly used in glass melting furnaces
- High waste loadings, typically between 25 and 50 mass%, depending on the waste.

The only other work continuing on phosphate glasses for waste disposal is in the USSR. Both borosilicate and phosphate glasses were studied from the mid-1950s until the startup of the Mayak facility in 1987. A ceramic melter without precalcination is used [41]. Glass systems including Na_2O–Al_2O_3–P_2O_5, Na_2O–Al_2O_3–B_2O_3–SiO_2, and Na_2O–CaO–Al_2O_3–B_2O_3–SiO_2 glasses were studied [23], but the aluminophosphate formulations have been pursued since the 1980s and into the present for the incorporation of high sodium–high aluminum type wastes [42].

6.7 Ceramic waste form development in various countries

Although ceramic waste forms have also been examined as hosts for the solidification of nuclear waste, these forms were difficult to process and not as flexible toward variations in waste composition as glass [25, 43–49]. The objective of the development of ceramics was to provide a waste form with chemical, thermal, and mechanical stability that was superior to glass. However, during ceramic processing, intergranular glassy phases often formed in the ceramic materials, especially when alkali-containing wastes were processed. This intergranular glass limited the product stability and durability [50–53]. However, both the historical development and the systems evaluation of glass ceramics and ceramics as solid waste forms parallel those of the vitreous waste forms and will be briefly discussed.

The concept of immobilizing the radioactive elements of nuclear waste in an assemblage of mineral phases was originally introducted by Hatch [54] at Brookhaven National Laboratory in 1953. The feasibility of making a ceramic of natural, mineralogically stable phases was demonstrated by McCarthy and Davidson [43, 44] and Roy [55, 56] at Pennsylvania State University between 1973 and 1976. Since that time, a number of other mineralogic–ceramic assemblages have been developed. Among them are the Sandia titanate-based ceramic [45], the Australian titanate-based ceramic 'SYNROC' [46, 57, 58], the silicate–phosphate supercalcine ceramics [59], the alumina-based tailored ceramics [23, 60], and the Pu pyrochlores [61]. Silicate glass ceramics were developed in the mid-1970s in Germany [49]. Silicate and phosphate glass ceramics were also developed in the USSR [62], silicate glass ceramics in Japan [63], and titanium aluminosilicate glass ceramics in Canada [64].

Since the turn of the twenty-first century, the public's interest in sources of clean energy has led to increased interest in advanced nuclear power production, often referred to as the 'nuclear renaissance'. The development of advanced waste forms is a necessary component of this new strategy. Therefore, advanced nuclear waste forms can be designed for robust disposal strategies. This renaissance has led to renewed interest in forming glass composite materials (GCMs) [65, 66] by JHM, AJHM, CCIM or HIPing which allow crystals to form in a glassy matrix. Implicit in ceramic and glass ceramic waste form development is the idea of using additives to 'tailor' the waste chemically so that the desired host radionuclide phases are produced after consolidation.

6.8 References

1. F.L. Parker, R.E. Broshears, and J. Pasztor, *The Disposal of High-Level Radioactive Waste*, Vol. I, Beijer Institute, Stockholm, Sweden (October 1984).
2. J.E. Mendel, 'The Storage and Disposal of Radioactive Waste as Glass in Canisters', US DOE Report PNL 3946, Battelle Pacific Northwest Laboratories, Richland, WA (December 1978).
3. M.J. Plodinec, G.G. Wicks, and N.E. Bibler, 'Borosilicate glass as a matrix for the immobilization of Savannah River Plant waste', pp. 336–345 in *The Technology of High-Level Nuclear Waste Disposal*, Vol. 2, ed. P.L. Hofmann, US Department of Energy, Washington, DC (1982).
4. C.M. Jantzen and M.J. Plodinec, 'Thermodynamic model of natural, medieval, and nuclear waste glass durability', *J. Non-Cryst. Solids*, 67, 207–233 (1984).
5. M.I. Goldman, J.A. Servizi, R.S. Daniels, T.H.Y. Tebbutt, R.T. Burns, and R.A. Lauderdale, 'Retention of fission products in ceramic-glaze-type fusions', *Proc. 2nd UN International Conference on Peaceful Uses of Atomic Energy*, Geneva, 1958, 1827, United Nations, New York, 27 (1958).
6. R. Eliassen and M.I. Goldman, 'Disposal of high-level wastes by fixation in fused ceramics', in *Hearings on Industrial Radioactive Waste Disposal*, Vol. 3, ed.

R.L. Doan, US Government Printing Office, Washington, DC, 1966–1979 (1959).

7. C.A. Mawson, *Management of Radioactive Wastes*, Van Nostrand, Princeton, NJ, 196 pp. (1965).
8. J.L. McElroy, W.J. Bjorklund, and W.F. Bonner, 'Waste vitrification, a historical perspective', in *The Treatment and Handling of Radioactive Wastes*, ed. A.G. Blasewitz, J.M. Davis, and M.R. Smith, Springer, New York, 171–177 (1982).
9. J.R. Grover and B.E. Chidley, 'Glasses Suitable for the Long Term Storage of Fission Products', British Report no. AERE-R 3178, Atomic Energy Research Establishment, Harwell, UK (1960).
10. W. Bocola, A. Donato, and G. Sgalambro, 'Survey of the present state of studies on the solidification of fission product solutions in Italy', p. 449 in *Symposium on the Management of Radioactive Wastes from Fuel Reprocessing*, International Atomic Energy Agency, Vienna (1972).
11. J.L. McElroy, K.J. Schneider, J.N. Hartley, J.E. Mendel, G.L. Richardson, R.W. McKee, and A.G. Blasewitz, 'Evaluation of WSEP (Waste Solidification Engineering Prototypes) High Level Waste Solidification Processes', *Waste Solidification Program Summary Report*, Vol. 11, US DOE Report BNWL-1667, 529 pp. (July 1972).
12. J.A. Kelley, 'Evaluation of Glass as a Matrix for Solidification of Savannah River Plant Waste', US DOE Report DP-1382, E.I. DuPont de Nemours and Co., Savannah River Laboratory, Aiken, SC, 28 pp. (May 1975).
13. J.M. White and G. Hahaie, 'Ultimate Fission Product Disposal: The Disposal of Curie Quantities of Fission Products in Siliceous Materials', AECL-391, 18 pp. (March 1955).
14. K.B. Harvey, 'The Development of Borosilicate Glasses as Media for the Immobilization of High-Level Recycle Wastes, 1. Literature Survey', AECL Technical Record TR-239, 73 pp. (January 1984).
15. R.W. Durham, 'Disposal of fission products in glass', *Second Nuclear Engineering and Scientific Conference*, AECL no. 476, 354–358 (1957).
16. W.F. Merritt, 'The Leaching of Radioactivity from Highly Radioactive Glass Blocks Buried Below the Water Table: Fifteen Years of Results', Atomic Energy of Canada Ltd, Report no. AECL-5317, Chalk River, Ontario, Canada (1976).
17. A.R. Bancroft and J.D. Gamble, 'Initiation of a Field Burial Test of the Disposal of Fission Products Incorporated into Glass', Atomic Energy of Canada Ltd, Report no. AECL-718, Chalk River, Ontario, Canada (1978).
18. T.W. Melnyk, F.B. Walton, and L.H. Johnson, 'High level waste glass field burial test: Leaching and migration of fission products', *Nucl. Chem. Waste Management*, 5, 49–62 (1984).
19. J.C. Tait, W.H. Hocking, J.S. Betteridge, and G. Bart, 'Field burial results and SIMS analysis of the Chalk River glass blocks', *Advances in Ceramics, Vol. 20: Nuclear Waste Management II*, ed. D.E. Clark, W.B. White, and A.J. Machiels, American Ceramic Society, Columbus, OH, 559–565 (1986).
20. C.M. Jantzen, 'Systems approach to nuclear waste glass development', *J. Non-Cryst. Solids*, 84(1–3), 215–225 (1986).
21. J. Boulton, 'Management of Radioactive Fuel Wastes: The Canadian Disposal Program', Report no. AECL-6314 (1978).
22. F.P. Sargent, R.B. Lyon, and L.H. Johnson, 'Status of the Canadian Nuclear Fuel Waste Management Program', *WM86*, Vol. 1, 73–83 (1986).

23. W. Lutze and R.C. Ewing, *Radioactive Waste Forms for the Future*, North-Holland, Amsterdam, 778 pp. (1988).
24. E.J. Tuthill, G.G. Weth, L.C. Emma, G. Strickland, and L.P. Hatch, 'Phosphate glass process for disposal of high level radioactive wastes', *Ind. Eng. Chem. Proc. Des. Dev.*, 6(3), 314–321 (1967).
25. W. Lutze, J. Borchardt, and A.K. De, 'Characterization of glass and glass ceramic nuclear waste forms', in *Scientific Basis for Nuclear Waste Management I*, ed. G.J. McCarthy, Plenum Press, New York, 69–81 (1979).
26. W. Heimerl, 'Solidification of HLW solutions with the PAMELA process', *Proc. Int. Symp. on Ceramics in Nuclear Waste Management*, CONF-790420, US DOE, Cincinnati, OH, 97–101 (1979).
27. B.C. Sales and L.A. Boatner, 'Lead-iron-phosphate glass: a stable storage medium for high-level nuclear waste', *Science*, 226, 45–48 (1984).
28. B.C. Sales and L.A. Boatner, 'Physical and chemical characteristics of lead-iron-phosphate nuclear waste glasses', *J. Non-Cryst. Solids*, 79, 83–116 (1986).
29. B.C. Sales and L.A. Boatner, 'Lead phosphate glass as a stable medium for the immobilization and disposal of high-level nuclear waste', *Mater. Lett.*, 2(4B), 301–304 (1984).
30. B.C. Sales and L.A. Boatner, 'Physical and Chemical Characteristics of Lead-Iron-Phosphate Nuclear Waste Glasses', US DOE Report ORNL-6168, Martin Marietta Energy Systems, Inc., Oak Ridge, TN (May 1985).
31. B.C. Sales and L.A. Boatner, 'Structural properties of lead-iron-phosphate glasses', *J. Non-Cryst. Solids*, 71, 103–112 (1985).
32. C.M. Jantzen, 'Investigation of lead-iron-phosphate glass for SRP waste', in *Advances in Ceramics, 20*, ed. D.E. Clark, W.B. White and A.J. Machiels, American Ceramic Society, Westerville, OH, 157–165 (1986).
33. L. Kahl, 'Hydrolytic durability of lead-iron-phosphate glasses', in *Advances in Ceramics, 20*, ed. D.E. Clark, W.B. White and A.J. Machiels, American Ceramic Society, Westerville, OH, 141–148 (1986).
34. L.A. Chick, L.R. Bunnell, D.M. Strachan, H.E. Kissinger, and F.N. Hodges, 'Evaluation of lead-iron-phosphate glass as a high level waste form', in *Advances in Ceramics, 20*, ed. D.E. Clark, W.B. White and A.J. Machiels, American Ceramic Society, Westerville, OH, 149–156 (1986).
35. D.E. Day, X. Yu, G.J. Long, and R.K. Brow, 'Properties and structure of sodium-iron phosphate glasses', *J. Non-Cryst. Solids*, 215(1), 21–31 (1997).
36. M. Mesko, D.E. Day, and B.C. Bunker, 'Immobilization of CsCl and SrF_2 in iron phosphate glass', *Waste Management*, 20(4), 271–278 (2000).
37. G.K. Marasinghe, M. Karabulut, X. Fang, C.S. Ray, and D.E. Day, 'Vitrified iron phosphate nuclear waste forms containing multiple waste components', *Ceramic Transactions*, 107, 115–122. American Ceramic Society, Westerville, OH (2000).
38. M. Karabulut, G.K. Marasinghe, C.S. Ray, D.E. Day, O. Ozturk, and G.D. Waddill, 'X-ray photoelectron and Mossbauer spectroscopic studies of iron phosphate glasses containing U, Cs, and Bi', *J. Non-Cryst. Solids*, 249(2–3), 106–116 (1999).
39. F. Chen and D.E. Day, 'Corrosion of selected refractories by iron phosphate melts', *Ceramic Transactions*, 93, 213–220, American Ceramic Society, Westerville, OH (1999).
40. D.E. Day and C.W. Kim, 'Reaction of Inconel 690 and 693 in Iron Phosphate Melts: Alternative Glasses for Waste Vitrification', Final Report for Contract DE-FG02–04ER63831 Project 0010255 (2005).

41. D.J. Bradley, *Behind the Nuclear Curtain: Radioactive Waste Management in the Former Soviet Union*, Battelle Press, Columbus, OH, 716 pp. (1997).
42. N.E. Brezneva, A.A. Minaev, and S.N. Oziraner, 'Vitrification of high sodium-aluminum wastes: Composition ranges and properties', in *Scientific Basis for Nuclear Waste Management I*, ed. G.J. McCarthy, Plenum Press, New York, 43–50 (1979).
43. G.J. McCarthy, 'Quartz-matrix isolation of radioactive wastes', *J. Mater. Sci.*, 8, 1358–1359 (1973).
44. G.J. McCarthy and M.T. Davidson, 'Ceramic nuclear waste forms: I. Crystal chemistry and phase formation', *Bull. Am. Ceram. Soc.*, 54, 782–786 (1975).
45. R.O. Schoebel, 'Stabilization of high level waste in ceramic form', *Bull. Am. Ceram. Soc.*, 54(4), 459 (1975).
46. A.E. Ringwood, V.M. Oversby and S.E. Kesson, 'SYNROC: Leaching performance and process technology', in *Proc. Seminar on Chemistry and Process Engineering for High-Level Liquid Waste Solidification*, ed. R. Odoj and E. Merz, Julich Conference 42, vol. 1, 495–506 (1981).
47. P.E.D. Morgan, D.R. Clarke, C.M. Jantzen, and A.B. Harker, 'High-alumina tailored nuclear waste ceramics', *J. Am. Ceram. Soc.*, 64(5), 249–258 (1981).
48. J.B. Dunson Jr., A.M. Eisenberg, R.L. Schuyler III, H.G. Haight Jr., V.E. Mello, T.H. Gould Jr., J.L. Butler, and J.B. Pickett, 'Assessment of Processes, Facilities, and Costs for Alternative Solid Forms for Immobilization of SRP Defense Wastes', US DOE Report DP-1625, E.I. DuPont de Nemours & Co., Savannah River Laboratory, Aiken, SC (March 1982).
49. A.K. De, B. Luckscheiter, W. Lutze, G. Malow, and E. Schiewer, 'Development of glass ceramics for the incorporation of fission products', *Ceramic Bulletin*, 55, 500–503 (1976).
50. D.R. Clarke, 'Preferential dissolution of an intergranular amorphous phase in a nuclear waste ceramic', *J. Am. Ceram. Soc.*, 64(6), C89–C90 (1981).
51. Z. Zhang and M.L. Carter, 'An X-ray photoelectron spectroscopy investigation of highly soluble grain-boundary impurity films in hollandite', *J. Am. Ceram. Soc.*, 93(3), 894–899 (2010).
52. W.J. Buykx, K. Hawkins, D.M. Levins, H. Mitamura, R. St C. Smart, G.T. Stevens, K.G. Watson, D. Weedon, and T.J. White, 'Titanate ceramics for the immobilization of sodium-bearing high-level nuclear waste', *J. Am. Ceram. Soc.*, 71(8), 678–688 (1988).
53. J.A. Cooper, D.R. Cousens, J.A. Hanna, R.A. Lewis, S. Myhra, R.L. Segall, R. St C. Smart, P.S. Turner, and T.J. White, 'Intergranular films and pore surfaces in Synroc C: Structure, composition, and dissolution characteristics', *J. Am. Ceram. Soc.*, 69(4), 347–352 (1986).
54. L.P. Hatch, 'Ultimate disposal of radioactive wastes', *Am. Sci.*, 41, 410–421 (1953).
55. R. Roy, 'Ceramic science of nuclear waste fixation', *Bull. Am. Ceram. Soc.*, 54, 459 (1975).
56. R. Roy, 'Rational molecular engineering of ceramic materials', *J. Am. Ceram. Soc.*, 60, 350–363 (1977).
57. A.E. Ringwood, *Safe Disposal of High Level Nuclear Reactor Wastes: A New Strategy*, Australian Nuclear University Press, Canberra, Australia, 1–64 (1978).
58. A.E. Ringwood, S.E. Kesson, N.G. Ware, W.O. Hibberson, and A. Major, 'The SYNROC process: a geochemical approach to nuclear waste immobilization', *Geochemical Journal*, 13, 141–165 (1979).

59. G.J. McCarthy, J.G. Pepin, D.E. Pfoertsch, and D.R. Clarke, 'Crystal Chemistry of the Synthetic Minerals in Current Supercalcine-Ceramics', US DOE Report Conf-790420, 315–320 (1979).
60. C.M. Jantzen, J. Flintoff, P.E.D. Morgan, A.B. Harker, and D.R. Clarke, 'Ceramic nuclear waste forms', in *Proc. Seminar on Chemistry and Process Engineering for High-Level Liquid Waste Solidification*, ed. R. Odoj and E. Merz, Julich Conference 42, vol. 2, 693–706 (1981).
61. P.E. Raison, R.G. Haire, T. Sato, and T. Ogawa, 'Fundamental and technological aspects of actinide oxide pyrochlores: Relevance for immobilization matrices', in *Scientific Basis for Nuclear Waste Management XXII, Symp. Proc.*, Vol. 556, Materials Research Society, Warrendale, PA, 3–10 (1999).
62. A.A. Minaev, S.N. Oziraner, and N.P. Prrokhorova, 'The Use of Glass-Ceramic Materials for the Fixation of Radioactive Wastes', US DOE Report Conf-790420, 229–232 (1979).
63. N. Ninomiya, T. Yamanaka, T. Sakane, M. Hora, S. Nakamura, and S. Kawamura, 'Diopside glass-ceramic material for the immobilization of radioactive wastes', in *Proc. Seminar on Chemistry and Process Engineering for High-Level Liquid Waste Solidification*, ed. R. Odoj and E. Merz, Julich Conference 42, vol. 2, 675–693 (1981).
64. R.A. Speranzini and P.J. Hayward, 'Development of sphene-based ceramics for disposal of some canadian wastes', *Adv. Ceram.*, 8, 273–281 (1984).
65. W.E. Lee, M.I. Ojovan, M.C. Stennett, and N.C. Hyatt, 'Immobilisation of radioactive waste in glasses, glass composite materials and ceramics', *Advances in Applied Ceramics*, 105(1), 3–12 (2006).
66. M.T. Peters, R.C. Ewing, and C.I. Steefel, 'GNEP Waste Form Campaign Science and Technology and Modeling and Simulation Program: Roadmap With Rationale and Recommendations', GNEP-M50-3040-303 (March 2008).

7

Decommissioning of nuclear facilities and environmental remediation: generation and management of radioactive and other wastes

M. LARAIA, International Atomic Energy Agency (IAEA),
Austria

Abstract: This chapter focuses on radioactive and other waste generated from the decommissioning of nuclear facilities. The chapter first reviews the whole process of decommissioning from a facility's permanent shutdown to site release, and strategic options. The chapter then highlights the inventory of decommissioning waste and how it can be minimized at the design stage and during operation. Typical techniques used in decommissioning are then presented with details of how they affect the generation and management of waste. Environmental remediation is illustrated as an important component of decommissioning. Trends, sources of additional information and a list of references complete the chapter.

Key words: decommissioning, decontamination, dismantling, environmental remediation, waste generation.

7.1 Introduction

All industrial facilities, whether or not they contain radioactive materials, will eventually face decommissioning. There is expertise and experience in all countries of the taking out of service, dismantling and demolishing of disused industrial and other facilities. However, those responsible for nuclear and related facilities face the particular challenges associated with managing their radioactive inventory. These not only include meeting normal engineering, economic and industrial safety goals but may also necessitate satisfying nuclear regulators and other stakeholders on the impact of decommissioning on the economy, health, safety and environment of the local area. Although the decommissioning industry cannot yet be regarded as fully mature in terms of delivering a standard package, the key elements of strategy development, waste treatment, dismantling and de-licensing have been separately demonstrated as achievable.

7.2 What is decommissioning?

A definition of nuclear decommissioning based only on industrial aspects of the process is as follows: 'The work required for the planned permanent retirement of a nuclear facility from active service' (IAEA 1983). In recognition of the actual or potential hazards associated with a shutdown facility, a safety-driven definition was developed by the IAEA, resulting eventually in the following: 'Administrative and technical actions taken to allow the removal of some or all of the regulatory controls from a facility (except for a repository or for certain nuclear facilities used for the disposal of residues from the mining and processing of radioactive material, which are "closed" and not "decommissioned")' (IAEA 2007a). Incidentally, this definition limits the scope of this chapter to decommissioning of nuclear facilities, leaving out mining and milling tailings or large territories contaminated by nuclear accidents (e.g. Chernobyl). It is currently recognized that the two main objectives of decommissioning are to render the site permanently safe and to restore it, as far as practicable, for reuse (WNA 2006).

7.2.1 Decommissioning strategies

The first step towards a successful decommissioning project is to develop an early strategy that is both acceptable to the regulator, and achievable in terms of programme and cost. This must then be followed by the appropriate survey and preparatory work in order to specify the task, and then to select the most effective approach while minimizing waste handling. The starting conditions and desired outcomes must be clearly defined and the decommissioning operations correctly sequenced.

The IAEA publications, e.g. IAEA (1999a), refer to three primary decommissioning options that are to be considered in implementing a decommissioning strategy for a particular site or facility. These primary options are immediate dismantling, deferred dismantling and entombment. Combinations or variations of these three primary options may also be considered.

Immediate dismantling

Immediate dismantling is the strategy in which the equipment, structures, and parts of a nuclear facility containing radioactive contaminants are removed or decontaminated to a level that permits the facility to be released for unrestricted use, or with restrictions imposed by the regulatory body, and activities begin shortly after permanent termination of operations. It implies prompt and complete decommissioning and involves the removal and processing of all radioactive material from the facility to another new or existing nuclear facility for either long-term storage or disposal.

Deferred dismantling

Deferred dismantling (sometimes called safe storage or safe enclosure) is the strategy in which parts of a nuclear facility containing radioactive contaminants are either processed or placed into such a condition that they can be safely stored and maintained until they can subsequently be decontaminated and/or dismantled to levels that permit the facility to be released for other use.

Entombment

Entombment is the strategy in which radioactive contaminants are encased in a structurally long-life material until the radioactivity decays to a level permitting unrestricted release, or release with restrictions imposed by the regulatory body, of the nuclear facility. Because radioactive material will remain on the site, the facility will eventually become designated as a near-surface waste disposal site.

7.2.2 Decommissioning planning

Ideally, an outline plan for decommissioning should be prepared during the early stages of construction or licensing (IAEA 1999a), otherwise the task will require commencement during the operational lifetime of the facility. Ideally, detailed planning and preparation of a final decommissioning plan for a large facility should begin some years before its permanent shutdown, although in practice, work on the decommissioning plan is sometimes delayed until operation has already ceased.

A structured approach to planning for decommissioning is essential. Before the final decommissioning plan can be drafted, a number of preparatory tasks should be undertaken. Most of these tasks will be taken forward in the period of transition from operation to decommissioning of the facility (IAEA 2004a, 2004b).

The decommissioning plan should be viewed as a 'living document' which may require refinements or amendments as decommissioning proceeds. The decommissioning plan should evolve from a preliminary plan to a detailed one with respect to changed circumstances, operational experience and information reflecting improved technology. IAEA (2005) provides a description of the contents of a final decommissioning plan.

A timely application should be made to the relevant regulatory body to obtain any necessary permission to dispose of decommissioning waste, especially where disposal routes are identified that were not previously utilized when disposing of waste from operational activities. The solution must of course include any necessary waste transport containers, vehicles and associated infrastructure.

7.2.3 Decommissioning implementation

It is desirable that a dedicated project team, adequate resources and suitable training are arranged before any significant planning work is commenced. With regard to selecting appropriate resources for implementing the decommissioning plan, key staff should include members of the team that operated the facility that is to be decommissioned. This minimizes the chances of a surprise incident due to work being performed on an 'unknown' hazard. However, contractors are generally essential for larger decommissioning projects, and the right mix of contractors and operational staff is often the best recipe to the success of decommissioning (IAEA 2000a).

7.3 Generation of decommissioning waste

As a result of decommissioning activities, a wide range of materials arise. Some of them will be radioactive; some will continue to have an economic value and/or are in a form that can be recycled or reused. Others will have little or no economic value, and these are the wastes that have to be disposed of, or which must be stored if no accepted method of disposal is available. Waste minimization can be considered a strategy for avoiding, as much as possible, the production of these undesirable by-products. Where by-products are unavoidable, steps are required to minimize their volumes (IAEA 2001).

It has long been recognized that waste management is a critical aspect of the decommissioning process. Managing many thousands of tonnes of decommissioning waste is not trivial and requires a dedicated organization. Besides, the cost of radioactive waste management is a significant element of the overall decommissioning costs and may dominate in some cases. In Germany it has been estimated that about 60% of the decommissioning costs are attributable to the costs of waste management, although the materials declared as radioactive waste comprise only some 2% of the materials associated with decommissioning activities. This fact alone indicates the need for an accurate radiological characterization of materials and of maximizing opportunities for reuse or recycle of materials and minimizing the amount of materials requiring treatment, storage and disposal as radioactive waste (NEA 2002).

As regards the large quantities of waste containing only small concentrations of radioisotopes and suspect waste, there are substantial incentives to maximize use of the principle of clearance. Firstly, sustainable development considerations demand maximum reutilization of non-renewable resources by way of direct reuse of equipment or buildings and by the recycling of useful materials. Furthermore, the intrinsic value of the materials for recycling, in the case of metals, or for use in construction in the case of concrete, is considerable (NEA 2002). Also the disposal of conventional (non-radioactive) waste is generally much cheaper than that of radioactive waste (IAEA 2004c). Despite the inherent benefits of the clearance policy, the costs of reclaiming the scrap, equipment and other materials can be significant and include *inter alia* the costs (and extra exposures) of labour resulting from decontamination and monitoring to ensure compliance with clearance criteria; the costs of administering the recycling programme; and the costs and other implications of managing the secondary waste associated with these practices. In addition these costs will increase as the clearance levels decrease owing to greater measurement difficulty at lower activity levels and the substantially greater decontamination effort required for achieving lower levels.

In other words, clearance is not a panacea. It may or may not be profitably applied to the disposition of one or more waste streams from the decommissioning of a given nuclear facility. Other strategies such as restricted release, nuclear reuse, storage for decay and release, on-site disposal or disposal as very low-level radioactive waste (VLLW) may be more cost-effective than clearance in some circumstances and for defined types and amounts of decommissioning waste. Ideally those in charge of decommissioning should be given access to a variety of options to maximize flexibility and cost-effectiveness of the disposition strategies (IAEA 2008).

7.3.1 Design and operation to facilitate decommissioning

Features that will benefit or facilitate decommissioning vary in importance. Some will be inherent in the design and would be introduced for operational and maintenance reasons and some will be introduced as representing ‘good practice’. Some factors, however, will have cost and programme implications for design and construction and sometimes for operation and plant reliability as well. A selection of the most important features relevant to waste management is highlighted below (IAEA 2007b, 2010).

Minimization of activated products

The need to minimize trace elements that will give rise to activation products from neutron flux has been well known in the nuclear industry for many decades. There are, however, still attempts to minimize this even further. Cobalt and nickel are particular problems for when high-strength corrosion-resistant steels are necessary.

Rigorous contamination control

There are numerous reports of lessons learned regarding the decommissioning of contaminated facilities where it was emphasized that good working practices could have avoided generation of waste and costly clean-up activities. In many instances decommissioning has been delayed by the discovery of unexpected contamination in inaccessible places. Surface coatings are now routinely used as a barrier against penetration of contamination.

Modular design for easy removal

It has been suggested that design and construction in modular form would greatly facilitate removal and reduce exposure to operators. It is appreciated that modular construction is likely to be more costly and may reduce reliability or integrity if prone to leakage or other faults and a compromise must be reached.

Segregation of contaminated items

There are likely to be a number of plant items and components that are delivered to site as large intact items such as heat exchangers, cooling pumps and motors. The ability to handle these as a unit may facilitate removal during decommissioning. This will require attention to the access pathways such as airlocks. Quite often pumps have integral motors and can become contaminated internally. This leads to mixed (radioactive and chemically toxic) waste due to the various complex materials used for electrical wiring and insulation and may become a waste management problem. Lubricating oils should only be used in non-contaminating situations to avoid the managing of radioactive oil.

One-piece removal

In general, intact removal of large components, e.g. reactor vessels or steam generators, has the potential of reducing occupational exposures and the volumes of waste. There have been a number of decommissioning projects where the whole reactor vessel has been removed intact, in Germany, the USA and elsewhere (Fig. 7.1). It may not always be possible to give adequate access for intact removal of components due to requirements of the design, considerations of safety, or the integrity of the shielding or containment. There may also be layout complications or inadequate access for lifting equipment.

7.1 One-piece removal of steam generator from Bruce NPP, Canada.

Ducts and piping

Numerous problems have been reported concerning the build-up of crud and contamination in ducting systems and piping due to lack of attention to physical configuration and layout. Particular problems are low areas or inverts where deposits can build up and become radiological hot-spots. The problem can be exacerbated when facilities are shut down for long periods and there is a delay in the start of decommissioning. Sludge and deposits can solidify in pockets in the piping. In addition to the above, the embedding of pipes and ducts in walls and floors should be avoided as far as possible. If necessary, for dose reduction and avoiding the spread of contamination, concentric pipes or ducts or similar confinement should be provided. Leak monitors should also be provided. Where it is necessary to seal penetrations through walls and floors, design features should be devised to ease final removal without the need to cut concrete or masonry structures. Cutting of concrete to remove embedded contaminated pipes or ducts usually requires hands-on action by operators with the consequent risk of spreading contamination and increasing exposure to radiation.

Limiting the provision of underground services and equipment

It is recognized that not all underground services can be avoided but they could be minimized or alternatives adopted. It is possible that these could corrode and/or develop leaks after many years of operation and some

7.2 Removal of underground piping at Argonne National Laboratory, USA.

would be almost impossible to remove or decontaminate (Fig. 7.2). A preferred arrangement, beneficial to decommissioning, would be to convey contaminated drains in double-walled pipes to removable sumps or alternatively, instead of gravity drainage, to arrange to pump liquids through accessible piping to higher-level tanks.

7.3.2 Inventory and waste characterization

An essential component of successful decommissioning planning and implementation is the acquisition of a thorough, adequate facility inventory and physical/radiological characterization. At permanent shutdown, the inventory of a reactor consists of corrosion/activation and contamination products. Non-reactor facilities will have only contamination. For neutron-induced activation, characterization is best carried out through a combination of theoretical models and sampling to validate the model accuracy.

7.3 Underground characterization tool.

Sampling is essential since models have a lot of unavoidable uncertainties (e.g. neutron fluxes at various locations and trace impurities in structures). Such methodologies are described in detail in IAEA (1998).

Even at facilities where extensive surveys have been routinely performed over the years, there will be a need to gather additional characterization data in view of decommissioning. Locations where waste collects over time (sumps, drain traps, etc.), cracks in surfaces (e.g., floor joints, surface cracks, penetrations through walls), roof areas, leakage to the foundations, sub-soil or groundwater, underground piping (Fig. 7.3), floor coverings, and where past clean-up actions have 'fixed' residual radioactivity in place – all of these are places where unexpected contamination can be present and increase the waste inventory.

The site characterization phase of a decommissioning effort is very important in order to:

- Identify what areas can be eliminated from the scope of the decommissioning
- Provide data needed to evaluate decontamination alternatives (e.g., the depth of penetration of contamination into structural surfaces, the ease of removing the contamination from surfaces, the presence of problem materials such as asbestos)
- Establish the amounts and types of waste that will be generated (e.g., what other constituents may be present in the waste), evaluate how they might be treated, and collect data needed by waste disposal facilities
- Set the total cost of the clean-up effort (IEM 2001).

7.4 Waste from dismantling of nuclear facilities

During decommissioning of nuclear facilities, large quantities of materials and equipment and some buildings become available for recycling or reuse or for disposal if economic and practical considerations prevent recycling or reuse. Typical categories of decommissioning waste include:

- Radioactive waste which has no economic or practical value. This waste would be sent for disposal as low level waste (LLW) or very low level waste (VLLW), depending on contamination levels, national policy and classification of radioactive waste, available infrastructure, and other factors and constraints. High level waste is relatively modest in amounts for reactors but more significant for nuclear fuel cycle facilities.
- Components that are inactive or have been decontaminated to bring their activity to below clearance levels. These items can be released for unrestricted use if it is economical and practical or sent for disposal as inactive waste (e.g. in a municipal landfill site). Depending on their chemical/toxic contents, the latter (mixed waste) may be subject to special disposal provisions.
- Components whose activity levels can be reduced to levels acceptable for restricted nuclear use or restricted destination or use in the non-nuclear domain (e.g. for smelting, for recycling under predetermined conditions, or for controlled disposal).
- Materials and waste kept in storage for radioactive decay and declassification to below clearance levels or from LLW to VLLW. This interim strategy can also be pursued pending the availability of one or more of the three above-mentioned options.

In many countries there are strong economic incentives to minimize the generation and release of decommissioning waste. It should be clear, however, that recycle and reuse practices are a typical example of industrial activities that are governed by multiple, conflicting factors. Consequently, some level of optimization is an inherent part of determining whether recycle and reuse practices could be applied (IAEA 2000b).

A wide range of techniques and equipment for use in the decontamination and demolition of concrete and metal structures during the decommissioning of nuclear facilities is given in IAEA (1999b). An overview of cutting techniques is given in Tables V and VI of that report for general orientation of the reader. Conditioning techniques for solids can include compaction, incineration, encapsulation within a solid matrix, direct packaging, dismantling and segmenting, melting, and chemical and biodegradation. Relevant sections of IAEA (1999b) are highlighted below with focus on waste management.

7.4.1 Mechanical cutting techniques

These are techniques whereby the direct action of the tool on the workpiece produces a cut. This is achieved by the tool fracturing, cleaving or eroding the workpiece surface. With the exception of grinding and explosive cutting, these techniques produce easily handled secondary waste streams which can be collected by local extraction systems. They also produce far fewer airborne fumes than thermal techniques, thus simplifying viewing of the cutting operation, although cutting speeds are generally lower.

Shears

Shears can be manually, pneumatically, hydraulically or electrically actuated and are used for segmenting metal and crushing concrete. In terms of construction there are three basic types, namely: (1) a two-bladed device; (2) a blade and anvil device; and (3) demolition shears. Shearing produces either no secondary waste or waste in the form of discrete sections, punched from the workpiece, which can be readily handled and retrieved. The drawbacks of shearing are the size of the tools compared with their relative cutting capacity, and the fact that the action of the shear tends to crush the component being cut. Crimp shears, as well as cutting the tube, also crimp it, thereby sealing the end of the tube and preventing the escape of loose contamination from internal surfaces.

Power nibblers

A nibbler is a punch-and-die cutting tool that normally reciprocates at a high rate, with the punch moving against the die. The process is not influenced by internal stresses in the workpiece and can be considered a mature technology.

Mechanical saws

Sawing techniques make use of shearing processes, normally produced when a hard cutting edge bears against a softer material which is to be separated. Mechanical sawing machines range in size from small hand-held hacksaws to very large and heavy band-saws capable of cutting steam generators (Fig. 7.4). There are three main mechanical saw types: reciprocating saws (including hacksaws and guillotine saws), band-saws and circular saws. They produce narrow kerfs and minimal heat and the cutting residues are in the form of large particles which can be easily collected. Also there is minimal production of aerosols. One disadvantage is that cutting speeds are relatively slow by comparison with techniques such as plasma arc.

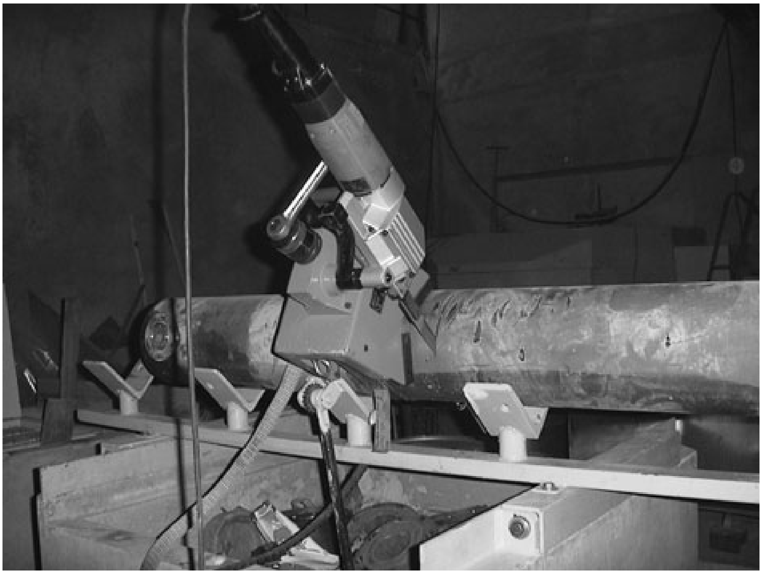

7.4 Sabre saw cutting pipe.

Orbital cutters

Orbital cutters can be manually actuated devices or self-propelled units that cut as they move around the outside or inside circumference of a pipe or vessel. They are an effective means of segmenting pipes and circular vessels. Three different types of tool are used for orbital cutting: swaging cutters, lathe tools and milling tools.

Abrasive cutting wheels, blades, wires and core drills

These are electrically, hydraulically or pneumatically powered wheels, beads or chain links containing abrasive held in a semi-rigid supporting matrix. Typical abrasives used include aluminium oxide, silicon carbide or diamond and these cut the workpiece by local shearing at multiple cutting points (Fig. 7.5). Abrasive cutters can be used either dry or with a coolant, such as water, which is often recirculated to reduce secondary waste volumes.

Explosives

Explosive dismantling or cutting is well known and the three main types of charge employed are conventional explosives, shaped explosives, and linear shaped charges.

7.5 Use of diamond saw at ORIS decommissioning project (France).

7.4.2 Thermal cutting techniques

In general, the main advantages of thermal techniques over other methods such as mechanical cutting are that:

- The cutting speeds are generally faster
- Remote operation is often possible because the equipment is lightweight
- The deployment system has to accommodate only small reaction forces during cutting as the tools do not require physical contact with the workpiece.

The main disadvantage is the production of aerosols, dust and dross which create issues of concern with respect to worker and environmental protection, visibility problems (mainly in underwater applications), and the production of large volumes of primary (owing to the thickness of the kerfs) and secondary waste. An additional drawback with the cutting of contaminated components which are to be decontaminated is the danger of the contamination being incorporated within the solidified slag on the cut workpiece. For underwater cutting, it is necessary to have efficient water filtration processes to maintain water quality and to use filters working in series with decreasing holding capacity but with increasing performance in order to minimize the total waste volume. For cutting in air, it is necessary to have efficient air filtration, either locally or in the cutting containment, and to have regenerative pre-filtration processes to protect the main ventilation filters, which can be rapidly blinded by the aerosols produced.

Plasma arc cutting

Plasma arc cutting is based on the establishment of a direct current arc between a tungsten electrode and the surface of a conducting metal. The arc is created by ionizing a gas (plasma gas) and then blowing the ionized plasma towards the surface of the workpiece in order to form a conductive pathway down which the main plasma current passes. The heat generated by the impingement of the arc on the workpiece causes local melting, and the force created by the velocity of the plasma gas stream blows the molten metal away from the melt pool, thereby creating the cut.

Flame cutting

Flame cutting is a well-established and mature technology and uses a flowing mixture of a fuel gas (acetylene, hydrogen, propane) or fuel vapour (gasoline), and oxygen, which are mixed and ignited to produce a high-temperature flame. In the case of carbon steels the flame is brought into contact with the surface of the workpiece, which is allowed to heat up before the cutting oxygen is injected into the centre of the flame, oxidizing the workpiece. As iron oxide melts at a lower temperature than the parent metal, the oxide melts and is blown from the melt pool by the flame, thereby producing a cut.

Powder injection flame cutting

Powder injection flame cutting is a variant of the standard flame cutting process reported above. Powder injection flame cutting involves the introduction of iron or a mixed iron/aluminium powder directly into the central oxygen jet of the fuel gas flame, causing an exothermic reaction. This increases the flame temperature and gas momentum, allowing the cutting of a variety of materials such as thick sections of stainless steel and concrete.

Thermic lance

The thermic lance consists of an iron pipe packed with a combination of steel, aluminium and magnesium wires through which a flow of oxygen gas is maintained. The lance cuts are achieved by thermite reactions at the tip of the lance in which all constituents are consumed.

7.4.3 Electrical cutting techniques

Electrical cutting techniques are based on metal evaporation, in contrast with thermal cutting techniques which melt the metal. Electrical techniques do not generate any metal flow in the melt pool but they do generate a larger volume of aerosols, and hydrosols under water, compared with thermal techniques.

Electro-discharge machining (EDM)

EDM is based on the principle of the thermo-mechanical erosion of metals through the accurate control of sparks. It is applicable to all materials which possess sufficient electrical conductivity and is ideally suited to underwater applications.

Consumable electrode

The consumable electrode technique consists of a wire being continuously fed from a coil into the kerf, an arc being initiated by a short-circuit between the wire and the workpiece. Three methods are in use:

- Oxygen jet cutting (mainly with mild steel wire)
- Water jet cutting (all metals)
- Water jet gouging (all metals).

Contact arc metal cutting

In the contact arc metal cutting process, the electrode is moved continuously towards the workpiece until contact is made between the two, thereby causing a short-circuit. The electrode is then fed into the material to be cut. The high density of the current in the arc heats the workpiece, causing the material to evaporate.

Arc saw cutting

Arc saw cutting uses a circular, toothless saw blade to cut conductive metals without making physical contact with the workpiece. This is achieved by maintaining a high-current electric arc between the blade and the material being cut. It is effective in cutting high-conductivity materials.

7.4.4 Emerging technologies

The following paragraphs present two techniques that are currently being developed and have not been fully evaluated as to their cost-effectiveness.

Liquefied gas cutting

Liquefied gas cutting is similar in principle to water jet cutting, except that the carrier medium is a liquefied gas. The perceived advantages of this method include lack of a secondary waste stream, favourable economics, and the absence of hazards from explosion, fire or oxidation.

Laser cutting

Laser cutting is a process by which a laser beam is used to heat locally a metal beyond its melting point, thereby cutting it. The technique can cut almost any material but is currently limited in its technical performance and by the high capital cost of the equipment.

7.5 Waste from decontamination for decommissioning purposes

An overview of many of the techniques and equipment used for decontamination and demolition of concrete and metal structures during the decommissioning of nuclear facilities was published by the IAEA in 1999 (IAEA 1999b). It should be noted first that decontamination is not a must. The selection of an inappropriate decontamination method may even add constituents to the waste that will create waste management issues that did not exist prior to the start of the project. One obvious example is the addition of hazardous constituents resulting in generation of a mixed waste. For example, the use of an organic solvent to remove contaminated paint layers from walls may seem like the most efficient thing to do, but it will surely result in the generation of a waste type that is significantly more difficult to dispose of. The alternative use of a water-based solvent, even though it might require more effort to implement, may actually save money in the long run. And one should not forget the acceptance criteria for the waste disposal facility. Most of them will not accept materials that contain substances like standing liquids, chelating agents and biodegradable materials.

As a general orientation to the reader, Tables I–IV of IAEA (1999b) indicate typical decontamination techniques and their main applications.

The tables also direct the reader to relevant sections of that report where general information on, and references related to, experience in the use of a given technique are provided. Conditioning and treatment techniques for decontamination liquids can include bituminization, drying, evaporation, cementation and incineration. In some cases pre-treatment of decontaminants is required to get to a chemical form compatible with subsequent processes. The following description is mostly an elaboration from IAEA (1999b) with a focus on waste generation and management. Another useful reference on decontamination is EPA (2006). It should be noted that many proprietary technologies exist and their omission here does not reflect adversely on the capabilities of any of these processes.

7.5.1 Chemical decontamination

Chemical solutions are generally most effective on non-porous surfaces. The choice of decontamination agents is based upon the chemistry of the contaminant, the chemistry of the substrate and the ability to manage the waste generated during the process. Many chemicals are hazardous substances due to their corrosivity (Section 7.6). A short review of chemical decontamination systems is provided in the following.

Strong mineral acids

The main purpose of these is to attack and dissolve metal oxide films and lower the pH of solutions in order to increase solubility or ion exchange of metal ions. Typical strong mineral acids include nitric acid, sulphuric acid, sometimes in combination with cerium(IV) ions, phosphoric acid (though the resulting waste may create a difficult treatment problem), and, more recently developed for decommissioning, fluor boric acid and fluor nitric acid.

Acid salts

The salts of various weak and strong acids can be used in place of the acids themselves or, more effectively, in combination with various acids to decontaminate metal surfaces. Possible salts include sodium phosphates and polyphosphates, sodium bisulphate, sodium sulphate, ammonium oxalate, ammonium citrate, sodium fluoride, etc.

Organic acids

The use of organic acids is widespread in the nuclear industry for decontamination, mainly during plant operation, and to a lesser extent for decommissioning activities. Examples include formic acid, oxalic acid, oxalic peroxide and citric acid.

Bases and alkaline salts

Caustic compounds are used both by themselves and in solution with other compounds to remove grease and oil films, to neutralize acids, to act as surface passivators, to remove paint and other coatings, to remove rust from mild steel, to act as a solvent for species that are soluble at high pH, and as a means of providing the right chemical environment for other agents, mainly oxidizing ones. Examples include potassium hydroxide, sodium hydroxide, sodium carbonate, trisodium phosphate, and ammonium carbonate.

Complexing agents

Complexing agents form stable complexes with metal ions, solubilize them, and prevent their redeposition out of solution. Problems may occur with the conditioning if the secondary waste contains complexing agents, i.e. solidification of concrete and stability of resins.

Detergents and surfactants

Detergents are effective, mild, all-purpose cleaners for treating all facility surfaces, equipment, clothes and glassware. They are not effective in dealing with metal corrosion and long-standing contamination. Surfactants are used as wetting agents, detergents and emulsifiers.

Organic solvents

Solvents are used in decontamination for removing organic materials, for example grease, wax, oil and paint, from surfaces and for cleaning clothes.

Multiphase treatment processes

Multiphase treatment processes combine a variety of chemicals and processes to achieve a more effective decontamination and are widely used. A few of these processes are described in IAEA (1999b) and they include techniques such as: (1) reducing–oxidizing (Redox) agents; (2) low oxidation state of metal ions (LOMI); (3) alkaline permanganate alone or followed by ammonium citrate, citric acid or oxalic acid; (4) chemical oxidizing/reducing decontamination (CORD) and PWR oxidizing decontamination (POD) multistep processes; (5) nitric acid, permanganate and hydrofluoric acid; and (6) strong oxidizing decontamination process.

Foam decontamination

Foam, such as that produced by detergents and wetting agents, is used on its own or as a carrier for chemical decontamination agents. This process is well developed and widely used, especially for large components with complex shapes or large volumes. It can be applied to surfaces in any orientation and produces low volumes of secondary waste.

Chemical gels

Chemical gels are used as carriers of chemical decontamination agents and are sprayed or brushed onto a surface, allowed to work, then scrubbed, wiped, rinsed or peeled off. This method is effective in situations where long contact times are required, together with the need to minimize secondary waste. Gel spraying has been found to be a good process for dealing with beta/gamma emitters on mild steel pipes with simple geometry.

Decontamination by pastes

Pastes are widely used for treating metal surfaces, particularly stainless steel. They consist of a filler, a carrier, and an acid or mixture of acids as the active agent. A variation on this method involves the inclusion of an abrasive within the paste. Mechanical action with the abrasive assists in breaking down surface films, increasing the effectiveness of the chemical reagents.

7.5.2 Mechanical decontamination

In general, mechanical decontamination methods can be used on any surface where contamination is limited to near-surface material. The following list represents the current summary status of each technique.

Flushing with water

As a decontaminant, water acts by dissolving chemical species or by eroding and flushing loose debris from the surface. Flushing with water, which can be used for areas that are too large for wiping or scrubbing, involves flooding a surface with hot or cold water, followed by water collection. Processing of large amounts of contaminated water and the potential for spreading contamination are drawbacks of this technique.

Dusting/vacuuming/wiping/scrubbing

Dusting, vacuuming, wiping and scrubbing involve the physical removal of dust, aerosols and particles from building and equipment surfaces using common cleaning techniques. Suction cleaning is most useful as a pre-treatment for removing large quantities of loose contaminants. Specially designed vacuum cleaners incorporating air filtration systems are widely used.

Strippable coatings

The strippable coating technique consists of a two-stage process: (1) the application of a polymer and decontaminant mixture to a contaminated surface, and (2) the removal of the stabilized polymer layer after setting. It is applicable to a wide range of contaminants and materials, with the best results achieved on large non-porous surfaces. This technique can also be used as a fixative for contamination control purposes in order to simplify future dismantling. It produces limited amounts of (solid) secondary waste.

Steam cleaning

Steam cleaning combines the solvent action of hot water with the kinetic energy effect of blasting. It is recommended for removing contamination from complex shapes and large surfaces, even if grease or similar substances are present. Secondary waste volumes produced by the process are relatively low as the steam can be collected by vacuum extract, and condensed.

Abrasive cleaning

This process uses an abrasive medium such as plastic, glass or steel beads, or grit such as garnet, soda or aluminium oxide. It is used to remove contamination from metal surfaces such as structural steel components and hand tools and also from concrete surfaces and coatings. In the case of concrete surfaces and coatings, a significant amount of the base material is also removed. This process is most effective on flat surfaces and can also be used on 'hard to reach' areas such as ceilings or behind equipment. The process produces comparatively large amounts of secondary waste. The decontamination process can be carried out wet or dry, with the abrasive medium being driven against the surface by mechanical means, e.g. a vibrating bed for small objects (also known as vibratory finishing), or blasted onto the surface using water or compressed air as the propellant.

Sponge blasting

Sponges made of water-based urethane, when blasted onto a surface, create a scrubbing effect by expanding and contracting. An 'aggressive' grade of sponge, impregnated with abrasives, can be used to erode material such as paints, protective coatings and rust.

CO_2 blasting

Carbon dioxide blasting is a variation of grit blasting, in which CO_2 pellets are used as the cleaning medium. The technique has proven effective with plastics, ceramics, composites and stainless steel, although soft materials can be damaged by the process and brittle materials may shatter. One advantage of the process is that the bulk of the secondary waste is in the form of a gas.

High-pressure liquid nitrogen blasting

High-pressure liquid nitrogen blasting is a variation of grit blasting whereby abrasive is injected into a liquid nitrogen jet, the jet propelling the grit onto the surface to be decontaminated. The contamination is removed by the embrittlement induced by the liquid nitrogen and the abrasive action of the grit. Secondary waste is airborne.

Wet ice blasting

Wet ice blasting is a variation of grit blasting where a compressed air jet is used to propel a mixture of water and ice crystals onto the surface to be decontaminated. This technique will remove coatings and some fixed surface contaminants but will not remove more than the surface layer from concrete. As secondary waste, water carrying contamination will be easier to treat than chemicals.

High-pressure and ultra-high-pressure water jets

High-pressure water processes use a pressurized water jet to remove contamination from the surface of the workpiece, the contamination being removed by the force of the jet. Pressures can range from 10^5 Pa to more than 10^8 Pa, the pressures and flow rates being optimized for individual requirements. Recirculation and treatment systems can also be used to minimize secondary waste production. Typical applications include the cleaning of inaccessible surfaces such as the interiors of pipes, structural steelwork and cell interiors.

Grinding/shaving

Grinding/shaving uses coarse-grained abrasives in the form of either water-cooled or dry diamond grinding wheels or multiple tungsten carbide surfacing discs. It is recommended for use where thin layers of contamination need to be removed.

Scarifying, scabbling and planing

Scarifying, scabbling and planing are used to abrade the surface of concrete structures to remove contamination. One method uses scabblers, consisting of several pneumatically operated piston heads, to strike simultaneously a concrete surface. Another method is a needle gun, which is used on both concrete and steel surfaces and consists of uniform sets of needles several millimetres long, which are pneumatically driven. These processes are very effective for removing the thin contaminated layer from the surface of concrete.

Milling

Metal milling uses rotating cutters to shave off layers of material and is most effective where there are a large number of similarly shaped items, or large areas, requiring decontamination.

Drilling and spalling

The drilling and spalling technique involves drilling holes into which a hydraulically operated spalling tool having an expandable tube is inserted. A tapered mandrel is then hydraulically forced into the hole to spread the 'fingers' and spall off the concrete. It is mainly applicable to concrete and is recommended for removing contamination which penetrates a few centimetres below the surface.

Expansive grout

Expansive grout is used as a dismantling technique but can also be used for decontamination through its ability to remove a thick layer of contaminated concrete.

Paving breaker and chipping hammer

Equipment such as the paving breaker and the chipping hammer is primarily used in demolition activities and is also referred to as a 'jackhammer'. It is mainly used to remove surface contamination, and the surface left on completion of operations may be very rough.

7.5.3 Other established decontamination techniques

Detailed descriptions and applications for each of the following techniques can be found in IAEA (1999b) with further references to the sources of information. Thermo-chemical decontamination techniques have been in use for over a decade in the Russian Federation. Thermo-chemical techniques were noted in IAEA (1999b) as emerging and have now remarkable results to report.

Electro-polishing

Electro-polishing is generally an anodic dissolution technique where a controlled amount of material is stripped from the surface of the workpiece along with the contamination. The process works for any conductive metal, providing protective surface coatings are not present, but the choice of electrolyte is important. The components are decontaminated following removal by immersing them in a bath of fluid or treated *in situ* using closed-circuit systems. The electrolyte can be filtered and recycled and the small amounts of contaminated residues treated separately.

Ultrasonic cleaning

In ultrasonic cleaning, high-frequency energy is converted into low-amplitude mechanical energy, i.e. vibrations. The vigorous scrubbing action produced by the cavitations of a cleaning solution is then imparted to a submerged object. This technique is usually applied to small objects with primarily loose deposits and adhered contamination. It is not applicable for concrete or for materials which absorb ultrasonic energy.

Melting

To some extent, melting can be considered a decontamination technique. In reality it is a technique with a threefold purpose. While the main goal of the process is the recycling of metals, simultaneous decontamination of the metal occurs during melting because many of the radioactive isotopes separate from the melt and concentrate in the slag. Other isotopes volatilize. Melting also provides a means of volume reduction and this aspect is of growing interest as waste disposal costs increase.

Thermo-chemical treatment technologies

Thermo-chemical treatment technologies are intended for decontamination of metals, asphalt and concrete, and treatment and conditioning of specific types of radioactive and toxic waste. Thermo-chemical processing uses the energy of exothermic reactions in a mixture of radioactive or hazardous waste with powder metal fuels (PMF). Generally, the PMF consist of combustible powder metals, oxygen-containing components and some additives. In decontamination this technology is particularly suitable when the radioactive contamination is strongly bonded in the near-surface layers where conventional decontamination methods cannot efficiently remove the radionuclides. Thermo-chemical decontamination is based on thermal treatment of a superficial layer of contaminated material by the heat generated from combustion of a layer of PMF covering the surface. The heat volatilizes most of the radionuclides, which are then trapped by the resulting slag layer that is formed as a result of PMF combustion (Ojovan 2004).

7.6 Problematic decommissioning waste

The scope of this section is to review the available experience and information concerning the management of hazardous and toxic waste generated during the decommissioning of nuclear facilities. The information presented below is mostly elaborated and excerpted from IAEA (2006). Graphite is dealt with separately.

7.6.1 Beryllium

Beryllium metal or beryllium oxide is used for the moderators and reflectors of many research reactors. The principal concern is the toxic and carcinogenic effects caused by the inhalation of airborne particulates. Current practice for the management of the beryllium metal and beryllium oxide components generated during decommissioning is their interim storage awaiting final disposal. These components are placed in cans and the void between the component and the can is filled with quartz sand, which ensures the mechanical stability of the packaged waste. It is not recommended to directly immobilize beryllium in cement, since it reacts with water in the basic cementitious matrices, leading to high levels of hydrogen gas generation and volume expansion.

7.6.2 Sodium and sodium–potassium alloy

Sodium or sodium–potassium alloy waste in the nuclear industry, including decommissioning activities, is closely associated with the development of the liquid metal fast breeder reactor. Besides the risk associated with the manipulation of radioactive products, nuclear alkali metal waste generates specific risks due to its chemical properties. The reactions of sodium and potassium with water, air and oxygen are generally violent and produce hazardous by-products such as hydrogen and caustic products. Alkali metal from reactor main circuits, for which the difficulties encountered are in general associated with the large quantities involved, must be transferred into a chemically stable form, with the resulting question of how to handle large quantities of the resulting reaction products.

7.6.3 Lead

Lead is widely used in nuclear facilities as a shielding material in the form of bricks, sheets, wool or shot. In addition, lead-based paints and primers were routinely used during the construction of many facilities. The principal health concern in the decommissioning of nuclear facilities is the inhalation of lead dust. If lead cannot be decontaminated for recovery and reuse, it is disposed of as radioactive waste. As a solid it can easily be incorporated into a cement matrix for disposal or used as shielding in a waste container.

7.6.4 Cyanide

Cyanide is a carbon–nitrogen chemical unit that combines with many organic and inorganic compounds. Different types of cyanide-containing material are quite often used in the nuclear industry, in particular in waste management practices, e.g. for the selective removal of caesium from various liquid waste streams. There are significant long-term health effects of cyanide. Alkaline chlorination is the most widely used method for the destruction of cyanides. This process is suitable for destroying free dissolved hydrogen cyanide and for oxidizing all simple and some complex inorganic cyanides in aqueous media. An obvious disadvantage of this method is that it requires the storage of large quantities of hazardous chlorine gas or hypochlorite solutions.

7.6.5 Decontamination chemicals

A general description of typical decontamination chemicals is given in Section 7.5. The major hazard with the use of acids is their corrosivity, causing severe damage to human tissue. Simple processes involving neutralization and filtration of reagents are often sufficient to remove the heavy metals and radioisotopes that precipitate out of solution; the liquid waste stream can then be discharged. The corresponding sludge waste stream can be immobilized in a cementitious matrix and stored pending disposal.

7.6.6 Asbestos

Asbestos is the name of a family of naturally occurring minerals that consist of silicates and varying amounts of other elements. Each asbestos mineral forms long, thin needle-like fibres. Reactor pressure vessels and nuclear piping were commonly insulated with material containing asbestos. Asbestos is only a concern when the fibres become airborne, because it is only when the fibres are present in the air that people can inhale them. The most significant medical problems are asbestosis, lung cancer, mesothelioma and other cancers. The removal of contaminated asbestos from piping, vessels, walls, etc., has to be carried out by an authorized specialized firm. After removal, the contractor places the asbestos and any contaminated material into sealed heavy-duty, labelled plastic bags. 'Wrap and cut' refers to a method of asbestos abatement. This method is used when a facility component, such as a length of piping with asbestos-containing material on it, is first wrapped in plastic sheeting. The entire wrapped component is then removed from the building.

7.6.7 Polychlorinated biphenyls

A commonly realized problem during decommissioning is the occurrence of polychlorinated biphenyls (PCBs). Due to their superior technical properties and their low cost, PCBs were widely used. PCBs are a group of very stable organic compounds, and because of this they are persistent in the environment and the food chain. PCBs are soluble in lipids and therefore are enriched in lipid tissue when incorporated. PCBs are suspected to be carcinogenic. During decommissioning the initial removal of PCB-containing material and its processing are the biggest problems with respect to the personal protection of workers from exposure to these types of material. Once PCB-containing waste is removed it should be incinerated at temperatures exceeding 1200°C.

7.6.8 Graphite

Although not a toxic material comparable to the elements described above, dismantling of graphite components can be a serious decommissioning problem in reactors having significant amounts of graphite. Its flammability should be taken into account when considering cutting techniques. This is of particular concern where the possibility of stored Wigner energy exists, and where an uncontrolled temperature rise could occur. Dismantling of graphite elements may produce airborne particulates and surface dust, which can be limited by using containment, ventilation and filtration systems. Disposal of graphite can be a special problem due to the very long half-life of C^{14} and contamination by fission and activation products. Incineration will release C^{14} to the atmosphere, resulting in global irradiation, although at very low levels. Other techniques have been proposed such as in-depth disposal and/or high-integrity confinement.

7.7 Environmental remediation as a decommissioning component

'Remediation' refers to any measures to reduce the radiation exposure from existing contamination of land areas (IAEA 2007a). Decommissioning and remediation activities are subject to some common driving forces that influence the ability of decommissioning and remediation programmes to achieve predetermined end-states (i.e. facility or site reuse). In order to achieve optimization of available resources, it is necessary that the goals of individual decommissioning and remediation activities are aligned and integrated. As compared to decommissioning waste that would be predominantly metallic and concrete waste, remediation may generate large quantities of contaminated soil. Recent plant design trends aim at facilitating decommissioning, which often provide for easier land remediation as well. For instance, pipework is not put underground, where it is difficult to monitor and repair (Section 7.3.1). In the case of the older nuclear facilities such (chronic) events may have led to the contamination of the surrounding soils, the remediation of which may generate large volumes of waste see IAEA (2009).

This section presents particulars on environmental restoration technologies (control and treatment). The technologies addressed can be categorized as follows:

- In situ treatment
- Removal of contamination
- Ex-situ treatment.

Details of these technologies can be found in IAEA (1999c).

7.7.1 In-situ remediation technologies

In-situ remediation technologies for control or treatment of soils and groundwater are increasingly being investigated because they offer the potential for:

- Significant cost reduction of clean-up by eliminating or minimizing excavation, transportation and disposal of waste
- Reduction of health impacts on workers and the public by minimizing exposure to waste during excavation and processing
- Significant reduction in ecological impacts
- Remediation of inaccessible sites, including deep sub-surfaces and in, under and around buildings.

In-situ technologies can be subdivided into three major groups:

1. Containment technologies (surface caps, cut-off walls, bottom barriers, hydraulic control measures)
2. Stabilization/immobilization technologies (in-situ encapsulation, in-situ compaction)
3. Treatment technologies (biological treatment, physical–chemical treatment, thermal treatment).

7.7.2 Materials removal technologies

- Removal of vegetation
- Removal of surface soil (standard or remote excavation, cryogenic removal, dust control, etc.).

7.7.3 Ex-situ treatment technologies

- Physical processes (physical retrieval, overpacking/repackaging/redrumming, screening, soil washing, high-gradient magnetic separation, solidification, vitrification/ceramics, incineration, filtration/ultra-filtration, reverse osmosis/membrane processes, solar evaporation)
- Chemical processes (chemical/solvent extraction, heap leaching, enhanced soil washing, enhanced soil leaching, chemical precipitation, ion exchange, electrodialysis, adsorption, aeration)
- Biological processes.

7.8 Future trends

In recent times, some countries (e.g. France and Spain) have developed disposal facilities and other provisions for very low level waste (VLLW), which is going to simplify the dismantling of nuclear facilities (Fig. 7.6). See

7.6 Disposal operations at a very low level waste facility.

also Section 7.3. The VLLW category allows inexpensive disposal of most decommissioning waste and is therefore an incentive to immediate, total dismantling. A recent IAEA report (IAEA 2008) describes VLLW, restricted release modes and other opportunities facilitating the management and release of slightly contaminated decommissioning waste.

If no suitable disposal facilities for the amounts and categories of waste are available, then the following options exist:

- Maintain the facility in safe storage
- Dismantle the facility, condition the waste and store in appropriate waste stores.

A major strategic change should be noted here. In former times, safe storage of the waste was not considered to be an alternative strategy to the utilization of a disposal site for decommissioning waste. The picture is different now, in that several countries lacking a disposal site have resorted to, or are planning to resort to, safe storage of their decommissioning waste. One such country is Germany.

It should be noted that disposal facilities now exist in many countries, e.g. France, Spain, the UK and the USA. This may have contributed to a general trend towards immediate dismantling. However, other countries do not have waste disposal sites and therefore have decided for long-term safe storage of their shutdown facilities. Even countries having some waste disposal options may not have disposal options for all types of decommissioning waste. For example, the reactor building of Vandellos NPP in Spain is being kept in a dormancy condition, one of the arguments being the unavailability of graphite disposal stores; so the Vandellos graphite is kept in segregated vaults inside the reactor building. Plans for graphite disposal are well underway in France.

In decommissioning, clearance criteria are critical regulatory requirements. Such criteria are now available in most countries, e.g. Germany, Spain and the UK. In some cases they are part of the legislative framework; in others they were established for specific projects. International recommendations were issued by the IAEA (IAEA 2004c) and the European Commission. However, institutions having established and legally enforced national criteria, often after excruciating domestic struggles, are reluctant to adopt new criteria. It is encouraging that countries having recently started large decommissioning programmes have taken on board international recommendations. The authorized release of radioactive materials to specified destinations in the public domain is still a rare event, due to expected public opposition (Laraia 2009).

As far as environmental remediation is concerned, existing technologies are adequate in many cases. The most obvious intervention is the simple removal of contaminated material. However, this may lead to a high cost of contaminant removal and treatment and storage of removed material. The challenge is to find reliable methods which minimize the amount of contaminated material to be removed or to allow the contaminated material to remain onsite, without major impact on the planned land use. Contaminant migration to areas surrounding a pollution source is a major environmental concern and methods are needed to control the spread of pollution. These technologies could provide short-term containment while the source plume is being remediated or long-term containment for sites presenting no immediate danger. High priority is placed on treating plumes *in situ*, so that potential worker and public exposure is eliminated. In-situ methods minimize waste material and reduce costs. Biological remediation systems utilize the natural ability of plants or microbes to metabolize, absorb, oxidize or reduce radioactive compounds, and may produce significant cost savings.

Improved methods of constructing impermeable barriers at greater depths and new methods of installing sub-surface containment barriers are necessary to reduce construction costs and increase their depth of application. New methods to simplify maintenance of reactive and temporary barriers are desirable.

7.9 Sources of further information and advice

Publications listed in Section 7.10 refer to specialist aspects of decommissioning. An all-inclusive list of electronic references to decommissioning and environmental remediation, including issues, technical reports, and ongoing projects, is available at the website http://www.radwaste.org/decom.htm. Each of the following publications provides a comprehensive overview of all technical subjects and lessons learned relevant to the decommissioning of nuclear facilities.

Bayliss, C. and Langley, K., *Nuclear Decommissioning, Waste Management, and Environmental Site Remediation*, Elsevier, 2003, ISBN-13: 978-0-7506-7744-8.

Cumo, M., Tripputi, I. and Spezia, U., *Nuclear Plant Decommissioning*, Università di Roma 'La Sapienza', Rome, Italy, 2004, ISBN: 88-900812-0-1.

European Commission, *Handbook on Decommissioning of Nuclear Installations*, EUR 16211, Luxembourg, 1995, ISBN: 92-827-0389-4.

Interstate Technology and Regulatory Council, Decontamination and Decommissioning of Radiologically Contaminated Facilities, 2008, http://www.itrcweb.org/Documents/RAD5.pdf (accessed 26 November 2009).

Taboas, A.L., Moghissi, A.A. and Laguardia, T.S. (eds), *Decommissioning Handbook*, ASME, 2004, ISBN: 0791802248.

The publication below is an overview of environmental remediation techniques:

Avogadro, A. and Ragaini, R.C. (eds), Technologies for Environmental Cleanup: Soil and Groundwater, Euro Courses, *Environmental Management*, vol. 1, Kluwer Academic Publishers, 1993, ISBN: 0-7923-2145-6.

7.10 References

EPA (2006) Technology Reference Guide for Radiologically Contaminated Surfaces, US Environmental Protection Agency, EPA-402-R-06-003, 2006, http://www.epa.gov/radiation/docs/cleanup/402-r-06-003.pdf (accessed 26 November 2009)

IAEA (1983) Decommissioning of Nuclear Facilities: Decontamination, Disassembly and Waste Management, Technical Reports Series No. 230, IAEA, Vienna.

IAEA (1998) Radiological Characterization of Shutdown Nuclear Reactors for Decommissioning Purposes, Technical Reports Series No. 389, IAEA, Vienna.

IAEA (1999a) Decommissioning of Nuclear Power Plants and Research Reactors, Safety Standards Series No. WS-G-2.1, IAEA, Vienna.

IAEA (1999b) State-of-the-Art Technology for Decontamination and Dismantling of Nuclear Facilities, Technical Reports Series No. 395, IAEA, Vienna.

IAEA (1999c) Technologies for Remediation of Radioactively Contaminated Sites, TECDOC-1086, IAEA, Vienna.

IAEA (2000a) Organization and Management for the Decommissioning of Large Nuclear Facilities, Technical Reports Series No. 399, IAEA, Vienna.

IAEA (2000b) Recycle and Reuse of Materials and Components from Waste Streams of Nuclear Fuel Cycle Facilities, TECDOC-1130, IAEA, Vienna.

IAEA (2001) Methods for the Minimization of Radioactive Waste from Decontamination and Decommissioning of Nuclear Facilities, Technical Reports Series, No. 401, IAEA, Vienna.

IAEA (2004a) Safety Considerations in the Transition from Operation to Decommissioning of Nuclear Facilities, Safety Reports Series No. 36, IAEA, Vienna.

IAEA (2004b) Transition from Operation to Decommissioning of Nuclear Installations, Technical Reports Series No. 420, IAEA, Vienna.

IAEA (2004c) Application of the Concepts of Exclusion, Exemption and Clearance, Safety Standards Series, No. RS-G-1.7, IAEA, Vienna.

IAEA (2005) Standard Format and Content for Safety Related Decommissioning Documents, Safety Reports Series No. 45, IAEA, Vienna.

IAEA (2006) Management of Problematic Waste and Material Generated During the Decommissioning of Nuclear Facilities, Technical Reports Series No. 441, IAEA, Vienna.

IAEA (2007a) Safety Glossary Terminology Used in Nuclear Safety and Radiation Protection, 2007 edition, IAEA, Vienna.

IAEA (2007b) Considerations for Waste Minimization at the Design Stage of Nuclear Facilities, Technical Reports Series No. 460, IAEA, Vienna.

IAEA (2008) Managing Low Radioactivity Material from the Decommissioning of Nuclear Facilities, Technical Reports Series No. 462, IAEA, Vienna.

IAEA (2009) Integrated Approach to Planning the Remediation of Sites Undergoing Decommissioning, Nuclear Energy Series No. NW-T-3.3, IAEA, Vienna.

IAEA (2010) Design Lessons Drawn from the Decommissioning of Nuclear Facilities, TECDOC (approved for publication).

IEM (2001) *Decommissioning: Advice for Staying Ahead During a Challenging Process*, Integrated Environmental Management, Inc., Knoxville, TN.

Laraia, M. (2009) Decommissioning strategies worldwide: a re-visited overview of relevant factors, *12th Int. Conf. on Environmental Remediation and Radioactive Waste Management, ICEM'09*, Liverpool, UK, 11–15 October 2009, ICEM 2009-16016, ASME, 15 pp.

NEA (2002) *Decommissioning and Dismantling of Nuclear Facilities: Status, Approaches, Challenges*, OECD Nuclear Energy Agency, Paris, ISBN: 92-64-18488-0.

Ojovan, M.I. (2004) Thermochemical processing using powder metal fuels of radioactive and hazardous waste, *J. Process Mechanical Engineering*, 218E, 261–269.

WNA (2006) Safe Decommissioning of Civil Nuclear Industry Sites, WNA Position Statement, World Nuclear Association, London.

8

Development of geopolymers for nuclear waste immobilisation

E. R. VANCE AND D. S. PERERA, Australian Nuclear Science and Technology Organisation (ANSTO), Australia

Abstract: The usefulness of geopolymers for immobilisation of low-level and intermediate-level nuclear waste is considered. While the aqueous dissolution behaviour of geopolymers is a key feature, other important parameters are flash set and set inhibition, radiolytic hydrogen formation, fire resistance and freeze–thaw behaviour, and all these are discussed. Geopolymers are argued to have advantages over candidate materials for low- and intermediate-level nuclear waste immobilisation. Future work necessary to follow up these advantages is detailed, particularly in the area of understanding the fundamentals of the reaction between geopolymers and water.

Key words: geopolymers, nuclear waste immobilisation, aqueous dissolution.

Note: This chapter is a revised and updated version of Chapter 18 'Geopolymers for nuclear waste immobilisation' by E. R. Vance and D. S. Perera, originally published in *Geopolymers: structures, processing, properties and industrial applications*, eds J. L. Provis and J. S. J. van Deventer, Woodhead Publishing Limited, 2009, ISBN: 978-1-84569-449-4.

8.1 Nuclear wastes around the world

Before discussing the role of geopolymers in nuclear waste immobilisation, we need to discuss nuclear waste on a worldwide basis. There are over 440 operating nuclear power reactors around the world and spent nuclear fuel accumulates at around 30 T/yr for a 1 GW plant, so since nuclear power currently runs at ~400 GW worldwide, ~12,000 T/yr of spent fuel is produced (Herbert and Hopley, 2007, p. 33). The spent fuel is mostly solid UO_2 and contains a few wt% of fission products and transuranic elements, many of which are highly radioactive. Table 8.1 shows some of the more important fission products and transuranic elements formed while the fuel is in the reactor and which persist for extended periods after removal of the fuel from the reactor.

Worldwide, only a relatively small fraction of spent fuel is currently reprocessed by chemical treatment to extract U and Pu for further nuclear fuel production. However, with climate change as a strong driver for

Table 8.1 Half-lives and principal decay modes of some of the more important fission products and actinides in nuclear wastes derived from the nuclear fuel cycle

Beta emitters	Half-life (yr)	Alpha emitters	Half-life (yr)
^{137}Cs	30	^{237}Np	2.1×10^6
^{90}Sr	30	^{235}U	7.0×10^8
^{99}Tc	2.1×10^5	^{238}U	4.5×10^9
^{135}Cs	2.3×10^6	^{238}Pu	88
^{129}I	1.7×10^7	^{239}Pu	2.4×10^4
^{79}Se	6.5×10^4	^{240}Pu	6.5×10^3
^{151}Sm	90	^{241}Pu	14
		^{241}Am	430
		^{243}Am	7.4×10^3
		^{244}Cm	18

additional construction of nuclear power plants, there is presently a lot more interest in reprocessing (commonly referred to as recycling) to (a) utilise the residual U and actinides in once-through spent fuel to make fresh fuel, and (b) minimise the volumes of waste for final disposition. In addition, high-level wastes (HLW) from Pu production for atomic weapons during the Cold War between Russia and the US constitute many millions of litres. This production involved relatively short (<1 yr) in-reactor times to maximise ^{239}Pu production, followed by various means of chemical reprocessing to extract the Pu from the irradiated fuel.

The categories of radioactive wastes around the world range from (a) HLW consisting of fission products, minor actinides and process chemicals from reprocessing of spent fuel from nuclear power plants or Pu production operations, and spent fuel itself, and (b) intermediate level waste (ILW) from nuclear reactor operations, to (c) low level wastes (LLW) from radioisotope production, contaminated laboratory apparatus, used radioactive sources, etc. ILW and particularly LLW have much larger volumes than HLW but only a few percent of the total radioactivity. LLW is normally stored in metal drums (see Fig. 8.1) before permanent disposal. Radioactive mine tailings from ore production are normally exempt from radioactive controls because of their relatively low radioactivity, but they may be chemically toxic.

The radioactivities of nuclear wastes decrease with increasing time after their production and are not precisely dependent on the class of waste but they range from roughly 10,000 to 1 Ci/L for HLW, from 10 to 10^{-3} Ci/L for ILW, and from 10^{-3} to 10^{-6} Ci/L for LLW (1 curie (Ci) = 3.7×10^{10} becquerels (decays/second)).

The most important fission products in nuclear wastes are not the ones with the highest specific activity as these are very short-lived (half-lives of a few days or less) and decay quickly to zero activity during the several

8.1 Drums containing LLW stored at ANSTO.

years of storage of spent nuclear fuel in water-cooled ponds or, later, in dry storage. Rather it is the isotopes which have half-lives of several tens of years which create the main problems in the context of human lifetimes and potential for human exposure as these have high specific activities and take several hundred years to decay to harmless levels. The radioactive species with very long half-lives are an obvious concern but their specific activities (inversely proportional to the decay half-life) are correspondingly less. It is noted in passing that non-radioactive toxic inorganic elements such as Pb and As have essentially infinitely long decay half-lives.

The disposition of HLW has been studied worldwide for over 50 years and work up to the mid-1980s is dealt with in Lutze and Ewing (1988). It is commonly, but not universally, agreed that these wastes should be ultimately disposed of in deep (>0.5 km) geological repositories in the Earth after a period of retrievable above-ground storage while much of the radioactivity decreases with time. Retrievable storage both allows the radioactivity to decay somewhat, making the final disposal easier, and gives the option of reworking the waste form if a significantly better waste form technology is developed in the future. Such repositories are envisaged to be constructed in clay deposits or crystalline rocks.

Liquid HLW from reprocessing would be converted to water-resistant glasses or ceramics (generally called waste forms) by the addition to the waste of glass- or ceramic-forming chemicals, followed by mixing and appropriate heat-treatment to consolidate and immobilise these wastes. Canisterised spent fuel from some nuclear countries – notably North

America – is targeted to be disposed of in the repository without further treatment.

Glass waste form production rates of T/day can be envisaged, and new facilities for this purpose are under construction at Hanford in the state of Washington, USA (Duncan, 2005). The baseline properties of glasses and ceramic alternatives for immobilised HLW can be summarised as follows: (a) loadings of ~10–50 wt% of waste in the glass or ceramic on a dry oxide basis; (b) production temperatures of 1000–1300°C via Joule- or cold-crucible for melting or sintering/hot-pressing; and (c) normalised leach rates in cold or warm water using a low waste form surface area to liquid volume (SA/V) of <1 g/m^2/day, corresponding to fractions of a micron per day. Normalised leach rates relate to the fractional inventory of the species being studied so that leach rates are defined as

$$\mathrm{LR} = w/(\mathrm{SA}.c.t) \tag{8.1}$$

where w = weight of leached species, SA = geometrical surface area of sample, c = concentration of species of interest in the waste form, and t = leaching time. These rates are typically 0.001–1 g/m^2/day, the usual unit of leaching rate in the context of radioactive waste immobilisation.

The dimensions of large solid bodies are simply measured to obtain the geometrical surface areas. For reasons of conservatism, geometrical surface areas of powders in measured particle size distributions are taken assuming the particles are cubes or spheres. These areas are used rather than surface areas of powders derived from Brunauer–Emmett–Teller (BET) measurements. It has been found in practice that BET surface areas of powders of solid materials are ~7 times the geometrical surface areas. However, the N_2 BET areas of porous materials such as cement might be tens of m^2/g (Odler, 2003), whereas the geometrical surface areas will be much smaller, depending on the particle size. Of course, the potential overall radionuclide extraction by water is minimised if the waste can be consolidated as large bodies of preferably non-porous material. The significant point about Equation 8.1 is that, unlike in the TCLP test (EPA, 1992) for hazardous waste testing, dilution of the waste radionuclide into a larger body of material not only has economic penalties but does not in first order change the leach rate, insofar as the gross leach rate is divided by the concentration of the element in question.

There is still widespread debate about whether glasses or ceramics are the most appropriate for given types of HLW, but generally speaking, both are within the zone of acceptability, as defined by national regulators and the IAEA (IAEA, 1996), and the main part of the debate is which approach has a smaller footprint and better economics. The protection of the biosphere after insertion of the HLW glasses or ceramics into the geological repository is further assured by the use of engineered barriers, which consist of resistant metal containers for the waste forms, possible surrounding of the containerised waste by clay to sorb any nuclides released from the containers, and finally concrete linings of the repository plus rock backfills if and when the repositories are to be finally sealed off.

No country has yet constructed a geological repository for HLW, though substantial progress is being made in Finland and Sweden. The selection by the US Congress in 2002 of Yucca Mountain in the US as a national HLW repository is also noteworthy, but the Obama administration has recently rejected this option.

8.2 Cementitious low-level waste (LLW)/intermediate-level waste (ILW) waste forms

The costs of producing glass and ceramics by high-temperature technologies for the vast volumes – millions of m^3 in the USA alone (Ewing, 2008) – of extant LLW/ILW waste would be huge, so there is a compelling driver to utilise 'cheap' low-temperature processes such as cementation and bitumenisation to immobilise these wastes. While ordinary Portland cements (OPC) have been examined for possible candidacy as immobilising agents for HLW, the normalised leach rates (US DOE, 1982), when referred to geometrical surface areas rather than those derived from BET measurements, are deemed as excessive for this purpose. For elements that do not form highly insoluble hydroxides (such as Cs), leach rates are in the order of 10–100 $g/m^2/day$ (corresponding to ~10–100 μm/day) in short-term HLW regulatory tests of a few days (see Section 8.2.2), although they decrease with increasing leaching time.

However, regulatory criteria for dealing with LLW/ILW are far less stringent than those applicable to HLW. So it is reasonable that OPC and variants thereof are being used around the world for immobilising LLW/ILW, and cementation should be considered as a baseline technology for this purpose.

As groundwater is a key medium for the transport of waste radioactivity to the human domain (the biosphere), LLW/ILW radioactive wastes for immobilisation need to be devoid of free water in the first instance. Such dewatering would also remove substantial fractions of organic material. They can then be incorporated in cementitious materials and metal drums, according to international standard practice.

Two basic strategies can be employed. Firstly, the waste can be directly mixed with a cementitious material in a metal drum. The cementitious material is then allowed to set and the drum is sealed. However, this approach has some risks, insofar as (a) certain possible waste components can cause flash setting or can prevent setting altogether, and (b) the water in the usual cementitious material yields radiolytic hydrogen and oxygen from the effect of radioactive decay of the nuclides being immobilised, and the hydrogen is a fire risk if it escapes and otherwise could deform the sealed container. On point (a), many wastes which have been in existence for many years are grossly inhomogeneous and the records of the chemical identities of the wastes are vague at best.

Hence a more popular practice is to dry the waste while it is contained in a drum, followed by uniaxial supercompaction of the drum to minimise the volume; drums are then put inside a concrete container and infilled with mortar for ultimate disposal in a shallow repository. Here there is no radiolytic hydrogen generated from aqueous material in the supercompacted drum (see below) and the radioactivity incident on the concrete container is relatively minor because of the shielding effect of the supercompacted drum and the distance of the concrete lining from the actual radioactivity. Figure 8.2 shows a schematic of this process.

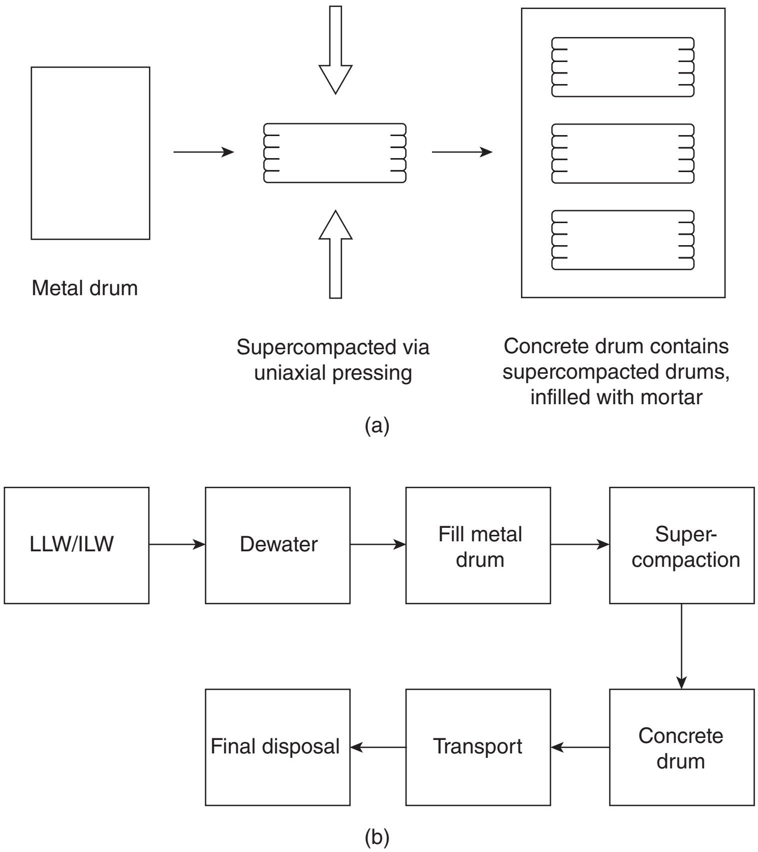

8.2 (a) Schematic of supercompaction process for LLW/ILW immobilisation; (b) flow sheet for LLW/ILW disposal.

So the main question for this chapter is whether geopolymers have potential to replace standard cement mixtures for containment of LLW/ILW. A second possible application is the replacement of cement by geopolymers in repositories for such waste, noting that repositories for LLW/ILW will be essentially close to the Earth's surface.

Geopolymers are a class of cementitious materials (Davidovits, 1982, 1991; Provis and van Deventer, 2009) that can be described as alkali-activated cements (Shi *et al.*, 2006). They are made by reacting at near-ambient temperatures aluminosilicates such as metakaolin, fly ash or ground blast-furnace slags with alkaline silicate solutions, usually strong NaOH solutions combined with soluble silicates such as water glass. The baseline stoichiometries for the geopolymeric products of the materials participating in the reaction are typically Na/Al = 1 and Si/Al = 2 on a molar basis, and a minimum amount of water (H_2O/Na ~7 on a molar basis) is used to make a thick paste to assure approximately a maximum amount of reaction and a minimum of porosity and bleed water. It is generally agreed that on a weight basis, the use of geopolymers produces only around 15% of CO_2 emissions compared to OPC, a very advantageous aspect of geopolymers from a greenhouse point of view.

The properties of geopolymers are relatively insensitive to variations in the molar ratios at the level of 10 or 20%. The aluminosilicates partly dissolve in the solutions and polymerise and solidify. Curing is carried out at 40–90°C. Geopolymers made using metakaolinite as the aluminosilicate source are X-ray amorphous (see Fig. 8.3), apart from minor crystalline impurities such as quartz and anatase, and are essentially featureless under

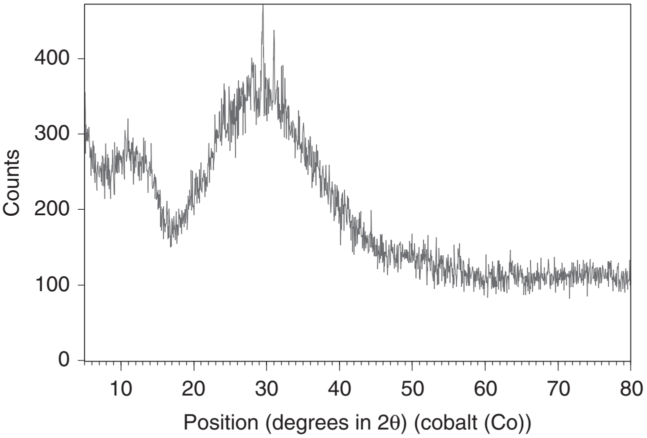

8.3 X-ray diffraction pattern of metakaolinite-based geopolymer with Na/Al = 1 and Si/Al = 2 molar ratios. Cu Kα radiation. Small diffuse peak near 10° in 2θ derives from instrumental background.

microscopic examination, apart from the impurities and pores. However, samples made using fly-ash show the crystalline species in the fly-ash, typically mullite, quartz and iron oxides in addition to the amorphous geopolymeric material.

Extensive studies by solid-state nuclear magnetic resonance have been carried out over the years together with porosity studies, so it is now accepted that geopolymers having Na/Al and Si/Al ratios of ~1 and 2 respectively consist of nanoporous three-dimensional aluminosilicate networks, with water in the pores (Barbosa *et al.*, 2000), although micro- and macro-porosity is also present. For Si/Al molar ratios of around 1 or less, crystalline zeolite formation is favoured, especially at higher curing temperatures, whereas when the Si/Al molar ratio significantly exceeds 2 or 3, extensive two-dimensional networks form, which have low strength.

While geopolymers have been known as potential building materials since the 1960s in the Ukraine and Russia (Glukhovsky, 1967), extensive international study was not made until the 1970s, when Davidovits in Europe began development of these materials in several areas, in terms of fire resistance and waste immobilisation as well as mechanical properties. Geopolymers can be readily made in quite large sections, such as railway sleepers, pipes, etc. (see Fig. 8.4), so there are no obvious problems in making large samples for radioactive waste immobilisation, other than assuring protection from the radioactivity by standard methods. Of course it must be remembered that when dealing with radioactive wastes the cost of the immobilising materials is only a small component of the total costs of the whole operation because of the safety aspects of shielding and general precautions in the handling of radioactive materials. However, the greenhouse advantage over cement for use in large-scale repository construction

8.4 Pipes made from geopolymers.

is direct because no radioactivity would be introduced before the repository construction would be completed. The basic steps in geopolymer production are summarised in Fig. 8.5.

The factors to be considered for LLW/ILW waste forms (solids for waste incorporation) are (a) knowledge of agents which give rise to flash set or set inhibition of geopolymers, (b) leach resistance relative to that of conventional cement, (c) the production of radiolytic hydrogen, (d) freeze–thaw behaviour, and (e) the immobilisation of possible chemically toxic entities accompanying the radioactive ions in the waste.

We have essentially dealt with (a) above already. But there could be some merit in combining waste directly with cementitious material if flash setting is not a problem. Ca and B are the possible agents of difficulty, together with water-soluble anions. When calcium salts were added to fly-ash-based geopolymers they set rapidly compared to those free of calcium salts (Lee and van Deventer, 2002). It has been shown that Class C fly-ash which is high in CaO (~22 wt%; Perera *et al.*, 2004) also sets rapidly (Nicholson *et al.*, 2005). However, the presence of Ca increases the strength in a geopolymer, hence the presence of a small amount of Ca (say 3–8 wt%) is beneficial (van Jaarsveld *et al.*, 2003; Dombrowski *et al.*, 2007). The addition of B-containing salts such as sodium tetraborate and lithium pyroborate increases the setting times significantly for OPC (Taylor, 1997) but does not significantly influence geopolymers in this regard (Palomo and de la Fuente, 2003). Boron is present as tetrahedral BO_4 entities in the geopolymer structure (Nicholson *et al.*, 2005). It was also found by Lee and van Deventer (2002) that anions such as Cl^- and CO_3^{2-} could possibly reduce the setting time for geopolymers, although the influence of cations accompanying these anions could well mask such effects.

Because of fire and radiation resistance criteria in nuclear regulatory tests (see Sections 8.5 and 8.6), waste form solids for immobilisation of nuclear waste preferably need to be inorganic and refractory. Water interactions with such solids can be very complex and are far from understood in detail.

8.2.1 Aqueous dissolution behaviour

While substances such as inorganic metal salts (e.g. NaCl) dissolve in water such that the cations and anions dissolve together on a stoichiometric basis until the solubility limit is reached (congruent dissolution), this is not the case for more complex compounds such as rocks, ceramics and metal alloys. Here some species dissolve preferentially, with this process being referred to as incongruent dissolution or more commonly as ‘leaching’. This process causes a nett alteration in the composition of the solid, particularly near the surface, and the whole process is diffusion controlled and non-linear in time.

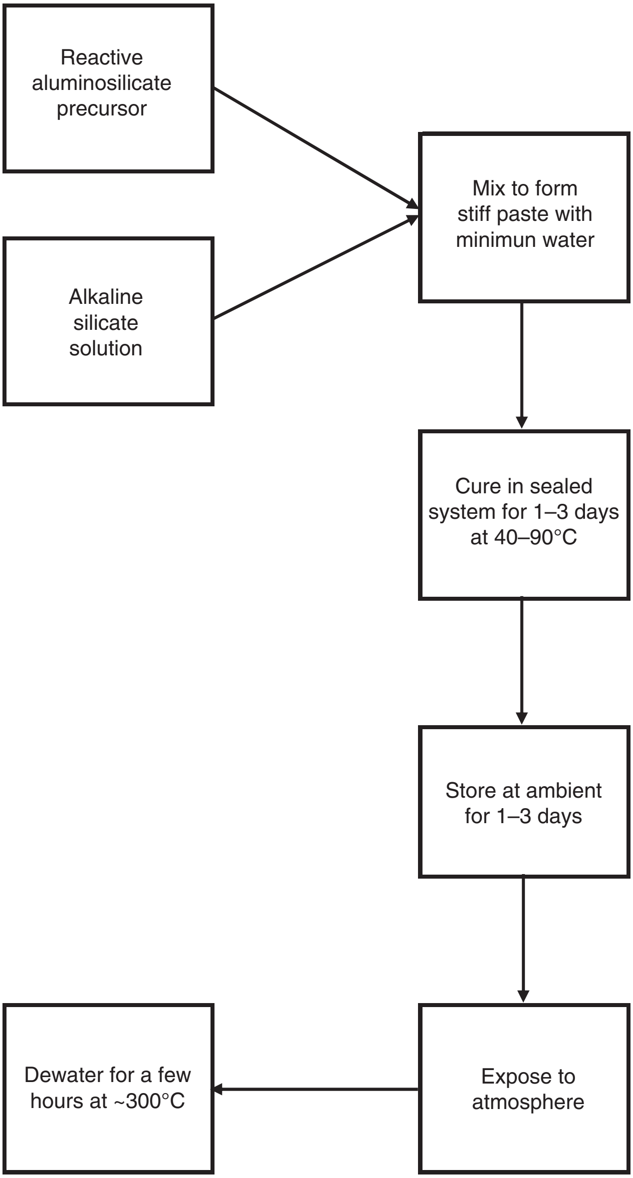

8.5 Schematic production route for geopolymers.

More generally, the dissolution rate of a solid is a complicated function of the ratio of the solid to liquid, sample surface area, pH, temperature, composition of the aqueous medium, and leaching reaction time. Thus the dissolution process is initially characterised by a forward reaction which can be characterised by the dissolution rate at zero time and zero concentration of dissolution products in the water. However, as dissolution proceeds, the reaction slows down because of a 'back-reaction' which tends to precipitate some of the dissolved species. Eventually equilibrium is reached between the solid dissolution products and the solution, depending on whether the system is essentially closed insofar as it is small and bounded by a water-free zone, or is essentially unbounded and therefore open. Further complications arise when leaching is carried out in groundwaters containing substantial amounts of salts.

One of the factors involved in the choice of a solid for regulation-dictated immobilisation of radioactivity is reproducibility of the solid, and for this reason we would argue that metakaolin is by far the most reproducible aluminosilicate precursor for geopolymers and should be used in candidate geopolymers for this purpose. A somewhat negative feature, however, is that the water demand is higher for geopolymers based on metakaolin as against fly-ash. While fly-ash is cheaper, its composition varies from one power station to the next and even on a day-to-day basis at a given power station. Moreover, fly-ash consists of a complex mixture of crystalline, cryptocrystalline and amorphous entities, which makes it very difficult to sort out collective aqueous dissolution mechanisms. Therefore we will mostly confine our remarks to metakaolin-based geopolymers.

The aqueous dissolution behaviour of (metakaolin-based) geopolymers is particularly complex because we are dealing with an aluminosilicate framework that contains pore water. So two basic processes contribute to the reaction of geopolymers with water: (a) the diffusion of the pore water into the external water solution, and (b) the leaching of the framework. However, it is clear from many studies that only partly reacted aluminosilicate precursors are usually also present in the geopolymer matrix and this further complicates the picture.

It is well known that 3-D polymerisation of geopolymers reaches a maximum at around a Si/Al molar ratio of ~2 and that for all the oxygen in the tetrahedral framework to be fully bonded the Na/Al molar ratio should be 1, to provide full charge compensation. Relevant studies include solid-state magic angle ^{27}Al and ^{29}Si nuclear magnetic resonance (Duxson *et al.*, 2005; Blackford *et al.*, 2007) as well as compressive strength measurements (Rowles and O'Connor, 2003). Not surprisingly, then, it has recently been found that aqueous dissolution also reaches a minimum for Si/Al values of around 2 (Aly *et al.*, 2008).

We will first consider the reaction of the tetrahedral aluminosilicate framework with water. To a first approximation, the framework can be likened to a porous aluminosilicate glass. When such a glass is immersed in water, the first indication of reaction is an increase in the pH of the water, and for solid glass this is attributed to ion exchange whereby alkali ions are transferred to the solution and protons (or H_3O^+ entities) replace the alkali ions in the glass. The continuation of this process is that the alkaline solution then attacks the aluminosilicate framework via a reaction such as:

$$SiO_2 + OH^- + H_2O \rightarrow SiO(OH)_3^- \tag{8.2}$$

Many studies have been made of borosilicate glasses in connection with the immobilisation of high-level nuclear waste (fission- product-rich waste derived from reprocessing of used nuclear power plant fuel – see above), and the process is basically well understood (Lutze and Ewing, 1988), although the fine detail of improvements to the nett leaching rate by the addition of small amounts of other cations such as Ti, Zr, Al, Fe, Li, Zn, etc., is still empirical to some extent.

When geopolymers are leached in water, it is found that the pH of the water quickly rises and the overall release rate in terms of fractional extraction of the inventory of a particular cation is by far the highest for the alkalis (Fig. 8.6 and see, e.g., Aly *et al.*, 2008; Ly *et al.*, 2006). But it has not proved easy to separate the contributions from framework dissolution and pore water dissolution to the total alkali release. However, it has been observed that, other things being equal, the release rate of the alkalis (and Al and Si) depends strongly on the surface area to liquid ratio even in relatively dilute

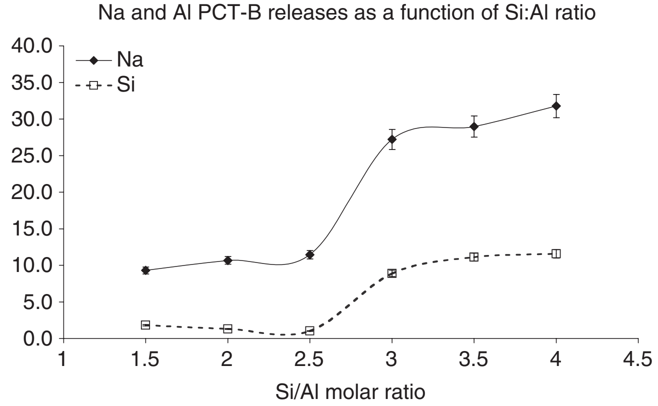

8.6 Percentage elemental extractions in PCT-B tests from metakaolin-based geopolymers with different Si/Al molar ratios. Al extractions all <0.4%. ANSTO unpublished work.

solutions (Vance *et al.*, 2007), something that would not be expected if pore water/solution exchange was the only contributor to the alkali release.

Although pore water can be nearly all removed by modest heating to ~300°C (Perera *et al.*, 2005), the pore structure would remain substantially unaltered and any salts in the pore water would crystallise on the sides of the pores: when the dried solid is immersed in water, the water could penetrate into the pore structure and dissolve the salts and then the salts can diffuse back into the leach water. Of course pore water transfer to an aqueous solution should be minimised if relatively large-scale porosity can be removed, so current efforts are directed to high-shear mixing to minimise water content and removing air bubbles.

Microstructures of geopolymers are discussed in other chapters and the essentials are that very fine meso- and macropores (2–50 nm and 50–200 nm respectively; Rouquerol *et al.*, 1999) are present even if millimetre-sized pores can be prevented from forming by vibration techniques. However, it is not all that likely that nanometre-sized pores would allow any significant pore water transfer to a leaching solution, in the absence of high external water pressures, so reduction of the larger-scale porosity would seem to have the most promise for improvement of the leaching resistance.

Experiments in the authors' laboratory are in progress to see how much water minimisation can be utilised in high-shear mixing of metakaolin-based geopolymers. It has been found (Walls and Kurlapski, private communication) that minimising water additions significantly beyond what can be readily attained by hand-mixing for setting does not improve performance in leaching tests and can cause samples to crack upon subsequent exposure to water. We have also investigated commercial geopolymers made with milled fly-ash, minimum water addition and high-shear mixing to maximise their strength, and found that they can fail even the HLW version of the PCT test (see Section 8.2.2), so it seems improbable that such water minimisation would lead to a large improvement in water leach resistance.

8.2.2 Conformance with regulatory tests

There are well-defined short-term International Atomic Energy Agency (IAEA) plus country-specific regulatory tests for the disposal of radioactive wastes, but scientific understanding of the behaviour of the disposed waste is still necessary to ensure that immobilisation will last for thousands of years or when all radioactive decay in the nominally immobilised waste has effectively ceased.

The main relevant regulatory tests are ANS 16.1 (ANS, 2003) and to a lesser extent the PCT-B test (ASTM, 2002). However, these are short-term tests and scientific understanding is still necessary to ensure the immobilisation of the particular wastes for periods of thousands of years. The ANS

16.1 test involves the use of cementitious samples of known composition ~1 × 1 × 5 cm in size and weighing ~20 g. These are immersed in ~200 mL of water at 20°C and leaching is allowed to proceed for 2, 7, 24, 48, 72, 96 and 120 h, with longer periods being optional. The solutions are then analysed for various cations, particularly the radioactive species. Assuming that <20% of the inventories have been leached out of the blocks (which can be deduced from knowing the composition), the fractional inventories leached out are plotted against the square root of leaching time and effective diffusion coefficients for various elements are derived. If the diffusion coefficients are all $<10^{-6}$ cm^2/s, the solid is deemed successful in immobilising the radionuclides of interest, assuming it has a compressive strength of >3.5 MPa (IAEA, 1996).

In the PCT-B test, the sample is powdered to achieve a fraction between 100 and 200 mesh (150–75 microns). Adherent fines are then removed by washing in ethanol/methanol/acetone or preferably a non-polar solvent to remove the chances of pre-dissolution of soluble species. For each gram of washed sample, 10 mL of deionised water is added and the samples are leached at 90°C for 7 days. The fractional inventories of the leached elements, notably Na and Si in the present context, are then measured and, assuming these elements are present, the material is a good candidate for HLW disposal if all leached inventories correspond to <~13% of the totals in the solid. The focus on these elements derives from the use of the PCT-B test as an indicator of the quality of HLW-bearing borosilicate glass, and it is also noteworthy that the SA/V ratio is relatively high (~40 cm^{-1}) in these tests. Borosilicate glasses typically give fractional release rates of the above-mentioned elements in the range of 0.1–10%.

The use of the PCT-B test for candidate solids containing LLW/ILW for near-surface disposal is identical in methodology but the 'pass mark' for elemental leaching is 2 g/m^2, a factor of 3–5 lower than that for HLW (depending on the waste form density), a criterion that is adjusted to account for LLW/ILW being disposable in a near-surface repository as against a deep repository containing multiple barriers to prevent radionuclide transport to the biosphere for HLW.

While waste-free geopolymers can be fabricated and pass the HLW version of the PCT test, and on occasion the LLW version, there are strong indications that the PCT test gives early saturation effects – at times of only 1 day (Vance *et al.*, 2007) – and this is consistent with the very high early release rates determined in tests in which the SA/V ratio is low.

8.2.3 Effect of anions

The US tank wastes from plutonium production during the Cold War (see Section 8.1) are classed as HLW in that country but their activities would fall into the ILW regime in many other nuclear countries. Accordingly there have been several attempts to demonstrate that geopolymers are a viable way to immobilise these wastes relative to vitrification which is the baseline technology in the US. The wastes under consideration are the liquid + sludge wastes at the Hanford site and the Savannah River Laboratory, and the calcines at Idaho National Laboratory. The liquid wastes consist of a metal hydroxide sludge containing most of the fission products and actinides, plus a supernatant solution of mainly sodium hydroxide, sodium nitrate, sodium nitrite and sodium aluminate, together with soluble fission products such as Cs and Tc. The calcines consist of mixtures of zirconia, alumina, calcium fluoride and dolomite, plus fission products and actinides. For the liquid wastes, geopolymer formulations have been devised to immobilise simulated wastes which have been calcined after mixing with clay and sugar as a reducing agent to maximise the removal of the nitrate/nitrite plus sulphate as well as organic species (Krishnamurthy *et al.*, 2001; Siemer *et al.*, 2001a,b; Bao and Grutzeck, 2007); the metakaolin-based geopolymers which were mostly treated by autoclaving at ~200ºC could pass the HLW version of the PCT test for sodium (the waste being classed as HLW in the USA), as well as display adequate compressive strength. Broadly similar results were obtained on geopolymers prepared from the Idaho National Laboratory calcines (Siemer *et al.*, 2001b).

The nitrate/nitrite and sulphate anions present in the liquid wastes normally exist in geopolymers as alkali salt solutions in the pore water and as such are very poorly immobilised when the geopolymer is exposed to water. Because these particular tank wastes have high alkali contents, it is difficult to remove the anions even by calcination without adding large amounts of other cations such as Al and/or reducing agents. However, fabrication of nitrate sodalites has been reported (Buhl and Lons, 1994, 1996; Buhl, 1991), although this was all done in hydrothermal preparations at temperatures well above 100ºC in which the nitrate was stoichiometrically in excess of the aluminosilicate components by factors of 10 or more. Nitrate, nitrite and sulphate ions can be incorporated in cancrinite structures derived from the basic sodalite structure and can evidently be immobilised in geopolymers with Na/Al/Si ratios of around unity (Krishnamurthy *et al.*, 2001; Siemer *et al.*, 2001a; Bao and Grutzeck, 2007). Moreover, barium hydroxide can be added to immobilise the sulphate as insoluble $BaSO_4$.

8.2.4 Comparison with ordinary Portland cements (OPC)

Caesium (Cs) is one of the most difficult radionuclides to immobilise because of its generally high water solubility as an alkali element, and in a PCT test on a geopolymer the extraction is roughly 2 g/L (Perera *et al.*, 2006) as against 80–100 g/L for Cs in cement (Hanna *et al.*, 2001). To try to lower the Cs leach rates for cement, attempts have been made to incorporate the Cs in zeolite which is in turn embodied in cement (El-Kamash *et al.*, 2006; Perera *et al.*, 2007).

In ANS 16.1 tests on geopolymers containing simulated LLW/ILW, we found *D* values (Perera *et al.*, 2007) of around 10 (i.e. considerably greater than the 'pass mark' of 6) for Al, Na, Si, Cs, Sr, Nd and Ba.

8.2.5 Radiolytic hydrogen

In cement, the main strength-building phase is the hydrated C-S-H (Ca-Si-oxide/hydrate) phase and radiolysis will generate hydrogen (Offerman, *et al.*, 1989). As mentioned above, such H_2 presents a hazard. In principle, the hydrogen can be largely removed by dehydrating the cement and this would ameriolate the radiolytic H_2 problem. However, heating to a few hundred degrees Celsius can seriously impact the cement structure and mechanical properties because water is a component of the C-S-H phase. By contrast, geopolymers can be almost completely dehydrated by heating at 300–400°C with virtually no effect on aqueous dissolution properties (Perera *et al.*, 2006). Any organic material would also be essentially removed by such treatment, so such heating should remove the problem of radiolytic H_2 generation. Effects of such heating on their mechanical properties have not been quantified (work is in progress) but are not anticipated to be very significant from laboratory observations of general friability.

8.2.6 Fire resistance

Fire resistance criteria for immobilising ILW/LLW are somewhat elastic but the IAEA recommends that attention be paid to this question (IAEA, 1996). Clearly, bituminous products (see page 223) would need to be contained in fireproof metal cans and even then the heat of a fire would produce potential for explosion and subsequent combustion. Geopolymers have adequate fire resistance and this is well documented (Kong *et al.*, 2007, 2008).

8.2.7 Freeze–thaw behaviour

Freeze–thaw problems are basically macroscopic cracking from the expansion/contraction of hydrous phases in cementitious materials. The freeze–thaw behaviour of OPC derivatives is an important parameter but, in the same way as the problem of radiolytic H_2 production can be minimised by heating geopolymers to ~300°C (Section 8.2.1), such heating also removes any potential problem of freeze–thaw behaviour in geopolymers, at least while they are not in contact with water.

8.2.8 Actual waste immobilisation in geopolymers

AllDeco Ltd of the Slovak Republic has developed a proprietary geopolymer matrix (called SIAL) for embedding various intermediate-level wastes resulting from Slovak power reactors (Majersy *et al.*, 2007). Some of the materials encapsulated in geopolymer matrices are bottom sludges from long-term storage of spent nuclear fuel elements, sludges from the sedimentation tank of a reactor and several other sludges. Some of the sludges are formed from an emulsified mixture of organic compounds from the cooling media and contain a large amount of calcium and magnesium hydrocarbonates. The activity of the ^{137}Cs in the sludges is ~$10^5 – 10^8$ Bq/L. Once these sludges were solidified in the geopolymer matrix and placed in 60 L drums, the surface dosage on the drums was 10–20 mGy/h. The *D* value for the ^{137}Cs in samples taken from the drum was >8 for the ANSI 16.1 test and the compressive strength was 25 MPa. About 20 wt% (on a dry basis) of waste was encapsulated.

Organic ion exchange resins on their own and in mixtures of sludges were also encapsulated in geopolymer matrices. It was possible to encapsulate ~20 wt% (on a dry basis) for geopolymers compared to 10 wt% for OPC. These were placed in 200 L drums. The dosages on the drum surfaces were 130–600 μGy/h and the *D* value for ^{137}Cs was >9 on cut samples from the drums. All the drums used were made from stainless steel. The SIAL matrix (geopolymer) has been accepted by the Slovak Nuclear Authority (UJDSR) and the Czech Nuclear Authority (SUJB) for placement in their respective repositories (Majersy *et al.*, 2007). AllDeco Ltd emplaced these drums in the Slovak repository in 2003.

8.2.9 Alternative low-temperature products for LLW/ILW immobilisation

Alternative ‘low-temperature’ products to OPC and geopolymers are the Argonne Mg-K-phosphate mixtures and bitumen, as well as modified cements. As mentioned previously, OPC is a baseline product for LLW/ILW immobilisation. OPC extenders are fly-ash and ground glass blast furnace slag and these have been studied extensively in this context – see, e.g., Quillin *et al.* (1994) and the reviews by Glasser (1992) and Milestone (2006). Again, however, the criticism of non-reproducibility of fly-ash and ground glass blast furnace slags will apply. Shi *et al.* (2006) have also discussed the use of alkali-activated cements for immobilising radioactive waste.

For bitumen, radiolytic H_2 production is generally perceived as a problem but bituminous products were used in Europe, with Eurobitum as a well-defined product (Chaix *et al.*, 2001; Valcke *et al.*, 2001; Sneyers and Van Iseghem, 1998). Oxalates and other radicals are radiolysis products (Valcke

Table 8.2 Key properties of candidate waste forms for immobilisation of LLW/ILW

Candidate	Leachability	Water/organic content	Fire resistance
Cement	Satisfactory	Yes	Binder weakened
Geopolymers	Better than OPC	Can be eliminated	Excellent
Mg-K-phosphate	Better than OPC	Yes	?
Bitumen	Better than OPC	Yes	No

et al., 2001); these will have complexing power and facilitate transfer of radionuclides in groundwater.

Mg-K-phosphates made by Argonne National Laboratory (ANL) workers involve combining calcined MgO with KH_2PO_4 via

$$MgO + 5H_2O + KH_2PO_4 \rightarrow MgKPO_4.6H_2O \qquad 8.3$$

as the major reaction (Singh *et al.*, 1994; Jeong *et al.*, 1996; Walker et al., 2000; Langton *et al.*, 2000). This material was seen as appropriate for the immobilisation of actinides and Cs incorporated in the CST ion exchanger (Singh *et al.*, 1994). It was also argued to be good for actinides (Jeong *et al.*, 1996), while the product was also widely applicable to the toxic components of the waste via passing TCLP tests. Radioactive stability was usually assessed by the ANS 16.1 tests.

Table 8.2 summarises the key properties of candidate waste forms. Cations which form insoluble hydroxides are clearly immobilised in non-acidic groundwaters, noting that the use of cement or geopolymers in the repository construction will promote alkalinity of any groundwater which enters the repository. Such alkalinity would not be fostered by the use of bitumen and probably not the ANL phosphate cements. It follows from Table 8.2 that potential advantages of geopolymers for LLW/ILW immobilisation can be summarised as follows:

- Geopolymers show generally better performance in regulatory leach tests. Essential removal of radiolytic H_2 production (and freeze–thaw problems) can be carried out by heating at very moderate temperatures such as 300°C without any serious effects on strength or leachability.
- Geopolymers have demonstrated excellent fire resistance.
- The alkalinity of geopolymers (and of course cements) would encourage the intrinsic formation of insoluble hydroxides for many fission products and actinides.

8.3 Future work

Current work in the authors' laboratory is investigating the dependence of leach rate in very low SA/V regimes of time, pH, water additives such as chloride and carbonate species, and temperatures between 25 and 90°C. Detailed studies of possible benefits of high-shear mixing and minimisation of water content are also in progress. Very recent work in this laboratory has shown that a change of chemistry to phosphate-based materials may also have considerable potential to improve on aluminosilicate geopolymers (Perera *et al.*, 2008).

8.4 Conclusions

Geopolymers can have significant advantages over cements (other than greenhouse gas emissions during production) and other candidates for the immobilisation of LLW/ILW, and it needs to be stressed that the existing volumes of these classes of nuclear waste far outweigh those of HLW. These advantages lie in lack of freeze–thaw problems and minimal production of radiolytic H_2 if a dewatering production step is inserted in the production cycle, fire resistance, and good immobilisation of radionuclides from the point of view of leaching resistance. There has been actual disposal of low-level nuclear waste in geopolymers on an industrial scale in the Slovak Republic. Even if advanced nuclear fuel cycles become widely implemented in, say, 40 or 50 years, there will always be very large amounts of LLW and ILW requiring immobilisation.

However, the aqueous dissolution behaviour of geopolymers containing a variety of LLW/ILWs in a range of groundwater types needs to be more widely investigated to ensure the long-term stability of the immobilised LLW/ILW. Research is especially needed to assess geopolymers' potential as engineered barriers in repositories for nuclear and hazardous wastes. Control and minimisation of porosity at the 0.1 μm scale and above is especially needed.

8.5 Sources of further information and advice

The book entitled *Radioactive Waste Forms for the Future*, edited by Lutze and Ewing, is an excellent source of materials-related research on nuclear waste immobilisation up to the mid-1980s. The Materials Research Society has held approximately annual symposia on radioactive waste management since 1978. Glasser (1992) and Milestone (2006) have given very useful reviews of research on cements as applied to immobilisation of radioactive waste. A recent book edited by Provis and van Deventer (2009) should also be highlighted.

8.6 Acknowledgements

We wish to thank D. Brew and P. Walls for helpful discussions, and Z. Aly for carrying out most of the leaching analyses. We also thank T. Gourley for figures. This work was supported in part by the Cooperative Research Centre for Sustainable Resource Processing, based at Curtin University, Perth, Western Australia.

8.7 References

Aly, Z, Vance, E R, Perera, D S, Davis, J, Durce, D, Hanna, J V and Griffith, C S (2008), 'Aqueous leachability of metakaolin-based geopolymers with molar ratios of Si/Al = 1.5 to 4', *J. Nucl. Mater.,* 378, 172–179.

ANS (2003), *Measurement of Leachability of Solidified Low Level Radioactive Wastes by Short-Term Test Procedure*, ANSI/ANS-16.1–2003, American Nuclear Society, La Grange Park, IL, USA.

ASTM (2002), Standard Test Methods for Determining Chemical Durability of Nuclear, Hazardous, and Mixed Waste Glasses and Multiphase Glass Ceramics: The Product Consistency Test (PCT), Designation C1285–02, ASTM International, PO Box C700, West Conshohocken, PA 19428–2959, USA.

Bao, Y and Grutzeck, M W (2007), 'Solidification of sodium bearing waste using hydroceramic and Portland cement binders', in Dunn, D, Poinssot, D C and Begg, B (eds), *Scientific Basis for Nuclear Waste Management XII*, Materials Research Society, Warrendale, PA, 233–242.

Barbosa, V F F, MacKenzie, K J D and Thaumaturgo, C (2000), 'Synthesis and characterization of materials based on inorganic polymers of alumina and silica: sodium polysialate polymers', *Int. J. Inorg. Mater.,* 2, 309–317.

Blackford, M G, Hanna, J V, Pike, K J, Vance, E R and Perera, D S (2007), 'Transmission electron microscopy and nuclear magnetic resonance in geopolymers for radioactive waste immobilisation', *J. Amer. Ceram. Soc.*, 90(4), 1193–1199.

Buhl, J-C (1991), 'The properties of salt-filled sodalites. Part 2. Synthesis, decomposition reactions and phase transitions of nitrate sodalite $Na_8[AlSiO_4]_6(NO_3)_2$', *Thermochim. Acta*, 189, 75–82.

Buhl, J-C and Lons, J (1994), 'Orientational disorder and heterogeneous reaction behaviour of NO_2^- and NO_3^- anions inside a sodalite matrix', *J. Solid State Chem.,* 112, 243–250.

Buhl, J-C and Lons, J (1996), 'Synthesis and crystal structure of nitrate enclathrated sodalite $Na_8[AlSiO_4]_6(NO_3)_2$', *J. Alloys and Compounds*, 235, 41–47.

Chaix, P, Camaro, S, Simondi, B, Vistoli, P P and Blanc, Y (2001), 'Long-term behaviour of bituminized waste: modelling of auto-irradiation and leaching', in Hart, K P and Lumpkin, G R (eds), *Scientific Basis for Nuclear Waste Management XXIV,* Materials Research Society, Warrendale, PA, 131–139.

Davidovits, J (1982), 'Mineral polymers and methods of making them', US Patent 4,349,386.

Davidovits, J (1991), 'Geopolymers – Inorganic polymeric new materials', *J. Therm. Anal.*, 37, 1633–1656.

Dombrowski, K, Buchwald, A and Weil, M (2007), 'The influence of calcium content on the structure and thermal performance of fly ash based-geopolymers', *J. Mater. Sci.*, 42, 3033–3043.

Duncan, G M (2005), 'The nation's largest construction project: Designing and constructing Hanford's waste treatment plant', *Radwaste Solutions*, Sept./Oct., 14–22.

Duxson, P, Lukey, G C, Separovic, F and van Deventer, J S J (2005), 'Effect of alkali cations on aluminum incorporation in geopolymeric gels', *Ind. Eng. Chem. Res.,* 44, 832–839.

EPA (1992), *Test Methods for Evaluating Solid Waste, Physical/Chemical Methods: Method 1311: Toxicity Control Leaching Procedure*, Document SW-846, US Environmental Protection Agency.

El-Kamash, A M, El-Naggar, M R and El-Dessouky, M I (2006), 'Immobilization of cesium and strontium radionuclides in zeolite-cement blends', *J. Hazardous Materials*, B136, 310–316.

Ewing, R C (2008), 'Nuclear fuel cycle: Environmental impact', *Materials Research Society Bulletin*, 33, 338–340.

Glasser, F P (1992), 'Progress in the immobilization of radioactive wastes in cement', *Cem. Concr. Res*., 22, 201–216.

Glukhovsky, V D (1967), *Soil Silicate Articles and Structures (Gruntosilikatnye vyroby I konstruktsii)*, Budivelnyk Publishers, Kiev, Ukraine.

Hanna, J V, Aldridge, L P and Vance, E R (2001), 'Cs speciation in cement', in Hart, K P and Lumpkin, G R (eds), *Scientific Basis for Nuclear Waste Management XXIV*, Materials Research Society, Warrendale, PA, 89–96.

Herbert, A M and Hopley, G W (2007), *Nuclear Energy Now*, John Wiley & Sons, Hoboken, NJ, p. 33.

IAEA (1996), *Requirements and methods for low and intermediate level waste package acceptability*, Report IAEA-TECDOC-864, IAEA, Vienna.

Jeong, S, Wagh, A S and Singh, D (1996), 'Chemically bonded phosphate ceramics for stabilizing low-level radioactive wastes', in Jain, V and Peeler, D (eds), *Environmental Issues and Waste Management Technologies in the Ceramic and Nuclear Industries II*, American Ceramic Society, Westerville, OH, 179–188.

Kong, D L Y, Sanjayan, J G and Sagoe-Crentsil, K (2007), 'Comparative performance of geopolymers made with metakaolin and fly ash after exposure to elevated temperatures', *Cem. Concr. Res.,* 37, 1583–1589.

Kong, D L Y, Sanjayan, J G and Sagoe-Crentsil, K (2008), 'Factors affecting the performance of metakaolin geopolymers exposed to elevated temperatures', *J. Mater. Sci.,* 43, 824–831.

Krishnamurthy, N, Grutzeck, M W and Kwan, S (2001), 'Hydroceramics for Savannah River Laboratory sodium-bearing waste', in Spearing, D R, Smith, G L and Putnam, R L (eds), *Environmental Issues and Waste Management Technologies in the Ceramic and Nuclear Industries VI*, American Ceramic Society, Westerville, OH, 337–344 .

Langton, C A, Singh, D, Wagh, A S, Tlustochowicz, M and Dwyer, K (2000), 'Phosphate ceramic solidification and stabilization of cesium-containing crystalline silicotitanate resins', in Chandler, G T and Feng, X (eds), *Environmental Issues and Waste Management Technologies in the Ceramic and Nuclear Industries V*, American Ceramic Society, Westerville, OH, 175–187.

Lee, W K W and van Deventer, J S J (2002), 'The effect of ionic contamination on the early-age properties of alkali-activated fly ash-based cements', *Cem. Concr. Res*., 32, 577–584.

Lutze, W and Ewing, R C (eds) (1988), *Radioactive Waste Forms for the Future,* North-Holland, Amsterdam.

Ly, L, Vance, E R, Perera, D S, Aly, Z and Olufson, K (2006), 'Leaching of geopolymers in deionised water', *Adv. in Mater. and Mater. Proc. J.,* 8, 236–247.

Majersy, D, Sekely, S and Breza, M (2007), 'Verified possibilities of specific and historical waste solidification', *IAEA RCM on Behaviour of Cementitious Materials in Long Term Storage and Disposal of Radioactive Waste Meeting,* 10–14 September, Moscow, CD ROM, IAEA, Vienna.

Milestone, N B (2006), 'Reactions in cement encapsulated nuclear wastes: Need for toolbox of different cement types', *Adv. App. Ceram.,* 105, 13–20.

Nicholson, C L, Murray, B J, Fletcher, R A, Brew, D R M, MacKenzie, K J D and Schmucker, M (2005), 'Novel geopolymer materials containing borate structural units', in Davidovits, J (ed.), *Proceedings World Congress Geopolymer 2005*, Saint-Quentin, France, 31–33.

Odler, I (2003), 'The BET-specific surface area of hydrated Portland cement and related materials', *Cem. Concr. Res.,* 33, 2049–2056.

Offermann, P (1989), 'Calculation of the radiolytic gas production in cemented waste', in Lutze, W and Ewing, R C (eds), *Scientific Basis for Nuclear Waste Management XII*, Materials Research Society, Pittsburgh, PA, 461–468.

Palomo, A and de la Fuente, J I L (2003), 'Alkali-activated cementitious materials: Alternative matrices for the immobilisation of hazardous wastes – Part 1. Stabilisation of boron', *Cem. Concr. Res.,* 33, 281–288.

Perera, D S, Nicholson, C L, Blackford, M G, Fletcher, R A and Trautman, R L (2004), 'Geopolymer made using New Zealand fly ash', *J. Jap. Ceram. Soc.*, 112(4), S108–S111.

Perera, D S, Vance, E R, Cassidy, D J, Blackford, M G, Hanna, J V and Trautman, R L (2005), 'The effect of heat on geopolymers made using fly ash and metakaolinite', in Singh, J P, Bansal, N P and Kriven, W M (eds), *Advances in Ceramic Matrix Composites X*, American Ceramic Society, Westerville, OH, 87–94.

Perera, D S, Vance, E R, Aly, Z, Davis, J and Nicholson, C L (2006), 'Immobilization of Cs and Sr in geopolymers with Si/Al molar ratios of ~2', in Herman, C C and Marra, S L (eds), *Environmental Issues and Waste Management Technologies in the Ceramic and Nuclear Industries XI*, American Ceramic Society, Columbus, OH, 91–96.

Perera, D S, Vance, E R, Kiyama, S, Aly, Z and Yee, P (2007), 'Geopolymers as candidates for low/intermediate level highly alkaline waste', in Dunn, D, Poinssot, C D and Begg, B (eds), *Scientific Basis for Nuclear Waste Management XXX*, Materials Research Society, Warrendale, PA, 361–366.

Perera, D S, Hanna, J V, Davis, J, Blackford, M G, Latella, B A, Sasaki, Y and Vance, E R (2008), 'Relative strengths of phosphoric-acid reacted and alkali-reacted metakaolin materials', *J. Mater. Sci.*, 43, 6562–6566.

Provis, J and van Deventer, J S J (eds) (2009), *Geopolymers: Structure, Processing, Properties and Applications*, Woodhead Publishing, Cambridge, UK.

Quillin, K C, Duerden, S L and Majumdar, A J (1994), 'Accelerated ageing of blended OPC cements', in Barkatt, A and Van Konynenburg, R A (eds), *Scientific*

Basis for Nuclear Waste Management XVII, Materials Research Society, Pittsburgh, PA, 341–348.

Rouquerol, F, Rouquerol, J and Sing, K (1999), *Adsorption by Powders and Porous Solids: Principles, Methodology and Applications*, Academic Press, San Diego, CA, p. 8.

Rowles, M A and O'Connor, B H (2003), 'Chemical optimisation of the compressive strength of aluminosilicate geopolymers synthesised by sodium silicate activation of metakaolinite', *J. Mater. Chem.,* 13, 1161–1165.

Shi, C, Krivenko, P V and Roy, D M (2006), *Alkali-Activated Cements and Concretes*, Taylor and Francis, London and New York, pp. 313–319.

Siemer, C D, Olanrewaju, J, Scheetz, B, Krishnamurthy, N and Grutzeck, M W (2001a), 'Development of hydroceramic waste forms', in Spearing, D R, Smith, G L and Putnam, R L (eds), *Environmental Issues and Waste Management Technologies in the Ceramic and Nuclear Industries VI,* American Ceramic Society, Westerville, OH, 383–390.

Siemer, C D, Olanrewaju, J, Scheetz, B, Krishnamurthy, N and Grutzeck, M W (2001b), 'Development of hydroceramic waste forms for INEEL calcined waste', in Spearing, D R, Smith, G L and Putnam, R L (eds), *Environmental Issues and Waste Management Technologies in the Ceramic and Nuclear Industries VI*, American Ceramic Society, Westerville, OH, 391–398.

Singh, D, Wagh, A S, Cunnane, J, Sutaria, M, Kurokawa, S and Mayberry, J (1994), 'Phosphate-bonded ceramics as candidate final waste form materials', in Bickford, D, Bates, S, Jain, V and Smith, G (eds), *Environmental and Waste Management Issues in the Ceramic Industry II,* American Ceramic Society, Westerville, OH, 165–174.

Sneyers, A and Van Iseghem, P (1998), 'The leaching behaviour of bituminized radioactive waste in the geologic disposal conditions of the boom clay formation', in McKinley, I G and McCombie, C (eds), *Scientific Basis for Nuclear Waste Management XXI,* Materials Research Society, Warrendale, PA, 565–572.

Taylor, H F W (1997), *Cement Chemistry*, 2nd edition, Thomas Telford, London.

US DOE (1982), *The Evaluation and Selection of Candidate High-level Waste Forms,* US Department of Energy Report DOE/TIC 11611.

Valcke, E, Sneyers, A and Van Iseghem, P (2001), 'The effect of radiolytic degradation products of Eurobitum on the solubility and sorption of Pu and Am in boom clay', in Hart, K P and Lumpkin, G R (eds), *Scientific Basis for Nuclear Waste Management XXIV*, Materials Research Society, Warrendale, PA, pp. 141–149.

van Jaarsveld, J G S, van Deventer, J S J and Lukey, G C (2003), 'The characterisation of source materials in fly ash-based geopolymers', *Mater. Lett.,* 57, 1272–1280.

Vance, E R, Perera, D S, Aly, Z, Walls, P A, Zhang, Y, Cassidy, D J and Griffith, C S (2007), 'Immobilisation of cations and anions in geopolymers', *Materials Science and Technology 2007 Conference and Exhibition*, 16–20 September Detroit, MI.

Walker, B W, Langton, C A and Singh, D (2000), 'Phosphate bonded solidification of radioactive incinerator wastes', in Chandler, G T and Feng, X (eds), *Environmental Issues and Waste Management Technologies in the Ceramic and Nuclear Industries V*, American Ceramic Society, Westerville, OH, 169–174.

Walls, P A and Kurlapski, I, private communication.

9

Development of glass matrices for high level radioactive wastes

C. M. JANTZEN, Savannah River National Laboratory, USA

Abstract: Vitrification is currently the most widely used technology for the treatment of high level radioactive wastes (HLW) throughout the world. Most of the nations that have generated HLW are immobilizing in either borosilicate glass or phosphate glass. One of the primary reasons that glass has become the most widely used immobilization medium is the relative simplicity of the vitrification process, e.g. melt waste plus glass-forming frit additives and cast. A second reason that glass has become widely used for HLW is that the short-range order (SRO) and medium-range order (MRO) found in glass atomistically bonds the radionuclides and governs the melt properties such as viscosity, resistivity, and sulfate solubility. The molecular structure of glass controls contaminant/radionuclide release by establishing the distribution of ion exchange sites and hydrolysis sites, and the access of water to those sites. The molecular structure is flexible and hence accounts for the flexibility of glass formulations to waste variability. Nuclear waste glasses melt between 1050 and 1150°C which minimizes the volatility of radioactive components such as Tc^{99}, Cs^{137}, and I^{129}. Nuclear waste glasses have good long-term stability including irradiation resistance. Process control models based on the molecular structure of glass have been mechanistically derived and have been demonstrated to be accurate enough to control the world's largest HLW Joule-heated ceramic melter in the US since 1996 at 95% confidence.

Key words: high level waste, HLW, glass, vitrification.

9.1 Introduction

Vitrification is currently the most widely used technology for the treatment of high level radioactive wastes (HLW) throughout the world. Most of the nations that have generated HLW are immobilizing in either borosilicate glass or phosphate glass. One of the primary reasons that glass has become the most widely used immobilization medium is the relative simplicity of the vitrification process, e.g. melt waste plus glass-forming frit additives and cast. Melting homogenizes the mixture and so this process is easier to perform remotely than a ceramic waste form process that requires powder handling, e.g. mechanical mixing of waste and ceramic additives and grinding for particle size control, followed by cold pressing and sintering or hot pressing at elevated temperatures. A second reason that glass has become widely used for HLW is that the amorphous and less rigid structure of glasses compared to ceramics enables the incorporation of a very large range of elements that are atomically bonded in the flexible glass structure. Thus glasses can accommodate larger waste composition fluctuations than ceramics.

Moreover, HLW glasses melt at lower temperatures (1050–1150°C) compared to higher ceramic waste form processing temperatures, which minimizes the volatility of radioactive components such as Tc^{99}, Cs^{137}, and I^{129}. Often in ceramics made by cold pressing and sintering or hot isostatic pressing, an intergranular glassy phase is produced on the ceramic grain boundaries and the radionuclides preferentially migrate to the glassy phase(s) [1–7]. While ceramics are often credited with having higher chemical durability than glasses, if the radionuclides are incorporated in the intergranular glassy phases, they leach at the same rates as those from glassy waste forms [8].

Lastly, nuclear waste glasses have good long-term stability including irradiation resistance and excellent chemical durability. In addition, the ease of modeling the durability of a homogeneous rather than a heterogeneous material in terms of having only one radionuclide source term is also an advantage. There are over 40 years of processing experience[1] with commercial borosilicate glasses, and borosilicate glasses have favorable systems evaluations in terms of both melting and product behavior. These attributes of borosilicate HLW glasses are discussed in more detail in the sections below.

9.1.1 HLW glass composition tolerance

Most nuclear nations have generated high level radioactive wastes from nuclear weapons programs and/or commercial nuclear power generation and most store waste materials from a variety of reprocessing flowsheets. The Plutonium and URanium EXtraction (PUREX) process[2] is the baseline for spent fuel reprocessing for most countries with active fuel cycle programs (see Chapter 1). France and the UK reprocess spent fuel for electric utilities from other countries using the PUREX process to recover uranium (U) and plutonium (Pu). Slight modifications to the PUREX

---

[1] Phosphate glasses (aluminophosphates and iron-phosphates) are not used commercially as frequently as the borosilicates and hence are not as well studied for applications to HLW stabilization.

[2] The PUREX process was developed in the United States in 1950 and the world's first operational full-scale PUREX separation plant began radioactive operations at the Savannah River Plant in 1954. The process ran continuously until the 1990s.

process can be made to recover U, Pu, Np, and Tc (if desired) and a number of countries (e.g., France, Japan, China, etc.) are developing solvent extraction processes to recover the minor actinides (Am and Cm) from spent fuel. Elimination of these actinides and fission products from the HLW reduces the long-term radiotoxicity and heat generation from an immobilized waste form once it is entombed in a geological repository.

In the US, a moratorium was placed on reprocessing of commercial spent nuclear fuel in 1977. A 2005 energy bill has revived the potential for reprocessing, but currently spent fuel rods (once through) are in storage pools across the US and destined for direct disposal in a deep geological repository. Hence, HLW in the US is primarily defense wastes of which 36 million US gallons (136,275 m^3) are stored at the Savannah River Site (SRS) in South Carolina and 50 million US gallons (189,270 m^3) are stored at the Hanford site in Richland, Washington (Fig. 9.1). While Hanford has more waste volume, Savannah River Site waste contains higher curie contents. Prior to the 1977 moratorium, a reprocessing facility had been built and initiated operation in West Valley, New York. The West Valley Demonstration Project (WVDP) created ~0.66 million US gallons (2500 m^3) of HLW from commercial nuclear fuel reprocessing using the PUREX and THOREX processes [9] (Fig. 9.1).

The nuclear nations' HLW streams are stored either as neutralized nitric acid streams in mild steel tanks (US and Russia) or as nitric acid streams in stainless steel tanks (France, UK, Japan, Russia). Although borosilicate glasses have become the preferred waste form for the immobilization of HLW solutions in the majority of the nuclear nations, the chemical variability of the wastes from the different reactor and reprocessing flowsheets

9.1 Distribution of HLW in the United States.

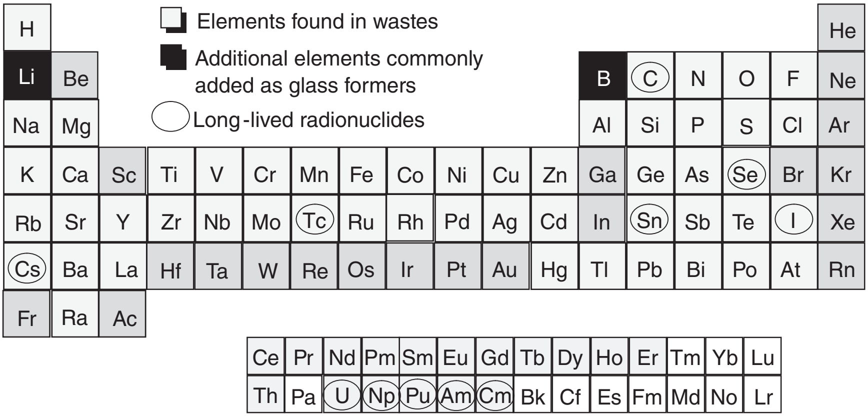

9.2 Elements in US HLW defense glass.

coupled with the additional variability imposed by neutralization vs. direct storage of acidic wastes has led to a diverse HLW chemistry, e.g. HLW contains about three-quarters of the elements in the periodic table (Fig. 9.2).

Some of these extreme differences in HLW waste chemistry from different facilities operating different flowsheets are shown in Table 9.1. When the HLW wastes are expressed as calcine oxides instead of on a liquid basis [10, 11] this wide variability is readily apparent (Table 9.1). To accommodate the differences in heat loads of the different HLW wastes (those produced by different reactor designs and those wastes processed immediately vs. those processed after neutralization and aging) different waste loadings are used (Table 9.1).

9.1.2 HLW glass adaptive structure

Glass has been found to be very flexible and to bond many of the HLW constituents (both radioactive and non-radioactive components) atomistically. Borosilicate waste glasses and melts possess short-range order (SRO; radius of influence ~1.6–3 Å) around a central atom, e.g. polyhedra such as tetrahedral and octahedral structural units (Fig. 9.3a), and medium-range order (MRO) [12] which encompasses second- and third-neighbor environments around a central atom (radius of influence ~3–6 Å; Fig. 9.3a). The polymerization of the SRO and MRO allows glasses to be more flexible in atomically bonding waste species than crystalline (ceramic or mineral) waste forms in which one must more rigorously know what crystalline structure each HLW waste component will reside in.

In glass, the central cation in the SRO tetrahedra is bonded covalently to the four surrounding oxygen atoms (Fig. 9.3a). The central cation in the

Table 9.1 HLW waste compositions in the US on a calcine oxide basis (wt%)

Oxide species (wt%)	DWPF high Fe (Purex HAW)[a]	DWPF high Al waste sludge (HM HAW)[a] before Al dissolution	DWPF high Al waste sludge (HM HAW)[a] after Al dissolution	West Valley, NY, reprocessing plant[c]
Waste loading (wt% calcine oxide)	28–38	28–38	28–38	25[b]
pH	Basic	Basic	Basic	Basic
Fission product oxides*	2.71 (0.53 RuO_2)	0.78 (0.04 RuO_2)	1.27 (0.08 RuO_2)	3.16 (0.34 RuO_2)
Actinides†	7.24 $UO_2 > ThO_2$	3.47 $UO_2 > ThO_2$	6.65 $UO_2 > ThO_2$	18.35 $ThO_2 > UO_2$
Al_2O_3	5.99	62.78	30.02	2.39
CaO	2.46	1.42	2.73	–
Cr_2O_3	0.71	0.24	0.46	2.92
CuO	0.17	0.06	0.11	–
Fe_2O_3	50.64	10.89	20.82	50.30
HgO	0.33	4.31	8.26	–
K_2O	0.16	0.15	0.29	0.44
MgO	0.56	0.27	0.51	–
MnO	12.70	3.05	5.83	1.34
Na_2O	6.33	3.48	7.04	6.77
NiO	6.52	1.17	2.24	2.01
PbO	0.68	0.01	0.02	–
P_2O_5	0.28	0.69	0.45	11.09
SiO_2	1.35	6.71	12.84	–
ZnO	0.28	0.06	–	–
F	–	0.16	0.30	–
Cl	0.18	–	–	0.10
SO_4	0.72	0.31	0.15	1.02
Total	100.00	100.00	100.00	100.00

* Fission product oxides (ZrO_2, SrO, Y_2O_3, MoO_3, TcO_2, Ag_2O, CdO, SnO_2, SeO_2, TeO_2, Rb_2O, Cs_2O, BaO, Ce_2O_3, Pr_2O_3, Nd_2O_3, La_2O_3, Sm_2O_3, Eu_2O_3, Gd_2O_3, Pm_2O_3, RuO_2, Rh_2O_3, PdO).
† Actinide oxides (UO_2, NpO_2, PuO_2, AmO_2, CmO_2, ThO_2) with oxides of Np, Pu, Am, Cm, Bk, Cf, Es, Fm, Md, No, and Lw being considered transuranic (TRU) in the United States.
Sources:
a. R.E. Eibling and J. R. Fowler, 'Updated Waste Composition at the Savannah River Plant', DPST-83-313 (February 1983).
b. R.A. Palmer, H., Smith, G. Smith, M. Smith, R. Russell, and G. Patello, 'Chemical and Physical characterization of the first West Valley demonstration project high-level waste feed batch', *Ceramic Transactions*, 132, 345–355 (2002); and V. Jain and S.M. Barnes, 'Radioactive waste solidification at the West Valley Demonstration Project (WVDP)', *Ceramic Transactions*, 29, 545–552 (1993).
c. C.C. Chapman, 'Design preferences for a slurry-fed ceramic melter suitable for vitrifying West Valley wastes', *Adv. Ceramics*, 8, 149–160 (1984).

Hanford 76–68[d]	INL HLW blended[e]	UK Magnox wastes (MW)[d]	French UOX1 reprocessed waste[f]	Belgian SM58[d]	Russian Myack[g]	Japanese Tokai[h]
32.5	17.7	25–31	16.5	11.1	~10	18.29
Basic	Acidic	Acidic	Acidic	Acidic	Acidic	Acidic
38.48 (5.60 ZrO_2)	80.1 (79.1 ZrO_2)	44.40 (3.46 RuO_2; 6.39 MoO_3)	72.24 (6.00 RuO_2)	54.95	37.91	65.01 (7.16 MoO_3; 12.14 Gd_2O_3; ~4.00 RuO_2)
13.95	0.33	1.60	2.25	–	–	5.41
–	8.9	19.60	–	–	–	–
–	0.45	–	–	–	–	–
1.21	–	1.60	3.15	–	0.58	1.69
–	0.36	–	–	–	–	–
29.09	0.26	10.00	18.06	10.81	6.07	9.02
–	–	–	–	–	–	–
–	6.29	–	–	–	22.00	
–	–	21.60	–	–	2.07	
–	–	–	–	–	–	
15.15	–	–	–	33.33	27.98	16.46
0.60	–	1.20	2.54	0.91	3.39	1.48
–	0.01	–	–	–	–	–
1.52	2.93	–	1.76	–	–	0.93
–	0.37	–	–	–	–	–
–	–	–	–	–	–	–
–	–	–	–	–	–	–
–	–	–	–	–	–	–
–	–	–	–	–	–	–
100.00	100.00	100.00	100.00	100.00	100.00	100.00

d. J.A.C. Marples, 'The preparation, properties, and disposal of vitrified high level waste from nuclear fuel reprocessing', *Glass Technology*, 29[6] (1988).

e. The 'all blend' composition given in this table assumes that the following wastes at INL are blended, e.g. sodium bearing waste (SBW), an Al-calcine, a Zr-calcine, solids, and ion-exchange resins–see D.K. Peeler, I. Reamer, J. Vienna, and J.A. Crum, 'Technical Status Report: Preliminary Glass Formulation Report for INEELHAW', US DOE Report WSRC-TR-98-00132 (March 1998) for details.

f. D. Caurant, P. Loiseau, O. Majérus, V. Aubin-Chevaldonnet, I. Bardez, and A. Quintas, *Glasses, Glass-Ceramics and Ceramics for Immobilization of high Radioactive Nuclear Waste*, Nova Science Publishers, New York, 359 pp. (2009).

g. M.I. Ojovan and W.E. Lee, *New Developments in Glassy Nuclear Wasteforms*, Nova Science Publishers, New York (2007).

h. Personal communication, IHI (2001).

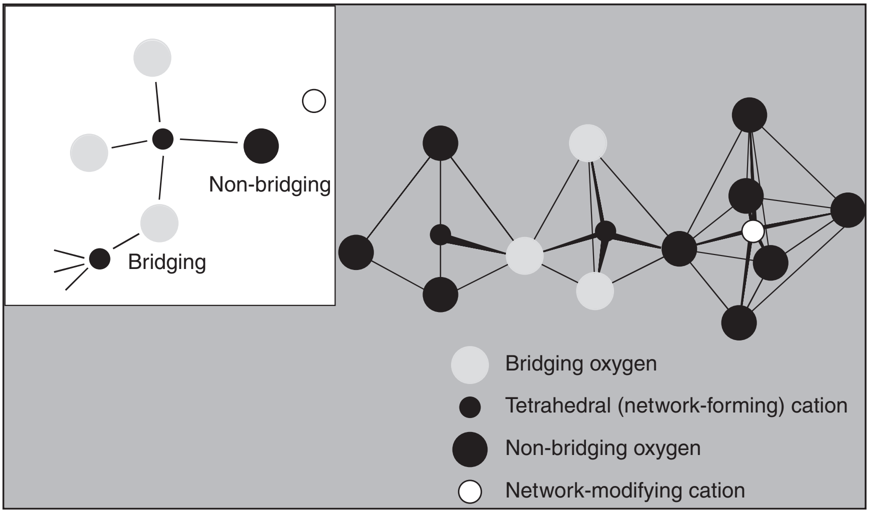

(a)

9.3 (a) An example of short-range order (SRO; tetrahedra and octahedra) and medium-range order (MRO; tetrahedra and octahedra with a network-modifying cation attracted to the non-bridging oxygen of the SRO tetrahedron in inset and two tetrahedra linked to an octahedron) structural units in glass and crystalline structures. Glass is a polymerized random structure of $(SiO_4)^{-4}$, $(AlO_4)^{-5}$, $(BO_4)^{-5}$ and $(PO_4)^{-3}$ tetrahedral and $(BO_3)^{-3}$ trigonal structural units. (b) Polymerization of SRO and MRO in the atomic structure of glass. The unshaded region shows formation of an alkali molybdate cluster (from Calas *et al.*, 2003 [27]). (c) A modified random network (MRN) for a glass of nominal composition $M_2O_3(G_2O_3)_2$, where M represents the modifying cations and G represents the tetrahedral cations. Covalent bonds are shown by the solid lines and ionic bonds by the dotted lines. The shaded regions are defined by the boundary which runs along the G–O non-bridging bonds. The unshaded regions represent the percolation channels defined by the M–O bonds that run through the glass network (Greaves, 1985 [21]).

SRO octahedra is bonded ionically to six surrounding oxygen atoms and is often a HLW constituent. The tetrahedra are linked to each other or to an octahedral SRO via a bridging oxygen bond (BO) (Fig. 9.3a inset). The non-bridging (NBO) atoms carry a negative charge and, in turn, bond positively charged cations like Cs^+, Sr^{+2} and Ca^{+2} and positively charged contaminants (hazardous and radioactive species) ionically (Fig. 9.3a inset).

The linkage of the SRO structural units creates the MRO structural groups such as (Cs,K,Na,Li)AlO_2, (Cs,K,Na,Li)FeO_2, (Cs,K,Na,Li)BO_2, and (Cs,K,Na,Li)SiO_4 [13] or (Cs,K,Na)$AlSiO_4$ [14] which form chains and rings in the glass structure (Fig. 9.3b). Experimentation has confirmed that glasses

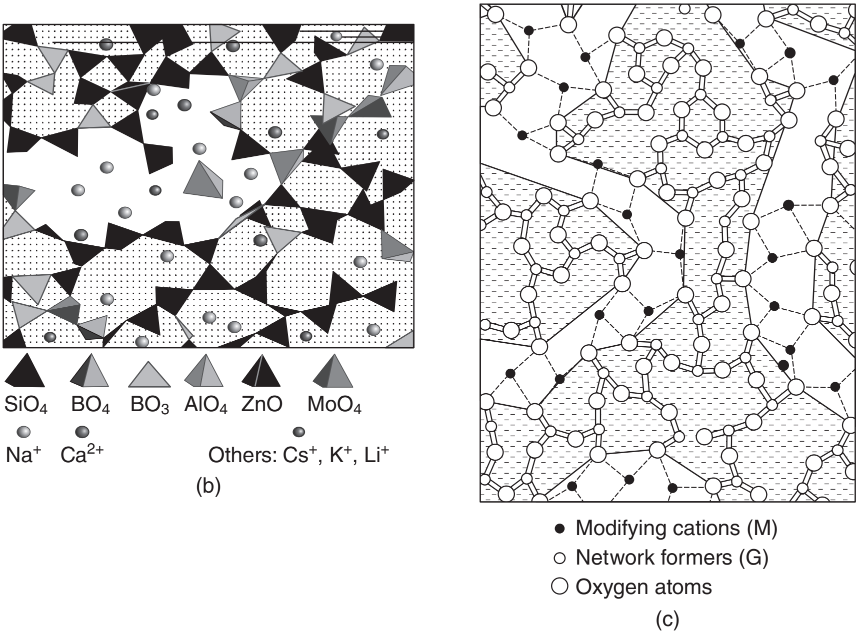

(b)

(c)

9.3 Continued

contain framework units, sheet-like units, chain-like units, and monomers [15] made up of tetrahedra of $(SiO_4)^{-4}$, boria as $(BO_4)^{-5}$ (where B is surrounded by four oxygen atoms or IV coordinated), $(PO_4)^{-3}$, $(AlO_4)^{-5}$, or $(BO_3)^{-3}$ trigonal units (where B is surrounded by three oxygen atoms or III coordinated) which are the same SRO structures found in crystalline minerals. The existence of MRO in melts and glasses led to a redefinition [16] of the widely accepted Zachariasen–Warren random-network structure model of glass [17–19] and its predecessor the crystallite structure model of glass [20]. The 'modified crystallite model' of glass structure treats the degree of medium-range order as spatial fluctuations in the glass network [16]. Similarly, Greaves [21] proposed a 'modified random network (MRN)' model which involves two interlacing 'sublattices'. One sublattice is more highly ordered (network regions) while the other is not (inter-network regions made up of large concentrations of network modifiers). The MRN model is able to describe the existence of large cation-rich clusters in glass, e.g. clusters of Ca in $CaSiO_3$ glasses [21] and Na_2MoO_4 (Fig. 9.3b). In the MRN, the tetrahedral SRO non-bridging oxygen atoms define the network regions, while the NBO-cation regions represent percolation channels that can act as ion-exchange paths for elements that are ionically bonded to the NBO (Fig. 9.3c). Such percolation channels are also found in rare-earth alumino-borosilicate glasses [22]. Thus, the molecular structure of glass controls contaminant release by establishing the distribution of ion exchange sites and hydrolysis sites, and the access of water to those sites.

In glass, the more highly ordered regions of MRO, referred to as clusters or quasi-crystals, often have atomic arrangements that approach those of crystals [12, 23]. These clusters or quasi-crystals, in conjunction with the octahedral site preference energies [24, 25], govern which waste constituents have poor solubility in borosilicate glass [26–29] and which crystalline species may form at the liquidus or during cooling of the vitrified waste form [24, 25]. The same type of SRO and MRO bonding that occurs in glass occurs in mineral waste forms. The primary difference with crystalline waste forms (ceramics/minerals) is that the SRO and MRO are more ordered and the crystallographic polyhedra have higher symmetry and so the mineral structures possess crystallographic long-range order (LRO), while the SRO and MRO in glasses have MRO distributions exhibiting polymerization into rings and chains and allow glass structures to accommodate the wide range of species existing in HLW wastes.

Vitreous waste forms can include silicate-based glasses, borosilicate glasses, phosphate glasses, etc. They are amorphous and leach congruently.[3] They can crystallize during cooling and thus can become glass ceramics or glass ceramic composites (GCMs) which leach incongruently. Vitreous waste forms can be made by a variety of melting technologies that include Joule-heated melters (this chapter) and cold crucible induction melters (CCIM; see Chapter 5).

9.1.3 HLW glass durability: a single source term

Glasses are homogeneous (one phase) and provide a single source term when testing glass and developing durability/leaching models. A basic assumption in all glass dissolution models, as well as in all mineral dissolution models, is that the solid being modeled comprises a single phase and so the durability response has only one source term. Therefore, phase separated glasses (with two source terms) cannot be easily modeled in this fashion. The approach to durability prediction for phase separated glasses is often referred to as mixed mechanism modeling, e.g., the separated phase for borosilicate glass is often boron rich and has a poorer durability than the bulk and/or the matrix phase. Having a poorly soluble second phase is not desirable for HLW

---

[3] Congruent dissolution of a waste form is the dissolving of species in their stoichiometric amounts. For congruent dissolution, the rate of release of a radionuclide from the waste form is proportional to both the dissolution rate of the waste form and the relative abundance of the radionuclide in the waste form. Thus for borosilicate glass ^{99}Tc is released at the same rate, congruently, as Na, Li, and B.

glasses where the distribution of the radionuclides in the two glassy phases would have to be known for every waste glass fabricated.

Additional mixed mechanism leaching can occur if crystals are present in a glass because crystals create grain boundaries that can (1) selectively undergo accelerated dissolution while the crystals themselves may have a different dissolution response [30] or (2) have compositions not representative of the bulk glass [31].

Glass formulations with only 1–2 wt% crystals are targeted for HLW in the US. Crystals such as iron spinels are 'inert' as they have little impact on glass durability, e.g. they are themselves very durable and cause minimal grain boundary dissolution since the spinels and the glass are both isotropic [30, 32]. However, for other phases such as nepheline, acmite, and lithium silicates, which are less durable than iron spinels and are not isotropic, the impact on glass durability from the crystal and the grain boundary can be pronounced. This is especially true if the crystal sequesters radionuclides as this gives a secondary source term for radionuclide release. Therefore, durability testing must be performed to confirm that any crystallization that might occur during canister cooling or during GCM formation has minimal impact [33–36]. This ensures that the last three terms in Equation 9.1 approximate to zero and that the dissolution response does not represent mixed mechanisms.

$$\sum \text{Durability} = \underbrace{\text{durability}_{(\text{homogeneous})}}_{\text{1st term}} + \underbrace{\text{durability}_{(\text{amorphous phase separation})}}_{\text{2nd term}} + \underbrace{\text{durability}_{(\text{crystallization})}}_{\text{3rd term}} + \underbrace{\text{durability}_{(\text{accelerated grain boundary})}}_{\text{4th term}} \qquad 9.1$$

9.2 High level radioactive waste (HLW) glass processing

9.2.1 Pre-processing of HLW acidic and neutralized HLW

The differences in HLW waste chemistry (Section 9.1.1 and Table 9.1) and storage methodologies (acidic vs. neutralized) have led to differences in waste pre-processing prior to and during vitrification. In acidic HLW wastes, the HLW contains free nitric acid and nitrate salts (Fig. 9.4a). In HLW neutralized with NaOH, the HLW contains primarily nitrate salts as a supernatant liquid that is less dense than the metal hydroxides formed during the neutralization (Fig. 9.4b). Thus in neutralized HLW, the excess neutralizing agent (NaOH) and nitrated salts must be treated separately from the sludge so that these non-radioactive constituents do not become part of the HLW vitrified product and take up valuable repository space (estimated at one million dollars burial costs per canister in the US).

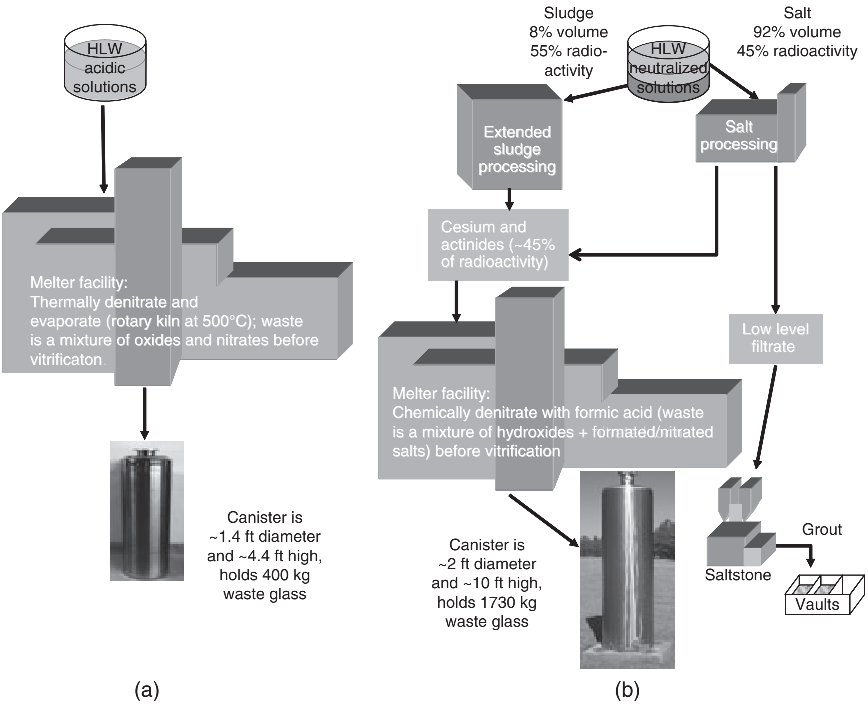

9.4 Typical vitrification flowsheets: (a) the AVM/AVH vitrification process for acid HLW wastes; (b) the Defense Waste Processing Facility (DWPF) vitrification process for neutralized HLW waste.

9.2.2 Removal of neutralizing agents from HLW: sludge washing

In neutralized HLW, the supernatant liquid is 92% of the waste volume and contains 45% of the radioactivity (primarily Cs^{137} and actinides) (see Fig. 9.4b). The hydroxide sludge formed after neutralization is only 8% of the waste volume and contains 55% of the radioactivity. Thus, the supernate is decanted and decontaminated (salt processing in Fig. 9.4b). After the supernatant is decanted from the top of the sludge, the sludge still contains residual supernatant in the interstitial regions. By mobilizing the sludge with water followed by a settling period, the resulting 'wash water' can be decanted and processed along with the supernates or evaporated [37] and returned to the tank farm for future processing. This minimizes the amount of soluble salts ($NaNO_3$, $NaNO_2$, NaOH, Na_2SO_4, $NaAlO_2$ and others) remaining with the HLW sludge and is known as 'sludge washing' [38, 39].

'Sludge washing' requires additional processing steps and the number of washing stages may be reduced or eliminated altogether. Typical 'sludge washing' scenarios are 2–5 wash cycles[4] and removal of soluble sodium salts including sodium sulfate. If the washing process is not as efficient as anticipated or fewer washing cycles are performed, additional sodium salts will become part of the sludge waste feed to the melter. In the following section the impact that this has on the calculation of the waste loading (WL) factors will be discussed. Sludge washing was performed at West Valley [40], is being performed routinely at the SRS, and may be performed at Hanford Waste Treatment Plant (WTP) in the US.

The radioactivity is usually removed from the supernates by the use of various combinations of ion exchange, selective precipitation, or solvent extraction and the radioactivity removed from the supernatant along with any spent ion exchange media is recombined with the sludge (Fig. 9.4b) to be vitrified as HLW. The low level waste filtrate, often referred to as the low activity waste (LAW) fraction of HLW, is either cemented (SRS or West Valley) or vitrified[5] (Hanford) and buried as low level waste at the individual sites. Alternate mineral waste forms being made by fluidized bed steam reforming (FBSR) are being examined for the LAW fraction of HLW at Hanford, and the mineral waste form is being implemented at Idaho National Laboratory for their sodium bearing waste (SBW).

9.2.3 Removal of cladding elements from HLW: Al dissolution

Defense wastes are high in aluminum (see Table 9.1), as aluminum-clad fuel assemblies and targets were dissolved in order to recover the uranium, plutonium and other radioactive isotopes of interest for defense purposes. Because the waste has been neutralized, the aluminum is present as gibbsite/bayerite ($Al(OH)_3$) or has aged to boehmite/diaspore (AlOOH) [41]. Both gibbsite and boehmite are soluble in 19M NaOH at 55–85°C as the sodium hydroxide drives the pH into the stability field of soluble $NaAlO_2$. The NaOH is consumed in the conversion of the aluminum hydroxides to $NaAlO_2$ and water [37] and $NaAlO_2$ is one of the soluble salts that can be removed by sludge washing (see Section 9.2.2). A full-scale active demonstration of 'Al dissolution' was performed in 1982 [37, 42] in waste tank 51. This demonstration, which allowed NaOH to dissolve Al out of the sludge for 5 days, showed that up to 80% of the aluminum in the

---

[4] Dependent on sludge volume and settling times, smaller volumes with rapid settling times may be washed 9–11 times.

[5] At the Hanford Site, due to the Hanford Federal Facility Agreement and Consent Order (Tri-Party Agreement between Department of Energy-Richland, the Washington State Department of Ecology, and the Environmental Protection Agency) signed in 1989, the low level filtrate will be vitrified (either Joule heated or by bulk vitrification) instead of cemented and buried as done at SRS.

high alumina-defense wastes created in H-Area and M-Area (HM) at SRS could be removed. The alumina dissolution is performed before sludge washing for the high alumina-containing sludges and then the excess $NaAlO_2$ created becomes part of the low level waste filtrate that is sent to shallow land burial on site (Fig. 9.4b). Recent demonstrations in 2008 showed that this reduces the 8% HLW sludge volume at SRS by ~1% which translates to a saving of 1.56×10^6 kg of glass (900 canisters) out of 1.38×10^7 kg of glass (8000 canisters) [37] or 11.25% fewer HLW glass canisters to be buried in a deep geological repository.

9.2.4 Thermal denitration vs. chemical denitration

Both acid and neutralized HLW waste (after sludge washing and Al dissolution) must be denitrated before vitrification (Section 9.2.2). Denitration can be performed either thermally or by the use of chemical additives [43]. Prior to thermal denitration the acidic wastes are concentrated by evaporation, or evaporation and denitration can be achieved simultaneously in a rotary kiln (Fig. 9.4a). Thermal denitration via calcination can increase the volatility of certain species such as Ru^{101}, Ru^{102}, Ru^{104} and Tc^{99} depending on the temperature of the calcinations [43].

The use of various organic reductants (formic acid, formaldehyde and sugar) has been successful for denitration of HLW as well as electrolytic denitration. The use of chemical additives for denitration reduces the acid content of the waste (waste that has not been neutralized) and/or the nitrated salts in the waste (in the case of neutralized wastes). At AVM (Atelier de Vitrification de Marcoule)/AVH (Atelier de Vitrification de La Hague) thermal denitration via a rotary calciner is used in conjunction with chemical additives such as sugar that are co-processed in the rotary calciner, which allows the denitration to be performed at temperatures as low as 500°C (Fig. 9.4a).

At the Savannah River Site vitrification facility, the Defense Waste Processing Facility (DWPF), denitration occurs in the sludge receipt and adjustment tank (SRAT) via formic acid additions (Fig. 9.4b). Since this is a neutralized HLW sludge, the formic acid also improves the rheology of the hydroxide sludge, decomposes any carbonates which could create CO_2 foam during melting, reduces manganese from Mn^{+4} to Mn^{+2} to prevent oxygen foaming during melting, and reduces mercury to the metallic state so it can be steam-stripped before it is volatilized in the vitrification process [44–46].

At West Valley sugar was used for denitration and added to the feed preparation tank [9] along with the glass-forming additives. At Myack in Russia molasses was added to form a ‘cold cap’ and limit volatility [47]. At the Hanford WTP sugar is being used for denitration [48]. The sugar is added with the feed and the melter is bubbled to enhance reactions, release evolved gases, and improve melt convection and melt rate.

9.2.5 The evolution of melter designs [49]

Commercial glass melters are extremely large and generally built in place, e.g. where they are operated. HLW glass melters are generally smaller and constructed as integrated systems and moved to the operating facilities. At the facilities they are installed and removed using remotely operated cranes. Once installed, the maintenance of the HLW melters is limited to changing out of auxiliary devices and/or complete melter replacement (Fig. 9.7). This type of operating environment requires melters of limited size that produce glass of consistent quality at predictable rates.

Fig. 9.5 shows the types of HLW melter systems that have been developed over the last 40–45 years: batch melters, continuous pot melters, and Joule-heated ceramic-lined melters (JHCM). The first waste glass melters were designed for batch operations. These were unsuitable due to slow heat transfer from external heaters through the canister into the reacting batch. The batch melters also suffered from lack of agitation and non-uniform temperature distribution which inhibited the glass from melting homogeneously. Calcination of the feed before introduction into the batch melter increased the melt rate but also increased the tendency for crystals to form

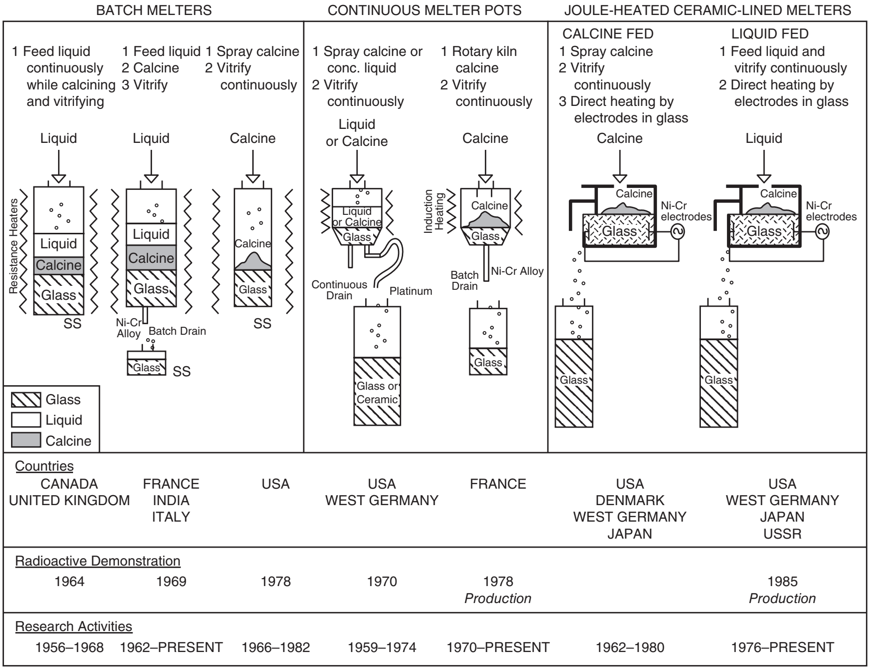

Countries						
CANADA UNITED KINGDOM	FRANCE INDIA ITALY	USA	USA WEST GERMANY	FRANCE	USA DENMARK WEST GERMANY JAPAN	USA WEST GERMANY JAPAN USSR
Radioactive Demonstration						
1964	1969	1978	1970	1978 *Production*		1985 *Production*
Research Activities						
1956–1968	1962–PRESENT	1966–1982	1959–1974	1970–PRESENT	1962–1980	1976–PRESENT

9.5 Evolution of HLW glass melter designs over time (from Bickford *et al.*, 1990 [49]).

in the glass. Solids entrainment of the batch materials (calcine and glass formers) was also problematic and the small size of the batch melters required that several be operated simultaneously to meet the production rates needed to immobilize the HLW inventories.

Continuous pot melters made of nickel-chrome alloy were tested in the US, Germany, and France. The diameter of the pot was larger than in batch melters and the pot was directly heated by radio frequency induction heating which increased the melt rate over batch melters. Continuous feeding of the raw materials was employed and gas bubblers were used to agitate the melt. The French AVH system is the largest melter of this type ever operated (Fig. 9.6). Melt temperature was limited to 1150°C due to the alloy used for the pot.

Joule-heated ceramic-lined melters (JHCMs) were tested in the US, Europe, Japan, and Russia (Table 9.3). These melters can be calcine-fed or slurry-fed and vitrification is continuous. The melter is lined with refractory material and the glass is Joule-heated by electricity transferred through the melt between nickel-chromium alloy electrodes. JHCMs have been selected for all the production melter systems in the US, Germany and Japan because of the high production rate and high glass quality. The size of these systems is limited only by the replacement crane capacity since all the structural support is provided by a stainless steel shell which contains the refractory material. The nominal melt temperature is 1150°C which is only 200°C lower than the electrode melting point (electrodes are usually made from Inconel alloys). The DWPF at SRS is the largest production melter of this type ever operated (Fig. 9.7) with a glass surface area of 226 ft^2 (20.996 m^2). Advanced Joule-heated melters (AJHMs) with larger surface areas will be discussed in Section 9.6.1.

Details about the melter designs in use in different countries can be found in recent compendiums by Ojovan and Lee [50, 51], Caurant *et al.* [22], and Jain [52]. There is additional information and historical detail in Chapter 6.

9.3 Glass formulation and waste loading

9.3.1 Structural similarity of glass formulations

While borosilicate glasses have been used in the US and Europe to immobilize radioactive HLW for ultimate geological disposal, aluminophosphate glasses are used in Russia for permanent disposal and/or long-term storage. Iron phosphate glasses have been proposed for HLW in the US but no wide-scale usage of this glass has yet to be implemented. It is believed this is due to the lack of commercial melting experience with this type of glass.

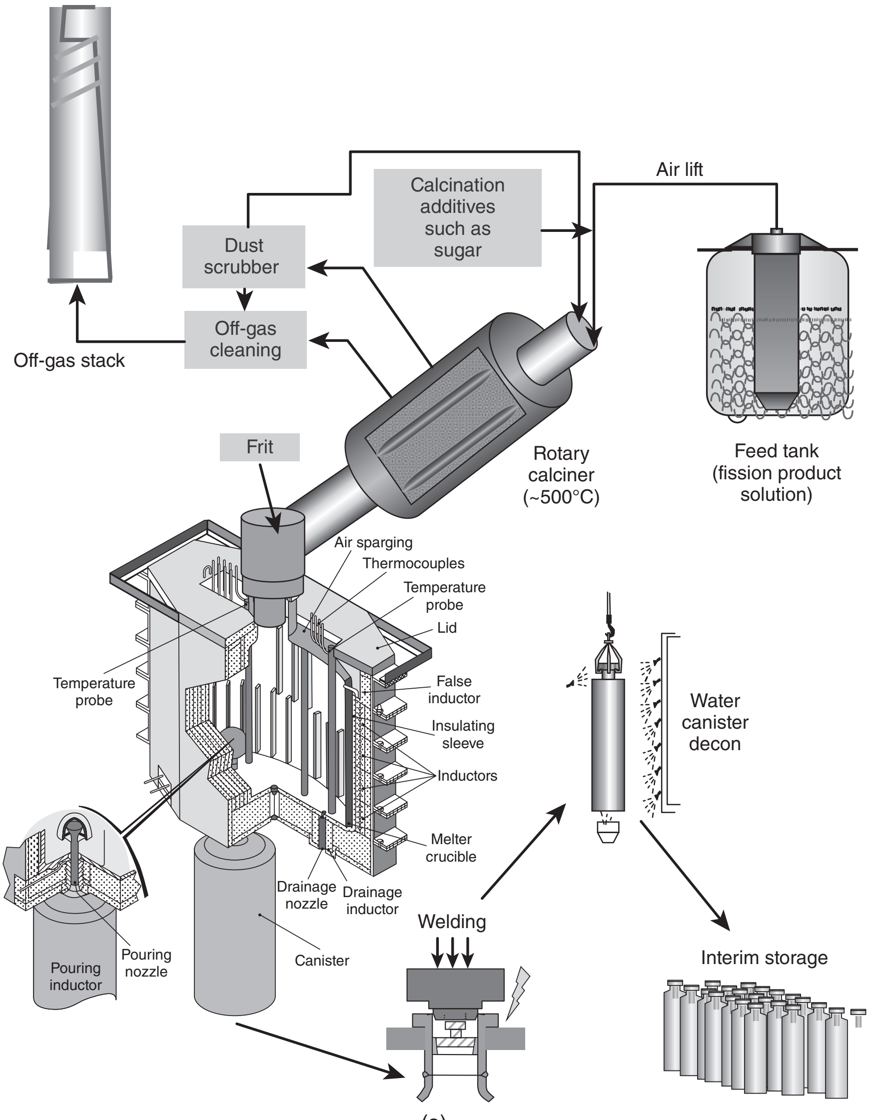

(a)

9.6 (**a**) Melter facility: thermally denitrate and evaporate (rotary kiln at 500°C); waste is a mixture of oxides and nitrates, mix with frit additives; induction-heated Inconel melter (1150°C). (**b**) Melter facility: chemically denitrate with formic acid; waste is a mixture of hydroxides and formated salts, mix with frit (or glass formers); Joule-heated melter, Inconel electrodes, refractory lined (1150°C).

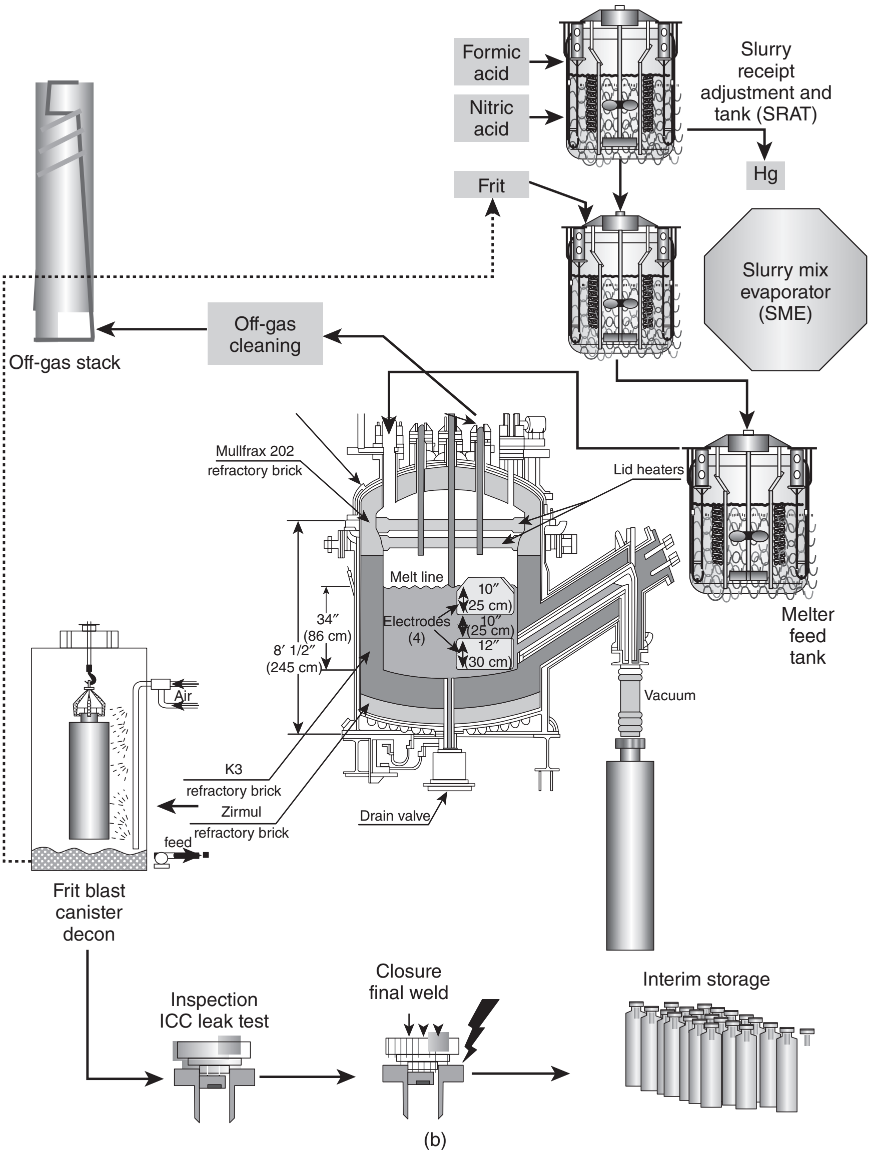

9.6 Continued

Waste glasses must be formulated to maximize the amount of waste to be vitrified so that waste glass volumes and the associated storage and disposal costs are reduced. The wastes generated by different reactor flowsheets were discussed above and are given in Table 9.1. For borosilicate glasses and phosphate glasses different frit additives and different waste loadings are used to accommodate the waste variability (Table 9.2).

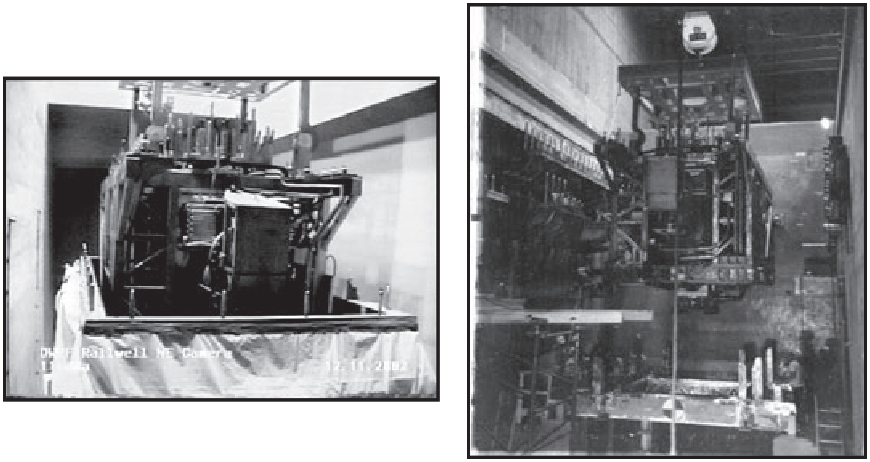

9.7 DWPF Melter One being disposed of after 9 years of operation. The melter was emptied through the emergency bottom drain and lifted out of the melt cell into a waste box for storage and eventual disposal (courtesy of Savannah River Site).

It is significant that the highly variable sludges (Table 9.1), when mixed with the highly variable frits (Table 9.2) at the highly variable waste loadings given in Tables 9.1 and 9.2, fall in a narrow glass-forming region in the borosilicate glass-forming system (Fig. 9.8a). In other words, successful HLW glass formulations contain 60 wt% or more of glass-forming oxides (SiO_2, B_2O_3, ZrO_2, Al_2O_3, P_2O_5 and fission products), >15 wt% glass modifier oxides (Na_2O, K_2O, Li_2O, CaO, MgO, SrO, and ZnO) and from 0 to 25 wt% glass intermediate oxides (Cr_2O_3, Fe_2O_3, CuO, NiO, MnO, PbO, TiO_2 and actinides). While Fig. 9.8a includes the radioactive glasses given in Tables 9.1 and 9.2 at the reference waste loadings given, this same glass-forming region was defined for simulated HLW glasses over an even broader range of glass compositions [53, 54] as shown in Fig. 9.8b.

9.3.2 HLW glass waste loadings

Waste loadings are generally expressed on a calcine waste oxide basis. In other words, if the nitrated or hydroxide wastes were heated to 1000°C and NO_x and H_2O or OH^- vaporized, then only calcine oxides would remain. The grams of calcine oxide waste per 100 grams of glass is referred to as the waste loading and expressed in weight percent. High heat wastes and acidic wastes that have not been neutralized have lower waste loadings, e.g. in the 10–25 wt% range (Table 9.1), as only the fission products and actinides are included in the waste loadings, e.g. the corrosion products such as

Table 9.2 Variations in frit additives on an oxide basis (wt%)

Oxide species (wt%)	DWPF high Fe (Purex HAW)[a]	DWPF high Al waste sludge (HM HAW)[a] before Al dissolution	DWPF high Al waste sludge (HM HAW)[a] after Al dissolution	West Valley, NY, reprocessing plant[c]	Hanford 76–68[d]
Waste loading (wt% calcine oxide)	28–38	28–38	28–38	25[b]	32.5
Al_2O_3	–	–	–	–	–
B_2O_3	10.00	10.00	10.00	15.4	14.18
CaO	–	–	–	–	2.99
K_2O	–	–	–	5.33	–
Li_2O	7.00	7.00	7.00	2.36	–
MgO	1.00	1.00	1.00	1.78	–
Na_2O	13.00	13.00	13.00	14.29	11.19
P_2O_5	–	–	–	–	–
SiO_2	68.00	68.00	68.00	59.35	59.7
TiO_2	–	–	–	1.49	4.48
ZnO	–	–	–	–	7.46
ZrO_2	1.00	1.00	1.00	–	–
Total alkali	20.00	20.00	20.00	21.98	11.19
Total	100.00	100.00	100.00	100.00	100.00

Source:
a. C.M. Jantzen, 'Glass Compositions and Frit Formulations Developed for DWPF', DPST-88-952 (November 1988).
b. L.R. Eisenstatt, 'Description of the West Valley Demonstration Project Reference High-Level Waste Form and Canister', US DOE Report WVDP-056, Rev. 0 (1986).
c. C.C. Chapman, 'Design preferences for a slurry-fed ceramic melter suitable for vitrifying West Valley wastes', *Adv. Ceramics*, 8, 149–160 (1984).
d. J.A.C. Marples, 'The preparation, properties, and disposal of vitrified high level waste from nuclear fuel reprocessing', *Glass Technology*, 29[6] (1988).
e. D.K. Peeler, I. Reamer, J. Vienna, and J.A. Crum, 'Technical Status Report: Preliminary Glass Formulation Report for INEELHAW', US DOE Report WSRC-TR-98-00132 (March 1998).
f. D. Caurant, P. Loiseau, O. Majérus, V. Aubin-Chevaldonnet, I. Bardez, and A. Quintas, *Glasses, Glass-Ceramics and Ceramics for Immobilization of High Radioactive Nuclear Waste*, Nova Science Publishers, New York, 359 pp. (2009).
g. M.I. Ojovan and W.E. Lee, *New Developments in Glassy Nuclear Wasteforms*, Nova Science Publishers, New York (2007).
h. Personal communication, IHI (2001).

INL HLW blended[e]	UK Magnox wastes (MW)[d]	French UOX1 reprocessed waste[f]	Belgian SM58[d]	Russian Myack[g]	Japanese Tokai[h]
17.7	25–31	16.5	11.1	~10	18.29
2.99	–	5.89	1.35	21.11	6.13
6.08	21.93	16.67	13.82	–	17.38
–	–	4.80	4.27	–	3.66
–	–	–	–	–	–
6.11	5.35	2.35	4.16	–	3.66
–	–	–	2.25	–	–
22.81	11.09	12.05	5.17	21.11	8.54
–	–	–	–	57.78	–
62.01	61.63	54.04	63.93	–	56.97
–	–	–	5.06		–
–	–	2.98	–	–	3.66
–	–	1.21	–	–	–
28.92	16.44	14.4	9.33	78.89	12.2
100.00	100.00	100.00	100.00	100.00	100.00

Fe_2O_3, Cr_2O_3, and NiO and any small amounts of alkali are not included in the waste loading. For the neutralized US defense wastes the corrosion products and Fe_2O_3 from the use of ferrous sulfamate during processing, and some of the alkali used for neutralization that cannot be washed out of the HLW sludge, is included in the waste loading calculations. Therefore, waste loadings up to 38–40 wt% on an oxide basis are achieved (Table 9.3). Table 9.3 demonstrates that the waste loadings for the US wastes are higher than those of the European and Russian wastes but the radionuclide content, expressed in tera-bequerels, is lower for the US wastes than for the European and Russian wastes.

9.3.3 Systems approach to glass formulation: basis for formulation similarities

The HLW glass formulations are driven by the need to simultaneously optimize [55–57] multiple product/process (P/P) constraints such as waste

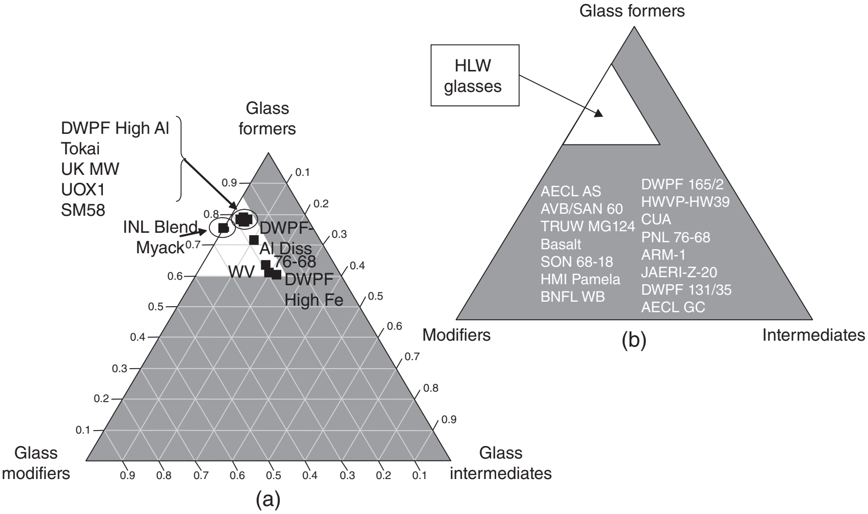

9.8 Ternary diagram depicting compositional similarities for a variety of HLW glasses expressed in terms of the structural components of the glasses.

component solubility, melt viscosity, melt corrosivity, melt volatility, liquidus and glass product durability (Table 9.4). A given HLW glass must simultaneously optimize all of the P/P constraints and not just have superior chemical durability while having poor thermal or mechanical stability or while being corrosive to all known melter materials of construction. In other words, one must look at the entire system using a 'systems approach', e.g. how does this waste form react during processing and how will the product produced react with the disposal environment and meet the regulatory requirements of the disposal system? Most P/P properties, other than melt temperature, cannot be measured directly. The waste streams are often highly variable and difficult to characterize. Therefore, often P/P models are used to relate glass composition to a given property, e.g. durability, viscosity, or liquidus. The 'systems approach' ensures that the final product safeguards the public, and that the production process used is safe to operate.

It is this inherent need to optimize the multiple P/P constraints that drives the diverse waste types and frits into a common region of glass formulation (see Section 9.3.1). For example, the discussion in Section 9.2.1 of the role that MRO in glass has on glass durability demonstrates that ion exchange occurs along percolation channels that exist in glass. The work of Greaves [21] demonstrated that the percolation channels in glass are defined by the NBO atoms, which ionically bond to the alkali, alkaline earth or contaminant species in a glass (Fig. 9.3c). As the cation species are preferentially leached out of the channels, the leachant can then preferentially attack the

Table 9.3 Data on HLW glass production

Vitrification plant	Location	Melting process	Waste glass produced (metric tons)	Waste loading range (wt%)	Size of canisters (meters)	Number of canisters	TBq[§]
Defense Waste Processing Facility (DWPF), Savannah River Site	Aiken, SC, USA	JHCM	5000*	28–40[c]	0.6 × 3	2845	7.7×10^5
West Valley Demonstration Project (WVDP)	West Valley, NY, USA	JHCM	~500**	~20.4–23.5[b]	0.6 × 3	275	8.9×10^5
Waste Vitrification Plant (WVP), BNFL	Sellafield, UK	Induction, hot crucible	~1800[†]	~25[a]	0.43 × 1.34	4319[††]	1.9×10^7
Areva NC (R7/T7)[d]	La Hague, France	Induction, hot crucible	5573 (1989–2008)	12–18[§]	0.43 × 1	14,045	2.38×10^8
AVM or Atelier de Vitrification de Marcoule[d]	Marcoule, France	Induction, hot crucible	1138 (1978–2008)	12–18[§]	0.43 × 1	3159	1.69×10^6
PAMELA	Mol, Belgium	JHCM	500 (1985–1991)	15–25[§]	0.30 × 1.2 0.43 × 1.34	2200	4.5×10^5
Tokai Vitrification Facility[e] (TVF)	Japan	JHCM	>100	20–30[§]	0.43 × 1	247 (1995–2006)	1.5×10^4
Mayak Vitrification Facility[f] (EP-500)	Ural Region, Russia	JHCM	~8000	33[§§]	0.57 × 1	17,600	3.33×10^7

* 1996–2009.

** 1996–2002 – mission complete.

[†] 1991–2007 at 150 L glass per canister and an assumed glass density of 2.75 g/cm3.

[††] Predicted mission completion is 6582 canisters.

[§] 1 tera-becquerel (TBq) = 1012 atoms decaying per second or transmutations per second.

[§§] Acidic waste loadings are comprised of fission products and minor actinides – corrosion products and alkali are not included as for neutralized wastes.

Sources:

a. A. Riley, S. Walker, and N.R. Gribble, 'Composition changes and future challenges for the Sellafield waste vitrification plant', in *Scientific Basis for Nuclear Waste Management, XXXIII*, Materials Research Society, Pittsburgh, PA, 267–273 (2009).

b. J.M. Perez, Jr., D.F. Bickford, D.E. Day, D.S. Kim, S.L. Lambert, S.L. Marra, D.K. Peeler, D.M. Strachan, M.B. Triplett, J.D. Vienna, and R.S. Wittman, 'High-Level Waste Melter Study Report', PNNL-13582 (2001).

c. C.M. Jantzen, A.D. Cozzi, and N.E. Bibler, 'High level waste processing experience with increased waste loadings', in *Environmental Issues and Waste Management Technologies X*, J.D. Vienna, C.C. Herman, and S.L. Marra (eds), *Ceramic Transactions*, 168, 31–49 (2005).

d. Caterine Veyer of AREVA, personal communication (2010).

e. Seiichiro Mitsui of JAEA, personal communication (2010).

f. P.P. Poluektor, private communication (2010).

Table 9.4 HLW waste glass product and process constraints

Product constraints	Process constraints
Chemical durability	Melt viscosity
Glass homogeneity	Liquidus
Thermal stability	Waste solubility
Regulatory compliance	Melt temperature/corrosivity
Mechanical stability	Radionuclide volatility
	REDOX*

* REDuction/OXidation which controls foaming and melt rate.

Si–O NBO bond. This is in agreement with the calculations of El-Shamy [58], which indicate that a silica content of ~67 mol% silica in alkali alkaline-earth silicate glasses corresponds to a composition at which every silicon atom in the glass becomes associated with a basic ion as a second neighbor. Thus, in glasses with <67 mol% silica, there is always an interconnected path of non-bridging +Si–O$^-$ sites that allows exchange of species between leachate solution and the glass. At >67 mol% silica, these sites are isolated from each other by the silica network +Si–O–Si+ groups in the glass that suppress the movement of ions involved in leaching. Therefore, to remain durable most waste glasses contain >67 wt% glass formers (Fig. 9.8) and thus minimize the interconnected paths by which non-matrix forming elements can leach.

9.4 Glass quality: feed-forward process control

When processing HLW glass, a production facility cannot wait until the melt or waste glass has been made to assess its acceptability, since by then no further changes to the glass composition and acceptability are possible. Therefore, the acceptability decision is made on the upstream process, rather than on the downstream *melt* or glass product. That is, it is based on 'feed-forward' statistical *process* control (SPC)[6] rather than statistical *quality* control (SQC).[7] In SPC, the feed composition to the melter is controlled *prior* to vitrification. In SQC, the glass product is sampled *after* it is vitrified. In addition, in the US, the P/P constraints must be satisfied to a very high degree of certainty (>95%) as the canister geometry (Table 9.3) makes rework (remelting) of the product impossible. With feed-forward process control, individual property models are used to transform constraints on the melt and product properties into constraints on the feed

[6] This controls the slurry feed to the melter *prior* to vitrification.

[7] This would adjudicate product release by sampling the glass *after* it has been made.

composition, e.g. the melter is treated as a 'black box' and the glass quality in the canister is controlled at 95% confidence from the incoming feed composition.

The successful 'systems approach' used at the Savannah River Sites HLW Defense Waste Processing Facility (DWPF) since 1996 is based on 'feed-forward statistical process control'. The feed composition to the melter is controlled *prior* to vitrification and a confirmatory glass sample is taken only when the feed tank composition changes, e.g. once every 1–3 years. The feed composition is used to calculate the P/P properties of a melter feed from mechanistic P/P models that relate the melt composition to the P/P properties [55, 56]. The P/P models depend on known relationships between glass bonding, thermodynamics, and glass structure. These models are the foundation of the SPC system used to monitor and control glass composition for HLW (Product Composition Control System) [59]. Since 1996, over 5000 metric tonnes (Table 9.3) of HLW glass has been successfully processed to stringent constraints (95% confidence) without any rework.

The mechanistic models can be extrapolated well outside the glass composition range for which they were developed [60] because they are based on known mechanisms. Therefore, mechanistic models allow more flexibility for process control than empirical models, e.g. empirical models are restricted to the compositional region over which they were developed. The P/P models presented below can, therefore, be directly applied to other types of HLW and borosilicate waste glasses.

9.4.1 Property/process models for borosilicate waste glasses

Glass durability

The most important glass product property is glass durability. The durability of a waste glass is the single most important variable controlling release of radionuclides and/or hazardous constituents. The intrusion of groundwater into, and passage through, a waste form burial site in which the waste forms are emplaced is the most likely mechanism by which constituents of concern may be removed from the waste glass and carried to the biosphere. Thus it is important that waste glasses be stable in the presence of groundwater.

For homogeneous borosilicate HLW glasses, acceptable performance is defined as an acceptably low dissolution rate, which is controlled by maintaining the glass composition within an acceptable range. The approach can be represented in terms of linking several relationships:

process control ↔ composition control ↔ dissolution rate control ↔ performance control ↔ acceptable performance

This linkage is appropriate for HLW waste glasses because the radionuclides are incorporated within the glass structure and are released congruently as the glass dissolves. In general, for any waste form it must be established that control of performance in a laboratory test predicts acceptable control of performance in a disposal system based on performance tests and modeling.

In the United States the durability and phase stability of vitrified HLW must be assessed during production [61] while the repository is interested in the 'maximum radionuclide release'. These are tied together by the linking relationships shown above that process and/or composition control translates into acceptable performance. The 'product quality constraint' on the HLW glass requires that the waste form producer demonstrate control of the waste form production by comparing production samples or process control information, separately or in combination to the Environmental Assessment benchmark glass [62, 63] using the Product Consistency Test (ASTM C1285–08) [64] or equivalent. For acceptance, the mean concentrations of lithium, sodium, and boron in the leachate, after normalization for the concentrations in the glass, shall be less than those of the benchmark glass. For congruent dissolution, the rate of release of a radionuclide from the waste form is proportional to both the dissolution rate of the waste form and the relative abundance of the radionuclide in the waste form [65]. Thus for borosilicate glass Tc^{99} is the radionuclide released at the fastest rate (Cs^{137} is released at a somewhat slower rate). However, extensive testing [66–76] demonstrated that Tc^{99} is released at the same rate, congruently, as Na, Li and B. This enables the Na, Li, and B to be measured in a glass durability test and be equated to the 'maximum radionuclide release'. These elements are not sequestered in precipitates that participate in surface alteration reactions, and are also not solubility limited. In the case of a multiphase glass ceramic waste form it may be important to analyze for elements from each significant phase present.

In vitreous and mineral waste forms, the molecular structure controls dissolution (contaminant release) by establishing the distribution of ion exchange sites, hydrolysis sites, and the access of water to those sites [77]. Thus the DWPF durability model, known as the Thermodynamic Hydration Energy Reaction MOdel (THERMO™) [78, 79], estimates the relative durability of silicate and borosilicate glasses based on their compositions. THERMO™ calculates the thermodynamic driving force of each glass component to hydrate based on the mechanistic role of that component during dissolution, e.g. ion exchange, matrix dissolution, accelerated matrix dissolution, surface layer formation, and/or oxidative dissolution. The overall tendency of a given glass to hydrate is expressed as a preliminary glass dissolution estimator, e.g. the change in the free energy of hydration of a glass (ΔG_p) based solely on its composition. ΔG_p is correlated to the response of a 7-day ASTM C1285 (Product Consistency Test). For glasses that undergo accelerated matrix dissolution, an accelerated hydration free energy, ΔG_a, can be calculated from known strong base (SB)–weak acid (WA) equilibrium. The ΔG_a term is additive to ΔG_p such that the overall durability of the glass, expressed as the final hydration free energy (ΔG_f), can be predicted, e.g. $\Delta G_f = \Delta G_p + \Delta G_a$. The more negative the ΔG_f the more readily the hydration reaction will occur and the less durable the glass. Improvements to the THERMO™ approach have been suggested by Conradt [80–82] in the form of a calculation that accounts for the free energy of formation of the crystalline reference state (c.r.s.) of a glassy material. This calculation improves the model fit between the ΔG_p parameter and the leachate response.

Recently, Jantzen and Pareizs [83] have proposed an Activated Complex Theory (ACT) durability model based on the early work of Helgeson *et al.* [84] and the more recent work of Oelkers and Sislason [85] on basalt glass dissolution. This approach attempts to define the activated complexes that participate in the irreversible formation of the glass gel layer based on the c.r.s. The formation of the hydrated gel layer is the irreversible step. The leached layer exhibits acid/base properties which are manifested as the pH dependence of the thickness and nature of the gel layer. The gel layer has been found to age into either clay mineral assemblages or zeolite mineral assemblages. The formation of one phase preferentially over the other has been experimentally related to changes in the pH of the leachant and related to the relative amounts of Al^{+3} and Fe^{+3} in a glass. The formation of ferrite clay mineral assemblages on the leached glass surface layers (lower pH and Fe^{+3}-rich glasses) causes the dissolution rate to slow to a long-term 'steady state' rate. The formation of zeolite mineral assemblages such as analcime (higher pH and Al^{+3}-rich glasses) on leached glass surface layers causes the dissolution rate to increase and return to the initial high forward rate. The return to the forward dissolution rate is undesirable for long-term performance of glass in a disposal environment.

The ACT approach [83] models the role of glass stoichiometry in terms of the quasi-crystalline mineral species (mineral moieties) in a glass. The stoichiometry of the mineral moieties in the parent glass appears to control the activated surface complexes that form in the leached layers, and these 'mineral' quasi-crystals (some Fe^{+3}-rich and some Al^{+3}-rich) play a role in whether or not clays or zeolites are the dominant species formed on the leached glass surface. The chemistry and structure, in terms of Q distributions of the parent glass, are well represented by the atomic ratios of the glass-forming components. Thus, glass dissolution modeling using simple atomic ratios and/or the c.r.s. are shown to represent the structural effects of the glass on the dissolution and the formation of activated complexes in the glass leached layer: both are related to the activated complexes on the surface by the law of mass action.

The geochemical code EQ3/EQ6 was used to model the leachate compositions from short- and long-term ASTM C1285 (PCT) tests to determine what phases could precipitate from the leachate, e.g. what phase was each leachate supersaturated with respect to. The EQ3/EQ6 predictions were coupled with the glass composition data in ACT and this provided a link between the atomic ratios of the glasses and the leachate supersaturation with respect to either analcime or ferrite phases [83]. Thus glass composition in terms of quasi-crystalline structural ratios could be used to determine whether or not a glass would form analcime and return to the forward rate. Since the pH of a static leachate is also driven by the glass composition and is a parameter entered into the EQ3/EQ6 model, it was not considered as a separate parameter during modeling. The use of the glass atomic ratios determined in this manner correctly predicted the well-studied PAMELA glasses SM58 and SAN60 [86] glasses. The former did not return to the forward rate but the latter glass did [87, 88].

The ACT durability model covers a wider composition range than both the THERMO™ durability model data and the THERMO™ validation data (see [60]). This allows either the ACT model or the THERMO™ model to be applied to broader composition ranges of LLW, TRU, and mixed waste glasses than either was developed for, since both models are based on known dissolution mechanisms for borosilicate glass.

Glass homogeneity

To ensure that borosilicate HLW glasses do not exhibit glass-in-glass phase separation, a minimum Al_2O_3 limit (wt% in the glass) is applied in the US.[8] The effect of insufficient Al_2O_3 was first hypothesized by French researchers [89] who determined that many glass durability models were non-linear, e.g., glasses had release rates far in excess of those predicted by most models in regions corresponding to low Al_2O_3 and in excess of 15 wt% B_2O_3 and this was later confirmed independently by Jantzen *et al.* [78, 79, 90]. The low Al_2O_3 was also shown to be a cause of glass-in-glass phase separation in Al_2O_3–Fe_2O_3–FeO–Na_2O–SiO_2 natural basalt systems [90].

---

[8] In glasses the competition for dominant tetrahedral role can cause one or more of the $(SiO_4)^{-4}$, $(BO_4)^{-5}$, and $(PO_4)^{-3}$ SRO tetrahedral units to phase separate, and contaminants/radionuclides can partition to the more soluble of the two or more glassy phases created. However, the presence of $(AlO_4)^{-5}$ tetrahedra in glass contracts the glass structure and inhibits phase separation.

Melt viscosity

The viscosity of a waste glass melt as a function of temperature is the single most important variable affecting the melt rate and pourability of the glass. The viscosity determines the rate of melting of the raw feed, the rate of glass bubble release (foaming and fining), the rate of homogenization, and thus, the quality of the final glass product. If the viscosity is too low, excessive convection currents can occur, increasing corrosion/erosion of the melter materials (refractories and electrodes) and making control of the waste glass melter more difficult. Waste glasses are usually poured continuously into steel canisters or cans for ultimate storage. Glasses with viscosities >500 poise do not readily pour. Moreover, too high a viscosity can reduce product quality by causing voids in the final glass. Therefore, a range of viscosities between 20 and 110 poise at T_{melt} are currently being used for Joule-heated waste glass melters at the DWPF. Different melter designs may have different ranges.

The approach taken in the development of the viscosity and resistivity process models [56, 91, 92] was based on glass structural considerations, expressed as a calculated non-bridging oxygen (NBO) term. This NBO parameter represents the amount of structural depolymerization in the glass (Equation 9.2). Oxide species were expressed in mole fraction and related to the viscosity–temperature dependence of the Fulcher equation [93, 94], also known as the Vogel–Fulcher–Tammann (VFT)[9] equation. The VFT relates the viscosity (η) of a glass to temperature (Equation 9.3) for Newtonian fluids.

$$\text{NBO} \equiv \frac{2\left\{[\text{Na}_2\text{O}]+[\text{K}_2\text{O}]+[\text{Cs}_2\text{O}]+[\text{Li}_2\text{O}]+[\text{Fe}_2\text{O}_3]-[\text{Al}_2\text{O}_3]\right\}+[\text{B}_2\text{O}_3]}{[\text{SiO}_2]} \tag{9.2}$$

$$\log_{10}\eta = A + \frac{B}{T - T_0} \tag{9.3}$$

In Equation 9.3, η is viscosity (poise or d · Pa[10]), T is temperature in °C, and A, B, and T_0 are fitted constants. It is well documented that the overall fit of the Fulcher equation is excellent for glasses but that it also overestimates viscosity at lower temperatures in the range of viscosities $>10^{10}$ Pa·s [95].

---

[9] Fulcher derived this expression to model viscosity of inorganic glasses in 1925. In 1921 Vogel (*Phys. Zeit.*, 22, 645–646) derived a similar expression for the viscosity of water, mercury, and oils, and Tammann and Hesse generated a similar equation for organic liquids in 1926 (*Z. Anorg. Allg. Chem.*, 156, 245–257). So all three are credited with the derivation of the mathematical expression and it is often referred to as the VFT equation.

[10] The c.g.s. unit of viscosity is the dyne second per square centimeter, which is called the poise. The SI unit for viscosity is the newton second per square meter, or pascal second; one of these units equals 10 poise.

Calculation of the NBO term from molar composition was combined with quantitative statistical analyses of response surfaces to express glass viscosity and resistivity as a function of melt temperature and glass composition (see the spline fit in Fig. 9.9a). The DWPF glass viscosity model is given by

$$\log \eta (\text{poise}) = -0.61 + \left(\frac{4472.45}{T(°\text{C})} \right) - (1.534 \times \text{NBO}) \qquad 9.4$$

with an $R^2 = 0.976$.

The DWPF viscosity model assumes that a pure SiO_2 glass is fully polymerized; i.e. there are no NBO and four BO bonds. Addition of other species, known as network modifiers, depolymerizes the glass, while network formers polymerize the glass. This approach was a simplification of an NBO term developed by White and Minser [96] to describe the structural features observed in Raman spectroscopy data of complex natural glasses (obsidians and tektites) which had no B_2O_3 and almost all FeO instead of Fe_2O_3, i.e.

$$\frac{\text{NBO}}{\text{T}} = \frac{2\{[\text{Na}_2\text{O}] + [\text{K}_2\text{O}] + [\text{CaO}] + [\text{MgO}] + [\text{FeO}] - [\text{Al}_2\text{O}_3] - [\text{Fe}_2\text{O}_3]\}}{[\text{SiO}_2] + 2[\text{Al}_2\text{O}_3] + [\text{Fe}_2\text{O}_3]} \qquad 9.5$$

Equation 9.5 is also consistent with the usage of a viscosity ratio (V_r) to model the viscosity of slags [97]. V_r is defined as

$$V_r \equiv \frac{\Sigma\left[Z/r(\text{charge/radius}) \times \text{at\% of the network formers}\right]}{\Sigma\left[Z/r(\text{charge/radius}) \times \text{at\% of the network modifiers}\right]}$$

In the DWPF viscosity model it is assumed that each mole of alkali oxide added creates two non-bridging oxygen bonds by forming metasilicate (Na_2SiO_3) structural units, thus depolymerizing the glass. While the exact number of non-bridging oxygen atoms depends on the molar ratio of all of the species in a waste glass to SiO_2, most DWPF glasses have an O^{2-}/Si^{4+} ratio of 2.6 to 3.3, which implies that disilicate and metasilicate structural units predominate for the alkali species in the waste glasses. Calculation of the O^{2-}/Si^{4+} ratio for DWPF glasses included contributions from Na, K, Li, and Cs alkali species and a Si^{4+} concentration that was depleted by the amount associated with B_2O_3 structural units.

The DWPF viscosity model further assumes that each mole of Al_2O_3 creates two bridging oxygen bonds (polymerizes the glass structure) by creating tetrahedral alumina groups that bond as $NaAlO_2$ structural groups. In Al_2O_3 and/or SiO_2 deficient glasses, Fe_2O_3 can take on a tetrahedral coordination and polymerize a glass by forming $NaFeO_2$ structural groups. However, if sufficient Al_2O_3 and SiO_2 are present in a glass such as DWPF waste glasses that typically contain >3 wt% Al_2O_3 and >40 wt% SiO_2, then

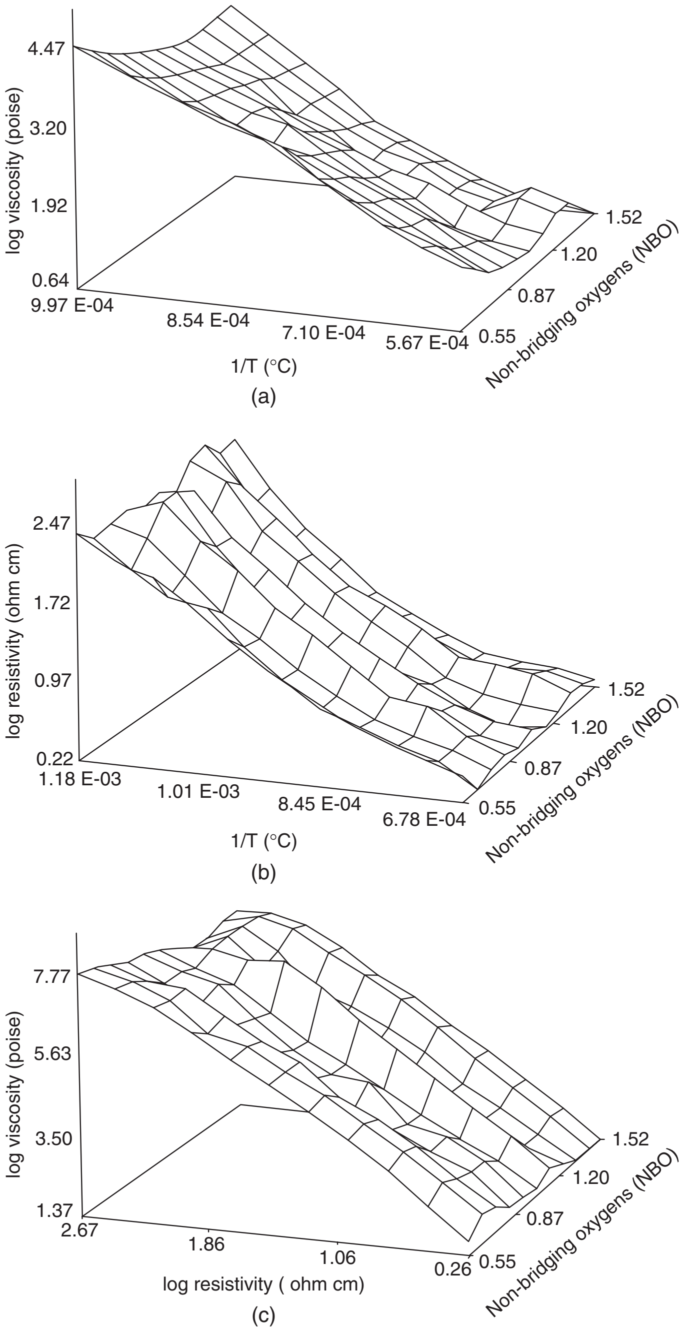

9.9 (a) Relationship between log viscosity (poise), inverse temperature, and NBO. (b) Relationship between log resistivity (ohm cm), inverse melt temperature, and NBO. (c) Relationship between log viscosity (poise), log resistivity (ohm cm), and NBO. From reference 55.

Fe_2O_3 is octahedral and creates two non-bridging oxygen bonds, i.e. it depolymerizes the glass matrix as assumed in the DWPF viscosity model (Equation 9.4). This is consistent with the work of Mysen *et al.* [98] who demonstrated that high iron magmas (iron silicate glasses) that contained levels of 10 wt% Fe_2O_3 decreased the melt viscosity. They concluded that $NaFeO_2$ structural groups were not incorporated into the silicate network to the same degree as $NaAlO_2$ structural groups [98]. Therefore, Fe_2O_3 is considered a network modifier and depolymerizer in the DWPF viscosity model. Since FeO is also known to act as a glass network depolymerizer, there is no need for a separate FeO term and all the iron in a given glass is calculated as if it were Fe_2O_3.

Lastly, the DWPF viscosity model assumes that each mole of B_2O_3 creates one non-bridging oxygen bond. This is based on data by Smets and Krol [99] and Konijnendijk [100] who demonstrated that for sodium silicate glasses with low B_2O_3 content the B_2O_3 enters the glass network as BO_4^- tetrahedral. At higher B_2O_3 concentrations these tetrahedra are converted into planar BO_3^- groups. Tetrahedral BO_4^- contributes no NBO while planar BO_3^- groups contribute one non-bridging oxygen atom [101].

In 1991 the model was developed on as-made compositions and revised [92] based on analyses of the same non-radioactive glasses and frits (220 viscosity–temperature measurements). During revision the model was validated [92] on an additional 200 glasses (radioactive and non-radioactive, and 1004 viscosity–temperature pairs) (Fig. 9.9a). Uranium was shown to have no impact on glass viscosity and ThO_2 at <1 wt% also had no impact on glass viscosity.

The viscosity model has been validated over composition and temperature regions (800–1500°C) well outside the regions for which it was developed (Fig. 9.9a) because it is based on known glass structural mechanisms. This affords the ability to use the viscosity model for the broader composition ranges of LLW, TRU, and mixed wastes.

Melt resistivity

The electrical resistivity of a waste glass melt as a function of temperature is the single most important variable affecting the establishment of Joule heating for electrically heated melters. The electrical resistivity controls the rate of melting after the establishment of Joule heating. At low temperatures, glasses are good insulators, while at high temperatures they conduct electric current relatively well. The current is transferred by ion migration: the mobility of modifying ions is much higher than that of network formers at all temperatures. The concentration of alkali ions contributes the most to the electrical conductivity. During passage of direct current though a glass melt, the alkali ions migrate to the cathode while the glass close to the anode is enriched with SiO_2 and the resistivity locally increases. These polarization effects are eliminated by the use of alternating current as used in JHCMs. However, the chemical composition of a melt thus has a significant effect on the electrical properties [102] and the melt rate at the melt temperature.

The same melt polymerization model was used for glass resistivity as was used for glass viscosity and a relationship was derived between the resistivity, the inverse of the melt temperature, and the NBO (Fig. 9.9b):

$$\log\phi(\Omega\text{cm}) = -2.48 + \left(\frac{4399.57}{T(°\text{C})}\right) - (0.45 \times \text{NBO}) \qquad 9.6$$

with $R^2 = 0.92$.

The measured viscosities and electrical resistivities are well correlated (Fig. 9.9c), i.e. if the viscosity is known, then the resistivity can be accurately calculated:

$$\log\eta(\text{poise}) = 1.82 - (0.67 \times \text{NBO}) + 2.42 \log\phi(\Omega\text{cm}) \qquad 9.7$$

With $R^2 = 0.95$.

This phenomenon had been noted previously in the commercial glass industry [102] where generally

$$\log\eta \cong 3 \log\phi \qquad 9.8$$

Melt REDuction/OXidation (REDOX)

Control of the REDuction/OXidation (REDOX) equilibrium in the DWPF melter is critical for processing high level liquid wastes. Foaming, cold cap roll-overs and off-gas surges all have an impact on pouring and melt rate during processing of waste glass. All of these phenomena can impact waste throughput and attainment. These phenomena are caused by gas–glass disequilibrium when components in the melter feeds convert to glass and liberate gases such as steam, CO_2, O_2, H_2, NO_x, and/or N_2. In order to minimize gas–glass disequilibrium a REDOX strategy is used to balance feed reductants and feed oxidants while controlling the REDOX between $0.09 \leq Fe^{+2}/\Sigma Fe \leq 0.33$. A $Fe^{+2}/\Sigma Fe$ ratio of ≤ 0.33 prevents metallic and sulfide-rich species from forming nodules that can accumulate on the floor of the melter. Control of foaming, due to deoxygenation of manganic species, is achieved by converting oxidized MnO_2 or Mn_2O_3 species to MnO during melter preprocessing. At the lower REDOX ratio of $Fe^{+2}/\Sigma Fe \sim 0.09$ about 99% of the Mn^{+4}/Mn^{+3} is converted to Mn^{+2} and foaming does not occur. Nominally a $Fe^{+2}/\Sigma Fe$ ratio of ~ 0.2 in the mid-range of 0.09–0.33 is targeted in the melt pool.

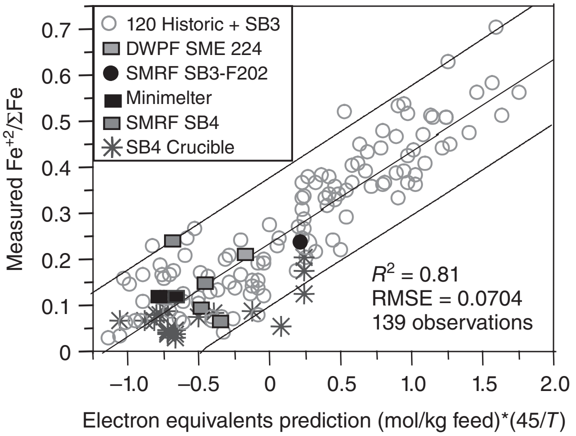

9.10 Correlation of glass REDOX expressed as $Fe^{+2}/\Sigma Fe$ versus melter feed oxidants and reductants expressed as electron equivalent transfers and weighted by the wt% solids in the slurry feed. Open circles and asterisks represent crucible data used to develop the model and the solid symbols represent melter testing including radioactive testing in the DWPF.

The REDOX model relates the $Fe^{+2}/\Sigma Fe$ ratio of the final glass to the molar concentrations of the oxidants and reductants in the melter feed. The REDOX model is based on electron equivalents (EE) that are exchanged during chemical reduction (making an atom or molecule less positive by electron transfer) (Fig. 9.10) and oxidation (making an atom or molecule more positive by electron transfer). Therefore, the number of electrons transferred for each REDOX reaction can be summed and an electron equivalent term for each organic and oxidant species defined [103–105]. The model accounts for reoxidation of the manganese by nitrate salts in the cold cap and takes the form

$$\frac{\mathrm{Fe}^{2+}}{\Sigma\mathrm{Fe}} = f\left[\left(2[\mathrm{F}]+4[C]+4[\mathrm{O_T}]-5[\mathrm{N}]-5[\mathrm{Mn}]\right)\frac{45}{T}\right] = f(\xi) \qquad 9.9$$

Where

f indicates a function

[F] = formate (mol/kg feed)

[C] = coal (carbon) (mol/kg feed)

[O_T] = $\text{oxalate}_{\text{Total}}$ (soluble and insoluble) (mol/kg feed)

[N] = nitrate + nitrite (mol/kg feed)

[Mn] = manganese (mol/kg feed)

T = total solids (wt%)

$$\xi = \left(2[\mathrm{F}] + 4[C] + 4[\mathrm{O_T}] - 5[\mathrm{N}] - 5[\mathrm{Mn}]\right)\frac{45}{T}$$

$$\frac{\mathrm{Fe}^{2+}}{\Sigma\mathrm{Fe}} = 0.2358 + 0.1999\xi$$

A model that includes sugar as a reductant can be found in reference 104.

Melt liquidus

A liquidus temperature model prevents melt pool or volume crystallization during operation. Volume crystallization needs to be avoided because it can involve almost simultaneous nucleation of the entire melt pool as volume crystallization can occur very rapidly. Furthermore, once iron spinel crystals are formed (the most ubiquitous liquidus phase occurring in US defense HLW), these crystals are refractory and cannot be redissolved into the melt pool. The presence of either the spinel or nepheline liquidus phases may cause the melt viscosity and resistivity to increase, which may cause difficulty in discharging glass from the melter as well as difficulty in melting via Joule heating. Once a significant amount of volume crystallization has occurred and the resulting crystalline material has settled to the melter floor, melting may be inhibited and the pour spout may become partially or completely blocked, making pouring difficult.

The crystal–melt equilibria were modeled based on quasi-crystalline concepts [24, 25]. A pseudobinary phase diagram between a ferrite spinel (an incongruent melt product of transition metal iron-rich acmite) and nepheline was defined. The pseudobinary lies within the Al_2O_3–Fe_2O_3–Na_2O–SiO_2 quaternary system that defines the crystallization of basalt glass melts (note that the basalt glass system is used as an analog for waste glass durability, liquidus, and the prevention of phase separation). The liquidus model developed based on these concepts has been used to prevent unwanted crystallization in the DWPF HLW melter for the past six years while allowing >10 wt% higher waste loadings to be processed. The liquidus model (Equation 9.10) and the pseudobinary (Fig. 9.11) are shown [24, 25] to be consistent with all of the thermal stability data generated on DWPF HLW glasses. The model was developed over a range of 105 different glass compositions and was validated over even wider ranges (161 glasses) [60].

$$\begin{aligned}\frac{1}{T_{\mathrm{L}}(\mathrm{K})_{\mathrm{spinel}}} &= -0.000260\ln(M_2) - 0.000566\ln(M_1) - 0.000153\ln(M_{\mathrm{T}}) - 0.00144\\ &= \ln\left\{(M_2)^{-0.000260}(M_1)^{-0.000566}(M_{\mathrm{T}})^{-0.000153}\right\} - 0.00144\end{aligned} \qquad 9.10$$

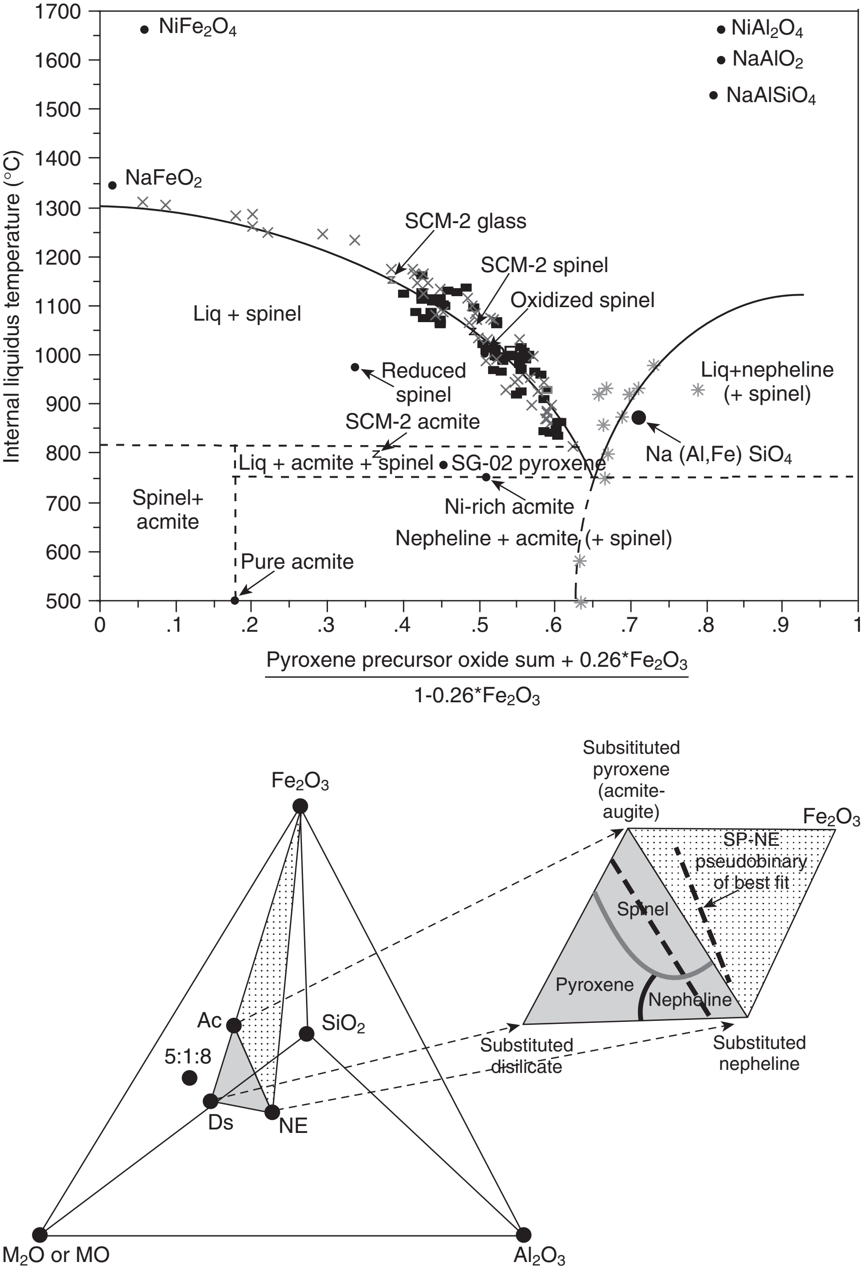

9.11 Pseudobinary phase diagram between acmite and nepheline expressed in terms of the pyroxene and nepheline quasi-crystalline precursor compositions (unnormalized mol%) on which the liquidus model is based. Inset shows the position of the pseudobinary in the quaternary (B_2O_3 free) system as B_2O_3 does not participate in the crystallization. From reference 25.

where

$$\Sigma_{\mathrm{MT}} \equiv \phi_{\mathrm{T,SiO_2}} Z_{\mathrm{SiO_2}} + \phi_{\mathrm{T,Al_2O_3}} Z_{\mathrm{Al_2O_3}} + \phi_{\mathrm{T,Fe_2O_3}} Z_{\mathrm{Fe_2O_3}}$$

$$\begin{aligned}\Sigma_{\mathrm{M1}} \equiv {} & \phi_{\mathrm{M1,Al_2O_3}} Z_{\mathrm{Al_2O_3}} + \phi_{\mathrm{M1,Fe_2O_3}} Z_{\mathrm{Fe_2O_3}} + \phi_{\mathrm{M1,TiO_2}} Z_{\mathrm{TiO_2}} + \phi_{\mathrm{M1,Cr_2O_3}} Z_{\mathrm{Cr_2O_3}} \\ & + \phi_{\mathrm{M1,ZrO_2}} Z_{\mathrm{ZrO_2}} + \phi_{\mathrm{M1,NiO}} Z_{\mathrm{NiO}} + \phi_{\mathrm{M1,MgO}} Z_{\mathrm{MgO}} + \phi_{\mathrm{M1,MnO}} Z_{\mathrm{MnO}}\end{aligned}$$

$$\begin{aligned}\Sigma_{\mathrm{M2}} \equiv {} & \phi_{\mathrm{M2,NiO}} Z_{\mathrm{NiO}} + \phi_{\mathrm{M2,MgO}} Z_{\mathrm{MgO}} + \phi_{\mathrm{M2,MnO}} Z_{\mathrm{MnO}} + \phi_{\mathrm{M2,CaO}} Z_{\mathrm{CaO}} \\ & + \phi_{\mathrm{M2,K_2O}} Z_{\mathrm{K_2O}} + \phi_{\mathrm{M2,Li_2O}} Z_{\mathrm{Li_2O}} + \phi_{\mathrm{M2,Na_2O}} Z_{\mathrm{Na_2O}}\end{aligned}$$

$$\Sigma_{\mathrm{T1}} \equiv \phi_{\mathrm{T1,SiO_2}} Z_{\mathrm{SiO_2}} + \phi_{\mathrm{T1,Al_2O_3}} Z_{\mathrm{Al_2O_3}} + \phi_{\mathrm{T1,Fe_2O_3}} Z_{\mathrm{Fe_2O_3}} + \phi_{\mathrm{T1,TiO_2}} Z_{\mathrm{TiO_2}}$$

$$\Sigma_{\mathrm{N1}} \equiv \phi_{\mathrm{N1,K_2O}} Z_{\mathrm{K_2O}} + \phi_{\mathrm{N1,Li_2O}} Z_{\mathrm{Li_2O}} + \phi_{\mathrm{N1,Na_2O}} Z_{\mathrm{Na_2O}}$$

$$\mathrm{M}_2 \equiv \frac{\Sigma_{\mathrm{M2}}}{\Sigma}, \mathrm{M}_1 \equiv \frac{\Sigma_{\mathrm{M1}}}{\Sigma}, \mathrm{M}_\mathrm{T} \equiv \frac{\Sigma_{\mathrm{MT}}}{\Sigma}$$

$$\Sigma \equiv \Sigma_{\mathrm{M2}} + \Sigma_{\mathrm{M1}} + \Sigma_{\mathrm{MT}} + \Sigma_{\mathrm{T1}} + \Sigma_{\mathrm{N1}}$$

and $R^2 = 0.89$. The details of the modeling are given elsewhere [106].

Melt sulfate solubility

Sulfate and sulfate-salts are not very soluble in borosilicate waste glass. When the glass is cooled, inclusions and/or phase separation of a sulfate-rich phase are often visible in the glass and often a layer of water-soluble sulfate is visible on the glass surface. When the glass is molten, the molten salt layer, known as gall, can float on the melt pool surface (Fig. 9.12a). Soluble sulfate salts are often enriched in cesium and strontium, which can impact radionuclide release from the cooled glass if the salts are present as inclusions or a frozen gall layer. The alkali and alkaline earth sulfate salts, in conjunction with alkali chlorides, collect on the melt surface as a low melting (600–800°C), low density, low viscosity melt phase. At moderate concentrations, the salts have a beneficial effect on melting rates. If a melter is slurry-fed, as is done in the US, steam can get trapped under the layer of gall and cause steam explosions, which are undesirable. At excessively high feed concentrations, molten alkali sulfates float on the surface of the melt pool or become trapped as inclusions in the glass.

The results of sulfate solubility measurements from both dynamic melter tests and static crucible tests performed with HLW wastes were compared. This data was also compared to slurry-fed melt rate furnace (SMRF) data generated on HLW melts. In addition, a survey was made of both dynamic and crucible tests for low activity wastes (LAW) and crucible tests were performed with commercial soda–lime–silica glasses. Phenomenological observations in the various studies, e.g. completeness or lack of gall and secondary sulfate phases, were categorized into melt conditions representing 'at saturation, oversaturation, and supersaturation'. This enabled modeling of the most

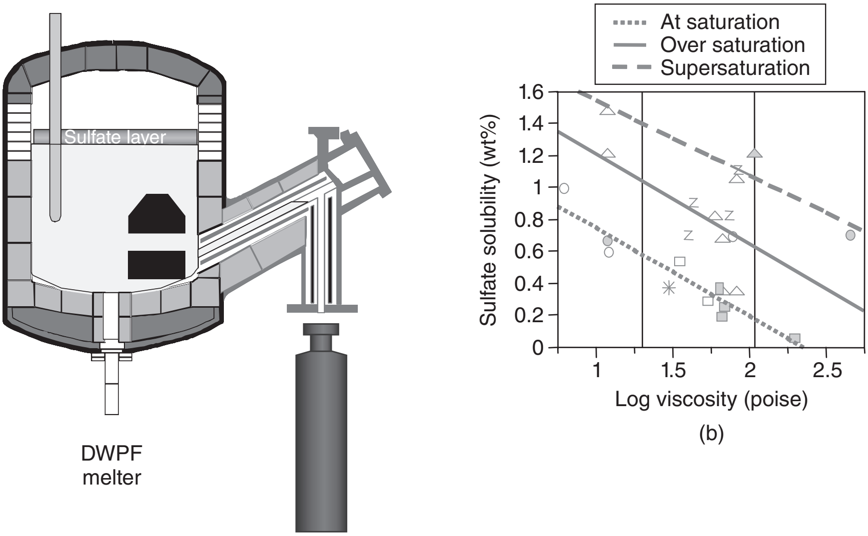

(a)

(b)

9.12 (a) Flotation of excess sulfate on the melt pool during supersaturation as gall and vesicles in the glass. This can cause operational problems and poor glass quality. (b) Relationships between the calculated melt viscosity at 1150°C and $SO_4^=$ solubility in DWPF HLW glasses as a function of sulfate saturation. From references 109 and 110.

desirable 'at saturation' conditions, e.g. no appearance of a sulfate layer on the melt pool, in relation to undesirable conditions of oversaturation (partial melt pool coverage) and supersaturation (almost complete melt pool coverage). Sulfate solubility is related to melt polymerization and temperature and so to the HLW viscosity model given in Equation 9.4. Using the viscosity model in Equation 9.4 allows models to be defined for sulfate solubility for the various degrees of sulfate saturation [107, 108] as shown in Fig. 9.12b.

Modeling of the sulfate solubility as a function of calculated viscosity (Equation 9.4) was performed. The glasses were grouped by sulfate saturation which provided a series of three parallel models, one at saturation, one at oversaturation, and one at supersaturation:

$$SO_4^= \text{solubility(saturation)} = 1.2360 - 0.5408 \log \text{viscosity}_{\text{calc}} \text{(poise)} \qquad 9.11$$

$$SO_4^= \text{solubility(supersaturation)} = 1.9605 - 0.5229 \log \text{viscosity}_{\text{calc}} \text{(poise)} \qquad 9.12$$

$$SO_4^= \text{solubility(oversaturation)} = 1.7539 - 0.5729 \log \text{viscosity}_{\text{calc}} \text{(poise)} \qquad 9.13$$

with R^2 values of 0.87, 0.96, and 0.86 respectively.

Product composition control system (PCCS) and process limits [57, 59]

While the individual P/P models are based on glass structural concepts of SRO, MRO and quasi-crystalline theory, the process limits are set for a given melter type and geometry by experience with non-radioactive pilot-scale melters. Multivariate statistical theory is used in conjunction with the P/P models to control within multidimensional composition space.

The regression lines for the individual properties, e.g. durability, liquidus temperature, and viscosity, can be back-solved to determine composition values, c_i, corresponding to the respective property limits. (No such solution is necessary for the homogeneity (including the limit on Al_2O_3), conservation, frit loading, or waste solubility constraints, since again they were originally formulated as limits on composition.) This transforms the constraints on properties into equivalent constraints, c_i^*, on composition. In turn, c_i^* transforms into a constraint on concentrations of individual constituent oxides. Describing all predicted oxide values for a given property that are acceptable defines the expected property acceptable region (EPAR) for that property (Fig. 9.13). It is denoted 'Expected' since it derives from the fitted line, which is the locus of the conditional *expectation* of the property given the composition. To incorporate modeling error, the appropriate 95% confidence band can also be back-solved to obtain a new limit on the property that includes the modeling error. This is defined as the property acceptable region (PAR) (Fig. 9.13).

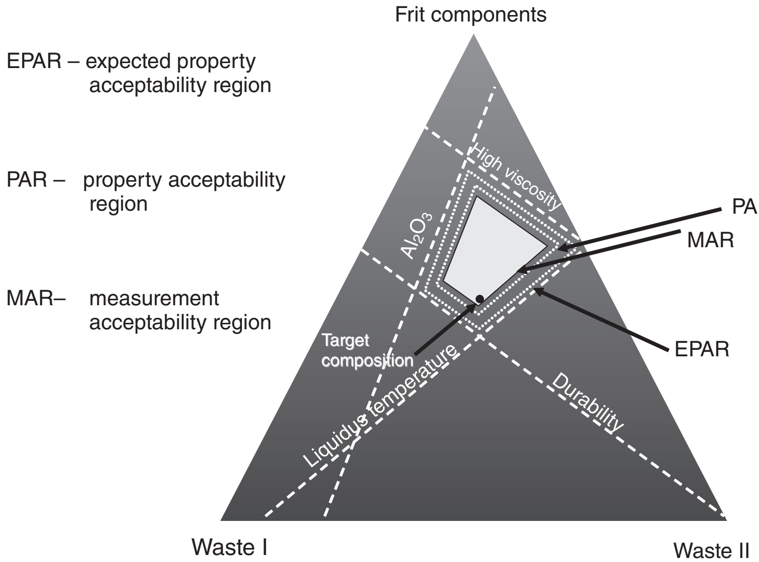

9.13 Product composition control system (PCCS).

Errors in measurement must also be accounted for. During operation, the feed compositions from which the properties must be predicted will not be known, but will be measured. There will be appreciable errors in composition arising from the DWPF sampling and measurement systems; therefore, these errors must be accounted for in order to achieve 95% confidence in the property predictions. In DWPF, a composition measurement is a vector of measurements taken for several constituents simultaneously (at least, these measurements are taken very close together in time and consequently may be considered simultaneous). Thus the description of compositional uncertainty requires multivariate statistical techniques. The concentrations of the individual constituents in the DWPF composition measurements are assumed to be multivariate Gaussian with a covariance matrix Σ_m and the solution can be solved with Student's *t*-test for all product and processing constraints incorporating all relevant constituent elements measured in the glass. The confluence of the regions described by the *t*-tests for all property constraints forms the measurement acceptable region (MAR) (Fig. 9.13) which includes all measurement errors, including tank transfer errors.

Glasses inside the MAR are durable and processable within 95% confidence. The ternary representation of the PCCS system demonstrates the flexibility to blend two different types of waste. In this case, the radionuclide-rich stream comes from the removal of these components from the salt supernates (waste I) and the sludge (waste II). This allows the waste glass formulations on the lower boundary of the MAR (Fig. 9.13) which maximizes waste sludge component loadings instead of waste glass formulations in the middle of the qualified MAR region. At the same time, it provides the basis for knowing, to within 95% confidence, that a given melter feed will be pourable, will not crystallize inside the melter, and will be durable and acceptable to the geological repository.

9.5 Other glasses

Borosilicate waste glasses contain $(SiO_4)^{-4}$, $(BO_4)^{-5}$, $(BO_3)^{-3}$and some $(AlO_4)^{-5}$ SRO structures that are bound together in MRO configurations. Glasses that contain only $(SiO_4)^{-4}$ and $(AlO_4)^{-5}$ SRO are aluminosilicate glasses, while glasses that contain $(BO_4)^{-5}$, $(BO_3)^{-3}$, and some $(AlO_4)^{-5}$ are aluminoborate glasses. Phosphate glasses contain no $(SiO_4)^{-4}$, $(BO_4)^{-5}$ or $(BO_3)^{-3}$ but contain $(PO_4)^{-3}$and $(AlO_4)^{-5}$ (aluminophosphate glasses) or $(PO_4)^{-3}$and $(FeO_4)^{-5}$ (iron phosphate glasses) instead.

9.5.1 Rare earth and lanthanum borosilicates

As melting technology improves (Section 9.6) both the melting temperature and the waste loading of waste in nuclear glasses will increase. The waste loading increase will translate into higher glass activity and heat loading and a higher canister temperature. Therefore, new nuclear glass compositions are being developed that will be able to immobilize higher waste concentrations than current glasses. Such glasses must exhibit excellent chemical durability and glass transformation temperatures that are higher than those of the current alkali borosilicate nuclear glasses in order to avoid crystallization risks (volume increase) during storage. As the concentration of actinide and rare earth (RE) elements will be greater in these wastes, researchers have begun to investigate rare earth-rich glassy matrices such as lanthanide aluminoborosilicate (LaBS) glasses and lanthanide aluminosilicate (RESiAlO) glasses [22, 109]. These glasses show very good performance, but their high melting temperature will likely increase the volatility of some fission products during melting. Therefore, glasses that melt around 1300°C have initially been investigated with compositions of approximately $51.0SiO_2–8.5B_2O_3–12.2Na_2O–4.3Al_2O_3–4.8CaO–3.2ZrO_2–16.0RE_2O_3$ where each RE was tested individually as was a mixture of La, Ce, Pr, and Nd.

LaBS glasses have also been used to immobilize PuO_2 and associated neutron absorbers such as Gd (Table 9.5, Frit A). Second-generation LaBS glasses for PuO_2 immobilization incorporated hafnium for improved criticality performance (Table 9.5, Frit B) [110]. Actinide solubility testing with the Frit B composition was primarily performed with combinations of plutonium and uranium to more accurately reflect the expected excess weapons-usable plutonium feed streams. The solubility of combinations of plutonium and uranium was shown to be even higher than for Pu only. For example, a homogeneous glass containing 9 wt% PuO_2 and 6 wt% UO_3 fabricated for a total actinide loading of 15 wt% [111] was shown to be very durable [112, 113].

The commercial lanthanide (rare earth) borosilicate glass upon which the PuO_2 LaBS glasses were based was first proposed by von Löffler [114, 115] for use in technical applications where dichroic glasses were needed or for use as decorative, highly colored glasses [114]. The lanthanide glasses are known to accommodate Cs, Y, La–Hf (i.e. the lanthanide elements La, Ce, Pr, Nd, Pm, Sm, Eu, Gd, Tb, Dy, Ho, Er, Tm, Yb, and Lu, indicated hereafter by the generic symbol Ln) and the actinides in relatively high concentrations [115]. This family of high lanthanide glasses has been used extensively in nuclear applications for protective purposes since many of the lanthanide elements have large thermal neutron cross-sections [115]. Therefore, several $La_2O_3–B_2O_3–SiO_2$ (LaBS) glasses based on the Löffler formulation were investigated.

The high lanthanide glasses were chosen for investigation rather than conventional borosilicate waste glasses that have inherently low solubilities for PuO_2 because of the ability of the lanthanide glasses to solubilize actinides. Von Löffler's glass is unique in that it combines lanthanide oxides

Table 9.5 Comparative oxide compositions (wt%) of lanthanide/plutonium borosilicate glasses

Oxide	Löffler Glass*	Ramsey Löffler ThO_2-1	Ramsey Löffler ThO_2-2	Meaker Löffler ThO_2	LaBS PNNL PuO_2	LaBS Frit A PuO_2	LaBS Frit B PuO_2	LaBS Frit X PuO_2	LaBS Frit B ZrO_2	LaBS Frit B HfO_2	LaBS Frit X HfO_2
Al_2O_3	9.0	9.08	3.58	16.25	19.04	19.46	19.27	9.05	20.35	19.17	9.00
BaO	2.0	2.02	2.14	–	–	–	–	–	–	–	–
B_2O_3	5.0	5.05	7.88	8.85	10.4	10.59	10.50	11.77	11.07	10.44	11.70
Ce_2O_3 (Pr_2O_3)	(3.2)	18.61	–	–	–	–	–	–	–	–	–
Gd_2O_3	–	–	–	17.16	7.61	7.78	11.58	12.22	12.23	11.52	12.15
HfO_2 (frit component)	–	–	–	–	–	–	5.97	6.34	6.23	5.94	6.30
HfO_2 (PuO_2 surrogate)	–	–	–	–	–	–	–	–	–	10.00	10.00
La_2O_3	18.3	0.91	1.21	3.80	11.01	11.22	7.33	17.20	7.70	7.29	17.10
Nd_2O_3	32.5	32.81	34.76	4.05	11.37	11.58	7.42	13.58	7.80	7.38	13.50
PbO	7.9	7.97	8.44	–	–	–	–	–	–	–	–
PuO_2 (Pu_2O_3)	–	–	–	–	11.39	9.50†	9.50	9.50	–	–	–
SiO_2	21.5	21.7	24.36	22.0	25.80	26.43	26.15	18.10	27.52	26.01	18.00
SrO (CaO + ZnO)	–	–	–	1.9	2.22	2.26	2.26	2.26	2.42	2.25	2.25
ThO_2 (PuO_2 surrogate)	–	1.85	17.62	25	11.39	–	–	–	–	–	–
ZrO_2 (frit component)	–	–	–	1	1.15	1.18	–	–	–	–	–
ZrO_2 (PuO_2 surrogate)	–	–	–	–	–	–	–	–	4.56	–	–
Na_2O and Li_2O	–	–	–	–	–	–	–	–	–	–	–
Melt temp. (°C)	1350	1400	1425	1475	1450–1500	1500	1500	1500	1500	1500	1500
Total Ln_2O_3	54.0	52.33	35.97	25.0	29.99	30.58	26.33	43.00	27.73	26.19	42.75
Ln_2O_3 + $(Th,Zr,Hf)O_2$	54.0	54.18	53.59	51.0	45.16	40.08	41.80	58.84	38.52	42.13	59.05
SiO_2 + Al_2O_3	30.5	30.78	27.94	38.25	44.84	45.89	45.42	27.15	47.87	45.18	27.00
Total	99.4	100	99.99	100.01	99.99	100	99.98	100.02	99.88	100.00	100.00

* This glass also has 0.1 wt% As2O5 as a fining agent.
† Maximum waste loading determined to be 13.4 wt% PuO2.
Source: Mara *et al.* [122].

as fluxes in an aluminosilicate-type glass in place of the usual alkali metal oxides [115]. The glasses melt at conventional melting temperatures (≥1350°C) but have an extraordinarily low viscosity. The Löffler glasses typically contain 10–70 wt% of some lanthanide oxides, and 9–20 wt% Al_2O_3, the remainder being SiO_2 (21.5–46 wt%).

The first Löffler glass formulations for PuO_2 stabilization were tested by Ramsey *et al.* [116] and were very similar to the Löffler composition given in Table 9.5. The Ramsey Löffler variants were able to stabilize any concentration from 1.85 to 17.62 wt% ThO_2 (a simulant for PuO_2). Ce_2O_3 was used in place of the La_2O_3 and Pr_2O_3 in the Löffler formulation, although a mixture of three lanthanide oxides was retained during all testing. Additional testing [117, 118] substituted a variety of different rare earth elements (always a minimum of three) with little impact on the solubility of ThO_2. This was consistent with the finding of the commercial glass industry that the substitution of various rare earths in the lanthanide borosilicate glasses had little effect on any measured physical properties [115].

The Löffler and early LaBS glasses contained hazardous metal oxides such as PbO and BaO. Subsequent formulations [119, 120] substituted Al_2O_3 and SrO for PbO and BaO and began to examine what combinations of lanthanide oxides (Gd_2O_3, La_2O_3, and Nd_2O_3) could be optimized with the actinides (ThO_2). The lanthanide Gd was chosen as a neutron absorber, and samarium and europium oxides were also investigated. A maximum ThO_2 loading of 25 wt% was achieved with one of the Al_2O_3/SrO formulations [120]. Further testing of Frit A glass at Pacific Northwest National Laboratory (PNNL) and Savannah River National Laboratory (SRNL) (Table 9.5) with PuO_2 revealed that the maximum PuO_2 concentration that could be accommodated in Frit A was 13.4 wt% and a concentration of 9.5 wt% was deemed acceptable for criticality concerns.

The change from the PbO/BaO bearing Löffler glasses to the SrO/Al_2O_3 Frit A glasses caused the total Ln_2O_3 content (Ln = lanthanide) of the glasses to decrease while the Al_2O_3+SiO_2 content increased (Table 9.5). The additional modification to Frit B which added HfO_2 in place of La_2O_3 caused a further decrease in the total La_2O_3 content (Table 9.5). At concentrations of lanthanide oxides, La_2O_3, in the range of 15 wt% the SRNL LaBS glass crystallized to lanthanum silicate phases, and amorphous phase separation (APS), known as glass-in-glass phase separation, was observed [120]. In addition, the liquidus temperatures of some of the LaBS formulations were shown to be too low, i.e. the glass easily crystallized lanthanum silicates and oxides during pouring [121]. Therefore, a glass formulation approach was needed that could be used to avoid regions of rare-earth silicate formation and regions of glass-in-glass phase separation.

None of the ternary oxide phase relations are known in the La_2O_3–B_2O_3–SiO_2 system. However, each of the binary oxide systems which comprise the binary sides of the ternary system are known, e.g. La_2O_3–SiO_2 and Sm_2O_3–SiO_2, La_2O_3–B_2O_3 , and B_2O_3–SiO_2. The phase diagrams for all the La_2O_3–SiO_2 systems are similar: each system has three stoichiometric compounds, 1:1, 2:3 and 1:2 La_2O_3:SiO_2. Each La_2O_3–SiO_2 system has a region of glass-in-glass phase separation at > 1:2 La_2O_3:SiO_2 with lower stability temperatures of ~1700°C. Each La_2O_3–SiO_2 system has one high-temperature congruent melting lanthanide silicate compound at 1:1 La_2O_3:SiO_2 and one incongruent melting lanthanide silicate compound at 1:2 La_2O_3:SiO_2. Likewise, all the La_2O_3–B_2O_3 binary phase diagrams are similar. The phase relations and regions of low melting eutectics in the La_2O_3–B_2O_3–SiO_2 system were inferred from the projections of the pertinent binary oxide systems (using the La_2O_3–SiO_2 and B_2O_3–SiO_2 systems as the prime example). In this manner the ternary phase relations regarding crystallization and phase separation were related to the composition of the fluid melts observed by von Löffler [122].

Since the known binary oxide systems are in mol% oxide, the compositions from Table 9.5 have been converted from oxide wt% to oxide mol%. All of the La_2O_3 have been grouped together and the phase equilibria analyzed with SiO_2 as the only glass former and with (SiO_2 + Al_2O_3) grouped with SiO_2 due to their similar structural role as glass formers. For the Löffler glass, this simplification of the glass chemistry (including the contribution of the Al_2O_3) accounts for 89.5 wt% of the glass components.

The potential ternary phase relations in the La_2O_3–B_2O_3–(SiO_2 + Al_2O_3) system are shown in Fig. 9.14. The 1:1 La_2O_3:SiO_2 stoichiometric compound which melts at 1975°C more than likely forms a high melting temperature ridge in the ternary system with the 1:1 La_2O_3:B_2O_3 stoichiometric compound which melts at 1660°C. In the La_2O_3–B_2O_3–(SiO_2 + Al_2O_3) system (Fig. 9.14) compositions in the proximity of this 1:1 stoichiometric (La_2O_3–B_2O_3):(La_2O_3–SiO_2) ridge will likely have high liquidus temperatures. The lowest melting temperature glasses can be formed in the La_2O_3–B_2O_3–(SiO_2 + Al_2O_3) system (Fig. 9.14) along a trough defined by a line joining the eutectic compositions at 1:3 La_2O_3:SiO_2 and ~1:3 La_2O_3:3B_2O_3. These eutectics melt at temperatures of 1625°C and ~1132–1136°C, respectively. Therefore, along the ~1:3 stoichiometric axis shown in Fig. 9.14 compositions higher in B_2O_3 will melt at a lower temperature than compositions enriched in (SiO_2 + Al_2O_3).

At compositions with less molar La_2O_3 than 22–25 mol% in Fig. 9.14, the regions of glass-in-glass (two-liquid) phase separation more than likely form a continuous dome as indicated by the shaded region in the figure. The lower stability temperature of the two liquid regions in the La_2O_3–SiO_2 system is ~1700°C, while the lower stability temperature of the two-liquid region in the La_2O_3–B_2O_3 system is 1136°C. This is a region of potential phase separation and should be avoided during glass formulation in this

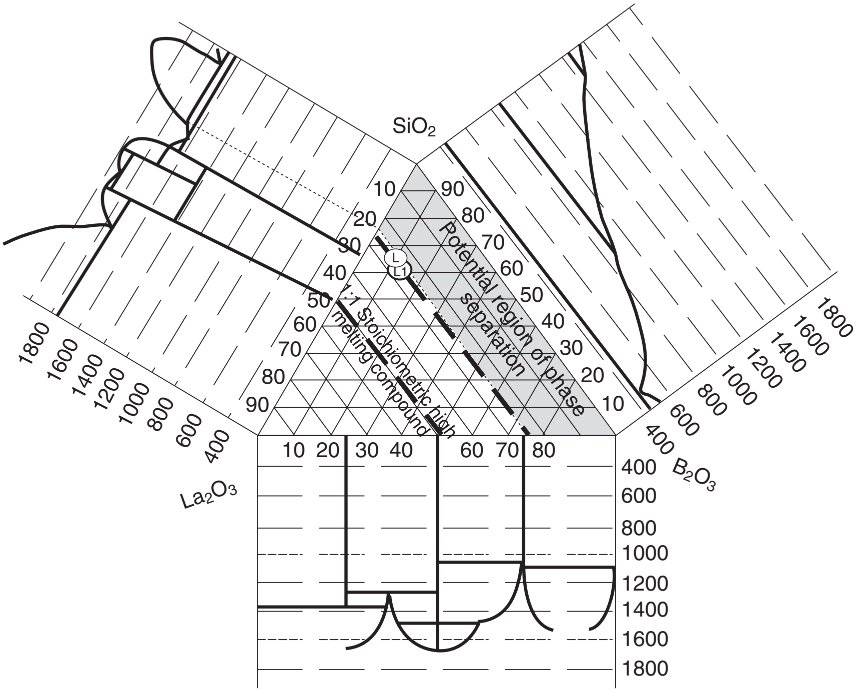

9.14 The inferred ternary oxide system La_2O_3–B_2O_3–SiO_2 (mol %) from the known binary oxide systems. Note that the Löffler glass formulation in the La_2O_3–B_2O_3–SiO_2 system is indicated in the circle by 'L1' and that if the ternary is generalized to include $SiO_2 + Al_2O_3$ at the apex then the Löffler glass formulation in the La_2O_3–B_2O_3–(SiO_2 + Al_2O_3) system is indicated as 'L'.

system. Even if a homogeneous glass of this composition can be made by rapid pouring and/or quenching, it will be metastable and tend to phase separate and/or crystallize when subjected to annealing and/or subsequent heat treatment.

Based on this phase equilibrium approach the following composition modifications to the LaBS formulations for PuO_2 were recommended [122]:

- La_2O_3 needs to be added and Al_2O_3 and SiO_2 content reduced to modify the glass composition so that it is no longer in the range of potential phase separation.
- Sufficient La_2O_3 should be added and Al_2O_3 and SiO_2 content reduced so that the final glass composition falls on or near the low melting eutectic trough delineated in Fig. 9.14 at ~1:3 stoichiometric axis in the La_2O_3–B_2O_3–(SiO_2 + Al_2O_3) system.

- Compositions lying along the 1:3 stoichiometric axis in the La_2O_3–B_2O_3–(SiO_2 + Al_2O_3) system (such as the composition shown below) should melt at lower temperatures than the current LaBS formulation and have lower liquidus temperatures:
  - 50 (SiO_2 + Al_2O_3) mol%
  - 25–30 La_2O_3 mol%
  - 20–25 B_2O_3 mol%.
- Mixed La_2O_3 should continue to be used instead of just La_2O_3 since the heat of mixing of the rare earth oxides will effectively lower the melt temperature.
- If 20–25% B_2O_3 is shown to be ineffective then compositions in the range of the original Löffler glass should be formulated as indicated below:
  - 65 (SiO_2 + Al_2O_3) mol%
  - 27 La_2O_3 mol%
  - 8 B_2O_3 mol%.

9.5.2 Phosphate glasses

Phosphate glasses have been studied in several countries (mainly Russia and the US) as potential waste forms to immobilize HLW solutions [11, 51, 123]. In general, the phosphate glasses have not been as well studied as the borosilicate glasses and hence processing knowledge, in terms of process models, is not available to accommodate the wide range of HLW wastes.

Phosphate glasses melt at lower temperatures and can incorporate high concentrations of actinides, rare-earth oxides, molybdates, and sulfates as discussed in [51]. However, phosphate melts are generally more corrosive and are less durable in aqueous environments than borosilicate systems [22, 55]. Phosphate glasses have lower thermal stability and a tendency to crystallize.

Aluminophosphates [124]

The delay in the development of phosphate glasses for use in waste disposal has been attributed to the lack of industrial usage of these types of glasses and hence the lack of commercial experience and technology such as exists for the silicate glasses. Aluminophosphate HLW glasses have been vitrified in Russia since 1987 in a JHCM, the EP-500 Mayak facility in the Ural Region [22, 125–128]. These glasses are primarily sodium phosphate glasses to which additions of Al_2O_3 have been shown to improve durability [129]. For HLW wastes with high Al_2O_3 content from dissolution of Al-cladding, these make good candidate waste forms as they can accept 17–25 wt% Al_2O_3 (Table 9.6). The first melter was put into operation in 1987 and

Table 9.6 Compositions of proposed phosphate glasses

Oxide	Russian alumino-phosphate[a]	Russian alumino-phosphate glass tested at SRNL[b]	Waste engineerring solidification prototypes (WSEP)[c]	Lead iron phosphate (LIP)*	Fe-P nominal†
Al_2O_3	19.0	17.0	0–35	1–2	5
Bi_2O_3					3–13
CaO		0.64			7–10
CaF_2					5
Cr_2O_3	0.1				3
Fe_2O_3	1.5	3.49			20–38
Fe_2O_3 + NiO + Cr_2O_3	1.6	4.81	0–30	6–13	
K_2O		0.4			5–10
La_2O_3					3
MgO		0.01			
MnO		0.09			
Mn_2O_3					5
MoO_3					4–8
Na_2O	21.2	22.2	5–25	1–2	10
NiO		1.23			6
PbO			0–30	36–53	
P_2O_5	52	51.2	30–55	25–42	42–50
SiO_2		0.07	0–6	0–0.25	10
ZrO_2		0.18			6
Fission products (Cs_2O + SrO)	6		30	0–0.25	20
Actinides (U_3O_8)		1.62	1–2.5		12
Melt temp. (°C)	1200	1150–1200	1050–1200	800–1050	950–1100

* The ratio $Fe_2O_3/(PbO \cdot P_2O_5) \cong 9$ wt%; B.C. Sales and L.A. Boatner, 'Physical and chemical characteristics of lead-iron-phosphate nuclear waste glasses', *J. Non-Crystalline Solids*, 79, 83–116 (1986).

† The O/P mole ratio of the final waste form should be in the range 3.4–3.8; the P_2O_5 content must be between 42 and 50 wt% and the Fe_2O_3 content must be at least 20 wt% although smaller amounts are permissible when Al_2O_3, Bi_2O_3, La_2O_3, U_3O_8 and other similar oxides are present. J.M. Perez, Jr., D.F. Bickford, D.E. Day, D.S. Kim, S.L. Lambert, S.L. Marra, D.K. Peeler, D.M. Strachan, M.B. Triplett, J.D. Vienna, and R.S. Wittman, 'High-Level Waste Melter Study Report', PNNL-13582 (2001).

Sources:

a. M.I. Ojovan and W.E. Lee, *New Developments in Glassy Nuclear Wasteforms*, Elsevier Publishers, Oxford, 315 pp. (2005).

b. N.E. Bibler, C.M. Jantzen, and W.G. Ramsey, 'Characterization of Two Russian Phosphate Waste Glasses – Interim Report', US DOE Report WSRC-RP-1213 (August 1993).

c. J.L. McElroy, K.J. Schneider, J.N. Hartley, J.E. Mendel, G.L. Richardson, R.W. McKee and A.G. Blasewitz, 'Waste Solidification Program Summary Report, Vol. 11, Evaluation of WSEP High Level Waste Solidification Processes', US DOE Report, BNWL-1667, Battelle Northwest Laboratories, Richland, WA 99352.

operated for 1.5 years. The composition of the glass-formers (in mass%) was reported as 22–26% Na_2O, 21–25% Al_2O_3, 47–53% P_2O_5, and up to 1.5% Fe_2O_3 [130]. After design changes, a second unit was constructed and placed into operation in 1991 and operated until 1997. A new JHCM melter was constructed and began operation in 2001 and operated until 2006. The JHCM is lined with ZrO_2–Al_2O_3 refractory material. Orthophosphate acid is mixed with the aqueous HLW and melted at a maximum temperature of 1200°C [51]. The EP-500 melters have produced 4000 metric tons of glass in 8800 canisters (Table 9.3).

Lead-iron phosphates

Research continued in the area of other phosphate glass compositions, specifically lead-iron-phosphate (LIP) glasses. Lead was added to decrease melt temperature and viscosity, and iron was added to increase durability and suppress the tendency towards crystallization. However, the low waste loading (typically <20 mass%), low corrosion resistance of crystallized glasses, and limited experience in melting LIP glasses resulted in this glass type not being used or considered as a viable waste form matrix for immobilization of HLW [131].

Jantzen [132, 133] found that there was limited solubility for alumina, silica, and uranium in the LIP glasses. Also, there is limited solubility for zirconia, which forms a zirconium-rich crystalline phase in the glass. With respect to defense HLW waste streams, the LIP glasses were not compatible with the silica-rich zeolite found in the waste (the zeolite did not dissolve in the melt and remained in the crucible after pouring). There were also issues with the melting-temperature range, the flexibility of the LIP glasses to handle all of the components found in the waste, the durability of the glasses processed at lower temperatures or in a reducing atmosphere, and the inhomogeneity of the waste form. It was also determined that the LIP glasses would be incompatible with the Joule-heated melter because the interactions with the Inconel 690 electrodes and with the refractories would cause inhomogeneous melts.

Concurrent research at PNNL showed that the glass crystallized when poured into canisters and that the Cs leach rate from the crystallized material was orders of magnitude greater than those from borosilicate glass [134]. This would have required special rapid cooling for the LIP glasses to prevent significant devitrification in the tall narrow stainless steel canisters proposed for HLW disposal (Table 9.3).

Testing performed in Germany on the corrosion (e.g., durability or resistance to aqueous attack) testing of the LIP glasses indicated that these glasses performed well in solutions of distilled water and groundwaters with pH levels between 5 and 9 and temperatures less than 150°C. Corrosion rates were significantly higher in saturated sodium chloride solutions (representing a salt repository brine) when compared to the same glass in distilled water [135]. Another fundamental issue with the LIP glasses is the fact that lead is a hazardous oxide constituent and, as such, the waste form must meet the TCLP, or it would be unacceptable for repository storage [136].

Iron phosphates

Within the last 15 years, numerous studies [137–145] have focused on the use of iron phosphate (FeP) glasses as a viable waste form host for HLW. In contrast to the lead-iron phosphate glasses, FeP glasses have been produced (on a laboratory scale) that contain in excess of 40 mass% of certain HLW components [139]. The atomic structure, specific structure–property relationships, REDOX equilibria, and crystallization characteristics of binary FeP glasses and those containing a single common waste component, such as Na_2O, UO_2, Cs_2O, SrO, or Bi_2O_3, have been reported [146–148]. Iron phosphate waste forms containing about nine different simulated nuclear wastes of complex composition have also been investigated [140]. Five of these simulated wastes are based on wastes at Hanford that are high in P_2O_5, Bi_2O_3, UO_2, etc. and/or compositions that were considered poorly suited for vitrification in borosilicate glass. Other simulated wastes vitrified to date in FeP glasses include aluminum-clad spent nuclear fuel (SNF), gunite waste from the Oak Ridge Reservation (ORR), a zirconia-rich calcine waste from the Idaho National Engineering and Environmental Laboratory (INEEL), and simulated plutonium wastes. Thus, an extensive body of data exists for FeP waste forms at this time. This section briefly describes some of the major differences of FeP glasses relative to other phosphate-based glass systems, as well as those properties that make them attractive candidates for vitrifying nuclear waste (at least some waste compositions). Some of the characteristics of FeP glasses that are important to waste vitrification are as follows:

- Their outstanding chemical durability [131, 139, 140, 149, 150]
- Their tendency to buffer the pH of solutions in which they may come into contact, thereby preventing the accelerated chemical corrosion that usually occurs when an alkali-containing glass is in contact with a solution whose pH typically increases with time
- Their inherently high solubility [144, 150, 151] for many heavy metals (uranium, chromium, zirconium, cesium, molybdenum, etc.), noble metals, and rare earths commonly present in nuclear waste
- Their low melting temperatures (950°C to 1100°C), rapid melting rates (few hours), capability of tolerating a wide range of furnace atmospheres (oxidizing to reducing), and high melt fluidity (viscosity typically

below one poise), which means that small furnaces can have reasonable throughput

- Their unexpectedly low corrosion of oxide refractories [141] commonly used in glass melting furnaces, such as high alumina, zircon, and mullite
- Their unexpectedly low corrosion of Inconel alloys [152] commonly used in glass melting furnaces
- Their high waste loading, typically between 25 and 50 mass%, depending on the waste, and their higher density, typically 3.0–3.4 g/cm^3 compared to borosilicate glasses of 2.75–2.80 g/cm^3 at 28–40 wt% waste loading, which combines to slightly minimize the volume of vitrified waste
- The influence of PO_4 on solubility of actinides in repository-like environments.

9.6 Future trends

9.6.1 Joule-heated melters (JHMs) vs. advanced Joule-heated melters (AJHMs)

Joule-heated melters have production rates that are approximately proportional to the surface area of the melt, but convection caused by the Joule heating is enhanced as the size of the melter is increased [49], so larger melters have proportionately higher melt rates. The melt temperature is limited by the materials of construction of the electrodes, generally Inconel™ 690. However, melt rate can be improved by:

1. adding lid heaters (Fig. 9.15) to increase the temperature of the melter plenum and enhance melting of the cold cap
2. adjusting the proportions of frit and cold chemical additions
3. increased use of reducing agents (formic acid/sugar) to control oxygen foaming (see page 262)
4. use of surface-active species such as sulfates and halides
5. increased melter convection by melting lower viscosity glasses, power skewing the bottom electrodes, or mechanical agitation (stirrer/bubblers/airlift pumps), and
6. dry feeding instead of slurry feeding [49]. In addition higher melt temperatures improve melt rate.

Round or oval melters avoid having cold corners and enhance natural convection, while square or oblong melters need agitation with bubblers or stirrers to enhance convection in the corners (Fig. 9.15). For example, the DWPF is fitted with an airlift bubbler [153] which increases the glass circulation while transferring additional energy from within the melt pool to the pool surface (cold cap) to better utilize electrode power.

The Hanford HLW melter will be fitted with eight twin-orifice melt bubblers that bubble air and thus improve melt rate and convection [154]. The

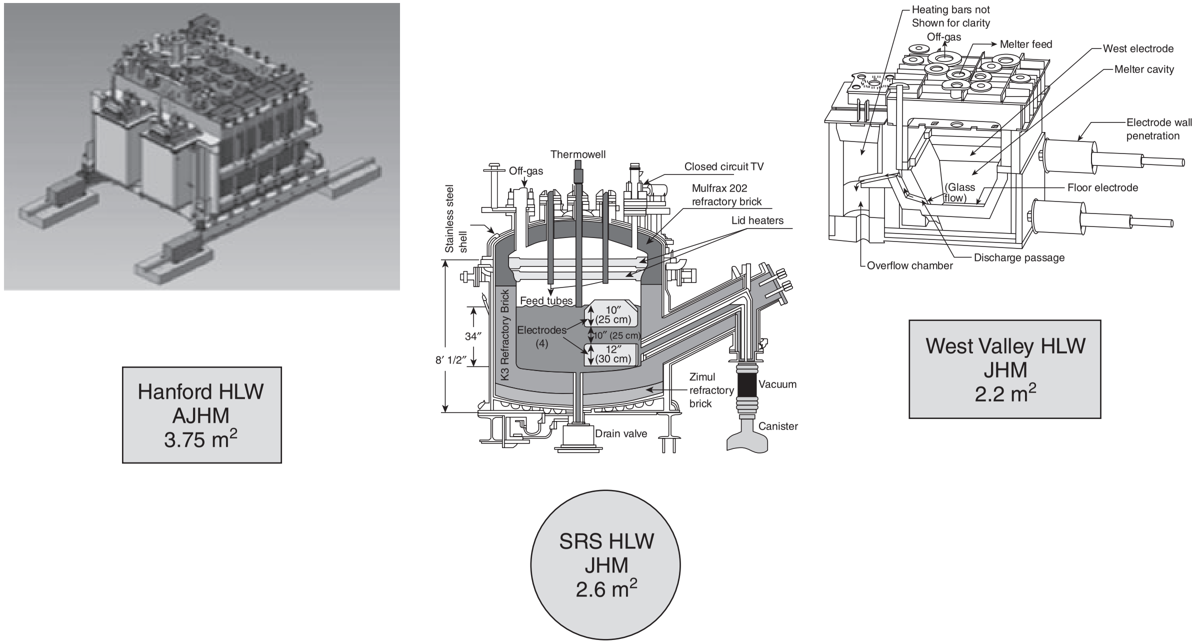

9.15 Joule-heated melters (JHMs) and advanced Joule-heated melters (AJHMs) for HLW. Boxes and circles are drawn to scale to represent melt pool surface area in m^2.

use of multiple bubblers with fairly frequent bubbler replacements is considered an advanced JHM design. While it has been well tested at the pilot scale, such an AJHM has yet to be demonstrated with actual radioactive waste.

It should be noted that the Hanford HLW melter shown in Fig. 9.15 is the largest JHM/AJHM in terms of melt pool surface area, 3.75 m^2. The DWPF melter is 1.5× smaller (2.6 m^2) and currently the largest HLW melter in operation. The DWPF could be lifted by a crane (Fig. 9.7) for replacement as could the West Valley Demonstration Project melter which had a melt pool surface area of 2.2 m^2. Therefore, replacement melters for Hanford must enter and be disposed of via a rail system which is visible in Fig. 9.15.

Joule-heated melters can be designed with sloped bottoms and bottom drains (with or without melt pool mixing) to facilitate periodic draining of noble metals that may precipitate, as was done with the Tokai JHM. JHMs can be operated at ~1200°C before different materials of construction are necessitated. However, increased melt pool volatility, refractory corrosion, and electrode corrosion are to be expected at higher operating temperatures. The increasing production capability is offset by increasing complexity of the melter system (Fig. 9.16).

Joule-heated melters are intolerant of crystal growth in the melt which causes slag formation [155]. Recently, Sellafield has shown the ability to go to 38 wt% waste loading [156] from 25 wt% waste loading [157] by allowing spinel formation in the melt, but the Sellafield melter is induction heated, not a JHM design. However, 1–2% crystallization of spinels is planned for Hanford's HLW AJHM and it is anticipated that the spinel crystals will stay buoyant from the melt pool agitation afforded by the bubblers [158, 159]. This strategy will likely work unless during long maintenance outages, the

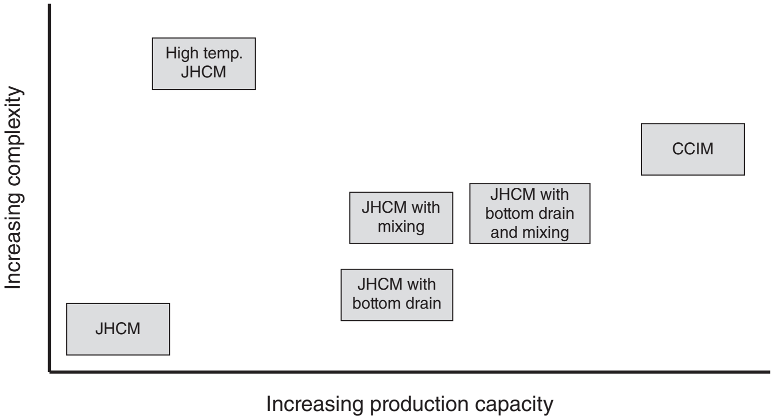

9.16 Representation of advanced melter technologies based on complexity and capability. From reference 124.

crystals grow larger than the size that the agitation can sustain or the melt pool will have to be diluted with components that dilute the spinel-forming tendencies, because JHMs and AJHMs cannot be drained without causing damage to the electrodes.

9.6.2 Advanced melter designs and GCMs

The cold crucible induction-heated melter (CCIM) is being pursued in Russia, France, and the US as an alternative to JHM and AJHM melter technology. The major advantages of CCIM over JHM/AJHM are higher productivity, higher temperatures, longer lifetime, smaller dimensions, and higher waste loadings while maintaining the same product quality. The CCIM is also capable of producing GCMs and mineral waste forms by a melt and controlled crystallization route [50, 51].

The melter is composed of water-cooled tubes that are arranged to form a crucible that is heated by induction heating. A slag forms along the crucible wall to form a barrier and container, and the inductor couples directly with the glass to provide melting. Presently, two different pour designs are being pursued for the CCIM technology: side pouring and a bottom drain. The side pouring method is similar to the overflow design used in the DWPF. The bottom drain configuration uses a plunger-type arrangement. It is water-cooled and unseated when ready to pour. It can also be used to clear the drain when plugging occurs. The CCIM technology targets a low viscosity glass (i.e., ~20 poise) to ensure pourability. Limited testing has also been performed with a stirrer in the CCIM, and preliminary data indicated increased productivity by ~15–20% [51]. While testing has been performed with the CCIM technology, the melter has not been installed for high level waste application. This technology has the potential to increase waste throughput and capacity with minimal complexity (Fig. 9.16). Additional discussion of this technology can be found in Chapter 5.

9.7 Sources of further information and advice

Textbooks such as those indicated in references 22, 50, 51, and the 1988 textbook given in reference 123 were especially helpful and many of the US DOE references can be obtained at www.osti.gov/bridge. Another excellent compendium about melter technology prior to 2001 is available in reference 124. An excellent compendium on glass durability not cited in the references below is J.K. Bates, C.R. Bradley, E.C. Buck, J.C. Cunnane, W.L. Ebert, X. Feng, J.J. Mazer, and D.J. Wronkiewicz, 'High-Level Waste Borosilicate Glass A Compendium of Corrosion Characteristics', Vols 1, 2 and 3, US DOE Office of Waste Management Report DOE-EM-0177 (March 1994).

9.8 References

1. D.R. Clarke, 'Preferential dissolution of an intergranular amorphous phase in a nuclear waste ceramic', *J. Am. Ceram. Soc.*, 64, C89–90 (1981).
2. J.A. Cooper, D.R. Cousens, J.A. Hanna, R.A. Lewis, S. Myhra, R.L. Segall, R.St.C. Smart, P.S. Turner, and T.J. White, 'Intergranular films and pore surfaces in Synroc C: Structure, composition, and dissolution characteristics', *J. Am. Ceram. Soc.*, 69[4], 347–352 (1986).
3. W.J. Buykx, K. Hawkins, D.M. Levins, H. Mitamura, R.St. C. Smart, G.T. Stevens, K.G. Watson, D. Weedon, and T.J. White, 'Titanate ceramics for the immobilization of sodium-bearing high-level nuclear waste,' *J. Am. Ceram. Soc.*, 71[8], 768–788 (1988).
4. F.J. Dickson, H. Mitamura, and T.J. White, 'Radiophase development in hot-pressed alkoxide-derived titanate ceramics for nuclear waste stabilization,' *J. Am. Ceram. Soc.*, 72[6], 1055–1059 (1989).
5. W.J. Buykx, D.M. Levins, R. St.C. Smart, K.L. Smith, G.T. Stevens, K.G. Watson, D. Weedon, and T.J. White, 'Interdependence of phase chemistry, microstructure, and oxygen fugacity in titanate nuclear waste ceramics,' *J. Am. Ceram. Soc.*, 73[5], 1201–1207 (1990).
6. W.J. Buykx, D.M. Levins, R. St.C. Smart, K.L. Smith, G.T. Stevens, K.G. Watson, and T.J. White, 'Processing impurities as phase assemblage modifiers in titanate nuclear waste ceramics,' *J. Am. Ceram. Soc.*, 73, 217–225 (1990).
7. H. Mitamura, S. Matsumoto, K.P. Hart, T. Miyazaki, E.R. Vance, Y. Tamura, Y. Togashi, and T.J. White, 'Aging effects on curium-doped titanate ceramics containing sodium-bearing high-level nuclear waste,' *J. Am. Ceram. Soc.*, 75[2], 392–400 (1992).
8. C.M. Jantzen, D.R. Clarke, P.E.D. Morgan, and A.B. Harker, 'Leaching of polyphase nuclear waste ceramics: Microstructural and phase characterization,' *J. Am. Ceram. Soc.*, 65[6], 292–300 (1982).
9. V. Jain and S.M. Barnes, 'Radioactive waste solidification at the West Valley Demonstration Project (WVDP),' *Ceram. Trans.*, 29, 545–552 (1993).
10. IAEA, 'Design and Operation of High Level Waste Vitrification and Storage Facilities,' IAEA Technical Reports Series No. 339 (1992).
11. I.W. Donald, B.L. Metcalfe, and R.N.J. Taylor, 'The immobilization of high level radioactive wastes using ceramics and glasses,' *J. Mater. Sci.*, 32, 5851–5887 (1997).
12. G.E. Brown, Jr., F. Farges, and G. Calas, 'X-ray scattering and X-ray spectroscopy studies of silicate melts,' in *Structure, Dynamics and Properties of Silicate Melts*, J.F. Stebbins, P.F. McMillan, and D.B. Dingwell (eds), *Reviews in Mineralogy*, 32, 317–410 (1995).
13. A.J.G. Ellison and A. Navrotsky, 'Thermochemistry and structure of model waste glass compositions,' in *Scientific Basis for Nuclear Waste Management, XIII*, V.M. Oversby and P.W. Brown (eds) Materials Research Society, Pittsburgh, PA, 193–207 (1990).
14. H. Li, Y. Su, J.D. Vienna, and P. Hrma, 'Raman spectroscopic study – Effects of B_2O_3, Na_2O, and SiO_2 on nepheline ($NaAlSiO_4$) crystallization in simulated high level waste glasses,' *Ceram. Trans.*, 107, 469–477 (2000).

15. W.B. White, ‘Glass structure and glass durability,’ in *Materials Stability and Environmental Degradation*, A. Barkatt, E.D. Vernik, and L.R. Smith (eds), *MRS Symposium Proceedings*, 125 (1988).
16. E.A. Porai-Koshits, *The Structure of Glass*, Consultants Bureau, New York (1958), p. 25.
17. W.H. Zachariasen, ‘The atomic arrangement in glass,’ *J. Am. Chem. Soc.*, 54, 3841–3851 (1932).
18. W.H. Zachariasen, ‘The vitreous state,’ *J. Chem. Phys.*, 3, 162–163 (1933).
19. B.E. Warren, ‘X-ray diffraction of vitreous silica,’ *Z. Krist.*, 86, 349–358 (1933).
20. A.C. Wright, ‘Neutron scattering from vitreous silica, V. The structure of vitreous silica: What have we learned from 60 years of diffraction studies?,’ *J. Non-Cryst. Solids*, 179, 84–115 (1994).
21. G.N. Greaves, ‘EXAFS and the structure of glass,’ *J. Non-Cryst. Solids*, 71, 203–217 (1985).
22. D. Caurant, P. Loiseau, O. Majerus, V. Aubin-Chevaldonnet, I. Bardez, and A. Quintas, ‘*Glasses, Glass-Ceramics and Ceramics for Immobilization of Highly Radioactive Nuclear Wastes*,’ Nova Science Publishers, New York, 359 pp. (2009).
23. C.W. Burnham, ‘The nature of multicomponent aluminosilicate melts,’ *Phys. Chem. Earth*, 13–14, 191–227 (1981).
24. C.M. Jantzen and K.G. Brown, ‘Predicting the spinel-nepheline liquidus for application to nuclear waste glass processing: Part I. Primary phase analysis, liquidus measurement, and quasicrystalline approach,’ *J. Am. Ceram. Soc.*, 90[6], 1866–1879 (2007).
25. C.M. Jantzen and K.G. Brown, ‘Predicting the spinel-nepheline liquidus for application to nuclear waste glass processing: Part II. Quasicrystalline freezing point depression model,’ *J. Am. Ceram. Soc.*, 90[6], 1880–1891 (2007).
26. R. Nyholm and L.O. Werme, ‘An ESCA investigation of molybdenum containing silicate and phosphate glasses,’ in *Scientific Basis of Nuclear Waste Management, III*, Plenum Press, New York (1981).
27. G. Calas, M. Le Grand, L. Galoisy, and D. Ghale, ‘Structural role of molybdenum in nuclear glasses: an EXAFS study’, *J. Nucl. Mater.*, 322, 15–20 (2003).
28. D. Caurant, O. Majérus, E. Fadel, A. Quintas, C. Gervais, and T. Charpentier, and D. Neuville, ‘Structural investigations of borosilicate glasses containing MoO_3 by MAS NMR and Raman spectroscopies,’ *J. Nucl. Mater.*, 396[1], 94–101 (2010).
29. N.C. Hyatt, R.J. Short, R.J. Hand, W.E. Lee, F. Livens, J.M. Charnock, and R.L. Bilsborrow, ‘The structural chemistry of molybdenum in model high level nuclear waste glasses, investigated by Mo K-edge X-ray absorption spectroscopy,’ *Ceram. Trans.*, 168, American Ceramic Society, Westerville, OH, 179–187 (2004).
30. C.M. Jantzen and D.F. Bickford, ‘Leaching of devitrified glass containing simulated SRP nuclear waste,’ in *Scientific Basis for Nuclear Waste Management, VIII*, C.M. Jantzen, J.A. Stone, and R.C. Ewing (eds), Materials Research Society, Pittsburgh, PA, 135–146 (1985).

31. M.J.D. Rushton, R.W. Grimes, and S.L. Owens, 'Changes to alkali ion content adjacent to crystal-glass interfaces,' in *Scientific Basis for Nuclear Waste Management, XXXI*, W.E. Lee, J.W. Roberts, N.C. Hyatt, and R.W. Grimes (eds), Materials Research Society, Pittsburgh, PA, 207–213 (2008).
32. M.I. Ojovan and W.E. Lee, 'Topologically disordered systems at the glass transition,' *J. Phys.: Condens. Matter*, 18, 11507–11520 (2006).
33. D.K. Peeler, 'Batch 1 Variability Study Using Twice Washed Tank 51 Sludge,' WSRC-RP-1045, Rev. 1 (January 1995).
34. D.K. Peeler, 'Batch 1 Variability Study Using Twice Washed Tank 51 Sludge and Frit 200,' WSRC-RP-96–20, Rev. 0 (1996).
35. J.R. Harbour, T.B. Edwards, and R.J. Workman, 'Summary of Results for Macrobatch 3 Variability Study', WSRC-TR-2000-00351, Rev. 0 (2000).
36. C.C. Herman, T.B. Edwards, and D.M. Marsh, 'Summary of Results for Expanded Macrobatch 3 Variability Study', WSRC-TR-2001-00511, Rev. 0 (2001).
37. M.T. Keefer, B.A. Hamm, and J.A. Pike, 'Low temperature aluminum dissolution of sludge waste,' WM2008 Conference Paper #8175 (2008).
38. J.A. Stone, J.A. Kelley, and T.S. McMillan, 'Sampling and Analyses of SRP High-Level Waste Sludges,' US DOE Report DP-1399, E.I. DuPont de Nemours & Co., Savannah River Laboratory, Aiken, SC (August 1976).
39. J.A. Stone, 'Separation of SRP Waste Sludge and Supernate,' US DOE Report DP-1441, E.I. DuPont de Nemours & Co., Savannah River Laboratory, Aiken, SC (November 1976).
40. C.C. Chapman, 'Design preferences for a slurry-fed ceramic melter suitable for vitrifying West Valley wastes,' *Adv. Ceram.*, 8, 149–160 (1984).
41. B.M. Rapko and G.J. Lumetta, 'Status Report on Phase Identification in Hanford Tank Sludges,' PNNL-13394 (December 2000).
42. T. Motyka, 'Technical Data Summary for In-Tank Sludge Processing,' US DOE Report DPSTD-84-100, E.I. DuPont de Nemours & Co., Savannah River Laboratory, Aiken, SC (April 1984).
43. E.R. Merz, 'Overview on the application of denitration in the nuclear field,' pp. 1–10 in *Denitration of Radioactive Liquid Waste*, L. Cecille and S. Halaszovich (eds) Graham & Trotman Ltd for the Commission of the European Communities, 180 pp. (1986).
44. C.M. Jantzen, J.R. Zamecnik, D.C.Koopman, C.C. Herman, and J.B. Pickett, 'Electron Equivalents Model for Controlling REDuction/OXidation (REDOX) Equilibrium during High Level Waste (HLW) Vitrification,' US DOE Report WSRC-TR-2003-00126, Rev. (9 May 2003).
45. C.M. Jantzen, D.C. Koopman, C.C. Herman, J.B. Pickett, and J.R. Zamecnik, 'Electron equivalents REDOX model for high level waste vitrification,' in *Environmental Issues and Waste Management Technologies IX*, J.D. Vienna and D.R. Spearing (eds), *Ceram. Trans.*, 155, 79–91 (2004).
46. C.M. Jantzen and M.E. Stone, 'Role of Manganese Reduction/Oxidation (REDOX) on Foaming and Melt Rate in High Level Waste (HLW) Melters,' US DOE Report WSRC-STI-2006-00066 (2007).
47. D.J. Bradley, '*Behind the Nuclear Curtain: Radioactive Waste Management in the Former Soviet Union*,' Battelle Press, Columbus, OH, 716 pp. (1997).
48. J.M. Perez, S.M. Barnes, S. Kelly, L. Petkus, and E.V. Morrey, 'Vitrification testing and demonstration for the Hanford waste treatment and immobilization plant,' *Ceram. Trans.*, 168, 3–21 (2005).

49. D.F. Bickford, P.Hrma, and B.W. Bowan II, 'Control of radioactive waste glass melters: II. Residence time and melt rate limitations,' *J. Am. Ceram. Soc.*, 73[10], 2903–2915 (1990).
50. M.I. Ojovan and W.E. Lee, '*An Introduction to Nuclear Waste Immobilization*,' Nova Science Publishers, Oxford, 315 pp. (2007).
51. M.I. Ojovan and W.E. Lee, '*New Developments in Glassy Nuclear Wasteforms*,' Elsevier Publishers, Oxford, 315 pp. (2005).
52. V. Jain, 'Survey of Solidification Process Technologies,' Report CNWRA 98-005, Center for Nuclear Waste Regulatory Analyses, San Antonio, Texas (April 1998).
53. W. G. Ramsey, 'Durability study of simulated radioactive waste glass in brine environment,' Unpublished M.S. Thesis, Clemson University, Clemson, SC, 101 pp. (1989).
54. G.G. Wicks, W.D. Rankin, and S.L. Gore, 'International waste glass study – Composition and leachability correlations,' in *Scientific Basis for Nuclear Waste Management, VIII*, C.M. Jantzen, J.A. Stone, and R.C. Ewing (eds), Materials Research Society, Pittsburgh, PA, 171–177 (1985).
55. C.M. Jantzen, 'Systems approach to nuclear waste glass development,' *J. Non-Cryst. Solids*, 84[1–3], 215–225 (1986).
56. C.M. Jantzen, 'Relationship of glass composition to glass viscosity, resistivity, liquidus temperature, and durability: First principles process–product models for vitrification of nuclear waste,' *Ceram. Trans.*, 23, American Ceramic Society, Westerville, OH, 37–51 (1991).
57. C.M. Jantzen and K.G. Brown, 'Statistical process control of glass manufactured for the disposal of nuclear and other wastes,' *Am. Ceram. Soc. Bull.*, 72, 55–59 (May 1993).
58. T.M. El-Shamy, 'The chemical durability of K_2O-CaO-MgO-SiO_2 glasses,' *Phys. Chem. Glasses*, 14[1], 1–5 (1973).
59. K.G. Brown and R.L. Postles, 'The DWPF product composition control system at Savannah River: Statistical process control algorithm,' *Ceram. Trans.*, 23, 559–568 (1991).
60. C.M. Jantzen and J.C. Marra, 'High level waste (HLW) vitrification experience in the US: Application of glass product/process control to other HLW and hazardous wastes,' in *Scientific Basis for Nuclear Waste Management, XXXI*, MRS Symposium Volume 1107, 183–190 (2008).
61. Department of Energy, 'Civilian Radioactive Waste Management System Waste Acceptance System Requirements Document, Revision 5,' US DOE Report DOE/RW-0351 Rev. 5 (March 2008).
62. C.M. Jantzen, N.E. Bibler, D.C. Beam, and M.A. Pickett, 'Characterization of the Defense Waste Processing Facility (DWPF) Environmental Assessment (EA) Glass Standard Reference Material,' US DOE Report WSRC-TR-92-346, Rev. 1, Westinghouse Savannah River Company, Aiken, SC (1993).
63. C.M. Jantzen, N.E. Bibler, D.C. Beam, and M.A. Pickett, 'Development and Characterization of the Defense Waste Processing Facility (DWPF) Environmental Assessment (EA) Glass Standard Reference Material,' in *Environmental and Waste Management Issues in the Ceramic Industry, Ceramic Transactions*, 39, American Ceramic Society, Westerville, OH (1994), 313–322.
64. ASTM C1285, 'Standard Test Methods for Determining Chemical Durability of Nuclear, Hazardous, and Mixed Waste Glasses and Multiphase Glass

Ceramics: The Product Consistency Test (PCT),' *Annual Book of ASTM Standards*, Vol. 12.01 (2008).

65. W.B. White, 'Theory of corrosion of glass and ceramics,' in *Corrosion of Glass, Ceramics, and Ceramic Superconductors*, D.E. Clark and B.K. Zoitos (eds), Noyes Publications, Park Ridge, NJ, 2–28 (1992).
66. W. Sinkler, T.P. O'Holleran, S.M. Frank, M.K. Richmann, and S.G. Johnson, 'Characterization of a glass-bonded ceramic waste form loaded with U and Pu,' in *Scientific Basis for Nuclear Waste Management, XXIII*, R.W. Smith and D.W. Shoesmith (eds), Materials Research Society, Pittsburgh, PA, 423–429 (2000).
67. T. Moschetti, W. Sinkler, T. Disanto, M.H. Hois, A.R. Warren, D. Cummings, S.G. Johnson, K.M. Goff, K.J. Bateman, and S.M. Frank, 'Characterization of a ceramic waste form encapsulating radioactive electrorefiner salt,' in *Scientific Basis for Nuclear Waste Management, XXIII*, R.W. Smith and D.W. Shoesmith (eds), Materials Research Society, Pittsburgh, PA, 577–582 (2000).
68. N.E. Bibler and J.K. Bates, 'Product consistency leach tests of Savannah River Site radioactive waste glasses,' in *Scientific Basis for Nuclear Waste Management, XIII*, V. M. Oversby and P. W. Brown (eds), Materials Research Society, Pittsburgh, PA, 327–338 (1990).
69. J.K. Bates, D.J. Lam, and M.J. Steindler, 'Extended leach studies of actinide-doped SRL 131 glass,' in *Scientific Basis for Nuclear Waste Management, VI*, D.G. Brookins (ed.), North-Holland, New York, 183–190 (1983).
70. N.E. Bibler and A.R. Jurgensen, 'Leaching Tc-99 from SRP glass in simulated tuff and salt groundwaters,' in *Scientific Basis for Nuclear Waste Management, XI*, M.J. Apted and R.E. Westerman (eds), Materials Research Society, Pittsburgh, PA, 585–593 (1988).
71. D.J. Bradley, C.O. Harvey, and R.P. Turcotte, 'Leaching of Actinides and Technetium from Simulated High-Level Waste Glass,' Pacific Northwest Laboratory Report, PNL-3152, Richland, WA (1979).
72. S. Fillet, J. Nogues, E. Vernaz, and N. Jacquet-Francillon, 'Leaching of actinides from the French LWR reference glass,' in *Scientific Basis for Nuclear Waste Management, IX*, L.O. Werme (ed.), Materials Research Society, Pittsburgh, PA, 211–218 (1985).
73. F. Bazan, J. Rego, and R.D. Aines, 'Leaching of actinide-doped nuclear waste glass in a tuff-dominated system,' in *Scientific Basis for Nuclear Waste Management, X*, J.K. Bates and W.B. Seefeldt (eds), Materials Research Society, Pittsburgh, PA, 447–458 (1987).
74. E.Y. Vernaz and N. Godon, 'Leaching of actinides from nuclear waste glass: French experience,' in *Scientific Basis for Nuclear Waste Management, XV*, C.G. Sombret (ed.), Materials Research Society, Pittsburgh, PA, 37–48 (1992).
75. W.L. Ebert, S.F. Wolf, and J.K. Bates, 'The release of technetium from defense waste processing facility glasses,' in *Scientific Basis for Nuclear Waste Management, XIX*, W.M. Murphy and D.A. Knecht (eds), Materials Research Society, Pittsburgh, PA, 221–227 (1996).
76. B.P. McGrail, 'Waste package component interactions with Savannah River defense waste glass in a low-magnesium salt brine,' *Nucl. Technol.*, 75, 168–186 (1986).
77. B.C. Bunker, G.W. Arnold, D.E. Day, and P.J. Bray, 'The effect of molecular structure on borosilicate glass leaching,' *J. Non-Cryst. Solids*, 87, 226–253 (1986).

78. C.M. Jantzen, K.G. Brown, T.B. Edwards, and J.B. Pickett, ‘Method of Determining Glass Durability (THERMO™),’ US Patent 5,846,278 (December 1998).
79. C.M. Jantzen, J.B. Pickett, K.G. Brown, T.B. Edwards, and D.C. Beam, ‘Process/Product Models for the Defense Waste Processing Facility (DWPF): Part I. Predicting Glass Durability from Composition Using a Thermodynamic Hydration Energy Reaction MOdel (THERMO),’ US DOE Report WSRC-TR-93-0672, Westinghouse Savannah River Co., Aiken, SC, 464 pp. (September 1995).
80. R. Conradt, ‘A proposition for an improved theoretical treatment of the corrosion of multi-component glasses,’ *J. Nucl. Mater.*, 298, 19–26 (2001).
81. R. Conradt, ‘Chemical structure, medium range order, and crystalline reference state of multicomponent oxide liquids and glasses,’ *J. Non-Cryst. Solids*, 345–346, 16–23 (2004).
82. R. Conradt, ‘Chemical durability of oxide glasses in aqueous solutions: a review,’ *J. Am. Ceram. Soc.*, 91[3], 728–735 (2008).
83. C.M. Jantzen and J.M. Pareizs, ‘Glass durability modeling: The role of activated complexes and quasicrystalline structural ratios’ (accepted *J. Nucl. Mater.*).
84. H.C. Helgeson, W.M. Murphy, and P. Aagaard, ‘Thermodynamic and kinetic constraints on reaction rates among minerals and aqueous solutions, II. Rate constants, effective surface area, and the hydrolysis of feldspar,’ *Geochim. Cosmochim. Acta*, 48, 2405–2432 (1984).
85. E.H. Oelkers and S.R. Sislason, ‘The mechanism, rates, and consequences of basaltic glass dissolution: I. An experimental study of the dissolution rates of basaltic glass as a function of aqueous Al, Si, and oxalic acid concentration at 25°C and pH = 3 and 11,’ *Geochim. Cosmochim. Acta*, 65[21], 3671–3681 (2001).
86. P. Van Iseghem and B. Grambow, ‘The long-term corrosion and modeling of two simulated Belgian reference high-level waste glasses,’in *Scientific Basis for Nuclear Waste Management, XI*, Materials Research Society, Pittsburgh, PA, 631–639 (1987).
87. C.M. Jantzen, D.I. Kaplan, N.E. Bibler, D.K. Peeler, and M.J. Plodinec, ‘Performance of a radioactive high level waste glass after 24 years burial,’ *J. Nucl. Mater.*, 378, 244–256 (2008).
88. C.M. Jantzen, K.G. Brown, and J.B. Pickett, ‘Durable glass for thousands of years,’ *Int. J. Appl. Glass Sci.*, 1[1], 38–62 (March 2010).
89. I. Tovena, T. Advocat, D. Ghaleb, E. Vernaz, and F. Larche, ‘Thermodynamic and structural models compared with the initial dissolution rate of SON glass samples,’ in *Scientific Basis for Nuclear Waste Management, XVII*, A. Barkatt and R.A. Van Konynenburg (eds), Materials Research Society, Pittsburgh, PA, 595–602 (1994).
90. C.M. Jantzen and K.G. Brown, ‘Impact of phase separation on waste glass durability,’ in *Environmental Issues and Waste Management Technologies in the Ceramic and Nuclear Industries, V*, G.T. Chandler (eds), *Ceram. Trans.*, 107, 289–300 (2000).
91. C.M. Jantzen, ‘Method for Controlling Glass Viscosity,’ US Patent 5,102,439 (April 1992).
92. C.M. Jantzen, ‘The Impacts of Uranium and Thorium on the Defense Waste Processing Facility (DWPF) Viscosity Model,’ US DOE Report WSRC-TR-2004-00311 (February 2005).

93. G.S. Fulcher, 'Analysis of recent measurements of the viscosity of glasses,' *J. Am. Ceram. Soc.*, 8, 339–355 (1925).
94. G.S. Fulcher, 'Analysis of recent measuements of the viscosity of glasses, II,' *J. Am. Ceram. Soc.*, 8[12], 789–794 (1925).
95. G.W. Scherer, 'Editorial comments on a paper by Gordon S. Fulcher,' *J. Am. Ceram. Soc.*, 75[5], 1060–1062 (1992).
96. W.B. White and D.G. Minser, 'Raman spectra and structure of natural glasses,' *J. Non-Cryst. Solids*, 67, 45–59 (1984).
97. E.T. Turkdogan, *Physicochemical Properties of Molten Slags and Glasses*, The Metals Society, London (1983).
98. B.O. Mysen, D. Virgo, C.M. Scarfe, and D.J. Cronin, 'Viscosity and structure of iron- and aluminum-bearing calcium silicate melts at 1 atm.,' *Am. Mineralogist*, 70, 487–498 (1985).
99. B.M.J. Smets and D.M. Krol, 'Group III ions in sodium silicate glass. Part 1. X-ray photoelectron spectroscopy study,' *Phys. Chem. Glasses*, 25[5], 113–118 (1984).
100. W.L. Konijnendijk, 'Structural differences between borosilicate and aluminosilicate glasses studied by Raman scattering,' *Glastechn. Ber.*, 48[10], 216–218 (1975).
101. T. Furukawa and W.B. White, 'Raman spectroscopic investigation of sodium borosilicate glass structure,' *J. Mater. Sci.*, 16, 2689–2700 (1981).
102. J. Hlavac, *The Technology of Glass and Ceramics: An Introduction*, Elsevier Scientific Publishing Company, Amsterdam (1983).
103. C.M. Jantzen, J.R. Zamecnik, D.C. Koopman, C.C. Herman, and J.B. Pickett, 'Electron Equivalents Model for Controlling REDuction/OXidation (REDOX) Equilibrium During High Level Waste (HLW) Vitrification,' US DOE Report WSRC-TR-2003-00126, Rev. 0 (May 2003).
104. C.M. Jantzen, D.C. Koopman, C.C. Herman, J.B. Pickett, and J.R. Zamecnik, 'Electron equivalents REDOX model for high level waste vitrification,' in *Environmental Issues and Waste Management Technologies IX*, J.D. Vienna and D.R. Spearing (eds), *Ceram. Trans.*, 155, 79–91 (2004).
105. C.M. Jantzen and M.E. Stone, 'Role of Manganese Reduction/Oxidation (REDOX) on Foaming and Melt Rate in High Level Waste (HLW) Melters,' US DOE Report WSRC-STI-2006-00066 (2007).
106. K.G. Brown, C.M. Jantzen, and G. Ritzhaupt, 'Relating Liquidus Temperature to Composition for Defense Waste Processing Facility (DWPF) Process Control,' US DOE Report WSRC-TR-2001-00520, Rev. 0, Westinghouse Savannah River Company, Aiken, SC (October 2001).
107. C.M. Jantzen and M.E. Smith, 'Revision of the Defense Waste Processing Facility (DWPF) Sulfate Solubility Limit,' US DOE Report WSRC-TR-2003-00518 (January 2004).
108. C.M. Jantzen, D.K. Peeler, and M.E. Smith, 'Dependency of sulfate solubility on melt composition and melt polymerization,' *Ceram. Trans.*, 168, 141–151 (2005).
109. I. Bardez, D. Caurant, J.L. Dussossoy, P. Loiseau, C. Gervais, F. Ribot, D.R. Neuville, N. Baffier, and C. Fillet, 'Development and characterization of rare earth-rich glassy matrices envisaged for the immobilization of concentrated nuclear waste solutions,' *Nucl. Sci. Eng.*, 153, 272–284 (2006).

110. T.F. Meaker and N.E. Bibler, 'Characterization and product consistency leach tests on lanthanide borosilicate glasses containing plutonium and uranium or impurities,' in *Plutonium Immobilization: The Glass Option – A Compendium of Reports and Presentations*, WSRC-RP-97-00902, Westinghouse Savannah River Company, Aiken, SC (1997).
111. T.F. Meaker and D.K. Peeler, 'Solubility of independent plutonium bearing feed streams in a Hf-based LaBS frit,' in *Plutonium Immobilization: The Glass Option – A Compendium of Reports and Presentations*, WSRC-RP-97-00902, Westinghouse Savannah River Company, Aiken, SC (1997).
112. T.F. Meaker and N. E. Bibler, 'Comparison of the durabilities and microstructures of an amorphous and devitrified plutonium bearing lanthanide borosilicate glass,' in *Plutonium Immobilization: The Glass Option – A Compendium of Reports and Presentations*, WSRC-RP-97-00902, Westinghouse Savannah River Company, Aiken, SC (1997).
113. T.F. Meaker and N.E. Bibler, 'Characterization and product consistency leach tests of lanthanide borosilicate glasses containing plutonium and uranium or impurities,' in *Plutonium Immobilization: The Glass Option – A Compendium of Reports and Presentations*, WSRC-RP-97-00902, Westinghouse Savannah River Company, Aiken, SC (1997).
114. J. von Löffler, 'Chemical decolorization,' *Glastechn. Ber.*, 10 (1932).
115. M.B. Volf, *Chemical Approach to Glass*, Glass Science and Technology, Vol. 7, Elsevier Science Publishing Co., New York (1984).
116. W.G. Ramsey, N.E. Bibler, and T.F. Meaker, 'Compositions and durabilities of glasses for immobilization of plutonium and uranium,' *Waste Management '95*, Record 23828-23907, WM Symposia, Inc., Tucson, AZ (1995).
117. N.E. Bibler, W.G. Ramsey, T.F. Meaker, and J.M. Pareizs, 'Durabilities and microstructures of radioactive glasses for immobilization of excess actinides at the Savannah River Site,' *Mater. Res. Soc. Symp. Proc.*, Vol. 412, Materials Research Society, Pittsburgh, PA (1995).
118. T.F. Meaker, W.G. Ramsey, J.M. Pareizs, and D.G. Karraker, 'Composition development for vitreous plutonium products,' *Ceram. Trans.*, 72, American Ceramic Society, Westerville, OH (1996).
119. T.F. Meaker, 'Compositional Development of a Plutonium Surrogate Glass without Listed RCRA Elements (Lead and Barium),' WSRC-TR-96-0322, Westinghouse Savannah River Company, Aiken, SC (1996).
120. T.F. Meaker, 'Homogeneous Glass Processing Region Defined for a Lanthanide Borosilicate Glass Composition for the Immobilization of Plutonium Using Thorium as a Surrogate,' WSRC-TR-96-0323, Westinghouse Savannah River Company, Aiken, SC (1996).
121. T. Jones, J.C. Marra, D. Immel, and B. Meers, 'Glass Macrocracking Determination in Prototypic Cans Containing Lanthanide Borosilicate Glass,' WSRC-TR-06-00015, Washington Savannah River Company, Aiken, SC (2006).
122. J.C. Marra, D.K. Peeler, and C.M. Jantzen, 'Development of an Alternate Glass Formulation for Vitrification of Excess Plutonium,' US DOE Report WSRC-TR-2006-00031 (January 2006).
123. B.C. Sales and L.A. Boatner, 'Lead-iron phosphate glass,' Chapter 3 in R.C. Ewing and W.Lutze (eds), *Radioactive Waste Forms for the Future*, North Holland, Amsterdam, 193–231 (1988).

124. J.M. Perez, Jr., D.F. Bickford, D.E. Day, D.S. Kim, S.L. Lambert, S.L. Marra, D.K. Peeler, D.M. Strachan, M.B. Triplett, J.D. Vienna, and R.S. Wittman, 'High-Level Waste Melter Study Report,' PNNL-13582 (2001).
125. International Atomic Energy Agency (IAEA), 'Design and Operation of HLW Vitrification and Storage Facilities,' TRS N339, IAEA, Vienna (1992).
126. A.S. Aloy, B.Y. Galkin, and B.S. Kuznetsov, 'Fractioning of liquid high-radioactive waste and incorporation of long-lived radionuclides into ceramics and vitreous compositions,' in *Waste Management'89*, 677–681, University of Arizona, Tucson, AZ (1989).
127. A.S. Aloy, A.V. Trofimenko, and O.A. Iskhakova, 'The development of a glass matrix for the immobilization of simulated strontium and cesium concentrate after HLW separation,' in *International Topical Meeting on Nuclear and Hazardous Waste Management (SPECTRUM '94)*, 1, 791–764, American Nuclear Society, Atlanta, GA (1994).
128. Y.A. Revenko, L.N. Lazarev, and V.N. Romanovsky, 'Radioactive waste management of the radiochemical plant under construction near Krasnoyarsk,' in *International Topical Meeting on Nuclear and Hazardous Waste Management (SPECTRUM '94)*, 3, 2015–2018, American Nuclear Society, Atlanta, GA (1994).
129. H. Scholze, *Glass: Nature, Structure, and Properties*, Springer-Verlag, New York (1990).
130. A.S. Aloy, V.A. Bel'yukov, A.V. Demin, and Y.A. Revenko, 'Experiences with vitrification of HLW and development of new approaches in Russia,' in *Glass as a Waste Form and Vitrification Technology: Summary of an International Workshop*, pp. E.50–E.51, National Academy Press, Washington, DC (1996).
131. G.K. Marasinghe, M. Karabulut, X. Fang, C.S. Ray, and D.E. Day, 'Vitrified iron phosphate nuclear waste forms containing multiple waste components,' *Ceram. Trans.*, 107, 115–122, American Ceramic Society, Westerville, OH (2000).
132. C.M. Jantzen, 'Investigation of Lead-Iron-Phosphate Glass for SRP Waste,' DP-1729, Savannah River Site, Aiken, SC (1986).
133. C.M. Jantzen, 'Investigation of lead-iron-phosphate glass for SRP waste,' in *Advances in Ceramics, 20*, D.E. Clark, W.B. White, and A.J. Machiels (eds), American Ceramic Society, Westerville, OH, 157–165 (1986).
134. L.A. Chick, L.R. Bunnell, D.M. Strachan, H.E. Kissinger, and F.N. Hodges, 'Evaluation of lead-iron-phosphate glass as a high level waste form,' in *Advances in Ceramics, 20*, D.E. Clark, W.B. White, and A.J. Machiels (eds), American Ceramic Society, Westerville, OH, 149–156 (1986).
135. L. Kahl, 'Hydrolytic durability of lead-iron-phosphate glasses,' in *Advances in Ceramics, 20*, D.E. Clark, W.B. White, and A.J. Machiels (eds), American Ceramic Society, Westerville, OH, 141–148 (1986).
136. Lawrence Livermore National Laboratory (LLNL), 'Fissile Material Disposition Program – Screening of Alternate Immobilization Candidates for Disposition of Surplus Fissile Materials,' UCRL-ID-118819, L-20790-1, Lawrence Livermore National Laboratory, Livermore, CA (1996).
137. X. Yu and D.E. Day, 'Effect of raw materials on the redox state of iron and properties of iron phosphate glasses,' in *Proceedings of the 17th International Congress on Glass*, 2, 45–51, International Academic Publishers, Beijing (1995).
138. A. Mogus-Milankovic, M. Fajic, A. Drasner, R. Tojiko, and D.E. Day, 'Crystallization of iron phosphate glasses,' *Phys. Chem. Glasses*, 39[2], 70–75 (1998).

139. D.E. Day, Z. Wu, C.S. Ray, and P.R. Hrma, 'Chemically durable iron phosphate glass wasteforms,' *J. Non-Cryst. Solids*, 241[1], 1–12 (1998).
140. M. Mesko, D.E. Day, and B.C. Bunker, 'Immobilization of high-level radioactive sludges in iron phosphate glasses,' in *Science and Technology for Disposal of Radioactive Tank Waste*, W.W. Schulz and N.J. Lombardo (eds), Plenum Publishing, New York (1998), 379–390.
141. F. Chen and D.E. Day, 'Corrosion of selected refractories by iron phosphate melts,' *Ceram. Trans.*, 93, 213–220, American Ceramic Society, Westerville, OH (1999).
142. C.R. Ray, X. Fang, M. Karabulut, G.K. Marasinghe, and D.E. Day, 'Iron redox and crystallization of iron phosphate glass,' *Ceram. Trans.*, 43, 187–194, American Ceramic Society, Westerville, OH (1999).
143. M. Mesko and D.E. Day, 'Immobilization of spent nuclear fuel in iron phosphate glass,' *J. Nucl. Mater.*, 273[1], 27–36 (1999).
144. Y. Badyal, M. Karabulut, G.K. Marasinghe, M.L. Saboungi, D. Haeffner, S. Shastri, D.E. Day, and C.S. Ray, 'The effects of uranium oxide high-level waste on the structure of iron phosphate glasses,' in *Scientific Basis for Nuclear Waste Management, XXII*, 556, 297–303, Materials Research Society, Pittsburgh, PA (1999).
145. G.K. Marasinghe, M. Karabulut, X. Fang, C.S. Ray, and D.E. Day, 'Iron phosphate glasses: an alternative to borosilicate glasses for vitrifying certain nuclear wastes,' *Environmental Issues and Waste Management Technologies VI*; *Ceram. Trans.*, 361–368 (2001).
146. G.K. Marasinghe, M. Karabulut, C.S. Ray, D.E. Day, M.G. Shumsky, W.B. Yelon, C.H. Booth, P.G. Allen, and D.K. Shuh, 'Structural features of iron phosphate glasses,' *J. Non-Cryst. Solids*, 222, 144–152 (1997).
147. G.K. Marasinghe, M. Karabulut, C.S. Ray, D.E. Day, C.H. Booth, P.G. Allen, and D.K. Shuh, 'Redox characteristics and structural properties of iron phosphate glasses: a potential host matrix for vitrifying high level nuclear waste,' *Ceram. Trans.*, 87, 261–270, American Ceramic Society, Westerville, OH (1998).
148. G.K. Marasinghe, M. Karabulut, C.S. Ray, D.E. Day, P.G. Allen, J.J. Bucher, D.K. Shuh, Y. Bagyal, M.L. Saboungi, M. Grimsditch, S. Shastri, and D. Heaffner, 'Effects of nuclear waste composition on redox equilibria, structural features, and crystallization characteristics of iron phosphate glasses,' *Ceram. Trans.*, 93, 195–202, American Ceramic Society, Westerville, OH (1999).
149. D.E. Day, X. Yu, G.J. Long, and R.K. Brow, 'Properties and structure of sodium-iron phosphate glasses,' *J. Non-Cryst. Solids*, 215[1], 21–31 (1997).
150. M. Mesko, D.E. Day, and B.C. Bunker, 'Immobilization of CsCl and SrF_2 in iron phosphate glass,' *Waste Management*, 20[4], 271–278 (2000).
151. M. Karabulut, G.K. Marasinghe, C.S. Ray, D.E. Day, O. Ozturk, and G.D. Waddill, 'X-ray photoelectron and Mossbauer spectroscopic studies of iron phosphate glasses containing U, Cs, and Bi,' *J. Non-Cryst. Solids*, 249[2–3], 106–116 (1999).
152. D.E. Day and C.W. Kim, 'Reaction of Inconel 690 and 693 in Iron Phosphate Melts: Alternative Glasses for Waste Vitrification,' Final Report for Contract DE-FG02-04ER63831 Project 0010255 (2005).
153. D.C. Witt, T.M. Jones, and D.F. Bickford, 'Airlift Mini-Bubbler Testing in the Slurry Fed Melt Rate Furnace,' US DOE Report WSRC-TR-2002-00494, Rev. 0 (2002).

154. B.W. Bowan, R. Meigs, and E.C. Smith, 'Bubbling as a means to enhance Joule heated ceramic melter production rates for vitrifying radioactive wastes,' *Ceram. Trans.*, 168, 21–30 (2005).
155. C.M. Jantzen, 'Lack of Slag Formation in the Scale Glass Melter,' US DOE Report DPST-87-373, E.I. DuPont de Nemours & Co., Savannah River Laboratory, Aiken, SC (April 1987).
156. N.R. Gribble, R. Short, E. Turner, and A.D. Riley, 'The impact of increased waste loading on vitrified HLW quality and durability,' in *Scientific Basis for Nuclear Waste Management, XXXIII*, Materials Research Society, Pittsburgh, PA, 283–289 (2009).
157. A. Riley, S. Walker, and N.R. Gribble, 'Composition changes and future challenges for the Sellafield waste vitrification plant,' in *Scientific Basis for Nuclear Waste Management, XXXIII*, Materials Research Society, Pittsburgh, PA, 267–273 (2009).
158. P. Hrma, P. Schill, and L. Nemec, 'Settling of Spinel in a High-Level Waste Glass Melter,' Final Report, US DOE Contract DE-AC06-76RL01830, Project 65422 (2001).
159. J.D. Vienna, T.B. Edwards, J.V. Crum, D.S. Kim, and D.K. Peeler, 'Liquidus temperature and one percent crystal content models for initial Hanford HLW glasses,' *Ceram. Trans.*, 168, 133–140 (2005).

10

Development of ceramic matrices for high level radioactive wastes

H. KINOSHITA, The University of Sheffield, UK

Abstract: Some of the naturally occurring minerals have an ability to incorporate radioactive elements in their crystal structures. Many of them are thermodynamically stable and chemically durable. A variety of ceramic phases based on such natural minerals have been investigated worldwide in order to apply them as a hot matrix for nuclear wastes. In this chapter, selections of potential ceramic phases for nuclear waste immobilisation are introduced together with some of the recent data on the key properties such as hosting capability, synthesis technique, leaching properties and irradiation effects.

Key words: ceramic waste form, crystalline waste form, natural minerals, high level wastes, nuclear waste disposal, single phase, polyphase.

10.1 Introduction

10.1.1 Basic concept

The underlying objective of the waste form is to keep the radionuclides in one place in a stable form so that we can monitor, to a certain extent, the approximate condition of the radionuclides, i.e., how much of such nuclides exist in what form and where. Some of the radionuclides have an extremely long half-life (^{239}Pu 2.411 × 10^4 years, ^{237}Np 2.140 × 10^6 years, ^{99}Tc 2.13 × 10^5 years, ^{129}I 1.57 × 10^7 years), and they have to be isolated from the biosphere for a correspondingly long time, on a geological timescale. The basic concept of ceramic waste matrices is to utilise the naturally occurring minerals and phases that have survived in the natural environment for a geological timescale, to immobilise radionuclides. It is known that some of the natural minerals contain a significant amount of actinide elements, e.g., U and Th, and retain them for such a long time.

The advantages and disadvantages of using ceramic matrices for nuclear wastes are summarised in Table 10.1. Because the incorporation of radionuclides is in the crystalline structure level, there are both advantages and disadvantages associated with this fundamental nature of the ceramics. For example, to immobilise highly fissile nuclides such as ^{239}Pu or ^{235}U, neutron absorbers such as Gd and Hf also have to be incorporated in the waste form

Table 10.1 Advantages and disadvantages of ceramic matrices

Advantages
1. Ceramic waste forms are durable.
2. It is possible to tailor the matrices for certain types of wastes.
3. Natural analogues can help us to understand the long-term behaviour.

Disadvantages
1. High-temperature process is usually required for fabrication.
2. Hosting capability is restricted by the crystal structure.
3. It is difficult to incorporate mixed wastes in a single phase.

to avoid criticality. Because of the incorporation in the crystalline structure level, the fissile and the neutron poisoning elements always remain in the relevant proximity. On the other hand, it may be challenging to apply ceramic matrices for more chemically complex mixed waste streams, as certain types of crystal structure accept only certain types of elements.

10.1.2 Research on ceramic matrices

Ewing [1] mentioned essential questions, in his recent review of ceramic matrices for Pu disposition, which materials scientists and mineralogists should keep in mind for the development of ceramic waste forms, i.e., 'Are there actinide-bearing phases of demonstrable chemical and physical durability that can be used for the long-term immobilization and disposal of plutonium? Are there naturally occurring analogue structures, minerals that contain U and Th that can be used to confirm the long-term performance of the actinide waste form?' Although these questions were intended for Pu immobilisation, the principle of the questions is applicable for any types of radionuclide immobilisation, which leads to important aspects for the ceramic matrices as summarised in Table 10.2.

Based on these aspects, various types of ceramic phases have been examined. Table 10.3 shows examples of ceramic phases investigated as a host matrix for radionuclides [1–5]. The formulae in the table are simple examples shown as a guide to assist the understanding of the basic crystal structure of the ceramic phases, and they may not represent the exact formulae of the minerals and phases. There are four 'types' of basic crystal structure that are often investigated: (1) apatite-type, (2) zircon-type, (3) fluorite-type and (4) other types. They can be further categorised into four 'groups' based on the main cation across four types of basic crystal, namely (i) silicate, (ii) phosphate, (iii) zirconia-based and (iv) titania-based groups.

Trocellier compared the chemical bonding of the elements and oxygen (M–O bond strength) related to the ceramic waste forms [3]. The M–O bond

Table 10.2 Important aspects of ceramic waste form matrices

Aspects	Description	Factors
Capacity to host waste elements	Capable of hosting waste elements within their crystal structure	Crystal structure, ionic radii, oxidation state
Stability under natural environment	Thermodynamically stable and chemically durable for a long time	Leaching rate, sorption behaviour
Integrity under irradiation	Integrity under irradiation especially from the α-decay events from actinides	Irradiation-induced damages, amorphisation
Reliable synthesis	Simple processes to minimise the possible contamination and exposure	Activity level, melting temperature

Table 10.3 Examples of ceramic matrix phases and their formulae

	Silicate	Phosphate	Zirconia-based	Titania-based
Apatite-type * X denotes O, OH, F, Cl, I	Britholite* [$Ca_2Ln_8(SiO_4)_6X_2$]	Apatite* [$Ca_{10}(PO_4)_6X_2$]		
Zircon-type ** Monazite has a distorted zircon structure	Zircon [$ZrSiO_4$] Thorite [$ThSiO_4$]	Xenotime [YPO_4] Monazite** [$LnPO_4$]		
Fluorite-type *** Baddeleyite and zirconolite have monoclinic structures			Cubic zirconia [ZrO_{2-X}] Baddeleyite*** [ZrO_2]	Pyrochlore [$Ln_2Ti_2O_7$] Zirconolite*** [$CaZrTi_2O_7$]
Other types	Garnet [$Ca_3Al_2(SiO_4)_3$]	NZP [$NaZr_2(PO_4)_3$]		Perovskite [$CaTiO_3$] Hollandite [$BaAl_2Ti_6O_{16}$]

The formulae in this table are simple examples shown only as a guide to assist the understanding of the basic crystal structure of the ceramic matrices, and may not represent the exact formulae of the minerals.

Table 10.4 Bond strength of elements with oxygen

M–O bond	Bond strength (kJ/mol)	M–O bond	Bond strength (kJ/mol)
Al–O	222–422	Nd–O	285
Ba–O	136	P–O	370–462
Ca–O	134	Si–O	443
Ce–O	257	Th–O	270
Gd–O	285	Ti–O	303
Hf–O	264	U–O	279
La–O	242	Y–O	208
Mg–O	155	Zr–O	338–507
Na–O	84		

Source: reference 3.

strength is equal to the oxide dissociation energy divided by the coordination number. As shown in Table 10.4, the strong M–O bonds (>300 kJ/mol) are assured for P–O, Si–O, Ti–O and Zr–O. It is, therefore, not surprising to see that silicate, phosphate, zirconia-based and titania-based groups have been the main focus of the research for ceramic matrices. In the following sections, selections of ceramic phases from Table 10.3 are further described together with data from recent publications.

10.2 Ceramic phases

10.2.1 Apatite

Table 10.5 shows the basic information for the apatite phase. The basic formula of apatite is $A_{10}(BO_4)_6X_2$, and various types of elements can be incorporated. One of the interesting features of this structure comes from the (BO_4) unit which is usually $(PO_4)^{3-}$ or $(SiO_4)^{4-}$. They can be interchangeable depending on the size and valence of the cations on the A-site. Examples are shown in Table 10.6. Boughzala *et al.* [7] produced $Sr_{10-x}La_x(PO_4)_{6-x}(SiO_4)$ xF_2 and $Sr_{10-x}La_x(PO_4)_{6-x}(SiO_4)_xO$ by replacing the (Sr^{2+}, PO_4^{3-}) pair in the strontium fluor- and oxyapatite with a (La^{3+}, SiO_4^{4-}) pair using standard calcination (900°C for 12 hours) and sintering (1200–1400°C) processes. The oxidation state of the elements is also important as it has an effect not only on the charge balance but also on the effective ionic radius. Terra *et al.* [8] experienced difficulty in incorporating U^{4+} in $Ca_9Nd_1(PO_4)_5(SiO_4)_1F_2$ by replacing the (Nd^{3+}, PO_4^{3+}) pair with a (U^{4+}, SiO_4^{4+}) pair. This was considered to be because of the oxidation of U^{4+} into U^{6+} during the synthesis. When all of the $(PO_4)^{3-}$ is replaced by $(SiO_4)^{4-}$ due to the introduction of tri-and/or tetravalent cations, this phase is often referred as britholite.

Table 10.5 Basic information for apatite

Basic formula*	$A_{10}(BO_4)_6X_2$
Site occupation	A: (Ca, Ln, An, Pb, Na Sr), B: (P, Si, V), X: (O, OH, I, F)
Structure	Hexagonal $P6_3/m$
Typical leaching rate	2×10^{-7} g/cm^2/day [6]
Radiation durability	0.24 dpa [6]

*Cations are expressed by A, B, C,…, whereas anions are X, Y, Z. O always denotes the oxygen ion.

Table 10.6 Examples of component substitution in apatite

Base apatite	Removing components	Adding components	Product	Ref.
$Sr_{10}(PO_4)_6F_2$	Sr^{2+}, PO_4^{3+}	La^{3+}, SiO_4^{4+}	$Sr_{10-x}La_x(PO_4)_{6-x}(SiO_4)xF_2$	[10]
$Sr_{10}(PO_4)_6O$	Sr^{2+}, PO_4^{3+}	La^{3+}, SiO_4^{4+}	$Sr_{10-x}La_x(PO_4)_{6-x}(SiO_4)xO$	[10]
$Ca_9Nd_1(PO_4)_5(SiO_4)_1F_2$	Nd^{3+}, PO_4^{3+}	U^{4+}, SiO_4^{4+}	$Ca_9Nd_{1-x}U_x(PO_4)_{5-x}(SiO_4)_{1+x}F_2$	[11]

Because the apatite structure is capable of accommodating monovalent anions, it has also been a subject of research as a host matrix for ^{129}I in the form of $Pb_{10}(VO_4)_6I_2$ [9–11]. The most important aspect for ^{129}I immobilisation is the process temperature during the synthesis. As shown in Table 10.7, common compounds of iodine have rather low melting temperatures. Therefore, sealing and pressuring are often applied during the heating process. Table 10.8 summarises some of such processes that have successfully incorporated iodine in apatite structures. Audubert *et al.* [9] used hot-pressing at 700°C with various pressures, and concluded that 25 MPa was most successful as the higher pressure caused phase transitions during the process and lead to broken products. Uno *et al.* [10] used a vacuum-sealed quartz ampoule to retain reactants during the synthesis. They further applied a uniaxial hot pressing to make a pellet with 9 MPa at 350 or 500°C. The final product was thermally stable up to about 800°C, and the leaching rate of iodine was 3.98×10^{-5} g/cm^2/day whereas that from AgI glass was 4.0×10^{-7} g/cm^2/day. Zhang *et al.* [11] have also been successful in incorporating iodine in an apatite structure using hot isostatic pressing (HIP) in copper cans at 700°C at 200 MPa. They used an excess amount of β-$Pb_3(VO_4)_2$ towards PbI_2 to ensure the incorporation of iodine.

Another interesting aspect of apatite is the response towards irradiation, especially effects of α-decay. Figure 10.1 shows the amorphisation dose for silicate apatite obtained by Weber *et al.* [12]. It suggests that the silicate apatite would not become amorphous above about 30°C. Because of such

Table 10.7 Melting temperatures of common compounds of volatile species

Element	Common compounds	Melting temperature (°C)	Element	Common compounds	Melting temperature (°C)
I	AgI,	558	Mo	MoO_3	795
	PbI_2	400	Tc	Tc_2O_7	119.5
Na	Na_2O	1132		TcO_2	1000
Cs	Cs_2O	490	Ru	RuO_2	1200*
Te	TeO_2	733		RuO_4	130**
	TeO_3	430			

* Sublime temperature.
** Boiling temperature.

Table 10.8 Process used to produce $Pb_{10}(VO_4)_6I_2$

Starting materials	Pressure, etc.	Heating process	Product	Ref.
PbI_2, $Pb_3(VO_4)_2$	25, 200, 350, 500 MPa	700°C	$Pb_{10}(VO_4)_6I_2$	[9]
PbO, PbI_2, V_2O_5	Vacuum-sealed ampoule	700°C, 5 h	$Pb_{10}(VO_4)_6I_2$	[10]
	9 MPa	350, 500°C, 5 h	Bulk $Pb_{10}(VO_4)_6I_2$	[10]
β-$Pb_3(VO_4)_2$, PbI_2	Excess β-$Pb_3(VO_4)_2$, 200 MPa (HIP)	700°C, 2 h	$Pb_5(VO_4)_5I$	[11]

a low critical temperature for amorphisation, apatite can be α-radiation resistant. For example, Metcalfe *et al.* [13] synthesised chlorapatite $Ca_5(PO_4)_3Cl$ and spodiosite $Ca_2(PO_4)Cl$ containing ^{241}Am and ^{239}Pu (or ^{238}Pu) to investigate a process for the immobilisation of ILW containing a significant quantity of chloride. Although the leach tests showed an increase in the release rates of P and Ca, any apparent changes in the XRD spectra of apatite samples (thus, no apparent change in crystal structures) was observed even after an α radiation fluence of 4×10^{18} g^{-1} from ^{238}Pu. Their phosphate-base apatite must have had a low critical temperature for amorphisation similar to the silicate apatite shown in Fig. 10.1 and most likely remained crystalline due to the high thermal recovery rates.

10.2.2 Zircon

As shown in Table 10.9, the basic formula of zircon is ABO_4. The A-site can accept tri-and/or tetravalent cations, and the B-site is usually occupied by

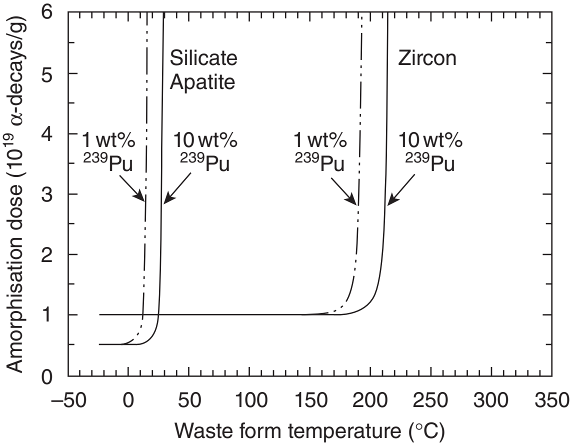

10.1 Critical amorphisation dose as a function of storage temperature (after Weber *et al.* [12]) for silicate apatite and zircon phases containing 1 and 10 wt% ^{239}Pu.

Table 10.9 Basic information for zircon

Basic formula*	ABO_4
Site occupation	A: (Zr, Ln, An, Hf), B: (Si)
Structure	Tetragonal I4/amd
Typical leaching rate	4×10^{-7} g/cm^2/day [6]
Radiation durability	0.2–0.6 dpa [14]

*Cations are expressed by A, B, C,..., whereas anions are X, Y, Z. O always denotes the oxygen ion.

Si. Similar to the apatite structure, the $(SiO_4)^{4-}$ unit in zircon can be replaced by $(PO_4)^{3-}$ depending on the size and valence of the cations on the A-site. When all of the $(SiO_4)^{4-}$ is replaced by $(PO_4)^{3-}$ due to introduction of tetravalent cations, this phase becomes monazite which usually has a monoclinic structure.

Important aspects of zircon as a host matrix for actinide elements have been reviewed by Ewing [14]. In his review, the capacity of zircon to incorporate actinide elements, which is one of the most important aspects as a host matrix, was discussed. The key points mentioned in the review include: (1) although U and Th replace the Zr in low concentrations in nature (typically up to 5000 ppm), zircon doped with a significant amount of actinide elements has been synthesised, e.g., 9.2 at% Pu (10 wt% Pu) [14 (and reference therein)]; and (2) $ASiO_4$ (A = Zr, Hf, Th, Pa, U, Np, Pu, Am) have been

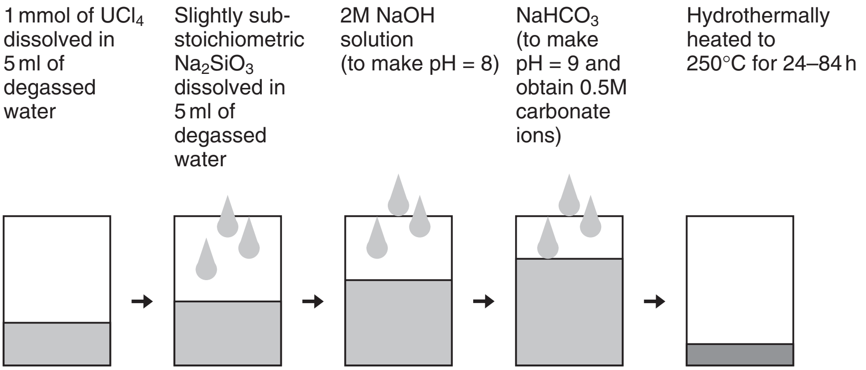

10.2 Example of the $USiO_4$ synthesis based on the process by Pointeau *et al.* [15].

synthesised [14 (and reference therein)]. A recent example of coffinite ($USiO_4$) synthesis using a hydrothermal process by Pointeau *et al.* [15] is depicted in Fig. 10.2. Forster [16] has reported natural thorite ($ThSiO_4$) containing up to 18.8 wt% Y_2O_3, 16.1 wt% of ZrO_2 and 23.3 wt% of UO_2 and zircon incorporating up to 41.8 wt% ThO_2.

Ewing [14] also mentioned that zircon undergoes a radiation-induced transformation from a periodic to an aperiodic state (metamict state) at doses over the range of 10^{18}–10^{19} α-decay events/g (=0.2–0.6 dpa) [14 (and reference therein)]. Metamictisation involves various types of atomic reorganisation, e.g., loss of well-defined medium-range order and a decrease in the average Zr-coordination number as well as tilting and distortion of the SiO_4 polyhedral. It is also suggested that the impurities lower the dose required for amorphisation and increase the temperature above which a material cannot be amorphised [14 (and reference therein)]. Such an effect of impurities can be seen in some of the recent examples with natural zircon. Geisler *et al.* [17] reported that epitaxial recrystallisation was not activated in natural zircon with a metamict state by dry annealing experiments at 600°C even though it could happen on zircon doped with 10 wt% Pu as shown in Fig. 10.1 [12] (See Section 10.2.1). Geisler *et al.* [18] have also shown, via X-ray diffraction measurements, that the only disordered crystalline fractions were recovered in the natural zircon upon hydrothermal treatment at 175°C, as shown in Fig. 10.3, whereas the amorphous phase recrystallised in the ^{238}Pu-doped synthetic zircon.

Our common interest is, then, how such radiation-induced changes effect the properties of zircon, especially the performance of zircon as a host matrix for nuclear wastes. Geisler *et al.* [19] observed the intensive fracturing inside the reaction rim of a partially metamicted natural zircon, during the hydrothermal process at 175°C with 2M $AlCl_3$ and 1M HCl–$CaCl_2$ solu-

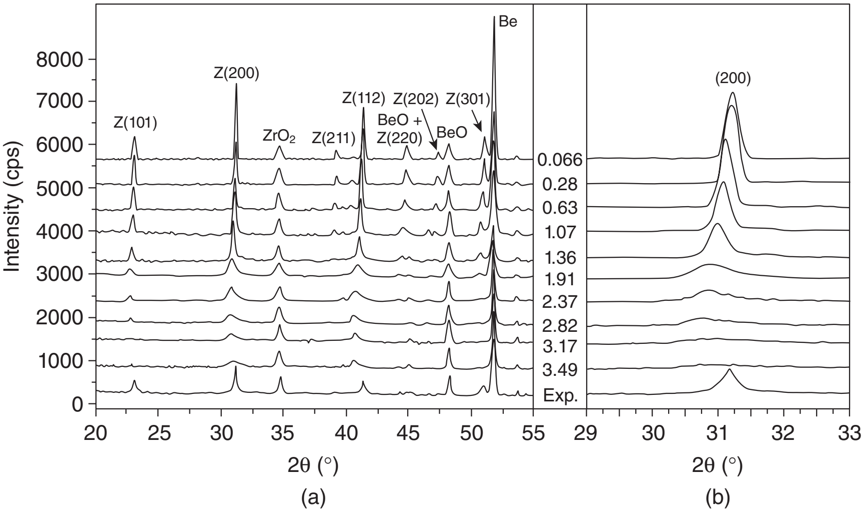

10.3 X-ray diffraction patterns, after Geisler *et al.* [18]. ^{238}Pu-doped zircon after the accumulation of different self-irradiation doses (given in 10^{18} α-decays/g) and after the hydrothermal treatment (labelled Exp.): (a) between 20° and 55° 2υ, and (b) between 29° and 30° 2θ.

tions. They explained that it was due to the volume reduction associated with the recovery of the disordered crystalline material. It is known that the density of zircon decreases in the metamict state and its volume expands by 18% [14 (and therein)]. Nasdala *et al.* [20] found highly porous regions typically in the centre of the natural zircon crystals as shown in Fig. 10.4, which are, in general, depleted in Zr, Si and U, and are notably enriched in Ca and Fe. They suggested that the accessibility of fluids to the micro-areas with higher levels of radiation damage drove such an ion exchange.

Some of the resent examples of leaching tests are shown in Table 10.10 [21, 22]. Although the leach rate of zircon increases with α-decay damage by one to two orders of magnitude, it is still considerably lower than that of glass [14 (and therein)].

10.2.3 Monazite

Table 10.11 shows the basic information for the monazite phase. The basic formula of monazite is APO_4, and the A-site can accept tri- and/or tetravalent cations with the B-site usually occupied by P. This mineral and crystal structure is strongly related to that of zircon, and is described as a distortion of the zircon structure [1]. Mullica *et al.* [23] studied seven types of $(Ln^aLn^b)PO_4$ compounds (Ln^a:Ln^b = 1:1) and reported that (Ce/Tb)PO_4, (Nd/Tb)PO_4 and (Sm/Tb)PO_4 formed monazite structures in monoclinic systems

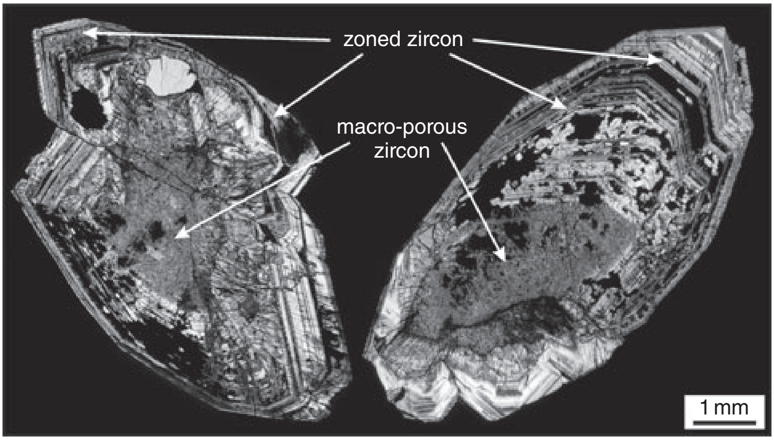

10.4 Photomicrograph (transmitted, cross-polarised light) of heterogeneous zircon crystals showing two distinctive regions formed by the secondary chemical alterations: zoned and macro-porous regions (courtesy of L. Nasdala). Further details can be found in Nasdala *et al.* [20].

Table 10.10 Examples of leaching tests on zircon-related materials

Material	Condition	Duration	Leaching rate (g/cm^2/day)	Ref.
Natural zircon	Deionised water, 96°C	1 month	Si: 1.2×10^{-6} Zr: 1.5×10^{-10}	[21]
Synthetic Zr-Pu(Am)-silicate gel (in a very similar state to the metamict zircon)	Deionised water, 90°C	3 days	Pu: 1.3×10^{-8} (0.0004 g/m^2) Am: 7×10^{-7} (0.021 g/m^2)	[22]
		14 days	Pu: 5.7×10^{-9} (0.0008 g/m^2) Am: 7.1×10^{-9} (0.001 g/m^2)	
		28 days	Pu: 4×10^{-9} (0.0013 g/m^2) Am: 7×10^{-9} (0.002 g/m^2)	

Source: references 21 and 22.

Table 10.11 Basic information for monazite

Basic formula*	ABO_4
Site occupation	A: (Ln, An, Ca), B: (P)
Structure	Monoclinic $P2_1/n$
Typical leaching rate	10^{-7} g/cm^2/day [6]
Radiation durability	>10 dpa [6]

*Cations are expressed byA, B, C,..., whereas anions are X, Y, Z. O always denotes the oxygen ion.

Table 10.12 Ionic radii of Ln^{3+} related to $(Ln^aLn^b)PO_4$ studied by Mullica *et al.* [23]

Ions	Ionic radii* (nm)	$(Ln^aLn^b)PO_4$	Ln^a–Ln^b average ionic radii* (nm)	Structure type
Ce^{3+}	0.1010	$(Ce/Tb)PO_4$	0.0967	Monazite
Nd	0.0983	$(Nd/Tb)PO_4$	0.0953	
Sm	0.0958	$(Sm/Tb)PO_4$	0.0941	
Tb	0.0923	$(Nd/Er)PO_4$	0.0937	Zircon
Er	0.0890	$(Sm/Er)PO_4$	0.0924	
Yb	0.0868	$(Sm/Yb)PO_4$	0.0913	
Lu	0.0861	$(Sm/Lu)PO_4$	0.0910	

*Values are for six-coordination shown only for comparison from [24].

whereas $(Nd/Er)PO_4$, $(Sm/Er)PO_4$, $(Sm/Yb)PO_4$ and $(Sm/Lu)PO_4$ formed zircon structures in tetragonal systems as shown in Table 10.12. To incorporate tetravalent cations, Montel *et al.* [25] replaced two of the A-site cations with a di- and tetravalent cation pair and synthesised $M^{2+}Th^{4+}(PO_4)_2$ (M^{2+} = Ca, Cd, Sr, Pb, Ba).

Monazite phases with various compositions have been synthesised via solid-state reactions as shown in Table 10.13 [26–30]. Although Bregiroux *et al.* [27] highlighted that the solid-state route is an efficient way in order to obtain very pure and very well-crystallised monazite powder, they also reported that the synthesis of the monazite phase containing several lanthanides was more difficult due to the different reaction temperature of lanthanides, leading to the formation of heterogeneous powders. The calcination/sintering atmosphere is also an important factor. Bregiroux *et al.* [28] obtained different products when processed in different atmospheres due to the redox condition of Pu as shown in Table 10.13. Aqueous processes

Table 10.13 Solid-state processes recently used to produce monazite phases

Starting materials	Process temperature	Products	Ref.
CeO_2, La_2O_3, ThO_2, $CaCO_3$, $NH_4H_2PO_4$	Above 1100°C	$Ca_{0.092}Th_{0.092}Ce_{0.089}La_{0.727}PO_4$	[26]
Ln_2O_3, $NH_4H_2PO_4$	1350°C	$LnPO_4$ (Ln = La, Ce, Pr, Nd, Sm, Eu, Gd)	[27]
PuO_2, $NH_4H_2PO_4$	1400°C in argon	$Pu^{3+}PO_4$	[28]
	1400°C in air	$Pu^{3+}PO_4$, $Pu^{4+}P_2O_7$	
PuO_2, CaO, $NH_4H_2PO_4$	1400°C in argon	$Pu^{3+}{}_{0.4}Pu^{4+}{}_{0.3}Ca_{0.3}PO_4$	[28]
	1400°C in air	$Pu^{4+}{}_{0.5}Ca^{2+}{}_{0.5}PO_4$	
$RECl_3$, $NH_4H_2PO_4$, LiCl–KCl eutectic	500°C in air	(RE)PO_4 (RE = La, Ce, Pr, Nd, Lu) and LiCl–KCl eutectic	[29]
CeO_2, ThO_2, $CaCO_3$, $La(PO_3)_3$, $LaPO_4$	1450°C for 4 h	$La_{0.91}Ce_{0.09}PO_4$ and $La_{0.73}Ce_{0.09}Th_{0.09}Ca_{0.09}PO_4$	[30]

Sources: references 26–30.

have also been applied to obtain homogeneous products as shown in Table 10.14 [25, 31].

Despite the similarity in their structures, monazite and zircon respond differently to ion irradiation and thermal- and irradiation-enhanced annealing [32]. Monazite cannot be amorphised by 800 keV Kr^{1+} ions at temperatures greater than 175°C whereas zircon can be amorphised at temperatures up to 740°C. This higher irradiation resistance of monazite compared with that of zircon can give an interesting insight into the study by Burakov *et al.* [31]. They compared the self-irradiation behaviour of monazite using ^{238}Pu-doped (La,Pu)PO_4 and $PuPO_4$. The (La,Pu)PO_4 monazite remained crystalline at ambient temperature up to a cumulative dose of 1.19×10^{25} α-decays/m^3. On the other hand, the $PuPO_4$ monazite became nearly completely amorphous at a lower dose of 4.2×10^{24} α-decays/m^3 as shown in Fig. 10.5. Although the difference between La^{3+} and Pu^{3+} is small (La^{3+}: 0.103 nm; Pu^{3+}: 0.100 nm [24]), the decrease in the average ionic radii of A-site cations could move the monazite structure towards the zircon structure as shown in Table 10.12, and could help the zircon-like behaviour of $PuPO_4$ monazite. The PuP_2O_7 in the system may also suggest the existence of Pu^{4+} (La^{4+}: 0.086 nm) in the $PuPO_4$ as an impurity, which should have a negative effect on the radiation resistance. Picot *et al.* [33] reported that both $LaPO_4$ and $La_{0.73}Ce_{0.27}PO_4$ exhibited a volume expansion of about

Table 10.14 Aqueous processes used to produce monazite phases

Starting materials	Processes	Products	Ref.
Nitrate (La, Pb, Sr, Cd, Th), carbonate (Ca) aqueous solutions	1. Gel formation by adding $(NH_4)_2HPO_4$ 2. Drying/calcination at 700–800°C 3. Heat treatment at 1200°C for 24 h	$M^{2+}Th(PO_4)_2$ (M^{2+} = Ca, Cd, Sr, Pb, Ba)	[25]
La and/or Pu from their nitrate aqueous solutions	1. Precipitation by adding ammonium hydro-phosphate 2. Drying in air at 100°C for 1 h 3. Calcination in air at 700°C for 1 h 4. Milling and cold pressing into pellets 5. Sintering in air at 1200–1250°C for 2 h	(La, Pu)PO_4 and $PuPO_4$	[31]

Sources: references 25 and 31.

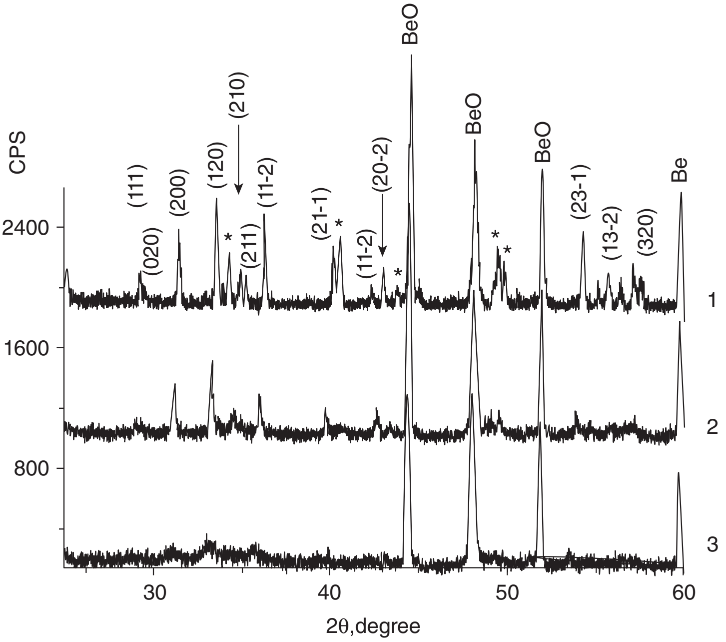

10.5 XRD patterns of $PuPO_4$, containing 7.2 wt% ^{238}Pu (content of all Pu isotopes 65.2 wt% el.), after Burakov *et al.* [31]. Cumulative dose ($\times 10^{23}$ α-decays/m^3) of (1) 1.3, (2) 17, (3) 42. Reflections from the minor phase, PuP_2O_7, are marked (*). BeO and Be are reflections from the Be-window that covered the ceramic sample.

Table 10.15 Basic information for garnet

Basic formula*	$A_3B_2(CO_4)_3$
Site occupation	A: (Ca, U, Gd, Y, Mg, Fe, Mn), B: (Al, U, Zr, Hf, Ti, Cr, Ca), C: (Si, Fe, Al)
Structure	Cubic Ia3d
Typical leaching rate (g/cm^2/day)	No recent data available
Radiation durability	0.2 dpa [6]

*Cations are expressed by A, B, C,…, whereas anions are X, Y, Z. O always denotes the oxygen ion.

8.1%, a drop in hardness by 59% and structure amorphisation by gold ions at a damage level of 6.7 dpa.

10.2.4 Garnet

Table 10.15 shows the basic information for the garnet phase. The basic formula of garnet is $A_3B_2(CO_4)_3$ with the A-site occupied by larger divalent cations and the B-site by smaller trivalent ones, although the valence is not too strict as long as the total charge on the cations matches that on the anions.

An interesting effect of cation size can be seen in a study by Yudintsev *et al.* [34], on the garnet of the $CaO–Fe_2O_3–Al_2O_3–SiO_2–ZrO_2–Gd_2O_3–UO_2$ system. They reported that introduction of Si into Ca–Zr–Fe garnet reduced the solubility of U from 16–18 wt% to 0.6–0.8 wt%. The size of the Si ion is much smaller than that of other cations that can usually occupy the C-site, and the introduction of Si into the system tends to restrict the solubility of the cation, especially that on the B-site. They also found that U enters both the A- and B-sites of the structure whereas Gd and Zr occupy only the A-site and the B-site, respectively. As shown in Table 10.16, the ionic radii of Gd^{3+} and Zr^{4+} are 0.094 nm and 0.072 nm for six fold-coordination (CN = 6) [24], respectively. The ionic radius of U^{4+} is 0.089 nm for CN = 6 [24].

A solid-state reaction is often used to synthesise garnet phases. Yudintsev *et al.* [34] mentioned above, have synthesised their garnet phases in air at 1400–1500°C. Utsunomiya *et al.* [35] synthesised garnet phases of $(Ca, Gd, Ce)_3(Zr, Fe)_2(FeO_4)_3$ and $(Ca, Gd, Th)_3(Zr, Fe)_2(FeO_4)_3$ systems by cold pressing at 200 MPa followed by sintering in air at 1600 K for 5 hours. Whittle *et al.* [36] synthesised $Ca_3Zr_2(Fe,Al,Si)O_{12}$ and $Ca_3Hf_2(Fe,Al,Si)O_{12}$ from stoichiometric mixtures of $CaCO_3$, SiO_2, Al_2O_3, Fe_2O_3, ZrO_2 and HfO_2 by calcination as pellets at 850°C for 24 hours, grinding and repelletisation, and sintering at 1400°C for 48 hours.

Table 10.16 Ionic radii of cations relevant to the system studied by Yudintsev *et al.* [34]

Cation	Ionic radii* (nm)		Cation	Ionic radii* (nm)	
	CN = 4	CN = 6		CN = 4	CN = 6
Ca^{2+}	–	0.100	Al^{3+}	0.039	0.054
Zr^{4+}	–	0.072	Si^{4+}	0.026	0.040
Gd^{3+}	–	0.094	Fe^{2+}	0.063	0.078
U^{4+}	–	0.089	Fe^{3+}	0.049	0.065

*Ionic radii data are from [24].

Irradiation effects on garnet have also been studied using 1.0 MeV Kr^{2+} irradiation [34, 35, 37]. Utsunomiya *et al.* [37] compared the radiation effects in four natural ferrate garnets containing Ca, Fe, Mg, Mn, Cr Al and Si with zircon and found that the average amorphisation dose of garnet (0.20 dpa) was lower than that of zircon (0.37 dpa) at room temperature. For synthetic garnet, $(Ca, Gd, Ce)_3(Zr, Fe)_2(FeO_4)_3$ and $(Ca, Gd, Th)_3(Zr, Fe)_2(FeO_4)_3$ systems have been reported to become amorphous at 0.17–0.19 dpa [35]. Uranium-containing garnet also has a similar dose for amorphisation of 0.18 dpa (1.63×10^{14} ions/cm^2) [34].

10.2.5 NZP

The name NZP originates from $NaZr_2(PO_4)_3$, a sodium zirconium phosphate. Because this phase does not occur naturally, it does not have a mineral name [1]. Table 10.17 shows the basic information for the NZP phase. The basic formula of NZP is $AB_2(CO_4)_3$ with the A-site occupied by larger monovalent cations and the B-site by smaller tetravalent ones. NZP has a characteristic three-dimensional hexagonal framework of PO_4 tetrahedra sharing corners with ZrO_6 octahedra, which forms a hole (A-sites) to accommodate the larger alkali or alkaline earth cations. In this three-dimensional framework, there are two other holes (A′-sites) which are not filled in conventional NZP. Therefore, NZP is sometimes expressed as $AA'_2B_2(CO_4)_3$ [38]. The A′-sites become filled only when additional cations are needed for charge compensation.

NZP can be synthesised through the usual ceramic techniques as well as less conventional techniques. Scheetz *et al.* [38] reviewed the NZP phase as a potential host material for nuclear waste immobilisation and mentioned the sol-gel (aqueous) method, the solid-state reaction method and the hydrothermal method as potential synthesis techniques. Table 10.18 shows

Table 10.17 Basic information for NZP

Basic formula*	$AB_2(CO_4)_3$
Site occupation	A: (Na, Sr, Cs, K, Ca), B: (Zr, Hf, Th), C: (P, Si, Al)
Structure	Hexagonal R3′c [3]
Typical leaching rate	10^{-5} g/cm^2/day
Radiation durability (dpa)	No recent data available

* Catinons are expressed by A, B, C,…, whereas anions are X, Y, Z.O always denotes the oxygen ion.

Table 10.18 Examples of different methods for NZP synthesis

Types of method	Processes	Products	Ref.
Aqueous method	1. R_2O_3 in a diluted nitric acid solution 2. Mixed with a $ZrOCl_2$ (92.136 g/l of Zr^{4+}) solution 3. H_3PO_4 solution (8.5%) added under constant stirring and heating 4. Precipitates dried and heated at 400°C (24 h), 600°C (24 h) and 800°C (24 h) in air with a grinding between each stage 5. Products pressed into pellets and repeatedly heated at 800°C (20 h)	$R_{1/3}Zr_2(PO_4)_3$ (R = La, Nd, Eu, Lu)	[39]
Solid-state method	1. $ZrO(NO_3)_2{\cdot}2H_2O$ and $NH_4H_2PO_4$ mixed with $NaNO_3$ and/or $Sr(NO_3)_2$ 2. Calcined up to 650°C 3. Pelletised and sintered at 950°C (48 h)	$NaZr_2(PO_4)_3$, $Sr_{0.5}Zr_2(PO_4)_3$, $Na_{0.93}Sr_{0.035}Zr_2(PO_4)_3$	[40]
Hydrothermal method	1. $HZr_2(PO_4)_3$ mixed with a $CsNO_3$ or $Sr(NO_3)_2$ aqueous solution 2. The mixture thermally treated in an autoclave at 200–300°C (6–200 h)	$(Cs,H)Zr_2(PO_4)_3$, $(Sr,H)Zr_2(PO_4)_3$	[41]

Sources: references 39–41.

examples of these three types of methods [39–41]. The aqueous method has an advantage in preparing homogeneous materials whereas the conventional solid-state method has an advantage in its simple procedure. The process temperature is also a key factor for the method of synthesis. As described in Section 10.2.1, special care is required to synthesise ceramic phases containing elements when their compounds are rather volatile.

Due to its capability of incorporating large cations, NZP has been studied as a candidate material for immobilisation of alkaline and alkaline earth elements, e.g., Na, Cs and Sr [40–42]. Table 10.19 shows examples of leaching tests performed on NZP phases [40–43]. Reasonably low reach rates for Na, Cs and Sr suggest a potential of NZP as a host matrix for Na, Cs and Sr. Table 10.19 also shows the leaching rate for other elements, which are widely spread from 10^{-6} to 10^{-11} g/cm^2/day. Incongruent behaviour of NZP in leaching has been reported [44, 45].

The most unique aspect of NZP is its flexibility in structure which can accommodate many different types of elements. Scheetz *et al.* [38] summarised the flexibility of NZP as 'it is the only structure so far studied which could accept (virtually) the entire set of cations in high level waste without further partitioning, in concentrations in the 1–10% range into a single crystalline radiophase.' Its great potential has been recently demonstrated

Table 10.19 Examples of leaching tests on NZP phases

Material	Media	Condition	Leaching rate (g/cm^2/day)	Ref.
$NaZr_2(PO_4)_3$ $Sr_{0.5}Zr_2(PO_4)_3$	Distilled water	95°C, 6 h	Na: 6×10^{-8} Sr: 5×10^{-7}	[40]
$Na_{0.93}Sr_{0.035}Zr_2(PO_4)_3$			Na: 6×10^{-7} Sr: 2×10^{-5}	[40]
$(Cs,H)Zr_2(PO_4)_3$ $(Sr,H)Zr_2(PO_4)_3$	1 M HCl solution	160°C, 24 h	Cs: $1–7 \times 10^{-7}$ Sr: $1–3 \times 10^{-7}$	[41]
$SrZr_4(PO_4)_6$	Deionised water	160°C, 24 h	Sr: $<10^{-10}$	[42]
	Sea water		Sr: 1.3×10^{-8}	
	1 mol/l/HCl		Sr: 2.0×10^{-7}	
	1 mol/l/NH_3		Sr: $<10^{-10}$	
$La_{1/3}Zr_2(PO_4)_3$	Deionised water	96°C, 1 month	La: 7.3×10^{-10} Zr: 1.9×10^{-10} P: 2.3×10^{-7}	[43]
		96°C, 2 months	La: 3.6×10^{-10} Zr: 4.7×10^{-11} P: 1.6×10^{-6}	[43]

Sources: references 40–43.

by Chourasia *et al.* [46]. They have incorporated up to 20 wt% of FBR waste simulants composed of 24 different oxides (shown in Table 10.20) into the NZP structure via a ceramic synthesis route at 1200°C.

10.2.6 Cubic zirconia

Zirconia can form in monoclinic, tetragonal and cubic structures (Fig. 10. 6) depending on the temperature. In nature, it occurs as baddeleyite with a monoclinic structure. Various aspects of baddeleyite as a potential host for nuclear wastes have been reviewed by Lumpkin [47], and significantly less geochemical alteration compared to other mineral phases and a possibility of high resistance towards α-decay damage have been reported.

Table 10.20 Chemical composition of NZP matrix and waste simulants used by Chourasia *et al.* [46]

	Oxide	(wt%)	Oxide	(wt%)	Oxide	(wt%)	Total (wt%)
NZP matrix	Na_2O	6.3106	ZrO_2	50.265	P_2O_5	43.424	100
Waste simulants	Ag_2O	15.626	MoO_3	13.986	SrO	1.2664	100
	BaO	4.0177	Ru_2O_3	0.87049	TeO_3	1.3347	
	CdO	0.34981	Pr_6O_{11}	6.7273	NiO	0.82225	
	Ce_2O_3	6.7248	Ru_2O	0.54434	Fe_2O_3	2.9797	
	Cs_2O	11.158	Sb_2O_5	0.15247	Cr_2O_3	0.52981	
	Nd_2O_3	13.666	SeO_2	0.16139	TiO_2	0.16598	
	Gd_2O_3	0.26618	Sm_2O_3	4.5972	MnO_2	0.15731	
	La_2O_3	4.3545	SnO_2	0.43700	ZrO_2	9.1046	

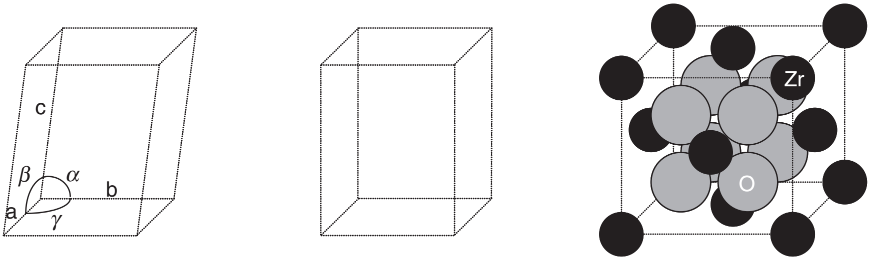

Monoclinic
$a = b \neq c$
$\alpha \neq 90°\ \beta, \gamma = 90°$

Tetragonal
$a = b \neq c$
$\alpha, \beta, \gamma = 90°$

Cubic
$a = b = c$
$\alpha, \beta, \gamma = 90°$

10.6 Crystal structures of pure ZrO_2 at different temperatures: the structure becomes more symmetric as temperature increases and the structure changes from monoclinic towards cubic.

The research on zirconia as a host matrix for actinide elements has been dominantly on the cubic phase rather than the monoclinic one. One of the reasons was that the solubility of actinide elements in the monoclinic phase is very low whereas that in the high temperature cubic phase with a fluorite structure is much larger as shown in Fig 10.7 [48]. It is possible to obtain this high-temperature cubic phase at lower temperatures by introducing other cations so-called stabiliser, typically di- or trivalent with a larger ionic radius. The cubic zirconia phase, therefore, as shown in Table 10.21, has the basic formula of AX_2 with the A-site occupied by di-, tri- and tetravalent cations and the X-site by oxygen ions or vacancies to keep the charge balance.

Table 10.22 shows some of the recent examples of cubic zirconia phases doped with actinide elements [49–53]. Gong *et al.* [49] used Gd as a stabi-

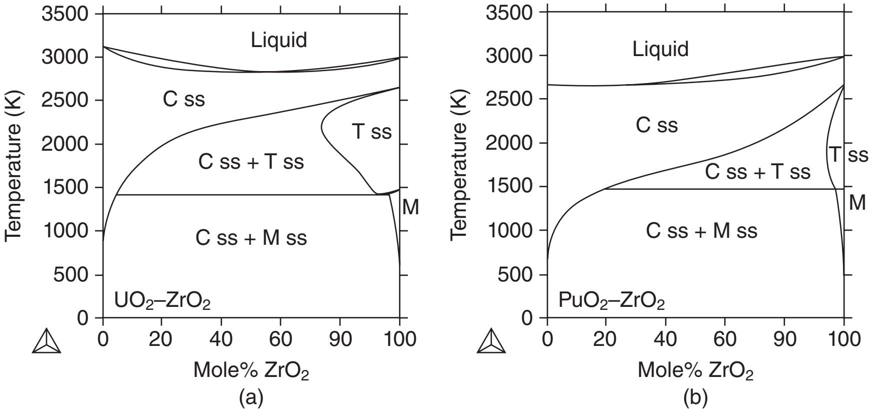

10.7 Phase diagrams for (a) UO_2–ZrO_2 and (b) PuO_2–ZrO_2 systems [48]: Css, Tss and Mss denote cubic, tetragonal and monoclinic solid solutions, respectively.

Table 10.21 Basic information for cubic zirconia

Basic formula*	AX_2
Site occupation	A: (Zr, An, Ln, REE, Ca), X: (O, O-vacancy)
Structure	Cubic Fm3m
Typical leaching rate	10^{-6} g/cm^2/day
Radiation durability	>10 dpa [6]

*Cations are expressed by A, B, C,…, whereas anions are X, Y, Z. O always denotes the oxygen ion.

Table 10.22 Examples of cubic zirconia phases containing actinide elements

	Stabiliser/ (Zr + stabiliser)	Actinide composition	Initial reaction and heating condition	Ref.
$Zr_{0.75}Gd_{0.15}Th_{0.10}O_{1.925}$	0.17	0.1	Sol-gel, 1500°C (3–36 h)	[49]
$Zr_{0.70}Gd_{0.15}U_{0.15}O_{1.925}$	0.18	0.15	Sol-gel, 1400°C (3–36 h)	
$(Zr_{0.86}Y_{0.14})_{1-x}Np_xO_{2-y}$	0.14	$x \leq 0.4$	Solid-state, 1773 K (80 h)	[50]
$(Zr_{0.77}Ca_{0.23})_{1-x}U_xO_{2-y}$	0.23	$x \leq 0.3$	Solid-state, 1400°C (–)	[51]
$(Zr_{0.85}Ca_{0.15})_{1-x}Pu_xO_{2-y}$	0.15	$x \leq 0.3$	Solid-state, 1400°C (1–3 h)	
$(Zr_{0.6}Y_{0.4})_{1-x}Am_xO_{1.88+0.2x}$	0.4	$x \leq 0.6$	Solid-state, 1775 K (20 h)	[52]
$(Zr_{0.75}Y_{0.25})_{1-x}Th_xO_{2-y}$	0.25	$x < 0.1$*	Solid-state, 1400°C (48 h)	[53]

* A single phase was not synthesised: phase separation (Zr-rich fluorite and Th-rich fluorite) occurred.
Sources: references 49–53.

liser to incorporate Th or U into a single cubic phase. Utilisation of Gd is particularly advantageous as it can serve also as a neutron absorber to immobilise fissile nuclides such as ^{239}Pu or ^{235}U. A large quantity of Np has also been incorporated into cubic zirconia [50]. Np^{4+} is stable in the stabilised zirconia matrix in both oxidising and reducing atmospheres [50, 54]. Walter *et al.* [54] has shown the possible oxidation of Np^{4+} in yttria-stabilised zirconia (YSZ) matrix to Np^{6+} only when the host lattice has enough oxygen vacancies probably to accommodate O^{2-} to be introduced into the lattice for charge balance. Cubic zirconia can incorporate Pu and Am in high concentrations as well [51, 52]. The incorporation of Th into YSZ, however, appears to be rather difficult. Grover *et al.* [53] showed that the YSZ–ThO_2 system separates into Zr-rich and Th-rich fluorite phases at 10 mol% of ThO_2. Perhaps the difference in the ionic radii between Th^{4+} and the cations in the host matrix (Zr, Y) was too large, as Gong *et al.* [49] successfully synthesised a single phase with exactly the same composition but using Gd^{3+} instead of Y^{3+} (Gd^{3+}: 0.105 nm; Y^{3+}: 0.102 nm; both CN = 8 [24]).

One of the most interesting features of cubic zirconia is its resistance towards radiation-induced amorphisation. Sickafus *et al.* [55] and Afanasyev-Charkin and Sickafus [56] observed no amorphisation in the cubic zirconia

Table 10.23 Examples of leaching rates of elements from cubic zirconia phases

	Irradiation (α-decays/m^3)	Leaching condition	Leaching rate (g/cm^2/day)	Ref.
$(Zr_{0.86}Y_{0.14})_{1-x}Np_xO_{2-y}$ ($x \leq 0.4$)	–	Deionised water at 150°C for 84 days	Np: $<10^{-9}$ Y: $<10^{-9}$ Zr: $<10^{-11}$	[59]
$Zr_{0.79}Gd_{0.14}Pu_{0.07}O_{1.99}$	11	Deionised water at 90°C for 28 days	Pu: 1.43×10^{-7}	[57]
	56		Pu: 1.25×10^{-6}	
	81		Pu: 1.32×10^{-6}	
	127		Pu: 8.57×10^{-7}	

Sources: references 57 and 59.

(stabilised by Y, Ca or Y/Er) single crystals upon 340 keV Xe^{2+} ion irradiation of 5×10^{18} ions/m^2 (2 dpa) [55] at 170–300 K and 1.5×10^{21} ions/m^2 [56], respectively. For polycrystalline materials, Burakov *et al.* [57] found that Gd-stabilised zirconia doped with ^{238}Pu (approximate composition of $Zr_{0.79}Gd_{0.14}Pu_{0.07}O_{1.99}$) retained its cubic structure even after high self-irradiation of 277×10^{23} α-decays/m^3. Although cubic zirconia is able to maintain the fluorite structure under irradiation, a microstructure evolution of a bulk material under irradiation has been reported. Large defect clusters were found by Yasuda *et al.* [58] in YSZ (13 mol% Y_2O_3, 87 mol% ZrO_2) under electron irradiation subsequent to ion irradiation (300 keV O^+, 100 keV He^+ and 4 keV Ar^+ ions).

Favourable chemical durability of cubic zirconia containing actinide elements has also been reported. Table 10.23 shows some of the examples [57, 59]. The leaching rate of Np and other cations from cubic zirconia was less than those from glass waste forms and other ceramic waste forms, e.g. Synroc [59]. The advantage of the resistance towards radiation-induced damage can be seen also in the chemical durability of the cubic zirconia. Burakov *et al.* [57] observed a low leaching rate of Pu from Gd-stabilised zirconia even after a high dose of self-irradiation. Mechanical integrity of YSZ doped with a high amount of NpO_2 has also been reported [60].

Cubic zirconia ceramics have been synthesised via both wet-chemical and solid-state processes as shown in Table 10.22. Examples of different factors affecting fabrication are also shown in Table 10.24. As well as the final sintering temperature, other conditions such as the preparation of powder and the calcination process have effects on the final products. Hellwig *et al.* [61] reported that the homogeneity in samples from the co-precipitation process was nearly perfect for the preparation of YSZ containing PuO_2,

Table 10.24 Various factors affecting fabrication of cubic zirconia ceramics

Materials	Factors studied	Outcomes	Ref.
PuO_2–Er_2O_3–YSZ	Solid-state preparation + sintering at 1723 K in CO_2	88.4% T.D. (theoretical density)	[61]
	Co-precipitation + sintering at 1973 K in N_2 with 8% H_2	87.6% T.D. (theoretical density)	[61]
8 mol% CeO_2–$(Zr_{0.84}Y_{0.16})O_{1.92}$	Co-precipitation + different calcination temperatures + sintering at 1600°C in air for 5 h	Calcination at 110–600$^{\circ\mathrm{C}}$ led to the highest densities. Fractionation of the powder in acetone was also found to be effective	[62]
$(Zr_{0.73}Y_{0.14}Er_{0.05}Ce_{0.08})O_2$ $(Zr_{0.73}La_{0.14}Er_{0.05}Ce_{0.08})O_2$ $(Zr_{0.73}Pr_{0.05}Er_{0.07}Ce_{0.15})O_2$	Densification temperature	Intensive densification took place at 1200–1700 K	[63]
10 mol% CeO_2–$(Zr_{0.854}Y_{0.46})O_{1.93}$	Wet-chemical process + sintering at 1450°C in air for 12–168 h	97.2–97.5% T.D. Homogeneity in Ce and pore distributions	[64]
	Wet-chemical process + sintering at 1600°C in air for 5–168 h	96.4–96.8% T.D. Homogeneity in Ce and pore distributions	[64]
	Wet-chemical process + HIP of 160 MPa argon pressure at 1400°C for 3 h	97.3% T.D. Heterogeneities in Ce and pore distributions. Reduction of Ce^{4+} to Ce^{3+}	[64]

Sources: references 61–64.

although the process was rather complicated and it was difficult to achieve high densities. Bukaemskiy *et al.* [62] found that the calcination at low temperatures from 110 to 600°C before sintering was most effective in obtaining high densities and good morphological structure for 8 mol% CeO_2–YSZ. Kamel *et al.* [63] showed that most of the densification for the different cubic zirconia ceramics occurs in the temperature range of 1127–1427°C. According to Menvie Bekale *et al.* [64], hot isostatic pressing (HIP) was not advantageous for 10 mol% CeO_2–YSZ as it led to heterogeneities in the Ce and pore distributions as shown in Fig. 10.8. They also found that HIP performed in argon caused the reduction of Ce^{4+} to Ce^{3+}, thus inducing volume modification, stresses and microcrack propagation.

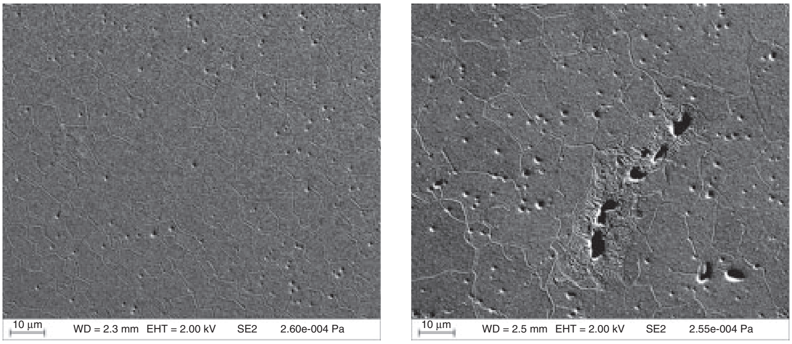

(a) (b)

10.8 SEM micrograph of 10Ce–8YSZ doped ceramics (courtesy of G. Sattonay): (a) after sintering at 1450°C for 12 h and (b) after HIP treatment under 160 MPa Ar pressure at 1400°C for 3 h. Further details can be found in Menvie Bekale *et al.* [64].

Table 10.25 Basic information for pyrochlore

Basic formula*	$A_2B_2O_6X$
Site occupation	A: (An, Ln, Zr, Ti, Na, Ca), B: (Ti, Al, Zr, An), X: (O, OH, F)
Structure	Cubic Fd3m [3]
Typical leaching rate	1.5×10^{-6} g/cm^2/day [6]
Radiation durability	0.3–0.4 dpa [6]

*Cations are expressed by A, B, C,..., whereas anions are X, Y, Z. O always denotes the oxygen ion.

10.2.7 Pyrochlore

Table 10.25 shows the basic information for the pyrochlore phase. The basic formula of pyrochlore is $A_2B_2O_6X$ with the A-site usually occupied by larger trivalent cations and the B-site by smaller tetravalent cations. The X-site is often occupied by another oxygen ion, which gives a more familiar formula of $A_2B_2O_7$. Similar to the cubic zirconia, pyrochlore is strongly related to the cubic fluorite structure. Oxygen vacancies are randomly distributed in the cubic zirconia, whereas the distribution of oxygen vacancies is ordered in pyrochlore as shown in Fig. 10.9.

The stability of the pyrochlore phase is often discussed with the ionic radius ratio of A-site and B-site cations (R_A/R_B ratio). Some of the examples are shown in Table 10.26. The ordered pyrochlore structure becomes less stable when the R_A/R_B ratio increases. With the A-site cation substitution,

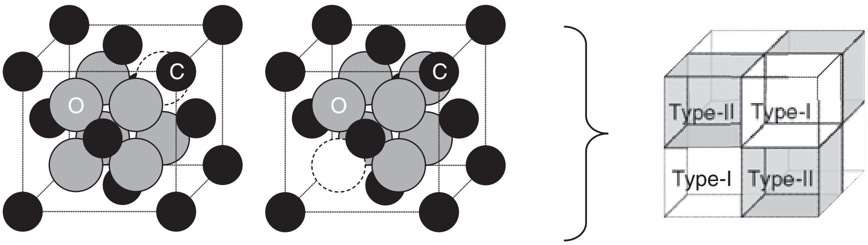

Type-I octant Type-II octant Pyrochlore unit cell

10.9 Basic crystal structure of pyrochlore: the unit cell is composed of two types of octants, both of which can be considered as an-oxygen-deficient fluorite structure.

Table 10.26 Examples of pyrochlore phases containing An and Ln

System	R_A/R_B ratio* (corresponding composition)	Synthesis procedure	Ref.
$(Pu_{1-x}La_x)_2Zr_2O_7$	$1.57^{**} \leq R_A/R_B \leq 1.58$ $(0 \leq x \leq 1)$	Solid-state: heating at 1400°C in a reducing atmosphere	[65]
$(Gd_{1-x}Nd_x)_2Ti_2O_7$	$1.74 \leq R_A/R_B \leq 1.78$ $(0 \leq x \leq 0.4)$	Solid-state: heating at 1200°C for 36 h + 1300°C for 36 h + 1400°C for 48 h	[66]
$(Nd_{1-x}La_x)_2Zr_2O_7$	$1.54 \leq R_A/R_B \leq 1.58$ $(0 \leq x \leq 1)$	Solid-state: Heating at 1500°C for 48 h	[67]
$Nd_2(Zr_{1-x}Ti_x)_2O_7$	$1.54 \leq R_A/R_B \leq 1.69$ $(0 \leq x \leq 0.56)$		
$(Gd_{1-x}Nd_x)_2Zr_2O_7$	$1.46 \leq R_A/R_B \leq 1.54$ $(0 \leq x \leq 1)$	Solid-state: heating at 1200°C for 36 h + 1300°C for 36 h + 1400°C for 48 h	[68]

* R_A/R_B ratio was calculated using data for A^{3+} (CN = 8) and B^{4+} (CN = 6) from [24].
** R_A for Pu^{3+} (CN = 8) was estimated from the data for Ce^{3+} [24].
Sources: references 65–68.

$R_A/R_B = 1.78$ is known to be the upper limit. On the other hand, with the B-site cation substitution, the upper limit appears to be $R_A/R_B = 1.69$, which suggests that B-site is more sensitive towards the stability of the pyrochlore structure. The ordered structure may not be stable when R_A/R_B ratio becomes small, either. Mandal *et al.* [68] reported possible disordering of cations at $R_A/R_B \leq 1.47$ in the $(Gd_{1-x}Nd_x)_2Zr_2O_7$ system.

Incorporation of di- or tetravalent cations in pyrochlore is more complex as it also involves the excess/vacancy of oxygen ions introduced for charge balance. The solubility of Sr^{2+} in $Gd_2Zr_2O_7$ is rather low (about 1.25 mol%) and increases only slightly (to 2.5 mol%) when substituted in combination with Ce^{4+} [69]. The issues related to the charge balance could be overcome, at least partially, as Nastren *et al.* [70] recently showed, using Th, U, Np, Pu and Am in a $(Nd_{1.8}An_{0.2})Zr_2O_{7+x}$ pyrochlore, that the valence of actinides in pyrochlore is controllable by the sintering atmosphere: Th^{4+}, U^{4+}, Np^{4+}, Pu^{3+} and Am^{3} obtained in Ar/H_2 at 1600°C, and Th^{4+}, $U^{5+,\,6+}$, Np^{5+}, Pu^{4+} and Am^{4+} by annealing in air at 800°C.

Since Wang *et al.* [71] reported $Gd_2Zr_2O_7$-based pyrochlore phases ($Gd_2Zr_2O_7$, $Gd_2Zr_{1.8}Mg_{0.2}O_{6.8}$, $Gd_{1.9}Sr_{0.1}Zr_{1.9}Mg_{0.1}O_{6.85}$ and $Gd_{1.9}Sr_{0.1}Zr_{1.8}Mg_{0.2}O_{6.75}$) which could not be amorphised by 1 MeV Kr^+ irradiation even at temperature as low as 25 K, the radiation-induced amorphisation of pyrochlore has been studied intensively. Lian *et al.* [72] showed a close relation between the critical amorphisation temperature, above which amorphisation occurs, and the R_A/R_B ratio using 1 MeV Kr^{2+} ion irradiation on U-, Th- and Ce-doped pyrochlores as shown in Fig. 10.10. The relationship between the radiation tolerance and the ionicity of the chemical bond in the crystal structure has also been reported by Lumpkin *et al.* [73].

Sickafus *et al.* [74] explained the radiation resistance of zirconate ceramics with $A_2B_2O_7$ stoichiometry from the energy for disordering. Their calculation suggests that the antisite energy, the energy required to exchange the position of A-site and B-site cations, becomes smaller as the A-site cation

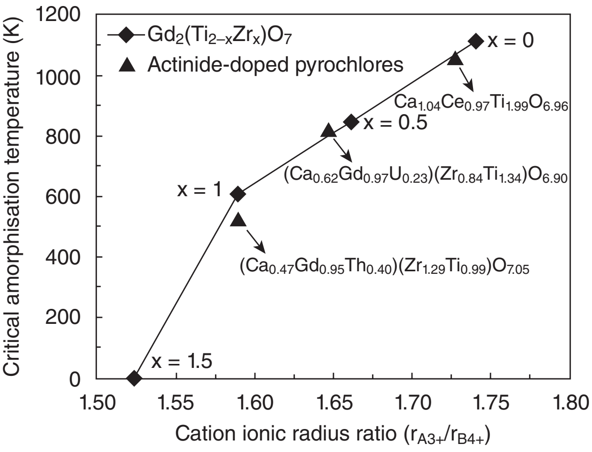

10.10 Critical amorphisation temperatures of pyrochlore phases as a function of the ionic radius ratio of A-site and B-site cations (R_A/R_B ratio), after Lian *et al.* [72].

Table 10.27 Leaching rate of actinides from pyrochlore phases after Vinokurov *et al.* [76]

Host material	Actinides	Leaching condition	Leaching rate ($g/cm^2/d$)
$Y_2Ti_2O_7$ pyrochlore with small amount of Mo produced by self-propagating high-temperature synthesis (SHS)	10 wt% $^{237}NpO_2$	MCC-1, in 90°C for 28 days	Np: 1.1×10^{-7}
	7 wt% $^{238}UO_2$ and 3 wt% $^{239}PuO_2$		U: 5.4×10^{-7} Pu: 4.1×10^{-7}
	9.7 wt% $^{238}UO_2$ and 0.3 wt% $^{241}Am_2O_3$		U: 8.1×10^{-7} Am: 7.0×10^{-8}
	10 wt% $^{239}PuO_2$ and 0.2 wt% $^{241}Am_2O_3$		Pu: 7.0×10^{-8} Am: 1.5×10^{-8}

becomes smaller and the B-site cation becomes larger, which means that the compounds with a smaller R_A/R_B ratio can accommodate the defects in the lattice more easily than those with a larger R_A/R_B ratio. Based on this, they have concluded that the fluorite structure should accept radiation-induced defects into the lattices more readily than the pyrochlore structure, and demonstrated the resistance of $Er_2Zr_2O_7$ with a fluorite structure to a high dose of Xe^{2+} irradiation. Interestingly, Belin *et al.* [75] found that the $^{241}Am_2Zr_2O_7$ pyrochlore phase evolved from the pyrochlore to a defect fluorite structure phase due to self-irradiation after about 200 days (1.24×10^{17} α-decay events/g) and remained unchanged afterwards, and concluded that the resulting fluorite structure was resistant to self-irradiation within the time limit of the experiment.

The chemical durability of the pyrochlore phase has also been studied. Vinokurov *et al.* [76] showed that the leaching rates of actinide elements from $Y_2Ti_2O_7$ pyrochlore containing 10 wt% of actinides were comparable with those from Synroc (10^{-8}–10^{-9} $g/cm^2/d$) and PNL76-68 glass (10^{-4}–10^{-5} $g/cm^2/d$) as shown in Table 10.27. Their materials were produced by self-propagating high-temperature synthesis (SHS), based on the locally induced exothermal chemical reaction resulting in a rapid self-propagating process in a narrow zone moving spontaneously with 0.1–15 cm/s at 1700–3000°C.

The effect of irradiation on the chemical durability of pyrochlore seems rather small. Begg *et al.* [77] observed a phase transformation of pyrochlore to fluorite as well as amorphisation after 0.18 dpa of 2 MeV Au^{2+}; the dissolution rate of Gd and Lu in pH 2 solution at 90°C increased from about 1×10^{-6} $g/cm^2/d$ to 1×10^{-5} $g/cm^2/d$ and that of Y remained at 1×10^{-5} $g/cm^2/d$ regardless of amorphisation, as shown in Table 10.28. Similarly, Strachan *et al.* [78] observed no significant change in the leaching rate of Pu and U from a pyrochlore phase containing ^{238}Pu even though the specimen became amorphous after about 2×10^{18} α-events/g of self-irradiation.

Table 10.28 Effect of irradiation on leaching

System	Type of irradiation	Effects on crystal structure	Effects on leaching (g/cm^2/d)	Ref.
$Y_2Ti_2O_7$	2 MeV Au^{2+} (5 ions/nm^2)	Transformation to fluorite and amorphisation after about 0.18 dpa	No change, 1×10^{-5} in pH 2 solution at 90°C	[77]
$Gd_2Ti_2O_7$, $Lu_2Ti_2O_7$			Increased from 1×10^{-6} to 1×10^{-5} in pH 2 solution at 90°C	[77]
$(Ca_{0.565}Gd_{0.11}Hf_{0.06}Pu_{0.12}U_{0.2})_2(Ti_{0.95}Hf_{0.05})_2O_7$ + 20 wt% $Ti_{0.9}Hf_{0.1}O_2$	Self-irradiation from ^{238}Pu	Amorphisation after about 2×10^{18} α/g	No change, Pu: 8.2×10^{-9}, U: 8.9×10^{-8} in pH 2 solution at 85°C	[78]

Sources: references 77, 78.

Table 10.29 Basic information for zirconolite

Basic formula*	ABC_2O_7
Site occupation	A: (Ca, An, REE), B: (Zr, An, REE), C: (Ti, Al, Fe, Mg)
Structure	Monoclinic C2/c
Typical leaching rate	4.5×10^{-6} g/cm^2/day [6]
Radiation durability	0.2–0.3 dpa [6]

*Cations are expressed by A, B, C,…, whereas anions are X, Y, Z. O always denotes the oxygen ion.

10.2.8 Zirconolite

Table 10.29 shows the basic information for the zirconolite phase. The basic formula of zirconolite is ABC_2O_7 with the A-site occupied by large, the B-site by medium and the C-site by small cations in general. Like pyrochlore, zirconolite can be described as an oxygen-deficient superstructure based on the fluorite structure, but it is less symmetrical and forms in a monoclinic system. Zirconolite is also described as a layered structure with hexagonal tungsten bronze (HTB)-type layers [79]. Three polytypes of zirconolite are often referred as zirconolite-2M, zirconolite-3T and zirconolite-4M depending on the number of HTB-type layers (two, three, or four) and basic structures (monoclinic or trigonal).

Zirconolite is known as the main host phase for actinides in Synroc which forms about 30–35 wt% of the host matrix in Synroc-B and -C, and is capable of accepting 27 wt% UO_2, 20 wt% ThO_2 and at least 29 wt% rare earth oxides [80, 81]. Fillet *et al.* [82] described the potential of the zirconolite phase as a host matrix for minor actinides as:

- capable of incorporating the respective radionuclides in the crystalline structure
- producible by conventional sintering in air
- chemically durable with very low initial and final dissolution rates.

Geochemical alteration and α-decay damage on the zirconolite phase have been reviewed by Lumpkin [83], and alteration in crystal structure including amorphisation has been mentioned. Smith *et al.* [79] showed, using 1.5 MeV Kr^+ on various types of zirconolite including U- and Th-doped ones, that the average critical doses at which the zirconolite phases became fully amorphous were in the range of $3.5–6.1 \times 10^{18}$ ions/m^2. Zirconolite phase can also be transformed to pyrochlore and further to fluorite structures depending on the irradiation condition. Wang *et al.* [84] observed that, concurrent with amorphisation, $CaZrTi_2O_7$ transformed into a partially cation-disordered pyrochlore structure and then a completely cation-disordered fluorite structure, followed by complete amorphisation upon in-situ 1.5 MeV Xe^+, 1 MeV Kr^+, and 0.6 MeV Ar^+ irradiation at 20 to 1073 K. Reid *et al.* [85] recently showed that such irradiation could reproduce the naturally occurring radiation damage on the zirconolite phase, i.e., the formation of a five-fold Ti coordination environment, which is often observed in metamict natural zirconolite, using $CaZrTi_2O_7$ with 2 MeV Kr^+ irradiation.

Although amorphisation may cause some alteration in the physical properties of zirconolite, including potential helium gas evolution from α-decay events [86], amorphisation itself seems to have little effect on the chemical durability of the zirconolite phase. Fillet *et al.* [82] reported that the high chemical durability is conserved, i.e., approximately 10^{-10} g/cm^2/d even after amorphisation by external irradiation with heavy ions or by self-irradiation in natural zirconolites 550 million years old. Strachan *et al.* [87] also reported that, although $CaHfTi_2O_7$ based zirconolite samples doped with 4–5 mol% $^{238}PuO_2$ experienced a significant swelling, the dissolution rate of the material was 1.7×10^{-7} g/cm^2/d in a pH 2 solution regardless of the amount of irradiation-induced damage.

10.2.9 Perovskite

Perovskite forms about 20–25 wt% of the host matrix in Synroc-B and -C primarily to host Sr and Ba [6, 80, 81]. Table 10.30 shows the basic information for the perovskite phase. The basic formula of perovskite is ABO_3 with the A-site often occupied by larger divalent cations and the B-site by smaller tetravalent cations, although this structure is flexible with the

Table 10.30 Basic information for perovskite

Basic formula*	ABO_3
Site occupation	A: (Ca, An, Ln, Na, Sr), B: (Ti, Al)
Structure	Cubic Im3 [6]
Typical leaching rate	2.5×10^{-8} g/cm^2/day [6]
Radiation durability	0.4–1 dpa [6]

*Cations are expressed by A, B, C,..., whereas anions are X, Y, Z. O always denotes the oxygen ion.

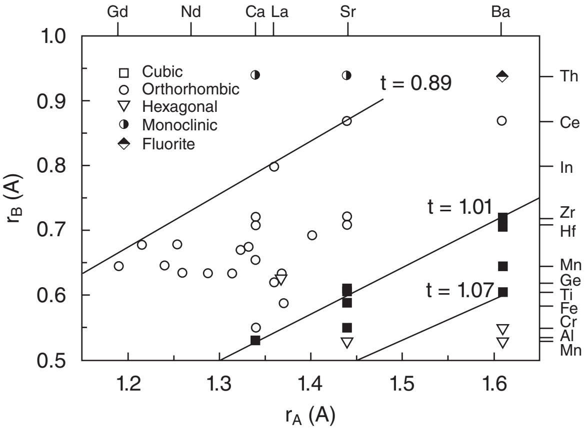

10.11 Relation of ionic radii and crystal structure for air-sintered ABO_3, after Ullmann *et al.* [88].

valence of cations. ABO_3 perovskite can form in different structures depending on the ionic radii of A-site and B-site cations as shown in Fig. 10.11 [88]. The stability of perovskite phases is often discussed using Goldschmidt's [89] tolerance factor (t), i.e.,

$$t = \frac{(R_A + R_O)}{\sqrt{2}(R_B + R_O)}$$

where R_A, R_B and R_O denote the ionic radii of the A-site cation (12-fold coordination), the B-site cation (six-fold coordination) and the oxygen ion, respectively.

Examples of perovskite phases containing actinide (An) and lanthanide (Ln) elements are shown in Table 10.31 [90–93]. To accommodate a trivalent An on the A-site, a trivalent cation is introduced on the B-site. Similarly, to incorporate a tetravalent An on the A-site, two trivalent cations should be

Table 10.31 Examples of perovskite phases containing An and Ln

Produced perovskite phase	Host perovskite	Substitution type	Synthesis	Ref.
$(Ca_{0.99}Cm_{0.01})(Ti_{0.99}Al_{0.01})O_3$	$CaTiO_3$	A: $Ca^{2+} \rightarrow Cm^{3+}$ B: $Ti^{4+} \rightarrow Al^{3+}$	Hot-pressed at 1250°C, 29 MPa for 2 h in N_2	[90]
$(Ca_{1-x}U_x)(Ti_{1-2x}A1_{2x})O_3$, $0 \leq x \leq 0.05$	$CaTiO_3$	A: $Ca^{2+} \rightarrow U^{4+}$ B: $2Ti^{4+} \rightarrow 2Al^{3+}$	Heated at 1600 K for 100 h in Ar	[91]
$(Ca_{1-x}Np_x)(Ti_{1-2x}Al_{2x})O_3$, $0 \leq x \leq 0.1$	$CaTiO_3$	A: $Ca^{2+} \rightarrow Np^{4+}$ B: $2Ti^{4+} \rightarrow 2Al^{3+}$	Heated at 1773 K for 6 h in Ar with 8% H_2 (repeating)	[92]
$(Na_{1/2+x}La_{1/2-3x}Th_{2x})TiO_3$, $0 \leq x \leq 1/6$	–	A: $(\frac{1}{2}Na^+, \frac{1}{2}La^{3+}) \rightarrow (\frac{2}{3}Na^+, \frac{1}{3}Th^{4+})$	Heated at 1000°C for 24 h in air + heated at 1200°C for 48 h in air	[93]

Sources: references 90–93.

introduced on the B-site. Hanajiri *et al.* [91] reported that the incorporation of U in $CaTiO_3$ was increased from 0–3 mol% to 5–7.5 mol% by introducing Al^{3+} into the B-site. It is also possible to maintain the charge balance by introducing monovalent cation on the A-site together with tri- or tetravalent cations.

Another potential method to maintain the charge balance in perovskite is to change the valence of certain cations. Sintering atmosphere could be used to control the oxidation state of An. Begg *et al.* [94] reported that Pu^{4+} in a perovskite phase produced in air was changed to Pu^{3+} by sintering at 1200°C in N_2 with 3.5% H_2 for 10 hours. They also reported the production of Np^{3+} using the same procedure.

Because perovskite is capable of accepting large cations on the A-site, the incorporation of alkaline and alkaline earth elements has also been investigated. Kulkarni *et al.* [95] synthesised perovskite phases of $Na_{0.5}Nd_{0.5}ZrO_3$, $Ca_{0.44}Na_{0.28}Nd_{0.28}ZrO_3$ and $Sr_{0.6}Na_{0.2}Nd_{0.2}ZrO_3$ by a so-called gel combustion method using glycerol, which is a highly exothermic reaction involving complexes of reactants. A large amount of gases evolved during the combustion reaction give a highly porous and reactive product. The release of Na from $Sr_{0.6}Na_{0.2}Nd_{0.2}ZrO_3$ perovskite was significantly higher than that from $Ca_{0.44}Na_{0.28}Nd_{0.28}ZrO_3$ perovskite in a 7-day leaching test in distilled water at 70°C.

Irradiation has significant effects on some of the physical properties of perovskite phases. Kuramoto *et al.* [90] found that the decrease in the

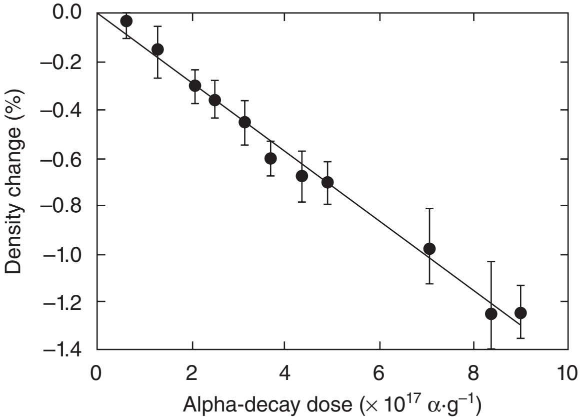

10.12 Density change in Cm-doped perovskite with α-decay dose, after Kuramoto *et al.* [90].

Table 10.32 Basic information for hollandite

Basic formula*	AB_8O_{16}
Site occupation	A: (Ba, Sr, Na, K, Rb, Cs, Pb), B: (Ti, Al, Fe, Cr, Sc)
Structure	Monoclinic I4/m [6]
Typical leaching rate	10^{-6} g/cm^2/day [6]
Radiation durability (dpa)	No recent data available

*Cations are expressed by A, B, C,…, whereas anions are X, Y, Z. O always denotes the oxygen ion.

density of $(Ca_{0.99}Cm_{0.01})(Ti_{0.99}Al_{0.01})O_3$ reached 1.3% after a self-irradiation dose of 9 × 10^{17} α-decays/g as shown in Fig. 10.12. They also reported that the leaching rates of perovskite specimens in an MCC-1 leach test in pH 2 solution at 90°C for 2 months were 1.7×10^{-4}, 2.3×10^{-4} and 3.0×10^{-4} g/cm^2/day with accumulated doses of 1.6×10^{17}, 4.0×10^{17} and 8.3×10^{17} α-decays/g, respectively.

10.2.10 Hollandite

Table 10.32 shows the basic information for the hollandite phase. The basic formula of hollandite is AB_8O_{16} with the A-site often occupied by larger mono- and/or divalent cations and the B-site by smaller tri- and/or tetravalent cations. The symmetry of the crystal structure can be either tetragonal or monoclinic depending on the composition. By differentiating the smaller cations, hollandite can also be described as $A^{2+}B^{3+}{}_2C^{4+}{}_6O_{16}$. The stability of hollandite phases can be estimated using the tolerance factor (t_H) defined by Kesson and White [96], i.e.,

$$t_H = \frac{\sqrt{(R_A + R_O)^2 - \frac{1}{2}(R_A + R_O)^2}}{\sqrt{\frac{3}{2}}(R_B + R_O)}$$

where R_A, R_B and R_O denote the ionic radii of the A-site cation (eight-fold coordination), B-site cation (six-fold coordination) and oxygen ion, respectively. Structures with t_H close to 1 should be more stable. Hollandite forms about 35–40 wt% of the host matrix in Synroc-B and -C, primarily to host Cs [6, 80, 81].

Although hollandite is able to host Cs, the synthesis of hollandite phase for practical applications needs extra care as the conventional synthetic method requires high reaction temperatures, which may cause volatilisation of Cs species. Consequently, different methodologies to produce hollandite phase have been investigated. Table 10.33 shows some examples. Leinekugel-le-Cocq *et al.* [97] compared an alkoxide route and a dry route to synthesise $(Ba_1Cs_{0.28})(Fe_{0.82}Al_{1.46}Ti_{5.72})O_{16}$ hollandite. They found that these two different synthesis routes gave the same final product, a tetragonal hollandite, after sintering at 1200°C, although the precursor obtained from calcination at 1000°C prior to the sintering was different: the precursor obtained from the alkoxide route had a monoclinic phase containing only Cs and a phase containing only Ba with a weak coherence length, in addition to a tetragonal phase containing Cs and Ba which was the only product obtained in the case of the oxide route. Aubin-Chevaldonnet *et al.* [98] synthesised $(Ba_{1.04}Cs_{0.24})(Fe_{2.32}Ti_{5.68})O_{16}$ via a solid-state reaction. Interestingly, only 63% and 46% of the designed Cs incorporation ($Cs_{0.24}$) were achieved when Fe^{3+} (0.0645 nm, CN = 6 [24]) was replaced by Ga^{3+} (0.0620 nm, CN = 6 [24]) and Cr^{3+} (0.0615 nm, CN = 6 [24]), respectively. Electrochemical synthesis using a mixture of Cs_2MoO_4 and TiO_2 in ambient atmosphere at 900°C has been suggested by Abe *et al.* [99]. With this technique, the crystals grow directly on the electrode as shown in Fig. 10.13, and a high Cs content of $Cs_{1.35}Ti_8O_{16}$ was achieved in the resultant single-crystalline, which is comparable with the highest Cs solubility in the polycrystalline of $Cs_{1.36 \pm 0.03}Ti_8O_{16}$ prepared by the conventional synthetic method.

Good chemical durability of the hollandite phase has been confirmed. Angeli *et al.* [100] studied the corrosion behaviour of $(Ba_1Cs_{0.28})(Fe_{0.82}Al_{1.46}Ti_{5.72})O_{16}$ in aqueous solution at 90°C for up to three years with pH varying from 1 to 10 and the ratio of sample surface area to solution volume varying from 0.1 cm^{-1} to 1200 cm^{-1}. They observed a low alteration rate of about 10^{-9} $g/cm^2/d$ at pH = 2–10 whereas a higher rate of 5 ×

Table 10.33 Examples of different synthetic techniques for hollandite phases containing Cs

Hollandite phase	Synthetic techniques applied	Ref.
$(Ba_1Cs_{0.28})(Fe_{0.82}Al_{1.46}Ti_{5.72})O_{16}$	*Alkoxide route:* • Alkoxide of Al and Ti, mixed in ethanol • Mixed solution poured into aqueous nitrate solution of Fe, Ba and Cs drop by drop • Stirring followed by evaporation of solvents and drying at 100°C • The dried product fired at 1000°C for 2 h • Milled, pressed into pellet under 120 MPa and sintered at 1200°C for 15 h. *Dry (solid-state oxide) route:* • TiO_2, $Al(NO_3)_3{\cdot}9H_2O$, $Fe(NO_3)_3{\cdot}9H_2O$, $CsNO_3$ and $BaCO_3$, mixed in an agate mortar • Calcined at 1000°C for 6 h (1°C/min) • Milled, pressed into pellet under 120 MPa and sintered at 1200°C for 15 h.	[97]
$(Ba_{1.04}Cs_{0.24})(Fe_{2.32}Ti_{5.68})O_{16}$	*Solid-state oxide route:* • TiO_2, Fe_2O_3, $CsNO_3$ and $BaCO_3$, mixed, ground in an agate mortar • Mixture pelletised and calcined at 810°C for 4 h in air • Ground again for 1 h with an attrition mill • Pelletised under 30 MPa and sintered at 1200°C for 30 h in air	[98]
$Cs_{1.35}Ti_8O_{16}$	*Electrochemical route:* • An electrolysis cell composed of an alumina boat with working, counter and reference electrodes of Pt was used • The cell filled with powdered Cs_2MoO_4 (4.0 g) and Anatase-type TiO_2 (0.1 g) • The cell introduced into a tubular furnace and electrolysis performed at 900°C for 1 h with Cs_2MoO_4 in molten state	[99]

Sources: references 97–99.

10^{-7} g/cm^2/d was observed at pH = 1. They also observed congruent release of Cs and Ba at pH = 1 and the congruency decreased as pH increased.

10.2.11 Synroc

Synroc is not one of the phases indicated in Table 3, but a combination of some of the phases in Table 10.3. It can be seen as a titanate-based

10.13 Optical microscope image of hollandite crystals grown at the tip of the working electrode observed by Abe *et al.* [99].

polyphase ceramic assemblage developed as 'synthetic rock' to incorporate different radionuclides in high level wastes (HLW) in one process [80, 81]. As shown in Table 10.34, Synroc is composed of four main phases, i.e., zirconolite ($CaZrTi_2O_7$), perovskite ($CaTiO_3$), hollandite ($BaA1_2Ti_6O_{16}$) and rutile (TiO_2) with a small amount of metallic phases. Most of the radionuclides in HLW including fission products and actinides are incorporated in these phases. Depending on the type of waste elements, the assemblage can be tailored, and other phases, e.g. nepheline $(Na, K)AlSiO_4$ and pyrochlore $(Ln)_2Ti_2O_7$, can also form in Synroc [6].

Because of the polyphase nature of the matrix, the distribution of the waste elements in each phase has been of interest. As shown in Table 10.35, Lumpkin *et al.* [101] studied the effects of additives to Synroc on the distribution of rare-earth elements (REE) and U in HLW simulants. In general, the distribution of waste elements was controlled mainly by the ionic radius, e.g., with smaller Y, Gd, and U ions having a preference for zirconolite and the larger Ce and Nd ions favouring perovskite. Lumpkin *et al.* reported that the element partitioning of REE was not strongly affected by the impurities, metal addition or waste loading they had tested. On the other hand, additions of up to ~3.6 wt% Na_2O led to an increase in the amount of perovskite phase and a decrease of zirconolite phase, which resulted in the shift of partitioning for REE and U from zirconolite to perovskite. For

Table 10.34 Typical main phases in Synroc

Phase	Formula	Composition	Waste elements to host
Zirconolite	$CaZrTi_2O_7$	30–35 wt%	An
Perovskite	$CaTiO_3$	20–25 wt%	Sr, Ba, An
Hollandite	$BaA1_2Ti_6O_{16}$	35–40 wt%	Cs, K, Rb, Ba
Rutile	TiO_2	~15 wt%	–

Sources: references 6, 80 and 81.

Table 10.35 Effect of waste loading and impurities in Synroc studied by Lumpkin *et al.* [101]

Matrix	Ti (wt%)	HLW simulant (wt%)	Impurity/ additives	Effects on phase assembly	Effects on waste distribution
Synroc	2	10	–	–	–
		10, 15, 19, 23	–	Decrease in rutile phase	No significant effect
		10	F, MgO, P_2O_5, Fe_2O_3	No significant effect	No significant effect
		10	Na_2O	Increase in perovskite, decrease in zirconolite	Y, U, Gd, Nd, Ce distribution in zirconolite decreased
		10	Al, Ni, Ti	No significant effect	No significant effect

10 wt% HLW with ~0.5 wt% Na_2O, the average relative partitioning coefficients ($D^{z/p}$), defined as

$$D^{z/p} = \frac{\text{wt\% metal oxide in zirconolite}}{\text{wt\% metal oxide in perovskite}}$$

were 0.14± 0.01 for Ce^{3+}, 0.39 ± 0.03 for Nd^{3+}, 1.7 ± 0.2 for Gd^{3+}, 3.8 ± 1.0 for Y^{3+} and 2.2 ± 0.8 for U^{4+} (Ce^{3+}: 0.114 nm; Nd^{3+}: 0.111 nm; Gd^{3+}: 0.105 nm; Y^{3+}: 0.102 nm; U^{4+}: 0.100 nm; all for CN = 8 [24]).

Synroc can be produced via both melting and sintering processes. The process temperature is about 1400–1550°C for the melting process whereas the sintering process requires about 1100–1300°C [6, 80, 81, 101]. Zhang *et al.* [102] recently incorporated U (4.51 wt%), Th (4.41 wt%) and Pu (13.00 wt%) in Synroc-like waste forms composed of 90% zirconolite and 10% hollandite using a sintering process. The designated proportions of oxides were mixed, calcined at 700°C for 2 hours in air, sealed in a vacuumed HIP can, and hot isostatically pressed (HIPed) at 1280°C for 3 hours under 100 MPa in an argon atmosphere. They reported that the normalised elemental release rates of U and Th were both $<10^{-7}$ g/cm^2/d in deionised water at 90°C for 28 days. The release rate of Pu was $<10^{-9}$ g/cm^2/d in the same condition. They also reported comparable release rates for both U/Gd and Pu/Hf pairs, which is favourable in decreasing the risk of criticality during interim storage and long-term geological disposal.

10.3 Ceramic waste forms for the future

10.3.1 Selection of ceramic matrices

It is clear, as demonstrated in the former sections, that we now have a variety of potential ceramic phases capable of hosting nuclear waste elements, which enables us to select good matrices for different types of nuclear wastes. The most important task to us is to make a wise selection of ceramic matrices for appropriate use.

Table 10.36 shows important aspects to be considered for the selection of ceramic matrices. The nature of wastes has an effect on the matrix and synthesis. If actinides and lanthanides are still mixed with other elements in HLW, e.g. FPs and corrosion products, it may be difficult to incorporate in a single phase. If the waste contains fissile elements, neutron absorbers such as Hf and Gd have to be incorporated as well. If it contains volatile species, the synthesis has to be under a certain temperature. The ceramic matrices have to be able to accept waste elements, thermodynamically and chemically stable, and possibly to synthesise with a simple procedure. Also, depending on the application of the ceramic forms, different aspects

Table 10.36 Aspects to be considered for the selection of ceramic matrices

Aspects	Key points
Properties of wastes	• Waste stream (pure, mixed) • Waste elements (An, REE) • Nuclear properties (fissile, high/low activity) • Chemical properties (volatile, water soluble)
Properties of ceramic matrices	• Capacity of waste elements (crystal structure) • Chemical durability (low leaching rate) • Radiation effects (amorphisation resistance) • Reliable synthetic process (large/small scale)
Application of products	• To irradiate in the reactor (stability under high temperature/pressure/irradiation, thermal conductivity) • To store and dispose as waste form (compatibility with repository, hydrothermal condition, redox condition)

have to be considered. Stabilities under high temperature, pressure and irradiation environments are important if the form is to be irradiated in the reactor as a component of nuclear fuel. Thermal properties such as heat capacity and thermal conductivity are also important in such a case. If the ceramic form is produced with the aim of nuclear waste disposal, the compatibility with the repository environment, under certain hydrothermal and redox conditions, is naturally one of the most important aspects.

10.3.2 Polyphase matrices and phase equilibrium

As the waste stream becomes more complex while the treatment of nuclear wastes is required to be simple, it may become necessary to incorporate the waste elements in combinations of different host phases. Synroc is one such example. This is an effective way to identify ceramic phases suitable for certain waste elements, as the waste elements find the host matrices that are thermodynamically most stable to be incorporated in.

In such a polyphase system, phase equilibrium becomes a much more important aspect in understanding the nature of the system and resultant products. As mentioned in Section 10.2.11, for example, the same waste elements can be distributed to different phases, and small quantity of additive can also change the assemblage of the host phases and the distribution of waste elements [101].

This would introduce another dimension to the design of ceramic waste forms, especially to identify the appropriate matrix composition and amount of waste loading. Figure 10.14(a), (b) and (c) shows the three possible relations of Gibbs energy curves for a simple two-phase equilibrium: the main host phase and a potential secondary host phase. In the case of (a), where

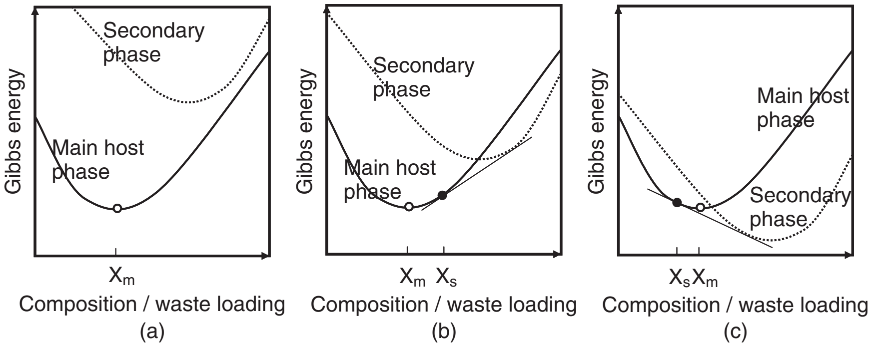

10.14 Schematic diagrams for the different relations of Gibbs energy curves between host phase (solid line) and secondary phase (dotted line). The common tangent for the two curves determines the solubility of the waste element in the main host phase.

the Gibbs energy of the potential secondary phase is much higher than that of the main host phase, the secondary phase would not form. Thus, the waste element could be incorporated freely in the main host phase, and the most stable composition is identified as X_m which provides the lowest Gibbs energy of the main host phase. In the case of (b), the waste element can be incorporated up to composition X_s which is determined by the common tangent of the Gibbs energy curves of both phases, and it would start forming a solid solution with the secondary phase above this composition. The most stable composition for the main host phase, X_m, is still available in this case. On the other hand, the in case of (c), the solubility limit of the waste element X_s in the main host phase becomes very low, and X_m, the most stable composition for the main host phase, is no longer achievable. These simple examples demonstrate two important aspects of polyphase assemblage: (1) the solubility limit of the waste elements in a phase is determined by the stability of other phases, and therefore the relations among the stability of phases become very important, and (2) waste loading itself may change the balance of the phase assemblage in the polyphase matrix.

10.3.3 Alternative synthesis techniques

Production of ceramic phases usually involves the initial mixing of raw materials in either dry or wet processes, followed by calcination and compaction and usually completing with the final sintering process at high temperatures, which can be time-consuming and also energy-consuming. There are a number of alternative processes that have been investigated to produce ceramic waste forms. For example, hot isostatic pressing (HIP) is a good way to reduce the sintering temperature and time.

The melting process is one of such alternatives. The advantage of the melting process is that the equilibrium of the system can be reached much faster than in the conventional solid-state sintering process. One of the challenges of such a process is the reduction of the melting temperature, as most of the potential host ceramic matrices for nuclear wastes have a high melting temperature as shown in Table 10.37. It is possible to reduce the melting temperature by introducing different constituents into the system [103], and usually the product is a polyphase ceramic material similar to Synroc. The melting process can be, therefore, a good process when aiming host matrix is a polyphase system.

The thermochemical process can offer a choice of self-sustaining processes. There are many variations on the thermochemical process, e.g., self-sustaining immobilisation (SSI) [6], self-propagating high-temperature synthesis [104] and self-propagating high-temperature synthesis (SHS) [76]. The basic principle of these processes is to use the strong exothermic reaction of the raw materials to heat the system and sustain this heating process.

Table 10.37 Melting temperatures of potential host ceramic phases

Phase	Melting temperature (°C)	Phase	Melting temperature (°C)
Zirconia, ZrO_2	2650 [3]	Perovskite, $CaTiO_3$	1975 [3]
Alumina, Al_2O_3	2100 [3]	Zirconolite, $CaZr_2TiO_7$	1530 [6]
Titania, TiO_2	1850 [3]	Hollandite, $BaAl_2Ti_6O_{16}$	1600 [3]
Apatite, $Ca_{10}(PO_4)_6X_2$	1700 [3]	Synroc-B and -C	1400–1550 [6]

Sources: references 3 and 6.

Table 10.38 Examples of thermochemical processes studied by Glagovskii *et al.* [104]

Raw materials	Products
$(Y_2O_3, Gd_2O_3, UO_2, ZrO_2) + MoO_3 + Zr$	Fluorite-like oxide, Mo inclusion
$(Y_2O_3, ZrO_2) + MoO_3 + Zr$	Fluorite-like oxide, Mo inclusion
$(Y_2O_3, TiO_2) + MoO_3 + Ti$	Pyrochlore, Mo inclusion

Vinokurov *et al.* [76], for example, used the following reaction to incorporate U, Np, Pu and Am in a phrochlore-type phase:

$$(2-x)Ti + xTiO_2 + Y_2O_3 + \frac{2(2-x)}{3}MoO_3 \rightarrow Y_2Ti_2O_7 + \frac{2(2-x)}{3}Mo$$

Different types of host phase can be produced via a thermochemical process as shown in Table 10.38 [104], and the process can be in the molten state as well depending on the system [105]. Although the product ceramic forms are often rather porous, the leaching rates of actinide elements are comparable with that from glass and Synroc [76].

10.4 Sources of further information and advice

M. I. Ojovan and W. E. Lee, *An Introduction to Nuclear Waste Immobilisation* (Elsevier Ltd, 2005), is a good resource for an overall introduction to nuclear waste management. Much of the basic information for the potential phases are from this book. The most dedicated information for Synroc can be obtained from W. Lutze and R. C. Ewing, *Radioactive Waste Forms for the Future* (North Holland Physics Publishing, 1998). I. W. Donald, *Waste Immobilisation in Glass and Ceramic Based Hosts* (Wiley Blackwell, 2010) contains the most recent information on ceramic matrices.

10.5 Acknowledgement

The author would like to thank Mr Ken-ichi Kuramoto, who worked together with him on Np-containing YSZ waste from the Japan Atomic Energy Research Institute (currently Japan Atomic Energy Agency). Without his guidance at that time, the author would not have established his current knowledge of ceramic waste matrices, and it would not have been possible to produce this chapter.

10.6 References

[1] R. C. Ewing, 'Ceramic matrices for plutonium disposition', *Progress in Nuclear Energy* 49 (2007) pp. 635–643.

[2] G. R. Lumpkin, 'Alpha-decay damage and aqueous durability of actinide host phases in natural systems', *J. Nucl. Mater.* 289 (2001) pp. 136–166.

[3] P. Trocellier, 'Immobilisation of radionuclides in single-phase crystalline waste forms: a review on their intrinsic properties and long term behaviour', *Ann. Chim. Sci. Mat.* 25 (2000) pp. 321–337.

[4] R. C. Ewing, 'Nuclear waste forms for actinides', *Proc. Natl Acad. Sci. USA* 96 (1999) pp. 3432–3439.

[5] I. W. Donald, B. L. Metcalfe, R. N. J. Taylor, 'Review: The immobilization of high level radioactive wastes using ceramics and glasses', *J. Mater. Sci.* 32 (1997) pp. 5851–5887.

[6] M. I. Ojovan and W. E. Lee, *An Introduction to Nuclear Waste Immobilisation*, Oxford, Elsevier (2005).

[7] K. Boughzala, E. Ben Salem, A. Ben Chrifa, E. Gaudin, K. Bouzouita, 'Synthesis and characterization of strontium–lanthanum apatites', *Mater. Res. Bull.* 42 (2007) pp. 1221–1229.

[8] O. Terra, F. Audubert, N. Dacheux, C. Guy, R. Podor, 'Synthesis and characterization of uranium-bearing britholites', *J. Nucl. Mater.* 366 (2007) pp. 70–86.

[9] F. Audubert, J. Carpena, J. L. Lacout, F. Tetard, 'Elaboration of an iodine-bearing apatite, iodine diffusion into a $Pb_3(VO_4)_2$ matrix', *Solid State Ionics* 95 (1997) pp. 113–119.

[10] M. Uno, M. Shinohara, K. Kurosaki, S. Yamanaka, 'Some properties of lead vanado-iodoapatite $Pb_{10}(VO_4)_6I_2$', *J. Nucl. Mater.* 294 (2001) pp. 119–122.

[11] M. Zhang, E. R. Maddrell, P. K. Abraitis, E. K. H. Salje, 'Impact of leach on lead vanado-iodoapatite [$Pb_5(VO_4)_3I$]: An infrared and Raman spectroscopic study', *Mater. Sci. Eng.* B 137 (2007) pp. 149–155.

[12] W. J. Weber, R. C. Ewing, A. Meldrum, 'The kinetics of alpha-decay-induced amorphization in zircon and apatite containing weapons-grade plutonium or other actinides', *J. Nucl. Mater.* 250 (1997) pp. 147–155.

[13] B. L. Metcalfe, I. W. Donald, S. K. Fong, L. A. Gerrard, D. M. Strachan, R. D. Scheele, 'Ageing of a phosphate ceramic used to immobilize chloride contaminated actinide waste', *J. Nucl. Mater.* 385 (2009) pp. 485–488.

[14] R. C. Ewing, 'Nuclear waste forms for actinides', *Proc. Natl Acad. Sci. USA* 96 (1999) pp. 3432–3439.

[15] V. Pointeau, A. P. Deditius, F. Miserque, D. Renock, U. Becker, J. Zhang, N. Clavier, N. Dacheux, C. Poinssot, R. C. Ewing, 'Synthesis and characterization of coffinite', *J. Nucl. Mater.* 393 (2009) pp. 449–458.

[16] H.-J. Forster, 'Composition and origin of intermediate solid solutions in the system thorite–xenotime–zircon–coffinite', *Lithos* 88 (2006) pp. 35–55.

[17] T. Geisler, K. Trachenko, S. Rios, M. T. Dove, E. K. H. Salje, 'Impact of self-irradiation damage on the aqueous durability of zircon ($ZrSiO_4$): Implications for its suitability as a nuclear waste form', *J. Phys. Cond. Matter* 15 (2003) pp. L597–L605.

[18] T. Geisler, B. Burakov, M. Yagovkina, V. Garbuzov, M. Zamoryanskaya, V. Zirlin, L. Nikolaeva, 'Structural recovery of self-irradiated natural and ^{238}Pu-doped zircon in an acidic solution at 175°C', *J. Nucl. Mater.* 336 (2005) pp. 22–30.

[19] T. Geisler, R. T. Pidgeon, W. van Bronswijk, R. Kurtz, 'Transport of uranium, thorium, and lead in metamict zircon under low-temperature hydrothermal conditions', *Chemical Geology* 191 (2002) pp. 141–154.

[20] L. Nasdala, J. M. Hanchar, D. Rhede, A. K. Kennedy, T. Váczi, 'Retention of uranium in complexly altered zircon: an example from Bancroft, Ontario', *Chemical Geology* 269 (2010) pp. 290–300.

[21] P. Trocellier and R. Delmas, 'Chemical durability of zircon', *Nucl. Instr. Meth. Phys. Res. B* 181 (2001) pp. 408–412.

[22] B. E. Burakov, A. Ph. Smetannikov, E. B. Anderson, A. Yu. Alexeev, 'Investigation of natural and artificial Zr-silicate gels', *Mat. Res. Soc. Symp. Proc.* 932 (2006) pp. 1017–1024.

[23] D. F. Mullica, E. L. Sappenfield, L. A. Boatner, 'Monazite- and zircon-type structures of seven mixed (Ln/Ln) PO_4 compounds', *Inorganica Chimica Acta* 244 (1996) pp. 247–252.

[24] R. D. Shannon, 'Revised effective ionic radii and systematic studies of interatomic distances in halides and chaleogenides', *Acta Cryst.* A32 (1976) pp. 751–767.

[25] J.-M. Montel, J.-L. Devidal, D. Avignan, 'X-ray diffraction study of brabantite–monazite solid solutions', *Chemical Geology* 191 (2002) pp. 89–104.

[26] J.-M. Montel, B. Glorieux, A.-M. Seydoux-Guillaume, R. Wirth, 'Synthesis and sintering of a monazite–brabantite solid solution ceramic for nuclear waste storage', *J. Phys. Chem. Sol.* 67 (2006) pp. 2489–2500.

[27] D. Bregiroux, F. Audubert, T. Charpentier, D. Sakellariou, D. Bernache-Assollant, 'Solid-state synthesis of monazite-type compounds $LnPO_4$ (Ln = La to Gd)', *Solid State Sciences* 9 (2007) pp. 432–439.

[28] D. Bregiroux, R. Belin, P. Valenza, F. Audubert, D. Bernache-Assollant, 'Plutonium and americium monazite materials: Solid state synthesis and X-ray diffraction study', *J. Nucl. Mater.* 366 (2007) pp. 52–57.

[29] D. Hudry, I. Bardez, A. Rakhmatullin, C. Bessada, F. Bart, S. Jobic, P Deniard, 'Synthesis of rare earth phosphates in molten LiCl–KCl eutectic: Application to preliminary treatment of chlorinated waste streams containing fission products', *J. Nucl. Mater.* 381 (2008) pp. 284–289.

[30] B. Glorieux, J. M. Montel, M. Matecki, 'Synthesis and sintering of a monazite–brabantite solid solution ceramics using metaphosphate', *J. Euro. Ceram. Soc.* 29 (2009) pp. 1679–1686.

[31] B. E. Burakov, M. A. Yagovkina, V. M. Garbuzov, A. A. Kitsay, V. A. Zirlin, 'Self-irradiation of monazite ceramics: Contrasting behavior of $PuPO_4$

and (La,Pu)PO_4 doped with Pu-238', *Mater. Res. Soc. Symp. Proc.* 824 (2005) pp. 219–224.

[32] A. Meldrum, L. A. Boatner, W. J. Weber, R. C. Ewing, 'Radiation damage in zircon and monazite', *Geochim. Cosmochim. Acta,* 62[14] (1998) pp. 2509–2520.

[33] V. Picot, X. Deschanels, S. Peuget, B. Glorieux, A. M. Seydoux-Guillaume, R. Wirth, 'Ion beam radiation effects in monazite', *J. Nucl. Mater.* 381 (2008) pp. 290–296.

[34] S. V. Yudintsev, M. I. Lapina, A. G. Ptashkin, T. S. Ioudintseva, S. Utsunomiya, L. M. Wang, R. C. Ewing, 'Accommodation of uranium into the garnet structure', *Mater. Res. Soc. Symp. Proc.* 713 (2002) p. 477.

[35] S. Utsunomiya, S. Yudintsev, R. C. Ewing, 'Radiation effects in ferrate garnet', *J. Nucl. Mater.* 336 (2005) pp. 251–260.

[36] K. R. Whittle, G. R. Lumpkin, F. J. Berry, G. Oates, K. L. Smith, S. Yudintsev, N. J. Zaluzece, 'The structure and ordering of zirconium and hafnium containing garnets studied by electron channelling, neutron diffraction and Mossbauer spectroscopy', *J. Solid State Chem.* 180 (2007) pp. 785–791.

[37] S. Utsunomiya, L. M. Wang, R. C. Ewing, 'Ion irradiation effects in natural garnets: Comparison with zircon', *Nucl. Instr. Meth. Phys. Res. B* 191 (2002) pp. 600–605.

[38] B. E. Scheetz, D. K. Agrawal, E. Breval, R. Roy, 'Sodium zirconium phosphate (NZP) as a host structure for nuclear waste immobilisation: a review', *Waste Management* 14[6] (1994) pp. 489–505.

[39] D. M. Bykov, R. J. M. Konings, A. I. Orlova, 'High-temperature investigations of the rare earth NZP phosphates $R_{1/3}Zr_2(PO_4)_3$ (R = La, Nd, Eu, Lu) by drop calorimetry', *J. Alloy. Comp.* 439 (2007) pp. 376–379.

[40] M. Ishida, K. Kikuchi, T. Yanagi, R. Terai, 'Leaching behaviour of crystalline phosphate waste forms', *Nucl. Chem. Waste Management* 16 (1986) pp. 127–131.

[41] C. Hashimoto, S. Nakayama, 'Immobilization of Cs and Sr to $HZr_2(PO_4)_3$ using an autoclave', *J. Nucl Mater.* 396 (2010) pp. 197–201.

[42] S. Nakayama, K. Itoh, 'Immobilization of strontium by crystalline zirconium phosphate', *J. Euro. Ceram. Soc.* 23 (2003) pp. 1047–1052.

[43] L. Bois, M. J. Guittet, F. Carrot, P. Trocellier, M. Gautier-Soyer, 'Preliminary results on the leaching process of phosphate ceramics, potential hosts for actinide immobilisation', *J. Nucl. Mater.* 297 (2001) pp. 129–137.

[44] M. Sugantha, N. R. S. Kumar, U. V. Varadaraju, 'Synthesis and leachability studies of NZP and eulytine phases', *Waste Management* 18 (1998) pp. 275–279.

[45] G. Buvaneswari and U. V. Varadaraju, 'Low leachability phosphate lattices for fixation of select metal ions', *Mater. Res. Bull.* 35 (2000) pp. 1313–1323.

[46] R. Chourasia, O. P. Shrivastava, R. D. Ambashta, P. K. Wattal, 'Crystal chemistry of immobilization of fast breeder reactor (FBR) simulated waste in sodium zirconium phosphate (NZP) ceramic matrix', *Annals of Nuclear Energy* 37 (2010) pp. 103–112.

[47] G. R. Lumpkin, 'Physical and chemical characteristics of baddeleyite (monoclinic zirconia) in natural environments: an overview and case study', *J. Nucl. Mater.* 274 (1999) pp. 206–217.

[48] H. Kinoshita, M. Uno, S. Yamanaka, 'Stability evaluation of fluorite structure phases in ZrO_2–MO_2 (M = Th, U, Pu, Ce) systems by thermodynamic modelling', *J. Alloy. Comp.* 370 (2004) pp. 25–30.

[49] W. L. Gong, W. Lutze, R. C. Ewing, 'Zirconia ceramics for excess weapons plutonium waste', *J. Nucl. Mater.* 277 (2000) pp. 239–249.

[50] H. Kinoshita, K. Kuramoto, M. Uno, T. Yanagi, S. Yamanaka, H. Mitamura, T. Banba, 'Phase stability of yttria-stabilized zirconia with dissolved cerium and neptunium oxides under oxidizing and reducing atmospheres', *J. Am. Ceram. Soc.* 83[2] (2000) pp. 391–396.

[51] N. K. Kulkarni, S. Sampath, V. Venugopal, 'Studies on stabilised zirconia as host phase for the fixation of actinides, rare-earths and sodium', *Ceramics International* 27 (2001) pp. 839–846.

[52] P. E. Raison and R. G. Haire, 'Zirconia-based materials for transmutation of americium and curium: Cubic stabilized zirconia and zirconium oxide pyrochlores', *Prog. Nucl. Energy* 38[3–4] (2001) pp. 251–254.

[53] V. Grover, P. Sengupta, A.K. Tyagi, 'Sub-solidus phase relations in CeO_2–YSZ and ThO_2–YSZ systems: XRD, high temperature-XRD and EPMA studies', *Mater. Sci. Eng. B* 138 (2007) pp. 246–250.

[54] M. Walter, J. Somers, D. Bouexiere, P. Gaczynski, B. Brendebach, 'Oxidation behaviour of uranium and neptunium in stabilised zirconia', *J. Solid State Chem.* 182 (2009) pp. 3305–3311.

[55] K. E. Sickafus, Hj. Matzke, Th. Hartmann, K. Yasuda, J.A. Valdez, P. Chodak III, M. Nastasi, R. A. Verrall, 'Radiation damage effects in zirconia', *J. Nucl. Mater.* 274 (1999) pp. 66–77.

[56] I. V. Afanasyev-Charkin and K. E. Sickafus, 'Effect of sputtering in Xe ion irradiated yttria-stabilized zirconia', *J. Nucl. Mater.* 306 (2002) pp. 112–120.

[57] B. E. Burakov, M. A. Yagovkina, M. V. Zamoryanskaya, A. A. Kitsay, V. M. Garbuzov, E. B. Anderson, A. S. Pankov, 'Behavior of ^{238}Pu-doped cubic zirconia under self-irradiation', *Mat. Res. Soc. Symp. Proc.* 804 (2004) pp. 213–217.

[58] K. Yasuda, C. Kinoshita, S. Matsumura, A. I. Ryazanov, 'Radiation-induced defect clusters in fully stabilized zirconia irradiated with ions and/or electrons', *J. Nucl. Mater.* 319 (2003) pp. 74–80.

[59] H. Kinoshita, K. Kuramoto, M. Uno, S. Yamanaka, H. Mitamura, T. Banba, 'Durability of yttria-stabilized zirconia for highly concentrated TRU wastes', *Mat. Res. Soc. Symp. Proc.* 608 (2000) 393–398.

[60] H. Kinoshita, K. Kuramoto, M. Uno, S. Yamanaka, H. Mitamura, T. Banba, 'Mechanical integrity of yttria-stabilised zirconia doped with Np oxide', *Mat. Res. Soc. Symp. Proc.* 932 (2006) pp. 647–654.

[61] Ch. Hellwig, M. Pouchon, R. Restani, F. Ingold, G. Bart, 'Fabrication and microstructure characterization of inert matrix fuel based on yttria stabilized zirconia', *J. Nucl. Mater.* 340 (2005) pp. 163–170.

[62] A. A. Bukaemskiy, D. Barrier, G. Modolo, 'Physical properties of 8 mol% ceria doped yttria stabilised zirconia powder and ceramic and their behaviour during annealing and sintering', *J. Euro. Ceram. Soc.* 26 (2006) pp. 1507–1515.

[63] N. Kamel, H. Ait-Amar, M. Taouinet, C. Benazzouz, Z. Kamel, H. Fodil-Cherif, S. Telmoune, R. Slimani, A. Zahri, D. Sahel, 'Comparative study of simulated

zirconia inert matrix fuel stabilized with yttrium, lanthanum or praseodymium: synthesis and leaching tests', *Prog. Nucl. Energy* 48 (2006) pp. 70–84.

[64] V. Menvie Bekale, C. Legros, C. Haut, G. Sattonnay, A. M. Huntz, 'Processing and microstructure characterization of ceria-doped yttria-stabilized zirconia powder and ceramics', *Solid State Ionics* 177 (2006) pp. 3339–3347.

[65] N. K. Kulkarni, S. Sampath, V. Venugopal, 'Preparation and characterisation of Pu-pyrochlore: $[La_{1-x}Pu_x]_2Zr_2O_7$ (x = 0–1)', *J. Nucl. Mater.* 281 (2000) pp. 248–250.

[66] B. P. Mandal and A. K. Tyagi, 'Phase relations and high temperature-XRD studies of $Gd_{2-x}Nd_xTi_2O_7$ solid solutions', *Mater. Sci. Eng. B* 136 (2007) 46–49.

[67] E. J. Harvey, K. R. Whittle, G. R. Lumpkin, R. I. Smith, S. A.T. Redfern, 'Solid solubilities of $(La, Nd)_2(Zr,Ti)_2O_7$ phases deduced by neutron diffraction', *J. Solid State Chem.* 178 (2005) pp. 800–810.

[68] B. P. Mandal, A. Banerji, V. Sathe, S. K. Deb, A. K. Tyagi, 'Order–disorder transition in $Nd_{2-y}Gd_yZr_2O_7$ pyrochlore solid solution: An X-ray diffraction and Raman spectroscopic study', *J. Solid State Chem.* 180 (2007) pp. 2643–2648.

[69] S. J. Patwe and A. K. Tyagi, 'Solubility of Ce^{4+} and Sr^{2+} in the pyrochlore lattice of $Gd_2Zr_2O_7$ for simulation of Pu and alkaline earth metal', *Ceramics International* 32 (2006) pp. 545–548.

[70] C. Nastren, R. Jardin, J. Somers, M. Walter, B. Brendebach, 'Actinide incorporation in a zirconia based pyrochlore $(Nd_{1.8}An_{0.2})Zr_2O_{7+x}$ (An = Th, U, Np, Pu, Am)', *J. Solid State Chem.* 182 (2009) pp. 1–7.

[71] S. X. Wang, B. D. Begg, L. M. Wang, R. C. Ewing, W. J. Weber, K. V. Govidan Kutty, 'Radiation stability of gadolinium zirconate: a waste form for plutonium disposition', *J. Mater. Res.* 14 (1999) 4470–4473.

[72] J. Lian, S. V. Yudintsev, S. V. Stefanovsky, L. M. Wang, R. C. Ewing, 'Ion beam irradiation of U-, Th- and Ce-doped pyrochlores', *J. Alloy. Comp.* 444–445 (2007) pp. 429–433.

[73] G. R. Lumpkin, M. Pruneda, S. Rios, K. L. Smith, K. Trachenko, K. R. Whittlea, N. J. Zaluzec, 'Nature of the chemical bond and prediction of radiation tolerance in pyrochlore and defect fluorite compounds', *J. Solid State Chem.* 180 (2007) pp. 1512–1518.

[74] K. E. Sickafus, L. Minervini, R. W. Grimes, J. A. Valdez, M. Ishimaru, F. Li, K. J. McClellan, T. Hartmann, 'Radiation tolerance of complex oxides', *Science* 289 (2000) pp. 748–751.

[75] R. C. Belin, P. J. Valenza, P. E. Raison, 'Structure of the americium pyrochlore $Am_2Zr_2O_7$ and its evolution under alpha self-irradiation', *Recent Advances in Actinide Science, Proc. Actinides* 2005, RSC Publishing (2006) pp. 352–354.

[76] S. E. Vinokurov, Yu. M. Kulyako, S. A. Perevalov, B. F. Myasoedov, 'Immobilization of actinides in pyrochlore-type matrices produced by self-propagating high-temperature synthesis', *C. R. Chimie* 10 (2007) 1128–1130.

[77] B. D. Begg, N. J. Hess, W. J. Weber, R. Devanathan, J. P. Icenhower, S. Thevuthasan, B. P. McGrail, 'Heavy-ion irradiation effects on structures and acid dissolution of pyrochlores', *J. Nucl. Mater.* 288 (2001) pp. 208–216.

[78] D. M. Strachan, R. D. Scheele, E. C. Buck, J. P. Icenhower, A. E. Kozelisky, R. L. Sell, R. J. Elovich, W. C. Buchmiller, 'Radiation damage effects in candidate titanates for Pu disposition: Pyrochlore', *J. Nucl. Mater.* 345 (2005) pp. 109–135.

[79] K. L. Smith, N. J. Zaluzec, G. R. Lumpkin, 'In situ studies of ion irradiated zirconolite, pyrochlore and perovskite', *J. Nucl. Mater.* 250 (1997) pp. 36–52.

[80] S. E. Kessol, W. J. Sinclair, A. E. Ringwood, 'Solid solution limits in synroc zirconolite', *Nucl. Chem. Waste Manag.* 4 (1983) pp. 259–265.

[81] A. E. Ringwood, S. E. Kesson, K. D. Reeve, D. M. Levins, E. J. Ramm, 'Synroc', in: *Radioactive Waste Forms for the Future*, ed. W. Lutze and R. C. Ewing, Amsterdam, North Holland Physics Publishing (1988) pp. 233–334.

[82] C. Fillet, T. Advocat, F. Bart, G. Leturcq, H. Rabiller, 'Titanate-based ceramics for separated long-lived radionuclides', *C. R. Chimie* 7 (2004) pp. 1165–1172.

[83] G. R. Lumpkin, 'Alpha-decay damage and aqueous durability of actinide host phases in natural systems', *J. Nucl. Mater.* 289 (2001) pp. 136–166.

[84] S. X. Wang, L. M. Wang, R. C. Ewing, G. S. Was, G. R. Lumpkin, 'Ion irradiation-induced phase transformation of pyrochlore and zirconolite', *Nucl. Instrum. Meth. Phys. Res. B* 148 (1999) pp. 704–709.

[85] D. P. Reid, M. C. Stennett, B. Ravel, J. C. Woicik, N. Peng, E. R. Maddrell, N. C. Hyatt, 'The structure of ion beam amorphised zirconolite studied by grazing angle X-ray absorption spectroscopy', *Nucl. Instr. Meth. Phys. Res. B* 268 (2010) 1847–1852.

[86] T. Wiss, X. Deschanels, J.-P. Hiernaut, D. Roudil, S. Peuget, V. V. Rondinella, 'Helium release from plutonium and curium-doped zirconolite', *J. Nucl. Mater.* 362 (2007) 431–437.

[87] D. M. Strachan, R. D. Scheele, E. C. Buck, A. E. Kozelisky, R. L. Sell, R. J. Elovich, W. C. Buchmiller, 'Radiation damage effects in candidate titanates for Pu disposition: Zirconolite', *J. Nucl. Mater.* 372 (2008) pp. 16–31.

[88] H. Ullmann and N. Trofimenko, 'Estimation of effective ionic radii in highly defective perovskite-type oxides from experimental data', *J. Alloy. Comp.* 316 (2001) pp. 153–158.

[89] V. M. Goldschmidt, *Fortschr. Min.* 15 (1931) p. 73.

[90] K. Kuramoto, H. Mitamura, T. Banba, S. Muraoka, 'Development of ceramic waste forms for actinide-rich waste', *Prog. Nucl. Energy* 32[3–4] (1998) pp. 509–516.

[91] Y. Hanajiri, H. Yokoi, T. Matsui, Y. Arita, T. Nagasaki, H. Shigematsu, 'Phase equilibria of $CaTiO_3$ doped with Ce, Nd and U', *J. Nucl. Mater*. 247 (1997) pp. 285–288.

[92] T. Sato, T. Yamashita, T. Matsui, 'Phase equilibria and thermal expansion of $CaTiO_3$ doped with neptunium', *J. Nucl. Mater.* 344 (2005) pp. 67–72.

[93] R. H. Mitchell and A. R. Chakhmouradian, 'Structural study of the perovskite series Na1/2-x La1/2-3x Th2x TiO3', *J. Solid State Chem.* 138 (1998) pp. 307–312.

[94] B. D. Begg, E. R. Vance, S. D. Conradson, 'The incorporation of plutonium and neptunium in zirconolite and perovskite', *J. Alloy. Comp.* 271–273 (1998) pp. 221–226.

[95] N. K. Kulkarni, S. K. Sali, K. D. Singh Mudher, V. Venugopal, 'Preparation and characterization of sodium bearing perovskite phases', *Mater. Res. Bull.* 43 (2008) pp. 222–229.

[96] S. E. Kesson and T. J. White, 'Radius ratio tolerance factors and the stability of hollandites', *J. Solid State Chem.* 63 (1986) pp. 122–125.

[97] A. Y. Leinekugel-le-Cocq, P. Deniard, S. Jobic, R. Cerny, F. Bart, H. Emerich, 'Synthesis and characterization of hollandite-type material intended for the

specific containment of radioactive cesium,' *J. Solid State Chem.* 179 (2006) pp. 3196–3208.

[98] V. Aubin-Chevaldonnet, D. Caurant, A. Dannoux, D. Gourier, T. Charpentier, L. Mazerolles, T. Advocat, 'Preparation and characterization of (Ba,Cs)(M,Ti)8O16(M = Al^{3+}, Fe^{3+}, Ga^{3+}, Cr^{3+}, Sc^{3+}, Mg^{2+}) hollandite ceramics developed for radioactive cesium immobilization,' *J. Nucl. Mater.* 366 (2007) pp. 137–160.

[99] H. Abe, A. Satoh, K. Nishida, E. Abe, T. Naka, M. Imai, H. Kitazawa, 'Electrochemical immobilization of Cs in single-crystalline SYNROC,' *J. Solid State Chem.* 179 (2006) pp. 1521–1524.

[100] F. Angeli, P. McGlinn, P. Frugier, 'Chemical durability of hollandite ceramic for conditioning caesium,' *J. Nucl. Mater.* 380 (2008) pp. 59–69.

[101] G. R. Lumpkin, K. L. Smith, M. G. Blackford, 'Partitioning of uranium and rare earth elements in Synroc: effect of impurities, metal additive, and waste loading,' *J. Nucl. Mater.* 224 (1995) pp. 31–42.

[102] Y. Zhang, M. W. A. Stewart, H. Li, M. L. Carter, E. R. Vance, S. Moricca, 'Zirconolite-rich titanate ceramics for immobilisation of actinides – Waste form/HIP can interactions and chemical durability,' *J. Nucl. Mater.* 395 (2009) pp. 69–74.

[103] H. Kinoshita, M. Uno, S. Yamanaka, W. E. Lee, 'Molten ceramic solidification during molten state processing of HLW,' *Mat. Res. Soc. Symp. Proc.* 932 (2006) pp. 655–659.

[104] E. M. Glagovskii, S. V. Yudintsev, A. V. Kuprin, L. P. Pelevin, E. E. Konovalov, V. I. Velichkin, B. F. Myasoedov, 'Crystalline host phases for actinides, obtained by self-propagating high-temperature synthesis,' *Radiochemistry* 43[6] (2001) pp. 632–638.

[105] Yu. M. Kulyako, S. A. Perevalov, S. E. Vinokurov, B. F. Myasoedov, G. A. Petrov, M. I. Ozhovan, S. A. Dmitriev, I. A. Sobolev, 'Properties of host matrices with incorporated U and Pu oxides, prepared by melting of a zircon-containing heterogeneous mixture (by virtue of exo effect of burning metallic fuel),' *Radiochemistry* 43[6] (2001) pp. 626–631.

11

Development of waste packages for the disposal of radioactive waste: French experience

G. OUZOUNIAN AND R. POISSON, National Agency for the Management of Radioactive Wastes (Andra), France

Abstract: This chapter deals with the packages used in France to dispose of radioactive waste. The chapter first presents packages that are produced and used for the disposing of low-level and intermediate-level short-lived waste in existing repositories. It then presents packages that are under development for the disposal of all other types of radioactive waste (including high-level and long-lived waste), and for which the repositories are in the design phase.

Key words: disposal, repository, disposal waste package.

11.1 Introduction

11.1.1 Classification of waste

The management of radioactive waste in France is organized according to the classification scheme given in Table 11.1 taking into account both level of activity and the radioactive lifetimes of the radionuclides contained by the waste (PNGMDR, 2006).

Repositories exist for low-level short-lived waste and intermediate-level short-lived waste. For all other categories of waste, the repositories are currently being developed (as stated in Table 11.1). Applying this logic, disposal waste packages are therefore in two categories:

- Being produced and used for the disposal of low-level short-lived waste and intermediate-level short-lived waste
- Being designed for all other types of waste.

This chapter follows the same logic (Sections 11.2 and 11.3) before dealing with future trends and further reading (Sections 11.4 and 11.5).

11.1.2 Radioactive waste packaging

Waste packaging is achieved through the use of a disposal package. A typical disposal package comprises the external container, and its internal

Table 11.1 Waste classification matrix

	Short lived	Long lived
Low-level waste	This waste is disposed of in the existing repository (Centre de l'Aube)	The repository for this waste is being designed
Intermediate-level waste	This waste is disposed of in the existing repository (Centre de l'Aube)	The repository for this waste is being designed
High-level waste	The repository for this waste is being designed. The proposed solution is a deep underground geological repository	The repository for this waste is being designed. The proposed solution is a deep underground geological repository

elements (see glossary of terms used in Section 11.6). Internal elements can include:

- Internal casing (for example, the concrete liner of a metallic package)
- The waste in either homogeneous (for example, spent resins in a cement-based confining matrix) or heterogeneous form (for example, separate pieces of contaminated equipment or also metallic drums)
- Grouting used to immobilize and/or confine the contents of the waste package.

Note that waste packages are used to confine radioactive waste over long periods of time, and Andra sets limits concerning their radiological content, both overall and also for each radionuclide. This subject is not covered in this chapter; however, the details of these limits for the Aube facility are given in the official document stating the rules of operations for this facility.

11.2 Existing waste packages used for the disposal of short-lived low- and intermediate-level waste

This type of waste is disposed of in the Centre de l'Aube facility (Andra, 2007). This facility has been operational since 1992, and the majority of waste packages that are disposed of on this site have been in production for a significant time. However, new waste packages are being developed to handle new types of waste and the process of qualifying new waste packages for this type of waste is ongoing.

The disposal packages that are disposed of in the Centre de l'Aube are generally manufactured by the producer (in this case the primary package and the disposal package are the same), transported to the repository and, after acceptance control, transferred to the repository disposal vaults. The disposal package is considered as either durable, if the container is made of concrete, or non-durable, if the container is metallic. The vaults are different in one case or the other since a better confinement capacity is required in the second case to compensate the lesser confinement level of the metallic container.

11.2.1 Metallic-type waste packages

There is a further distinction between:

- Metallic waste packages in which the waste is inside an internal casing that has a confinement capacity
- Metallic waste packages in which the waste is embedded in a confining matrix.

Requirements for a disposal package with an internal casing with a confinement capacity

In this case the confinement of the disposal package relies on the confinement capacity of the internal envelope. The target material for this envelope is concrete, although another material satisfying the requirements could be used provided it proved suitable. The confinement capacity of this envelope is specified through a requirement on the diffusion coefficient to tritiated water of the material used. Added requirements for this internal casing are as follows:

- Its thickness
- The physical characteristics of the material used (shrinkage, permeability to gas)
- The mechanical characteristics of the material used (compressive and traction strengths)
- Its homogeneity (size of cracks, density)
- Its resistance to irradiation
- Its resistance to thermal cycling.

Other requirements concern the contents (the waste plus matrix block) of the internal casing:

- In the case of homogeneous waste, the waste bloc must have low water content, and a minimal compression strength (permeability to gas and porosity must also be measured and the results supplied to Andra).
- In the case of non-homogeneous waste, the waste must be correctly immobilized (the package must have as low a void volume as possible

and the waste must not be dispersible) and a minimal compression strength and shrinkage are required for the immobilizing material.

In all cases the material used for the internal casing must resist irradiation (between 5 and 25 × 10^{-2} G/s during approximately 25 days with minor modification of the samples) and thermal cycling (100 cycles from +9°C to –18°C for eight samples with minor modifications to the samples).

The final waste package, once completed, must have less than 3% void and must also resist a 0.35 MPa load.

Requirements for a waste package with a matrix with a confinement capacity

In this case the confinement capacity of the waste package is due to the use of the appropriate matrix to immobilize the waste (below a certain radioactivity level for the waste, this approach is simplified). The target material is a hydraulic binder (OPC CEM I type), although another material satisfying the requirements could be used provided it proved suitable (polymers and bitumen have also been used).

In the case of homogeneous waste, the confinement capacity of the waste block (waste and matrix) is specified through the setting of a maximum acceptable value for the apparent diffusion coefficient (D_a in m^2/s). This value depends on the type of radionuclide and also on the quantity of radionuclides the waste form contains.

In the case of non-homogeneous waste, the confinement is guaranteed by the homogeneous physical and chemical characteristics of the waste and the even repartition of the radioactivity inside the waste. The measurement of the leach rate leads to the evaluation of the apparent diffusion coefficient inside the waste block and the limits used for homogeneous waste concerning this parameter then apply.

The other requirements for the waste block depend on the level of homogeneity of the waste and are similar to those stated on page 341.

The finished waste package must then have less than 3% void and resist must a 0.35 MPa load.

Manufacturing process and sealing

The overall geometries of the different types of waste packages that are currently produced and disposed of in Andra's facilities are given in Table 11.2. If the waste package is of the drum type, then it generally contains either heterogeneous waste, or waste in a conditioning matrix, the drum being closed with a metallic cover. The manufacturing process is straightforward. If the waste package is of the box type, then there are three possibilities for the manufacturing process:

Table 11.2 Different types of metallic waste packages

Type of waste package	Size	Weight of the final waste package
200 l metallic drum	Diameter: 600 mm Height: 915 mm	750 kg
450 l metallic drum	Diameter: 740 mm Height: 1130 mm	1500 kg
870 l metallic drum	Diameter: 1050 mm Height: 1170 mm	4000 kg
5 m^3 metallic box	1700 mm cube	16,000 kg
10 m^3 metallic box	Cube of 1700 × 1700 × 3400 mm	32,000 kg

1. The first is that the box contains an internal concrete casing, the waste is inside this internal casing, and grout is then injected (or not if the waste is already immobilized).
2. Alternatively, the waste is in a metallic basket positioned inside the box, and the grout is injected around this basket, providing there is a space left between the bottom of the metallic basket and the bottom of the box for correct penetration of the grout around the basket.
3. Lastly, the waste is contained by metallic drums and these drums are inserted inside the box before the grout injection, providing there is a space left between the bottom of the drums and the bottom of the box for correct grouting.

11.2.2 Concrete-type waste packages

Requirements

In this case the container has a confinement capacity and requirements are set by Andra both for the confinement capacity of the waste package (the container itself and possibly the potential internal envelope and the waste itself) and also for the durability of this performance level in time. For this last requirement, this leads to the setting of requirements for the following:

- The mechanical performance of the empty container (its thickness must be superior to 5 cm if it has a regular shape)
- For the chemical durability of the empty container (its walls will have a minimal thickness that includes a part, representing the wasted portion due to chemical alterations, this wasted part depending on the characteristics of the material used for the manufacture of the container).

The confinement capacity of the waste package is specified through a requirement on the diffusion coefficient to tritiated water of the waste package. This requirement is a function of the thickness of concrete involved in the confinement (container or container + internal envelope) and depends on whether the contained waste plus matrix block has a confinement capacity.

Concerning the container, added requirements are set by Andra concerning:

- The type of cement to be used (mostly with respect to the standards system that concerns cement in France), the type of aggregates used, the type of additives used and lastly the type of mixing water
- The concrete mix
- The characteristics of the concrete (shrinking levels, etc.).

Obviously if the container includes a plug, then requirements exist concerning both the plug and also the watertightness of the plug–container link.

Should there be an internal envelope and should it have confinement requirements then Andra also specifies:

- A minimal thickness
- The characteristics of the material used (shrinking levels, etc.)
- Mechanical characteristics.

Lastly, the requirements concerning the homogeneity of the block of matrix plus waste are very similar to those concerning the metallic container (see Section 11.2.1). Should a confinement performance level be expected of this block, then the value for the leaching parameter is specified.

Fabrication process and sealing

The overall geometries of the different types of waste packages that are currently produced and disposed of in Andra's facilities are given in the Table 11.3. The manufacturing process for all these different types of waste packages varies. However, the following manufacturing steps are common:

1. The waste package and associated plug are manufactured and delivered to the waste producing site.
2. The waste is inserted into the empty container. The waste can be
   - either contained in a metallic drum, if the initial waste is very active (in this case a spacer is installed below the metallic drum to guarantee that the grout to be injected will constitute a continuous envelope),
   - or a mixture of a cement matrix and waste (in this case the next operations are not necessary),
   - or heterogeneous waste.

Table 11.3 Different types of concrete containers

Type of waste package	Size	Weight of the final waste package
Cylindrical, reinforced concrete	Diameter: 1400 mm Height: 1300 mm Thickness of the concrete for the waste package: 160, 319, 411, 150 mm	6000–8000 kg
Cylindrical, fibred concrete	Diameter: 840 or 1000 mm Height: 1500 mm	2000–5000 kg
Cubic, fibred concrete	1700 mm cube	16,000 kg

3. Should there be grouting, an element is included in the container to prevent the waste from floating when the grouting is injected (the grout having a higher density than the waste).
4. The grout is injected into the container.
5. The plug is put onto the container.

11.2.3 Quality control for short-lived low- and intermediate-level waste

The waste manager's requirements for a future disposal package, during the disposal package design, are discussed during the agreement process. Through this process the waste manager verifies that the disposal package fits his specifications, that the production and Quality Control process guarantee that produced packages will also fit his specifications and that all disposal packages arriving at the Centre de l'Aube are adequate to be disposed of in the facility.

The acceptance process

Parameters that are specified by Andra are of two types (Dutzer, 2002):

- Either they can be monitored directly on the waste package or during the process. For instance, the weight of a package can be measured and compared with the maximum specified weight; dose rates can also be measured.
- Alternatively, it is not possible to control them directly during the fabrication process of the package. This is the case for containment parameters (leaching rate, diffusion coefficient). For these parameters it would be necessary to destroy the package and then to perform experiments that could last more than one year.

Therefore during the agreement process investigations are made to identify operational parameters of the packaging or of the conditioning process that can be monitored during the fabrication of the packages and that will ensure indirectly compliance with Andra's requirements (including the parameters that are not directly controllable). For the diffusion coefficient example these operational parameters may be the composition of the cement used to make the diffusion barrier, or its water content.

The choice of the operational parameters relies on a qualification step. Experiments are performed on prototype packages or samples and must demonstrate compliance with waste acceptance criteria. Note that the waste generator may choose to qualify the package in a wide or a narrow range. Such an investigation is performed by the waste generator, with Andra's support, for each technical requirement for disposal.

All these operational parameters are grouped in a list that gives a suitable description (or 'specification') of the package relevant with Andra's requirements. This list, including the parameters and their values, is called a 'Contractual requirements sheet' or 'CRS'. It gives the description of the package that the generator agrees to manufacture and that Andra agrees to take in charge in the disposal facility (see Fig. 11.1). Supplying, fabrication or control procedures are then derived to ensure that actual packages will meet the CRS. In that way the agreement process leads to an operational definition of the package complying with Andra's requirements and to relevant QA procedures.

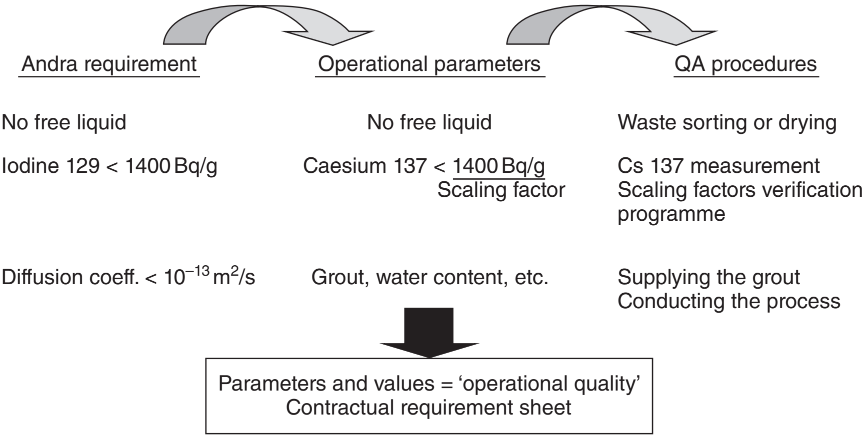

Andra requirement	Operational parameters	QA procedures
No free liquid	No free liquid	Waste sorting or drying
Iodine 129 < 1400 Bq/g	Caesium 137 < $\frac{1400\ \text{Bq/g}}{\text{Scaling factor}}$	Cs 137 measurement Scaling factors verification programme
Diffusion coeff. < $10^{-13}\ \text{m}^2/\text{s}$	Grout, water content, etc.	Supplying the grout Conducting the process

Parameters and values = 'operational quality'
Contractual requirement sheet

11.1 Transformation of Andra's requirements into QA procedures.

Package quality surveillance by Andra

By the agreement process, Andra obtains confidence in the ability of the waste generators to produce waste packages. This confidence must be maintained by surveillance of package quality. Different means are implemented for surveillance:

- *Computer check of package declaration by the waste generator.* Each package to be delivered to the Centre de l'Aube facility must be first declared by the waste generator in a computer tracking system. Identification of the package, the type of envelope, volume, mass, physical nature of waste, and activity of nuclides are declared.
- *Control of packages an delivery to the Centre de l'Aube facility.* Controls are performed on dose rate and surface contamination of packages.
- *Audits at the waste-producing facility.* 'Process/product audits' are performed by Andra in waste-producing facilities. References for these audits are QA procedures derived from the CRS. About 60 audits are performed per year, so all main waste-producing facilities are 'visited' at least once a year. Deviations are analysed according to the CRS with a follow-up of corrective actions.
- *Destructive and non-destructive tests on actual packages.* These tests are an important aspect of Andra's surveillance. Packages that are investigated are taken from those delivered to the disposal facility. About 150 to 300 non-destructive tests and 10 to 15 destructive tests are performed annually (Bouchet *et al.*, 2002). In view of the 25,000 to 30,000 packages that are delivered and to the 130 agreement files, such tests cannot have a statistical meaning. However, data collected in the 1500 non-destructive tests and 200 destructive tests undertaken since 1984 provide significant information that may be used to adjust some conditioning processes or parameter evaluations (such as scaling factors). A criterion to select packages to investigate is their contribution to the radioactive inventory. Tests also focus on recently agreed packages.

Depending on the type of packages, non-destructive tests consist of weight and dimensional controls, dose rate, surface contamination, gamma spectrometry, gamma-graphy, X-radiography or neutron measurements (see Fig. 11.2).

Destructive tests are used to investigate the waste content of packages and general quality of conditioning (see Fig. 11.3). 'Carrots' or core samples are taken to perform measurements on mechanical strength, diffusion coefficient and leaching rate (see Fig. 11.4). Alpha or beta emitters (particularly long-lived beta emitters) or chemical compounds are investigated. Destructive tests provide important information on parameters that are used in the safety assessment for the industrial packages.

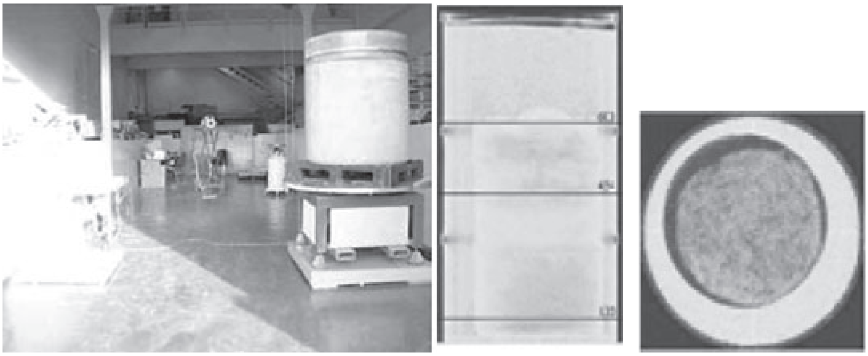

11.2 Non-destructive tests (gamma spectrometry, tomography).

11.3 Waste packages being developed for other types of radioactive waste

11.3.1 Low-level long-lived waste

Low-level long-lived (LL-LL) waste includes two categories of waste: graphite waste originating from decommissioned reactors being dismantled, and radium-bearing waste resulting from the waste produced by industrial uses of rare earths (Ozanam *et al.*, 2009). The repository for this type of waste is in the very preliminary design phase. We shall describe here only the packaging principles for graphite waste. For this type of waste the objective is that the primary waste package should also be the disposal waste package. The current design of the disposal package is a container made of reinforced or fibred concrete with a volume of 10 m^3. The waste is first inserted into a metal basket and this basket is then inserted in the 10 m^3 concrete container. Cement grout is injected in the container and a concrete cover is cast to seal the overall assembly (see Fig. 11.5).

Requirements for LL-LL waste packages

Requirements for LL-LL waste packages are related to their safety, transportability and mechanical strength.

Regarding the main function, that is the safety, the package contributes or guarantees two main safety functions, first upstream during the operation of the disposal facility and then downstream after its closure (during a sufficient time period). These are:

- The containment of the radioactive materials
- The limitation of irradiation of workers and members of the public.

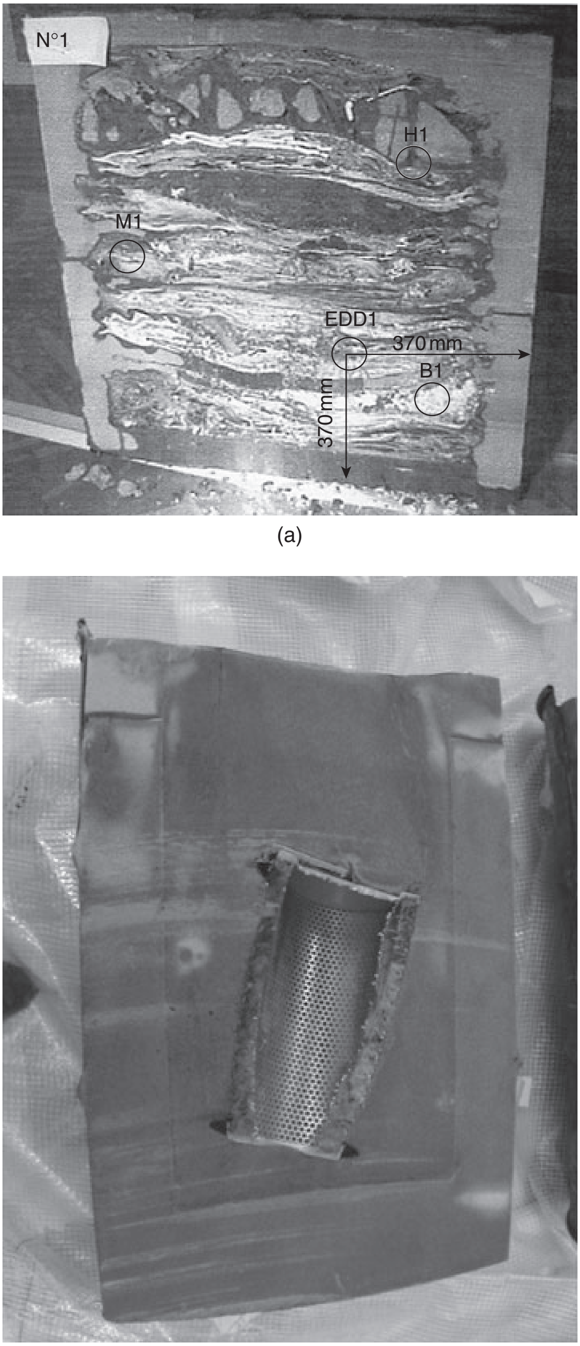

(a)

(b)

11.3 Destructive tests of concrete waste packages.

11.4 Destructive tests.

In order to contain radioactive materials, the concrete container (cover plus container itself) must be free of any through-cracks (including at the interface between the cover and the container), with a low permeability level ($<5 \times 10^{-18}$ m^2). Shrinkage must be slight (<400 mm/m after 28 days). These requirements extend over a period of a few centuries.

With regard to radiation protection, the expected performance is 2 mSv/h when in contact with the waste package and 0.1 mSv/h at 2 m from the waste package contained by a standard IP2 transport package.

As far as transport is concerned, the plan is to select standard exclusive transport (see international regulations) in the 20-feet metal IP2 containers and, consequently, with a maximum payload of 22 t.

Lastly, with regard to mechanical aspects, the design must sustain:

- Potential stacking of three disposal packages
- Drop under realistic conditions (drop on one corner, cover upwards low point at 50 cm from a concrete slab, high point of the bottom face at 1 m). In such a case, the waste must be neither dispersed nor exposed,

11.5 Design of the low-level long-lived waste package (photograph of a prototype).

the final plug must remain effective and there must not be any significant run-through cracking.

Design options

EDF, in conjunction with Andra, is investigating different design variations, notably containers made of reinforced or fibrous concrete. Prototype-fabrication tests were performed and two of the four reinforced-concrete prototypes are being submitted to drop tests on a corner.

The external dimensions of the 10 m^3 package are as follows: 2.9 m in length, 1.9 m in width and 1.8 m in height; its maximum weight is 24 t. The characteristics of the current prototypes are summarized in Table 11.4. The first results show not only that the prototypes meet all functional requirements described on page 348, but that they are also feasible from an industrial standpoint.

11.3.2 Intermediate-level long-lived waste

The intermediate-level long-lived (IL-LL) waste repository is in the design phase (see Section 11.1). For this waste, the primary waste packages are

Table 11.4 Characteristics of the low-level long-lived prototypes

	Concept with reinforced concrete	Concept with fibrous concrete
Container and cover	C50/60-class concrete, black steel reinforcement	Fibrous concrete
Backfill of containers	Immobilizing mortar (grout) with a formulation close to that of the concrete for the container	Immobilizing mortar (grout) with a formulation close to that of the concrete for the container

very diverse in size (diameters from 0.4 m to 1.5 m, heights from 0.7 m to 1.7 m and weights from 0.3 tons to 7 tons), materials used (steel, alloyed steel, concrete, fibred concrete, reinforced concrete) and radiological content. In view of this diversity and in view of the objectives for the repository, this has led to examining the need for an overpack (for the definition, see Section 11.6).

Requirements for IL-LL waste packages

The relevant safety functions for packaging IL-LL waste do not necessarily include enhancing the primary packaging to confine radionuclides over the long term. However, the compactness and reversibility objectives (reversibility is the possibility of removing the disposal package from its emplacement in the repository at a later stage, should the need arise) of the IL-LL waste repository have led to examine the need for an overpack to simplify operational procedures in the underground installations.

Most IL-LL waste is irradiating. In order to be protected against this radiation, a significant thickness of shielding material (e.g., about 1 m of concrete) is necessary to mitigate satisfactorily such radiation. Although an overpack provides that protection, it does not alleviate the need in most cases for handling operations in the disposal cell to be automated (no human presence) in view of the high radiation level, due to the large number of waste packages inside the cell. Consequently, all operations dealing with the emplacement of waste packages in disposal cells must be as simple as possible in order to:

- facilitate the automation of repetitive actions, such as emplacing packages, and
- perform such operations under very safe conditions.

Seeking simplicity and reliability implies two conditions, as follows:

- Limited streams of waste packages to be handled
- As low as possible physical diversity of the items placed in the same disposal cell.

Therefore the waste overpack must simplify and enhance the reliability of the waste-disposal procedure: not only does the gathering of the smaller primary packages in a larger container reduce the disposal package stream being handled in the disposal cells, but the use of an overpack also homogenizes the size and the handling devices of such items.

The overpack must also contribute to minimizing residual voids in the disposal cell in order to limit long-term deformations in the rock surrounding the waste. It must also limit internal voids around primary packages, except for the required clearances for emplacement purposes. Lastly, the overpack design must include the reversibility objective and chosen materials must suffer minimal alterations under repository conditions in order to facilitate a potential retrieval (this retrieval must be feasible for a period that is in the hundreds of years range).

Design principle of the waste package

While studying potential solutions, several options were reviewed. The arguments for the choices made are described below in relation to three fundamental aspects: geometric shape, constituting material, and size and weight.

Geometric shape

Two shapes (cylinders and parallelepipeds) were examined. The first shape has the major inconvenience of leaving relatively significant voids between packages within disposal cells, even when these are placed in close contact with each other. On the contrary, the second shape is more favourable with respect to the concern for compactness and void limitation. The regularity of the voids between disposal packages once emplaced in disposal cells limits the void fraction and avoids the need for backfill.

Constituting material

Concrete was chosen as the constituting material for disposal packages, since it lends itself readily to large volumes, is resistant, has a relatively low density and fills voids between primary packages. Another advantage is that the alkaline environment brought by the concrete generally reduces the release of radionuclides towards the geological environment, providing that the pH be limited to less than 12.5. Moreover, choosing concrete ensures mechanical integrity over a minimum period of about 100 years, in case the waste has to be retrieved. One must note that the concrete formulation must limit the quantity of water and organic matter contained, notably with regard to radiolysis.

Size and weight
The overpack, which may vary in size, will significantly reduce the number of items to be managed underground and will minimize the waste streams being transferred to disposal cells. The dimensional and radiological characteristics of the primary waste packages, taking into account limits in terms of (1) transfer capacity from surface installations down to disposal and (2) handling structure in disposal cell capacity, will lead to appropriate sizing of the overpack, therefore defining its capacity in terms of number of primary packages contained.

Transfer from surface installations down to the disposal cell
The disposal package is conveyed from the surface down to the disposal cell under a transfer hood providing radiation protection. The disposal package does not therefore have to ensure biological protection against external irradiations.

Handling and emplacement in the disposal cell
Disposal packages are designed in parallel with means of handling and emplacement in disposal cells. The sizing of disposal cells and the handling conditions of packages, including the number of packages to be stacked, affect directly the package design.

Selected solution

A disposal waste package consists of two pre-cast concrete components (see Fig. 11.6), as follows:

- A body with internal dividing walls
- A cover.

The generic concept is to build a body with internal dividers separating the fitted housings shaped for the primary packages. The functional clearance between each housing and the primary package is large enough to ensure the emplacement of the primary packages, and the residual void is small enough not to require backfill once the primary package is emplaced. This approach facilitates the retrievability of primary packages and avoids the use of a grouting process in an irradiating environment.

A design variation also exists for an overpack specific to small waste volumes of primary packages (the result represents a small volume of the overall inventory), so as not to have to develop a specific mould. In this case, a multi-purpose package has been developed. It has no dividers and

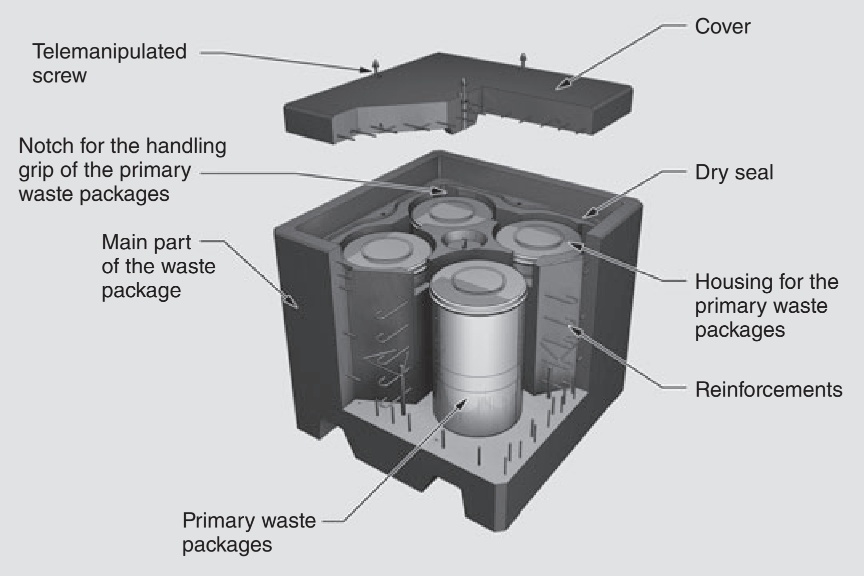

11.6 Disposal waste package for IL waste packages.

accommodates only packages with standard dimensions. Ultimately, a blocking material (grout) is poured in order to limit any residual voids in the finished package.

For primary packages releasing radiolytic hydrogen, the risk of excessive concentrations in the waste package may be avoided by installing vents in the overpack. It should be noted that, as long as the concrete is under a dry atmosphere, the sole porosity of the concrete would be sufficient to release the produced amount of hydrogen.

Disposal packages include a more or less large number of primary packages with a maximum weight in the order of 25 t, bearing in mind that the handling procedure may slightly affect the geometry of the disposal package, as follows:

- In the case of individual handling (see Fig. 11.6), the package is equipped with notches in its bottom section for letting the pallet forks through.
- In the case of stack handling, the package is equipped with lateral notches.

11.3.3 Containers for high-level waste

As for the intermediate-level waste repository (see Section 11.3.2), the high-level waste repository is currently in the preliminary design phase. For this repository, Andra has decided to use an overpack (for the definition, see Section 11.6) and is therefore developing such a type of container for the primary high-level waste package (Andra, 2005a).

The design of the cells and general architecture of the high-level waste repository zones aim to meet the various long-term operational and safety requirements. In particular, the management of the heat released by the waste and the long-term safety requirements (protecting packages in order to restrict the release of radioactive nuclides, repository organization and disposal reversibility) appear to be the dimensioning factors for the container characteristics.

The requirements

Preventing water reaching the glass during the thermal phase

The high level of β–γ activity of vitrified HL waste results in a considerable amount of heat being released by the primary package. This heat release decreases over time according to the isotope decay. The heat release phenomenon could last a millennium. It induces a temperature increase in the repository, which is liable to:

- *increase the glass alterability* (glass in which the radioactive nuclides are trapped, whose constituents, particularly silica, are sensitive to heat and dissolve progressively when in contact with water), and
- *modify the behaviour of the radionuclides* which would be released into the water after the heat release has induced glass alteration.

Consequently, Andra decided to prevent water reaching the glass for a period of several thousand years, by adding an overpack to the HL primary waste package in order to:

- avoid the risk of piercing the primary stainless steel waste package by corrosion through water contact, which could occur after several decades, and a dissemination of radioactive nuclides which would make package retrievability operations trickier (reversible management), and
- prevent early alteration of the glass, accelerated by the temperature, which would be accompanied by radionuclide release (safety).

The duration of container watertightness is longer than that of the thermal phase of HL waste, i.e. the period following waste emplacement in the repository, during which glass core temperature is in excess of 50°C.

Providing long-term post-closure safety

In order to fulfil the long-term safety function, the cell design and construction procedures aim at the following.

- *Protecting the disposal packages.* A primary objective is to maintain a physico-chemical environment that favours the overpack durability objective and, thus, to prevent corrosion. In order to reduce the period during which the corrosion rate is highest (aqueous corrosion under oxidizing conditions), air (and thus oxygen) must be prevented from re-entering the cell from the ventilated access drift. Once the overpack is damaged and water is in contact with the glass, the cell must also maintain conditions that favour a slow glass dissolution rate and a slow release of radionuclides by the glass (Andra, 2005b). Another objective is thus to restrict the renewal of the water in contact with the glass after the cell has been closed. Also, once the waste package envelope is damaged, water flowing out of the cell (means of transport of the radionuclides released by the packages) must also be restricted. In the long term, after re-saturation, this restriction relies on the low permeability of argillites and on the cell seal watertightness.
- *Limiting mechanical distortion in the medium* by reducing the residual void spaces in the cells and in the disposal package to prevent, in the long run, their resorption due to the alteration of materials causing distortions that damage the argillites.
- *Controlling physico-chemical disturbances.* The disposal waste package is designed to prevent water arriving in contact with the primary package and avoid a premature alteration of the glass during the thermal phase. It is also essential to ensure that the waste package materials do not cause excessive disturbances of the glass and its environment in the longer term, particularly the water pH, which is expected to be kept between 7 and 9 (the glass dissolution rate is very sensitive to this parameter).

Note that three corrosion phases have been identified inside the disposal cell:

- *Dry oxidizing conditions* (confined air) causing hardly any corrosion
- *Next, aqueous corrosion under oxidizing conditions* which means a steel corrosion rate (concentrated at the cell head) of several tens of microns per year. This phase is very limited in duration
- *Finally, corrosion under anoxic and reducing conditions* during which the steel corrosion rate is reduced to a few microns (or even less than a micron) per year.

Ensuring reversibility and allowing package retrievability

The objective is to retain the ability, for at least a century, to retrieve the packages, to intervene in the operation and closure of the repository and to modify its design. The ability to withdraw packages essentially requires the disposal packages and structure geometry to be ‘maintained in condition'. The mechanical and geometrical durability of the components surrounding the packages (disposal cell sleeve) must be maintained to take account of corrosion and the increased pressure exerted by the argillite. This involves:

- limiting corrosion, by reducing the duration of the aqueous corrosion period under oxidizing conditions in which the corrosion rate is high, and
- maintaining a functional clearance around the disposal packages inside the cell, dimensioned at best in order to prevent damaging the argillite in the long term through resorption of void spaces.

In addition, the modularity of the architecture provides flexibility in repository management.

Description of the waste package

Andra has opted for an individual cylindrical non-alloyed steel container containing a single high-level waste primary package. Andra had previously studied other metallic materials for the container: metals (copper, titanium) or chrome, nickel and manganese-based passivable alloys (property achieved through the formation at the metal surface of a fine corroded layer that then protects the metal), that present very low corrosion sensitivity and can be used in small thicknesses. The studies into passivable alloys showed a greater sensitivity to the repository environment (highly oxidizing conditions, temperature, presence of aggressive species such as chlorides, etc.) and the possibility of corrosion by pitting. Furthermore, as with noble metals, they require innovative techniques in order to use them to form a watertight envelope. Therefore the solution of passivable metals was not chosen, but work carried out on these alloys is being actively monitored.

The rationale behind this choice is the following:

- An individual container offers great flexibility in cell design (particularly their thermal dimensioning) and package management. It minimizes the dimensions of the objects to be handled, which is possible due to primary package standardization.
- Non-alloyed steel (P235) presents two advantages that limit the risk of failure damaging the container tightness and durability, particularly along welds:
  - This type of material presents robust behaviour and its corrosion processes are well understood. As far as aqueous corrosion is concerned, experimental results and modelling indicate that generalized corrosion is the dominant mechanism in the medium and long term

and that its rate can be quantified based on experimentally validated models. Iron archaeological analogues over 2000 years old support the assessment of the corrosion processes and provide a temporal reference with respect to the durability of steel over a significant timescale. In addition, as non-alloyed steel corrosion models are only very slightly sensitive to water chemistry, they require less precision concerning the chemical environmental conditions (in particular, they are compatible with uncertainties concerning the composition of the Callovo-Oxfordian interstitial water), and with respect to the composition of the metal and its structural and surface condition.

– Its use (metallurgy, weldability, control) is based on industrially proven technologies. Andra chose P235 non-alloyed steel because of its good welding properties and adequate mechanical characteristics with respect to the dimensioning of disposal packages.

The High Level waste container therefore has a P235 non-alloyed steel casing fitted with ceramic runners (pads) and a P235 non-alloyed steel lid (welded to the casing by electron beam) to meet tightness requirements.

- The casing consist of an envelope (55 mm thick) providing confinement over a period of 4000 years based on conservative models, notably by assuming corrosion inception as of its emplacement in the repository, then corrosion in an oxidizing medium for a decade or so. Its interior is designed to limit any void spaces and, on the outside, ceramic sliding runners allowing its handling in the disposal cell through a pushing technique. They prevent direct steel/steel friction between the package and the cell sleeve, which may damage the package during its transfer, facilitate sliding and thus limit the pushing forces.
- The lid is 55 mm thick. Its internal shape, adapted to the primary package profile, helps to limit the amount of void space. A groove machined into the outside enables its vertical and horizontal handling using a grapple; it is dimensioned to leave sufficient room for deploying the grapple fingers, even in the event of corrosion (for possible retrieval within the reversibility context).

Manufacturing the high-level waste container

HL waste packages can be manufactured in two phases. In the first phase, the container casing and lid are prefabricated. For the casing, it was preferred to obtain a casing body and bottom with a single piece using an industrially proven technique, boring and hot-drawing a solid steel block (cavity obtained by metal deformation). In the second phase, the disposal packages are made up in shielded cells in the repository surface installations: emplacing the vitrified waste primary package into the container, fitting the lid and welding it through an electron beam technique, inspecting the weld before transfer to the disposal cells.

Andra studied several lid welding processes:

- Welding with filler metal based around several processes: laser/YAG, used for thin steel but still under development for welding large thicknesses of steel; TIG processes (tungsten inert gas arc welding); and MIG, MAG (metal inert/active gas welding), though welding times are not, however, suitable for thick pieces.
- Welding without filler metal, using electron beam (EBW process) and friction processes. The latter, currently under development in Sweden by SKB for welding 50 mm thick copper containers, is not directly transposable to thick steel welding.

At this stage, Andra has preferred electron beam welding (EBW) under vacuum, which has the following advantages:

- The process requires no filler metal (well suited for use in a shielded cell)
- It is an industrially proven process on thick steels (up to 200 mm)
- A small area is thermally affected by welding
- There is a low risk of cold fissuration (welding under vacuum)
- The process can be automated
- Welding is carried out in a single pass (high welding speed) and high productivity (welding 5 to 10 times faster than the TIG and MIG processes).

Given the similarity to the container planned for spent fuel, the electron beam welding technique and its associated inspection processes were qualified in 2004–2005 as part of an Andra/EDF/CEA demonstration programme, through two full-scale spent fuel package disposal container demonstrators.

11.4 Future trends

The disposal packages for radioactive waste described in this chapter are either already in production or being designed. It is not expected that the design of the first type will be changed. However, new designs could be developed over time, to standardize the number of disposal package types, for example (as stated in Section 11.2, it is significant with more than 15 types of waste packages handled by the Centre de l'Aube facility).

Regarding the disposal packages currently in the design phase (for all high-level and long-lived waste), the design process will continue. In view of the current target dates for the associated repositories to become operational (in the 2020s decade for both projects), it is expected that these designs will change with modifications of the solutions described in this text.

11.5 Sources of further information and advice

A significant amount of further information on disposal waste packages for intermediate- and high-level long-lived waste is available from Andra's Internet website: the 'dossier' published in 2005 describes in great detail the packages themselves, the handling process, the justification for their design, the chemical and physical behaviour of the waste, and the chemical and physical behaviour of the rock formation. A new 'dossier' was published in 2009, and it will upgrade to some extent the previous information.

Information on low-level and intermediate-level short-lived waste packages can be obtained from the main producers of these packages (these packages are used in production): AREVA and Electricité de France.

11.6 Glossary of terms

Conditioning matrix (also embedding matrix, encapsulation matrix, immobilizing matrix): Solid material used to immobilize or to condition radioactive waste

Confining matrix: Used to describe the conditioning matrix when it is expected to have a confinement capacity

Container (also canister): Closed recipient used for transport, storage or disposal of waste

Disposal waste package: Radioactive waste package that can be placed unchanged into a waste disposal facility. An overpack can be used to transform a primary waste package into a disposal waste package

Internal envelope: Envelope contained by a waste package to enhance the waste package functionalities (generally the confinement capacity)

Overpack: Used to transform a primary waste package into a disposal package

Primary waste package: Waste package as it is produced on the waste producer's conditioning facility

Transport package: The package including both the packaging and its radioactive contents, as used for transport purposes.

11.7 References

Andra (2005a), 'Synthesis Argile Evaluation of the feasibility of a geological repository in an argillaceous formation', published by Andra in 2005 (part of the 'Dossier 2005' available in pdf format in September 2010 on the site in English: www.andra.fr)

Andra (2005b), 'Phenomenological evolution of a geological repository', published by Andra in 2005 (part of the 'Dossier 2005' available in pdf format in September 2010 on the site in English: www.andra.fr)

Andra (2007), Description of the Centre de l'Aube facility, published by Andra in 2007 (available in December 2009 as reference 208 VA on www.andra.fr)

Bouchet, C., Cédon, G., Félix, B., Langlois, G. (2002), 'The evolution in the LL and IL radioactive waste management in France and its impact in Andra's acceptance criteria at the Centre de l'Aube disposal facility' *WM'00 Conference*, Tucson, AZ, 27 to 2 March, 2000

Dutzer, M. (2002), 'From waste packages acceptance criteria to waste packages. Acceptance process at the Centre de l'Aube disposal facility', *Proceedings of WADRAP 2002*, 23–26 September 2002

Ozanam, O., Hoorelbeke, J.-M., Ouzounian, G. (2009), 'Progress of the graphite and radium bearing waste disposal Project', Paper 9268, *Proceedings of Global 2009*, Paris

PNGMDR (2006), 'National plan on management of radioactive materials and waste', updated 6 October 2009, published by the French Safety Authority in 2006 (available in pdf format in September 2010 on the site in English: www.asn.fr)

12

Development and use of metal containers for the disposal of radioactive wastes

I. G. CROSSLAND, Crossland Consulting, UK

Abstract: The chapter describes the metal containers that are used for the packaging of solid radioactive waste with a focus on containers intended for disposal. One of the safety functions of a container is physical containment and the three ways of achieving this are outlined. The chapter provides an overview of metal corrosion theory and then describes some of the many container designs that are already in use or proposed for use in the future, grouping these by material. Approaches to quality management and possible future developments are also discussed.

Key words: metal containers, radioactive waste, radioactive waste disposal.

12.1 Introduction

12.1.1 Outline of the chapter

Metal containers or canisters have long been used for the packaging of radioactive waste. Until the early 1980s the main aim was to contain the wastes during storage. Since then it has become increasingly recognised that storage – even extended storage – is no more than a temporary solution that only passes the burden of management on to others, some of whom may not yet be born. Today, therefore, managers of radioactive waste strive to package their waste once only and to do so in a way that is suitable for both storage and disposal. The latter is defined by the International Atomic Energy Agency as 'emplacement of waste in an appropriate facility without the intention of retrieval' (IAEA, 2003). Disposal aims to provide a permanently safe solution that relieves future generations of the burden – both physical and financial – of waste management.

In settling on an appropriate waste package design, many different factors will need to be considered. These include the nature of the waste which may, for instance, require the package to have built-in radiation shielding, the storage period, the environmental conditions during storage and disposal and, not least, the regulatory regime. While waste package designs vary widely, the metallic materials used in waste containers are relatively few in number. They consist of carbon or low alloy steels, cast iron, various grades of stainless steel, nickel-based superalloys and copper. The presence of materials such as plain carbon steel in this list shows that it is not always necessary to seek a material with very low corrodibility. The optimum material will combine adequate corrosion resistance with other properties such as availability, weldability and affordability. In this chapter we aim to describe the principles that lie behind the choice of waste packaging and illustrate those principles through practical examples of waste containers in use today. Throughout, the focus is on waste packaging for disposal.

12.1.2 Content of each section

Section 12.2 describes the nature of radioactive waste and the various forms that disposal can take. It also outlines key safety principles relevant to containers for radioactive waste. Section 12.3 presents the three approaches that can be used to provide physical containment of waste and highlights the importance of other issues such as container geometry and the need, or not, for radiation shielding. Section 12.4 is an introduction to electrochemical corrosion that draws from classical texts. Section 12.5 describes some of the many containers that are in use or proposed, grouping these according to the type of metal used. Section 12.6 discusses quality management and Section 12.7 outlines some possible future trends.

12.2 Safety in radioactive waste disposal

12.2.1 Nature of radioactive waste and its influence on the form of disposal

Radioactive waste comes in many forms: the UK National Inventory of Radioactive Waste, for example, lists more than 1000 solid waste steams that exist in many different chemical forms. It is usual to categorise these wastes according to the concentration and nature of the radionuclides that they contain. This is helpful in terms of waste handling and storage because it provides an indication of the measures that must be taken to protect workers. At the same time it is useful if the waste categories also provide an indication of the eventual disposal route. An important consideration here is whether the waste will still be sufficiently radioactive to be hazardous at a time when institutional control over a disposal facility lapses. This time is generally taken to be a few hundred years (often 300 years). It follows that two parameters are important in the categorisation of waste: specific activity and half-life. This leads, typically, to the waste categories indicated in Table 12.1.

Table 12.1 Typical waste categorisation scheme

Waste category	Abbreviation	Disposal type
High-level waste – heat generating*	HLW	Deep
Intermediate-level waste – long-lived†	ILW-LL	Deep
Intermediate-level waste – short-lived†	ILW-SL	
Higher specific activity		Deep
Lower specific activity‡		Near-surface
Low-level waste‡	LLW	Near-surface
Very low-level waste	VLLW	Landfill
Very short-lived waste (usually consists of disused sealed sources)	VSLW	Decay storage followed by recycling or landfill disposal
Exempt waste	EW	Recycling/landfill

* Radioactivity always generates heat but the demarcation between heat-generating and (so-called) non-heat-generating waste is normally set at 2 kW m^{-3}, this being the level above which it usually becomes necessary to specifically provide for heat dissipation in the design of a store or repository. For a radionuclide that emits an alpha particle with an energy of 4 MeV, this corresponds to an activity of around 3×10^{15} Bq m^{-3}.

† For disposal purposes, short-lived radionuclides are generally taken to have a half-life of less than about 30 years.

‡ Lower-activity ILW-SL and LLW, both of which could be disposed to a near-surface facility, are sometimes combined into one category that is abbreviated to LILW.

In most circumstances, high-level waste (HLW) needs to be contained for many thousands of years if it is not to be a danger to humans and the environment. On the other hand, very low-level waste may contain insignificant amounts of radioactivity within a few decades of its disposal at which time it represents a negligible hazard. From this it is clear that these two categories of waste will require quite different treatment and packaging.

12.2.2 Containment

It is useful to consider two kinds of containment. The first follows the ordinary meaning of the word and simply means that radionuclides are prevented from migrating by some kind of physical barrier such as a container; we call this physical containment. The second meaning recognises the fact that, even in the absence of a physical barrier, a radionuclide may have low solubility in the surrounding groundwater or be chemically attracted to the materials with which it comes into contact, i.e. it may sorb to them. Solubility and sorption reduce the rate of migration so that the radionuclide has a longer time-span over which it may decay before coming into contact with the human environment; we call this chemical containment. A waste container clearly provides physical containment but, even when it is totally corroded, it may still provide chemical containment because of the strong attraction between migrating radionuclides and the oxides and hydroxides (i.e. the corrosion products) of iron (Gillespie, 2001). Exclusively, however, it is physical containment that will be discussed in this chapter.

The IAEA 'Requirements' document for deep geological disposal (IAEA, 2006a) names 'containment' as one of a number of mandatory 'safety design principles'. The design life of the containment is to be decided with respect to the properties of the waste, in particular heat generation and radioactive decay. The containment will be designed to avoid all but minimal releases of radionuclides from the waste, prevent water ingress and, generally, preserve the physical integrity of the waste form. Situations where this translates into a requirement for long-lived, absolute physical containment are usually confined to disposal of the most highly concentrated radioactive wastes such as spent nuclear fuel (SNF) and vitrified HLW from SNF reprocessing.

12.2.3 Passive safety

IAEA documents (IAEA, 2006a, 2006b) and some regulatory regimes stress the importance of 'passive safety' during both storage and disposal. IAEA does not provide a formal definition of passive safety but one might broadly describe it as minimising the need for human intervention to ensure safety. It follows that waste containers should at least be designed to have lifetimes that are commensurate with the expected storage period and the expected storage conditions. With respect to disposal, post-closure safety is (almost by definition) entirely dependent on passive means and, therefore, on the ability of the natural and engineered barriers, acting in concert, to provide the required level of radionuclide containment. In general, it is advantageous in terms of cost and passive safety (thinking, in particular, of radiation dose to workers) if the package in which the wastes are stored is also acceptable for final disposal.

12.2.4 Multiple safety functions

Another IAEA Requirement for the safe disposal of radioactive waste is the provision of multiple safety functions (IAEA, 2006a): '[t]hat is, safety shall be provided by means of multiple barriers whose performance is achieved by diverse physical and chemical processes. The overall performance of the geological disposal system shall not be unduly dependent on a single barrier or function.' Barriers fall into two types, natural and engineered, and the waste container will be one of the engineered barriers,

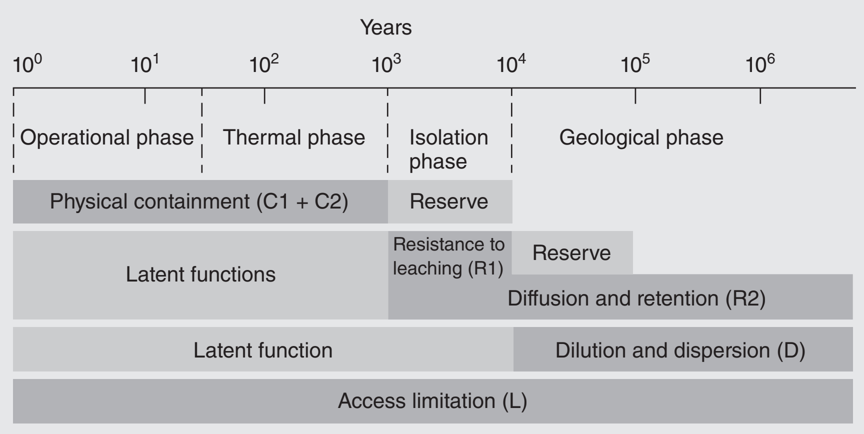

12.1 Safety functions in relation to repository evolution (after Ondraf-Niras, Belgium).

possibly the principal one. It is useful if barriers are relatively independent, since this will provide a degree of redundancy, but more important is the need to ensure that the various barriers work in concert and that one barrier does not have a detrimental effect on another. If, for instance, the disposal concept entails the use of large quantities of concrete backfill made from Portland cement, the other barriers must be capable of tolerating high-pH conditions. It is normal to find that the different engineered barriers perform their allotted functions over different timescales with physical containment (provided by the waste container) being the first to come into play (Fig. 12.1).

12.3 Approaches to physical containment of radioactive waste

12.3.1 General

There are, broadly, three ways of achieving the desired period of physical containment (Savage, 1995). The first is the use of a material such as copper that is stable under repository conditions. The main advantage of this approach is that simple arguments for longevity can be made on the grounds of fundamental thermodynamics and mass balance. Furthermore, this argument can be supported by natural analogues such as the occurrence of native copper of great antiquity.

The second way is to use a material such as stainless steel that is corrosively passive under repository conditions. Invariably, this is because of the formation of a thin, adherent, non-conducting oxide. The main advantage of this approach is that containers can be made in relatively thin sections from ordinary engineering materials, principally stainless steel. Depending on the choice of material, it may be relatively inexpensive, widely available and easily fabricated. The main difficulty with such materials is that they are often susceptible to localised corrosion (see Section 12.4).

The third way is to choose a material that corrodes at a moderately low rate but to fabricate the container with sufficient thickness to provide the required container lifetime. This approach usually entails the use of iron-based materials (especially cast iron and forged steel) that have the advantages of well-developed technology, high availability and low cost. The ubiquity of these materials means that their corrosion is well understood and data exist that span many hundreds of years.

Whichever of the three approaches is chosen, containment depends not only on the material used but on the prevailing environmental conditions. In general, would-be repository operators will aim to show that the adopted design is robust to all reasonably anticipated environmental changes.

12.3.2 Influence of corrosion on repository environmental conditions

Once a repository has been covered over or backfilled and sealed, corrosion of the waste containers will both depend on and, to some extent, determine the environmental conditions. Specifically, where metallic corrosion occurs it will consume oxygen and lower the redox potential (Chambers *et al.*, 2002). This effect acts to progressively reduce the corrosion rate and, importantly, suppress the solubility of certain radionuclides, notably the actinides. In a repository where containers are made from a non-corroding material, oxygen removal will also occur but the kinetics are more likely to be governed by microbial and other processes (Puigdomenech *et al.*, 2001).

12.3.3 Container geometry

Container geometry is especially important for low- and intermediate-level wastes which tend to be stacked within the repository vaults so as to use all the available volume. In a HLW repository, by contrast, waste containers have to be separated so as to diminish the intensity of the heat loading. Consequently, efficiency in terms of space filling is less important. In a low- and intermediate-level repository, therefore, it is advantageous if space-filling rectilinear containers are used. Large rectilinear containers, e.g. cubes of side greater than 1 m, also aid the waste packaging process because they may eliminate some of the need for size reduction of the waste. In practice, however, through force of habit and availability, it is the 200 and 500 litre drums that are most commonly encountered. Often, these are placed, four at a time, inside a stackable steel crate (sometimes called a stillage) or a rectilinear concrete container. Of course, putting these drums within a space-filling overpack does not improve the efficiency of utilisation of the available repository volume and it is common to find that less than 50% of the available repository volume is actually occupied by waste.

12.3.4 Shielded containers

SNF and the HLW produced by SNF reprocessing are intensely radioactive and the gamma field they produce is a very great hazard. Indeed, even after decades of cooling, the strength of the gamma field demands very thick shielding if humans are to be allowed to come into close proximity. Such shielding may not always be convenient for underground working (where space is limited) so that remote handling will sometimes be a necessity. Intermediate-level wastes emit a lower, though often still significant, gamma field and here the repository operator always has a choice between handling the containers remotely or packaging the wastes inside a shielded container. The shielding may be in the form of a concrete insert within the container; often it is possible to adjust the thickness of this to suit the intensity of the radiation emitted by the waste. Of course, the use of a shielded waste container will reduce the filling efficiency of the repository. On the other hand, where unshielded containers are used this will often create a need for remote handling equipment and for reusable shielded transport containers so that the waste containers can be conveyed, through the public domain, from the site of production to the site of storage or disposal.

12.3.5 Container closure

For SNF and HLW it is invariably the case that containers are seal-welded. As with the copper/steel containers used in the Swedish KBS-3 concept (see later), this may require specialised welding techniques to be developed. For other categories of waste, the need for absolute containment is less pressing and container lids may be simply bolted into place or, in the case of drums, held in place by a metal closure band that fastens the lid to the lip of the drum. For such wastes, metal containers are usually no more than a few millimetres thick, so that other issues must be considered, notably pressure increases due to gas production, stackability and, for deep disposal, the hydrostatic stresses that will occur when the repository resaturates. In some circumstances it may be advisable to provide a means for gas escape and pressure equalisation. Normally this will consist of a hole in the container lid that is covered by a fine metal gauze filter to prevent egress of particulate matter.

12.3.6 Demonstrating long-term container integrity

Especially in the case of long-lived wastes (SNF, HLW and long-lived intermediate-level waste) there will often be an expectation that the waste container will provide absolute physical containment over thousands of years. By combining corrosion rates measured under simulated repository conditions and the known thickness of the container material, it is obviously possible to estimate the expected container lifetime. The difficulty, of course, is that this entails an extrapolation in terms of timescale of, perhaps, a million times. This is a common problem in radioactive waste disposal that is usually addressed by means of natural analogues. The classic example is the natural nuclear reactors found in the 1960s in Gabon. These have been studied extensively and used to demonstrate, for instance, the way that commonly encountered minerals can retard the migration of actinides in the natural environment (Salas and Ayora, 2004). Natural analogues can also be used to demonstrate the long-term corrosion properties of naturally occurring metals, primarily copper and iron. This is a significant advantage that can influence the choice of container material for long-lived wastes.

12.4 Metal corrosion: an overview

12.4.1 Electrochemical processes and localised corrosion

Following Evans (1981), we imagine a piece of iron covered by some kind of electrically conducting coating such as an oxide scale formed during high-temperature treatment (Fig. 12.2). When this is immersed in sodium chloride solution, it is found that, if the scale has been scratched to reveal the iron below, the iron will rust very rapidly at this point; indeed, it will rust many times quicker than a piece of uncoated iron. This observation cannot be explained using a straightforward, and seemingly obvious, corrosion model in which metal simply reacts with oxygen to form an oxide. Rather, it exemplifies the electrochemical nature of aqueous corrosion and, as we shall see, serves to explain the corrosion of iron under aerobic conditions.

Electrochemical corrosion theory proposes the existence of complementary chemical reactions. Under the conditions presented in Fig. 12.2, these are

$\mathrm{Fe} \rightarrow \mathrm{Fe}^{++} + 2e^-$, i.e. metal dissolution – the anodic reaction

$2e^- + \mathrm{O} + \mathrm{H_2O} \rightarrow 2\mathrm{OH}^-$, i.e. electron consumption – the cathodic reaction

When the metal ions dissolve, their charge is balanced by chloride ions that migrate towards the area of attack, attracted by the positively charged ions being formed there. Iron chloride is soluble in water so that a solution

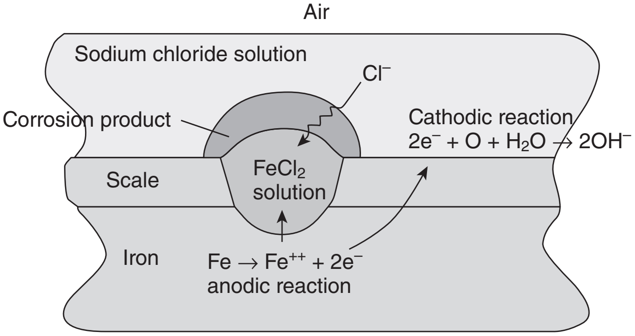

12.2 Corrosion at a break in the scale covering a piece of iron immersed in sodium chloride solution.

of iron chloride forms locally. This forms no barrier to further corrosion; indeed, because iron chloride solution is very acidic (because of the process known as metal hydrolysis), it accelerates the rate of attack. But, as the Fe^{++} ions move away from this locality, they encounter hydroxyl ions – either present in the water naturally or formed by the cathodic reaction – and precipitate as ferrous hydroxide, $Fe(OH)_2$. In the presence of dissolved oxygen, this is quickly oxidised further to ferric oxy-hydroxide:

$$2Fe(OH)_2 + O \rightarrow 2FeOOH + H_2O$$

Ferric oxy-hydroxide may be written as FeOOH or $Fe_2O_3.H_2O$.

The important things to recognise from this example are that (i) three reactions occur in the rusting of iron and (ii) they take place in three different places, namely:

- The corrosion (anodic) reaction occurs at the place of metal loss.
- The cathodic reaction occurs where oxygen dissolved in water can accept electrons.
- The solid corrosion product is produced at some other place.

The current flow from the cathodic and anodic reactions must be the same, otherwise there would be a build-up of charge in the metal sample. It follows that if the area of the cathode is very much greater than the area of the anode (as in Fig. 12.2), the depth of attack will be very much greater than it would be if the cathode and anode were of roughly equal size.

12.4.2 Localised corrosion of stainless steel

In Fig. 12.2 the layer of scale mostly serves to isolate the iron surface from the oxygen; it does not take part in any of the corrosion reactions. This example has some parallels with the important case of corrosion-resistant alloys such as stainless steel, whose surface is covered by a thin, non-porous and adherent film. In higher-chromium steels this film consists primarily of chromic oxide, Cr_2O_3. It forms rapidly and, because diffusion of ions through this film is negligible, it quickly reaches a limiting thickness. Further metal corrosion is governed by the rate of film dissolution, which is also very slow under chemically neutral and alkaline conditions. If the film is damaged, by scratching for instance, it quickly re-forms, accounting for the excellent corrosion resistance of stainless steels (Sedriks, 1996, p. 389).

In the case shown Fig. 12.2, localised corrosion was initiated by the presence of the scratch in the surface layer of scale; subsequent propagation depended on the preservation of the acidic, highly corrosive liquid within the scratched area. Whereas in iron corrosion the acidity is produced by hydrolysis of iron ions, in stainless steel corrosion it is primarily chromium ion hydrolysis that is responsible (Sedriks, 1996, p. 178). In dilute chloride solutions it is known that areas of local film breakdown continually form. These may occur, for instance, at inclusions, second-phase particles, or inhomogeneities in composition (e.g. local chromium depletion). These are quickly stifled by the reformation of a protective film of oxide (a process known as repassivation). Under more aggressive chemical conditions, however, not all the areas of film breakdown will repassivate; instead, some will form areas of localised corrosion (pits) where the attack goes deep into the metal. The parameters that influence pit initiation are well understood in global terms but the level of understanding is not so advanced that it can yet be modelled mathematically with any accuracy.

Unlike initiation, propagation of localised corrosion is sufficiently well understood for predictive models to be useful and Fig. 12.3 illustrates the main features of these models. The figure shows a propagating pit below a cap of dirt or corrosion products that serves to preserve the localised chemistry at the point of attack by preventing mixing with the bulk solution. The pitting corrosion model depicted in Fig. 12.3 can be applied, with relatively little modification, to other types of localised corrosion so that the anodic reaction now takes place within a crevice or stress corrosion crack (where the constricted nature of the crevice or crack provides the necessary isolation from the bulk solution) or below a biological membrane. It is also worth noting that stress corrosion cracks often start from the base of a pit. The build-up of positive charge within the pit (due to the flow of electrons through the metal to the cathodic regions) causes a counter-flow of negatively charged ions (A^- in Fig. 12.3) into the pit from the bulk solution. Depending on the identity of the negatively charged species, this can increase or decrease the pitting rate. Chloride ions, for instance, are well known to increase pitting for reasons explained above.

As before, the anodic reaction within the pit is balanced by a cathodic reaction on the 'open' metal surface and, because of the large disparity

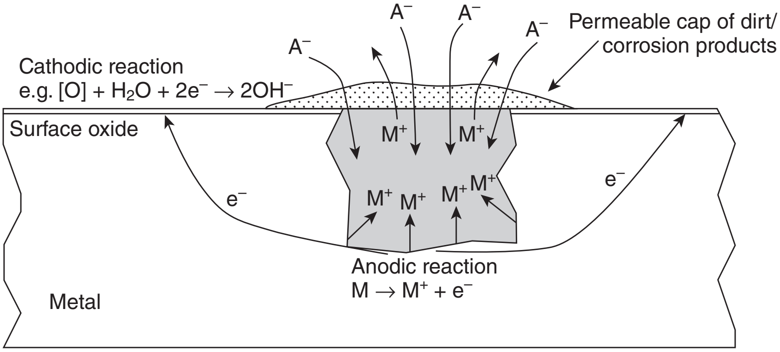

12.3 Growth of a pit in a metal sample.

between the cathodic and anodic areas, the rate of pitting can be high. There are, however, a number of processes that can cause localised corrosion to cease through, for instance, loss of the localised chemistry. These processes include:

- A slowing of the cathodic reaction due to loss of dissolved oxygen in the bulk solution
- Loss of the cap
- Thickening of the cap
- Precipitation of solid corrosion products within the pit
- Over-deepening of the pit, leading (for instance) to a reduced counterflow of anions.

The net result of these processes is that the rate of pit deepening typically falls off with time (t), i.e. pit depth (d) obeys an equation of the form

$$d = kt^n$$

where k and n (<1) depend on the material and the corrosion environment (Newman and Franz, 1984).

12.4.3 General (uniform) corrosion

As explained, the electrochemical theory of corrosion proposes that both electron-producing (anodic) and electron-consuming (cathodic) reactions are necessary for corrosion to occur. In metals, where electron flow occurs easily, these reactions can occur at widely separated positions, provided also that there is a continuous moisture path between the cathode and the anode. Figure 12.4 illustrates the point that, even in the absence of the chemical micro-environments that characterise true 'localised corrosion' (in the sense of the previous sections), it is still expected that anode and

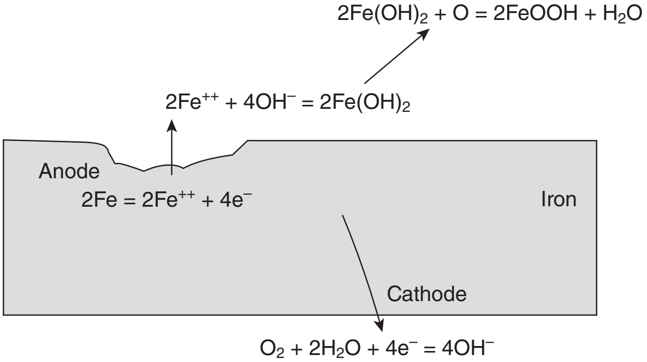

12.4 Nominally uniform aqueous corrosion of iron.

cathode will be separated in space so that the anodic reaction will always be localised to some extent. The factors that may cause one part of the metal to be anodic and another part to be cathodic are diverse and include:

- Local cold deformation of the metal – this constitutes a point of higher energy that will be anodic
- Welds
- Occlusion of the solution, which may allow locally acidic conditions or differential aeration to develop
- The aspect of an object with respect to the prevailing weather – often the weather side is cathodic because rain washes off any loose deposits
- Differential aeration – if one part of the surface has easier access to oxygen, cathodic reactions will usually occur there.

An example of the last factor occurs in the corrosion of large underground pipelines: the soil adjacent to the upper part of the pipe will contain higher levels of oxygen which will favour the cathodic reaction. Consequently, such pipes are often more corroded on the underside.

Over a long period of time, dissolution of 'preferred' anodic areas and the build-up of corrosion products around the anodic surface may cause the anodic and cathodic areas to change position. So, even though at any one time only certain parts of an object will be undergoing corrosion, over an extended period the corrosion may appear to be relatively uniform.

In heavily corroded iron it can be difficult to distinguish between uniform and localised corrosion – indeed, it is possible to argue that localised corrosion is the prime corrosion mechanism, with the metal surface being consumed by the sideways growth of pits. The propensity to pitting corrosion is sometimes expressed through a 'pitting factor' which expresses the ratio between mean pit depth and the uniform metal loss. In iron the pitting factor is typically 3 or 4. In stainless steel, on the other hand, when pitting occurs, it can be orders of magnitude faster than uniform corrosion.

12.4.4 Influence of storage or disposal environment

The anticipated disposal environment will clearly be a major determinant of the container design and, in particular, the container material. Regardless of how it is to be disposed, however, a waste container will need to be designed to maintain its integrity under a range of environmental conditions. Partly, this is because, as previously described, it is advantageous from the perspectives of cost and worker radiation doses if a waste package can serve for both storage and disposal. Additionally, it is invariably the case that closure of a repository (i.e. backfilling and sealing) will occur some time after the first waste emplacements. For many repository designs, this means that waste containers will, in effect, be subject to a period of on-site storage whilst repository operations continue. This operational period could persist for many decades during which waste packages must be preserved. This may require control of humidity and salinity levels in the repository environment.

12.5 Radioactive waste containers in use or proposed

12.5.1 Thick-walled iron and steel containers

Thick-walled iron or steel containers have been used for many years in the storage and transportation of SNF. Most well known, perhaps, is the so-called CASTOR container (Cask for Storage and Transport) developed in Germany. These are made from ductile cast iron, are 30–40 cm thick and are equipped with fins to aid cooling; they are approximately 6 metres long, have a diameter of about 2 metres and can weigh up to 140 tonnes when loaded (e.g. Droste, 2001). Similar, though more recent, is the POLLUX container, which was developed by the Gesellschaft für Nuklear-Behälter mbH (GNB) for transport, storage and deep geological disposal of SNF. This consists of an inner and an outer container and weighs up to 65 tonnes when laden (Fig. 12.5). For the purpose of disposal, the fuel assemblies are dismantled and the fuel rods are loaded into baskets within the inner container, which can hold rods from up to 10 PWR or 30 BWR fuel assemblies (Droste, 1995; Filbert and Bollingerfehr, 2008). The inner container is forged in one piece from low-alloy steel of nominal composition 1.5% manganese and 0.63% nickel. It has a thick wall section and two lids – one screwed on and the other welded into place. Welding may be performed using a variety of techniques (tungsten inert gas, electron beam, submerged arc, etc.). The

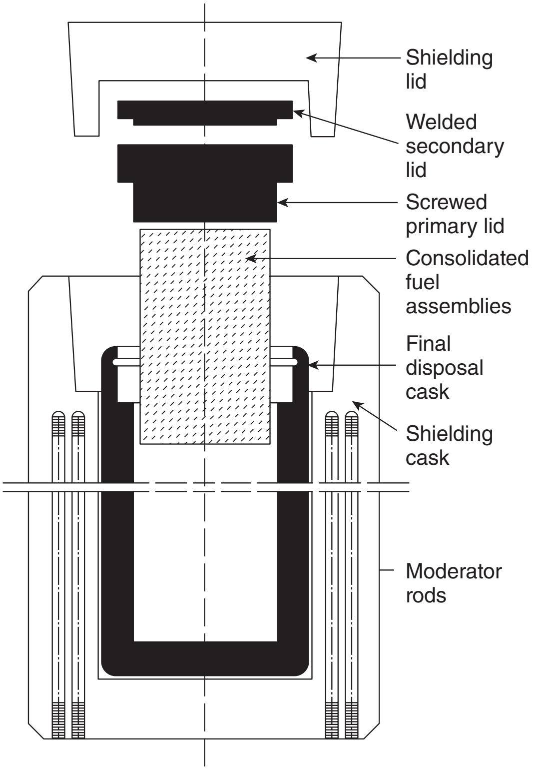

12.5 POLLUX container for storage, transport and disposal of spent nuclear fuel (courtesy Dr Bernhard Droste, BAM, Berlin, Germany).

outer container is similar in thickness to a CASTOR container and, like the CASTOR, is made from ductile cast iron and incorporates an array of moderator rods. This is closed with a massive cap that serves to provide radiation shielding during transport and repository operation. The German concept for disposal of SNF entails emplacement of the inner container in an underground salt formation (Witherspoon and Bodvarsson, 2001). This would be a low-humidity environment where corrosion rates would be extremely slow but, to cover the possibility that the salt formation could suffer a major water intrusion at some time, corrosion tests are also performed in brine solutions. Under these conditions, iron and steel have the general advantage that they are resistant to localised corrosion. An alternative design, which departs from the corrosion allowance approach and aims to deploy a material that is resistant to corrosion, is briefly described in Section 12.5.6.

The use of thick iron-based containers for disposal of heat-generating HLW and SNF is also being considered in France (Andra, 2005), Switzerland

12.6 Stainless steel container (primary waste package) for vitrified high-level waste in France and UK (courtesy Sellafield Ltd, UK).

(Nagra, 2004) and Japan (JNC, 2000). The primary waste package for vitrified HLW (so-called Type C waste) in France is a thin-walled stainless steel container that is 1.34 m long and 0.43 m in diameter (Fig. 12.6). For the purpose of disposal it is proposed to seal each one inside a 55 mm thick carbon steel overpack with a welded-on lid (Fig. 12.7). The overpacks are fitted with external ceramic runners (pads) that allow the overpacks to be pushed into, and slide along, a horizontal emplacement borehole drilled from an underground gallery. The 55 mm thickness is intended to provide a design lifetime of 4,000 years.

For SNF, Andra proposes much larger containers capable of taking either one or four fuel assemblies; again these are made from carbon steel. The intended physical containment period is 10,000 years and, as a result, the container wall thickness is increased to either 120 or 130 mm. In this case the lid has a thickness that is more than double that of the walls. This is for reasons of strength and handling, and to provide a weld root face.

In Switzerland, the container for vitrified HLW or SNF would most probably be a forged or cast steel cylinder, 5 m long and 1.05 m in diameter, with a wall thickness of at least 15 cm and a welded-on lid. This container

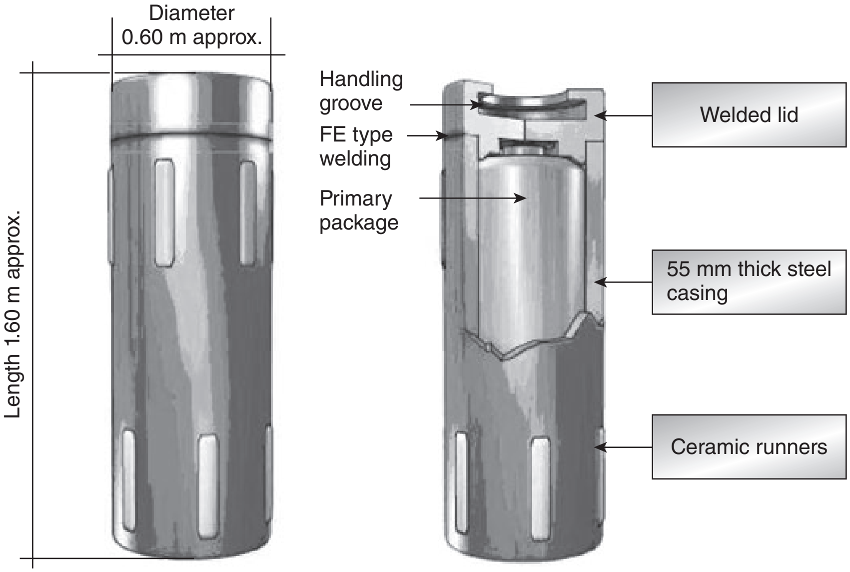

12.7 Overpack for vitrified waste primary package in France (courtesy Andra, France).

would be dual purpose, serving the needs of both transport to the disposal site and disposal itself. Assuming disposal was in an indurated clay formation, the containers would be expected to remain intact for at least 10,000 years (Nagra, 2004). A specific issue with respect to iron-based containers is the evolution of hydrogen caused by the reduction of water by iron under anaerobic conditions and, in particular, the effect this could have on evolution of the near-field environment. A recent Nagra report acknowledges the need for further work on this and for a comprehensive programme on the evaluation of technological solutions for fabrication, welding, surface finishing and stress mitigation of thick-walled steel canisters (Landolt *et al.*, 2009).

12.5.2 Stainless steel

General

Austenitic stainless steel is a widely available material that is corrosion resistant, ductile and easily welded. It is not surprising, therefore, that it has come to be used for the manufacture of waste containers. Almost invariably, AISI 304 (18%Cr, 8%Ni) or, more recently, AISI 316 (16%Cr, 10%Ni, 2%Mo) are used in the low-carbon (304L and 316L) or stabilised-carbon grades. These grades help to prevent the formation of chromium carbides and, therefore, adjacent chromium-depleted zones, during heat treatment. The replacement, in type 316 steel, of some of the chromium with molybdenum improves the resistance to localised corrosion. Where it is anticipated that the container will experience higher temperatures, as in the case of vitrified HLW, AISI 309 steel (22%Cr, 12%Ni) may be used. The higher chromium content provides adequate corrosion resistance at the higher temperature while the nickel is increased to maintain the austenitic structure.

Primary waste containers for vitrified HLW and compacted long-lived wastes

Vitrified HLW is produced as a result of the reprocessing of SNF. It consists primarily of fission products dissolved in borosilicate glass, which is poured into the containers at a temperature of around 1100°C. The containers are fabricated from 3 mm thick sheets of AISI 309 steel. The vitrified HLW is intensely radioactive so that filling and sealing operations must be done remotely. The capacity of each container, known as a CSD-V container in France, is 0.15 m^3. These same containers, with a change in name to CSD-C, are also used in France as primary waste packages for compacted technological wastes such as fuel assembly components, hulls and ends, etc., remaining from reprocessing (Andra, 2005). Sealing is effected using electron beam welding.

According to German workers, if disposal is in a suitable salt formation, it is possible to use these primary waste packages as disposal packages (Filbert *et al*., 2008). This assertion is based on the very low humidity levels that pertain in salt formations and the resulting absence of localised corrosion. As indicated in the previous section, however, if disposal is not in salt, then the primary waste container will usually require some form of overpack before it can be emplaced in a deep geological repository. A particularly interesting concept for disposal of vitrified HLW is the 'supercontainer' developed by Niras-Ondraf (Belgium). This consists of a sealed, 30 mm thick, carbon steel overpack capable of containing two CSD-V primary waste packages. This, in turn, is surrounded by a thick concrete outer shell (Bel *et al*., 2006; Niras-Ondraf, 2008). Such an arrangement provides both containment and shielding.

Containers for long-lived intermediate-level wastes

Containers made from type 316 stainless steel are widely used in the UK for packaging the long-lived intermediate-level wastes produced by SNF reprocessing. The Nuclear Decommissioning Authority (NDA), the UK's national waste management organisation, has developed a range of stainless

12.8 UK 4 metre box (courtesy NDA, UK).

steel packages for disposal of these wastes. Typical examples are the 4-metre box (Fig. 12.8) and the 500-litre drum (Fig. 12.9) (Nirex, 2001). The latter comes in a number of variants. The one shown in Fig. 12.9 contains an internal paddle that allows the waste and encapsulation matrix to be homogenised by stirring. The paddle remains in the drum after mixing. Another variant receives the wasteform pre-mixed and, therefore, does not have a paddle; and a third, used to hold smaller drums that have been supercompacted into 'pucks', is made with an in-situ concrete liner (Fig. 12.10).

All these containers are vented to prevent the build-up of pressure due to gas generation, indicating that absolute physical containment is not a safety objective. As made clear by the NDA waste package specifications (Barlow *et al.*, 2000), stainless steel is chosen not for reasons of post-closure safety, but to preserve the handle-ability and mechanical integrity of the packages during the period (perhaps 100 years) leading up to repository closure.

IAEA BOSS concept

Sealed radioactive sources are used throughout the world for a wide range of industrial, medical, agricultural and research purposes. In modern practice it is usual for the manufacturer to agree to take back the source for disposal or recycling at the end of its useful life. To allow this, the manufacturer may include the cost of disposal or recycling in the price of the source. There exist, however, many thousands of old disused sources that were created before such arrangements were established. A particular problem exists with disused radium needles previously used in medical therapies: radium-226 is fairly long-lived (1600 years half-life), its salts are usually soluble and, often, the needles are sealed with nothing more substantial than gold foil. As a means of promoting the safe storage and disposal of these and other radioactive sealed sources, IAEA has developed the BOSS concept (Nel, 2005; Nel and Potier, 2005). The concept has been

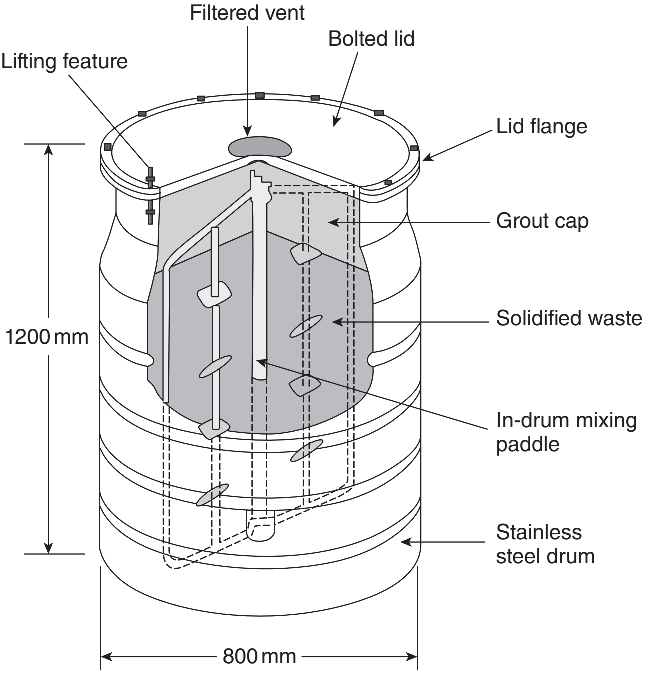

12.9 In-drum mixing version of UK 500 litre drum (courtesy NDA, UK).

extensively tested but has yet to be deployed to the extent of an actual disposal.

According to the BOSS concept, disused sealed sources are first conditioned for storage by sealing them inside a 3 mm thick type 316L stainless steel capsule. The conditioned sources are then placed within a concrete insert inside a 6 mm thick 316L stainless steel container (Fig. 12.11), which, like the capsule, is also sealed by welding. Given appropriate geochemical (e.g. anaerobic) conditions, the combined thicknesses of the capsule and container (9 mm) should be capable of providing absolute physical containment for hundreds of thousands of years, which is more than enough to allow radium-226 (for instance) to decay to exemption levels.

12.5.3 Copper containers for HLW and SNF

The use of copper canisters for disposal of SNF is an integral part of the KBS-3 concept developed by the Swedish radioactive waste management organisation, Svensk Kärnbranslehäntering AB (SKB). This concept has also been adopted in Finland and, as a reference concept, in the UK. The complete container consists of a cast iron insert, which holds around 2

12.10 Sectioned waste package consisting of a series of 'pucks' (supercompacted 200 litre drums) cemented into a larger stainless steel drum (courtesy Sellafield Ltd, UK).

12.11 BOSS capsule and container with concrete insert. The lids of the container and capsule can be seen at the bottom of the picture.

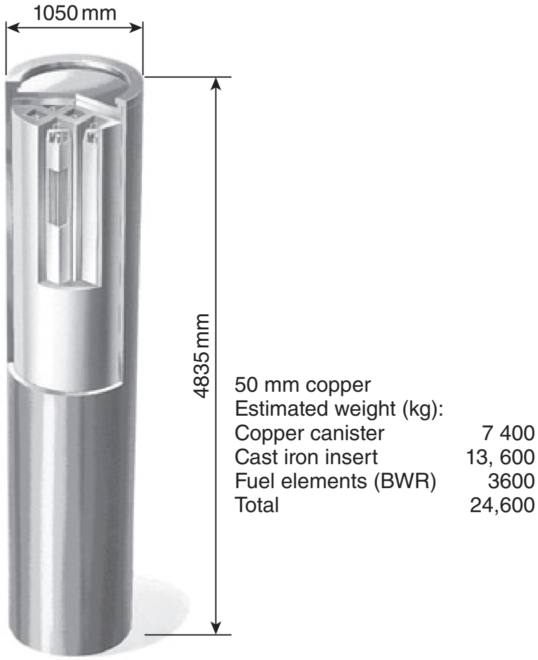

50 mm copper
Estimated weight (kg):

Copper canister	7 400
Cast iron insert	13, 600
Fuel elements (BWR)	3600
Total	24,600

12.12 Schematic of copper canister used in the Swedish KBS-3 disposal concept (courtesy SKB, Sweden).

tonnes of SNF, surrounded by an external 50 mm thick copper canister (Fig. 12.12). A filled container weighs more than 24 tonnes.

Four possible methods for fabrication of the copper tube have been investigated by SKB: roll forming of copper plate to form two halves which are welded together, seamless tubes formed by extrusion, pierce and draw processing, and forging. All these methods produce a copper cylinder that must be machined internally, externally and on the end surface to obtain the desired dimensions. Lids and bottoms are machined from hot-forged blanks. The thickness of the copper and its high thermal conductivity make conventional welding difficult. Consequently, friction stir welding and/or electron beam welding are likely to be deployed (SKB, 2006).

In the KBS-3 concept, disposal is effected by placing each container into an oversized deposition hole drilled into the floor (or in the 'horizontal' variant, the wall) of an underground gallery. The gap between the container and the surrounding rock is filled with a compacted bentonite clay 'buffer' that, on rehydration (following resaturation of the repository), swells to form a barrier that protects the containers from minor rock movement. Copper (unlike iron) is not oxidised by pure water and the low permeability buffer also limits the inflow of potentially corrosive agents in groundwater.

In so doing it provides a benign environment in which, even in a million year perspective, corrosion is insufficient to cause canister failure.

12.5.4 High-duty alloys for HLW and SNF

The Yucca Mountain facility, located at the Nevada Test Site, USA, was, until recently, being developed for the disposal of commercial and military SNF and HLW. While the project was abandoned in 2010, it is still worth describing here because it represents the world's most highly developed concept for disposal of HLW and SNF under unsaturated conditions. The proposed repository would have been located 300 m below the surface but still, because this is an arid region, 300 m above the groundwater table. Following waste emplacement, the disposal tunnels were to be sealed but not backfilled. The presence of water in the repository would have been limited to small quantities of infiltrating meteoric water and water already present in the rock. During the operational period, suitable environmental conditions within the repository were to have been maintained by forced ventilation. After closure, the conditions would have evolved naturally in response to the heat generated by the SNF and HLW. The combination of hot, aerobic, humid conditions made it necessary to use corrosion-resistant container materials. Potentially, the most severe corrosion conditions would have been reached some hundreds of years after closure when temperatures would be high enough to significantly increase corrosion rates but not so high that water would boil at the rock wall (i.e. the surface of the vault), which would prevent it from dripping from the vault roof onto the waste packages (Payer, 2004).

Wastes mostly consisted of SNF assemblies with smaller quantities of vitrified HLW in stainless steel canisters. These would have mostly arrived at site in a primary waste container known as a transportation, aging and disposal (TAD) container. These would then be enclosed in an overpack made in a range of geometries to suit the various kinds of TAD container. The overpack was specifically intended for good corrosion resistance in elevated temperature, unsaturated conditions with a double wall design. The inner wall was 50 mm thick and made from type 316, low-carbon, low-nitrogen stainless steel with a 65 to 130 mm thick lid. This inner wall supported the outer wall which was made from 20 to 25 mm thick corrosion-resistant nickel alloy (so-called restricted Alloy-22, see below). The outer wall had a 25 mm thick closure lid, also made from restricted Alloy 22 (Doering and Pasupathi, 2002; Witherspoon and Bodvarsson, 2001). Both lids were to be welded in place using gas tungsten arc welding. To divert dripping water away from the waste packages and thereby extend their life, Titanium Grade 7 drip shields were to have been placed over the waste packages shortly before repository closure (Fig. 12.13). Both the inner and

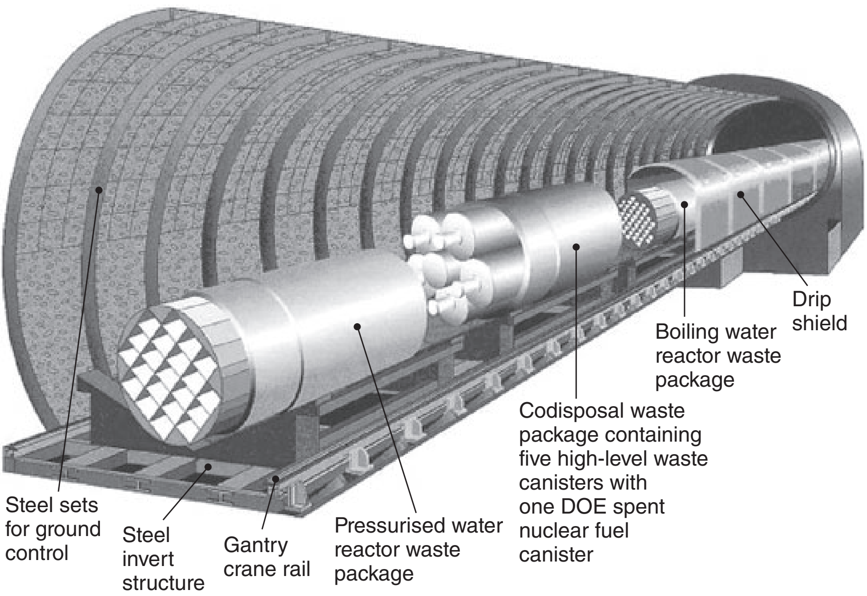

12.13 Cutaway view of waste packages in a Yucca Mountain disposal drift (courtesy US DOE).

outer containers of the overpack were to be fabricated from sheet material to pressure vessel standards (even though the outer container was needed to function only as a corrosion barrier).

Restricted Alloy 22, so-called because its composition is more tightly controlled than normal Alloy 22, has the following composition: (a) chromium = 20.0% to 21.4%, (b) molybdenum = 12.5% to 13.5%, (c) tungsten = 2.5% to 3.0%, (d) iron = 2.0% to 4.5%, with the balance of nickel. Like stainless steel, general corrosion rates of Alloy 22 are extremely low and, under the conditions envisaged for Yucca Mountain, resistance to localised corrosion was likely to be the more exacting criterion, especially if water could have dripped from the roof of the vault onto the hot waste packages. The purpose of the drip shields was to prevent this but, even in their absence, it is possible that the waste packages would have had sufficient corrosion resistance to provide adequate physical containment (Payer, 2004).

12.5.5 Mild and low-alloy steel for LILW

Containers for low-level and short-lived intermediate-level waste (LILW) are made in a range of sizes and shapes. Most frequently encountered is the open-topped ‘200 litre’ (actually 210 litre) steel drum which comes with a close-fitting lid that can be secured in place using a hoop device that fits around the rim of the drum. The principal advantages of the 200 litre drum are cost and availability; it is also the largest size of container that can be moved with simple manual handling equipment. On the other hand, its limited size may require waste items to be reduced in size, its shape results in inefficient use of repository space, and its thin section (usually around 1 mm) and corrodibility demands good storage conditions if it is not to be soon penetrated. Depending on the nature of the disposal site, it may be possible to dispose of the drums directly without further treatment, as happens for transuranic wastes at the WIPP repository in New Mexico. In many circumstances, however, storage and disposal space will be more efficiently utilised if the drums are supercompacted and then cemented into larger containers, as illustrated in Fig. 12.10.

A second example of a mild steel container used for radioactive waste is the half-height standard ISO container used at the near-surface repository near Drigg, north-west England (Fig. 12.14). With the top of the ISO container removed, wastes are emplaced and, when full, the lid is put into place and any voidage within the container is filled by flooding it with a liquid

12.14 A waste container being handled by forklift in Vault 8 at the UK near-surface repository for LLW in north-west England (courtesy LLW Repository Ltd, UK).

cement grout. The containers are stacked in the repository vault which, at closure, is to be covered with a low permeability cap.

A final example of a mild or low-alloy steel container used for radioactive waste – in this case used for storage – comes from nuclear power plants (NPPs) of Russian design. These NPPs are common in former Soviet countries and usually recycle waste water using a method known as deep evaporation. This produces a solid residue, sometimes known as 'fusion cake', that is at the lower end of the intermediate-level waste range. It largely consists of sodium and potassium nitrates and borates contaminated with radionuclides such as Cs-137, Co-60, etc. The fusion cake is poured in its hot, molten state through a hole in the lid of a specially made container. Such containers are usually made from 6–8 mm thick low-alloy steel and have a capacity between 100 and 300 litres. After filling, a steel plate is welded over the hole. Nitrates and borates have a passivating effect on mild steel and, while the design lifetime is said to be 15 years, experience in Ukrainian NPPs suggests that, when painted on the outside and kept in a suitable storage environment, container integrity may be retained for significantly longer than this.

12.5.6 Container materials considered or in development

Kursten *et al.* (2004a with a summary at 2004b) describe the outcome of a number of programmes designed to identify suitable materials for radioactive waste containers. In addition to the materials already described above, these include low-alloy steels, so-called Ni-resists, Cr-Ni stainless steels, cupronickel, a number of standard Ni-base alloys and the titanium alloy Ti99.8-Pd. Low alloy steels may be preferred over plain carbon steels because of their superior mechanical properties but, because their corrosion properties and methods of fabrication are essentially the same as those of unalloyed steel, they are not discussed further here (but see Section 12.5.1). Similarly, Cr-Ni stainless steels have already been discussed and are not described further.

Cupronickel (specifically, copper with 30% nickel) was investigated as part of the Spanish programme of research into candidate materials for disposal of SNF in granite. Comparing the results with oxygen-free copper, the cupronickel data indicated a stronger dependence of corrosion on temperature, more localised attack at the highest temperature (100°C) and a susceptibility to stress-corrosion cracking. For this reason cupronickel was rejected as a candidate material.

In support of the German disposal concept of emplacement in deep salt formations, corrosion and stress corrosion tests were performed in brine solutions (45 wt% $MgCl_2$) at a temperature of 170°C on a number of already available alloys. The intended use of these alloys was as a 3–4 mm thick corrosion-resistant cladding to be placed over a steel inner housing. The test conditions essentially represent a fault situation in which brine intrusion occurs into a part of the (normally dry) repository. The alloys tested included Ni-resist alloys, three superalloys (Hastelloy C-4, Inconel 625 and Incoloy 825) and titanium + 0.2% palladium ('Ti99.8-Pd'), which is the most corrosion-resistant alloy of titanium. Only two of the alloys – Hastelloy C-4 and Ti99.8-Pd – were found to be sufficiently resistant to localised corrosion to justify more comprehensive testing. This subsequent testing programme revealed that, while Hastelloy C-4 has satisfactorily low uniform corrosion rates, at high gamma dose rates[1] it is susceptible to pitting at a rate of 1 mm per year. In the absence of radiation, 0.2 mm deep pits were seen after 3 years at the highest test temperature (200°C). Similar tests conducted on the titanium alloy Ti99.8-Pd failed to show any evidence of localised corrosion. The highest uniform corrosion rates, though still less than 1 μm per year, were observed in the presence of high gamma fields.

12.6 Quality management of metal containers

12.6.1 General

The application of a rigorous quality management system (i.e. the combination of quality assurance and quality control) is essential for safety-sensitive operations such as steps leading to the packaging of radioactive waste (IAEA, 2008). The management system should aim to ensure the application of appropriate quality assurance and quality control measures during the various packaging stages, including the manufacture of containers and their sealing. Such measures will probably be demanded by the waste acceptance criteria and are almost certain to be an important element of regulatory compliance. The regime represented by ISO 9001:2000 (ISO, 2000) provides a well-recognised and auditable standard and is widely used by organisations tasked with radioactive waste management. Compliance with ISO 9001 requires that quality management should be embedded into the operations of the enterprise and this will be reflected, for instance, in company mission statements, company objectives and job descriptions.

Application of a quality management approach will usually begin with an analysis of the company activities and a categorisation of these activities

---

[1] The effect of radiation on water is to cause it to dissociate, producing electrons and a series of radicals of which the most reactive are the uncharged hydroxyl and hydrogen radicals. A series of secondary reactions then lead to the formation of H_2, which is relatively unreactive, and oxidisers such as hydrogen peroxide. Consequently, radiolysis usually leads to an increase in oxidation potential and often, therefore, an increase in corrosion rate (Turner, 2004).

according to their relevance to the company mission. For a company that is tasked with radioactive waste management, this usually equates to a ranking according to relevance to safety. Procedures for the various activities are then prepared, introducing into the procedures measures to provide the required level of assurance. These measures may include controls such as monitoring and inspection. In applying the procedures, an important element is the creation of records that individuals must sign to say that the procedures have been followed and that the activity has been satisfactorily completed. This provides both an audit trail and personal accountability.

12.6.2 Quality and waste containers

It is important to recognise that there is no one-size-fits-all solution when applying quality management to container design and manufacture. What is needed is a graded approach in which the level of assurance is commensurate with the required safety functions of the container – see, for example, Appendix II of IAEA (2008). These safety functions are most effectively defined through comprehensive safety assessments for storage, transport and disposal. It is clear, for example, that there is no point in designing a container whose service life greatly exceeds the longevity of the hazard represented by the waste and, indeed, a waste container could have a service life that was much shorter than the longevity of the hazard provided that the repository design introduced other safety functions that obviated the need for a container. If it were intended, for example, to enclose the primary waste container in a high-integrity overpack, the primary container may not itself need to retain its leak-tightness over a long period, so that the quality management measures for the primary container would be focused on the need for them to retain their integrity until the overpack is put in place. Similarly, some disposal concepts, especially those using deep salt formations, can achieve the required level of long-term safety without needing to rely on long-term physical containment. In these circumstances, the quality measures will reflect this and the container properties will most likely be determined by considerations of transport, storage and handling at the disposal site.

In all cases, when applying a quality management system to waste containers, one expects attention to be focused on three main aspects: material supply, the condition of the as-supplied containers, and final sealing (e.g. fitting of a lid) after the container has been filled. Measures designed to control material supply would aim to demonstrate that the container body, the lid and, where applicable, welding consumables and fixings were made from the correctly specified grade of material. The minimum requirement in terms of material supply is likely to consist of the analyses provided by the supplier of the steel and, where applicable, the weld metal. At the other extreme, high-integrity containers for disposal of SNF or HLW could be made from a special type of material and may require more than one chemical analysis for each individual container.

When it comes to the condition of the as-supplied containers, similar considerations apply. The minimum requirements are manufacture under a quality management regime to specified standards on wall thickness, painting, leakage rates, etc., that had previously been shown to be adequate. Where high-integrity containers are concerned, it is likely that detailed records will be required describing the manufacture of each individual container, results of non-destructive testing, examinations of samples and so on.

Finally, fixing of the container lid is likely to be performed by the waste producer or the disposer. Again, the level of detail required by the waste acceptance criteria will vary depending on how the container is supposed to perform. In the 'minimum' case it may be sufficient to record that an approved means of closure was used. At the other extreme, and taking the example of the Swedish KBS-3 concept, we can see the kind of measures that will be necessary. Because of the high radiation field, all procedures must be performed remotely. The SNF is first placed in the steel insert, which is closed using a bolt-on lid. Next, the lid of the outer copper container is welded into place and radiographic and/or ultrasonic non-destructive testing techniques are then used to verify the integrity of the weld. These procedures require extensive research, development and demonstration.

12.7 Future trends

Radioactive waste management is an inevitable but nonetheless unwanted outcome of nuclear power and nuclear technologies. It is an activity that has the potential to impact unfavourably on human life and the environment yet, at the same time, it yields no income or profit to the waste generator; indeed, it is a drain on resources. In part, this is why radioactive waste management is so highly regulated; it is also the reason why it is important to consider the 'back end' before initiating any new nuclear project. All this underlines the importance of waste avoidance (usually, though misleadingly, called waste minimisation) and the need to reduce the costs of waste management when this can be done safely.

So, with respect to future trends in waste container technology, reduction in costs (while maintaining safety) is a clear priority. There are a number of ways in which this may be achieved. One is through economies of scale brought about by fixing on a small number of standard container designs for the various waste types. Given that most countries do not allow importation of radioactive waste, this will normally be done on a national basis but there is, nonetheless, no reason why some waste container designs should not be common to several countries, much as happens with the CASTOR container and some that occur throughout the former Soviet Union. As explained previously, while the 200 litre drum is ubiquitous, it does not lead to the efficient use of available repository space. The standardisation of waste containers could lead to the introduction of larger containers that partly remove the need to size-reduce the wastes and, being rectangular parallelepiped, are space filling and so make better use of the repository volume.

An increased focus on cost reduction is likely to place greater reliance on lower-cost materials such as steel and cast iron provided, of course, that the needs of safety can be met. A saturated deep geological repository will almost always provide anaerobic conditions, in which case an iron or steel container with a wall thickness of 400 mm is likely to provide physical containment for, perhaps, 100,000 years. Such a solution will be cheaper (in materials at least) than, say, a 50 mm thick copper container or even a much thinner container made from titanium. It also has the advantage of support from natural analogue data and does not lead to the burial of valuable metals as waste.[2] For these reasons a move to superalloys or more unusual materials such as Ti99.8-Pd seems unlikely. Another lower-cost alternative is the use of concrete containers, which is described elsewhere in this book.

Another means of cost reduction is design optimisation, which may also be described as the avoidance of over-specification in the container design. Clearly, though, this has the potential to impact on safety and therefore needs detailed consideration through safety assessment, which may be used to define the safety functions that are required of the containers. As the technology of deep geological disposal becomes mature, however, we should expect to see developments of this kind.

12.8 Sources of further information and advice

Much of the information that is relevant to containers for radioactive waste is published by national waste management agencies. Almost without exception, these agencies have transparency policies that require them to provide virtually free access to their reports and research findings. Many of these reports are available in English and most of them can be freely downloaded from the Internet. Hard copies can also be requested although, here, there may be a charge to cover administrative costs and postage. The British, Finnish, French, Swedish and US agencies (DOE) are particularly useful in

---

[2] While it is sometimes said that wider use of copper containers could create difficulties with respect to copper supply, this seems unlikely. Together, the world's nuclear reactors discharge a few thousand tonnes of spent fuel annually. Some of this is sent for reprocessing but, even if all of it were to be encapsulated in copper, this would still use less than 0.1% of annual world mined copper production.

this respect. The relevant organisations, addresses and websites are listed below. The website of the Belgian research organisation SCK/CEN is also a useful source, as is that of BAM, which contains information on the large waste containers (CASTOR, POLLUX, etc.) originating from the German programme.

Two other useful sources, for both international regulatory standards and technical information are the IAEA and OECD-NEA. Virtually all IAEA reports (including all those listed in the references) and even some draft safety standards are available in downloadable form.

The contact details or relevant organisations are given below.

- Andra. Agence Nationale pour la Gestion des Déchets Radioactifs, 1/7, rue Jean Monnet, Parc de la Croix-Blanche, 92298 Châtenay-Malabry, Cedex, France (www.andra.fr).
- BAM. Federal Institute for Materials Research and Testing, Unter den Eichen 87, 12205 Berlin, Germany (www.bam.de).
- IAEA. International Atomic Energy Agency, Wagramer Strasse 5, PO Box 100, Vienna, Austria (www.ieae.org).
- NDA. Nuclear Decommissioning Authority, Waste Management Division (formerly UK Nirex Ltd), Curie Avenue, Harwell, Didcot, Oxon, UK (www.nda.gov.uk).
- NEA-OECD. Nuclear Energy Agency of the Organisation for Economic Development and Cooperation, Issy-les-Moulineaux, Paris, France (www.nea.fr).
- Posiva. Posiva Oy, Olkiluoto, FI-27160 Eurajoki, Finland (www.posiva.fi).
- SCK-CEN. Studiecentrum voor Kernenergie / Centre d'Etude de l'Energie Nucléaire, Boeretang 200, BE-2400 MOL, Belgium (www.sckcen.be).
- SKB. Svensk Kärnbränslehantering, Blekholmstorget 30, Box 250, SE-101 24 Stockholm Savedom (www.skb.se).
- US DOE. US Department of Energy, 1000 Independence Ave., SW, Washington, DC 20585, USA (www.energy.gov).

12.9 References

Andra, 2005, Synthesis Argile: Evaluation of the feasibility of a geological repository in an argillaceous formation, part of the 'Dossier 2005' available in pdf format in September 2010 in English on the website www.andrm.fr.

Barlow SV, Carr NA and Wisbey SJ, 2000, *Waste Package Specification for Intermediate Level Waste*, Nirex Report N/007, May 2000.

Bel JJP, Wickham SM and Gens RMF, 2006, Development of the supercontainer design for deep geological disposal of high-level heat emitting radioactive waste in Belgium, *Mat. Res. Soc. Symp. Proc.*, Vol. 932.

Chambers AV, Ilett DJ, Tearle WM and Tweed CJ, 2002, *Modelling the Evolution of Repository Redox Potential*, AEA Technology Report for Nirex (available on request from Nuclear Decommissioning Authority, UK), AEAT/ERRA 0333.

Doering TW and Pasupathi V, 2002, *Waste Package and Material Testing for the Proposed Yucca Mountain High Level Waste Repository* (available from US DOE Office of Scientific and Technical Information, Oak Ridge, PO Box 62, TN 37831, USA).

Droste B, 1995, Safety assessment of HLW and spent fuel transport and storage casks, Vol. 1, pp. 243–248, in Proc. *Fifth Int. Conf. on Radioactive Waste Management and Environmental Remediation, ICEM'95*, Berlin, 3–7 September 1995, ed. S Slate, F Feizollahi and J Creer. Published by American Society of Mechanical Engineers, New York.

Droste B, 2001, Bauartprüfung, Qualitätssicherung und Sonderversuche mit CASTOR-Behältern, pp. 141–194 in *Fachtagung Standortnahe Zwischenlager*, 14–15 March 2001, Bonn (in German). IBSN 3-926956-43-7, published by Deutsches Atomforum e.v., Bonn.

Evans UA, 1981, *An Introduction to Metallic Corrosion*, 3rd edition, Edward Arnold, London.

Filbert W and Bollingerfehr W, 2008, Demonstration tests for direct disposal of spent fuel, presented at *2008 East Asia Forum on Radwaste Management Conference (2008 EAFORM Conference)*, 20–23 October, Session 13B.

Filbert W, Bollingerfehr W and Wehrmann J, 2008, Demonstration of the emplacement technology for the direct disposal of spent fuel into deep vertical boreholes, *Transactions of Research Reactor Fuel Management (RRFM) Conference*, Hamburg, 2–5 March 2008, ISBN 978-92-95064-04-1, published by European Nuclear Society, Brussels. Also downloadable from www.euronuclear.org.

Gillespie MR, 2001, *Potential for Secondary Iron Oxyhydroxide Minerals to Retard Radionuclide Migration: A Literature Review and Assessment*, Nirex Report NSS/R294, available from NDA, Harwell, Oxon, UK, www.nda.gov.uk.

IAEA, 2003, *Radioactive Waste Management Glossary*, 2003 edition, International Atomic Energy Agency, Vienna.

IAEA, 2006a, *Geological Disposal of Radioactive Waste*, IAEA Safety Standard Series WS-R-4, International Atomic Energy Agency, Vienna.

IAEA, 2006b, *Storage of Radioactive Waste*, IAEA Safety Standard Series No. WS-G-6.1, International Atomic Energy Agency, Vienna.

IAEA, 2008, *The Management System for the Processing, Handling and Storage of Radioactive Waste*, IAEA Safety Standards, Safety Guide GS-G-3.3, International Atomic Energy Agency, Vienna.

ISO, 2000, *Quality Management Systems — Requirements*, ISO 9001:2000, International Organization for Standardization, Geneva.

JNC, 2000, *H12: Project to Establish the Scientific and Technical Basis for HLW Disposal in Japan. Project Overview Report*, Second Progress Report on Research and Development for the Geological Disposal of HLW in Japan, JNC TN1410 2000-001, Japan Nuclear Cycle Development Institute.

Kursten B, Smailos E, Azkarate I, Werme L, Smart NR and Santarini G, 2004a, *State-of-the-art document on the COrrosion BEhaviour of COntainer MAterials*, European Commission 5th Euratom Framework Programme 1998–2002, COBECOMA Project Final Report, October 2004.

Kursten B, Smailos E, Azkarate I, Werme L, Smart NR, Marx G, Cunado MA and Santarini G, 2004b, Corrosion evaluation of metallic materials for long-lived HLW/spent fuel disposal containers: Review of 15–20 years of research, pp. 185–195, in *Nuclear Science and Technology, Euradwaste '04, Radioactive Waste Management – Community Policy and Research Initiatives, Proceedings of the Sixth European Commission Conference on the Management and Disposal of Radioactive Waste*, Luxembourg, 29–31 March 2004, ed. C. Davies, European Commission EUR 21027.

Landolt D, Davenport A, Payer J and Shoesmith D, 2009, *A Review of Materials and Corrosion Issues Regarding Canisters for Disposal of Spent Fuel and High-level Waste in Opalinus Clay*, Nagra Technical Report 09-02, January 2009.

Nagra, 2004, *Nagra Bulletin*, No. 35, May, p.27.

Nel B vd L, 2005, *Design of the Borehole Disposal Concept*, Necsa Report GEA 1623, Nuclear Energy Corporation of South Africa, Pretoria, July 2005.

Nel B vd L and Potier J-M, 2005, Development of the borehole disposal concept, in *Safety and Security of Radioactive Sources: Towards a Global System for the Continuous Control of Sources throughout their Life Cycle*, Proceedings of an International Conference held in Bordeaux, France, 27 June–1 July 2005, p. 471.

Newman RC and Franz EM, 1984, Growth and repassivation of single corrosion pits in stainless steel, *Corrosion*, 40, 325–330.

Niras-Ondraf, 2008, *Evolution of the Near-Field of the ONDRAF/NIRAS Repository Concept for Category C Wastes*, first full draft report, ed. S Wickham, NIROND-TR 2007-07E, April 2008.

Nirex, 2001, *Generic Phased Disposal System Documentation, Repository Design*, Nirex Report N/028, Volume 2 (Appendices), March 2001.

Payer JH, 2004, paper presented to US Nuclear Waste Technical Review Board, 18–19 May, 2004, available from US DOE Office of Scientific and Technical Information, Oak Ridge, PO Box 62, TN 37831, USA. Also Paper #32 at MRS 2005, 29th International Symposium on the Scientific Basis for Nuclear Waste Management, 12–15 September, 2005, Ghent, Belgium.

Puigdomenech I, Ambrosi J-P, Eisenlohr L, Lartigue J-E, Banwart SA, Bateman K, Milodowski AE, West JM, Griffault L, Gustafsson E, Hama K, Yoshida H, Kotelnikova S, Pedersen K, Michaud V, Trotignon L, Rivas Perez J and Tullborg E-L, 2001, *O_2 Depletion in Granitic Media, The REX Project*, SKB Technical Report TR-01-05, February 2001.

Salas J and Ayora C, 2004, Groundwater chemistry of the Okelobondo Uraninite-Deposit Area (Oklo, Gabón): Two dimensional reactive transport modelling, *J. Contaminant Hydrol.*, 69: 117–137.

Savage D (ed.), 1995, *The Scientific and Regulatory Basis for the Geological Disposal of Radioactive Waste*, Wiley, New York.

Sedriks AJ, 1996, *Corrosion of Stainless Steels*, 2nd edition, Wiley, New York.

SKB, 2006, *Long-term Safety for KBS-3 Repositories at Forsmark and Laxemar – a First Evaluation*, SKB Technical Report TR-06-09, October 2006.

Turner JE, 2004, *Atoms, Radiation and Radiation Protection*, 2nd edition, pp. 386–388, Wiley-VCH Verlag, Weinheim, Germany.

Witherspoon PA and Bodvarsson GS, 2001, *Geological Challenges in Radioactive Waste Isolation*, Lawrence Berkeley National Laboratory Report LBNL-49767, December 2001.

13

Failure mechanisms of high level nuclear waste forms in storage and geological disposal conditions

V. V. RONDINELLA,
European Commission
Joint Research Centre, Germany

Abstract: A schematic description of the main aspects constituting the back-end of the nuclear fuel cycle is provided: concepts and stages available or envisaged for the treatment of spent fuel, and main radionuclides (transuranics, fission and activation products) determining the properties of the waste form relevant for the storage/disposal concepts are mentioned. Nuclear fission determines the inventory, and, together with the irradiation conditions/history, the physical and chemical state of spent fuel at discharge. Radioactive decay determines the changes occurring after discharge; in particular, alpha-decay governs the accumulation of defects and damage in the waste; it also produces helium, whose accumulation behaviour over long time periods has to be assessed. The evolution of properties as a function of time is described in terms of mechanical stability and evolution of solid state properties; the main features characterizing the corrosion behaviour of high level waste are also described, including source term, radiolysis effects and chemical reactions occurring at the waste/water interface.

Key words: high level waste, HLW, spent fuel, nuclear waste glass, transuranium elements, fission products, waste storage, waste disposal, α-decay damage, corrosion behaviour, instant release fraction, radiolysis.

13.1 Introduction: the main aspects of the back-end of the nuclear fuel cycle

All existing and future concepts of nuclear fuel cycles share the requirement of physical concentration and sequestration from the biosphere of radiotoxic nuclides generated during the operation of nuclear reactors. This constitutes a key safety aspect which has a strong impact on the public perception of nuclear technology and on its full acceptance as a viable and effective source to ensure a sustainable supply of energy for future generations. Nuclear waste forms (spent fuel, glass or other matrices containing radionuclides) contribute to the fulfilment of this task together with all containment barriers (both engineered and natural) envisaged for all stages of treatment and disposal. Therefore, it is important to identify the boundary conditions defining the safe performance of the waste form and to assess any relevant mechanism which may cause its failure. The failure modes not related to deliberate human action which could lead to a mobilization of radiotoxic species for a given waste form are essentially associated with the following:

- Criticality events
- Power (heat) induced alterations in the waste package (waste form and containers)
- Radiation damage induced alterations causing loss of the mechanical integrity of the waste package
- Chemical corrosion processes.

Neutron irradiation is responsible for the generation of radioactive and radiotoxic nuclides which constitute the main source of hazard associated with high level nuclear waste. Table 13.1 lists the typical inventory of spent fuel from a light water reactor (LWR) at different burnup levels, while Table 13.2 illustrates the composition of a reference high level waste (HLW) glass (HLW consists of spent fuel in the case of open nuclear fuel cycle (direct disposal) or vitrified waste from reprocessing of spent fuel). Fission products and transuranics (produced by neutron absorption in actinide nuclei) dominate the radioactivity and the potential hazard of spent fuel and other waste forms. Radioactive decay, in turn, governs the behaviour

Table 13.1 Spent fuel inventory ($kg\,t_{HM}^{-1}$ of transuranic elements and relevant fission products) of LWR (PWR) fuel at different burn-up ten years after discharge from the reactor; data obtained from the Nucleonica database (www.nucleonica.net)

Fuel, Burn-up	UO_2 35 GWd/t_{HM}	UO_2 55 GWd/t_{HM}	MOX 50 GWd/t_{HM}
Initial fissile content	3.25% ^{235}U	4.7% ^{235}U	4.2% Pu
Pu	9.49	11.04	40.95
Np	0.48	0.83	0.20
Am	0.70	0.94	6.06
Cm	0.02	0.07	1.08
^{79}Se	0.002	0.004	0.003
^{90}Sr	0.447	0.693	0.281
^{93}Zr	0.756	1.187	0.737
^{99}Tc	0.857	1.284	1.144
^{107}Pd	0.240	0.364	0.807
^{126}Sn	0.025	0.039	0.070
^{129}I	0.171	0.265	0.320
^{135}Cs	0.388	0.739	1.125
^{137}Cs	1.038	1.595	1.437

Table 13.2 Composition of Areva NC R7/T7 reference vitrified HLW (Gras *et al.* 2007; see also waste glass composition table in IAEA 2008)

Component	Fraction (wt%)
SiO_2	45.1
B_2O_3	13.9
Al_2O_3	4.9
Na_2O	10
Fe_2O_3	2.9
NiO	0.4
Cr_2O_3	0.5
Fission products	12.4
Actinides (oxide)	0.37
Metal particles	1.6

and determines the safety requirements related to all aspects concerning the handling, storage and disposal of nuclear waste. In particular, radioactive decay governs the property evolution of the waste material as a function of time. The half-life and other relevant properties of key radionuclides are reported in Table 13.3.

The so-called back-end of the nuclear fuel cycle includes all activities affecting the fuel after the end of its operation in-pile. Right after discharge from the reactor core, spent fuel elements are too hot to be dry-handled or reprocessed, due to the decay power of short-lived nuclides produced during reactor operation (see Table 13.3); therefore, they are kept in wet storage facilities (cooling ponds) at the reactor site for several years or decades. Once the spent fuel has cooled down to a level allowing handling and transportation (but still requiring remote manipulation and appropriate shielding for the operators), different options are considered:

- Direct disposal of spent fuel elements
- Recycling of U and Pu through spent fuel reprocessing (IAEA 2008) followed by disposal of vitrified HLW, typically borosilicate glass (Lutze and Ewing 1988, Godon 2004; see also Chapters 6 and 9), containing minor actinides (MA – Np, Am, Cm) and fission products
- Recycling of U and Pu including separation of MA (and, in some cases, also long-lived fission products) for burning in nuclear reactors (partitioning and transmutation (P&T)) followed by disposal of the resulting waste (Kubota *et al.* 1993, Bychkov *et al.* 1997, Inoue and Tanaka 1997, Koch *et al.* 1999, Warin 2007, Grouiller *et al.* 2003, CEA 2004).

All the options considered for the back-end of the nuclear fuel cycle have in common three main steps:

Table 13.3 Selected properties of relevant radionuclides present in HLW; data obtained from the Nucleonica database (www.nucleonica.net)

Nuclide	$T_{1/2}$ (y)	Main decay mode	Spontaneous fission rate ($s^{-1}g^{-1}$)	Specific activity (Bq g^{-1})	Specific power (W g^{-1})
^{234}U	$2.46 \cdot 10^{6}$	α	$3.91 \cdot 10^{-3}$	$2.3 \cdot 10^{8}$	$1.79 \cdot 10^{-4}$
^{235}U	$7.04 \cdot 10^{8}$	α	$1.6 \cdot 10^{-6}$	$8.00 \cdot 10^{4}$	$6.0 \cdot 10^{-8}$
^{237}Np	$2.1 \cdot 10^{6}$	α	$5.1 \cdot 10^{-5}$	$2.61 \cdot 10^{7}$	$2.06 \cdot 10^{-5}$
^{238}Pu	87.7	α	$1.18 \cdot 10^{3}$	$6.33 \cdot 10^{11}$	0.567
^{239}Pu	$2.41 \cdot 10^{4}$	α	$1.0 \cdot 10^{-2}$	$2.3 \cdot 10^{9}$	$1.93 \cdot 10^{-3}$
^{240}Pu	6564	α	479	$8.4 \cdot 10^{10}$	$7.06 \cdot 10^{-3}$
^{241}Pu	14.3	β^{-}	$9.19 \cdot 10^{-4}$	$3.82 \cdot 10^{12}$	$3.28 \cdot 10^{-3}$
^{242}Pu	$3.75 \cdot 10^{5}$	α	805	$1.46 \cdot 10^{8}$	$1.17 \cdot 10^{-4}$
^{241}Am	432.7	α	0.545	$1.27 \cdot 10^{11}$	0.114
^{242m}Am	140	α, β^{-}	62	$3.88 \cdot 10^{11}$	$4.65 \cdot 10^{-3}$
^{243}Am	7370	α	0.27	$7.33 \cdot 10^{9}$	$6.43 \cdot 10^{-3}$
^{242}Cm	0.45	α	$7.47 \cdot 10^{6}$	$1.23 \cdot 10^{14}$	122
^{244}Cm	18.1	α	$4.0 \cdot 10^{6}$	$3 \cdot 10^{12}$	2.83
^{14}C	$5.7 \cdot 10^{4}$	β^{-}	–	$1.66 \cdot 10^{11}$	$1.31 \cdot 10^{-3}$
^{36}Cl	$3.01 \cdot 10^{5}$	β^{-}	–	$1.22 \cdot 10^{9}$	$5.34 \cdot 10^{-5}$
^{59}Ni	$7.6 \cdot 10^{4}$	β^{-}	–	$2.95 \cdot 10^{9}$	$3.39 \cdot 10^{-6}$
^{79}Se	$1.1 \cdot 10^{6}$	β^{-}	–	$1.52 \cdot 10^{8}$	$1.36 \cdot 10^{-6}$
^{90}Sr	28.81	β^{-}	–	$5.11 \cdot 10^{12}$	0.142
^{90}Y	$7.3 \cdot 10^{-3}$	β^{-}	–	$2.01 \cdot 10^{16}$	3010
^{93}Zr	$1.5 \cdot 10^{6}$	β^{-}	–	$9.31 \cdot 10^{7}$	$2.86 \cdot 10^{-7}$
^{93m}Nb	16.14	β^{-}	–	$8.83 \cdot 10^{12}$	$4.37 \cdot 10^{-2}$
^{94}Nb	$2 \cdot 10^{4}$	γ	–	$7.05 \cdot 10^{9}$	$1.96 \cdot 10^{-3}$
^{99}Tc	$2.1 \cdot 10^{5}$	β^{-}	–	$6.25 \cdot 10^{8}$	$8.54 \cdot 10^{-6}$
^{107}Pd	$6.5 \cdot 10^{6}$	β^{-}	–	$1.9 \cdot 10^{7}$	$2.8 \cdot 10^{-8}$
^{126}Sn	$2.3 \cdot 10^{5}$	γ	–	$4.57 \cdot 10^{8}$	$1.31 \cdot 10^{-5}$
^{126m}Sb	$3.5 \cdot 10^{-6}$	γ	–	$2.89 \cdot 10^{18}$	$1.02 \cdot 10^{6}$
^{129}I	$1.6 \cdot 10^{7}$	β^{-},γ	–	$6.37 \cdot 10^{6}$	$8.9 \cdot 10^{-8}$
^{135}Cs	$2.3 \cdot 10^{6}$	β^{-}	–	$4.26 \cdot 10^{7}$	$6.1 \cdot 10^{-7}$
^{137}Cs	30.06	β^{-}	–	$3.22 \cdot 10^{12}$	0.0967
^{137m}Ba	$4.9 \cdot 10^{-5}$	γ	–	$1.99 \cdot 10^{19}$	$2.1 \cdot 10^{6}$

- Handling and transportation
- Storage in a temporary (or interim) storage facility
- Final disposal in a geologic repository.

These three steps can be discriminated based on their duration and on the timescale (age of the waste form) involved; they are affected by the evolving properties of the waste form (spent fuel, waste glass or another waste matrix). This, in turn, defines the nature of the reference events/processes to be considered in safety design and assessment to ensure that radionuclide isolation is maintained under different relevant scenarios. The first two steps and all activities related to final disposal of HLW up to the time limit of active human control of the repository occur under strict monitoring and within well-defined operation safety limits. Any significant deviation from safe operation scenarios has to be considered an accident. Accidents should be viewed as singularities limited in time and extension. Appropriate safety and security procedures, together with the design of multiple containment barriers capable of withstanding reference accident conditions, should minimize the actual likelihood and impact of such events. The third step, especially in the case of spent fuel or HLW containing long-lived radionuclides, extends to timescales well beyond the duration of human civilization. This poses a limitation to the extent of active human control (and, if necessary, intervention) to ensure the long term safety of the disposal that can be guaranteed. Therefore, it must be assumed that in the long term the radionuclide sequestration function can be fulfilled by the geologic repository system also without active human monitoring and intervention.

13.1.1 Main radionuclides affecting the properties of the waste

Potential criticality risks are associated with the presence of fissile (or fissionable) species in the waste; therefore, criticality safety assessment is relevant in the case of spent fuel or conditioning matrices containing plutonium and/or other actinides. Criticality concerns can be tackled by ensuring that an appropriate spacing is present between waste elements or by introducing neutron-absorbing materials in the design of the waste package or in the layout of the storage or repository site (see e.g. Oversby 1998).

Different families of radionuclides govern radioactivity and thermal output of HLW at different timescales (see Tables 13.1, 13.2 and 13.3). During the first century after discharge, relatively short-lived fission products (namely Sr-90, Y-90, Cs-137 and Ba-137m) together with short-lived actinides are the main contributors to the radioactivity and the heat load of spent fuel and vitrified waste. The heat production is a key factor limiting the loading fraction of these fission products into specific waste forms (Gras *et al.* 2007). In particular, radiogenic heat in the case of HLW glass may induce devitrification processes, or extend recrystallization phenomena occurring during vitrified waste fabrication (Ojovan *et al.* 2004; see refs 2–7 in Rose *et al.* 2004; see also Caurant *et al.* 2006), resulting in the degradation of durability and overall performance of the waste form. The relatively fast decay rate of the fission products limits the long-term relevance of the heat dissipation issue in the case of HLW not containing Pu and minor actinides. In spent fuel, the heat production due to actinides becomes equivalent to that from fission products after ~70 years and is governed by Pu isotopes for the subsequent 100,000 years. Am-241 contributes significantly to the heat load up to ~1000 years. Figure 13.1 shows the heat load in the repository of different types of

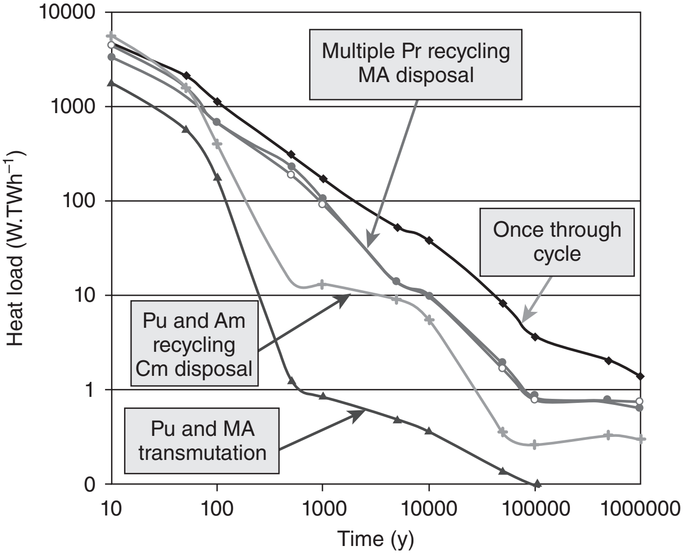

13.1 Evolution of heat in a repository for different types of HLW corresponding to different levels of separation and recycling of Pu and minor actinides (MA) from fission products (FP) (Gras *et al.* 2007).

HLW as a function of time. The curves highlight the potential reduction of the long-term heat load associated with separation and recycling of Pu and MA.

If present in the waste form, the contribution to the radioactivity by long-lived actinides (Pu-239, Pu-240, Am-241) becomes predominant after a few hundred years. In particular Pu-239 dominates the activity up to ~10^5 y. After a very long time from discharge, up to 10^6 years, actinides like U-234, Np-237 and Pu-242 constitute most of the radioactivity in spent fuel. Radioactive fission products present after ≥10^5 years are Pd-107, Sn-126 and Sb-126m.

In terms of long-term radiotoxicity, however, long-lived fission products like Tc-99 and I-129, together with Se-79 and Cs-135, are the main contributors in addition to the above-mentioned actinides, and dominate the potential hazard in the case of HLW not containing actinides. Figure 13.2 compares the radiotoxicity as a function of time for spent fuel, HLW from today's reprocessing (recycling of U and Pu), and the resulting HLW from a P&T concept. The curves on the diagram are normalized to a natural uranium ore and reveal the drastic reduction (from millions down to hundreds of years) of the time necessary to reduce the radiotoxicity to a level corresponding to 'natural' environments if adopting P&T.

Neutron activation products generated in structural components (e.g. grids, spacers, etc.) or from impurities in the reactor core contribute to a

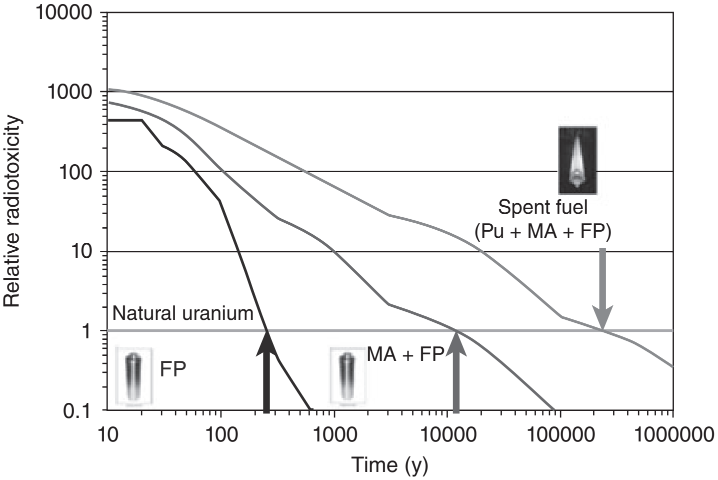

13.2 Evolution of radiotoxicity in a repository normalized to natural uranium for spent fuel, vitrified waste containing minor actinides (MA) and fission products (FP), and HLW containing only FP (Gras *et al.* 2007).

small extent to the radioactivity and the heat production in the HLW, and would be part of the HLW only in the case of direct disposal of spent fuel assemblies. Over the long term (≥10^5 years), Ni-59, and, in smaller amounts, Nb-94 will be present, together with Zr-93 and Nb-93m, which are both activation and fission products. C-14 and Cl-36 are also relevant due to their relatively high radiotoxicity.

13.1.2 Handling, transportation and interim storage

Handling and transportation have limited duration and occur when the waste form is relatively 'young'. The property evolution timescale for the waste package (including the waste form itself and the related containers: see Chapters 11 and 12) that has to be considered spans over the duration of the interim storage, if one assumes that no further handling/transport will take place after emplacement of the waste in the geologic repository.[1]

[1] Additional handling and transport must be considered in the case of retrievable disposal scenarios. This option has become more popular in recent years, and responds mainly to two concerns: the first is the possibility that what today is considered as waste could become a resource for tomorrow's advanced technologies; the second is related to a better acceptance by the public of disposal concepts in which HLW remains retrievable, e.g., for advanced treatment options aimed at reducing its radiotoxic lifetime.

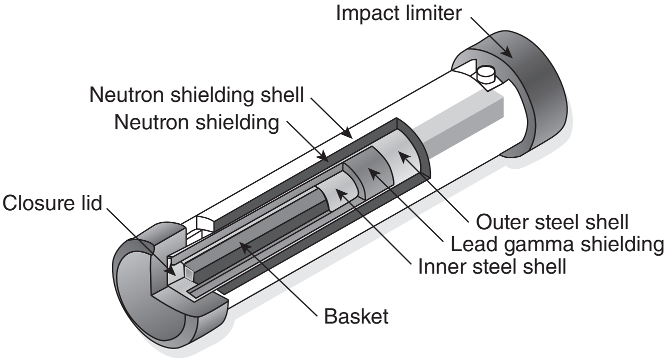

13.3 Schematic of a spent fuel road transportation cask (NRC). Weight including fuel: 25 tons; cask diameter: 1.22 m; diameter including impact limiters: 1.83 m; length including impact limiters: 6.10 m; capacity: up to four PWR or nine BWR fuel assemblies.

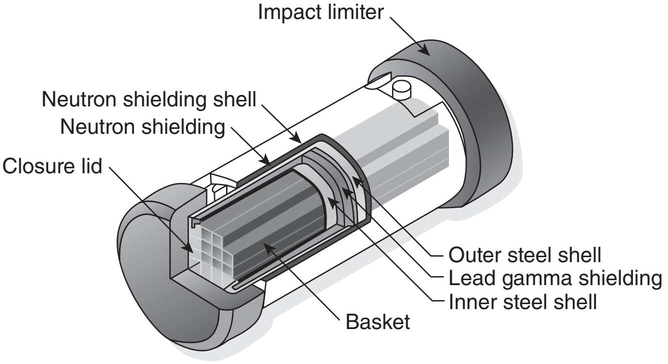

13.4 Schematic of a spent fuel rail transportation cask (NRC). Weight including fuel: 125 tons; cask diameter: 2.44 m; diameter including impact limiters: 3.35 m; length including impact limiters: 7.62 m; capacity: up to 26 PWR or 61 BWR fuel assemblies.

The reference scenarios that have to be considered for the safety assessment of these activities are accidental situations, which would be associated with isolated events. The design of relevant procedures and components (containers, barriers) aims at avoiding radiological dispersion in the environment as a consequence of such accidents. Figures 13.3 and 13.4 show a schematic configuration of transportation casks for spent fuel for truck and rail transportation, respectively (source: NRC).

The purpose of the interim storage stage is the temporary insulation of the waste up to a time when the waste can be transported to a reprocessing facility or to the geologic repository for final disposal. The timescale of interim

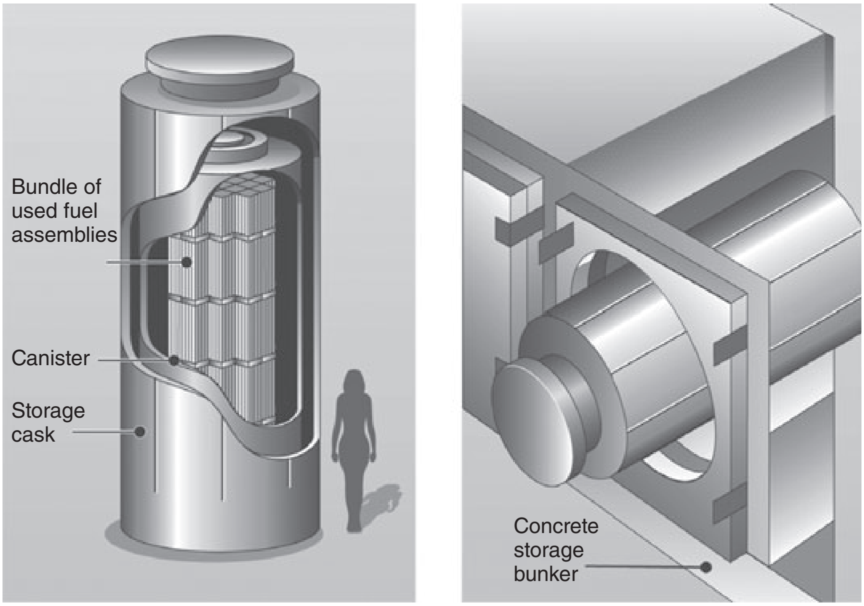

(a) (b)

13.5 Schematic views of (a) a dry storage cask for spent fuel and (b) a horizontal emplacement concept (source: NRC 2010).

storage ranges from a few decades (e.g. 40 years in the German concept) up to a few centuries (e.g. up to 300 years in the French concept) (Helie *et al.* 2006, Helie 2007). The fulfilment of the isolation requirement during storage is ensured by the physical layout and the containment barriers envisaged in the design of the containers (see Chapters 11 and 12; IAEA 2002) and the facility, and by maintaining appropriate operation conditions (in terms of temperature, humidity and container corrosion rate) during the storage time, through, e.g., cooling (dry or wet) and insulation from external water and chemical corrosion agents. Figures 13.5 and 13.6 show the schematic layout of a dry storage cask for spent nuclear fuel (NRC 2010).

The layout of the storage facility is affected by criticality and heat load considerations, which determine the spacing and overall volume occupied by the waste containers. The operation of the facility is designed to ensure that the waste form retains the necessary physico-chemical stability over the storage duration and in view of the subsequent handling/transport to the reprocessing facility or to the geologic repository. The engineering criteria to be fulfilled are defined in terms of maximum deformation and stress conditions to be acceptable over the duration of the storage period. For instance, German regulations define a maximum deformation of 1% and a

13.6 Dry storage casks facility for spent fuel (source: NRC 2010).

maximum level of circumferential stress of 120 MPa for the cladding of spent fuel rods during 40 years of dry storage (IAEA 2002). This, in turn, determines the temperature range for the safe operation of the facility. In addition to the assessment of accidental events, the duration of interim storage encompasses a certain evolution of the waste form properties. The stability of the waste form depends on some properties of the waste material, in particular its composition, chemical state and radioactivity level. In the case of spent fuel, the irradiation history and conditions (burn-up, temperature) determine the properties and behaviour of the spent fuel rod (fuel plus cladding) during storage.

13.1.3 Geologic repository

Figures 13.7 and 13.8 illustrate two examples of a geologic repository which refer to two concepts developed in Europe and in the USA, respectively (source: SKB, DOE, respectively). Figure 13.7 shows the schematic of the KBS-3 disposal concept, based on a deep, chemically reducing granite repository in the saturated zone as envisaged (among others) in the Scandinavian countries (SKB website, SKB 1983, 2008), while Figure 13.8 schematically depicts a chemically oxidative repository concept in the unsaturated zone as considered (but finally abandoned) for the Yucca Mountain site in Nevada, USA (US DOE 2008, Swift *et al.* 2009).

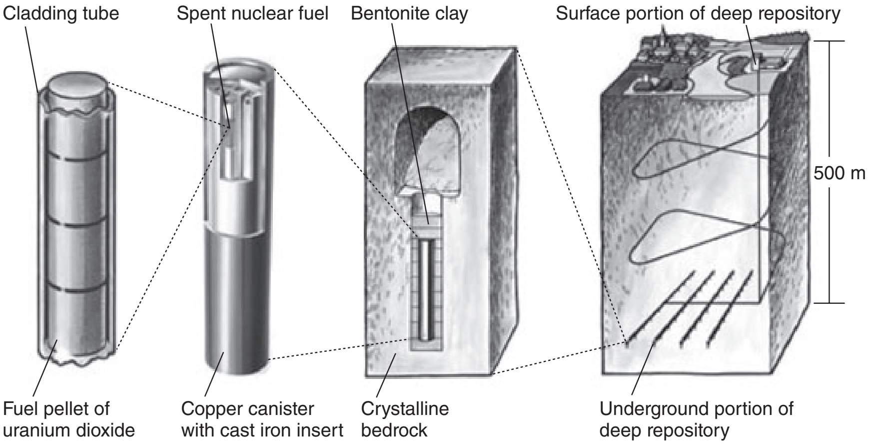

13.7 Schematic view of the emplacement of spent fuel in a deep geolgic repository. The scheme depicted in this figure refers to the ~500 m deep Swedish KBS-3 repository project (source: SKB).

The purpose of the final disposal stage is the insulation of the waste from the biosphere up to a time when the radiotoxicity of the waste will have decayed down to levels that will not constitute a source of hazard. This timeframe can be of the order of 10^5–10^6 years. The layout of the HLW emplacement in the repository is designed to satisfy the safety requirements in terms of criticality (if fissile species are present in the waste form) and thermal load effects. The radionuclide insulation goal will be achieved by the combined action of engineered waste containment barriers, environmental conditions characteristic of the selected repository site, and properties of the geologic media separating the repository and the biosphere. All these factors, acting individually or in synergy, will contribute to retarding the exposure of the waste to groundwater, minimizing the corrosion and mobilization rates of radiotoxic species away from the waste material, and finally minimizing the transport velocity of the mobilized radionuclides through the geologic media. The main characteristics of the waste form that will affect its corrosion behaviour in contact with groundwater will be composition, chemical state, morphology (surface area), and radioactivity level.

The sites selected as possible host for a geologic repository have undergone a thorough preliminary investigation in terms of intrinsic geologic stability over very long time periods. This analysis is combined with the evaluation of likelihood and potential impact of disruptive (and locally unlikely) events such as volcanism, glaciations, etc. The safety assessment of the final disposal concepts in terms of behaviour of the waste form and

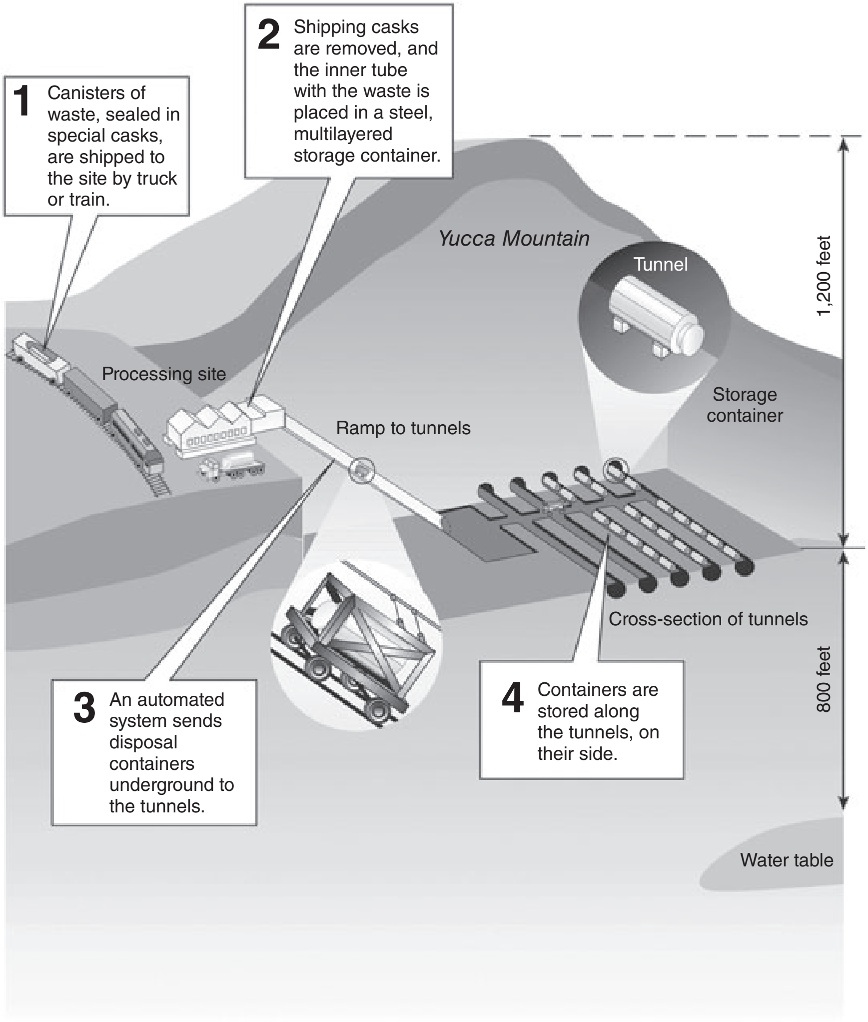

13.8 Schematic view of the emplacement of HLW in a geologic repository. The scheme depicted refers to the Yucca Mountain repository project in the USA (NRC, 2006). Used with permission of NEI, December 2010.

the waste package includes short-term events associated with accident scenarios (see Section 13.2.1). However, in the case of the open-ended final disposal the consideration of singularity events affecting individual waste packages is relatively not important; the main scope of the safety investigation is associated with the long-term 'natural' evolution of the waste form and all the engineered barriers. This constitutes an extrapolation to the remote future of the *global* performance of the repository, including all the emplaced waste. The deterministic prediction of the evolution of a complex system over geologic time intervals constitutes a formidable challenge, given the uncertainties associated with such a long timeframe (see Chapter 14). The safety guarantee is ultimately provided by adopting redundancy criteria in the configuration of the repository, including both man-made and natural factors active *in situ*. It is also based on the outcome of the combined evaluation of material properties, physico-chemical and thermodynamic studies, geologic information referring to the specific repository site and to natural analogue systems rich in actinide and decay-daughter minerals, and on short-term experimental studies testing relevant aspects of the behaviour of specific components of the waste/repository system.

13.2 Effects of radiation on properties relevant for storage and disposal of high level waste (HLW)

The main concern associated with neutron radiation from spontaneous fission of actinides present in HLW is related to criticality safety (see Section 13.1.1). β- and γ-emissions are characteristic of fission products and dominate the radiation field in and around HLW during the first centuries. These emissions are associated with short-term heat effects discussed in the previous sections like devitrification (for waste glass), and, in the case of γ-radiation, are responsible for the heavy shielding and radioprotection measures related to handling of the HLW. In the case of waste resulting from partitioning and transmutation (P&T) cycles, in which U, Pu and MA are not present, β- and γ-radiation from long-lived fission products constitute also the main long-term component of the radioactivity (Marivoet and Weetjens 2009).

In the case of spent fuel or HLW containing actinides, α-emissions become the dominating component of the radiation field after a few hundred years and thereafter, due to the long half-life of many α-emitters. Alpha-decay is the mechanism responsible for most microstructural damage in the waste material and for potentially significant alterations of the behaviour of the waste form (Rondinella *et al.* 2003, 2007, Peuget *et al.* 2004, Johnson *et al.* 2005, Wiss *et al.* 2007, Ferry *et al.* 2005).

13.2.1 Characterization of waste form candidate materials

All candidate waste form materials are tested to verify their radiation resistance quality. Such testing can occur essentially following four investigation approaches:

- Fabricate a ‘real’ waste form (or studying spent fuel) with the envisaged standard composition and loading fraction of radionuclides, and test it under conditions relevant for storage or disposal. This approach allows optimizing fabrication routes and handling procedures in view of industrial scale-up, and allows determining the starting properties of the waste form. However, it may not be representative of the long- or very long-term evolution of the material.

- Accelerated testing by α-doping the waste form with short-lived emitters (Gray 1987, Wald and Weber 1984, Weber *et al.* 1985, Rondinella *et al.* 1999). This allows reproducing long-term evolution within timescales acceptable for laboratory testing. Moreover, it allows singling out specific effects (e.g. α- vs. β- and γ-decay). However, there are limits to the acceleration of the rate of accumulation of decay damage that must not be exceeded (Rondinella *et al.* 2007).
- Accelerated testing by ion beam irradiation at accelerator facilities. The advantages of this approach are similar to those of α-doping. Additionally, the absence of radioactive nuclides in this approach makes available all options for characterization, avoiding adoption of radioprotection measures as in the previous case. However, ion beam irradiation is not isotropic. Moreover, the range of α-particles and especially of recoil atoms with energy reproducing α-decay events is very shallow, thus limiting the possibilities for specific α-decay simulation (Weber 1981, Matzke 1982, Weber *et al.* 1998).
- Characterization of natural analogues, i.e. natural minerals containing actinides and their daughters (Evron *et al.* 1994, Payne *et al.* 2007, Gin *et al.* 2009). Such minerals can have ages of the order of billions of years. Finding actinides (U, Th) or decay daughters still incorporated in crystalline mineral phase after geologic eras have elapsed is a strong indicator for a potentially effective HLW host matrix. This approach is very useful to identify candidate compounds to be considered as possible hosts for Pu, minor actinides and also long-lived or relevant fission products. However, uncertainties are related to the thermal history of the natural minerals; moreover, often practical limitations are found to the use of synthetic compounds mimicking natural minerals for actual incorporation of radioactive species in terms of waste loading, fabrication routes, chemical compatibility and finally also resistance against specific dose rate at relatively low temperature.

13.2.2 Effects of α-decay

Alpha-decay consists of the emission of a highly energetic (typically ~5 MeV) α-particle (a helium nucleus) and a recoil atom with energy of the order of 100 keV. The α-particle (a nucleus of helium) has a typical range of tens of μm (~10–20 μm in UO_2, ~40 μm in water) and loses energy mainly by electronic loss mechanisms causing relatively isolated defects

(~200 displacements) in the microstructure. The recoil atom has a much shorter range, of the order of 20 nm in UO_2, and slows down mainly by nuclear energy loss mechanisms, i.e. by direct collisions with other atoms, causing a cloud of ~1500 displacements. Most of the displacements caused by an α-decay event recombine rapidly. Some of them (typically 100–200 in the case of UO_2) remain as 'stable' point defects, e.g. as Frenkel pairs (an interstitial atom and a vacancy). Point defects close enough to each other can also cluster and arrange themselves into linear defects like dislocations. Various types of linear, bi- and tri-dimensional extended defects can be formed (Olander 1976, Weber 1981, Matzke 1982, Sickafus 2007). An important family of 3D defects is porosity, formed by clustering vacancies.

Depending on the specific α-activity of the waste, the accumulation of microstructural damage (typically measured in displacements per atom (dpa)) at relatively low temperatures and of He atoms can reach significant levels over different timescales, potentially affecting macroscopic properties and the behaviour of the waste during various stages of the back-end of the fuel cycle. Effects associated with accumulation of decay damage can be characterized by measuring the evolution (usually degradation) of properties such as, for example, hardness (Rondinella *et al.* 2007) or thermal transport (Staicu *et al.* 2010). These effects can also be quantified and deconvoluted into contributions due to different types of defects by performing thermal annealing tests on the damaged material (Weber 1981, Staicu *et al.* 2010).

The most important negative consequences that might be induced in a solid waste form by accumulation of defects and He, and may eventually compromise the mechanical integrity of the material, are:

- Excessive swelling
- Amorphization (in the case of crystalline waste forms).[2]

A bias in the evolution of the Frenkel pairs due to trapping mechanisms in the material, such as, e.g., the interaction of interstitials to form dislocation loops (i.e. portions of extra planes of atoms in the lattice), may cause accumulation of vacancies, which may ultimately coalesce into pores and cause swelling of the material. The evolution of the bias condition with increasing dose contributes to determining the long-term behaviour of the waste material: if a 'saturation equilibrium' between interstitials and vacancies is

---

[2] An indirect consequence (through long-term heat effects) of high dose rate α-decay in vitrified waste material could be partial crystallization of phases associated with specific radionuclides. This process would overlap and extend possible partial recrystallization phenomena occurring during glass fabrication (see also Chapters 6 and 9).

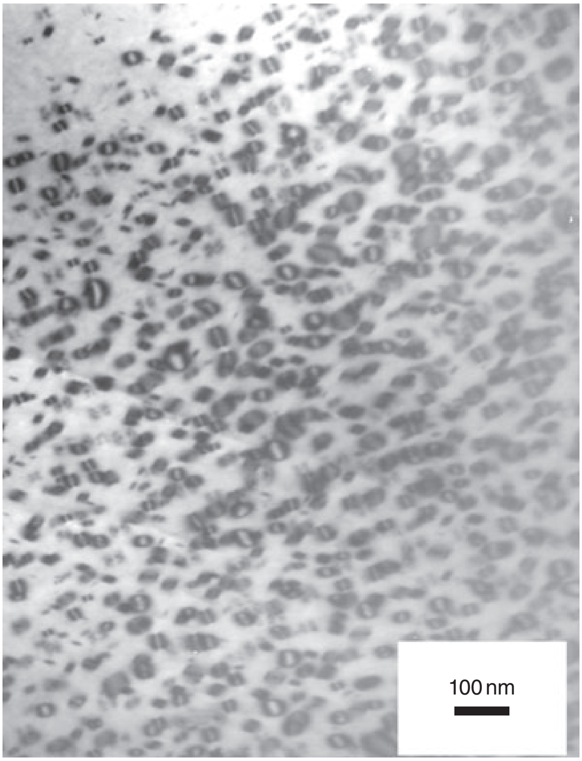

13.9 Transmission electron microscopy image showing dislocation loops induced in UO_2 by α-decay damage (10^{-5} dpa).

achieved, the material reaches a sort of steady-state condition, and the alteration of the relevant properties levels off; if the imbalance between families of point defects continues to grow, the integrity of the waste form will be compromised and one (or both) of the above-mentioned negative effects will ultimately cause a failure of the waste (Sickafus 2007).

Figure 13.9 shows a transmission electron microscopy (TEM) image of the microstructure of UO_2 after a very small α-decay dose corresponding to ~10^{-5} dpa. The dark round features visible in the micrograph are dislocation loops.

13.2.3 Swelling

Figures 13.10 and 13.11 illustrate examples of swelling associated with α-decay damage for $(U,Pu)O_2$ (Rondinella *et al.* 2003, 2007) and for vitrified HLW (Gras *et al.* 2007), respectively. In both cases α-doped materials were used, i.e. materials containing appropriate fractions of short-lived α-emitters

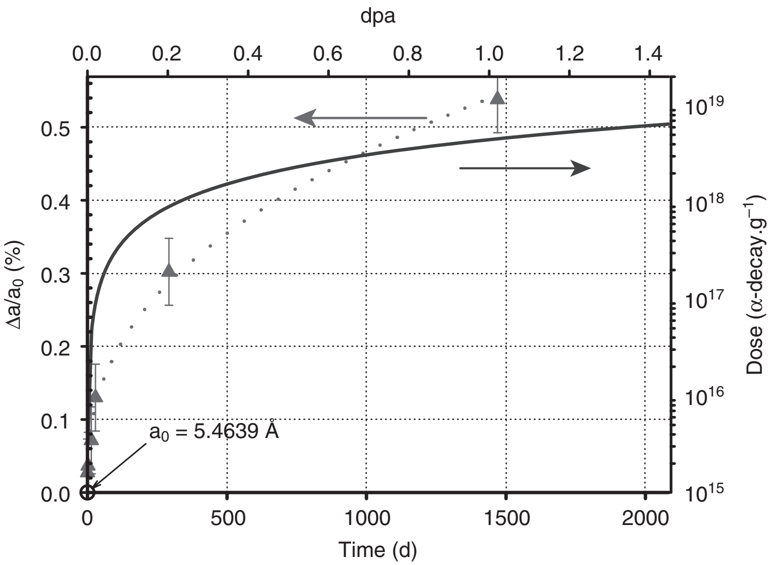

13.10 Alpha-decay dose and corresponding microstructure (lattice parameter) swelling as a function of time or accumulated damage (expressed as displacements per atom, dpa) for $(U_{0.9},{}^{238}Pu_{0.1})O_2$. The lattice parameter was calculated from X-ray diffraction measurements (Rondinella *et al.* 2007).

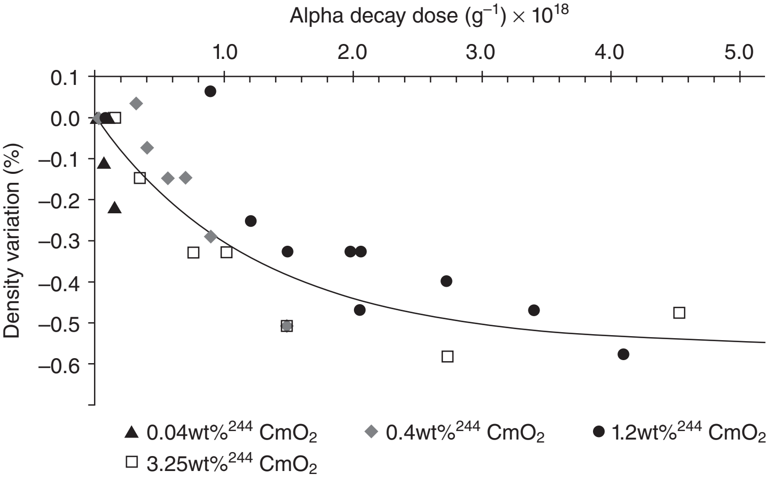

13.11 Swelling as a function of α-decay dose for waste glass containing different fractions of ^{244}Cm (Peuget *et al.* 2004, Gras *et al.* 2007).

to produce accelerated damage accumulation conditions. In the case of the mixed U-Pu oxide shown in Fig. 13.10, the damage level of ~1 dpa reached after slightly more than 4 years corresponds to the damage accumulated in medium burn-up UO_2 after more than 1000 years of storage (Rondinella *et al.* 2003).

In both cases illustrated in Figures 13.10 and 13.11 the waste material retained its function without losing its mechanical integrity after accumulating the maximum dose. Both swelling curves show a trend towards saturation at high dose, corresponding to a higher likelihood for recombination of displaced atoms once a condition characterized by a high density of point defects is reached (Noe and Fuger 1974, Weber 1981, Matzke 1982, Evron *et al.* 1994, Peuget *et al.* 2004). The capability of responding to accumulating microstructural damage through recombination or restructuring without losing the mechanical integrity is a key property to ensure that a waste form fulfils its radionuclide retention function (Eyal 1997, Sickafus *et al.* 2000, Sickafus 2007).

13.2.4 Amorphization

Generally, the fluorite structure characterizing, e.g., oxides of U, Th and Zr, shows the capability to resist against extreme levels of decay damage. UO_2 remains crystalline up to a dose level much higher than that shown in Fig. 13.10, corresponding to geologic ages for standard light water reactor spent fuel. Many other crystalline solids respond to a high α-decay dose by turning into an amorphous phase (Wald and Weber 1984, Sickafus *et al.* 2000, Lian *et al.* 2003, Wiss *et al.* 2007). Although it avoids a complete loss of mechanical integrity, amorphization presents significant disadvantages: in many cases it entails swelling; furthermore, it reduces the chemical corrosion resistance in groundwater by several orders of magnitude (see next section). A dose of the order of 10^{18} α-decays/g is often above the threshold for amorphization. Figure 13.12 (Muller *et al.* 2001) compares the amorphization resistance of three compounds (titanate and zirconate pyrochlore and zircon) considered for possible applications as conditioning matrices for Pu and/or minor actinides (see Chapter 10). It shows that among the three compounds tested only zirconate pyrochlore can withstand high α-decay dose without amorphizing (Wang *et al.* 1999, Weber and Ewing 2000, Lutique *et al.* 2003, Ewing *et al.* 2004, Belin *et al.* 2008).

13.2.5 Helium accumulation effects

At the end of its range, the α-particle is a He atom, i.e. a noble gas atom located in the material. Helium has a relatively low solubility in matrices

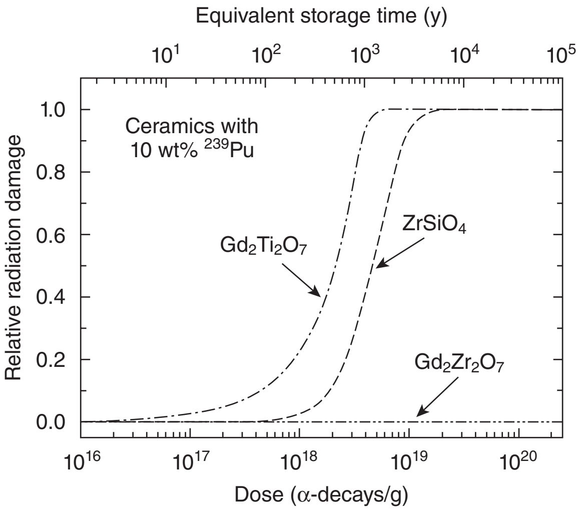

13.12 Amorphized fraction as a function of α-decay dose or time for candidate conditioning matrices containing 10 wt% ^{239}Pu (Muller *et al.* 2001). Only zirconate pyrochlore exhibits good resistance against decay damage (Wang *et al.* 1999, Weber and Ewing 2000).

like UO_2 (Maugeri *et al.* 2009). Differently from displaced atoms, He accumulation is not subjected to recombination. It is therefore important to be able to predict the effects associated with the cumulative long-term production of helium (Rondinella *et al.* 2003, Ronchi and Hiernaut 2004, Roudil *et al.* 2004, Wiss *et al.* 2007, Ferry *et al.* 2005, 2007, Yakub *et al.* 2010, Chamssedine *et al.* 2010). There are two possible negative consequences affected by He behaviour:

- If helium is retained in the waste form material, it may contribute significantly to swelling and possibly (as an extreme consequence) cracking of the material.
- If He is released from the waste material, it could determine pressurization of the cladding or the waste container up to its eventual failure.

Depending on the amount of α-emitters present in the waste, and hence on the cumulative amount of helium produced, these extreme effects may become relevant. In the case of low-medium burn-up UO_2 all experimental indications confirm that the long-term behaviour of the HLW (in this case spent fuel) will be benign (see e.g. Ferry *et al.* 2005). This positive conclusion has to be fully verified in the case of other systems, including high specific α-activity waste matrices, or fuels from advanced fuel cycle concepts containing a high fraction of α-emitters, associated, e.g., with the recycling of minor actinides. In the latter case, the issue of He accumulation effects may be highly relevant also for fuel storage *prior* to reactor irradiation (see, e.g., Babelot and Chauvin 1996).

13.3 Chemical corrosion of high level waste (HLW) in presence of water

Release/transport of radionuclides to the biosphere in the gas phase at ambient temperature would include only fission or, depending on the type and the age of the waste form, decay gases and would constitute a relatively mild source of hazard, compared to release events occurring at high temperature, which could also result in the mobilization of volatile species like Cs, I and Rb. Such events would be relevant only during the first decades after spent fuel discharge (or waste form fabrication), and would thus belong to the category of accidental occurrences. Accidents during handling, transport or interim storage may also involve exposure of HLW to water and potential release in the liquid medium.

Transport by aqueous phase is considered the main natural process which could cause release of radionuclides into the biosphere after emplacement of the waste package in a geologic repository. This section is focused on the main failure modes of the waste form, i.e. on the corrosion behaviour of HLW exposed to groundwater in the repository. As mentioned in Section 13.1.3, the design and the properties of a geologic repository aim at ensuring that contact between the waste and the groundwater will not take place in the first thousands or tens of thousands of years after closure of the repository. The exact time for this event to occur cannot be predicted with accuracy, due to the uncertainties associated with the long timescale of the prediction. Assumptions are thus made, adopting more or less conservative approaches, on the time of the contact and the corresponding behaviour of the waste form.

Thermodynamic and physical quantities like temperature and pressure, presence, amount, pathways and flow rate of the groundwater will play a major role in determining the modes of interaction between waste and groundwater. The chemical configuration in the repository, including composition of groundwater, overall redox condition, composition and behaviour of the mineral phases in the geologic medium and the materials in the engineered barriers surrounding the waste package, and the properties of the waste form at the time of the water exposure will govern the corrosion process.

Before interacting with the waste form, the groundwater will have to corrode through the metallic canister (see King and Shoesmith 2010). In the case of spent fuel disposal, the first potential source for radionuclide release will be the corrosion of the fuel rod cladding[3] and of the structural steel components (grids, spacers) of the fuel element. The radionuclides that may be released would be activation products and impurities (see Section 13.1.1) present in the metallic alloy or in the thin outer oxide layer which forms on the cladding during in-pile operation.

Table 13.4 summarizes chemical properties of thorium, uranium, transuranium elements and long-lived fission and activation products relevant for long-term corrosion in aqueous environments. Indicative range of solubilities or, for Pu, apparent concentration ranges are listed (Neck *et al.* 2007), referring to oxidizing and reducing conditions associated with different types of geologic repositories. The sorption behaviour is also indicated. A high sorption corresponds to a significantly lower rate of transport through the geologic media.

13.3.1 HLW glass corrosion in a geologic repository

The release of radionuclides from HLW glass is determined by the rate of alteration of the glass matrix. This, in turn, is affected by the following parameters (Gin *et al.* 2004, 2010, Godon 2004):

- Temperature
- pH
- Glass composition and alteration (decay damage effects) that occurred prior to contact with water
- Surface area (cracking)
- Groundwater flow
- Availability of sorption sites for dissolved silica.

The first two quantities govern the hydrolysis process responsible for congruent glass dissolution. However, additional mechanisms are also contributing to the overall glass corrosion process (Vernaz *et al.* 2001).

Interdiffusion of water in glass and ion exchange resulting in alkali depletion in the glass network is the first interaction between water and glass, together with the onset of the hydrolysis process. As long as dissolved silica can be effectively removed from the glass surface, e.g. through sorption mechanisms on the corrosion products of the waste containers, or due to relatively high water flow rates, the alteration rate remains relatively high, of the order of 1.5–3 $g\ m^{-2}d^{-1}$ (refs 9 and 10 in Peuget *et al.* 2004), or ~40 $nm\ h^{-1}$ (Gin *et al.* 2010). In practice, the nature of the repository site and the presence of materials like clay exclude the possibility of having high

---

[3] The cladding of LWR fuel rods is made of zircaloy, a metallic alloy containing > 98 wt% Zr, 1.2–1.7% Sn and smaller amounts of Cr, Fe, Ni or Nb. The cladding of fast reactor rods is austenitic steel.

Table 13.4 Summary of relevant properties of actinide elements and long-lived fission products in water at near neutral pH. Different behaviour/values corresponding to oxidizing and reducing conditions are indicated

Element	Indicative solubility range (mol/l)	Sorption	Oxidation states in aqueous solution	Remarks
Th	10^{-8}	High	+4	Not redox sensitive; solubility affected by the formation of colloids
U	10^{-3} *oxidizing*, 10^{-10} *reducing*	High	+4, +6	Redox sensitive, strongly affected by the presence of complexing agents (e.g. carbonates)
Pu	10^{-8}–10^{-7}* *oxidizing*, $<10^{-9}$ *reducing* (however, high solubility for Pu^{3+})	High	+3,+4,+5,+6	Redox sensitive, relatively high amounts can be found in the groundwater*; low solubility, high sorption, colloid transport
Np	10^{-6}–10^{-3} *oxidizing*, $<10^{-8}$ *reducing*	Low *oxidizing*, high *reducing*	+4, +5, +6	Redox sensitive, high solubility under oxidizing conditions, low sorption, colloid transport
Am	10^{-9}–10^{-3}	High	+3, +5	Oxidation state +3 up to very strong oxidizing conditions
Cm			+3, (+4)	Oxidation state +4 is not stable
Tc	10 *oxidizing*, 10^{-8} *reducing*	Low *oxidizing*, high *reducing*	(−1, +2), +3, +4, (+5, +6), +7	Redox sensitive; disproportionation of +5 and +6 states; +4 and +7 are most common states; humic acid complexation can increase solubility under reducing conditions
I	Highly soluble as I^-_3	Low	−1, +1, +3, +5, +7	Not redox sensitive; highly mobile
Cs	High	High	+1 (+2, +3)	Not redox sensitive

*The total amount of plutonium that can be measured when analysing a groundwater solution by spectrometric methods represents an 'apparent' concentration. This apparent concentration includes contributions from colloids and sorbed Pu, in excess of actual dissolved plutonium ions.

water flow regimes (in fact, according to Gin *et al.* 2004, the conditions to be expected in a clay repository are best simulated by leaching experiments under static conditions). Therefore, the initial alteration rate of the HLW glass will last until saturation of the sorption sites surrounding the HLW is achieved.

Subsequent corrosion will be affected by the formation of a porous hydrated silica gel layer condensed on the glass surface acting as a barrier limiting transport of the reaction products to and from the unaltered glass surface. The formation of such a 'protective layer' will result in a drop by about four orders of magnitude of the alteration rate of the glass (down to a level of ~$3 \cdot \times 10^{-3}$ nm h^{-1}; Gin *et al.* 2010).

Precipitation of secondary phases, mainly containing glass-forming species like Si and Al, will also occur. Figure 13.13 illustrates the expected evolution of the fraction of altered glass as a function of time for the R7T7 HLW glass envisaged in the French disposal programme (see Table 13.2) under very conservative assumptions (Gin *et al.* 2010). Two alteration curves are shown, which highlight the impact on the extent of glass alteration during the initial reaction period deriving from the inclusion of the

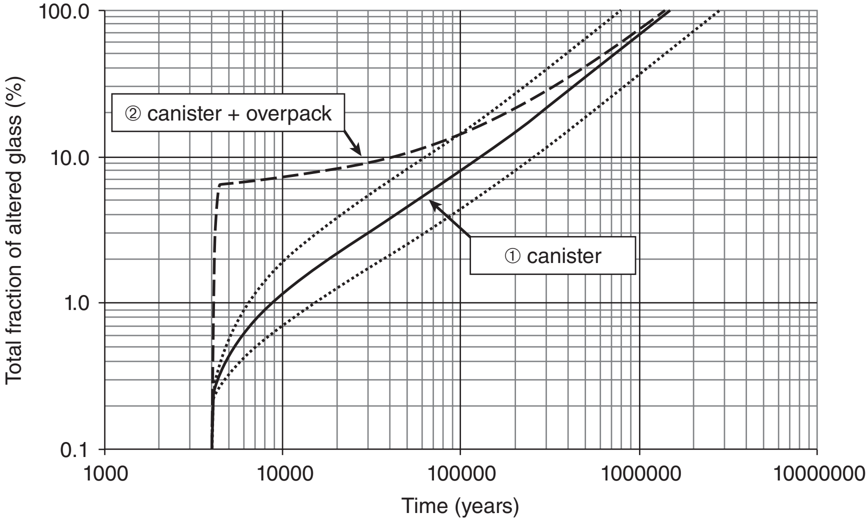

13.13 Fraction of altered glass as a function of time for R7T7 HLW glass in a geologic repository. The solid and the dashed lines correspond to the alteration expected considering as available sorption sites for dissolved silica the corrosion products only of the glass container (canister) or also of the overpack material, respectively. The dotted lines represent the uncertainties for the alteration curve including only the canister corrosion products (Gin *et al.* 2010).

corrosion products of the overpack materials as sites available for silica sorption. The diagram corresponds to the assumption that first contact of HLW and groundwater occurs after 4000 years. If only the waste canister corrosion products are considered as sorption sites for silica, the initial alteration rate (of the order of 1.5–3 g $m^{-2}d^{-1}$, or ~40 nm h^{-1}) will affect ~0.25% of the waste, and total alteration of the HLW package will have occurred after a time > 10^6 years. The inclusion of the overpack materials as sorption sites would dramatically increase the extent of the initial alteration rate, but would not change the total lifetime of the waste.

The curves in Fig. 13.13 are calculated under the assumption that the release of all radionuclides will take place at the same rate as that for boron and the alkali elements, i.e. without considering specific (benign) properties of various radionuclides, which would result in significant retention mechanisms to become active, thus significantly delaying the release of many radiotoxic species. By including these mechanisms, the results of the corresponding performance assessment indicate a reduction of up to two orders of magnitude of the radiotoxicity released between 10^3 and 10^4 years (Gin *et al.* 2010).

While the overall mechanisms affecting the corrosion process of waste glass are well characterized, various aspects are still a matter of debate. In particular, the exact description of the interaction of all agents and quantities active in the near field of the geologic repository (i.e. the region hosting the engineered barriers surrounding the waste package), the evolution of the protective gel layer and the description of the role of the precipitated secondary phases are still objects of investigation, both experimentally and theoretically.

13.3.2 Spent fuel corrosion in a geologic repository

The mobilization of radionuclides from oxide spent fuel (essentially UO_2) in contact with groundwater depends on the amount of water contacting the fuel (total mass, flow rate), on the total surface area available for reaction with water at a given time, and on the corresponding source term, i.e. on the amount of radionuclides associated with the reaction area. The release can be attributed to two main modes: the so-called instant release and the fuel matrix dissolution.

The instant release corresponds to the rapid dissolution of nuclides present in easily accessible regions first exposed to groundwater, namely the gap region between fuel pellet and cladding, the open surfaces (cracks, crevices), and the grain boundaries. Given the fact that the first contact with water is expected only after tens or hundreds of thousands of years have elapsed since closure of the repository, the source term for this initial release, called the instant release fraction (IRF), is characterized by the presence of a few percent of the total inventory of long-lived fission products I-129, Cs-135, Se-79 and Sn-126, together with impurities like Cl-36 (Tait *et al.* 1997) or other relevant nuclides like C-14 (Stroes-Gascoyne *et al.* 1992). Highly soluble, volatile fission products that can readily be removed by water like Cs and I are the key species responsible for the first spike of release. The IRF is determined by the initial composition and irradiation history of the fuel (burn-up, power rating, temperature) and by the post-irradiation evolution of the material (decay damage/helium accumulation, temperature, time, oxidation conditions) (Ferry *et al.* 2009).

Important features are associated with the properties and behaviour of spent fuel with high burn-up. Above ~45 GWd t^{-1} fuel swelling during irradiation causes a progressive closure of the gap between fuel pellet and zircaloy cladding. A transition oxide region is formed rich in zirconium, fission products like Cs (Walker *et al.* 1996), uranium and actinide oxides. Moreover, due to the radial burn-up gradient occurring in LWR fuel, the burn-up level is significantly higher at the outer periphery (or rim) of the fuel pellet. At local burnup around 70–75 GWd t^{-1} the relatively colder pellet rim has undergone a dramatic restructuring process, characterized by the subdivision of the original fuel grains (with dimensions of the order of ≥10 μm) into smaller sub-micron grains. This transformation, called also high burn-up or rim structure, is accompanied by the relocation of fission gases into a new family of intergranular pores, and by other modifications of the properties of the fuel (Sonoda *et al.* 2002, Kinoshita *et al.* 2004, Rondinella and Wiss 2010). As a result, a compact, but highly porous, small-grained fuel, with a large grain boundary surface area and a high relative inventory of fission products, is the material that will be first exposed to groundwater in a hypothetical 'first contact' scenario.

Different assumptions and considerations have been made to define the IRF. Values stemming from 'realistic' to 'ultraconservative' assumptions have been proposed and fed into performance assessment exercises for different types of repository. Specific source term studies have been focused on spent fuel from different types of reactor (LWR, CANDU), and on different types of fuel (UO_2, MOX) and on different components or special configurations of the IRF (grain boundaries, gap). Detailed treatment and discussion on IRF can be found elsewhere (Stroes-Gascoyne *et al.* 1992, Jégou *et al.* 2001, Johnson *et al.* 2004, 2005, Poinssot *et al.* 2005, Ferry *et al.* 2008, Rondinella *et al.* 2008, Roudil *et al.* 2009, SKI 2007, de Pablo *et al.* 2009). As an example, Table 13.5 summarizes IRF estimates for fission products and relevant impurities for LWR UO_2 fuel at different burn-up (SKI 2007). Generally, experimental results confirm that only a few percent of the total inventory of mobile nuclides would be available as IRF under the expected conditions in a repository. Moreover, specific studies on the leaching behaviour of rim-structure fuel samples indicate that in spite of

Table 13.5 Instant release fraction values (% of total inventory) for UO_2 from a pressurized water reactor fuel as proposed for the Swedish disposal concept (SKI 2007). The values in parentheses represent conservative estimations

Burnup (GWd/t U)	41	48	60	75
Fission gas	1 (2)	2 (4)	4 (8)	8 (16)
^{14}C	10	10	10	10
^{36}Cl	5	10	16	26
^{90}Sr	1 (2)	1 (3)	1 (5)	1 (9)
^{99}Tc, ^{107}Pd	0.1 (1)	0.1 (3)	0.1 (5)	0.1 (9)
^{129}I	1 (3)	2 (4)	4 (8)	8 (16)
^{135}Cs, ^{137}Cs	1 (2)	2 (4)	4 (8)	8 (16)

the higher grain boundary area and higher inventory of fission products and transuranics the release is not enhanced, being actually lower in many cases than that of unrestructured fuel samples (de Pablo *et al.* 2009, Roudil *et al.* 2009). This may be related to the tight configuration of the high burn-up structure (which retains most of the fission gas inventory in the intragranular porosity) or to the oxidation stabilizing effect of the UO_2 matrix due to the relatively high content of fission products like Zr. The investigation of this fascinating aspect of nuclear fuel is continuing (Rondinella and Wiss 2010).

Although the IRF represents the initial burst of radiotoxicity that becomes available for transport through engineered and natural media, most of the radiotoxicity of spent fuel is incorporated and contained in the UO_2 matrix. Matrix dissolution is therefore the long-term process which would account for the mobilization of the largest portion of radionuclides. In addition to the factors affecting the IRF, matrix dissolution in groundwater is governed by the oxidation state of the fuel (Loida *et al.* 2004). As shown in Table 13.4, the solubility of U(VI) in water is several orders of magnitude higher than that for U(IV) (being also strongly enhanced by the action of complexing agents like carbonates). Reported values of matrix (U) dissolution rate obtained in leaching studies on spent fuel under different conditions range from 10^{-4} mg $m^{-2}d^{-1}$ under reducing conditions to ~6 mg $m^{-2}d^{-1}$ under oxidizing conditions (Carbol *et al.* 2005, Johnson *et al.* 2005). It can be said that that under reducing conditions UO_2 constitutes a valid additional barrier against the release of radionuclides. This is the reason for selecting geologic repository formations (granite, clay, salt) characterized by highly reducing conditions.

Given this positive property of the spent fuel matrix, the focus of many investigation campaigns is on factors that may potentially alter the oxidation condition of the fuel matrix during in-pile operation (fission effects) and/or after discharge from the reactor (decay effects). Oxygen potential

(Walker *et al.* 2005, Rondinella *et al.* 1999) and other measurements (Ferry *et al.* 2005, 2009) confirm that no significant oxidation of the fuel matrix has to be expected as long as the fuel rod remains sealed.

The main cause for potential local oxidation at the spent fuel surface is water radiolysis. By the time an interaction between fuel and groundwater may occur, the radiation field in and around spent fuel will be dominated by α-decay. The range of α-particles in water is limited to ~40 μm. The radiolysis process causes the formation of highly active molecular and radical species which tend to react relatively rapidly. Their generation near the fuel surface causes a relatively high probability of interaction of oxidizing species like, e.g., hydrogen peroxide and UO_2. Enhancement of UO_2 dissolution specifically associated with α-radiolysis has been observed experimentally in leaching tests using α-doped UO_2 (Rondinella *et al.* 1999, 2000, 2001, 2004, 2005, Cobos *et al.* 2002, Jégou *et al*. 2005, Stroes-Gascoyne *et al.* 2005, Gray 1987). Radiolytic corrosion enhancement was observed also for other types of HLW, e.g. for zirconolite under ion beam irradiation (Tribet *et al.* 2007).

In single-effect studies, i.e. by looking at the radiolysis effect in the absence of other conditions expected in the repository, the radiolysis enhancement could cause an increase of the dissolution rate of UO_2 fuel up to 3–4 orders of magnitude (Rondinella *et al.* 2004, Carbol *et al.* 2005), essentially reproducing the range of dissolution rates described above by varying the specific activity of the samples. Surface area and radiolysis effects possibly constitute the key properties of spent fuel determining its corrosion behaviour. If radiolysis alone were determining the corrosion behaviour of spent fuel, it would be a cause for concern. However, several factors contribute to offset or minimize the ultimate impact of this mechanism:

- The radioactive decay will cause a progressive decrease of the α-activity of spent fuel. Experiments under deaerated conditions revealed the presence of an α-activity threshold between $\sim 3 \times 10^6$ Bq/g and $\sim 4 \times 10^7$ Bq/g below which no significant radiolytic dissolution enhancement is observed (Rondinella *et al.* 2004, Johnson *et al.* 2005). This corresponds to UO_2 spent fuel with an age ranging from a few thousand to a few tens of thousands of years (calculated for 36 GWd t^{-1} and 60 GWd t^{-1}, respectively). If the containment barriers can be designed to maintain their integrity over this timescale, by the time water would react with the fuel the corrosion would be chemically controlled, and radiolysis effects could be neglected.
- As mentioned in the previous section, it is expected that the reaction between fuel and groundwater will be characterized by relatively high fuel surface to water volume (S/V) ratios. It has been observed that

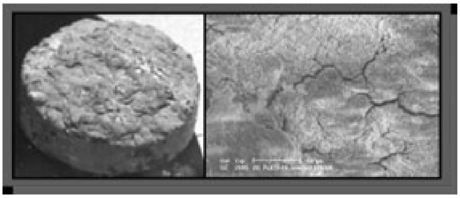

13.14 Optical (left) and scanning electron (right) microscopy images of UO_2 containing 10 wt% Pu-238 after approximately 2 months of leaching in demineralized water. Phase analysis confirmed that the phase covering the surface is studtite (Cobos *et al.* 2003).

under such conditions saturation and reprecipitation of secondary phases on the fuel surface would contribute to reduce the surface available for further reaction or limit the dissolution rate. Figure 13.14 shows the appearance of a disk of α-doped UO_2 containing ~10 wt% Pu-238 after ~60 days of leaching in water under relatively high S/V conditions: the surface is completely covered by studtite (uranium peroxide) (Cobos *et al.* 2003). The full surface coverage corresponds to saturation of the concentration in solution of dissolved species. The role of surface phases like studtite for possible retention of radionuclides is being investigated (see e.g. Gimenez *et al.* 2009).

- Radiolysis effects and other properties of the fuel are only some of the factors active in the repository environment. When combining together the dissolution enhancing effects of radiolysis with all the contrasting effects active in the near-field system, the beneficial reducing and re-immobilizing effects will prevail and dominate the overall behaviour of the repository. In particular, this is due to the presence of strongly reducing (and re-immobilizing) species like Fe(II) minerals and corrosion products of containment materials (Cui *et al.* 2009); additionally, hydrogen overpressure generated by iron corrosion in water will cause a suppression of the UO_2 matrix corrosion (Carbol *et al.* 2005, 2009, Fors *et al.* 2009) through catalytically activated mechanisms (Cui *et al.* 2010) that are the object of current investigation.

13.4 Future trends

Increasing fuel burn-up is a trend common to current and evolutionary Gen III types of reactors. For LWR, burn-up around 60 GWd t^{-1} is a possible option. Also advanced CANDU reactors envisage low enriched uranium dioxide fuel with a burn-up of the order of 20 GWd t^{-1}. Higher burn-up allows improved utilization of the fuel and provides economic benefits for energy production. In terms of spent fuel properties, higher burn-up for

LWR fuel implies higher loads for the cladding material, the full closure of the pellet–cladding gap and a higher specific (and long-term) activity for spent fuel associated with a higher inventory of fission products and transuranics. It is important to evaluate the impact of this trend on the various steps of the back-end of the fuel cycle, namely possible effects due to decay damage and helium accumulation during storage and eventual effects due to higher IRF and higher α-activity on the corrosion in the repository. The extended use of mixed oxide fuel (MOX and/or possibly Th-Pu oxide) will also have relevance for the evolution of HLW concepts based on spent fuel disposal.

Considering current reprocessing routes, increasing the load fraction in waste glass of actinides and fission products would allow limiting the increase of HLW volume per spent fuel assembly required to treat higher burn-up fuel. Today's HLW glass typically contains ~15% of radionuclides from spent fuel (Table 13.2). In order to increase this fraction the glass fabrication process would have to be modified. Moreover, the effects associated with higher decay dose, He production and higher thermal load would have to be assessed.

The evolution of other types of HLW is closely related to the evolution of the fuel cycle. If separation processes of minor actinides and fission products are introduced in the back-end of the fuel cycle, specific waste forms tailored to immobilize different fission products could be considered for possible implementation. In particular, host matrices to immobilize short-lived fission products like Cs-137 and Sr-90, metallic species like Tc-99, iodine, and actinides not considered for transmutation concepts are being studied (McCarthy 1977, Ringwood *et al.* 1979, Muller *et al.* 2001, Ewing *et al.* 2004, Vance 2007, Gombert *et al.* 2008, Weber *et al.* 2009, Rard 2005, Boyer *et al.* 1997, Wang *et al.* 1999). The development of various lines of waste forms for immobilization of families of radionuclides has to be evaluated in terms of technical effectiveness and also economic feasibility (see e.g. Gombert *et al.* 2009).

13.5 Sources of further information and advice

A large amount of information is available from national organizations and authorities dealing with nuclear waste disposal. Below is a short list of national organizations: www.nrc.gov; www.doe.gov (USA); www.cea.fr; www.andra.fr (France); www.skb.se; www.ski.se (Sweden); www.posiva.fi (Finland); www.nagra.ch (Switzerland); www.nirond.be (Belgium); www.enresa.es (Spain); www.nda.gov.uk (UK); www.bfs.de (Germany); www.nwmo.ca (Canada); www.numo.or.jp (Japan).

International organizations like IAEA (www.iaea.org) and the Nuclear Energy Agency of OECD (www.oecd.org) provide a comprehensive collection of data and publications reporting on the state of the art concerning nuclear waste management options in different countries.

In Europe, the European Commission supports international projects dealing with, among others, nuclear waste management and disposal issues as 'indirect actions' within its multi-annual Framework Programmes (FP). A list and contact information on relevant projects during the current and previous FP can be found at http://cordis.europa.eu/fp7/euratom-fission/home_en.html.

A useful link to perform calculations of inventories, decay, dose and shielding is the web portal www.nucleonica.net. Nucleonica is also host of the Karlsruhe Nuclide Chart, a valuable tool to obtain specific data and background information on radionuclides.

Several scientific conferences and related proceedings/publications provide a useful forum to collect updated information on national programmes and scientific advances in all subjects mentioned in this chapter:

Symposium on Scientific Basis for Nuclear Waste Disposal, Materials Research Society www.mrs.org

Migration: International Conference on the Chemistry and Migration Behaviour of Actinides and Fission Products in the Geosphere

IHLRWM: International High-Level Radioactive Waste Management Conference and other sessions/symposia in meetings/conferences organized by the American Nuclear Society (www.ans.org)

ICEM: International conference on environmental remediation and radioactive waste management: www.icemconf.com.

13.6 References

Babelot J F and Chauvin N (1996), Rapport de synthèse commun CEA/ITU sur l'expérience SUPERFACT 1, in *Note Technique* SDC/LEMC 96-2028, CEA Cadarache

Belin R C, Valenza P J, Raison P E and Tillard M (2008), Synthesis and Rietveld structure refinement of americium pyrochlore $Am_2Zr_2O_7$, *J. Alloys and Compounds* 448, 321–324

Boyer L, Carpena J and Lacout J L (1997), Synthesis of phosphate-silicate apatites at atmospheric pressure, *Solid State Ionics* 95, 121–129

Bychkov A V, Vavilov S K, Skiba O V, Porodnov P T, Pravdin A K, Popkov G P, Suzuki K, Shoji Y and Kobayashi T (1997), Pyroelectrochemical processing of irradiated FBR MOX fuel. III. Experiment on high burn-up fuel of the BOR-60 reactor, *Proc. Int. Conf. on Future Nuclear Systems, GLOBAL '97*, Yokohama, Japan, Vol. 2, pp. 912–917

Carbol P, Cobos-Sabate J, Glatz J P, Ronchi C, Rondinella V V, Wegen D H, Wiss T, Loida A, Metz V, Kienzler B, Spahiu K, Grambow B, Quinones J and Martinez-Esparza A (2005), The effect of dissolved hydrogen on the dissolution of ^{233}U doped UO_2(s), high burnup spent fuel and MOX fuel, Technical report SKB TR-05-09, SKB

Carbol P, Fors P, Van Winckel S and Spahiu K (2009), Corrosion of irradiated MOX fuel in presence of dissolved H_2, *J. Nucl. Mater.* 392, 45–54

Caurant D, Majerus O, Loiseau P, Bardez I, Baffier N and Dussossoy J L (2006), Crystallization of neodymium-rich phases in silicate glasses developed for nuclear waste immobilization, *J. Nucl. Mater.* 354, 143–162

CEA (2004), Les déchets radioactifs à haute activité et à vie longue / Recherches et résultats, Rapport CEA/DEN/DDIN/2004-642

Chamssedine F, Sauvage T, Peuget S, Fares T and Martin G (2010), Helium diffusion coefficient measurements in R7T7 nuclear glass by $^3He(d,\alpha)^1H$ nuclear reaction analysis, *J. Nucl. Mater.* 400, 195–181

Cobos J, Havela L, Rondinella V V, de Pablo J, Gouder T, Glatz J P, Carbol P and Matzke Hj (2002), Corrosion and dissolution studies of UO_2 containing α-emitters, *Radiochim. Acta* 90, 597–602

Cobos J, Wiss T, Gouder T and Rondinella V V (2003), XPS and SEM studies on the corrosion of UO_2 containing plutonium in demineralized and carbonated water, *Mat. Res. Soc. Symp. Proc.* 757, 365–375

Cui D, Ranebo Y, Low J, Rondinella V V, Pan J and Spahiu K (2009), Immobilization of radionuclides on iron canister material at simulated near-field conditions, *Mat. Res. Soc. Symp. Proc.* 1124, 111–116

Cui D, Low J, Rondinella V V and Spahiu K (2010), Hydrogen catalytic effects of nanostructured alloy particles in spent fuel on radionuclide immobilization, *Applied Catalysis B* 94, 173–178

de Pablo J, Serrano-Purroy D, Gonzalez-Robles E, Martinez-Esparza A, Wegen D H, Casas I, Christiansen B, Glatz J P and Gimenez J (2009), Effect of HBS structure in fast release fraction of 48 GWd/tU PWR fuel, *Mat. Res. Soc. Symp. Proc.* 1193, 613–620

Evron R, Kimmel G and Eyal E (1994), Thermal recovery of self radiation damage in uraninite and thorianite, *J. Nucl. Mater.* 217, 54–66

Ewing R C, Weber W J and Lian J (2004), Nuclear waste disposal-pyrochlore ($A_2B_2O_7$): Nuclear waste form for the immobilization of plutonium and 'minor' actinides, *J. Appl. Phys.* 95, 5949–5971

Eyal Y (1997), A radiation annealing model for maintenance of crystallinity in self-damaged actinide dioxides, in *Radioactive Waste Management and Environmental Remediation*, Baker R, Slate S and Benda G (eds), American Society of Mechanical Engineers, New York, 303–307

Ferry C, Poinssot C, Broudic V, Cappelaere C, Desgranges L, Garcia P, Jegou C, Lovera P, Marimbeau P, Piron J-P, Poulesquen A, Roudil D, Gras J-M and Bouffioux P (2005), *Synthesis On The Spent Fuel Long Term Evolution*, Rapport CEA-R-6084, CEA Saclay, France

Ferry C, Piron J P and Stout R (2007), Effect of helium accumulation on the spent fuel microstructure, *Mat. Res. Soc. Symp. Proc.* 985, NN-05-01

Ferry C, Piron J P, Poulesquen A and Poinssot C (2008), Radionuclides release from the spent fuel under disposal conditions: re-evaluation of the instant release fraction, *Mat. Res. Soc. Symp. Proc.* 1107, 447–454

Ferry C, Cappelaere C, Jégou C, Piron J P, Firon M and Ambard A (2009), Overview of the French research on the evolution of spent fuel rod after discharge from the reactor, *Mat. Res. Soc. Symp. Proc.* 1193, 605–612

Fors P, Carbol P, Van Winckel S and Spahiu K (2009), Corrosion of high burn-up structured UO_2 fuel in presence of dissolved H_2, *J. Nucl. Mater.* 394, 1–8

Gimenez J, Sureda R, de Pablo J, Casas I, Martinez-Llado X, Rovira M and Martinez-Esparza A (2009), The role of uranium peroxide studtite on the retention of Cs, Sr and Se(VI), *Mat. Res. Soc. Symp. Proc.* 1193, 621–626

Gin S, Godon N, Ribet I, Jollivet P, Minet Y, Frugier P, Vernaz E, Cavedon J M, Bonin B and Do Quang R (2004), Long-term behavior of R7T7-type nuclear glass: Current state of knowledge and outlook, *Mat. Res. Soc. Symp. Proc.* 824, 327–332

Gin S, Verney-Carron A and Libourel G (2009), Use of archaeological glass to predict the long-term behavior of HLW, *Mat. Res. Soc. Symp. Proc.* 1193, 239–247

Gin S, Ribet I, Frugier P, Chave T, Angeli F, Lartigue J E, de Combarieu G and Godon N (2010), Assessment of nuclear glass behavior in geological disposal conditions: Current state of knowledge and recent advances, *Proceedings of the 13th International Conference on Water-rock Interaction,* WR113, Guanajuato, Mexico, 10–20 August 2010, 641–644

Godon N (2004), Dossier de référence sur le comportement à long terme des verres nucléaires, Rapport technique DTCD 2004/06, CEA 2004

Gombert II D, Carter J, Cozzi A, Jones R, Matthern G, Nutt M, Priebe S and Sorenson K (2008), Global Nuclear Energy Partnership Integrated Waste Management Strategy, GNEP-WAST-AI-RT-2008-000214, US-DOE

Gombert D, Carter J, Ebert B, Piet S, Trickel T and Vienna J (2009), A trade study for waste concepts to minimize HLW volume, *Mat. Res. Soc. Symp. Proc.* 1124, Q01–03

Gras J M, Quang R D, Masson H, Lieven T, Ferry C, Poinssot C, Debes M and Delbecq J M (2007), Perspectives on the closed fuel cycle – Implications for high-level waste matrices, *J. Nucl. Mater.* 362, 383–394

Gray W J (1987), Comparison of uranium release from spent fuel and unirradiated UO_2 in salt brine, *Mat. Res. Soc. Symp. Proc.* 84 141–151

Grouiller J P, Pillon S, de Saint Jean C, Varaine F, Leyval L, Vambenepe G and Carlier B (2003), Minor actinides transmutation scenario studies with PWRs, FRs and moderated targets, *J. Nucl. Mater.* 320, 163–169

Helie M (2007), A review of 25 years of corrosion studies on HLW container materials at the CEA, *Mat. Res. Soc. Symp. Proc.* 985, 269–274

Helie M, Desgranges C and Perrin S (2006), Prediction of corrosion behavior of HLW containers in the framework of the French interim storage concept, *Nucl. Technol.* 155(2), 120–132

IAEA (2002), Long term storage of spent nuclear fuel – survey and recommendations, Tecdoc 1293

IAEA (2008), Spent fuel reprocessing options, Tecdoc 1587

Inoue T and Tanaka H (1997), Recycling of actinides produced in LWR and FBR fuel cycles by applying pyrometallurgical process, *Proc. Int. Conf. on Future Nuclear Systems, GLOBAL '97*, Yokohama, Japan, Vol. 1, pp. 646–652

Jégou C, Peuget S, Lucchini J F, Corbel C, Broudic V and Bart J M (2001), Effect of spent fuel burnup and composition on alteration of the $U(Pu)O_2$ matrix, *Mat. Res. Soc. Symp. Proc.* 663, 399–408

Jégou C, Muzeau B, Broudic V, Peuget S, Poulesquen A, Roudil D and Corbel C (2005), Effect of external gamma irradiation on dissolution of the spent UO_2 fuel matrix, *J. Nucl. Mater.* 341, 62–82

Johnson L, Poinssot C, Ferry C and Lovera P (2004), Estimates of the instant release fraction for UO_2 and MOX fuel at $t = 0$, Nagra Technical Report, NTB 04-08, Nagra, Wettingen, Switzerland

Johnson L, Ferry C, Poinssot C and Lovera P (2005), Spent fuel radionuclide source-term model for assessing spent fuel performance in geological disposal. Part I: Assessment of the instant release fraction, *J. Nucl. Mater.* 346, 56–65

King F and Shoesmith D W (2010), in *Geological Repository Systems for Safe Disposal of Spent Nuclear Fuels and Radioactive Waste*, Chapter 16. Woodhead Publishing, in press

Kinoshita M, Sonoda T, Kitajima S, Sasahara A, Kameyama T, Matsumura T, Kolstad E, Rondinella V V, Ronchi C, Hiernaut J P, Wiss T, Kinnart F, Ejton J, Papaioannou D and Matzke Hj (2004), High burnup rim project (III). Completed scope and results, *Proc. Int. Conf. on LWR Fuel Performance*, ANS, Orlando, Fl, 19–22 September, 2004, paper 1102, 207–213

Koch L, Glatz J P, Konings R J M and Magill J (1999), Partitioning and Transmutation studies at ITU, *ITU Annual Report 1999*, EUR 19054, 34–47

Kubota M, Yamaguchi I, Morita Y, Kondo Y, Shirahashi K, Yamagishi I and Fujiwara T (1993), Development of a partitioning process for the management of high-level waste, *Proc. Global '93*, Seattle, WA, USA, Vol. 1, p. 588

Lian J, Chen J, Wang L M, Ewing R C, Farmer J M, Boatner L A and Helean K B (2003), Radiation-induced amorphization of rare-earth titanate pyrochlores, *Phys. Rev. Condensed Matter and Mater. Phys. B* 68, art. no. 134107

Loida A, Kienzler B and Geckeis H (2004), Corrosion behavior of pre-oxidized high burnup spent fuel in salt brine, *Mat. Res. Soc. Symp. Proc.* 807, 53–58

Lutique S, Konings R J M, Rondinella V V, Somers J, Staicu D and Wiss T (2003), Zirconate pyrochlore as a transmutation target: thermal behaviour and radiation resistance against fission fragment impact, *J. Nucl. Mater.* 319, 59–64

Lutze W and Ewing R C (1988), *Radioactive Waste Forms for the Future*, Elsevier Science Publishers BV, Amsterdam

Marivoet J and Weetjens E (2009), Impact of advanced fuel cycles on geological disposal, *Mat. Res. Soc. Symp. Proc.* 1193, 117–126

Matzke Hj (1982), Radiation damage in crystalline insulators, oxides and ceramic nuclear fuels, *Radiation Effects* 64, 3–33

Maugeri E, Wiss T, Hiernaut J P, Desai K, Thiriet C, Rondinella V V, Colle J Y and Konings R J M (2009), Helium solubility and behaviour in uranium dioxide, *J. Nucl. Mater.* 385, 461–466

McCarthy G J (1977), High level waste ceramics: Materials considerations, process simulation and product characterization, *Nucl. Technol.* 32, 92–105

Muller I, Weber W J, Vance E R, Wicks G and Karraker D (2001), Glass ceramics and composites, in *Advances in Plutonium Chemistry 1967–2000*, Hoffman D C (ed.), Chapter 10, 260–297, ANS

Neck V, Altmaier M and Fanghänel Th (2007), Solubility of plutonium hydroxides/hydrous oxides under reducing conditions and in the presence of oxygen, *C.R. Chimie* 10, 959–977

Noe M and Fuger J (1974), Self-radiation effects on the lattice parameter of $^{238}PuO_2$, *Inorg. Nucl. Chem. Letters* 10, 7–19

NRC (2006) *Information Digest 2006–2007*, NUREG-1350, vol. 18. US Nuclear Regulatory Commission, Washington

NRC (2010) *Information Digest 2010–2011*, NUREG-1350, vol. 22. US Nuclear Regulatory Commission, Washington

Ojovan M I, Hyatt N C and Lee W E (2004), Crystallisation within simulated high level waste borosilicate glass, *Mat. Res. Soc. Symp. Proc.* 824, 321–326

Olander D R (1976), Fundamental aspects of nuclear reactor fuel elements, Report TID-26711-P1, Technical Information Center, Energy Research and Development Administration, Oak Ridge, TN, USA

Oversby V M (1998), Criticality in a repository for spent fuel: lessons from Oklo, *Mat. Res. Soc. Symp. Proc.* 506, 781–788

Payne T E, Giere R, Hart K P, Lumpkin G R and McGlinn P (2007), Partitioning and leaching behaviour of actinides and rare earth elements in a zirconolite-bearing hydrothermal vein system, *Mat. Res. Soc. Symp. Proc.* 985, 347–352

Peuget S, Jégou C, Broudic V, Roudil D, Deschanels X and Bart J M (2004), Effect of alpha decay on nuclear borosilicate glass properties, *Mat. Res. Soc. Symp. Proc.* 824, 315–320

Poinssot, C, Ferry C, Kelm M, Grambow B, Martinez-Esparza A, Johnson L, Andriambololona Z, Bruno J, Cachoir C, Cavedon J M, Christensen H, Corbel C, Jégou C, Lemmens K, Loida A, Lovera P, Miserque F, de Pablo J, Poulesquen A, Quinones J, Rondinella V, Spahiu K and Wegen D (2005), Final Report of the European Project Spent Fuel Stability under Repository Conditions, Rapport CEA-R-6093, CEA Saclay, France.

Rard J A (2005), Current status of the thermodynamic data for technetium and its compounds and aqueous species, *J. Nucl. Radiochem. Sci.* 6(3), 197–204

Ringwood E, Kesson S E, Ware N G, Hibberson W and Major A (1979), Immobilisation of high level nuclear reactor wastes in SYNROC, *Nature* 278, 219–223

Ronchi C and Hiernaut J P (2004), Helium diffusion in uranium and plutonium oxides, *J. Nucl. Mater.* 325, 1–12

Rondinella V V and Wiss T (2010), The high burnup structure in nuclear fuel, *Materials Today* 13(12), 26–34

Rondinella V V, Matzke Hj, Cobos J and Wiss T (1999), α-Radiolysis and α-radiation damage effects on UO_2 dissolution under spent fuel storage conditions, *Mat. Res. Soc. Symp. Proc.* 556, 447–454

Rondinella V V, Matzke Hj, Cobos J and Wiss T (2000), Leaching behaviour of UO_2 containing α-emitting actinides, *Radiochim. Acta* 88, 527–531

Rondinella V V, Cobos J, Matzke Hj, Wiss T, Carbol P and Solatie D (2001), Leaching behaviour and α-decay damage accumulation of UO_2 containing short-lived actinides, *Mat. Res. Soc. Symp. Proc.* 663, 391–398

Rondinella V V, Cobos J, Wiss T and Hiernaut J P (2003), Studies on spent fuel alterations during storage and radiolysis effects on corrosion behaviour using alpha-doped UO_2, in *Proc. ICEM* 2003, paper 4593, Oxford, UK

Rondinella V V, Cobos J and Wiss T (2004), Leaching behaviour of low activity alpha-doped UO_2, *Mat. Res. Soc. Symp. Proc.* 824, 167–173

Rondinella V V, Cobos J, Wiss T and Staicu D (2005), Studies on spent fuel alterations during storage and effects on corrosion behaviour, in *Proc. ICEM 2005*, paper 1275, Glasgow, UK

Rondinella V V, Wiss T and Hiernaut J P (2007), Dose rate effects on the accumulation of radiation damage, in *Proc. ICEM 2007*, paper 12755-8, Bruges, Belgium

Rondinella V V, Serrano-Purroy D, Hiernaut J P, Wegen D, Papaioannou D and Barker M (2008), Grain boundary inventory and instant release fractions for SBR MOX, *Proc. Int. High-Level Radioactive Waste Management Conf.*, 7–9 September, 2008, Las Vegas, NV, USA, paper 195780, ANS CD-ROM

Rose P B, Ojovan M I, Hyatt N C and Lee W E (2004), Crystallisation within simulated high level waste borosilicate glass, *Mat. Res. Soc. Symp. Proc.* 824, 321–326

Roudil D, Deschanels X, Trocellier P, Jomard F, Boutry A, Jégou C, Peuget S, Gosset D and Nivet P (2004), Thermal diffusion of helium and volatile fission products in UO_2 and zirconolite nuclear ceramics, *Mat. Res. Soc. Symp. Proc.* 824, 195–201

Roudil D, Jégou C, Broudic V and Tribet M (2009), Rim instant release radionuclide inventory from french high burnup spent UOX fuel, *Mat. Res. Soc. Symp. Proc.* 1193, 627–633

Sickafus K E (2007), Radiation Damage Effects in Solids, Los Alamos Unclassified Report LA-UR-07-5573

Sickafus K E, Minervini L, Grimes R W, Valdez J A, Ishimura M, Li F, McClellan K J and Hartmann T (2000), Radiation tolerance of complex oxides. *Science* 289, 748–751

SKB (1983), Final storage of spent nuclear fuel – KBS-3, Swedish Nuclear Fuel Supply Co./Division KBS, Stockholm, Sweden

SKB (2008), Horizontal deposition of canisters for spent nuclear fuel. Summary of the KBS-3H Project 2004–2007, SKB TR-08-03, Stockholm, Sweden

SKB website: www.SKB.se

SKI (2007), Spent Fuel Dissolution and Source Term Modelling in Safety Assessment, SKI Report 2007:17, Swedish Nuclear Power Inspectorate (SKI), Stockholm, Sweden

Sonoda T, Kinoshita M, Ray I L F, Wiss T, Thiele H, Pellottiero D, Rondinella V V and Matzke Hj (2002), TEM observation on irradiation-induced microstructural evolution in high burn-up UO_2 disk fuel, *Nucl. Instr. Meth. Phys. Res. B* 191, 622–628

Staicu D, Wiss T, Rondinella V V, Hiernaut J P, Konings R J M and Ronchi C (2010), Impact of auto-irradiation on the thermophysical properties of oxide nuclear reactor fuels, *J. Nucl. Mater.* 397, 8–18

Stroes-Gascoyne S, Tait J C, Garisto N C, Porth R J, Ross J P M, Glowa G A and Barnsdale T R (1992), Instant release of ^{14}C, ^{99}Tc, and ^{137}Cs from used CANDU fuel at 25°C in distilled deionized water, *Mat. Res. Soc. Symp. Proc.* 257, 373–380

Stroes-Gascoyne S, Garisto F and Betteridge J S (2005), The effects of alpha-radiolysis on UO_2 dissolution determined from batch experiments with ^{238}Pu-doped UO_2, *J. Nucl. Mater.* 346, 5–15

Swift P N, Knowles K, McNeish J, Hansen C W, Howard R L, MacKinnon R and Sevougian S D (2009), Long-term performance of the proposed Yucca Mountain Repository, USA, *Mat. Res. Soc. Symp. Proc.* 1124, 3–14

Tait J C, Cornett B J J, Chant L A, Jirovec J, McConnell J and Wilkin D L (1997), Determination of Cl impurities and ^{36}Cl instant release from used CANDU fuels, *Mat. Res. Soc. Symp. Proc.* 465, 503–510

Tribet M, Toulhoat N, Moncoffre N, Toulhoat P, Jégou C, Corbel C, Bardez I and Leturcq G (2007), Enhancement of zirconolite dissolution due to water radiolysis, *Mat. Res. Soc. Symp. Proc.* 985, 335–340

US DOE (2008), Yucca Mountain Repository License Application, DOE/RW-0573, Rev 0

Vance E (2007), Development of ceramic waste forms for high-level nuclear waste over the last 30 years, *Mat. Res. Soc. Symp. Proc.* 135–140

Vernaz E, Gin S, Jégou C and Ribet I (2001), Present understanding of R7T7 glass alteration kinetics and their impact on long-term behavior modelling, *J. Nucl. Mater.* 298(1–2), 27–36

Wald J W and Weber W J (1984), Effects of self-radiation damage in Cm-doped $Gd_2Ti_2O_7$ and $CaZrTi_2O_7$, in Wicks G G and Ross W A (eds), *Advances in Ceramics*, Vol. 8, American Ceramic Society, pp. 71–75, Columbus, OH, USA

Walker C T, Bagger C and Mogensen M (1996), Observations on the release of cesium from UO_2 fuel, *J. Nucl. Mater.* 240, 32–42

Walker C T, Rondinella V V, Papaioannou D, van Winckel S, Goll W and Manzel R (2005), On the oxidation state of UO_2 nuclear fuel at a burn-up of around 100 MWd/kg HM, *J. Nucl. Mater.* 345,192–205

Wang S X, Begg B D, Wang L M, Ewing R C, Weber W J and Govidan Kutty K V (1999), Radiation stability of gadolinium zirconate: A waste form for plutonium disposition, *J. Mater. Res.* 14(12), 4470–4473

Warin D (2007), Status of the french research on partitioning and transmutation, *Mat. Res. Soc. Symp. Proc.* 985, 613–620

Weber W J (1981), Ingrowth of lattice defects in alpha irradiated UO_2 single crystals, *J. Nucl. Mater.* 98, 206–215

Weber W J and Ewing R C (2000), Plutonium immobilization and radiation effects [3], *Science* 289, 2051–2052

Weber W J, Wald J W and McVay G L (1985), Effects of alpha-radiolysis on leaching of a nuclear waste glass, *J. Am. Ceram. Soc.* 68(9), C253–C255

Weber W J, Ewing R C, Catlow C R A, Diaz de la Rubia T, Hobbs L W, Kinoshita C, Matzke Hj, Motta A T, Nastasi M, Salje E K H, Vance E R and Zinkle S J (1998), Radiation effects in crystalline ceramics for the immobilization of high-level nuclear waste and plutonium. *J. Mater. Res.* 13, 1434–1484

Weber W J, Navrotsky A, Stefanovsky S, Vance E R and Vernaz E (2009), Materials science of high-level nuclear waste immobilization, *MRS Bull.* 34, 46–53

Wiss T, Deschanels X, Hiernaut J P, Roudil D, Peuget S and Rondinella V V (2007), Helium release from plutonium and curium-doped zirconolite, *J. Nucl. Mater.* 362, 431–437

Yakub E, Ronchi C and Staicu D (2010), Diffusion of helium in non-stoichiometric uranium dioxide, *J. Nucl. Mater.* 400, 189–195

14

Development of long-term behavior models for radioactive waste forms

D. BACON AND E. PIERCE,
Pacific Northwest National Laboratory, USA

Abstract: The long-term performance of solid radioactive waste is measured by the release rate of radionuclides into the environment, which depends on corrosion or weathering rates of the solid waste form. The reactions involved depend on the characteristics of the solid matrix containing the radioactive waste, the radionuclides of interest, and their interaction with surrounding geologic materials. This chapter describes thermo-hydro-mechanical and reactive transport models related to the long-term performance of solid radioactive waste forms, including metal, ceramic, glass, steam reformer and cement. Future trends involving Monte-Carlo simulations and coupled/multi-scale process modeling are also discussed.

Key words: model, simulation, performance assessment, corrosion, source term, glass, metal, steam reformer, cement, cast stone, Monte-Carlo.

14.1 Introduction

Before solid radioactive waste may be placed in a subsurface disposal facility, a license must be obtained. Approval of the license is generally based on a performance assessment that determines the long-term impacts of the disposal facility on public health and environmental resources. A sound scientific basis for determining the long-term release rates of radionuclides from the radioactive waste forms must be developed if the performance assessment is to be accepted by regulatory agencies and the public. The long-term performance of solid radioactive waste is measured by the release rate of radionuclides into the environment, which in turn depends on corrosion or weathering rates of the solid waste form. These rates strongly depend on the subsurface temperature and flow of moisture through the disposal facility, as well as the reactive surface area of these solid materials. So, an effective performance assessment model is often some combination of a coupled thermo-hydro-mechanical model combined with a reactive transport model. The reactions involved depend on the characteristics of the solid matrix containing the radioactive waste, the radionuclides of interest, and their interaction with surrounding geologic materials. This chapter describes a number of models, of varying complexity, related to the long-term performance of solid radioactive waste forms, including metal, ceramic, glass, steam reformer and cement. Future trends involving Monte-Carlo simulations and coupled/multi-scale process modeling are also discussed.

14.2 Thermo-hydro-mechanical performance modeling

Coupled thermo-hydro-mechanical (THM) models are used to simulate the simultaneous flow of heat and water in deforming rocks or soils. These models have been applied to the safety assessment of waste repositories for radioactive waste disposal, as well as a number of other engineering fields. A number of THM computer codes have been developed. Some consider saturated or unsaturated water flow (Noorishad and Tsang, 1996; Ohnishi and Kobayashi, 1996; Nguyen, 1996; Borgesson, 1996; Thomas *et al*., 1996), while others also consider two-phase flow of water and air (Olivella *et al*., 1994; Rutqvist *et al*., 2001). A more recent approach considers multiphase flow of water and air in both the liquid and vapor phases, including the advection of water vapor (Rutqvist *et al*., 2002), but the thermo-hydro model (TOUGH) is loosely coupled with a separate rock mechanics code (FLAC3D). A more comprehensive, fully coupled approach is taken in the development of the ROLG code (Tong *et al*., 2010). The partially saturated medium is treated as a multiphase system (solid, liquid, and gas), and the multiphase medium is considered as a mixture wherein every phase is continuous and each spatial point in the mixture is assumed to be occupied simultaneously by a material point of every phase.

14.3 Corrosion modeling

The Yucca Mountain engineered barrier system corrosion model predicts the long-term performance of the titantium drip shield and the Alloy 22 waste packages (EBSCOM) (Glasser *et al*., 2008). EBSCOM includes several submodels of various corrosion processes: general corrosion and hydrogen-induced cracking of the drip shield, and general corrosion, localized corrosion, microbially influenced corrosion and stress corrosion cracking of the waste package. It is essentially a collection of process models, and not a multi-dimensional flow and transport code. The rates of the various processes are empirical relations derived from experimental data. The model considers cooling of the waste, and relative humidity of the surrounding air. Once the surface temperature drops below the dew point, seepage waters may drip into the engineered barrier system, and be concentrated by evaporation. The general corrosion of the drip shield is driven by oxidation of titanium, which, in the absence of free oxygen, may produce hydrogen. The produced hydrogen may be absorbed by the drip shield and lead to hydrogen-induced cracking. Microbially influenced corrosion is affected by the surrounding temperature and availability of water. General corrosion is a function of temperature defined by an Arrhenius relationship, whereas local corrosion occurs when the drip shield has failed and seepage water contacts the waste package. Stress corrosion cracking only affects the lid welds, and is a function of temperature, pH and chloride and nitrate concentration.

14.4 Source term release modeling

14.4.1 Commercial spent nuclear fuels

Modeling the release of radionuclides from spent nuclear fuel involves two main processes: an instant release fraction and a matrix alteration process (Johnson *et al.*, 2005). The instant release fraction represents the fraction of the inventory of radionuclides that may be rapidly released from the fuel and fuel assembly materials at the time of canister breaching. Matrix alteration is a slow, long-term process resulting from the dissolution of the uranium oxide matrix. An instant release fraction forms because during in-reactor irradiation, radionuclides produced in a nuclear fuel assembly may stay in the locations in which they are produced or may migrate due to various mechanisms, including recoil, diffusion, grain growth and rim restructuring. An estimate of the instant release fraction under geological disposal conditions was obtained by fitting an empirical model to experimental data of fission product leaching.

14.4.2 Glass

A large amount of information on the glass–water reaction collected over the past 25 years has been summarized in the 'glass compendium' (DOE, 1994) and numerous reviews (Barkatt *et al.*, 1986; Bourcier, 1991, 1994; Bunker *et al.*, 1988; Casey and Bunker, 1990; Hench *et al.*, 1986; Icenhower *et al.*, 2004; Chen *et al.*, 1997; Strachan and Croak, 2000; Werme *et al.*, 1990; Vernaz and Dussossoy, 1992; Vernaz *et al.*, 2001). Based on these reviews, the glass dissolution reaction can be divided into four regimes or stages (Fig. 14.1) that occur as the reaction proceeds (Stages I, II, III, and IV).

Stage I, commonly referred to as the initial rate, consists of the following processes: upon initial contact by water, alkali cations are extracted by interdiffusion, which is considered a diffusion-controlled reaction such that hydrogen or hydronium ions from the solution exchange for alkali ions contained in the glass. The process of interdiffusion is followed by two simultaneous reactions: hydration and dissolution of the glass network. In dilute solutions, the TST-based model successfully accounts for silicate

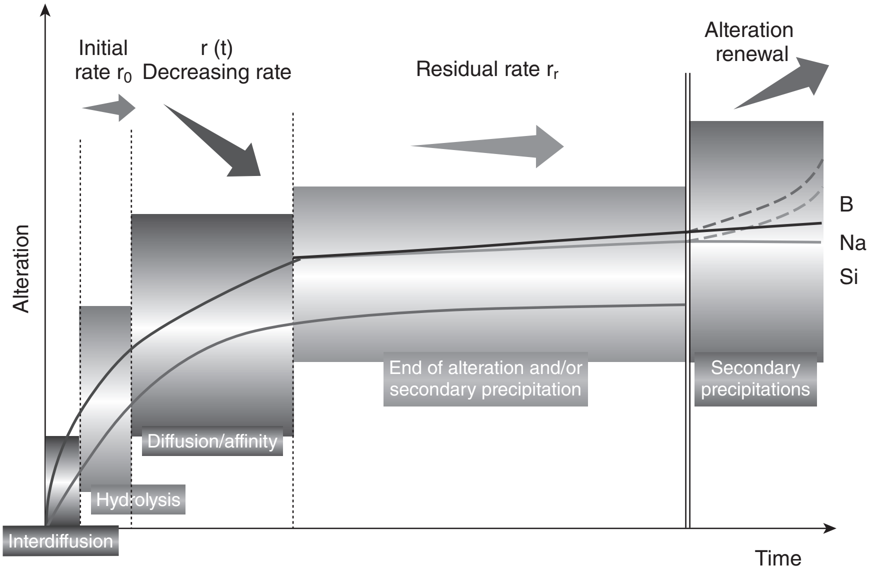

14.1 General schematic of the stages of glass–water reaction.

dissolution in terms of temperature, pH, and reactive surface area. As the concentration of dissolved components increases and the build-up of these components approaches the formation of a thermodynamically unstable phase (hydrated surface layer), Stage II is reached.

During Stage II the matrix dissolution rate becomes dependent on the solution saturation state (concentration of elements in solution). Therefore, the process of ion exchange reaches a relatively constant rate in accordance with a diffusion-controlled process as a hydrated surface layer (e.g., gel layer) develops on the surface of the glass over time (Ojovan *et al.*, 2006b). The hydrated surface layer forms when relatively insoluble glass components (i.e., Al, Fe, and Si) accumulate in the bulk solution and condense at the glass–water interface. Unlike the rate of ion exchange, the dissolution rate of the glass network decreases because of the common ion effect, i.e., as the solution becomes more concentrated in glass components, the difference in chemical potential between the glass and aqueous phase decreases, which decreases the dissolution rate. This decrease in the rate of matrix dissolution is partially due to the effect H_4SiO_4(aq) has on the dissolution rate and the formation of the hydrated surface layer (Pierce *et al.*, 2004, 2008; Abraitis *et al.*, 2000). In other words, as the activity of H_4SiO_4(aq) increases in the aqueous solution the rate of glass dissolution decreases. It is important to note that in the case of glass, the dissolution rate cannot become zero because silicate glasses are thermodynamically unstable in water.

During Stage III the solution becomes saturated and secondary minerals begin to form; the alteration phase is often a simple clay mineral, such as a smectite or chlorite. The precipitation kinetics associated with these phases can be complex, but in general the rate of secondary phase growth increases in response to the increase in magnitude of supersaturation (Nagy and Lasaga, 1993; Nagy, 2001). Depending on the type of alteration phase, the glass–water reaction can increase from the residual rate and return to the forward rate (e.g., Stage IV – alteration rate renewal). This type of behavior has been observed in accelerated weathering experiments and may be associated with the Al:Fe ratio of the glass formulation (Jantzen *et al*., 2008).

Kinetic rate equation

To predict the long-term fate of glass in the subsurface over the period of regulatory concern, a mathematical model that describes glass reactivity is needed. Over the last few decades, a general rate equation has been fashioned to describe the dissolution of glass (and more ordered materials) into aqueous solution. As described below, the equation is based upon the TST of chemical kinetics, in which the overall reaction rate is governed by the slowest elementary reaction. Elementary reactions have simple stoichiometry and can be combined as an overall reaction. In many cases, the elementary reactions can only be inferred. As an example of the elementary reaction, consider the dissolution of SiO_2 polymorphs to form silicic acid:

$$SiO_2(s) + 2H_2O \leftrightarrow SiO_2{\cdot}2H_2O^{\ddagger} \rightarrow H_4SiO_4(aq) \qquad (14.1)$$

in which $SiO_2{\cdot}2H_2O^{\ddagger}$ represents an activated complex. Note that the reactants and the activated complex in Equation 14.1 are linked by a double-headed arrow symbolizing a reversible reaction. Equation 14.1 also illustrates that the TST formulation assumes that the decay of the activated complex is an irreversible reaction.

Previous studies have established that the corrosion rate of silicate waste glasses is a complex process that depends strongly on temperature, pH, and the chemical composition of the aqueous solution contacting the glass. When the aqueous solution is dilute, the glass dissolves at a characteristic forward rate that depends only on glass composition, temperature, and solution pH (Chen *et al*., 1997). In static systems, or where the rates of mass transport by fluid flow are slow, dissolution releases glass components into the aqueous solution, and the concentration of these elements in the contacting fluid increases. The build-up of these dissolved components leads to slower glass corrosion rates as the contacting solution becomes more concentrated. As solution concentrations of dissolved elements continue to increase, solubility limits with respect to secondary phase(s) are reached, and these phases may begin to precipitate. Because silicate glasses are metastable solids, thermodynamics dictates that the glass will continue to dissolve or transform into more stable alteration phases. The key factor controlling long-term durability of waste glasses is the rate at which this process proceeds.

The rate law that appears to best describe this overall dissolution behavior developed by Aagaard and Helgeson (1982) and applied to glass by Grambow (1985) is presented as follows:

$$r_i = \bar{k}_o v_i a_{H^+}^{\eta} \exp\left(\frac{E_a}{RT}\right)\left[1-\left(\frac{Q}{K_g}\right)^{\sigma}\right]\prod_j a_j \qquad (14.2)$$

The chief virtue of Equation 14.2 is that it can be directly input into reaction-transport codes for predicting the long-term dissolution behavior of glass. Another benefit of Equation 14.2 is that it is solidly based on the TST of chemical kinetics, in which a series of reaction rates are governed by the slowest elementary reaction. Therefore, it is simply necessary to ascertain the ‘rate limiting’ step in dissolution, rather than attempt to fully understand all of the possible reactions and kinetic pathways that can occur during the reaction of glass with aqueous solution. Because this rate-limiting step is an ‘elementary reaction’, the stoichiometry of the reaction is typically simple and can easily be modeled.

Numerical simulator

The STORM code has been used to simulate the corrosion of waste forms containing radioactive glass at the Hanford Site in Richland, Washington (Bacon and McGrail, 2005). The STORM simulator was developed by coupling STOMP, a non-isothermal multiphase flow simulator (White and Oostrom, 1996), with AREST-CT Version 1.1, a reactive transport and porous medium alteration simulator (Chen *et al.*, 1995, 1997). The underlying mathematics in STORM is contained in a set of coupled, nonlinear, partial differential equations. They describe the rate of change of the solute concentrations of pore water in a variably saturated, non-isothermal porous medium. The STORM code capabilities include kinetic dissolution of glass, kinetic precipitation and dissolution of secondary phases, aqueous equilibrium speciation, gas-aqueous equilibria, two-phase flow (water and air), and dynamic hydraulic properties.

As previously stated and shown in Fig. 14.2, the capabilities of STORM include: (1) kinetic dissolution of glass, (2) kinetic precipitation and dissolution of secondary phases, (3) aqueous equilibrium speciation, (4) gas–aqueous equilibria, (5) two-phase flow (water and air), and (6) dynamic hydraulic properties. The use of this reactive chemical transport code (i.e.,

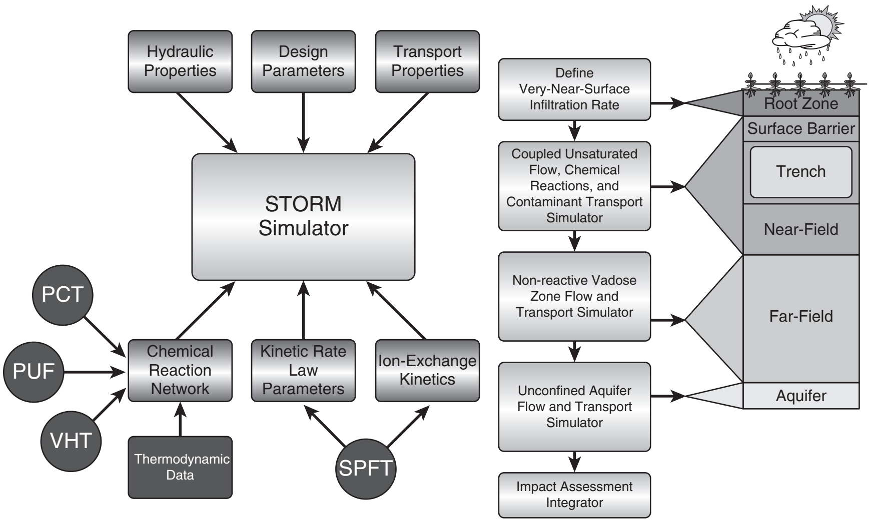

14.2 Schematic that describes the STORM simulator and the approach to modeling the near-field environment for the IDF PA.

STORM) integrates the results obtained from bench-scale laboratory test methods and results from long-term accelerated weathering tests to model the long-term weathering of glass and subsequent release of radionuclides from the engineered portion of IDF (e.g., surface barrier, trench, and near-field). The STORM code has the capability to simulate the special glass kinetic reaction in which many aqueous species are released, but equilibrium depends only on a few of these, such as silica and aluminum. Also, reactive transport in STORM is fully coupled with unsaturated flow; the unsaturated flow field may be altered by mineral dissolution and precipitation reactions. The STORM code runs efficiently in parallel on multi-core workstations and supercomputers, shortening execution times. The verification studies for STORM are documented in the STORM user's guide (Bacon *et al.*, 2004). Applications of the STORM simulator include weathering of vitrified waste at the Hanford site in Richland, Washington (Bacon and McGrail, 2003) and several field sites (McGrail *et al.*, 2003; Ojovan *et al.*, 2006a).

Bulk vitrification (BV)

As part of the strategy for immobilizing waste from the underground tanks at Hanford, selected wastes may be immobilized using BV. During analyses of the glass produced in engineering-scale tests, metal inclusions were found in the glass product. Experiments were designed to quantify the corrosion rates of metal inclusions found in the glass product from Test ES-32B (AMEC 2005) and simulations designed to compare the rate of Tc release from the metal inclusions to the release of Tc from glass produced with the BV process (Bacon *et al.*, 2006). Due to the probability of oxidizing conditions surrounding the waste packages in the IDF, in the simulations the Tc in the metal inclusions and the glass was conservatively assumed to be released congruently as soluble TcO_4^-. The experimental results and modeling calculations (Bacon and McGrail, 2005) show that the metal corrosion rate will, under all conceivable conditions at the IDF, be dominated by the presence of the passivating layer and corrosion products on the metal particles. As a result, the release of Tc from the metal particles at the surfaces of fractures in the glass occurs at a rate similar to that of the Tc present as a soluble salt (Mann *et al.*, 2003; Pierce *et al.*, 2004). The release of the remaining Tc in the metal is controlled by the dissolution of the glass matrix.

The dissolution kinetics of iron [Fe(0)] were quantified under conditions of constant dissolved O_2 [O_2(aq)] and in solutions that minimized the formation of a passive film on the metal surface. These tests were performed to determine the forward reaction rate for the metal inclusions in the BV glass. Single-pass flow through (SPFT) tests were conducted over the pH (23°C) range from 7.0 to 12.0 and temperature range from 23°C to 90°C. The presence of EDTA minimized the formation of a passive film and Fe-bearing secondary phase(s) during testing, allowing us to determine the forward dissolution rate. These results indicate that the corrosion of Fe(0) is relatively insensitive to pH and temperature and the forward rate is 3–4 orders of magnitude higher than when a passive film and corrosion products are present. Tests conducted with Amasteel (a low-carbon steel non-radioactive surrogate) and ES-32B metal indicated that the forward dissolution rates for both metals were similar, if not identical. In other words, the presence of P and ^{99}Tc in the ES-32B metal appeared to have little effect on the forward dissolution rate. These results indicate that the corrosion rate of the ES-32B metal at repository relevant conditions was not significantly less than that of the surrogate metal. Because the effects of temperature ($E_a = 15 \pm 5$ kJ/mol at pH (23°C) = 9.0 based on Fe release from ES-32B metal) and solution pH ($\eta = -0.13 \pm 0.02$ at 70°C based on Fe release from ES-32B metal) were determined to be relatively small under these test conditions, we were unable to obtain reliable rate-law parameters for the metal. Because of the difficulty in obtaining the forward dissolution rate, we conclude that under all conceivable conditions at the IDF a passive film and iron corrosion products will be present and will control metal inclusion dissolution rates. Thus, for the PA calculations a field-measured corrosion rate for low-carbon steel of 0.2 mil/y (0.11 g/(m^2·d)) was used for the maximum corrosion rate for the metals incorporated in the BV product.

A range of field-measured rates were used to simulate release rates of ^{99}Tc from metal inclusions in BV waste packages emplaced in the IDF. The results of these simulations indicate that ^{99}Tc release rates from metal inclusions are likely to be 2–4 orders of magnitude higher than release rates of ^{99}Tc from the glass itself, during the first 2000 years after waste packages have been breached. However, the release rates of Tc to the groundwater are insensitive to the corrosion rates assumed for the metal inclusions, because the corrosion rates are fast relative to travel times through the vadose zone. Technetium release rates from BV product with metal inclusions are sensitive to the size assumed for the inclusions, because the larger the radius of the metal inclusions, the more likely inclusions are to be exposed by a fracture in the glass. Based on the modeling studies, peak ^{99}Tc release rates from the metal inclusions are linearly proportional to the amount of metal in the glass waste packages, whereas long-term ^{99}Tc release rates from the metal inclusions are limited by the corrosion rate of glass. Elevated Tc concentrations due to glass corrosion may inhibit iron corrosion for 500 years, thus delaying the release of Tc from the metal. However, delaying the release of Tc in the metal by 500 years is unlikely to have a significant impact on final groundwater concentrations.

To summarize, the release of ^{99}Tc from the BV glass within precipitated Fe is directly proportional to the diameter of the Fe particles and to the amount of precipitated Fe. However, the main contribution to the Tc release from the iron particles is over the same time period as the release of the soluble Tc salt. For the base case used in this study (0.48 mass% of 0.5 mm diameter metal particles homogeneously distributed in the BV glass), the release of ^{99}Tc from the metal is approximately the same as the release from 0.3 mass% soluble Tc salt in the castable refractory block and occurs over the same time period as release from the salt. Therefore, to limit the impact of precipitated Fe on the release of ^{99}Tc, both the amount of precipitated Fe in the BV glass and the diameter of these particles should be minimized.

14.4.3 Steam reformer

A risk assessment of radionuclide release from the fluidized bed steam reformer product was conducted for Hanford waste (Mann *et al.*, 2003). The THOR$^{\text{TM}}$ FBSR process operates by introducing high sodium nitrate content tank wastes into a moderate temperature (650–800°C) fluidized bed. The tank waste is reacted with carbon and iron-based reductants to convert nitrates and nitrites directly to nitrogen gas. Radionuclides, alkali metals, sulfate, chloride, fluoride, and non-volatile heavy metals in the waste stream are reacted with clay (kaolinite) or other inorganic materials to produce a polycrystalline mineral product (Jantzen, 2002).

Extensive characterization and testing studies have been performed on a SR product manufactured in a 6-inch diameter, fluidized bed pilot plant at Hazen Research (Golden, Colorado) and the results documented by Jantzen (2002) and McGrail *et al.* (2003). The SR process produces a granular product with grain sizes ranging between 4 mm and 1 mm in diameter. The primary minerals in the product examined by Jantzen (2002) and McGrail *et al.* (2003) were nepheline ($NaAlSiO_4$) and nosean [$Na_8(AlSiO_4)_6SO_4$]; small amounts of hematite, magnetite, and corundum were also detected. From testing data and independent mineral synthesis work (Mattigod *et al.*, 2006), rhenium (Re) (chemical analog for Tc) was inferred to be located principally in the nosean phase. The packing efficiency of the SR product in its container was specified by THOR^{TM} at 70% pore space by volume, but the sample examined by McGrail *et al.* (2003) packed to a total porosity of 65%. Scanning electron microscopy of SR grains shows highly irregular surfaces and micropores in each grain that were confirmed by porosimetry measurements.

The physical properties of the SR product used for simulations in this risk assessment are documented in the report by McGrail *et al.* (2003). The kinetic rate law and solubility data for nepheline and nosean are provided in the companion testing report (Mann *et al.*, 2003). The waste package was assumed to be an 8 ft × 8 ft container cross-section for 2D simulations.

The steam reformer material was assumed to consist of two phases, nosean and nepheline. The dissolution reaction used for nosean in the waste form release calculations is:

$$\text{Nosean} \rightarrow 6AlO_2^- + 8Na^+ + 6SiO_2(aq) + 3.29 \times 10^{-6}TcO_4^- + SO_4^- \tag{14.3}$$

The kinetic rate constants used for this dissolution reaction were a forward rate constant of 0.25 mol/m^2/s, an activation energy of 48.6 kJ/mol, and a pH power law coefficient of 0. The log K assumed for this reaction was –92.1.

The dissolution reaction for the nepheline phase is

$$\begin{aligned}\text{Nepheline} \rightarrow\ & 0.9874AlO_2^- + 2.06 \times 10^{-2}Ca^+ + 1.37 \\ & \times 10^{-1}Fe(OH)_3(aq) + 2.25 \times 10^{-2}K^+ + 2.50 \times 10^{-2}Li^+ \\ & + 0.7225Na^+ + 0.77SiO_2(aq) + 0.307Ti(OH)_4(aq)\end{aligned} \tag{14.4}$$

The kinetic rate constants used for this dissolution reaction were a forward rate constant of 1 × 10^{-9} mol/m^2/s, an activation energy of 16.6, and a pH power law coefficient of –0.251. The log K assumed for this reaction was –9.39, assuming equilibrium with AlO_2^-, Na^+ and $SiO_2(aq)$. The other components were excluded from influencing the saturation state of the nepheline. No secondary phases were observed in laboratory experiments with the SR product (Mann *et al.*, 2003), so none were included in the simulations.

14.4.4 Cement

The durability of hydrated cement systems and their constituent phases has received significant attention from scientists and engineers (Glasser *et al.*, 2008; Mohammed and Hamada, 2003, 2004, 2006; Suryavanshi and Swamy, 1998; Suryavanshi *et al.*, 1995, 1996, 2002; Wee *et al.*, 1999, 2000; Birnin-Yauri and Glasser, 1998). Research has been conducted to improve our understanding of the physical and chemical processes that control the long-term performance of these materials under a variety of disposal conditions. A significant portion of these research activities has been conducted with a variety of cemented formulations using different mixtures of dry blend materials – such as slag and fly ash – which can affect the chemical, mineralogical, and microstructural properties of the cast waste form (Glasser, 1997), thereby impacting the degradation mechanisms.

The most common degradation mechanisms that must be captured when modeling the performance of cement-based waste forms include a series of physical and chemical processes. Physical degradation process includes shrinkage (e.g., volume contraction), thermal cracking resulting from temperature excursions, and freezing and thawing cracking which is caused by pore-water expansion (Pabalan *et al.*, 2009). Common chemical degradation processes involve chloride ingress, carbonation, decalcification, sulfate attack, and alkali silica reactions (Glasser *et al.*, 2008; Pabalan *et al.*, 2009). Each of these mechanisms is time- and temperature-dependent (Lothenbach *et al.*, 2008). Therefore, accurately capturing these processes in performance models across spatial and temporal scales requires improved approaches to measuring the interrelationships between these coupled processes. The majority of the modeling conducted to date uses a combination of distribution coefficients and diffusion-based equations that capture only a portion of the key processes that occur and can impact the behavior of the cement waste form over time.

Cast stone

Simulation of diffusion-controlled release of radionuclides from cast stone was conducted at the Integrated Disposal Facility at the Hanford Site in Richland, Washington (Mann *et al.*, 2003). Production of cast stone is performed by mixing dry reagents with low activity waste (LAW) feed (nominal 5M sodium) that has been concentrated to 10M sodium by evaporation. The dry reagents consist of: (1) Portland cement, (2) fly ash, (3) blast furnace slag (BFS), and (4) ferrous sulfate monohydrate. This formulation is essentially equivalent to salt stone grout formulations used at the Savannah River site (Langton, 1989; Langton *et al.*, 1988).

Hydration and set of the cast stone product begins upon mixing the concentrated LAW liquid waste with the dry reagents. Each component contributes to a complex set of chemical reactions that consume water, produce heat, and form calcium-silicate-hydrate (CSH) gel. A generalized reaction scheme is

$$Ca_3SiO_5 + 3H_2O = xCaH_2SiO_4\ (1 - x)SiO_2 + (3 - x)Ca(OH)_2 \tag{14.5}$$

$$Ca_2SiO_4 + 2H_2O = xCaH_2SiO_4\ (1 - x)SiO_2 + (2 - x)Ca(OH)_2 \tag{14.6}$$

where x is the Ca/Si ratio of the CSH gel. The CSH can be considered a solid solution consisting of a non-ideal mixture of the end-member components $CaH_2SiO_4(s)$ and $SiO_2(s)$ (Rahman *et al.*, 1999). The calcium hydroxide produced from reactions 14.5 and 14.6 reacts with silica and calcium aluminates in reactions such as

$$Ca_4Al_2Fe_2O_{10} + 4Ca(OH)_2 + 22H_2O = Ca_8Al_2Fe_2O_{14}\cdot 26H_2O \tag{14.7}$$

$$Ca_3Al_2O_6 + Ca(OH)_2 + 12H_2O = Ca_4Al_2O_7\cdot 13H_2O \tag{14.8}$$

Reactions 14.5–14.8 (along with many others) produce solid particles that continue to grow with time (Peterson *et al.*, 2002) and develop a macroscopic fine-scale pore structure, thereby trapping and limiting the transport of contaminants contained within the cast stone matrix. Hydration of BFS initially proceeds much slower than that of Portland cement, but the products of hydration are similar in terms of chemical make-up, i.e. CSH. Hydration of BFS depends on the activation of the glass component by hydroxyl and alkali ions available from the Portland cement hydration. Activation of the glass is relatively slow and causes a delay in the hydration of slag, which is reflected in slower setting and lower early strength development compared to Portland cement. BFS hydration products are generally found to be more gel-like, as compared to cement, and tend to fill voids, contributing denseness to the cement paste, increased strength, and enhanced durability.

For some radionuclides, solubility limits can be exceeded in the cement pore water, causing precipitation that controls their pore water concentration (Glasser, 1999). For ^{99}Tc, this is highly unlikely under oxidizing conditions. However, the blast furnace slag and $FeSO_4\cdot H_2O$ additives to the cast stone are reductants that have been shown to cause reduction of Tc(VII) to Tc(IV) in cements (Allen *et al.*, 1997; Gilliam *et al.*, 1990). Tc(IV) is highly insoluble and would be expected to precipitate as $TcO_2\cdot xH_2O$ or TcS_2 in cast stone (Allen *et al.*, 1997). However, the authors are unaware of any direct measurements of Re (or Tc) oxidation state in cast stone samples produced to date. If the Tc in cast stone is reduced, remobilization would require oxidation or complexation of the Tc(IV) with organic compounds (i.e. EDTA, HEDTA) present in LAW tank waste that are known to remain in cement pore water (Smillie and Glasser, 1999). Technetium reduction, if it occurs in cast stone, will be properly reflected in reduced effective diffusion coefficients measured with the ANS 16.1 method (Allen *et al.*, 1997; Gilliam *et al.*, 1990).

In Mann *et al.* (2003), a physical model of contaminant diffusion was adopted. Empirical effective diffusion coefficients measured in short-term laboratory experiments were used to model the long-term performance of the cast stone. However, there is no fundamental scientific reason why empirical diffusion coefficients based on short-term laboratory tests for each contaminant should accurately describe cast stone performance for 10,000 years. Cementitious waste forms, such as cast stone, are inherently a porous medium and so diffusion, advection, and chemical reactions within its pores can all be treated within the framework of reactive transport theory (Steefel and Lichtner, 1998). In fact, STORM has been used to model uranium and ^{14}C release from a grout disposal facility in Italy (Bacon *et al.*, 2002; Buck *et al.*, 2002). The chemical aging reactions and contaminant transport in cementitious forms are inherently coupled and so a reactive transport approach is well suited for modeling long-term degradation and contaminant release from cast stone.

A diffusion-controlled transport analysis in its continuous pore network coupled with diffusive-advective transport in idealized fractures was performed. This approach (treating the cementitious waste form as a porous medium with contaminants of concern instantly available in the pore water to be transported using advection and diffusion) is essentially equivalent to what has been performed for analysis of saltstone at the Savannah River site (Cook, 2000) and the past Hanford grout assessment (Kincaid *et al.*, 1995). Time-invariant effective diffusion coefficients measured in the ANS 16.1 laboratory test (data available for only 19 days of leaching) for selected radionuclides and chemical contaminants were used (Table 14.1). It is difficult to evaluate the uncertainty in using the simple effective diffusion coefficient release model to predict the evolving release of contaminants from the aging cast stone matrix, but the literature is replete with discussions of how short-term (from days to a few months) test-derived cumulative effective diffusion coefficients often are larger than cumulative effective diffusion coefficients measured after many months to a few years (Serne *et al.*, 1987, 1989, 1995). However, few have discussed the adequacy of the simple diffusion release model and available data to accurately predict behavior over time periods of thousands of years.

The temporal signature for a diffusion-controlled process is typically a high initial mass flux that declines with the square root of time. However,

Table 14.1 Recommended effective diffusion coefficients for cast stone

Contaminant	Effective diffusion coefficient – simulant basis (cm^2/s)	Effective diffusion coefficient – LAW basis (cm^2/s)	Recommended effective diffusion coefficient (cm^2/s)
NO_3 (nitrate)	2.0×10^{-8}	3.2×10^{-8}	2.5×10^{-8}
NO_2 (nitrite)	4.0×10^{-8}	2.5×10^{-8}	2.5×10^{-8}
Cr (total) (chromium)	$<1.6 \times 10^{-11}$	1.3×10^{-13}	1.6×10^{-11}
99-Tc	Not measured	3.2×10^{-10}	3.2×10^{-10}
129-I	Not measured	$<2.5 \times 10^{-9}$	2.5×10^{-9}
U (total) (uranium)	Not measured	Not measured	3.2×10^{-10}*

* Recommended effective diffusion coefficient set equal to the measured Tc-99 effective diffusion coefficient.

the cast stone blocks will crack over time. The effect of cracking considered in a previous Hanford grout PA was to increase the saturated hydraulic conductivity (Kincaid *et al.*, 1995) by 2–4 orders of magnitude. Diffusivity, porosity, and the relative unsaturated hydraulic conductivity were assumed to be unaffected by cracking (Kincaid *et al.*, 1995). These assumptions will alter the temporal signature from a purely $\sqrt{t}$ dependence at very long times in the simulations. The results from this study have shown that the fracturing of the cast stone has limited effects on the contaminant release.

Probably the most significant concern with the present cast stone release methodology is that reductants have been introduced that have been demonstrated to lower the rates of Tc release in short-term laboratory tests with saltstone (Allen *et al.*, 1997; Gilliam *et al.*, 1990). Technetium release rates are expected to be significantly higher than would be the case if Tc were not reduced. If the reducing properties of the cast stone were to remain effective over the time frame of interest in a risk assessment (thousands of years), use of the lower effective diffusion coefficients measured in short-term ANS 16.1 experiments would be appropriate for modeling long-term Tc release rates from cast stone. Unfortunately, maintenance of reducing conditions in cast stone pore water over these time frames, especially in a vadose zone environment, has not been demonstrated. In fact, modeling calculations performed by Smith and Walton (1993) and direct measurements conducted by Allen *et al.*, (1997) and Shuh *et al.* (2000) suggest that significant reoxidation of Tc occurs. Path lengths in containerized grout are much shorter than for very large blocks considered in prior studies at Hanford (Kincaid *et al.*, 1995). Thus oxygen may penetrate to significant depths in the cast stone blocks over the time frame of interest. Finally, cracks in the cast stone blocks are not expected to fill with water in a vadose zone environment. Cracks, therefore, represent a short-circuit pathway for gaseous oxygen diffusion into the interior of the cast stone. For all these reasons, the authors are concerned about the use of effective diffusion coefficients for Tc measured in very short-term laboratory tests with cast stone.

14.5 Future trends

14.5.1 Monte-Carlo simulations

A major difficulty in predicting the long-term weathering of glasses has been selecting and identifying secondary mineral phases that form from the glass–water reaction. The present inability to accurately predict secondary phase formation from glass composition means that uncertainty exists when accelerated test methods, like the VHT, are used to infer acceptability of glasses in the actual disposal system. Secondary phase formation is strongly linked to glass composition, temperature, and the prevailing chemical environment of fluids in contact with the glass.

Monte-Carlo simulations provide a new computational approach that allows for predicting secondary phase formation as a result of the glass–water reaction changing from a porous amorphous gel-layer to ordered crystalline phases. For example, MC models have been applied successfully to model glass dissolution (Devreux *et al.*, 2004; Arab *et al.*, 2008) and have provided insights into the microscopic processes of glass weathering (Aertsens and Ghaleb, 2001; Ledieu *et al.*, 2006; Lasaga and Lüttge, 2001, 2004; Icenhower *et al.*, 2004). The advantage of Monte-Carlo simulations is that they afford treatment of the interaction of a solid with an aqueous solution as a many-bodied, three-dimensional problem, thereby allowing the investigator to account for the structural properties of the glass and gel layer. This approach is expected to provide a critical missing step in the development of the gel layer and the processes involved in secondary phase formation.

14.5.2 Coupled/multi-scale processes

Quantifying the rate and extent of element or contaminant release from minerals, glasses, or other waste forms has been at the heart of predictive geochemistry studies for decades. The majority of the geochemistry studies have focused on understanding the weathering of primary minerals and basaltic glasses contained in the earth's crust for the purpose of predicting element cycles. The concepts and theories related to mineral and glass weathering developed within the geochemical community have been carried forward and used to predict the release of contaminants from waste forms and other engineered materials. The weathering of these materials is impacted by a series of sequential or simultaneous competing chemical and physical reactions or processes that may control the mass transfer of contaminants from the waste form into solution. These reactions and processes include, but are not limited to, the following:

- Diffusion/advection
- Dissolution/precipitation
- Adsorption/absorption/desorption
- Oxidation/reduction
- Paragenetic sequence of mineral transformation.

The overall impact of individual or coupled reactions and processes on the long-term performance of a waste form depends on a number of variables, such as the waste-form composition, the material's resistance to physical and chemical degradation, the dominant mechanism controlling release, and the disposal system. To improve future simulations of waste-form performance will require a more robust understanding of these processes, linking them across a wide variety of spatial scales. This is shown as an example in Fig. 14.3, which aims to improve our understanding of the coupled processes that affect the glass–water reaction across a variety of spatial scales.

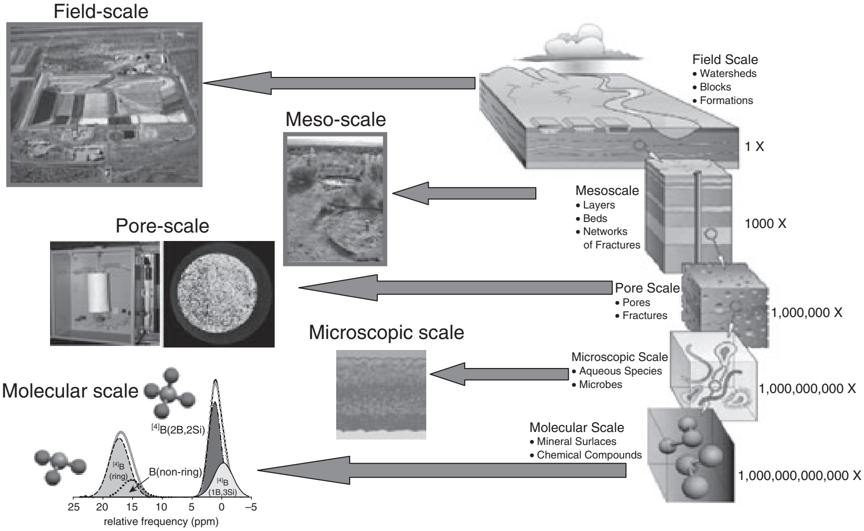

14.3 Example of length scales. This technical strategy increases temporal and spatial resolution to explain key coupled-processes across scales.

14.6 References

Aagaard, P. & Helgeson, H. C. (1982) Thermodynamic and kinetic constraints on reaction rates among minerals and aqueous solutions. I. Theoretical considerations. *American Journal of Science,* 282, 237–285.

Abraitis, P. K., Livens, F. R., Monteith, J. E., Small, J. S., Trivedi, D. P., Vaughan, D. J. & Wogelius, R. A. (2000) The kinetics and mechanisms of simulated British Magnox waste glass dissolution as a function of pH, silicic acid activity, and time in low temperature aqueous systems. *Applied Geochemistry,* 15, 1399–1416.

Aertsens, M. & Ghaleb, D. (2001) New techniques for modelling glass dissolution. *Journal of Nuclear Materials,* 2001, 37–46.

Allen, P. G., Siemering, G. S., Shuh, D. K., Bucher, J. J., Edelstein, N. M., Langton, C. A., Clark, S. B., Reich, T. & Denecke, M. A. (1997) Technetium speciation in cement waste forms determined by X-ray absorption fine structure spectroscopy. *Radiochimica Acta,* 76, 77–86.

AMEC (2005) *Engineering-Scale Quantitative Test Report, Test ES-32B Final Report*. AMEC Earth & Environmental, Inc., GeoMelt^{TM} Division: Richland, Washington, 35004-RT-0001, Rev. 1.

Arab, M., Cailleteau, C., Angeli, F., Devreux, F., Girard, L. & Spalla, O. (2008) Aqueous alteration of five-oxide silicate glasses: Experimental approach and Monte Carlo modeling. *Journal of Non-Crystalline Solids,* 354, 155–161.

Bacon, D. H. & McGrail, B. P. (2003) Lessons learned from reactive transport modeling of a low-activity waste glass disposal system. *Computers & Geosciences,* 29, 361–370.

Bacon, D. H. & McGrail, B. P. (2005) *Waste Form Release Calculations for the 2005 Integrated Disposal Facility Performance Assessment*, PNNL-15198, Richland, WA, Pacific Northwest National Laboratory.

Bacon, D. H., McGrail, B. P., Freedman, V. L., Ventura, G., Risoluti, P. & Krupka, K. M. (2002) Performance assessment of low-level waste disposal facilities using coupled unsaturated flow and reactive transport simulators. In McGrail, B. P. & Cragnolino, G. A. (eds) *2001 Materials Research Society Fall Meeting Proceedings, Symposium JJ, Scientific Basis for Nuclear Waste Management XXV.* Warrendale, PA, Materials Research Society.

Bacon, D. H., White, M. D. & McGrail, B. P. (2004) *Subsurface Transport Over Reactive Multiphases (STORM): A Parallel, Coupled, Nonisothermal Multiphase Flow, Reactive Transport, and Porous Medium Alteration Simulator, Version 3.0, User's Guide*, PNNL-14783, Richland, WA, Pacific Northwest National Laboratory.

Bacon, D. H., Pierce, E. M., Wellman, D. M., Strachan, D. M. & Josephson, G. B. (2006) *Corrosion of Metal Inclusions in Bulk Vitrification Waste Packages*, PNNL-15947, Richland, WA, Pacific Northwest National Laboratory.

Barkatt, A., Gibson, B. C., Macedo, P. B., Montrose, C. J., Sousanpour, W., Barkatt, A., Boroomand, M.-A., Rogers, V. & Penafiel, M. (1986) Mechanisms of defense waste glass dissolution. *Nuclear Technology,* 73, 140–164.

Birnin-Yauri, U. A. & Glasser, F. P. (1998) Friedel's salt, $Ca_2Al(OH)_6(Cl,OH)\cdot 2H_2O$: Its solid solutions and their role in chloride binding. *Cement and Concrete Research,* 28, 1713–1723.

Borgesson, L. (1996) ABAQUS. In Stephansson, O., Jing, L. & Tsang, C.-F. (eds) *Coupled Thermo-hydro-mechanical Processes of Fractured Media.* Amsterdam, Elsevier.

Bourcier, W. L. (1991) Overview of chemical modeling of nuclear waste glass dissolution. *Material Research Symposium Proceedings,* 212, 3–17.

Bourcier, W. L. (1994) Waste glass corrosion modeling: Comparison with experimental results. *Material Research Symposium Proceedings,* 333, 69–81.

Buck, J. W., McGrail, B. P., Bacon, D. H., Freedman, V. L., Ciabotti, P. & Hoopes, B. L. (2002) *Modeling Methodology for Preliminary Performance Assessment of Italian Low-Level Radioactive Waste Repository*, PNWD-3176, Richland, WA, Battelle Pacific Northwest Division.

Bunker, B. C., Tallant, D. R., Headley, T. J., Turner, G. L. & Kirkpatrick, R. J. (1988) The structure of leached sodium borosilicate glass. *Physics and Chemistry of Glasses,* 29, 106–120.

Casey, W. H. & Bunker, B. C. (1990) Leaching of mineral and glass surfaces during dissolution. In Hochella, M. F., Jr. & White, A. F. (eds) *Mineral–Water Interface Geochemistry.* Washington, DC, Mineralogical Society of America.

Chen, Y., Engel, D. W., McGrail, B. P. & Lessor, K. S. (1995) *AREST-CT V1.0 Software Verification*, PNL-10692, Richland, WA, Pacific Northwest Laboratory.

Chen, Y., McGrail, B. P. & Engel, D. W. (1997) Source-term analysis for Hanford low-activity tank waste using the reaction-transport code AREST-CT. In Gray, W. J. & Triay, I. (eds) *Scientific Basis for Nuclear Waste Management XX.* Pittsburgh, PA, Materials Research Society.

Cook, J. R. (2000) *Radiological Performance Assessment for the E-Area Vaults Disposal Facility*, Aiken, SC, Savannah River Site.

Devreux, F., Ledieu, A., Barboux, P. & Minet, Y. (2004) Leaching of borosilicate glasses. II. Model and Monte-Carlo simulations. *Journal of Non-Crystalline Solids,* 343, 13–25.

DOE (1994) *High-level Borosilicate Waste Glass: A Compendium of Corrosion Characteristics, vol. 1*, DOE-EM-0177, Springfield, VA, US Department of Energy Office of Waste Management.

Gilliam, T. M., Spence, R. D., Bostick, W. D. & Shoemaker, J. L. (1990) Solidification stabilization of technetium in cement-based grouts. *Journal of Hazardous Materials*, 24, 189–197.

Glasser, F. P. (1997) Fundamental aspects of cement solidification and stabilisation. *Journal of Hazardous Materials,* 52, 151–170.

Glasser, F. P. (1999) The solubility limited source term for cement-conditioned wastes: A status report. In Wronkiewicz, D. J. & Lee, J. H. (eds) *Scientific Basis for Nuclear Waste Management XXII.* Warrendale, PA, Materials Research Society.

Glasser, F. P., Marchand, J. & Samson, E. (2008) Durability of concrete – Degradation phenomena involving detrimental chemical reactions. *Cement and Concrete Research,* 38, 226–246.

Grambow, B. (1985) A general rate equation for nuclear waste glass corrosion. *Material Research Symposium Proceedings,* 44, 15–27.

Hench, L. L., Clark, D. E. & Harker, A. B. (1986) Nuclear waste solids. *Journal of Materials Science,* 21, 1457–1478.

Icenhower, J. P., Samson, S., Lüttge, A. & McGrail, B. P. (2004) Towards a consistent rate law: Glass corrosion kinetics near saturation. In Giere, R. & Stille, P. (eds) *Energy, Waste, and the Environment: A Geochemical Perspective.* Geological Society of London.

Jantzen, C. M. (2002) *Engineering Study of the Hanford Low Activity Waste (LAW) Steam Reforming Process*, WSRC-TR-2002-00317, Rev. 0, Aiken, SC, Westinghouse Savannah River Co.

Jantzen, C. M., Kaplan, D. I., Bibler, N. E., Peeler, D. K. & Plodinec, M. J. (2008) Performance of a buried radioactive high level waste (HLW) glass after 24 years. *Journal of Nuclear Materials,* 378, 244–256.

Johnson, L., Ferry, C., Poinssot, C. & Lovera, P. (2005) Spent fuel radionuclide source-term model for assessing spent fuel performance in geological disposal. Part I: Assessment of the instant release fraction. *Journal of Nuclear Materials,* 346, 56–65.

Kincaid, C. T., Voogd, J. A., Shade, J. W., Westsik, J. H., Jr., Whyatt, G. A., Freshley, M. D., Piepho, M. G., Blanchard, K. A., Rhoads, K. & Lauzon, B. G. (1995) *Volume 1: Performance Assessment of Grouted Double-Shell Tank Waste Disposal at Hanford*, WHC-SD-WM-EE-004, Richland, WA, Pacific Northwest Laboratory and Westinghouse Hanford Company.

Langton, C. A. (1989) *Slag-Based Materials for Toxic Metal and Radioactive Waste Stabilization*, DP-MS-87-95, Rev. 2, Aiken, SC, E. I. du Pont de Nemours & Co., Savannah River Laboratory.

Langton, C. A., Oblath, S. B., Peppe, D. W. & Wilhite, E. L. (1988) Waste salt disposal at the Savannah River Plant. *Chemical Engineering Communications,* 66, 189–199.

Lasaga, A. C. & Lüttge, A. (2001) Variation of crystal dissolution rate based on a dissolution stepwave model. *Science,* 291, 2400–2404.

Lasaga, A. C. & Lüttge, A. (2004) Mineralogical approaches to fundamental crystal dissolution kinetics. *American Mineralogist,* 89, 527–540.

Ledieu, A., Devreux, F., Barboux, P. & Minet, Y. (2006) Contribution of Monte Carlo modeling to understanding the alteration of nuclear glasses by water. *Nuclear Science and Engineering,* 153, 285–300.

Lothenbach, B., Matschei, T., Möschner, G. & Glasser, F. P. (2008) Thermodynamic modelling of the effect of temperature on the hydration and porosity of Portland cement. *Cement and Concrete Research,* 38, 1–18.

Mann, F. M., McGrail, B. P., Bacon, D. H., Serne, R. J., Krupka, K. M., Puigh, R. J., Khaleel, R. & Finfrock, S. (2003) *Risk Assessment Supporting the Decision on the Initial Selection of Supplemental ILAW Technologies*, RPP-17675, Richland, WA, CH2M Hill Hanford Group, Inc.

Mattigod, S. V., McGrail, B. P., McCread, D. E., Wang, L. Q., Parker, K. E. & Young, J. S. (2006) Synthesis and structure of perrhenate sodalite. *Microporous and Mesoporous Materials,* 91, 139–144.

McGrail, B. P., Bacon, D. H., Meyer, P. D., Ojovan, M. I., Strachan, D. M., Jovan, N. V. & Startceva, I. V. (2003) New developments in field studies of low activity waste glass corrosion and contaminant transport. In Finch, R. J. & Bullen, D. B. (eds) *Scientific Basis for Nuclear Waste Management XXVI*, Warrendale, PA, Materials Research Society.

Mohammed, T. U. & Hamada, H. (2003) Relationship between free chloride and total chloride contents in concrete. *Cement and Concrete Research,* 33, 1487–1490.

Mohammed, T. U. & Hamada, H. (2004) Long-term performance of alumina cement concrete mixed with tap water and seawater. *ACI Materials Journal,* 101, 226–232.

Mohammed, T. U. & Hamada, H. (2006) Corrosion of horizontal bars in concrete and method to delay early corrosion. *ACI Materials Journal,* 103, 303–311.

Nagy, K. L. (2001) Dissolution and precipitation kinetics of sheet silicates. In *Silicate Mineral Dissolution*, Washington, DC, Mineralogical Society of America.

Nagy, K. L. & Lasaga, A. C. (1993) Letter: Simulatneous precipitation kinetics of kaolinite and gibbsite at 80°C and pH 3. *Geochimica et Cosmochimica Acta,* 57, 4329–4335.

Nguyen, T. S. (1996) Description of the computer code FRACON. In Stephansson, O., Jing, L. & Tsang, C.-F. (eds) *Coupled Thermo-hydro-mechanical Processes of Fractured Media.* Amsterdam, Elsevier.

Noorishad, J. & Tsang, C.-F. (1996) ROCMAS-simulator: a thermohydromechanical computer code. In Stephansson, O., Jing, L. & Tsang, C.-F. (eds) *Coupled Thermo-hydro-mechanical Processes of Fractured Media.* Amsterdam, Elsevier.

Ohnishi, Y. & Kobayashi, A. (1996) THAMES. In Stephansson, O., Jing, L. & Tsang, C.-F. (eds) *Coupled Thermo-hydro-mechanical Processes of Fractured Media.* Amsterdam, Elsevier.

Ojovan, M. I., Lee, W. E., Barinov, A. S., Startceva, I. V., Bacon, D. H., McGrail, B. P. & Vienna, J. D. (2006a) Corrosion of low level vitrified radioactive waste in a loamy soil. *Glass Technology – European Journal of Glass Science and Technology Part A,* 47, 48–55.

Ojovan, M. I., Pankov, A. & Lee, W. E. (2006b) The ion exchange phase in corrosion of nuclear waste glasses. *Journal of Nuclear Materials,* 358, 57–68.

Olivella, S., Carrera, J., Gens, A. & Alonso, E. E. (1994) Nonisothermal multiphase flow of brine and gas through saline media. *Transport in Porous Media,* 15, 271–293.

Pabalan, R. T., Glasser, F. P., Pickett, D. A., Walter, G. R., Biswas, S., Juckett, M. R., Sabido, L. M. & Myers, J. L. (2009) *Review of Literature and Assessment of Factors Relevant to Performance of Grouted Systems for Radioactive Waste Disposal*, San Antonio, TX, Center for Nuclear Waste Regulatory Analyses.

Peterson, V., Hunter, B., Ray, A. & Aldridge, L. P. (2002) Rietveld refinement of neutron, synchrotron and combined powder diffraction data of cement clinker. *Applied Physics A–Mater. Sci. Process.,* 74, S1409-S1411.

Pierce, E. M., McGrail, B. P., Rodriguez, E. A., Schaef, H. T., Saripalli, K. P., Serne, R. J., Krupka, K. M., Martin, P. F., Baum, S. R., Geiszler, K. N., Reed, L. R. & Shaw, W. J. (2004) *Waste Form Release Data Package for the 2005 Integrated Disposal Facility Performance Assessment*, PNNL-14805, Richland, WA, Pacific Northwest National Laboratory.

Pierce, E. M., Richards, E. L., Davis, A. M., Reed, L. R. & Rodriguez, E. A. (2008) Aluminoborosilicate waste glass dissolution under alkaline conditions at 40°C: Implications for a chemical affinity-based rate equation. *Environmental Chemistry,* 5, 1–13.

Rahman, M. M., Nagasaki, S. & Tanaka, S. (1999) A model for dissolution of CaO-SiO_2-H_2O gel at Ca/Si < 1 by considering disordered structure. *Materials Research Society Symposium Proceedings,* 556, 1237–1244.

Rutqvist, J., Borgesson, L., Chijimatsu, M., Kobayashi, A., Jing, L., Nguyen, T. S., Noorishad, J. & Tsang, C. F. (2001) Thermohydromechanics of partially saturated geological media: governing equations and formulation of four finite element models. *International Journal of Rock Mechanics and Mining Sciences,* 38, 105–127.

Rutqvist, J., Wu, Y. S., Tsang, C. F. & Bodvarsson, G. (2002) A modeling approach for analysis of coupled multiphase fluid flow, heat transfer, and deformation in fractured porous rock. *International Journal of Rock Mechanics and Mining Sciences,* 39, 429–442.

Serne, R. J., Martin, W. J., McLaurine, S. B., Airhart, S. P., Legore, V. L. & Treat, R. L. (1987) *Laboratory Leach Tests of HFW Grout and Leachate Adsorption Tests Using Hanford Sediment*, PNL-6019, Richland, WA, Pacific Northwest Laboratory.

Serne, R. J., Martin, W. J., Legore, V. L., Lindenmeier, C. W., McLaurine, S. B., Martin, P. F. C. & Lokken, R. O. (1989) *Leach Tests on Grouts Made with Actual and Trace Metal-spiked Synthetic Phosphate/Sulfate Waste*, PNL-7121, Richland, WA, Pacific Northwest Laboratory.

Serne, R. J., Martin, W. J. & Legore, V. L. (1995) *Leach Test of Cladding Removal Waste Grout Using Hanford Groundwater*, PNL-10745, Richland, WA, Pacific Northwest Laboratory.

Shuh, D. K., Edelstein, N. M. Burns, C. J. Lukens, W. W. Bucher, J. J. Fickes, M. G. & Scott, B. L. (2000) *Research Program to Investigate the Fundamental Chemistry of Technetium*. Lawrence Berkeley National Laboratory: Berkeley, California, EMSP-60296.

Smillie, S. & Glasser, F. P. (1999) Reaction of EDTA, oxalic acid and citric acid with Portland cement. *Advances in Cement Research,* 11, 97–101.

Smith, R. W. & Walton, J. C. (1993) The role of oxygen diffusion in the release of technetium from reducing cementitious waste forms. In Interrante, C. G. & Pabalan, R. T. (eds) *Scientific Basis for Nuclear Waste Management XVI*, Warrendale, PA, Materials Research Society.

Steefel, C. I. & Lichtner, P. C. (1998) Multicomponent reactive transport in discrete fractures – II: Infiltration of hyperalkaline groundwater at Maqarin, Jordan, a natural analogue site. *Journal of Hydrology,* 209, 200–224.

Strachan, D. M. & Croak, T. L. (2000) Compositional effects on long-term dissolution of borosilicate glass. *Journal of Non-Crystalline Solids,* 272, 22–33.

Suryavanshi, A. K. & Swamy, R. N. (1998) Influence of penetrating chlorides on the pore structure of structural concrete. *Cement Concrete and Aggregates,* 20, 169–179.

Suryavanshi, A. K., Scantlebury, J. D. & Lyon, S. B. (1995) The binding of chloride-ions by sulfate resistant Portland-cement. *Cement and Concrete Research,* 25, 581–592.

Suryavanshi, A. K., Scantlebury, J. D. & Lyon, S. B. (1996) Mechanism of Friedel's salt formation in cements rich in tri-calcium aluminate. *Cement and Concrete Research,* 26, 717–727.

Suryavanshi, A. K., Swamy, R. N. & Cardew, G. E. (2002) Estimation of diffusion coefficients for chloride ion penetration into structural concrete. *ACI Materials Journal,* 99, 441–449.

Thomas, H. R., He, Y., Sansom, M. R. & Li, C. L. W. (1996) On the development of the thermo-mechanical-hydraulic behaviour of unsaturated soil. *Engineering Geology,* 41, 197–218.

Tong, F., Jing, L. & Zimmerman, R. W. (2010) A fully coupled thermo-hydro-mechanical model for simulating multiphase flow, deformation and heat transfer in buffer material and rock masses. *International Journal of Rock Mechanics and Mining Sciences,* 47, 205–217.

Vernaz, E. & Dussossoy, J. L. (1992) Current state of knowledge of nuclear waste glass corrosion mechanisms: The case of R7T7 glass. *Applied Geochemistry,* 1, 13–22.

Vernaz, E., Gin, S., Jégou, C. & Ribet, I. (2001) Present understanding of R7T7 glass alteration kinetics and their impact on long-term behavior modeling. *Journal of Nuclear Materials,* 298, 27–36.

Wee, T. H., Suryavanshi, A. K. & Tin, S. S. (1999) Influence of aggregate fraction in the mix on the reliability of the rapid chloride permeability test. *Cement and Concrete Composites,* 21, 59–72.

Wee, T. H., Suryavanshi, A. K. & Tin, S. S. (2000) Evaluation of rapid chloride permeability test (RCPT) results for concrete containing mineral admixtures. *ACI Materials Journal,* 97, 221–232.

Werme, L. O., Bjorner, I. K., Bart, G., Lutze, W., Ewing, R. C. & Magrabi, C. (1990) Chemical corrosion of highly radioactive borosilicate nuclear waste glass under simulated repository conditions. *Journal of Materials Research,* 5, 1130–1146.

White, M. D. & Oostrom, M. (1996) *STOMP: Subsurface Transport Over Multiple Phases, Theory Guide*, PNNL-11217, Richland, WA, Pacific Northwest National Laboratory.

15

Knowledge management for radioactive waste management organisations

P. GOWIN, J. KINKER, A. KOSILOV,
I. UPSHALL AND Y. YANEV,
International Atomic Energy Agency (IAEA), Austria

Abstract: The International Atomic Energy Agency (IAEA) is developing a guidance publication on knowledge management for radioactive waste management organisations. The publication is part of the IAEA Nuclear Energy Document Series at the level of Report. The purpose of the document is to provide guidance to the full range of decision makers (in both the public and private sectors) on planning, implementing and sustaining the critical nuclear and institutional knowledge needed for the safe and efficient management of radioactive waste. The guidance covers salient aspects of managing tacit, implicit and explicit knowledge, both in documented (record) form and as skills and experiences in human beings. It addresses information management, human resources, technical competence management, primary and continuing education, stakeholder involvement, management systems and approaches and knowledge analysis and integration.

Key words: knowledge management, long term, radioactive waste knowledge, radioactive waste management, techniques, tools.

15.1 Introduction

The management of radioactive waste is a long-term commitment comprising a number of stages, including waste creation, pre-treatment, treatment, conditioning, storage, transportation, and disposal. These stages may vary from country to country. Nevertheless, they are representative of the stages in a generic radioactive waste lifecycle.

There is a risk that a decision based on incomplete knowledge in one stage will have the potential to foreclose an option in a subsequent stage. Knowledge management will help identify where there are long-term interdependencies between the planning, designing, constructing, operating and decommissioning phases of a radioactive waste management facility.

The International Atomic Energy Agency (IAEA) is developing the guidance publication on *Knowledge Management for Radioactive Waste Management Organizations* [1]. The publication is part of the IAEA Nuclear Energy Document Series at the level of Report.

The purpose of the document is to provide guidance to the full range of decision makers (in both the public and private sectors) on planning, implementing and sustaining critical nuclear and institutional knowledge needed for the safe and efficient management of radioactive waste. The guidance covers salient aspects of managing tacit, implicit and explicit knowledge, both in documented (record) form and as skills and experiences in human beings. It addresses information management, human resources, technical competence management, primary and continuing education, stakeholder involvement, management systems and approaches, and knowledge analysis and integration.

15.2 Challenges for managing nuclear knowledge in radioactive waste management organisations

It is now generally accepted that the fundamental objective of radioactive waste management is to deal with the waste in a manner that protects human health and the environment now and in the future without imposing undue burdens on future generations. This objective first appeared in a 1995 IAEA Safety Series document [2]. The waste management principles that underpinned this objective have now been incorporated in a new generic Safety Standard and a review of the 10 new principles clearly demonstrates the need to adopt a working culture that is largely dependent on access to information and knowledge. Effective knowledge management can therefore have a very positive effect on maintaining and improving safety in our waste management activities.

Knowledge management in a radioactive waste management environment requires specifically defined processes and a framework that must be organised to support the planning, recording, dissemination and transfer of information (collectively 'management'). Knowledge management in radioactive waste management operations (and their regulation) is primarily concerned with ensuring that present and future generations of planners, decision makers and operators have access to appropriate sources of information and that the knowledge created can be efficiently and accurately disseminated and transferred. This must be done in such a way that key personnel are equipped with the necessary skills and competencies to understand and use the knowledge. The ultimate concern must be to support the long-term safe, efficient and cost-effective management of the radioactive waste management facilities and their contents.

Knowledge management will also make a major contribution to the retention and retrieval of information over the long periods of time peculiar to radioactive waste management. Retention of critical staff and knowledge transfer to new staff will clearly be necessary; this may be achieved through succession planning, training, mentoring, and other knowledge transfer processes.

Among the key benefits for implementing knowledge management as an integral part of the business and management culture of a radioactive waste management facility are safety, operating efficiency, and economic efficiency.

Of the three key driving forces for implementing knowledge management in radioactive waste management programmes, the most important stems from operational safety and long-term stewardship. Every treatment, storage and disposal facility operator must ensure that critical knowledge and skills related to safe operation are appropriately gained, maintained and transferred during the facility lifetime. This may span several decades for treatment and storage facilities and several centuries for disposal facilities. Knowledge management is not a generic application that can be 'installed' and implemented – the techniques used will be different depending on the facility, the organisation and Member State. The developers, operators and regulators of these facilities have specific knowledge requirements for meeting their respective responsibilities and these will largely determine the most effective techniques.

In addition to safe operation, radioactive waste management organisations are likely to be concerned with operational efficiency (or optimisation). Where this is the case the motivation for adopting knowledge management could be different. However, safety and operational efficiency can be complementary, based upon a skilled and sustained workforce – a serious challenge when considering the timescales relating to radioactive waste management. Loss of skills and knowledge resulting from an increasingly mobile workforce, in addition to natural wastage, is a particular concern.

Increasingly, government-funded waste management organisations have to demonstrate that they are investing public funds in an effective way. In commercial organisations, the economic effectiveness of an organisation is likely to be a significant factor in its long-term viability. Thus, having a knowledgeable workforce that is able to make justifiable and well-founded decisions can have an impact on economic efficiency.

Regulatory organisations need to be assured that key decisions are made on sound bases and that the outcomes are accurately transmitted and understood. Communicating the basis for a decision can be very important when it is considered that some will have an impact on future generations living and operating in a significantly different regulatory environment. This suggests that records containing the legislation of the day must be retained in order to enable a future society to interpret and understand the basis for historical decisions.

Facilities dealing with radioactive waste include the integration of two primary types of knowledge: about the facility itself; and about the waste and any associated processes carried out.

These two knowledge streams, and the associated documented information, will together represent the bulk of the input used in the decision-making process. For example, there will be many factors that will influence the evolving management strategy during the period for which the waste is subject to active management. These will include revised or updated technical data, changes to regulations, environmental considerations and so on, some of which are associated with the waste and some with the performance of the facility. Therefore, knowledge associated with all potential management strategies should be retained – even if there is a low possibility that they will be adopted. If new information brings into question the validity or appropriateness of an historical decision, national policy may require that it is necessary to review the basis of the decision in terms of the effect of contemporary knowledge.

Controlling potential long-term liability also requires knowledge to be preserved. Preserving the basis for decisions, for example, can protect a radioactive waste management facility operator and its legal successors over a long period of time against charges of negligence or capriciousness in making safety-related decisions. This also protects the legal interest of the public and the government regulatory organisation.

The report [1] outlines the challenges in managing nuclear knowledge that are specific to radioactive waste management organisations. They are:

1. Need to consider long timescales
2. Operating waste management facilities with limited experience
3. Integrating knowledge from multiple sources
4. Need to involve many stakeholders
5. Need for education and training in radioactive waste management.

15.3 Managing nuclear knowledge over very long timescales

Management timescales will vary depending on the disposal facility and the waste type. In order to illustrate typical timescales, Table 15.1 shows the differences between high level waste (HLW), including spent fuel, long-lived (LL) low and intermediate level wastes (LILW), short-lived (SL) LILW, and very low level waste (VLLW) (these waste types are not uniformly defined or recognised by Member States – they are used here simply to aid comparison).

It is necessary to consider that one cannot make judgements about the evolution of, for example, technology, knowledge, regulatory requirements,

Table 15.1 Typical time scales for aspects of various types of disposal systems/repositories

Waste type	HLW/long-lived intermediate level waste (LL-LILW)	Short-lived low and intermediate level waste (SL-LILW)	Very low level waste (VLLW)
Type of disposal system	Geological repository	Near-surface burial facility	Near surface burial facility
Implementation time	>100 years	Several decades (typically)	Several decades (typically)
Duration of potential risk	Several thousand to ~1 million years	100 to 300 years	A few decades
Status	Prospective: under development	Ongoing experience	Ongoing experience

stability of political interest or human society. Therefore, the principles underpinning the knowledge management system must be such that systems can be implemented to capture and process the knowledge necessary for the safe and effective operation of facilities over the various phases, including that of post-closure.

The very long timeframe involved in the HLW disposal facility lifecycle requires a phased or step-by-step decision-making approach to developing, managing and closing such a repository. This suggests that:

- Knowledge must be continuously validated for long-term waste disposal, whilst, in contrast, continuous assessment and improvement would be the best approach for managing SL-LILW disposal facilities (ongoing process with a number of facilities in various Member States with the sharing of lessons learned).
- The knowledge management system for a HLW disposal facility needs to be evaluated in terms of its relation or potential importance to the main goals and lifecycles of the radioactive waste management system ('grading' its importance to safety is a common approach to help allocate resources most effectively).

15.3.1 Knowledge about radioactive waste in perspective

Information about radioactive waste is created in all phases of its management – from its generation, through processing, storage and transportation, disposal and post-facility closure. It is not known how long it will be necessary to undertake extended environmental monitoring and disposal facility performance evaluation but it could amount to many decades.

Systems for the disposal of radioactive waste must meet a set of minimum standards for the long-term protection of human health and the environment. These standards may evolve over time and the systems must be suitably flexible and robust to provide the necessary assurances to society. The IAEA's implementation guidance for its HLW repository safety standards [3] states that the application of a long-term monitoring programme would be a reasonable societal expectation as long as there are appropriate institutions to perform the task. This post-closure monitoring will require that adequate knowledge about disposal sites is made available for as long as these programmes are in place.

The knowledge management arrangements are driven not just by the immediate needs of the present waste custodian but also to whom responsibility falls in the future. The relevance of the information passed on may become less obvious as time goes by, therefore it becomes increasingly important to also transfer contextual information:

> 'To make it possible for future generations to read, understand and interpret the information, it will be important to retain and transmit contextual information (for example, policy for regulating waste, rationale for safety arguments and choices, language and technical terminology, scientific understanding, methods for collecting, analysing and interpreting measurements) as well as the actual recorded data.' [4]

This ongoing requirement means that radioactive waste managers need to work with each other, and their licensing and regulatory authorities, to ensure that the right information is created and maintained at each appropriate step along the way.

15.3.2 Knowledge at various stages of radioactive waste management

The major sources of information are the waste generator and the waste conditioner/packager. Waste generation – and consequently the generation of important information – has typically preceded the start of planned waste management programmes. Whilst there is a certain amount of historical information to be managed, all future activities should recognise the information management needs. For the waste management knowledge management system it is essential to ensure that the information acquisition, managing and processing to support the generation of adequate knowledge also supports its transfer for use in the next stage of the waste lifecycle and/or for the next generation of managers and workers [4, 5].

15.4 Implementing knowledge management in radioactive waste management organisations

Knowledge management is a business management concept which relies heavily on human resources, information technology and process. Therefore, knowledge management should leverage, and be integrated into, an organisation's culture, business processes, management strategy, operational structures, information technology, and stakeholder relationships. This means that any knowledge management strategy should be part of the corporate strategic and policy documents of the organisation and should receive clear commitment from the management team. The degree of success in adopting knowledge management should be measured against staff-based and organisational performance metrics. Particular processes and tools that bring benefits through knowledge sharing should be integrated into the business culture and social and intellectual networks where these have an impact on radioactive waste management.

Knowledge is, by definition, multidisciplinary and this characteristic is particularly apparent in the field of radioactive waste management. Where the purposes of specific knowledge management processes are not generally recognised for what they are, it may be necessary to highlight and tailor them and to phase them in over a period of time. The IAEA report [1] provides guidelines for phasing and structuring knowledge management practices into an existing and functioning radioactive waste management facility, including:

- The assessment of existing knowledge management practices and knowledge inventory analysis
- The development of a viable strategy that includes the assignment of roles and responsibilities
- Strategies for knowledge management contingency plans
- Performance measures of knowledge management success at both staff and organisational levels.

Ultimately, the benefits of knowledge management will only be realised when the practices become an integral part of the facility's everyday operating ethos. Success relies on staff to think from a knowledge management perspective when designing workflows and to look beyond performing just the task at hand to considering how knowledge can be captured and shared both now and in the future. This fundamental change in perspective will require top-level support from senior managers in the form of clear expectations, adequate resources, and rewards for desired behaviours and results.

Implementing an effective knowledge management strategy may require some fundamental changes to the facility's organisational culture. Although some benefits can be realised on a short timescale, major institutional changes of this nature can take several years to bed in. Because of the significance and duration of the change process, active change management is essential to the success of knowledge management. Managing the changes will require clear communications, top-down and bottom-up alignment, building momentum on early successes, and most importantly, leadership to direct the effort over the long term.

15.4.1 Organisational obligations

In an ideal implementation, all organisations forming the radioactive waste community with responsibilities for information preservation, transfer and knowledge creation would incorporate a fully compliant, standards-based integrated framework as the basis of their information management system. Specific organisational obligations would include:

- The creation and preservation of appropriate information resources in accordance with relevant standards
- The management of those resources in a system that documents and preserves the context of their creation and use
- Making available to the wider waste management community the information surrogates representing context entities in a form suitable for citation, linking and data exchange
- Linking to the relevant context surrogates in other sites or clusters in the broader radioactive waste information network
- The documentation of their information resource management system as part of quality management system processes
- Responsibility for the quality of the data and information in their own systems
- The sharing of any knowledge, technologies or systems they develop to facilitate the utilisation of contextual information
- Financing this activity as a part of standard operational practice.

Bodies that currently have responsibilities for the standards, protocols and training programmes that support the radioactive waste community should take on the responsibility for developing and managing such programmes that may be required to sustain the utilisation of integrated frameworks over time.

15.4.2 Implementation

If the radioactive waste community or any part of it decided to implement an integrated framework, their first task would be the development of an implementation strategy. The issues that such a strategy should consider include:

- Setting up a pilot project to evaluate the approach and develop a detailed implementation strategy
- Assessing the existing information resource management systems and planning their upgrade to include the required capabilities. Particular attention is to be paid to archival, record management and knowledge management systems
- Defining the purpose and limits of the integrated framework. These can be scaled or graded to meet particular needs and circumstances as required
- Gearing the contextual information system to work with existing information systems as far as possible without compromising functionality
- Reusing existing contextual information resources wherever possible to minimise duplication of effort
- Identifying and utilising the appropriate open-source or non-proprietary contextual information management tools
- Involving all staff concerned with the management of information, in particular the officer(s) responsible for the management system, knowledge managers, archivists, records managers, librarians and information officers
- Training of staff, including senior management, and defining new tasks and job descriptions
- Maintaining the hardware and software to support the system, including back-up strategies
- Establishing information quality review processes.

15.4.3 Benefits and risks

In addition to the generic benefits that stem from information managed in open network systems, it is possible to identify specific benefits that would arise from the implementation of the contextual information frameworks across the radioactive waste management community. These would include:

- Facilitating the capture of critical implicit technical knowledge, mutual learning, and the sharing of experience both within and between organisations
- Utilising existing technical and operational knowledge and information that has already been accumulated and therefore building on existing resources in a structured way
- Enabling all stakeholders to understand the bigger picture, thus promoting trust and confidence in the community
- Complementing existing practice as it is a non-invasive technique that builds frameworks that will enable much more to be done with existing information

- Helping avoid contradictory decisions being taken in the future and improving decision making more generally
- Enabling the informed appraisal and selection of information resources for future needs based on shared experience and information
- Enabling the informed, confident, systematic, responsible and registered destruction of information resources no longer deemed to be of value
- Providing a quality feedback mechanism
- Improving transparency both within the industry and to the wider community
- Facilitating indirect review of information content by regulatory and other appropriate external organisations.

However, all strategies and technologies have inherent risks that need to be considered and evaluated. The risks to such an approach could include:

- *Concern in the radioactive waste industry about the use of an open network to reference potentially sensitive information about radioactive materials.* Each organisation responsible for a contextual information framework would decide what primary information should be placed in the public domain. Much information that is required to make the framework effective is already in the public domain but not systematically managed. As time passes the security implications associated with much of the information are likely to reduce as they become of historical rather than operational value.
- *Concerns about the longevity of electronic information technologies.* It is indeed the case that the concept makes use of contemporary technologies and expertise and it is recognised that there is nervousness about using digital technologies and digital networks. However, critical information should be replicated in other systems using different technologies or media and this applies equally to contextual information.
- *Concerns that such strategies will lead to increased costs and increased workloads.* There is no question that this strategy will require adequate resourcing. It is contended that as the strategy makes better use of information that already exists, the system, once in place, will add significantly to administrative and governance productivity, and thus reduce costs over time.
- *Concerns about unintended consequences.* All new activities and technologies run the risk of experiencing unintended consequences. Web-based and networked information system technologies are in their infancy and their impact on society is only just becoming apparent. The adoption of the approach should be undertaken in a measured and self-reflective manner to ensure that they are not counterproductive.

There are also risks associated with the failure to implement an integrated information management strategy. The decision not to use this approach would, by default, leave the industry to continue to adopt unsustainable practices which have been shown to be inadequate. Indeed, it could be argued that the industry could be seen to be negligent if it failed to implement strategies that have been codified by international archival and records management standards. More specifically these risks could include:

- Increasing the degree of burden on future generations
- Criticism that the industry is not adequately addressing its responsibilities
- Increasing the likelihood of accidents
- Criticism for not using best practice tools and concepts
- Loss of critical information through poorly managed organisational change
- Duplication of work and inefficient use of resources
- Loss of implicit knowledge
- Increasing the likelihood of inaccurate information having a misleading influence on community attitudes and political decision making.

15.5 Knowledge management tools and techniques for use in radioactive waste management

Knowledge management in radioactive waste management processes, whether operational or regulatory, is just now being established. Therefore, the tools and techniques discussed here are taken from other applications in which knowledge management has been successfully established. It is suggested that the general principles can be adapted to the meet the particular aspects of waste management operations. In time, the experience gained will allow a review of the effectiveness of these techniques in a radioactive waste management environment.

As for these other domains that already apply knowledge management techniques, it is require to adopt robust planning and well-defined management processes within a business framework. The planning must involve all stakeholders, including knowledge owners and producers as well as knowledge users. The process must be organised to support the alignment, sharing, transfer and management of human resources and information related to radioactive waste management. This must be done in such a way that the people have not only access to information but the skills and competencies to understand and use it. The knowledge bases and the existing information must be appropriate to support a safe, efficient and cost-effective operation of the waste management facilities and their contents. Given that these facilities often have long lifecycles, it is important to maintain the knowledge for a long period of time. It is equally important that the lifetime plan is supported by effective staff succession planning, talent retention and competence management.

The report [1] lays out the aspects of knowledge management that may be usefully adapted for use in the management of radioactive waste. It includes discussions about knowledge-maintenance infrastructures as well as talent management and human resources.

15.6 Conclusions

Over the past years, it has become increasingly clear that managing nuclear knowledge is of prime importance for any nuclear endeavour. Good nuclear knowledge management programmes can – in most general terms – contribute to:

- Achieving safe operation and maintenance of all nuclear facilities
- Achieving gains in economics and operational performance through effective management of the resource knowledge
- Facilitating innovation to achieve significant improvements in the safe, economical operation of all new nuclear projects
- Maximising the flow of nuclear knowledge from one generation to the next and attracting, maintaining, and further developing a dedicated cadre of highly competent professional staff to sustain nuclear competence
- Achieving a high degree of transparency – regional, national, and international – and exchange of operational experience to ensure nuclear safety while simultaneously achieving appropriate safeguard requirements by avoiding the improper use of sensitive information.

The IAEA report [1] recommends that nuclear knowledge management programmes should be established also for radioactive waste management, both on the level of radioactive waste management organisations and also possibly as part of related national radioactive waste management programmes.

For doing so, the IAEA has already published a number of documents applicable to nuclear organisations in general. In particular IAEA-TECDOC-1510 on *Knowledge Management for Nuclear Industry Operating Organizations* [6] is applicable also to radioactive waste management organisations, contains relevant guidance and should be read together with this publication. Establishing and implementing nuclear knowledge management programmes in the context of radioactive waste management poses special challenges, however. The report [1] is meant as additional guidance for addressing these challenges, which are:

- The long timescales to be considered
- The need to run programmes based on limited experience gained to date
- The need to integrate relevant knowledge from different sources
- The desired involvement of stakeholders
- The need to develop adequate education and training programmes for radioactive waste management.

The report is written to be specific for nuclear knowledge management in a radioactive waste management context, and provides strategic advice to managers on how to embark on and implement nuclear knowledge management programmes in a radioactive waste management context.

15.7 Sources of further information and advice

1. P. Gowin, J. Kinker, A. Kosilov, I. Upshall, Y. Yanev, Knowledge management for radioactive waste management organisations. *International Journal of Nuclear Knowledge Management* 2009, Vol. 3, No. 2, pp. 157–169
2. International Atomic Energy Agency, Nuclear Fuel Cycle and Waste Technology website: http://www.iaea.org/OurWork/ST/NE/NEFW/index.html
3. International Atomic Energy Agency, Publications website: http://www.iaea.org/Publications/index.html
4. International Journal of Nuclear Knowledge Management, website: http://www.inderscience.com/index.php.
5. International Atomic Energy Agency, Nuclear Knowledge Management website: http://www.iaea.org/inisnkm/nkm/index.html
6. TVA Knowledge Retention, http://www.tva.com/knowledgeretention/index.html
7. ENTRAC – a Tool for Sharing Information Regarding Nuclear Training and Technology, http://entrac.iaea.org/Default.aspx
8. Interactive Training Course on Nuclear Knowledge Management, http://www.iaea.org/inisnkm/nkm/e_learning/2010/multimedia_TrainingCourse.htm
9. 2009 School of Nuclear Knowledge Management website: http://www.iaea.org/inisnkm/nkm/e_learning/2009/web_school/NKM_School_Trieste.htm
10. International Atomic Energy Agency, Radioactive Waste Management Information Systems website: http://www.iaea.org/OurWork/ST/NE/NEFW/wts_information.html
11. International Atomic Energy Agency, *Joint Convention on the Safety of Spent Fuel Management and on the Safety of Radioactive Waste Management*. Online: http://www.iaea.org/ns/rasanet/conventions/jointconven.htm

15.8 References

[1] International Atomic Energy Agency, *Knowledge Management for Radioactive Waste Management Organizations*, IAEA, Vienna (in preparation)

[2] International Atomic Energy Agency, *The Principles of Radioactive Waste Management*, Safety Series No. 111-F, IAEA, Vienna (1995)

[3] International Atomic Energy Agency, *Geological Disposal of Radioactive Waste*, IAEA Safety Guide (in preparation)

[4] International Atomic Energy Agency, *Management System for Geological Disposal of Radioactive Waste*, IAEA Safety Requirement (in preparation)

[5] International Atomic Energy Agency, *Records for Radioactive Waste Management up to Repository Closure: Managing the Primary Level Information (PLI) Set*, IAEA-TECDOC-1398, IAEA, Vienna (2004)

[6] International Atomic Energy Agency, *Knowledge Management for Nuclear Industry Operating Organizations*, IAEA-TECDOC-1510, IAEA, Vienna (2006)

Index